CRANFIELD UNIVERSITY

CRANFIELD POSTGRADUATE MEDICAL SCHOOL.
DEPARTMENT OF MATERIALS AND MEDICAL SCIENCES.

PhD THESIS

Academic Year 2005-2006.

Richard Barker Cook

Non-Invasively Assessed Skeletal Bone Status and its Relationship to the Biomechanical Properties and Condition of Cancellous Bone

Supervisor: Dr. P. Zioupos

December 2005-12-18

Abstract

Cancellous bone constitutes much of the volume of bone which makes up axial skeletal sites such as the vertebrae of the spine and the femoral neck. However the increased vascularity of cancellous bone compared with cortical bone means that it is more prone to drug, endocrine and metabolic related effects and therefore these skeletal sites are more prone to the bone condition osteoporosis. With the bone condition osteoporosis increasing in prevalence it is becoming far more important not only for those at risk of having the condition to be diagnosed earlier, but also for the effects of the condition to be better understood. There is a need for the better clinical management of fractures and for therapies and medical practices that will best avoid the low trauma fractures that are seen as a consequence of the condition.

This study is in two separate sections, the first constitutes an investigation into the diagnostic abilities of the CUBA Clinical and Sunlight Omnisense quantitative ultrasound systems; and on the other hand an examination of the osteoporotic risk factor questionnaires, Osteoporosis Risk Assessment Instrument (ORAI), Osteoporosis Index of Risk (OSIRIS), Osteoporosis Self-assessment Tool (OST), Patient Body Weight (pBW), Simple Calculated Osteoporosis Risk Estimation (SCORE) and the Study of Osteoporotic Fractures (SOFSURF). The skeletal status was assessed by DXA at the axial skeleton. The aim was to differentiate between the systems that could rationally be used to screen populations to identify those who needed DXA densitometry investigations, on the basis of ability.

The second section of the study focused on the biomechanics of cancellous bone, with the initial studies examining the compressive properties of both osteoporotic and osteoarthritic cancellous bone and the effects that the conditions have on the compressive mechanics of the bone. The later section is the first ever study into the K, G and J-integral fracture mechanics of cancellous bone. It used osteoporotic and osteoarthritic cancellous bone from the femoral head of a cohort of ultrasound scanned patients and of some equine vertebral cancellous bone. The study focused on the identification of the dominant independent material variables which affected the compressive and fracture mechanics of cancellous bone, and the differences that were seen between the two different skeletal conditions. In addition to the independent variables, quantitative ultrasound (QUS) scans were performed on the donors of the femoral heads which enabled investigation into QUS's ability to predict either the compressive or fracture mechanics of bone in-vivo.

The study demonstrated that the investigation of the calcaneus using the CUBA clinical system provided the highest level of diagnostic accuracy (AUC: 0.755 - 0.95), followed by the questionnaires, of which the OSIRIS questionnaire was the best performer (AUC: 0.74 – 0.866), and lastly the Sunlight Omnisense results. The best option for the prediction of the lowest feasible DXA T-score was a combination of the CUBA Clinical results, the individual's weight and the OSIRIS questionnaire (r^2 = 45.5%), with potential minor, but significant, support also added by the OST and SOFSURF questionnaires (r^2 = 46.8%).

The compressive testing demonstrated that osteoporotic and osteoarthritic bone both performed differently with respect to the apparent density, with the osteoporotic bone

adhering to the previously published power function relationships, but with the osteoarthritic bone having lower power functions.

The stress intensity factor for plane strain testing (K_Q or K_C) and the critical strain energy release rate results were both influenced primarily by the apparent density with the K values obeying a power relationship to the power of 1.5 and G a relationship to the power 2. However, both the composition and integrity of the collagen network, (demonstrated by collagen cross-link analysis), played roles in the explanation of the fracture mechanics results. The J-integral results were distinctly different to those of the K and G results with regard to their dependence on composition and it is hypothesised that this is due to the structure of the bone having more dominant effects than the apparent density.

In conclusion, the fracture mechanics of cancellous bone are contributed to by a complex combination of a number of variables, but with apparent density dominating the K and G fracture mechanics to a power function of between 1 and 2. Currently available QUS systems demonstrated an ability to relate to the Young's modulus and strength but also, in this study, to the fracture mechanics variables of the cancellous bone from the hip. This relationship is a profound outcome which may help the clinical management of the condition and the fractures when they occur. The dependence on fracture mechanic variables points to a clear causal relationship between the bone fracture parameters and bone condition as underlying factors of osteoporotic fractures.

Acknowledgements

This study was a huge undertaking for me and I never would have been able to perform the work that I have without the support I received. My first thanks must go to Dr. Peter Zioupos who almost four years ago took a Saturday afternoon to meet me and hasn't ceased in his support, mentoring and guidance since that day. Further thanks must go to those other individuals who have helped along the way; Dr. Chris Curwen and his team as well as Andy Williams and Sharon Wade for their support and organisation in gaining the human tissue from Gloucestershire Royal Hospital. Thanks also goes to the staff of the Radiography and Rheumatology departments at the Great Western Hospital, Swindon and in particular Julie Tucker and Dr. David Collins for their support with the clinical aspect of this study.

Slightly closer to home, I must thank the members of the Department of Materials and Medical Sciences in Shrivenham for their support; in particular Viv Wise for her support early on in the project, Colin Offer for the amazing work he did with the test rigs and jigs which made the testing possible; and my colleagues, past and present in Stephenson Lab 1-12.

Finally many thanks to my friends and girlfriend for there unwavering support and to my parents who inexplicably haven't thrown me out the house yet, and even proof read this thesis!

Forward

This project was undertaken as part of a project entitled “Bone Scanning for Occupant Safety” (BOSCOS). The BOSCOS project was funded by the Department for Transport as a Foresight Vehicle Project which was set to run from February 2002 until April 2005. The project consortium consisted of two universities (Cranfield and Loughborough), two research institutes (Nissan Technical Europe and Cranfield Impact Centre), two automotive restraint manufacturers (TRW Automotive and Autoliv), with the final consortium member being a clinical ultrasound manufacturer (McCue Plc.).

For many years the restraint systems within the automotive industry have been steadily improving, with new air bags, seat belt pre-tensioners and in-car sensing enabling far better protection of an individual in a crash situation. However the default set-up of the protection systems is based on the 50^{th} percentile Hybrid III dummy. The more elderly of the population and individuals with low bone density or bone conditions such as osteoporosis have impaired bone biomechanical properties compared to an average individual. Therefore a suitable restraint for the protection of an average occupant during a crash scenario could potentially result in the fracture of an older of less skeletally competent individual. The restraint manufacturers and automotive related research institutes recognised that in a number of crash scenarios, there was potential for adjustment of the restraint systems. These adjustments would enable the peak loads imposed on the body during deceleration in a crash to be reduced.

The premise of the project was to attempt to compare the biomechanical competence of human osteoporotic bone with respect to more normal individuals. This would enable the restraint manufacturers to understand the percentage load reduction that would be required to better protect the weak boned individual. In addition, it was decided to input a bone scanning system into the vehicle that would enable the acquisition of data for the skeletal condition of the occupant. The result of the scan would be included in the number of different restraint related parameters, to provide a more specific restraint system for the occupant which would provide the best fracture prevention in a crash situation.

The project aims, with respect to Cranfield University, were to work alongside McCue Plc. to help develop and validate a scanning system which could be inserted into a motor vehicle. In addition to this, work was to be performed to investigate the mechanics of osteoporotic bone so as to understand better the percentage reduction in competence occuring in osteoporosis with respect to normal average individuals. The final aspect was to relate the percentage drop in the ultrasound result obtained either by the prototype system or by another clinical QUS system with the relative percentage drop in the biomechanical competence of the bone.

The work was undertaken over the three year period of the project and six documents were written on different aspects of the project, with all documents submitted to the Department of Transport as project deliverables. The deliverable documents can be found in Appendix 15.

The work that is contained within this thesis is part of the work that was performed for the BOSCOS project, but it has been written so as to be relevant to the clinical and biomechanical fields of academia, rather than with reference to its benefits and significance

solely for the BOSCOS project. The work that is contained within this thesis has been presented both at international conferences and published within the scientific literature. All the following publications can be found in Appendix 16.

Conference Presentations

1. R. Cook, D. Collins, C. Curwen and P. Zioupos (2003) Comparison of Inter-Site Bone Densitometry Measurements, and the Short-Term Precision of Two Bone Quantitative Ultrasound Scanners.

IPEM Annual Scientific Meeting, 15-17 September 2003, University of Bath, Bath, UK

2. R. Cook, D. Collins, J. Tucker and P. Zioupos (2004) The Predictive Ability of Two Quantitative Ultrasound Bone Scanners in Comparison to DXA.

ESB 2004, 4-7 July 2004, Hertogenbosch, the Netherlands
(This paper was one of three selected to compete for the Clinical Biomechanics Award, and was presented at a special plenary session at the meeting.)

3. R. Cook, P. Zioupos, C. Curwen and T. Tasker (2005) Fracture Toughness of Femoral Head Cancellous Bone Material in Relation to Non-invasive Bone Assessment Measurements.

Biomech (2005) Applied Biomechanics, 1 - 3rd July 2005, Regensburg, Germany

Poster Presentations

1. R.B. Cook, D. Collins and P. Zioupos (2005) Comparison of Patient Screening Techniques for Dual-Energy X-ray Absorptiometry (DXA).

National Osteoporosis Society, 10th Conference on Osteoporosis, 28th November – 1st December 2005, Harrogate International Conference Center, Harrogate, UK

Automotive Conference Papers

1. J.W. Watson, R.N. Hardy, R. Frampton, O. Williams, P. Zioupos, R. Cook, A. Kennedy, P. Sproston, B. Forrester and S. Peach (2004) BOSCOS Bone Scanning for Occupant Safety.

Vehicle Safety Conference, Institute of Mechanical Engineers, December 2004.

2. R.N. Hardy, J.W. Watson, R. Cook, P. Zioupos, B. Forrester, R. Frampton, M. Page, A. Kennedy, S. Peach and P. Sproston (2005). Development and Assessment of a Bone Scanning Device to Enhance Restraint Performance.

Enhanced Safety of Vehicles (ESV) Conference, Washington June 2005

3. R.N. Hardy, J.W. Watson, R. Frampton, M. Page, P. Zioupos, R. Cook, A. Kennedy, P. Sproston, B. Forrester and S. Peach (2005). BOSCOS - Development and Benefits of a Bone Scanning System

IRCOBI Conference, Prague September 2005

Peer Reviewed Journal Articles

1. R.B. Cook, D. Collins, J. Tucker and P. Zioupos (2005) The Ability of Peripheral Quantitative Ultrasound to Identify Patients With Low Bone Mineral Density in the Hip or Spine. **Ultrasound in Medicine and Biology;** *Vol. 31*, No. 5, p.625-632

2. R.B. Cook, D. Collins, J. Tucker and P. Zioupos (2005) Comparison of Questionnaire and Quantitative Ultrasound Techniques as Screening Tools For DXA. **Osteoporosis International;** *Article in Press*

List of Contents

Chapter 1: Introduction **1**

Chapter 2: Bone **4**
2.1 The Macro-Structure of Bone 5
2.1.1 Cortical Bone 5
2.1.2 Cancellous Bone 6
2.2 Bone Composition 6
2.2.1 Organic Matrix 7
2.2.1.1 Non-collagenous Proteins 7
2.2.1.2 Collagen 8
2.2.2 Mineral Matrix 10
Concluding Remarks 11

Chapter 3: Biomechanics **12**
3.1 Trabecular Bone Material 12
3.2 Cancellous Bone 16
3.2.1 Compression Testing 16
3.2.1.1 Apparent Density 17
Young's Modulus / Stiffness 18
Strength 26
Other Mechanical Parameters 28
3.2.1.2 Apparent Ash Density (g cm^{-3}) 31
3.2.1.3 Bone Mineral Density (BMD) 36
3.2.1.4 Composition 38
3.2.1.5 Sources of Irregularity in Compression Testing 42
Bone Related Errors 42
Sample Design 44
Testing Errors 45
Loading Rate or Testing Conditions 47
3.2.2 Tensile Testing 48
3.2.3 Compression vs. Tension 51
3.2.4 Fracture Toughness Testing 52
3.2.4.1 Fracture toughness simulations 52
Concluding Remarks 58

Chapter 4: Bone Conditions **60**
4.1 Osteoporosis 60
4.1.1 Incidence and Scale of the Problem 60
4.1.2 Definition 60
4.1.3 Primary Osteoporosis 61
Type I or Postmenopausal Osteoporosis 61
Type II or Age-Related Osteoporosis 61
Idiopathic Osteoporosis 62
4.1.4 Secondary Osteoporosis 62
4.2 Osteoarthritis (OA) 64

4.2.1 Definition and Incidence 64
4.2.2 Primary OA 64
4.2.3 Secondary OA 65
4.3 The Effects of Osteoporosis and Osteoarthritis on Bone 65
4.3.1 Composition 65
4.3.2 Material Properties and Structure 68
4.4 Densitometry Assessment 69
4.4.1 Dual Energy X-ray Absorptiometry (DXA) 70
4.5 Diagnosis of Osteoporosis and Low Bone Density 71
4.6 Clinical Risk Factors 74
4.7 Questionnaire Systems 78
4.8 Quantitative Ultrasound (QUS) 86
4.8.1 Ultrasound Parameters 87
4.8.1.1 Broad-band Ultrasound Attenuation (BUA) 87
4.8.1.2 Velocity / Speed of Sound (VOS / SOS) 88
4.8.1.3 Stiffness Index, Quantitative Ultrasound Index, Estimated Heel BMD 88
4.8.2 The Utility of QUS 89
4.8.2.1 Precision 89
Factors Affecting Precision 96
4.8.2.2 Inter-site Correlations 98
4.8.2.3 Discriminatory Ability 102
4.8.2.4 Predictive Ability 106
4.8.2.5 Fracture Prediction and Fracture Risk 110
4.9 Biomechanics vs. Quantitative Ultrasound 118
4.9.1 QUS for the Determination of Modulus 118
4.9.2 Biomechanics vs. Clinical QUS 122
4.9.2.1 The Forearm 127
4.9.2.2 Intact Femurs 127
4.9.2.3 Vertebral Bodies 128
4.9.2.4 Sample Specific Testing 128
Concluding Remarks 130

Chapter 5 Materials and Methods: Clinical Studies 132
5.1 Ethical Approval 132
5.2 Quantitative Ultrasound Systems 132
5.2.1 CUBA Clinical 132
5.2.2 Sunlight Omnisense 133
5.2.3 Dual-Energy X-ray Absorptiometry (DXA) 134
5.3 Study Groups and Anthropometric Data 135
5.4 Study Designs 137
5.4.1 Precision Study 137
5.4.1.1 Precision Calculation 137
CV% 137
$_{RMS}$CV% 138
sCV% 140
5.4.2 Sensitivity and Specificity Study 140
5.4.2.1 Discriminatory Ability 141

5.4.2.2 Inter-site correlation 142
5.4.2.3 Diagnostic Ability Investigation 142
5.4.2.4 Cut-off / Threshold Selection 144
5.4.2.5 Screening Strategy 146
Concluding Remarks 147

Chapter 6: Materials and Methods: In-Vitro Testing 148
6.1 Compression Testing Parameters 148
6.2 Fracture Toughness Parameters 149
6.2.1 K_{IC} 149
6.2.2 G_{IC} 149
6.2.3 J-Integral 150
6.3 Fracture Toughness Sample Design and Calculation 150
6.3.1 Sample Design 150
6.3.1.1 Disk-Shaped Compact Specimen 151
6.3.1.2 Beam Specimens 152
6.3.2 Fracture Toughness Calculation 153
6.3.2.1 K_Q 154
Disk Samples (Section A6.5 ASTM Standard E399-90): 154
Beam Samples (Section A3.5 ASTM Standard E399-90): 154
Validation 155
6.3.2.2 G_{IC} Determination 156
6.3.2.3 J-Integral Determination 156
6.4 Subjects and Materials 160
6.4.1 Equine Material 160
6.4.2 Human Tissue 160
6.4.2.1 Osteoporotic + Scan Data (OP+): Gloucester Royal Hospital 161
6.4.2.2 Osteoporotic No Scan Data (OP-): Gloucester and Aberdeen 161
6.4.2.3 Osteoarthritic (OA): Standish Hospital 161
6.5 Sample Manufacture 163
6.5.1 Equine Vertebra Preparation 163
6.5.1.1 Central Slices. 164
6.5.1.2 Peripheral Slices 165
6.5.2 Human Femoral Head Preparation 166
6.5.2.1 Central Slices 166
6.5.3 Sample Sizing 168
6.5.4 Cleaning 171
6.6 Density Determination 172
6.7 Collagen Cross-Linking Analysis 174
6.7.1 Sample Preparation 174
6.7.2 Decalcification 175
6.7.3 Borohydride Reduction 175
6.7.4 Hydrolysis 175
6.7.5 Cross-link Analysis 176
6.7.6 Hydroxyproline Analysis 176
6.7.7 Glycated Cross-link Analysis 176
6.7.8 Substrate Zymography 176
6.8 Sample Testing Preparation 177
6.8.1 Notching 178

6.8.2 Loading and Extensometer Holes. 181
6.9 Compression Testing Samples 182
6.10 Testing Rigs 184
6.10.1 Three Point Bending Rig 184
6.10.2 Disk-Shaped Compact Specimen Test Rig 185
6.10.3 Compression Testing Rig 186
6.11 Mechanical Testing 187
6.11.1 Fracture Toughness Testing 187
6.11.2 Compression Testing 189
6.12 Compositional Testing 190
Concluding Remarks 191

Chapter 7: Results: Clinical Studies 193
7.1 Precision Study 193
7.2 Discriminatory Ability 194
7.2.1 Graphical Representation 195
7.2.2 Kappa Indices 196
7.3 Inter-site Correlation 199
7.4 Diagnostic Ability 201
7.4.1 ROC Curve Analysis 201
7.4.2 AUC Analysis 209
7.5 Threshold Selection 213
7.5.1 The Best Accuracy Method (Table 7.9) 213
7.5.2 The Best Sensitivity and Specificity Method (Table 7.9 / Table 7.10) 213
7.5.3 The 90% Sensitivity Method (Table 7.11) 214
7.6 Screening Strategy 218
Concluding Remarks 220

Chapter 8: Results: In-Vitro Testing 222
8.1 Compression Testing 222
8.1.1 Extensometer and Group Comparisons 223
8.1.2 Dependent and Independent Variable Relationships 226
8.1.2.1 Regression Analysis 226
Material Properties 226
Collagen Cross-linking Analysis 230
8.1.2.3 Power Functions 234
8.2 Fracture Toughness Testing 235
8.2.1 Fracture Toughness Validation 236
8.2.2 Study Group Comparisons 239
8.2.3 Linear and Logarithmic Regression Relationships 242
8.2.3.1 Material Properties 242
Apparent Density 242
Porosity 250
Material Density 251
8.2.3.2 Compositional Properties 251
Hydrated and Dehydrated Mineral and Organic Content 251
Collagen Cross-Link Analysis 252
8.2.4 Step-Wise Regression Relationships 253

8.2.5 The J-Integral 264
8.3 Material and Compositional Comparisons 267
8.3.1 Material Properties 267
8.3.2. Intra-group Sample Comparisons 270
8.3.2.1 Osteoporotic samples 270
8.3.2.2 Osteoarthritic Group 272
8.3.2.3 Equine Group 275
8.4 Compositional Properties 278
8.4.1 Mineral vs. Organic 278
8.5 Inter-material Property Relationship 281
8.6 Inter-material Property and Compositional Relationship 287
8.7 Collagen Cross-link Comparison 289
8.9 Biomechanics vs. QUS Assessments 291
8.9.1 Compression Testing vs. Age and Clinical QUS 291
8.9.2 Fracture Toughness Testing vs. Age and QUS Investigations 296
8.9.2.1 Age 296
8.9.2.2 QUS Investigation 296
8.10 Material Properties vs. QUS 305
Concluding Remarks 307

Chapter 9: Discussion 309
9.1 Clinical Work Discussion 309
9.1.1 Introduction 309
9.1.2 Precision Study 310
9.1.2.1 Alternative Error Sources 311
Repositioning 311
Oedema and Excess Soft Tissue 312
9.1.3 Discriminatory Ability 314
9.1.3.1 Kappa Indices 314
9.1.3.2 Graphical Representations 316
9.1.4 Inter-site Correlations 318
9.1.5 Diagnostic Ability 322
9.1.6 Threshold Selection 327
9.1.7 Screening Strategy 331
9.1.8 Study Limitations 333
9.2 In-Vitro Investigation Discussion 334
9.2.3 Compression Testing 334
9.2.4 Fracture Toughness Testing 339
9.2.4.1 Validity 340
9.2.4.2 Fracture Toughness Results 341
Material Properties and Compositional Effects 341
Composition 344
9.2.1 Material Property Investigations 346
9.2.2 Compositional Property Investigations 347
9.2.5 QUS vs. Material and Mechanical Properties. 348
9.2.5.1 Compression vs. QUS 348
9.2.5.2 QUS vs. Fracture Toughness 350
9.2.5.3 QUS vs. Material Properties 353

Chapter 10: Conclusions **355**
10.1 Clinical Studies. 355
10.2 In -Vitro Testing 356

References and Bibliography **359**

Appendices **Vol.2**

List of Figures

	Chapter 2	Page
Figure 2.1	Hierarchical structural organisation of bone (taken from J.-Y. Rho et al., 1998)	4
Figure 2.2	A: Image of the macrostructure of cortical bone from the femur of a 92 yr old male (Taken from J.Y. Rho et al. 2002) B: Image of the macrostructure of cancellous bone from the femoral head of a 69 Osteoarthritic male.	5
Figure 2.3	Tertiary diagram showing the relationships and variation between the different constituent components of bone and the variation that occurs within nature. (Taken from P. Zioupos (2005))	7
Figure 2.4	Schematic representation of fibrous nature of type 1 collagen showing the (A.) structure and the divalent immature cross-links within the newly formed collagen fibres and (B.) the trivalent mature cross-linking produced from the immature cross-links which link the microfibrils.	9
	Chapter 3	
Figure 3.1	Compressive stress-strain curves of three cancellous bone samples of different relative density, taken from L.J. Gibson and M.F. Ashby (1997a).	18
Figure 3.2	Young's moduli vs. relative density (Diagram taken from L.J. Gibson, 2005)	19
Figure 3.3	Compressive strength vs. relative density (Diagram taken from L.J. Gibson (2005))	26
	Chapter 4	
Figure 4.1	Cancellous bone samples from the neck of the femur of (A) a 54 year old female and (B) a 74 year old female.	69
	Chapter 6	
Figure 6.1	Load deformation curve demonstrating the points from which the compressive mechanical parameters are determined	148
Figure 6.2	Disk-shaped compact specimen adapted from ASTM standard E399-90, *C section was not removed leaving an area for the extensometer attachment.	152
Figure 6.3	Three point bending specimen adapted from ASTM standard E399-90	152
Figure 6.4	Principle types of load-displacement curves for the determination of P_5, P_Q and P_{max}. (Taken from ASTM standard E399-90).	153
Figure 6.5	Load vs. crack opening displacement curve from an osteoporotic disc sample, with the notch orientated to travel across the trabecular structure. Demonstrating the points P_Q and P_{max} with their corresponding displacements D_Q and D_{max}, as well as the fixed displacements (D1-D9).	157

Figure 6.6	Regression plot of the AUC values for displacement 1 vs. the initial notch length, taken form the OP+ scan groups disc samples orientated in the Ac direction, where the slope that was required is in bold (-0.0766).	158
Figure 6.7	Plot of the slopes vs displacements (the J-integral calibration curve), using the best regression equation, and demonstrating the methods for the insertion of D_Q and D_C.	159
Figure 6.8	Diagrammatic representation of the sectioning of the equine thoracic vertebrae	163
Figure 6.9	Diagrammatic representation of the sample manufacture from the central slice of the equine vertebrae	164
Figure 6.10	Central slices of an equine vertebra with two disk samples and two oblong blocks removed.	164
Figure 6.11	Diagrammatic representation of the sample manufacture from the peripheral slice of the equine vertebrae	165
Figure 6.12	Sectioning of the outer slice in the CC direction.	165
Figure 6.13	Osteoarthritic femoral head sectioned into 4 slices in the medial-lateral direction, showing the sections of tissue removed from the central slices for collagen analysis.	167
Figure 6.14	Central slice of an osteoarthritic femoral head, with a disk sample and three beam samples taken in the Ac direction (Ac: Notch across the trabecular structure)	167
Figure 6.15	Central slice of an osteoarthritic femoral head, with a disk sample and two beam samples taken in the AL direction. (AL: Notch along the trabecular structure).	168
Figure 6.16	The rotary pregrinder used for the grinding of samples to the correct size.	169
Figure 6.17	Beam sample from an osteoarthritic femoral head central slice, after polishing to size.	169
Figure 6.18	Disk sample from osteoarthritic femoral head central slice, after polishing to size.	169
Figure 6.19	Disk and beam samples from group 2 after the cleaning process, showing the cancellous bone structure free of marrow.	171
Figure 6.20	A. Mettler-Tolledo College B154 scales B. Density Determination Equipment	173
Figure 6.21	Jig for the preparation of disk-shaped compact specimens.	177
Figure 6.22	Jig for the preparation of beam samples.	177
Figure 6.23	Struers® Accutom 2 wafering saw with a 300μm thick diamond impregnated circular blade	178
Figure 6.24	Travelling microscope (W.G.Pye and Co. Ltd., Cambridge, UK)	180
Figure 6.25	Equine AC Beam sample with extensometer attachment holes and notch.	181
Figure 6.26	Equine AL disk with loading holes, extensometer attachment holes and notch.	182
Figure 6.27	Cleaned compression core from OP+	183
Figure 6.28	Compression core from OP+ with the addition of teak spacers to either end of the sample.	184
Figure 6.29	Schematic representation of the three-point bending rig.	185
Figure 6.30	Schematic representation of the test rig for the compact disk-shaped specimens.	186
Figure 6.31	a: Schematic of the compression testing rig, showing the articulated upper platen, an 1mm deep depressions on the loading platen surfaces. b: Image showing 1mm deep depressions on the loading platen.	187
Figure 6.32	A Miniature extensometer (Miniature Model 3442-006M-050ST, Epsilon Technology Corp., Jackson, WY, USA).	188
Figure 6.33	Tensile testing of the compact disk specimens showing the crack opening during testing	188
Figure 6.34	Three point bend testing of the beam specimens showing the crack opening during testing.	189
Figure 6.35	The compressive testing of a compression core, showing both the contact extensometer and the platens LVDT.	190

	Chapter 7	
Figure 7.1	Group 2 Discriminatory abilities.	195
Figure 7.2	Group 3 Discriminatory abilities.	196
Figure 7.3	ROC Curves for the Group 2 QUS results prediction of DXA Combined at a T-score of -2.5.	202
Figure 7.4	ROC Curves for the Group 2 QUS results prediction of DXA Combined at a T-score of -2.	202
Figure 7.5	ROC Curves for the Group 2 QUS results prediction of DXA Combined at a T-score of -1.5	203
Figure 7.6	ROC Curves for the Group 2 QUS results prediction of DXA Combined at a T-score of -1.	203
Figure 7.7	ROC Curves for the Group 3 QUS and questionnaire results prediction of DXA Combined at a T-score of -2.5	204
Figure 7.8	ROC Curves for the Group 3 QUS and questionnaire results prediction of DXA Combined at a T-score of -2	205
Figure 7.9	ROC Curves for the Group 3 QUS and questionnaire results prediction of DXA Combined at a T-score of -1	205
Figure 7.10	ROC Curves for the Group 3 QUS and questionnaire results prediction of Lumbar Spine DXA at a T-score of -2	206
Figure 7.11	ROC Curves for the Group 3 QUS and questionnaire results prediction of Lumbar Spine DXA at a T-score of -2	206
Figure 7.12	ROC Curves for the Group 3 QUS and questionnaire results prediction of Lumbar Spine DXA at a T-score of -1	207
Figure 7.13	ROC Curves for the Group 3 QUS and questionnaire results prediction of Total Hip DXA at a T-score of -2.5	207
Figure 7.14	ROC Curves for the Group 3 QUS and questionnaire results prediction of Total Hip DXA at a T-score of -2	208
Figure 7.15	ROC Curves for the Group 3 QUS and questionnaire results prediction of Total Hip DXA at a T-score of -1	208
	Chapter 8	
Figure 8.1	Loading curves obtained from the two different extension determining methods for the same osteoporotic compression core.	223
Figure 8.2	Load deformation curve comparisons from samples of the same initial notch length but with different apparent densities	264
Figure 8.3	The regression plot for the K_C fracture toughness results in relation to apparent density, using the loading curves in Figure 8.2	265
Figure 8.4	The regression plot for the J_C fracture toughness results in relation to apparent density, using the loading curves in Figure 8.2	265
Figure 8.5	Box plot displaying the comparison between the apparent densities (g cm-3) of the three study groups	268
Figure 8.6	Box plot displaying the comparison between the Material Densities (g cm-3) of the three study groups	269
Figure 8.7	Box plot displaying the comparison between the porosities (%) of the three study groups	269
Figure 8.8	Comparison between the apparent densities of the different sample designs and orientations of the osteoporotic group	271
Figure 8.9	Comparison between the material density of the different sample designs and orientations of the osteoporotic group	271

Figure 8.10	Comparison between the porosity of the different sample designs and orientations of the osteoporotic group	272
Figure 8.11	Comparison between the apparent densities of the different sample designs and orientations of the osteoarthritic group	273
Figure 8.12	Comparison between the material densities of the different sample designs and orientations of the osteoarthritic group	274
Figure 8.13	Comparison between the porosities of the different sample designs and orientations of the osteoarthritic group	274
Figure 8.14	Comparison between the apparent densities of the different sample designs and orientations of the equine group	276
Figure 8.15	Comparison between the material densities of the different sample designs and orientations of the equine group	276
Figure 8.16	Comparison between the apparent densities of the different sample designs and orientations of the equine group	277
Figure 8.17	Pie-charts for the comparisons between the average compositions of three different study groups.	279
Figure 8.18	Box plot displaying the comparison between the hydrated mineral contents (%) of the three study groups	280
Figure 8.19	Box plot displaying the comparison between the Dry organic content (%) of the three study groups	281
Figure 8.20	Linear regression between material density and apparent density of the osteoporotic samples	282
Figure 8.21	Linear regression between material density and apparent density of the osteoarthritic samples	282
Figure 8.22	Linear regression between material density and apparent density of the Equine samples	283
Figure 8.23	Linear regression between material density and porosity of the osteoporotic samples	283
Figure 8.24	Linear regression between material density and porosity of the osteoarthritic samples	284
Figure 8.25	Linear regression between material density and porosity of the equine samples	284
Figure 8.26	Box plot displaying the comparison between the collagen cross-linking of the osteoporotic and osteoarthritic study groups	290
Figure 8.27	Box plot displaying the comparison between the fmoles Pentosidine / pmole collagen of the osteoporotic and osteoarthritic study groups	290

List of Tables

	Chapter 3	**Page**
Table 3.1	Review of the published Young's Moduli of individual Trabeculae, or trabecular bone table adapted and modified from J.Y. Rho et al. 1993, 1998, L.J. Gibson and M.F. Ashby, 1997, H.H. Bayraktar et al., 2004.	14
Table 3.2	Linear and power function relationships between apparent density and Young's modulus and strength from the literature.	21
Table 3.3	Linear and power function relationships between apparent density and compressive mechanical properties of cancellous bone from the literature.	30
Table 3.4	Linear and power function relationships between apparent ash density (ρash) and the Young's Modulus of cancellous bone from the literature.	32

Table 3.5	Linear and power function relationships between apparent ash density (ρash) and strength of cancellous bone from the literature.	34
Table 3.6	Linear and power function relationships between apparent ash density and compressive mechanical properties of cancellous bone from the literature.	35
Table 3.7	Linear and power function relationships between BMD and the Young's modulus and strength of cancellous bone from the literature.	36
Table 3.8	Tensile mechanical properties and their relationships with density from within the literature	49
	Chapter 4	
Table 4.1	Diseases, and drug therapies linked to secondary osteoporosis, adapted from L.A. Fitzpatrick, 2002; D.M. Reid and J. Harvie, 1997; NOF, 2003.	63
Table 4.2	Expected levels (mol/mol) of collagen cross-links with the tissues of normal osteoporotic and osteoarthritic individuals	67
Table 4.3	Adapted from (S. Grampp et al., 1993; M. Jergas and H.K. Genant, 1993; C. Christiansen, 1995; D.T. Baran et al., 1997)	71
Table 4.4	Clinical referral criteria provided by the official groups related to osteoporosis and specialised centres for the study of Osteoporosis.	76
Table 4.5	Previously developed and validated questionnaire systems from within the literature, with their modes of calculation.	78
Table 4.6	AUC values for the performance of the OST / OSTA / FOSTA questionnaire system to screen individuals based on their DXA derived T-score.	81
Table 4.7	AUC values for the performance of the ORAI questionnaire system to screen individuals based on their DXA derived T-score.	81
Table 4.8	AUC values for the performance of the SCORE questionnaire system to screen individuals based on their DXA derived T-score.	82
Table 4.9	AUC values for the performance of the SOFSURF, OPERA and ABONE questionnaire systems to screen individuals based on their DXA derived T-score.	82
Table 4.10	AUC values for the performance of the OSIRIS and pBW questionnaire systems to screen individuals based on their DXA derived T-score.	83
Table 4.11	The manufacturers' published precisions. Adapted from C.F. Njeh et al. (1997).	90
Table 4.12	Precision of BUA assessment determined using calcaneal QUS machines. (Mean, Range).	92
Table 4.13	Precision of SOS assessment determined using calcaneal QUS machines. (Mean, Range).	93
Table 4.14	Precision of Manufacturer derived combination parameters, (Stiffness index, QUI, Est. Heel BMD, OSI) determined using calcaneal QUS machines. (Mean, Range).	94
Table 4.15	Precision of Distal Radius SOS assessment determined using the Sunlight Omnisense QUS machine. (Mean, Range).	94
Table 4.16	Precision of Proximal Phalanx SOS assessment determined using either the DBM Sonic 1200, the IGEA Bone Profiler or the Sunlight Omnisense QUS systems. (Mean, Range).	94
Table 4.17	Precision of Mid-Shaft Tibia SOS assessment determined using the SoundScan 2000 or the Sunlight Omnisense QUS machines. (Mean, Range).	95
Table 4.18	The potential repercussions of repositioning on the precision error (adapted from W.D. Evans et al., 1995).	97
Table 4.19	The range and mean Pearson's correlations for the QUS systems prediction of BMD at the forearm.	98
Table 4.20	The range and mean Pearson's correlations for the QUS systems prediction of BMD at the forearm.	99

Table 4.21	The range and mean Pearson's correlations for the QUS systems prediction of BMD at the Femoral Neck.	100
Table 4.22	The range and mean Pearson's correlations for the QUS systems prediction of BMD at the Total Hip.	101
Table 4.23	Previous studies and QUS systems utilised, that have shown a significant difference in QUS measurement results between DXA confirmed osteoporotic individuals and normal individuals.	103
Table 4.24	Kappa indices for the comparison between QUS diagnoses and DXA diagnoses.	104
Table 4.25	Area Under (AUC) Receiver Operating Characteristic (ROC) Curves for the prediction of T-scores ≤ -2.5, or T-scores ≤ -1, using BUA assessment of the Calcaneus.	106
Table 4.26	Area Under (AUC) Receiver Operating Characteristic (ROC) Curves for the prediction of T-scores ≤ -2.5, or T-scores ≤ -1, using SOS assessment of the Calcaneus.	107
Table 4.27	Area under (AUC) Receiver Operating Characteristic (ROC) Curves for the prediction of T-scores ≤ -2.5, or T-scores ≤ -1, using manufacturer derived combination parameters from the assessment of the Calcaneus.	107
Table 4.28	Area under (AUC) Receiver Operating Characteristic (ROC) Curves for the prediction of T-scores ≤ -2.5, or T-scores ≤ -1 using SOS assessment of the Distal Radius, Proximal Phalanx or Mid-Shaft Tibia.	108
Table 4.29	Table showing the studies in which the BUA results at the calcaneus were lower in individuals with fractures and the studies which provided OR and AUC values for the prediction fractures.	112
Table 4.30	Table showing the studies in which the VOS results at the calcaneus were lower in individuals with fractures and the studies which provided OR and AUC values for the prediction fractures.	114
Table 4.31	Table showing the studies in which the manufacturers combination parameter results from the calcaneus were lower in individuals with fractures and the studies which provided OR and AUC values for the prediction fractures.	115
Table 4.32	Table showing the studies in which the SOS from peripheral sites other than the calcaneus were lower in individuals with fractures and the studies which provided OR and AUC values for the prediction fractures.	116
Table 4.33	Modulus vs. Density relationships, determined from the ultrasonic determination of modulus	121
Table 4.34	Relationships between clinical QUS measurements and the biomechanics of human skeletal tissue from within the literature.	123
	Chapter 5	
Table 5.1	Anthropometric data for the study groups.	136
Table 5.2	Meaning of the Kappa indices taken from R.F. Mould (1998)	142
Table 5.3	Demonstration 2x2 table	143
Table 5.4	Table representing the meaning of an AUC value for a diagnostic technique	144
	Chapter 6	
Table 6.1	Study Group Demographics	161
Table 6.2	Average (Standard deviation) of the sample sizes for the equine vertebral disk and beam test samples.	170
Table 6.3	Average (Standard deviation) of the sample sizes for the human femoral disk and beam test samples	171

Table 6.4	a_o and a_o/W ratios for the equine disk and beam specimens	180
Table 6.5	Average (standard deviation) for the ao and ao/W ratios for the human disk specimens from the 4 different lengths.	180
Table 6.6	a_o and a_o/W ratios for the human beam specimens	181
Table 6.7	Range, average and standard deviation of the diameter and length of the compression cores, taken from the femoral heads of all groups.	183
Table 6.8	Range, standard deviation and average gauge lengths of the compression cores taken from the femoral heads of all groups after the addition of the teak spacers.	184
	Chapter 7	
Table 7.1	Short Term Precision of Group 1 (95% Confidence intervals)	193
Table 7.2	Short-Term Precision of Group 2 (95% Confidence intervals)	194
Table 7.3	Kappa scores for the comparison between group 2 measurement results	198
Table 7.4	Kappa scores for the comparison between group 3 assessment measures and DXA	198
Table 7.5	Pearson's correlations between the different techniques for group 2	199
Table 7.6	Pearson's correlations between the different techniques for group 2	200
Table 7.7	AUC Results for Group 2	210
Table 7.8	AUC results for Group 3 for the different diagnostic abilities of the systems in relation to DXA	212
Table 7.9	Group 2: Potential cut-off values for prediction of DXA and their associated numbers of false-positive and false-negative results	215
Table 7.10	The suggested cut-off points that allow for the best sensitivity and specificity balance within study group 3	216
Table 7.11	The suggested cut-off points that allow for a guaranteed 90% sensitivity level within study group 3	217
Table 7.12	Stepwise regression analysis for the three scenarios presented in section 5.4.2.5	219
	Chapter 8	
Table 8.1	ANOVA comparisons between the results of the two different extensometers.	224
Table 8.2	Comparison between the range, mean and standard deviations of the compressive mechanical properties of the two different study groups	225
Table 8.3	Pearson's correlations between the compressive mechanical parameters and the material properties and composition for the osteoporotic group	228
Table 8.4	Pearson's correlations between the compressive mechanical parameters and the material properties and composition for the osteoarthritic group	229
Table 8.5	Stepwise regression analysis of the Osteoporotic compression results vs. the 9 independent variables.	231
Table 8.6	Stepwise regression analysis of the Osteoarthritic compression results vs. the 9 independent variables.	233
Table 8.7	The powers of the logarithmic relationships between the compressive mechanical parameters and apparent density	234
Table 8.8	Validation P_{max} / P_Q ratio values	236
Table 8.9	Average (Standard Deviation) specimen strength ratios	237
Table 8.10	Comparison between the fracture toughness results of the beam samples from the different study groups	240
Table 8.11	Comparison between the fracture toughness results of the disk samples from the different study groups	241

Table 8.12	Pearson's correlations between the fracture toughness parameters from the equine beam samples, and the material and compositional properties	243
Table 8.13	Pearson's correlations between the fracture toughness parameters from the equine disk samples, and the material and compositional properties.	244
Table 8.14	Pearson's correlations between the fracture toughness parameters from the osteoporotic beam samples, the material and compositional properties and the collagen cross-linking analysis.	245
Table 8.15	Pearson's correlations between the fracture toughness parameters from the osteoporotic disk samples, the material and compositional properties and the collagen cross-linking analysis.	246
Table 8.16	Pearson's correlations between the fracture toughness parameters from the osteoarthritic beam samples, the material and compositional properties and the collagen cross-linking analysis.	247
Table 8.17	Pearson's correlations between the fracture toughness parameters from the osteoarthritic disk samples, the material and compositional properties and the collagen cross-linking analysis.	248
Table 8.18	Power functions of the relationships between the apparent density and relative density with respect to the fracture toughness parameters	250
Table 8.19	Stepwise regression analysis of the equine fracture toughness results from the beam samples in relation to the 6 independent variables	254
Table 8.20	Stepwise regression analysis of the equine fracture toughness results from the disk samples in relation to the 6 independent variables.	255
Table 8.21	Stepwise regression analysis of the osteoporotic fracture toughness results from the beam samples in the Ac direction in relation to the 12 independent variables.	257
Table 8.22	Stepwise regression analysis of the osteoporotic fracture toughness results from the beam samples in the AL direction in relation to the 12 independent variables.	258
Table 8.23	Stepwise regression analysis of the osteoporotic fracture toughness results from the disk samples in the Ac direction in relation to the 12 independent variables.	259
Table 8.24	Stepwise regression analysis of the osteoporotic fracture toughness results from the disk samples in the AL direction in relation to the 12 independent variables.	259
Table 8.25	Stepwise regression analysis of the osteoarthritic fracture toughness results from the beam samples in relation to the 12 independent variables.	260
Table 8.26	Stepwise regression analysis of the osteoarthritic fracture toughness results from the disk samples in the Ac direction, in relation to the 12 independent variables.	261
Table 8.27	Stepwise regression analysis of the osteoarthritic fracture toughness results from the disk samples in the AL direction, in relation to the 12 independent variables.	262
Table 8.28	Pearson's correlation coefficients for the comparisons between the P_Q and P_C extensions with apparent density	266
Table 8.29	Range, mean, standard deviation and ANOVA comparisons of the apparent densities, material densities, and porosities of the samples from the three study cohorts.	268
Table 8.30	Comparison between the material properties of the different sample designs and orientations of the osteoporotic group	270
Table 8.31	Comparison between the material properties of the different sample designs and orientations of the osteoarthritic group	272

Table 8.32	Comparison between the material properties of the different sample designs and orientations of the equine group	275
Table 8.33	Range, mean, standard deviation and ANOVA comparisons of the compositions of the samples from the three study cohorts	278
Table 8.34	Pearson's correlations between the compositional properties with respect to the material properties of the bone samples from the three groups	286
Table 8.35	Pearson's correlations between the material properties and compositions of the test samples from the three groups	287
Table 8.36	Mean, range, standard deviation and ANOVA comparison between the collagen cross-linking within the osteoporotic and osteoarthritic samples.	289
Table 8.37	Pearson's correlations between the compressive mechanical parameters, the age of the donor subject, and the QUS results obtained in-vivo on the donor subject for the osteoporotic group.	292
Table 8.38	Pearson's correlations between the compressive mechanical parameters, the age of the donor subject, and the QUS results obtained in-vivo on the donor subject for the osteoarthritic group.	293
Table 8.39	Pearson's correlations between the compressive mechanical parameters, the age of the donor subject, and the QUS results obtained in-vivo on the donor subject for the combined osteoporotic and osteoarthritic group.	294
Table 8.40	Pearson's Correlations between the fracture toughness parameters from the beam samples and the age and QUS values obtain from the donor subjects for the OP group.	298
Table 8.41	Pearson's Correlations between the fracture toughness parameters from the disk samples and the age and QUS values obtain from the donor subjects for the OP group.	299
Table 8.42	Pearson's Correlations between the fracture toughness parameters from the beam samples and the age and QUS values obtain from the donor subjects for the OA group.	300
Table 8.43	Pearson's Correlations between the fracture toughness parameters from the disk samples and the age and QUS values obtain from the donor subjects for the OA group.	301
Table 8.44	Pearson's Correlations between the fracture toughness parameters from the beam samples and the age and QUS values obtain from the donor subjects for the OP and OA groups combined.	303
Table 8.45	Pearson's Correlations between the fracture toughness parameters from the disk samples and the age and QUS values obtain from the donor subjects for the OP and OA groups combined.	304
Table 8.46	Pearson's correlation coefficients for the relationships between the averaged material properties of each osteoporotic individual vs. the clinical QUS results.	305
Table 8.47	Pearson's correlation coefficients for the relationships between the averaged material properties of each osteoarthritic individual vs. the clinical QUS results.	306

Chapter 1: Introduction

With an ever increasing elderly population around the world, the prevalence of the bone condition osteoporosis is escalating. The National Osteoporosis Society within the UK reports that 1 in 3 women and 1 in 12 men over the age of 50 are likely to suffer fractures caused by osteoporosis, with there being estimates of the number of sufferers reaching 3 million in the UK alone, and somewhere in the region of 7.8 million in the United States of America. The resultant diagnosis and treatment of the condition, with drug therapies, fracture repairs such as hip replacement surgery and the costs of care for sufferers, are estimated to cost the UK government approximately £1.7 billion each year.

The primary method for the diagnosis of osteoporosis currently lies in the measurement of bone density or bone mineral density (BMD), with the gold standard technique considered to be dual-energy X-ray absorptiometry (DXA), around which the World Health Organisation and other groups associated with osteoporosis have based their diagnostic guidelines and recommendations. However DXA systems are costly to purchase and run and have an inherent health risk, although minor, as they use X-rays to perform the measurements. The systems are therefore restricted to hospitals or specialised clinics, where the demand for their services is high.

It has therefore been desirable to develop either an alternative to DXA, or a new referral criteria / screening tool that will enable the pre-selection of individuals at risk of, or who suffer from, osteoporosis. The current referral criteria vary depending on the country of origin and encompass almost every possible risk factor for osteoporosis, and in doing so do little to reduce the numbers of individuals being sent for unnecessary

DXA investigations. A number of different solutions were developed to ease the demands on DXA, the best of which was found in quantitative ultrasound (QUS). QUS offers a far cheaper, portable, radiation free and simple to use technique which provides quantitative assessments of the skeletal condition. However poor precision errors and the ability only to measure peripheral sites has meant that the use of QUS for the 'diagnosis' of osteoporosis and the monitoring of therapies or bone loss is not possible, and as such QUS has remained a poor and relatively underused technique. More recently it has been found that QUS results are highly predictive of an individual's fracture risk. At the same time QUS values are lower in individuals classified as osteoporotic by DXA and therefore offer a great deal of potential as a screening tool. The only other inexpensive method to compete with QUS as a screening tool is the risk factor questionnaires; these provide a free and informative prediction of an individual's skeletal condition based on just a few anthropometrical measurements and risk factors. Studies utilising the questionnaires have provided predictive abilities which would rival those of the QUS systems, but very few studies have performed any comparisons between the available questionnaire systems and QUS in relation to DXA. It is therefore one of the aims of this study to perform the first comprehensive review of the various questionnaires and the predictive abilities of two QUS techniques in order to determine the best performing technique in relation to DXA of the axial skeleton, and to attempt to use the results in combination to provide a screening tool.

The early diagnosis of low bone density is important as it enables the clinician to put into place preventative measures to stave off the symptom of osteoporosis which is low trauma fracture. Of the fractures which are most prevalent in osteoporosis most of them occur in areas of the skeleton made up predominantly of cancellous bone. The

compressive properties of cancellous bone have been extensively studied but few studies have investigated the properties of bone from individuals with conditions such as osteoporosis and osteoarthritis, both of which are known to adversely change bone from what could be considered normal. It is therefore desirable to investigate the effects of these conditions on the compressive properties of cancellous bone to provide additional information into an area of the literature which is lacking in content.

The site of interest in this study is the proximal femur and in particular the fracture of the femoral neck which occurs when a crack propagates across the cancellous bone structure. Yet the fracture toughness of cancellous bone has never been investigated or fully characterised and has only been modelled with respect to density. If fractures are to be prevented it is important that the mechanics that occur during fracture are understood and that the independent variables which affect the mechanics are known so that therapies can be designed to capitalize on relevant independent variables for the maximisation of fracture prevention. The aim of this study is to perform the first ever characterisation of the fracture toughness of cancellous bone and to investigate as many as possible of the independent variables which positively affect the fracture mechanics, so as to better understand what is required from any future therapies if they are to best prevent osteoporotic fractures.

Chapter 2: Bone

The human skeleton performs a number of crucial roles which enable the human body to function. It plays a vital part in the musculoskeletal system as it provides insertion points for muscles and tendons which allows for locomotion and other muscle action; it acts as a protective barrier for the vital organs such as the heart and brain while providing a network to support them; it acts as a storage supply for crucial minerals such as calcium, magnesium and phosphorus; and finally the medullary canals provide the site for bone marrow to produce the body's blood cells.

Bone is by no means a single phase solid; it has a hierarchical structure ranging from the sub-nanostructure of the collagen molecules and the mineral matrix, through to the macrostructure of the cancellous and cortical bone Figure 2.1 (J.-Y. Rho et al., 1998)

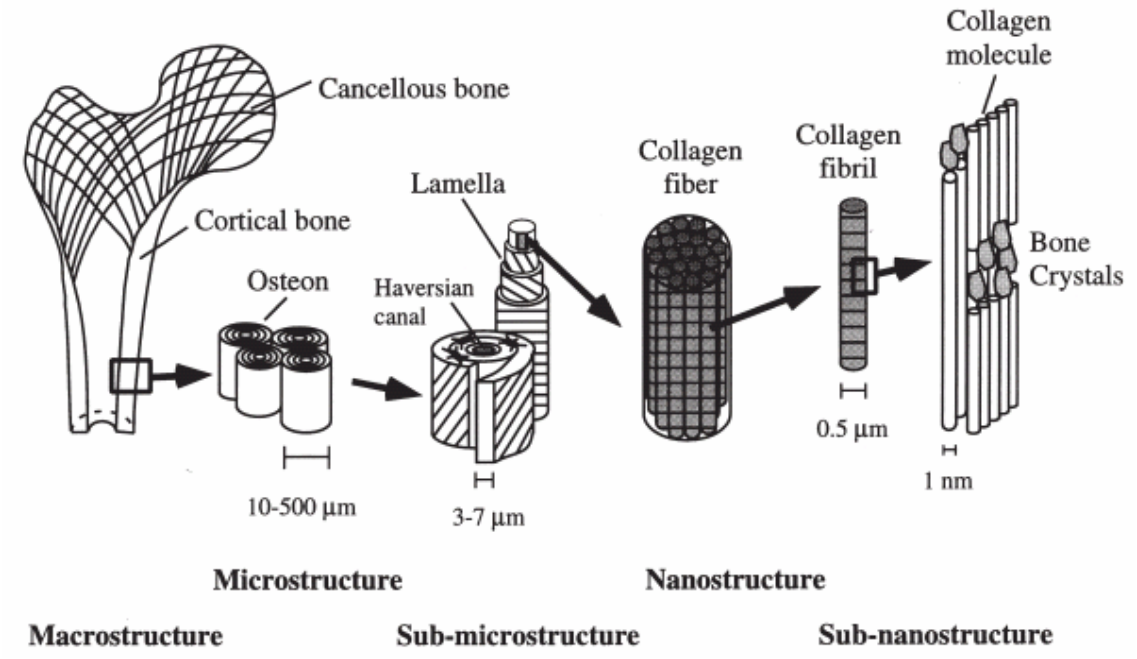

Figure 2.1 Hierarchical structural organisation of bone (taken from J.-Y. Rho et al., 1998)

2.1 The Macro-Structure of Bone

The macrostructure consists of two different types of bone, cortical bone (compact bone) and cancellous (spongy) bone. The difference between the two types of bone is set at 70% solid volume fraction, with anything greater than 70% considered to be compact bone and anything less than 70% cancellous bone (L.J. Gibson, 1985).

2.1.1 Cortical Bone

Much of the bone found in the body is of the cortical type, (Figure 2.2A), and can be considered to be a composite material with a matrix density in the region of 1.7-2.1 g cm^3, (P. Zioupos et al., 2000) an apparent density in the region of 1.8 g/cm^3 and a porosity of between 5 and 30% (E. Bonucci, 2000). The porosity with the cortical bone network is due to a number of different features such as the central canals of the haversian systems allowing for blood vessel passage, lacunae containing the osteocyte cells, canaliculi the interconnecting pathways between the lacunae, and any resorption cavities caused by the remodelling process that occurs in any bone (E. Bonucci, 2000).

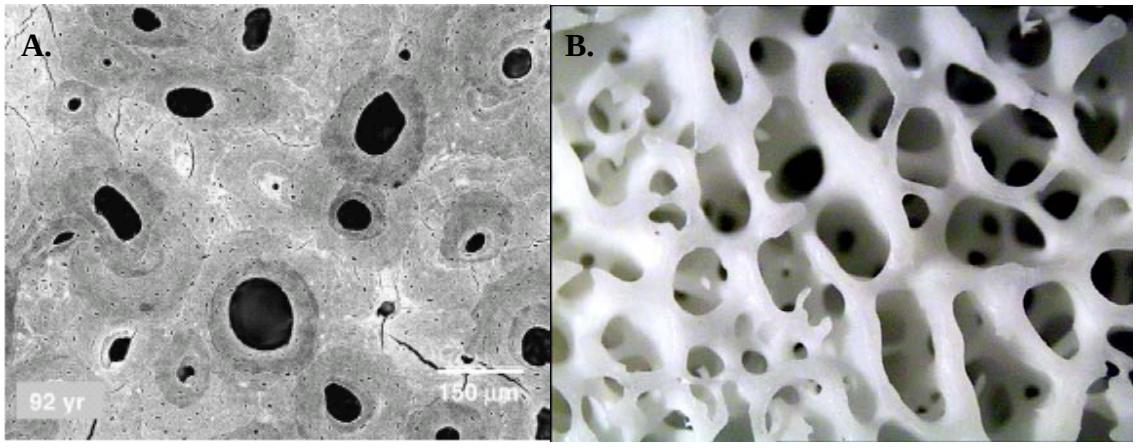

Figure 2.2 A: Image of the macrostructure of cortical bone from the femur of a 92 yr old male (Taken from J.Y. Rho et al. 2002) **B:** Image of the macrostructure of cancellous bone from the femoral head of a 69 Osteoarthritic male.

2.1.2 Cancellous Bone

Cancellous bone is a cellular solid composed of bone tissue in a complex network of rods and plates known as trabeculae (Figure 2.2B).

The material density (1.6-1.9 g cm^3) is not dissimilar to that of cortical bone, (P. Zioupos et al., 2000); but the cellular nature of the cancellous bone means the apparent density is reduced, between 0.1 to 0.6 g/cm^3 (F. Linde, 1994) and with a significantly greater porosity, ranging between 30% and 90% (E. Bonucci, 2000) both discernibly different to that of cortical bone.

2.2 Bone Composition

The material which makes up both cancellous and cortical bone has approximately the same composition (L.J. Gibson and M.F. Ashby, 1997). The compositional makeup of bone can be split into three distinct components, water, organic and mineral, with the percentage of each varying depending on the species and the requirements of the bone to fulfil its job. Figure 2.3 is a tertiary diagram showing the range of variation that occurs naturally between species, with the mineral content ranging from as little as 39.3% (Red deer antler) to 96% (Mesoplodon rostrum).

Within normal human cancellous bone from the proximal femur, the composition varies but is roughly 20%, 30% and 50% for water, organic and mineral respectively (B. Li and R.M. Aspen, 1997a,b,c). In dry bone matrix the percentage of organic and inorganic material is in the region of 33% and 67%.

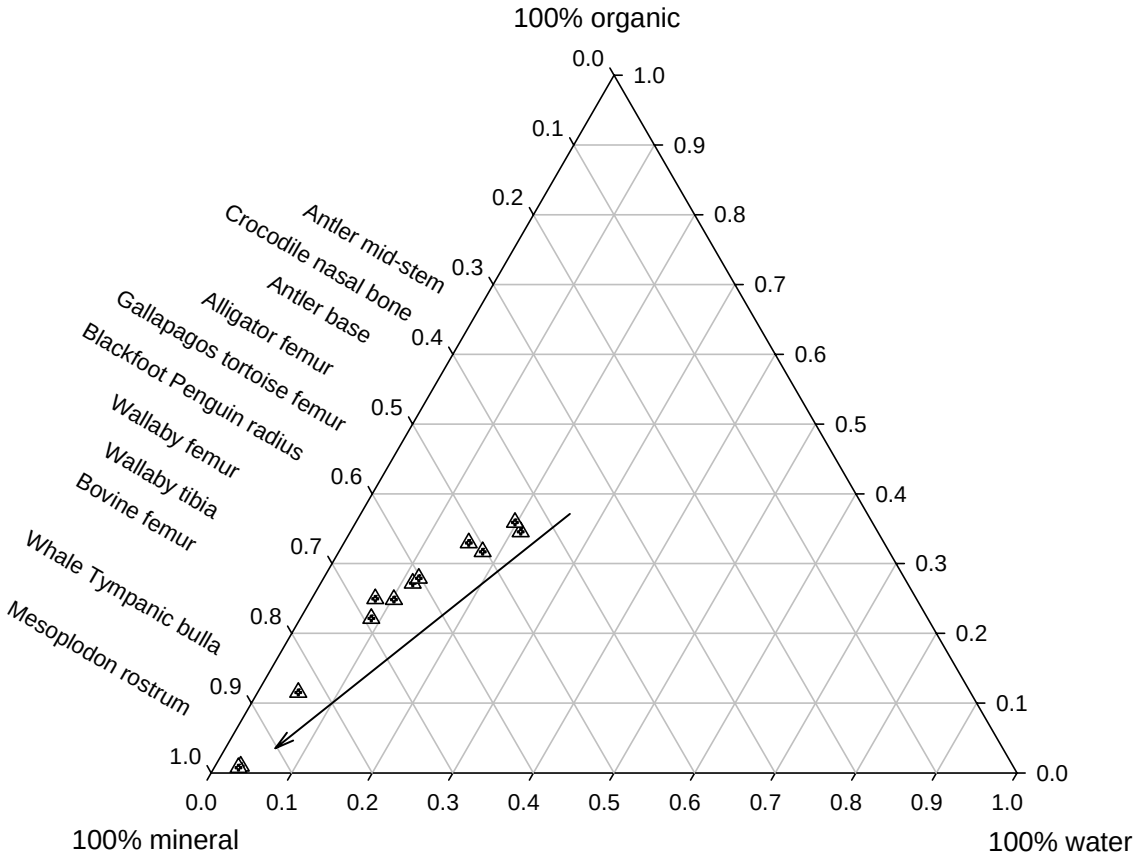

Figure 2.3 Tertiary diagram showing the relationships and variation between the different constituent components of bone and the variation that occurs within nature. (Taken from P. Zioupos (2005))

2.2.1 Organic Matrix

10% of the organic matrix is made up of made up of noncollagenous proteins, with the remaining 90% made up of type I collagen (H. Oxlund et al., 1996; L. Knott and A.J. Bailey, 1998; X. Banse et al., 2002a).

2.2.1.1 Noncollagenous Proteins

Although constituting 10% of the organic matrix of bone, the purpose of the noncollagenous proteins lies not in the direct mechanical competence of the tissue, but

in its maintenance. The proteoglycans and osteocalcin are linked with the remodelling process (W.T. Butler, 1984; E. Bonucci, 2000), the phospholipids and osteopontin are linked with the degree and the control of mineralization within the tissue (E. Bonucci, 2000), while the bone morphogenetic protein is linked to osteoinductive properties (E. Bonucci, 2000).

2.2.1.2 Collagen

The predominant form of collagen found in bone is Type I, with the presence of small quantities of type III, V and VI (B. Bätge et al., 1992; A.J. Bailey et al., 1993; A.J. Bailey and L.K. Knott, 1999). Type I collagen is composed of a triple helix, made up of two $\alpha 1$ and one α 2 chains, measuring approximately 300nm in length and 1.23nm in diameter, (J. Dow, 1996; J.-Y. Rho et al., 1998) and is generally regarded as a fibrous collagen due to the nature of its aggregated form (A.J. Bailey et al. 1998).

During bone formation, osteoblast cells synthesise collagen which, upon secretion from the cell, form into fibrils which have a characteristic structure and pattern; each molecule overlaps by 27 nm with the gaps between molecules being in the region of 40nm giving a characteristic 67nm periodic pattern (J.-Y. Rho et al., 1998) (Figure 2.4A). This spacing allows the tail of one molecule to be positioned next to the head of the molecule in an adjoining position, known as the quarter stagger array (J. Dow, 1996). The initial fibril formation is governed by the formation of immature non-covalent cross links between adjoining amino acid chains, but with time and enzymatic help the lysine residues of the molecules form mature covalent cross-links, providing secure support to the fibrils structure (B. Alberts et al., 1994; J. Dow, 1996; H. Oxlund et al., 1996) (Figure 2.4A).

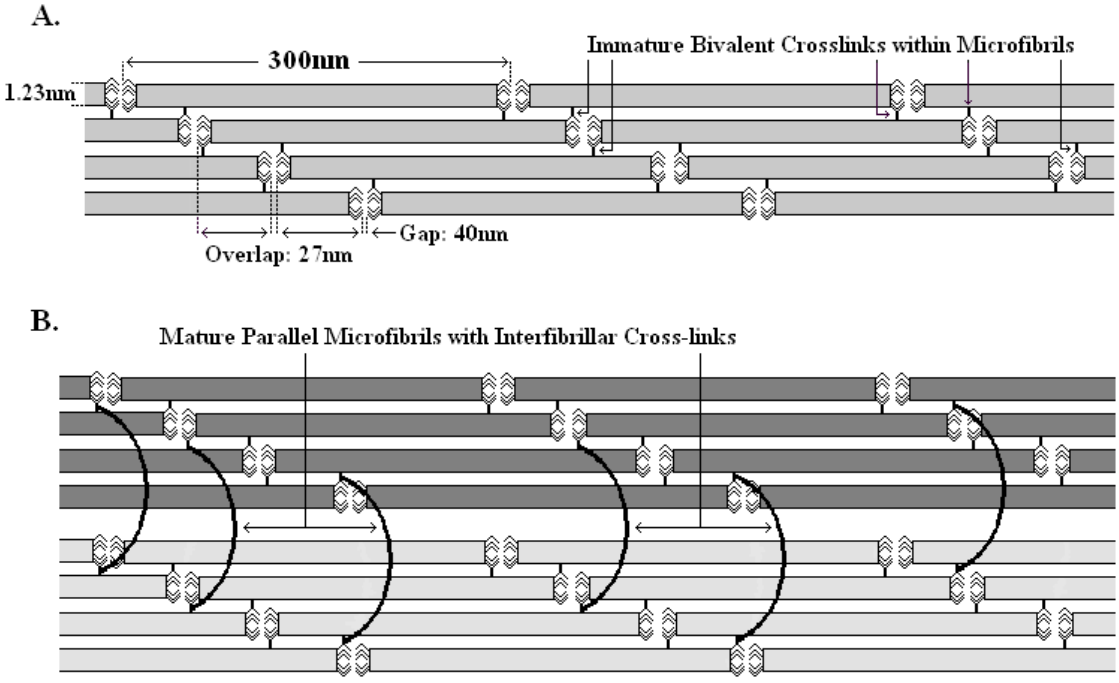

Figure 2.4 Schematic representation of fibrous nature of type 1 collagen showing the (A.) structure and the divalent immature cross-links within the newly formed collagen fibres and (B.) the trivalent mature cross-linking produced from the immature cross-links which link the microfibrils.

This study will investigate both the immature and the resultant mature cross-links, in terms of their volume within the tissue, with the information adapted from personal communication with the Collagen Research Group, University of Bristol, who performed the collagen analysis in this study. The immature or intermediate cross-links are split into two different groups, the Aldimines and the Ketoimines. The Aldimines are derived from lysine aldehyde reaction with hydroxylysine or lysine, and yield the hydroxylysinonorleucine (HLNL) and lysinonorleucine (LNL) cross-links, but only HLNL was investigated in this study. The Ketoimines are derived from hydroxylysine aldehyde reaction with hydroxylysine or lysine, and yield hydroxylysinoketonorleucine (HLKNL) or lysinoketonorleucine (LKNL) respectively. The levels of HLKNL were investigated in this study, but when LKNL is reduced it produces lysino-

hydroxynorleucine (LHNL) which is a structural isomer of HLNL and the two cannot be differentiated between; however its mature form (see below) was investigated.

The mature cross-links are, as mentioned previously, a further chemical reaction of the immature cross-link. The Aldimine or HLNL cross-link reacts with histidine to yield histidinohydroxylysinonorleucine (HHL). The Ketoimines are, however, far more complex and the resultant cross-link depends on the degree of hydroxylation of the tissue. The HLKNL and LKNL cross-links will react with hydroxylysine aldehyde to yield hydroxylysylpyridinoline (OHPyr) and lysylpyridinoline (Lys-Pyr) respectively, both of which were investigated in this study. However they will also react with lysine aldehyde to yield hydroxylysyl or lysyl pyrrole (OH & L-Pyrrole) respectively which were not investigated. The final cross-link which was investigated in this study was the level of Pentosidine within the tissue. Pentosidine is formed as part of a complex list of reactions, but is generally extremely low in concentration, and although investigated would not be expected to have any effects on the mechanics of the skeletal tissue. Full chemical reactions and in-depth explanations of the cross-links and their formations can be found in A.J. Bailey et al. (1998), L. Knott and A.J. Bailey (1998) and A.J. Bailey and L. Knott (1999).

2.2.2 Mineral Matrix

The collagen network forms the scaffold for the deposition of the mineral matrix which fills the 40nm gaps between the collagen molecules, and packs the spaces between the collagen fibrils. The mineral is a mixture of calcium phosphate ($Ca_3(PO_4)_2$), calcium hydroxide ($Ca(OH)_2$) and phosphate ions in the form of crystals of hydroxyapatite ($Ca_{10}(PO_4)_6(OH)_2$). The hydroxyapatite is, however, far from pure and

incorporated into the crystals are other ions and compounds such as HPO_4, Na, Mg, citrate, carbonate and K (J.-Y. Rho et al., 1998; J.E. Shea and S.C. Miller, 2005).

Concluding Remarks

This chapter has demonstrated that bone is a complex composite material made up primarily of two phases, a mineral phase laid down on an organic phase which together form a hierarchical structure. The human skeleton has evolved over time to enable humans to stand upright and move; in doing so, the skeletal tissue is subjected, during everyday physiological movements, to numerous different magnitude loads and loading conditions. In normal physiological loading the skeletal tissue is able to resist the forces; however conditions such as osteoporosis and osteoarthritis are known to adversely affect the skeletal tissue with, in particular, osteoporosis reducing the mechanical competence thereby causing an increased risk of fracture in sufferers. In the following two chapters the aim is to outline the previously determined biomechanics for normal, osteoporotic and osteoarthritic cancellous bone tissue, to review the effects of the conditions with respect to the skeletal tissue itself, to introduce the guidelines for the diagnosis of osteoporosis and to consider the abilities of the diagnostic methods available to the clinician for the prediction of DXA determined skeletal condition.

Chapter 3: Biomechanics

When referring to the mechanical properties of cancellous bone it is important to differentiate between the properties of the cancellous bone structure and the actual cancellous bone material. In order to differentiate between the two, cancellous bone will be used to refer to the properties relating to the structure, and trabecular bone will be considered to be the actual bone material.

3.1 Trabecular Bone Material

As mentioned previously, the material density of trabecular bone is not dissimilar to that of cortical bone; however the similarity between the mechanical properties of the materials is an area under discussion. There are a number of studies that have attempted to assess the mechanical properties of trabecular bone material by a number of different methods, including micro-mechanical methods, nanoindentation, microhardness, Finite Element Analysis (FEA) and ultrasonic methods. The results of these studies have been reviewed on a number of occasions over the years (J.Y. Rho et al. 1993; 1998; L.J. Gibson and M.F. Ashby, 1997; H.H. Bayraktar et al., 2004) and a combination of these reviews is shown in Table 3.1.

Of the studies that compared compact bone tissue with trabecular bone (J.C. Runkle and J. Pugh, 1975; J.L. Kuhn et al., 1989; P.L. Mente and J.L. Lewis, 1989; J.-Y. Rho et al., 1999; C.H. Turner et al., 1999; H.H. Bayraktar et al., 2004), the majority found that the difference between the Young's modulus of the two tissue types was significantly different. However C.H. Turner et al. (1999) using nanoindentation and acoustic microscopy on bone tissue from one human subject found that the Young's

moduli of the two tissues were within the same range. That said, the range of the Young's modulus from study to study is huge, from 1.30 GPa (J.L. Williams and J.L. Lewis, 1982) to 22.7 ± 3.12 GPa (J.-Y. Rho et al., 1999). One explanation for this range of values is the extraction of samples from different areas of the bone opening the opportunity for the natural variation in mineralization, composition and microstructure between sampling sites to affect the results. P.K. Zysset et al. (1999) showed that the elastic properties of the cortical bone from the femoral neck was half way between the values for the femoral neck trabecular bone and the diaphyseal cortical bone. The authors offer the explanation that this may prevent deleterious local deformation mismatches between the two different types of bone that could potentially have reduced the strength of the femoral neck. A further reason for this range can be explained by the methods used to characterise the mechanical properties of trabecular bone. A lot of the work is based on the micro-mechanical testing of individual trabeculae and the studies all note that working with a small sample size and the machining of samples, increases the potential sources of error.

Table 3.1 Review of the published Young's Moduli of individual Trabecula, or trabecular bone table adapted and modified from J.Y. Rho et al. 1993, 1998, L.J. Gibson and M.F. Ashby, 1997, H.H. Bayraktar et al., 2004.

Reference	Type of Bone	Test Method	Result Trabecular	Results Cortical
J.C. Runkle and J. Pugh (1975)	Human, Distal Femur	Buckling	8.69 ± 3.17 GPa (dry)	Compared to Literature
P.R. Townsend and R.M. Rose (1975)	Human, Proximal Tibia	Inelastic Buckling	11.38 GPa (wet) 14.13 GPa (dry)	
J.L. Williams and J.L. Lewis (1982)	Human, Proximal Tibia	2D FEA modelling	1.30 GPa	
J.L. Ku et al. (1987)	Fresh Frozen Human Tibia	Three-Point Bending	3.17 ± 1.5 GPa	
P.L. Mente and J.L. Lewis (1987)	Dried Human Femur and Fresh human Tibia	Cantilever Bending and FEA modelling	5.3 ± 2.6 GPa	
R.B. Ashman and J.Y. Rho (1988)	Human Femur	Ultrasonic Test Method	13.0 ± 1.5 GPa (wet)	
K. Choi et al. (1989)	Human Tibia	Three Point Bending	4.59 GPa	
R. Hodgskinson et al. (1989)		Microhardness	15 GPa (estimation)	
J.L. Kuhn et al. (1989)	Human Iliac Crests from a 23 year old and a 63 year old	Three Point Bending	23 yr old: 3.03 ± 1.63 GPa 63 yr old: 4.16 ± 2.02 GPa	23 yr old: 3.76 ± 1.68 GPa 63 yr old: 5.26 ± 2.09 GPa
P.L. Mente and J.L. Lewis (1989)	Dried Human Femur Fresh Human Tibia	Cantilever Bending and FEA Modelling	7.8 ± 5.4 GPa (dry)	18.2 ± 1.4GPa (dry) 12.4 ± 3.8GPa (wet)
K.S. Jensen et al. (1990)	Human Vertebra (L3)	3D FEA Modelling	3.8 GPa	
K. Choi et al. (1990)	Human Tibia	Four-Point Bending	Vertical: 4.87 ± 1.84 GPa	Vertical: 5.44 ± 1.25 GPa
			Horizontal: 3.83 ± 0.45 GPa	
			Total: 4.59 ± 1.6 GPa (wet)	
J.-Y. Rho et al. (1993)	Human Tibia	Tensile Testing	10.4 ± 3.5 GPa (dry)	18.6 ± 3.5 GPa
		Ultrasonic Testing	14.8 ± 1.4 GPa (wet)	20.7 ± 1.9 GPa

Table 3.1 Continued

Reference	Type of Bone	Test Method	Result Trabecular	Results Cortical
D. Ulrich et al. (1997)	Human Femoral Head	Experiment – FEA modelling	3.5 – 8.6 GPa	
J.-Y. Rho et al. (1997)	Human Vertebra	Nanoindentation	13.4 ± 2.0 GPa	
F.J. Hou et al. (1998)	Human Vertebra	Experiment – FEA modelling	5.7 ± 1.6 GPa	
A.J. Ladd et al. (1998)	Human Vertebra	Experiment – FEA modelling	6.6 ± 1.0 GPa	
J.-Y. Rho et al. (1999)	Human Vertebra	Nanoindentation Longitudinal:	19.4 ± 2.3 GPa	Osteons: : 22.4 ± 1.2 Interstitial Lamellae: 25.7 ± 1
		Nanoindentation Transverse:	15.0 ± 2.5 GPa	16.6 ± 1.1 GPa
M.E. Roy et al. (1999)*	Human Lumbar Vertebrae	Nanoindentation	ATL: 17.99 ± 2.2 GPa ATT: 22.7 ± 3.12 GPa RTL: 16.3 ± 2.41 GPa CTL: 15.7 ± 1.47 GPa	ECC: 18.1 ± 2.87 GPa ECS: 16.7 ± 2.86 GPa CSS: 16.9 ± 3.2 GPa CST: 18.1 ± 2.66 GPa
C.H. Turner et al. (1999)	Human Distal Femur	Nanoindentation	18.14 ± 1.7 GPa	Transverse: 16.58 ± 0.32 GPa Longitudinal: 23.45 ± 0.21 GPa Average: 20.02 ± 0.27 GPa
		Acoustic Microscopy	17.5 ± 1.1 GPa	Transverse: 14.91 ± 0.52 GPa Longitudinal: 20.55 ± 0.21 Average: 17.73 ± 0.22
P.K. Zysset et al. (1999)	Human Femoral Neck	Nanoindentation	11.4 ± 5.6 GPa	
F. Bini et al. (2002)	Human Greater Trochanter	Tensile Testing	1.41 – 1.89 GPa	
H.H. Bayraktar et al. (2004)	Human Femoral Neck	Experiment – FEA modelling	18.0 ± 2.8 GPa	19.9 ± 1.8 GPa

* ATL: Axial Trabeculae Longitudinal Section, ATT: Axial Trabeculae Transverse Section, RTL: Radial Trabeculae Longitudinal Section, CTL: Circumferential Trabeculae Transverse Section, ECC: Cortical Endplate Coronal Section, ECS: Cortical Endplate Sagittal Section, CSS: Cortical Shell Sagittal Section, CST: Cortical Shell Transverse Section

3.2 Cancellous Bone

3.2.1 Compression Testing

The most commonly performed test for the determination of the mechanical properties of cancellous bone tissue is the compression test, with the large volume of previous work having performed this as the principal biomechanical test.

The wide variation in the density of cancellous bone means that there can be no definitive value for the compressive properties of cancellous bone, such as a single Young's modulus (MPa), yield strain (%), strength (MPa) etc, but only relationships and equations with respect to different variables. The best explanation for this is that:

'Trabecular bone is classified from an engineering materials perspective as a composite, anisotropic, open porous cellular solid' T.M. Keaveny et al. (2001).

As such, its mechanical properties are affected by density (apparent and material), porosity, trabecular orientation and organisation (trabecular number, size and direction) and composition (mineral concentration).

The relationship between the variables forming either a power function relationship, which adheres to equation 3.1, or a linear function relationship which adheres to equation 3.2, where for both equations 'A' and 'B' are constants.

$$\text{Material Property} = A(\text{Density})^{B} \qquad \textbf{Equation 3.1}$$

$$\text{Material Property} = A(\text{Density}) + B \qquad \textbf{Equation 3.2}$$

3.2.1.1 Apparent Density

There is much discussion about the relationship between the apparent density of cancellous bone and its compressive mechanical properties, with linear and power functions both initially providing equally valid degrees of explanatory ability, depending on the mechanical property. The reason behind this uncertainty was best outlined by L.J. Gibson, (1985), who recognised that a change in the apparent density of the bone went hand in hand with a change in the structure of the bone. The cancellous bone with low density was made up of an open cell structure of rods, whereas the higher density bone was a closed-cell structure made up of plates, with the change between the two structures being a gradual effect but estimated to start at 0.35g cm^{-3}, with anything above this being a closed-cell foam of plates (L.J. Gibson, 1985; D.R. Carter and W.C. Hayes, 1977). The deformation of cancellous bone under compression occurs by the buckling of the rods or plates that make up the structure, (J.W. Pugh et al., 1973; J.L. Stone et al., 1983; L.J. Gibson, 1985) and as such, the two structures deform differently under applied loads.

This is best demonstrated using Figure 3.1 from L.J. Gibson and M.F. Ashby, (1997a), which shows the stress-strain curves of three different relative densities of cancellous bone, and their different deformations.

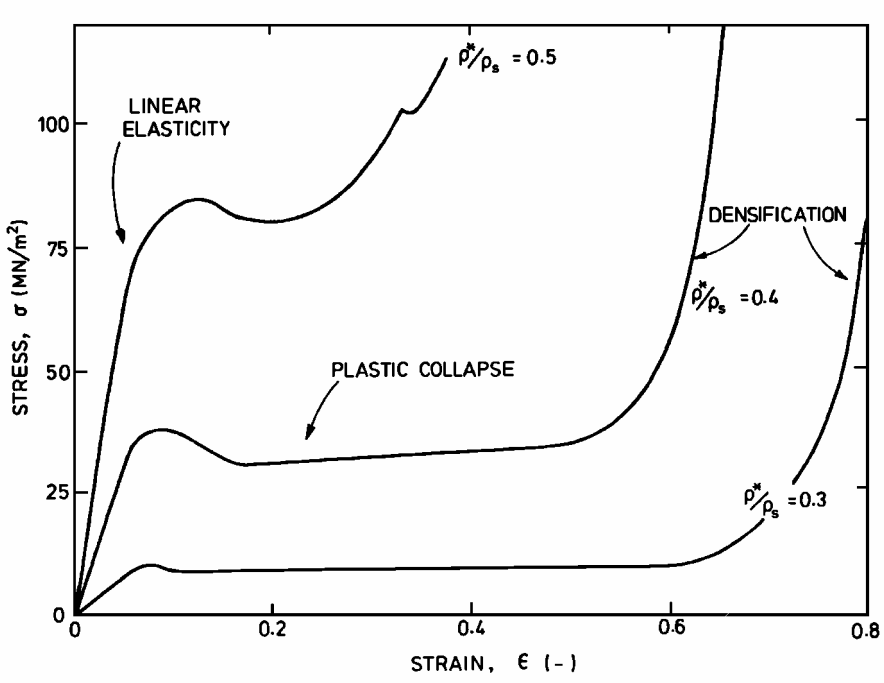

Figure 3.1 Compressive stress-strain curves of three cancellous bone samples of different relative density (ρ^*/ρ_s), taken from L.J. Gibson and M.F. Ashby (1997a).

The apparent density of the test sample has been shown to affect a number of different compressive properties of cancellous bone to different degrees. A. Nafei et al. (2000) demonstrated that the apparent density of ovine trabecular bone in compression could explain 64% of the variation in the Elastic Modulus, 70% in the Ultimate Strength and 53% of the Energy Absorption to Failure, although it explains very little of the variation in ultimate strain (10%).

Young's Modulus / Stiffness

The most quoted property of cancellous bone in relation to apparent density is the stiffness or Young's modulus. In a review of a number of different studies by L.J. Gibson and M.F. Ashby, (1988, 1997), and republished in 2005, the relationship

between relative density and the Young's modulus of cancellous bone was investigated with the resultant analysis providing a power function of roughly two (Figure 3.2).

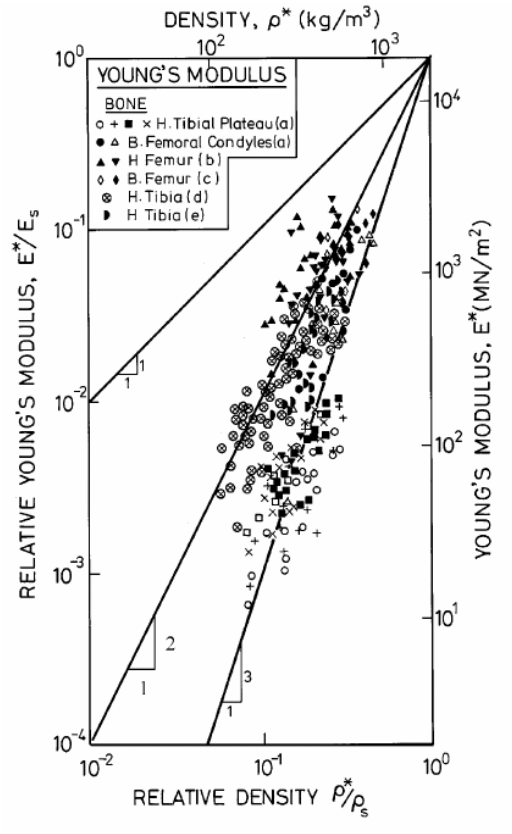

Figure 3.2 Young's moduli vs. relative density (Diagram taken from L.J. Gibson, 2005)

A further 17 studies (Table 3.2), provide either power function or linear regression equations for the relationship between Young's modulus and apparent density, with Young's modulus being determined by a number of different methods, including both destructive (DT) and non-destructive (NDT) compression testing, and in two cases an ultrasonic technique.

All the power function relationships from the literature (Table 3.2), ranged from between 1.06 (F. Linde et al., 1988) to 3.46 (T.S. Keller, 1994), with an average power of 1.98 (SD = 1.7) which is in close agreement to the work of L.J. Gibson and

M.F. Ashby, (1988, 1997). The correlation coefficients were all statistically significant, with the Pearson's correlations (r) ranging from 0.57 (T.M. Keaveny et al., 1993) to 0.92 (T.M. Keaveny et al., 1993, F. Linde and I. Hvid, 1989) and averaging 0.80 (SD = 0.09) and the r^2 values ranging from 0.57 (M.J. Ciarelli et al., 1991) to 0.941 (R. Hodgskinson and J.D. Currey, 1990a) and averaging 0.78 (SD = 0.11).

For the linear relationships between the Young's modulus and the apparent density, the strength of correlations was lower in comparison to those of the power function relationship with the r values ranging from 0.57 to 0.9 (T.M. Keaveny et al., 1993) and averaging 0.7 (SD =0.15), and the r^2 values ranging from 0.31 (T.M. Keaveny et al., 1997) to 0.92 (R. Hodgskinson and J.D. Currey, 1990a) and averaging 0.68 (SD = 0.19).

The difference between the linear and the power function relationships is with the closeness of agreement between the studies; on the most part the power function relationships are in fairly close agreement, with power functions within the expected range for the relationship. The linear relationships are, however, extremely variable with differences being in the order of 1000+ for both the A and B values, even after consideration of the units used in the studies. The reasons for this are errors related to differences in the testing conditions, be it destructive or non-destructive, with loading rate or strain rate, the application of conditioning prior to testing, the size and shape of the test sample, the data collection method, the source of the bone sample and the samples orientation, all providing sources of error and variation in the results; this will be introduced in more depth in section 3.1.2.5.

Table 3.2 Linear and power function relationships between apparent density and Young's modulus and strength from the literature.

Reference Extensometer	Type of Bone	Sample Design	Loading Regime Units	Linear Function Modulus			Power Function Modulus			Linear Function Strength			Power Function Strength		
				A	B	r or r^2	A	B	r or r^2	A	B	r or r^2	A	B	r or r^2
S.J. Kaplan et al. (1985) Test Machine **Units**: σ_{Ult}: MPa; ρ: g cm^{-3}	Bovine Humeri	Cylindrical Cores L = 5mm D = 20mm	**DT**: at 0.01 s^{-1}	-	-	-	-	-	-	-	-	-	32.4	1.85	$r^2 = 0.87$
K. Brear et al. (1988) Test Machine **Units**: E: GPa; σ_{Ult}: MPa, ρ: kg m^{-3}	Bovine Dist. Femur	Cubic S = 10mm	**DT**: 1 mm min^{-1} Cold conditions	0.0034	-0.806	$r^2 = 0.76$	$10^{-4.81}$	log 1.76	$r^2 = 0.76$	0.045	-10.5	$r^2 = 0.83$	$10^{-3.67}$	log 1.75	$r^2 = 0.85$
			DT: 1 mm min^{-1} Hot conditions	0.0034	-0.884	$r^2 = 0.80$	$10^{-5.41}$	log 1.96	$r^2 = 0.80$	0.038	-8.69	$r^2 = 0.88$	$10^{-3.83}$	log 1.79	$r^2 = 0.88$
F. Linde et al. (1988) Test Machine **Units**: E: MPa, σ_{Ult}: MPa, ρ: g cm^{-3}	Prox. Tibia	Cylindrical Cores L = 7.5mm D = 7.5mm	**DT**: 5mm min^{-1}, or 0.01s^{-1}, No preconditioning	-	-	-	1369	1.33	r = 0.79	-	-	-	25.3	1.50	r = 0.89
			NDT: 0.2Hz at 0.01s^{-1} between 5N and 0.6% strain	-	-	-	2560	1.47	r = 0.84	-	-	-	34.1	1.56	r = 0.89
			NDT: 0.2Hz at 0.01s^{-1} between 5N and 0.45% strain **DT**: 5mm min^{-1}, or 0.01s^{-1}, No preconditioning	-	-	-	1136	1.06	r = 0.76	-	-	-	24.7	1.32	r = 0.83
I. Hvid et al. (1989) Test Machine **Units**: E: MPa, σ_{Ult}: MPa, ρ: g cm^{-3}	Prox. Tibia	Cylindrical Cores L = 7.5mm D = 7.5mm	**Cond**: 0.2Hz at 0.01s^{-1} to 0.6% strain **NDT**: 0.2Hz at 0.01s^{-1} between 5N and 0.6% strain **DT**: 5mm min^{-1}, or 0.01s^{-1}	1173	-44.38	r = 0.744	1371	1.33	r = 0.74	18.99	-1.141	r = 0.863	25.30	1.494	r = 0.892
F. Linde et al., (1989) Platens Extensometer **Units**: E: MPa, σ_{Ult}: MPa, ρ: g cm^{-3}	Prox. Tibia	Cylindrical Cores L = 7.5mm D = 7.5mm	**Cond**: 0.2Hz at 0.01s^{-1} to 0.6% strain **NDT**: 0.2Hz at 0.01s^{-1} between 5N and 0.6% strain **DT**: 5mm min^{-1}, or 0.01s^{-1}	-	-	-	2561	1.47	r = 0.84	-	-	-	34.17	1.56	r = 0.89

Extensometers: Test Machine: The extensometer built into the test machine. **Platens Extensometer:** An extensometer connected directly to the loading platens either side of the test sample. **Contact Extensometer:** An extensometer attached directly to the bone samples surface.
Cond: Condition testing regime, **NDT:** Non-destructive testing regime, **DT:** Destructive testing regime.
Sample Design: L = Length, **D:** Diameter, **S:** Side Length

Table 3.2 Continued

Reference Extensometer	Type of Bone	Sample Design	Loading Regime	Linear Function Modulus			Power Function Modulus			Linear Function Strength			Power Function Strength		
				A	B	r or r^2	A	B	r or r^2	A	B	r or r^2	A	B	r or r^2
F. Linde & I. Hvid (1989) Test Machine **Units**: E: MPa, σ_{Ult}: MPa, ρ: g cm^{-3}	Prox. Tibia	Cylindrical Cores L = 7.5mm D = 7.5mm	**NDT**: 0.2Hz at 0.01s^{-1} between 5N and 0.8% strain **DT**: 5mm min -1, or 0.01s^{-1}	-	-	-	10256	2.5	r = 0.92	-	-	-	69	2.1	r = 0.94
A. Odgaard et al., (1989) Platens and Optical Extensometer **Units**: E: MPa, σ_{Ult}: MPa, ρ: g cm^{-3}	Prox. Tibia	Cylindrical Cores L = 7.5mm D = 5mm	**DT**: 0.00015s^{-1}	-	-	-	-	-	-	-	-	-	17.05	1.82	r = 0.91
R. Hodgskinson & J.D. Currey (1990a) Test Machine **Units**: E: MPa, ρ: kg m^{-3}	Prox.and Dist. Femur / Tibia	Cubic S = 10mm	**DT**: 0.0017 s^{-1}	1.96	-255	r^2 = 92.3	0.004	1.96	r^2 = 0.94	-	-	-	-	-	-
R. Hodgskinson & J.D. Currey (1990b) Test Machine **Units**: E: MPa, ρ: kg m^{-3}	Equine Prox. Tibia, Bovine Femur / Vertebra, Donkey Dist. Femur	Cubic S = 10mm	**DT**: 1. 1 mm min^{-1} or 0.0017s^{-1} 2. 2 mm min^{-1} or 0.0033 s^{-1}	2.03	-359	r^2 = 0.908	0.0015	2.09	r^2 = 0.91	-	-	-	-	-	-
M.J. Ciarelli et al. (1991) Test Machine **Units**: E: MPa, ρ: g cm^{-3}	Prox. Femur	Cubic S= 8mm	**Cond**: ~40-60% of the Ultimate Load **NDT**: ~1%/s	1276	n.a.	r^2 =0.54	n.a.	1.80	r^2 =0.57	-	-	-	-	-	-
	Dist. Femur			1019	n.a.	r^2 =0.77	n.a.	1.45	r^2 =0.80	-	-	-	-	-	-
	Prox. Tibia			693	n.a.	r^2 =0.52	n.a.	2.05	r^2 =0.68	-	-	-	-	-	-
	Prox. Humerus			761	n.a.	r^2 =0.72	n.a.	2.06	r^2 =0.83	-	-	-	-	-	-
	Dist. Radius			1019	n.a.	r^2 =0.88	n.a.	1.80	r^2 =0.89	-	-	-	-	-	-
M.J. Anderson et al. (1992) Test Machine **Units**: E: MPa, σ_{Ult}: MPa, ρ: g cm^{-3}	Prox.Tibia	Column 2 x 1x 1cm	**Cond**: 5N load, + 0.1mm cycles at 0.2mm s^{-1} **DT**: 1%/s	-	-	-	3890	2.08	-	-	-	-	51.3	2.09	-

Table 3.2 Continued

Reference Extensometer	Type of Bone	Sample Design	Loading Regime	Linear Function Modulus			Power Function Modulus			Linear Function Strength			Power Function Strength		
				A	B	r or r^2	A	B	r or r^2	A	B	r or r^2	A	B	r or r^2
F. Linde et al. (1992) Platens Extensometer **Units**: E: MPa, σ_{Ult}: MPa, ρ: g cm^{-3}	Prox. Tibia	Cylindrical Cores L, D = 6.5mm	**Cond**: 0.2Hz at 0.01s^{-1} to 0.4% strain **NDT**: 0.01s^{-1} between 0.12 MPa and 0.4% strain **DT**: 0.01 s^{-1}	-	-	-	1624	1.32	r = 0.70	-	-	-	25.4	1.60	r = 0.75
		Cubic Specimens S = 5.8mm		-	-	-	2374	1.60	r = 0.79	-	-	-	30.5	1.72	r = 0.84
		Cylindrical Cores L, D = 5.5mm	**Cond**: 0.2Hz at 0.01s^{-1} to 0.4% strain **NDT**: 0.01s^{-1} between 0.12 MPa and 0.4% strain	-	-	-	1236	1.45	r = 0.75	-	-	-	32.4	1.87	r = 0.80
		Cylindrical Cores L, D = 6.5mm		-	-	-	1364	1.39	r = 0.83	-	-	-	25.1	1.63	r = 0.90
		Cylindrical Cores L, D = 7.5mm		-	-	-	4778	1.99	r = 0.89	-	-	-	76.5	2.23	r = 0.94
T.M. Keaveny et al. (1993) Test Machine **Units**: E: MPa, σ_{Ult}: MPa, ρ: g cm^{-3}	Bovine Humerus	Cylindrical Cores L = 10mm D = 5.1mm	**No Cond** **DT**: 0.005 s^{-1}	3890	- 1110	r = 0.90	3380	2.21	r = 0.92	48.1	-13.1	r = 0.94	40.0	1.98	r = 0.95
		Cubic S = 5mm		4220	- 909	r = 0.57	3710	1.65	r = 0.57	58.8	-16.5	r = 0.82	54.1	2.14	r = 0.82
T.S. Keller (1994) Test Machine **Units**: E: GPa, σ_{Ult}: MPa, ρ: g cm^{-3}	Human Lumbar Spine	Cubic S = 1cm	**No Cond** **DT**: 5 mm min^{-1} or 0.005 s^{-1}	0.203	-0.00747	r^2 = 0.54	0.757	1.94	r^2 = 0.702	16.9	-0.971	r^2 = 0.739	97.9	2.30	r^2 = 0.788
	Prox. and Dist. Femur	Cubic S = 0.8cm	**No Cond** **DT**: 4 mm min^{-1} or 0.005 s^{-1}	11.1	-6.97	r^2 = 0.69	1.99	3.46	r^2 = 0.751	116	-70.6	r^2 = 0.907	26.9	3.05	r^2 = 0.815

Table 3.2 Continued

Reference Extensometer	Type of Bone	Sample Design	Loading Regime	Linear Function Modulus			Power Function Modulus			Linear Function Strength			Power Function Strength		
				A	B	r or r^2	A	B	r or r^2	A	B	r or r^2	A	B	r or r^2
M.-C. Hobatho et al. (1997) Extensometer n.a. **Units**: E: MPa, σ_{Ult}: MPa, ρ: kg m^{-3}	Prox. Tibia	Cubic Samples		-	-	-	-	-	-	0.021	-1.72	r^2 =0.73	0.000005	2.01	r^2 = 0.78
	Prox. Femur			-	-	-	-	-	-	0.018	-1.89	r^2 =0.81	0.000005	2.01	r^2 = 0.80
	Dist. Femur			-	-	-	-	-	-	0.02	-1.76	r^2 =0.73	0.000006	1.51	r^2 = 0.78
	Prox. Humerus			-	-	-	-	-	-	0.021	-2.42	r^2 =0.70	0.00002	1.51	r^2 = 0.71
	Patella			-	-	-	-	-	-	0.020	-6.77	r^2 =0.78	0.000002	2.27	r^2 = 0.85
	Lumbar Spine			-	-	-	-	-	-	0.013	-0.131	r^2 =0.61	0.003	1.26	r^2 = 0.63
T.M. Keaveny et al. (1997) Contact + Platens **Units**: E: MPa, ρ: g cm^{-3}	Human Lumbar Spine	Cylindrical Cores L = 35mm D = 8mm	**NDT**: 10 cycles between 0 and 0.3% strain at 0.005 s^{-1}	1540	-58	r^2 = 0.64	-	-	-	-	-	-	-	-	-
	Bovine Prox. Humerus		**NDT**: 10 cycles between 0 and 0.4% strain at 0.005 s^{-1} Brass End-Caps	2890	-509	r^2 = 0.90	-	-	-	-	-	-	-	-	-
	Bovine Prox. Tibia			7390	-1050	r^2 = 0.87	-	-	-	-	-	-	-	-	-
Platens	Human Lumbar Spine	Cylindrical Cores L = 16mm D = 8mm	**Cond**: 10 cycles between 0% strain at 5-10N to 0.8% strain **DT**: strain rate 0.003s^{-1}	935	15	r^2 = 0.31	-	-	-	-	-	-	-	-	-
	Bovine Prox. Humerus			2510	-611	r^2 = 0.91	-	-	-	-	-	-	-	-	-
	Bovine Prox. Tibia			5410	-989	r^2 = 0.56	-	-	-	-	-	-	-	-	-
	OA Femoral Heads			17.4	-13.1	r^2 = 0.39	-	-	-	-	-	-	-	-	-
	OP Femoral Heads			22.1	-21.4	r^2 = 0.40	-	-	-	-	-	-	-	-	-

Table 3.2 Continued

Reference Extensometer	Type of Bone	Sample Design	Loading Regime	Linear Function Modulus			Power Function Modulus			Linear Function Strength			Power Function Strength		
				A	B	r or r^2	A	B	r or r^2	A	B	r or r^2	A	B	r or r^2
B. Li & R.M. Aspden (1997b) Test Machine **Units**: E: MPa, ρ: g cm^{-3}	Normal Femoral Heads	Cylindrical Cores L =~7.7mm D = 9mm	**NDT**: 20% / min or 0.0033 s^{-1} Test stopped prior to yield	573	-9.4	$r^2 = 0.59$	-	-	-	-	-	-	-	-	-
	OA Femoral Heads			278	129	$r^2 = 0.33$	-	-	-	-	-	-	-	-	-
	OP Femoral Heads			587	6.3	$r^2 = 0.44$	-	-	-	-	-	-	-	-	-
R.W. McCalden et al. (1997) Test Machine **Units**: σ_{Ult}: MPa, ρ: kg m^{-3}	Human Femora	Cylindrical Cores L= 10mm D = 10mm	**DT**: 1mm min^{-1} or 0.0017 s^{-1}	-	-	-	-	-	-	0.0356	-5.649	$r^2 = 0.94$	-	-	-
D.L. Kopperdahl & T.M. Keaveny (1998) Platens + Contact Extensometer **Units**: E: MPa, σ_{Ult}: MPa, ρ: g cm^{-3}	Human Lumbar Spine	Cylindrical Cores L = 25mm D = 8mm	**NDT**: ±0.1% strain at 0.005 s^{-1} **DT**: 0.005 s^{-1} Brass End-Caps	2100	-	$r^2 = 0.61$	2350	1.20	r^2 =0.60	21.9	-1.46	$r^2 = 0.71$	33.2	1.53	$r^2 = 0.68$
E.F. Morgan et al. (2003) Platens + Contact Extensometer **Units**: E: MPa, ρ: g cm^{-3}	Vertebra (T10 – L5)	Cylindrical Cores L = 25mm D = 8mm	**Cond**: 3 cycles to 0.1% strain **NDT**: 0.005 s^{-1} tested to the yield point Brass End-Caps	-	-	-	4730	1.56	$r^2 = 0.73$	-	-	-	-	-	-
	Prox. Tibia			-	-	-	15520	1.93	$r^2 = 0.84$	-	-	-	-	-	-
	Greater Trochanter			-	-	-	15010	2.18	$r^2 = 0.82$	-	-	-	-	-	-
	Femoral Neck			-	-	-	6850	1.49	$r^2 = 0.85$	-	-	-	-	-	-

Strength

The relationship between compressive strength and density was also reviewed by L.J. Gibson and M.F. Ashby, (1988, 1997), and republished in 2005. This relationship also displayed a power function of 2 (Figure 3.3).

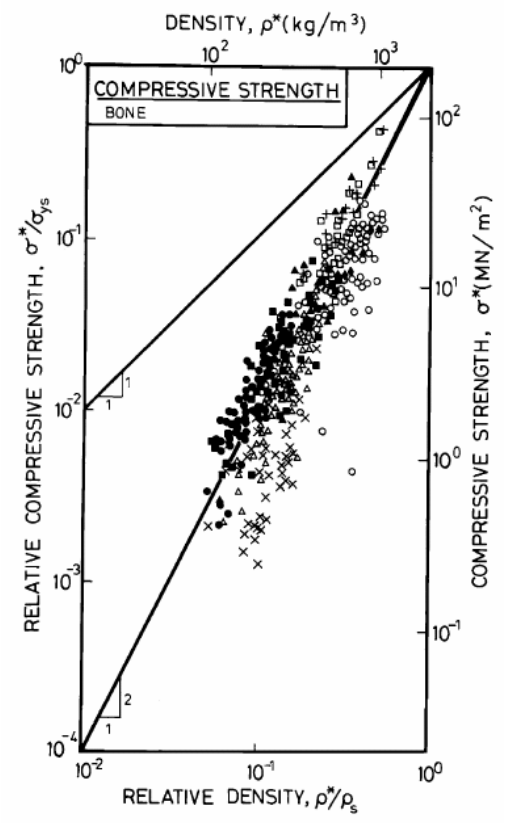

Figure 3.3 Compressive strength vs. relative density (Diagram taken from L.J. Gibson (2005))

Table 3.2 shows 13 studies which have investigated the relationship between the compressive strength of cancellous bone in relation to its apparent density. As with the Young's modulus results, both linear and power function relationships were presented. For the power function relationships the average power was 1.85 (SD = 0.39), range 1.32 (F. Linde et al., 1988) to 3.05 T.S. Keller (1994) almost identical to that seen for the Young's modulus relationship. The correlations for the power function

relationship were also similar to those seen for the Young's modulus. The Pearson's correlations ranged from 0.75 (F. Linde et al., 1992) to 0.95 (T.M. Keaveny et al., 1993) and averaged 0.87 (SD = 0.08). The r^2 values for the power function relationship ranged from 0.63 (M.-C. Hobatho et al., 1997) to 0.88 (K. Brear et al., 1988), and averaged 0.79 (SD = 0.08). The correlations for the linear functions were very similar to those of the power function relationships; for the linear relationships, the Pearson's correlations ranged from 0.82 to 0.94 (T.M. Keaveny et al., 1993) and averaged 0.87 (SD = 0.06), while the r^2 values ranged between 0.61 (M.-C. Hobatho et al., 1997) and 0.94 (R.W. McCalden et al., 1997) with an average of 0.78 (SD = 0.1).

Strength regressions and results are affected by a number of the same error sources that were introduced for the Young's modulus, with loading rate or strain rate, the application of conditioning prior to testing, the size and shape of the test sample, the source of the bone sample and the sample's orientation all providing sources of error and variation in the results, and will be introduced in more depth in section 3.1.2.5.

One noticeable difference is that unlike the regression equations for the Young's modulus, the A and B values for the equations are of the same order of magnitude. This is most likely due to the nature of the strength value in that it is determined from the peak load, which is easily defined, whereas the Young's modulus is based on the fitting of a tangent to, or the determination of, the slope of the linear portion of the loading curve, which is more prone to human error.

Of the studies introduced in Table 3.2 it is noticeable that only two (B. Li & R.M. Aspden, 1997b; T.M. Keaveny et al., 1997) performed any testing on tissue from individuals who were suffering from either osteoarthritis of osteoporosis. The studies are hard to compare as the sample designs and test methods were noticeably different

with T.M. Keaveny et al., (1997) using long thin cylindrical cores (L = 16mm, D = 8mm) which were destructively tested, while B. Li & R.M. Aspden, (1997b) used cores which were half the length and thicker (L = ~7.7mm, D = 9mm) and tested them non-destructively. Although the strain rate was virtually identical the results were different by a factor of 10. They did, however, both demonstrate that the modulus of the osteoarthritic bone samples was reduced in comparison to normal and osteoporotic bone, and although the osteoporotic bone in the T.M. Keaveny et al., (1997) was also reduced compared to bone from the lumbar spine, B. Li & R.M. Aspden, (1997b) they found that the modulus of the osteoporotic bone was superior to that of normal bone. This is not necessarily an incorrect result as it is feasible that the modulus of the tissue may be the same in compression, and it is the other compressive mechanical properties such as strain, yield stress and work to failure which are affected by the conditions; as such it is important to consider these alternative parameters.

Other Mechanical Parameters

The compressive Young's modulus and the strength of cancellous bone are not the only properties to be affected by apparent density; six other studies (Table 3.3) provide information on the relationships between apparent density and the yield stress and strain, the ultimate strain and the work to failure of cancellous bone.

The yield stress was strongly related to the apparent density, and as with the ultimate stress (strength) the power function relationship was between 1.5 and 2, with the power function providing a better correlation in comparison to the linear function relationship. The effect of the apparent density on the yield and ultimate strain was not as strong as that seen for the corresponding yield stress values. The yield strain appeared to be affected more than the ultimate strain by variation in apparent density

but the results were from different studies which utilised different strain rates, sample designs, test methods and sampling sites.

The final parameter investigated was the work to failure, or the energy (area below the load-displacement curve) required to cause failure in the sample. The results of the three studies in Table 3.3 show that work to failure increases with apparent density but that the nature of the relationship, be it linear or power function, is unclear. The study by I. Hvid et al. (1989) is the only one to provide any comparison and indicates that a power function of 1.69 is a better relationship than the corresponding linear relationship.

In addition to the two studies which were introduced in the previous section, S.J. Brown et al. (2002) provides further information on the yield stress of osteoarthritic bone, with respect to normal bone, of the femoral head and showed that there was no discernable difference caused by the condition, with the osteoarthritic bone only displaying slightly higher yield stress values.

Table 3.3 Linear and power function relationships between apparent density and compressive mechanical properties of cancellous bone from the literature.

Reference	Type of Bone	Loading Rate		A	B	r or r^2 value
Power Function: Yield Stress (MPa) = A(Apparent Density (g cm^{-3}))^B						
D.L. Kopperdahl & T.M. Keaveny (1998) Platens + Contact Extensometer	Human Lumbar Spine	Cylindrical Cores L = 25mm D = 8mm Brass End-Caps	**NDT**: ±0.1% strain at 0.005 s^{-1} **DT**: 0.005 s^{-1}	32.6	1.60	r^2 = 0.70
E.F, Morgan & T.M. Keaveny, (2001) Platens + Contact Extensometer	Vertebra (T10 – L5)	Cylindrical Cores L = 25mm D = 8mm	**Cond**: 3 cycles to 0.1% strain **NDT**: 0.005 s^{-1} tested to the yield point Brass End-Caps	37.1	1.74	r^2 = 0.80
	Prox. Tibia			90.2	2.17	r^2 = 0.90
	Greater Trochanter			85.5	2.26	r^2 = 0.92
	Femoral Neck			38.5	1.48	r^2 = 0.62
Linear: Yield Stress (MPa) = A(Apparent Density (g cm^{-3})) + B						
D.L. Kopperdahl & T.M. Keaveny (1998) Platens + Contact Extensometer	Human Lumbar Spine	Cylindrical Cores L = 25mm D = 8mm Brass End-Caps	**NDT**: ±0.1% strain at 0.005 s^{-1} **DT**: 0.005 s^{-1}	19.6	-1.40	r^2 = 0.73
S.J. Brown et al. (2002) Test Machine	Normal Femoral Heads	Cylindrical Cores L = 16mm D = 12mm	**DT**: 0.25 mm min^{-1}	6.0	- 1.3	r^2 = 0.77
	OA Femoral Heads			6.5	- 1.9	r^2 = 0.70
Power Function: Yield Strain (%) = A(Apparent Density (g cm^{-3}))^B						
D.L. Kopperdahl & T.M. Keaveny (1998) Platens + Contact Extensometer	Human Lumbar Spine	Cylindrical Cores L = 25mm D = 8mm Brass End-Caps	**NDT**: ±0.1% strain at 0.005 s^{-1} **DT**: 0.005 s^{-1}	1.24	0.21	r^2 = 0.48
Linear: Yield Strain (%) = A(Apparent Density (g cm^{-3})) + B						
D.L. Kopperdahl & T.M. Keaveny (1998) Platens + Contact Extensometer	Human Lumbar Spine	Cylindrical Cores L = 25mm D = 8mm Brass End-Caps	**NDT**: ±0.1% strain at 0.005 s^{-1} **DT**: 0.005 s^{-1}	1.09	0.66	r^2 = 0.49
Power Function: Ultimate Strain = A(Apparent Density (g cm^{-3}))^B						
I. Hvid et al. (1989) Test Machine	Prox. Tibia	Cylindrical Cores L = 7.5mm D = 7.5mm	**Cond**: 0.2Hz at 0.01s^{-1} to 0.6% strain **DT**: 5mm min^{-1}, or 0.01s^{-1}	0.0114	0.0175	r = 0.271
Linear: Ultimate Strain = A(Apparent Density (g cm^{-3})) + B						
K. Brear et al. (1988) Test Machine	Bovine Dist. Femur	Cubic S = 10mm	**DT**: 1 mm min^{-1} room temperature conditions (20-22^oC)	0.000024	0.015	r^2 = 0.35
			DT: 1 mm min^{-1} physiological conditions (37^oC)	0.000020	0.016	r^2 = 0.30
I. Hvid et al. (1989) Test Machine	Prox. Tibia	Cylindrical Cores L = 7.5mm D = 7.5mm	**Cond**: 0.2Hz at 0.01s^{-1} to 0.6% strain **DT**: 5mm min^{-1}, or 0.01s^{-1}	0.0114	0.0175	r = 0.271

Table 3.3 Continued

Reference	Type of Bone	Loading Rate		A	B	r or r^2 value
Power Function: Work to failure = A(Apparent Density (g cm^{-3}))^B						
I. Hvid et al. (1989) Test Machine	Prox. Tibia	Cylindrical Cores L = 7.5mm D = 7.5mm	**Cond**: 0.2Hz at 0.01s^{-1} to 0.6% strain **DT**: 5mm min^{-1}, or 0.01s^{-1}	432	1.69	r = 0.896
Linear Function: Work to failure = A(Apparent Density (g cm^{-3}))+ B						
K. Brear et al. (1988) Test Machine **Units:** MJ m^{-3}	Bovine Dist. Femur	Cubic S = 10mm	**DT**: 1 mm min^{-1} Cold conditions (20-22^oC)	0.00106	-0.383	r^2 = 0.74
			DT: 1 mm min^{-1} Hot conditions (37^oC)	0.00086	-0.239	r^2 = 0.89
I. Hvid et al. (1989) Test Machine **Units:** kJ m^{-3}	Prox. Tibia	Cylindrical Cores L = 7.5mm D = 7.5mm	**Cond**: 0.2Hz at 0.01s^{-1} to 0.6% strain **DT**: 5mm min^{-1}, or 0.01s^{-1}	296	-25.34	r = 0.859
F. Linde et al., (1989) Platens Extensometer **Units:** kJ m^{-3}	Prox. Tibia	Cylindrical Cores L = 7.5mm D = 7.5mm	**Cond**: 0.2Hz at 0.01s^{-1} to 0.6% strain **DT**: 5mm min^{-1}, or 0.01s^{-1}	446	1.67	r = 0.85

Test Machine: The extensometer built into the test machine.
Platens Extensometer: An extensometer connected directly to the platens either side of the sample.
Contact Extensometer: An extensometer attached directly to the bone samples surface.
Cond: Condition testing regime, **NDT:** Non-destructive testing regime, **DT:** Destructive testing regime.
Sample Design: L = Length, **D:** Diameter, **S:** Side Length

3.2.1.2 Apparent Ash Density (g cm^{-3})

Measured in the same units as the apparent density, but determined as the ash-weight per unit total sample volume, apparent ash density has the same predictive abilities as apparent density in terms of the bone biomechanics, with T.S. Kaneko et al. (2004) reporting its abilities to account for 79% and 88% of Young's modulus and strength respectively. The Young's modulus results in Table 3.4 show a relationship not dissimilar to that seen in Table 3.2 with the average power function being 1.76 (SD = 0.46) and the power function relationships providing superior correlations than the corresponding linear relationships.

Table 3.4 Linear and power function relationships between apparent ash density (ρ_{ash}) and the Young's Modulus of cancellous bone from the literature.

Reference	Type of Bone		Testing Conditions + Units	A	B	r or r^2 value
Power Function: Young's Modulus = A(Ash Density)^B						
I. Hvid et al. (1989) Test Machine	Prox. Tibia	Cylindrical Cores L = 7.5mm D = 7.5mm	**Cond**: 0.2Hz at 0.01s^{-1} to 0.6% strain **NDT**: 0.2Hz at 0.01s^{-1} between 5N and 0.6% strain **DT**: 5mm min^{-1}, or 0.01s^{-1} **Units:** E: MPa,ρ_{ash}: g cm^{-3}	3473	1.43	r = 0.82
M.J. Ciarelli et al. (1991) Test Machine	Proximal Femur	Cubic S= 8mm	**Cond**: ~40-60% of the Ultimate Load **NDT**: ~1%/s **Units:** E: MPa, ρ_{ash}: g cm^{-3}	n.a.	1.25	r^2 = 0.49
	Distal Femur			n.a.	1.57	r^2 = 0.78
	Proximal Tibia			n.a.	2.10	r^2 = 0.74
	Proximal Humerus			n.a.	0.91	r^2 = 0.73
	Distal Radius			n.a.	1.86	r^2 = 0.91
A. Odgaard and F. Linde (1991) Platens Extens.	Proximal Tibia	Columns 7.0x 6.0 x 6.0mm	**NDT**: Between 3N and 0.8% strain at 0.025 mm min^{-1}, 5.95x10^{-5} s^{-1} **Units:** E: MPa,ρ_{ash}: kg m^{-3}	0.0118	2.10	r = 0.85
Optical Extens.				0.0083	2.21	r = 0.85
T.S. Keller (1994) Test Machine	Human Lumbar Spine	Cubic S = 1cm	**No Cond** **DT**: 5 mm min^{-1} or 0.005 s^{-1} **Units:** E: MPa, ρ_{ash}: g cm^{-3}	1.89	1.92	r^2 = 0.70
	Prox. and Dist. Femur	Cubic S = 0.8cm	**No Cond** **DT**: 4 mm min^{-1} or 0.005 s^{-1}	10.5	2.29	r^2 = 0.85
J.H. Keyak et al. (1994) Platens Extens. SI Direction	Prox. Tibia	Cubic S = 15mm	**Cond**: Between 5N and 0.5% strain **NDT**: 5N to 0.67% strain at 0.15mm s^{-1} **Units**: E: MPa, ρ_{ash}: g cm^{-3}	33900	2.20	r = 0.92
AP Direction				1700	1.11	r = 0.85
ML Direction				7330	2.07	r = 2.07
Mean				11300	1.90	r = 1.90
T.S. Kaneko et al. (2004) Contact Extens. SI Direction	Dist. Femora	Cubic S = 15mm	**NDT**: 0.15mm s^{-1}, 0.001s^{-1} to 0.4% strain **DT**: 0.15mm s^{-1}, 0.001s^{-1} **Units:** σ_{Ult}: MPa ρ_{ash}: mg cm^{-3}	0.161	1.61	r = 0.78
AP Direction				0.0058	2.15	r = 0.84
ML Direction				0.0016	2.30	r = 0.74
Mean Direction				0.031	1.85	r = 0.89
Linear: Young's Modulus (MPa) = A(Ash Density) + B						
I. Hvid et al. (1989) Test Machine	Prox. Tibia	Cylindrical Cores L = 7.5mm D = 7.5mm	**Cond**: 0.2Hz at 0.01s^{-1} to 0.6% strain **NDT**: 0.2Hz at 0.01s^{-1} between 5N and 0.6% strain **DT**: 5mm min^{-1}, or 0.01s^{-1} **Units:** E: MPa, ρ_{ash}: g cm^{-3}	2278	-79.7	r = 0.78

Table 3.4 Continued

Reference	Type of Bone		Testing Conditions + Units	A	B	r or r^2 value
Linear: Young's Modulus (MPa) = A(Ash Density) + B						
M.J. Ciarelli et al. (1991) Test Machine	Proximal Femur	Cubic S= 8mm	**Cond**: ~40-60% of the Ultimate Load **NDT**: ~1%/s **Units:** E: MPa, ρ_{ash}: g cm^{-3}	1992	n.a.	$r^2 = 0.54$
	Distal Femur			1921	n.a.	$r^2 = 0.80$
	Proximal Tibia			1157	n.a.	$r^2 = 0.56$
	Proximal Humerus			1327	n.a.	$r^2 = 0.75$
	Distal Radius			1676	n.a.	$r^2 = 0.91$
E. Lespessailles et al. (1998) Test Machine	Human Calcanei	Cylindrical Cores L = 33.1mm D = 13.1mm	**DT**: 0.027 s^{-1} **Units:** E: MPa, ρ_{ash}: g cm^{-3}	595.49	-27.3	r = 0.78 $r^2 = 0.62$
T.S. Keller (1994) Test Machine	Human Lumbar Spine	Cubic S = 1cm	**No Cond** **DT**: 5 mm min^{-1} or 0.005 s^{-1} **Units:** E: MPa, ρ_{ash}: g cm^{-3}	0.334	-0.0076	$r^2 = 0.552$
	Prox. and Dist. Femur	Cubic S = 0.8cm	**No Cond** **DT**: 4 mm min^{-1} or 0.005 s^{-1}	14.1	-3.25	$r^2 = 0.707$

Test Machine: The extensometer built into the test machine.
Platens Extensometer: An extensometer connected directly to the platens either side of the sample.
Contact Extensometer: An extensometer attached directly to the bone samples surface.
Cond: Condition testing regime, **NDT:** Non-destructive testing regime, **DT:** Destructive testing regime.
Sample Design: L = Length, **D:** Diameter, **S:** Side Length

The strength results (Table 3.5) are also in agreement with those shown previously for apparent density. The power function relationships provide an average power that is virtually identical to that seen with the apparent density (1.88, SD = 0.23), with once again the superior level of correlation being attributed to the power function relationships.

Of the studies reviewed which used apparent ash density not one of them considered the biomechanics of osteoarthritic or osteoporotic bone, with most studies using cadaveric tissue and applying exclusion criteria to ensure that the two conditions were not present in any of the samples tested.

Table 3.5 Linear and power function relationships between apparent ash density (ρ_{ash}) and strength of cancellous bone from the literature.

Reference	Type of Bone		Loading Rate	A	B	r or r^2 value
Power Function: Strength / Ultimate Stress / Max Stress = A(Ash Density)^B						
L. Mosekilde et al. (1987) Test Machine	Lumbar Vertebra L1	Cylindrical Cores L = 5mm D = 7mm	**DT**: 2mm min^{-1} **Units:** σ_{Ult}: MPa, ρ_{ash}: g cm^{-3}	78.2	1.8	r = 0.91
I. Hvid et al. (1989) Test Machine	Prox. Tibia	Cylindrical Cores L = 7.5mm D = 7.5mm	**Cond**: 0.2Hz at 0.01s^{-1} to 0.6% strain **DT**: 5mm min^{-1}, or 0.01s^{-1} **Units:** σ_{Ult}: MPa, ρ_{ash}: g cm^{-3}	70.38	1.596	r = 0.908
T.S. Keller (1994) Test Machine	Human Lumbar Spine	Cubic S = 1cm	**No Cond** **DT**: 5 mm min^{-1} or 0.005 s^{-1} **Units:** σ_{Ult}: MPa, ρ: g cm^{-3}	284	2.27	r^2 = 0.785
	Prox. and Dist. Femur	Cubic S = 0.8cm	**No Cond** **DT**: 4 mm min^{-1} or 0.005 s^{-1}	116	2.03	r^2 = 0.932
J.H. Keyak et al. (1994) Platens Extens. SI Direction	Proximal Tibia	Cubic S = 0.8cm	**Cond**: Between 5N and 0.5% strain **DT**: 0.15mm s^{-1} **Units:** σ_{Ult}: MPa ρ_{ash}: g cm^{-3}	137	1.88	r = 0.956
AP Direction				58.0	1.64	r = 0.962
ML Direction				70.2	2.05	r = 0.894
T.S. Kaneko et al. (2004) Contact Extens.	Distal Femur	Cubic S = 15mm	**DT**: 0.15mm s^{-1} **Units:** σ_{Ult}: MPa ρ_{ash}: mg cm^{-3}	0.00059	1.75	r = 0.941
Linear: Strength / Ultimate Stress / Max Stress = A(Ash Density) + B						
L. Mosekilde et al. (1987) Test Machine	Lumbar Vertebra L1	Cylindrical Cores L = 5mm D = 7mm	**DT**: 2mm min^{-1} **Units:** σ_{Ult}: MPa, ρ_{ash}: g cm^{-3}	0.021	- 1.83	r = 0.69
I. Hvid et al. (1989) Test Machine	Prox. Tibia	Cylindrical Cores L = 7.5mm D = 7.5mm	**Cond**: 0.2Hz at 0.01s^{-1} to 0.6% strain **DT**: 5mm min^{-1}, or 0.01s^{-1} **Units:** σ_{Ult}: MPa, ρ_{ash}: g cm^{-3}	36.19	-1.6	r = 0.884
T.S. Keller (1994) Test Machine	Human Lumbar Spine	Cubic S = 1cm	**No Cond** **DT**: 5 mm min^{-1} or 0.005 s^{-1} **Units:** σ_{Ult}: MPa, ρ: g cm^{-3}	27.5	-0.95	r^2 = 0.736
	Prox. and Dist. Femur	Cubic S = 0.8cm	**No Cond** **DT**: 4 mm min^{-1} or 0.005 s^{-1}	147	-31.0	r^2 = 0.921
E. Lespessailles et al. (1998) Test Machine	Human Calcanei	Cylindrical Cores L = 33.1mm D = 13.1mm	**DT**: 0.027 s^{-1} **Units:** σ_{Ult}: MPa, ρ_{ash}: g cm^{-3}	15.45	-1.17	r = 0.84 r^2 = 0.71

The other mechanical properties such as the yield stress, ultimate strain and the work to failure are all in agreement with those seen in Table 3.6. Both the work to failure (the area under the load deformation curve at failure) and the yield stress are significantly affected by a change in density, with the ultimate strain demonstrating a weak but significant positive correlation.

Table 3.6 Linear and power function relationships between apparent ash density and compressive mechanical properties of cancellous bone from the literature.

Reference	Type of Bone		Loading Rate	A	B	r or r^2 value
Power Function: Yield Stress (MPa) = A(Ash Density (mg cm^{-3}))^B						
T.S. Kaneko et al. (2004) Contact Extens.	Distal Femur	Cubic S = 15mm	**DT**: 0.15mm s^{-1}	0.000831	1.68	r = 0.939
Power Function: Ultimate Strain = A(Ash Density (g cm^{-3}))^B						
I.Hvid et al. (1989) Test Machine	Prox. Tibia	Cylindrical Cores L = 7.5mm D = 7.5mm	**Cond**: 0.2Hz at 0.01s^{-1} to 0.6% strain **DT**: 5mm min^{-1}, or 0.01s^{-1}	0.0282	0.176	r = 0.313
Linear Function: Ultimate Strain = A(Ash Density (g cm^{-3})) + B						
I. Hvid et al. (1989) Test Machine	Prox. Tibia	Cylindrical Cores L = 7.5mm D = 7.5mm	**Cond**: 0.2Hz at 0.01s^{-1} to 0.6% strain **DT**: 5mm min^{-1}, or 0.01s^{-1}	0.02	0.0175	r = 0.255
Power Function: Work to failure (kJ m^{-3}) = A(Ash Density (g cm^{-3}))^B						
I. Hvid et al. (1989) Test Machine	Prox. Tibia	Cylindrical Cores L = 7.5mm D = 7.5mm	**Cond**: 0.2Hz at 0.01s^{-1} to 0.6% strain **DT**: 5mm min^{-1}, or 0.01s^{-1}	1344	1.80	r = 0.906
Linear Function: Work to failure (kJ m^{-3}) = A(Ash Density (g cm^{-3})) + B						
I. Hvid et al. (1989) Test Machine	Prox. Tibia	Cylindrical Cores L = 7.5mm D = 7.5mm	**Cond**: 0.2Hz at 0.01s^{-1} to 0.6% strain **DT**: 5mm min^{-1}, or 0.01s^{-1}	555	-30.95	r = 0.866

3.2.1.3 Bone Mineral Density (BMD)

The determination of BMD is performed using a specialised densitometry system, such as quantitative computed tomography (QCT) or Dual Energy X-ray Absorptiometry (DXA), a system which is used clinically for the determination of bone density in vivo (section 4.4.1). It is of note that BMD determined using DXA is not a volumetric measure, but measures areal density in g cm^{-2}. QCT however, does perform volumetric analysis of density.

Table 3.7 Linear and power function relationships between BMD and the Young's modulus and strength of cancellous bone from the literature.

Reference	Type of Bone	Samp. Design	Test Conditions	A	B	r or r^2 value
Power Function: Young's Modulus = $A(BMD)^B$						
M.J. Ciarelli et al. (1991) Test Machine	Proximal Femur	QCT Cubic S= 8mm	**Cond**: ~40-60% of the Ultimate Load **NDT**: ~1%/s **Units**: E: MPa, ρ: g cm^{-3}		1.10	r^2 =0.87
	Distal Femur				1.21	r^2 =0.79
	Proximal Humerus				0.75	r^2 =0.61
	Distal Radius				1.14	r^2 = 0.90
L. Røhl et al. (1991) Contact Extensometer	Prox.Tibia	QCT Column 9 x 9 x 20mm	**Cond**: Between 2N and 0.2% strain at 0.005 s^{-1} **NDT**: 4 cycles between 2N and 0.2% strain at 0.005 s^{-1} **DT**: 0.005 s^{-1} **Units**: E: MPa, ρ: r_o*	222	11.4	r = 0.80
Linear: Young's Modulus = A(BMD) + B						
M.J. Ciarelli et al. (1991) Test Machine	Proximal Femur	QCT Cubic S= 8mm	**Cond**: ~40-60% of the Ultimate Load **NDT**: ~1%/s **Units**: E: MPa, ρ: g cm^{-3}	1.567		r^2 =0.84
	Distal Femur			1.456		r^2 =0.77
	Proximal Humerus			0.738		r^2 =0.46
	Distal Radius			1.267		r^2 =0.92
P. Augat et al. (1998) Platens Extensometer	Lumbar Spine	QCT Cubic S= 12mm	**Cond**: between 0.001% and 0.1% strain **NDT**: between 5N and 0.4% strain at 0.05s^{-1} **Units**: E: MPa, ρ: g cm^{-3}	1.1	-53	r^2 = 0.82
	Proximal Femur			2.1	-230	r^2 = 0.83
	Distal Femur			0.6	17	r^2 = 0.24
E. Lespessailles et al. (1998) Test Machine	Human Calcanei	DXA Cylindrical Cores L = 33.1mm D = 13.1mm	**DT**: 0.027 s^{-1} **Units**: E: MPa, ρ: g cm^{-2}	558.37	-37.6	r = 0.78 r^2 = 0.61

Table 3.7 Continued

Reference	Type of Bone	Samp. Design	Test Conditions	A	B	r or r^2 value
Linear: Yield Strength (MPa) = A(BMD)+ B						
S.J. Brown et al. (2002) Test Machine	Normal Human Femoral Head	DXA Cylindrical Cores L = 16mm D = 12mm	**DT**: 0.25 mm min^{-1}	1216	- 344	$r^2 = 0.86$
	OA Human Femoral Head			1184	- 381	$r^2 = 0.66$
T.M. Keaveny et al. (1994b) Contact Extensometer	Bovine Proximal Tibia Brass End-caps	QCT Cylindrical Cores L = 40mm D = 8mm Reduced gauge length L = 8mm D = 6mm	**DT**: 0.005 s^{-1} **Units**: $\sigma_{Y.}$: MPa, ρ: gm cm^{-3} Θ	169	-184	$r^2 = 0.66$
S.J. Brown et al. (2002) Test Machine	Normal Human Femoral Head	DXA Cylindrical Cores L = 16mm D = 12mm	**DT**: 0.25 mm min^{-1} **Units**: $\sigma_{Y.}$: MPa, ρ: g cm^{-2}	554	- 101	$r^2 = 0.77$
	OA Human Femoral Head			560	- 144	$r^2 = 0.59$
Linear: Strength (MPa) = A(BMD)+ B						
T.M. Keaveny et al. (1994b) Contact Extensometer	Bovine Proximal Tibia Brass End-caps	QCT Cylindrical Cores L = 40mm D = 8mm Reduced gauge length L = 8mm D = 6mm	**DT**: 0.005 s^{-1} **Units**: $\sigma_{Ult.}$: MPa, ρ: gm cm^{-3} Θ	185	-201	$r^2 = 0.76$
P. Augat et al. (1998) Platens Extensometer	Lumbar Spine	QCT Cubic S= 12mm	**Cond**: between 0.001% and 0.1% strain **NDT**: between 5N and 0.4% strain at 0.05s^{-1} **Units**: $\sigma_{Ult.}$: MPa, ρ: g cm^{-3}	0.019	-0.9	$r^2 = 0.91$
	Proximal Femur			0.037	-3.9	$r^2 = 0.80$
	Distal Femur			0.022	-1.4	$r^2 = 0.54$
E. Lespessailles et al. (1998) Test Machine	Human Calcanei	DXA Cylindrical Cores L = 33.1mm D = 13.1mm	**DT**: 0.027 s^{-1} **Units**: σ_{Ult}: MPa, ρ: mg cm^{-2}	15.2	-1.68	r = 0.86 $r^2 = 0.75$
Power: Strength = $A(BMD)^B$						
L. Røhl et al. (1991) Contact Extensometer	Prox.Tibia	QCT Column 9 x 9 x 20mm	**Cond**: Between 2N and 0.2% strain at 0.005 s^{-1} **NDT**: 4 cycles between 2N and 0.2% strain at 0.005 s^{-1} **DT**: 0.005 s^{-1} **Units:** σ_{Ult} : MPa, ρ: r_o*	1.2	12.2	r = 0.88

* r_o is the relative linear attenuation coefficient, Θ gm cm^{-3} converted from g ml^{-1} of $K_2 PO_4$

With the number of studies for each relationship being minimal, and with differences in the test methods and bone sources, it is difficult to visualise any links with the previous results or to compare directly the regressions between studies, but the

relationships between BMD with the Young's modulus and the strength are of the same magnitude and the correlations are comparable to those achieved for both the apparent ash density and the apparent density. The exception to the rule is the study by L. Røhl et al. (1991) which displayed a far higher power than the other studies for both strength and modulus, due to the use of relative linear attenuation coefficient (r_o) instead of a volumetric density link BMD.

Of the three different density measures, apparent density, apparent ash density and BMD, the basic relationship outlined originally for the modulus and strength, that they relate with a power function of ~2 for normal bone, is well proven. However only three studies (T.M. Keaveny et al., 1997; B. Li & R.M. Aspden, 1997b; S.J. Brown et al., 2002) out of the numerous studies which were reviewed, attempted any mechanical testing of bone from osteoporotic or osteoarthritic individuals. When one considers that L.J. Gibson, (1985) and D.R. Carter and W.C. Hayes (1977) demonstrated a change in the structure occurs at a density of 0.35g cm^{-3}, which is coupled with a change in the mode of deformation, it is feasible that the extrapolation of the current power function relationships might not provide the correct fit for the results at the extremes of density seen in osteoporosis and osteoarthritis. It is also of note that the composition of bone in these conditions is also affected (Section 4.3) and, as such, the investigation of the effects of composition on the mechanics of the bone is also important.

3.2.1.4 Composition

The information in the literature with reference to the relationships between the composition of the bone, namely the mineral and organic contents and the mechanics of the bone is less well documented. The study by A. Nafei et al. (2000) does, however, attribute 80 % of the variation in the Young's modulus of ovine trabecular bone to the

bone mineral content, with 84 % of the variation in Young's modulus and 81% of the variation in strength explainable by the collagen content of the bone.

The effect of the mineral content or the degree of mineralization has varied depending on the mechanical testing performed and the type of bone under investigation. J.D. Currey (1969) demonstrated that for cortical bone, both the strength and the modulus of elasticity in three-point bending were positively related to the mineral content, but in relation to the modulus of impact (impact energy normalised for the sample area), a definitive peak of about 66.5% ash content was optimal.

The relationship between the mineral content (I. Hvid et al., 1985) and the degree of mineralization (DMB) (H. Follet et al., 2004), with mechanical parameters from compressive testing, have both been investigated with relation to cancellous bone. I. Hvid et al., (1985) demonstrated that there was a significant linear relationship between the mineral content and a number of the compressive mechanical parameters, the yield strength ($r = 0.892$), the ultimate strength ($r = 0.915$), Elastic Modulus ($r = 0.819$), Ultimate Energy ($r = 0.792$) and the yield energy ($r = 0.727$), but that the mineral content failed to affect the strain at which the samples yielded or failed. The DMB results presented by H. Follet et al., (2004) were relatively similar to those seen for mineral content with positive relationships between modulus ($r^2 = 0.69$), strength ($r^2 = 0.69$) and work to fracture ($r^2 = 0.43$), but the effects of DMB on strain were not included. The findings clearly show that an increase in mineralization results in an increase in the modulus, strength and work to fracture of bone.

The volume of collagen in the tissue, the amount of cross-linking and the stability of the network within the bone matrix varies between the different types of tissue and the age of the donor. There are four studies which have investigated the

effects of the collagen network and levels of cross-linking on cortical bone tissue. Two of the studies (P. Zioupos et al., 1999, X. Wang et al., 2001) utilised heat denaturation as a method of investigating the stability of the collagen network, and the effects of a reduction in stability on the mechanics. Both studies demonstrated that in three-point bending the effects of the collagen network on modulus were non-significant; however, P. Zioupos et al. (1999) also found no significant link with strength, which was in contrast to X. Wang et al. (2001) who demonstrated a negative effect on the yield and ultimate strength as well as the work of fracture. The studies on cortical bone with respect to the individual cross-links have mainly focused on the mature cross-links such as pyridinoline and pentosidine. Once again, P. Zioupos et al. (1999) found that the levels of the cross-link pyridinoline were positively related with the modulus ($r = 0.40$) and strength ($r = 0.46$) in three-point bending, but not significantly. The study by P. Garnero et al. (2005) was in disagreement with the trends of this study and found that the modulus and yield strength in bending were significantly and negatively affected ($r = -0.41$ and -0.55 respectively), as well as showing that pyridinoline was also significantly correlated with the modulus ($r = -0.40$), yield strength ($r = -0.57$), ultimate strength ($r = -0.45$) and the post-yield energy absorption ($r = 0.45$) when tested in compression. With respect to the levels of pentosidine both P. Garnero et al. (2005) and X. Wang et al. (2002) were in agreement that the effects were significant and negative in nature with respect to the yield strength in bending but not modulus. The work to failure results were in contrast, X. Wang et al. (2002) showed the relationship to be significant but negative with respect to the three point bending, whereas it was significant and positive when tested in compression (P. Garnero et al., 2005). The compressive yield and ultimate strength were also found to be negatively correlated (P.

Garnero et al. 2005). It is clear from these results that the integrity and the degree of cross-linking in cortical bone has a significant effect on the biomechanics of the tissue, with different effects depending on the loading applied.

Whilst the previous studies all focused on cortical bone, the effects of cancellous bone have also been investigated in two further studies. The first study by A.J. Bailey et al. (1999) focused mainly on the relationship between the percentage of collagen content with respect to the mechanics and found that the content affected the ultimate stress (female r = 0.71, male r = 0.68), modulus (female r = 0.69, male r = 0.60) and work to failure (female r = 0.63, male r = 0.67). The second study X. Banse et al. (2002b) investigated both the percentage collagen content and the individual cross-links within the tissue, and demonstrated that unlike the previous study on the modulus, the vertebral tissue was affected by the percentage of collagen (r = 0.26). The individual cross-links that were investigated correlated poorly with the mechanical parameters, with only the levels of OHPyr and Lys-Pyr correlating with ultimate strain (r = 0.37 and 0.39 respectively). As with the results for the cortical bone, it is clear that the collagen content and the degree of cross-linking with cancellous bone are important parameters for the mechanical competence of the bone.

This section of the literature review has demonstrated that apparent density is highly important for the mechanics of cancellous bone tissue, but that apparent density alone can not explain the differences seen in the mechanics of the tissue. Other factors such as the degree of mineralization, the organic content and the cross-linking of the collagen network all have effects which should not be ignored, and in particular when considering bone conditions such as osteoporosis and osteoarthritis where all of these possible variables are affected. This is even more important when considering the

normal use of these results is for the basis of FEA models, upon which prosthesis design and other medical devices can be based. If osteoporotic and osteoarthritic bone have distinctly different mechanical properties it might be necessary to provide prosthesis specific to the condition of the bone, to prevent stress-shielding and other side effects of prosthesis insertion. It is also important when considering potential preventative therapies, as the predominant aim of most therapies at the moment is based on the maintenance of bone density, with little consideration given to the integrity and maintenance of the collagen network which provides a discernable percentage explanation of the bone mechanics. One of the aims of this study is to try and ensure that all these different variables are taken into consideration during the analysis of the compression testing results to show that, although apparent density may be the dominant variable, other variables play crucial roles in the mechanics of cancellous bone.

3.2.1.5 Sources of Irregularity in Compression Testing

The sources of irregularity with the compression testing of cancellous bone are high and not surprisingly are generated from the sample design, the test rig, the method of data collection and the actual bone itself.

Bone Related Errors

The density of the bone has already been discussed as having a big effect on the mechanics of cancellous bone, but the structure of the cancellous bone is of importance too. In many cases, the structure of the cancellous bone is highly orientated so as to manage with the normal physiological loading condition imparted upon it,

which leads to anisotropy within the material, with different properties in different directions.

The level of anisotropy within the material is noted in a number of studies, such as J.H. Keyak et al. (1994), M. Ding et al. (1997), H. Sugita et al. (1999) and T.S. Kaneko et al. (2004) but not quantified. Other studies have provided a quantitative value for the level of anisotropy; E.B.W. Giesen et al. (2001) showed that within the mandibular condyles, the bone orientated in the axial direction was 3.4 times stiffer and 2.8 times stronger than a sample orientated in the transverse direction. M.J. Ciarelli et al. (1991) tested bone from a number of different sites; the results showed that a sample orientated in the superior-inferior direction was 2.5 times greater than that of a sample in the anterior posterior direction, which was in turn 1.45 times greater than one in the medial-lateral direction.

Other studies have utilised the anisotropy ratio, or the result of dividing the mechanical result from one direction to another. M.-C. Hobatho et al. (1997) tested a wide range of bone samples from 6 different skeletal sources and demonstrated that for the group as a whole the anisotropy ranged between ~2 and ~4, with the more load bearing sites having a greater anisotropy ratio (proximal tibia, 4.22) than that of non-load bearing sites (proximal humerus, 1.80). This study is closely supported by two further studies; L. Mosekilde et al. (1985) investigated thoracic and lumbar vertebrae as well as samples from the iliac crest and showed an anisotropy ratio of between 2.95 and 4.19 for the lumbar vertebrae, but only 1.31-1.40 for the iliac crest samples; while F. Linde et al. (1990) tested samples from the proximal tibia and found an anisotropy ratio of 3.7. The final study that provided any anisotropy ratio values was P. Augat et al. (1998) who assessed both the distal femur and the lumbar spine and found anisotropy

ratios as high as 10.3 and 8.7 respectively, but the average was closer to those shown previously ranging form 0.3 to 3.5 for the proximal femur and 0.4 to 2.7 for the lumbar spine, depending on the orientations which were being compared.

In addition to the anisotropy ratio, the site the sample was taken from is important as studies by R.L. Wixson et al., (1989), M.Ding et al. (1997) show that variation can occur from one area of the proximal tibia to another, and C.M. Schoenfeld et al. (1974), and S.J. Brown et al. (2002) showed that variation in density and mechanical properties can occur within the same femoral head.

These irregularities go some way towards explaining the variation within the regressions seen previously, but highlight the importance of sample orientation and sampling site when preparing test samples.

Sample Design

As can be seen from Table 3.2 to Table 3.7 the two main sample designs are either cylinders or cubes of bone, both of which have their own advantages. The cubes allow for non-destructive testing to be performed in all three orthogonal directions on the same sample, but they require a great deal more time and effort to prepare. The cylinders on the other hand are simple to manufacture using a core drill, but they are unidirectional. The opinion within the literature is mixed, with the two main research groups differing slightly. F. Linde et al. (1992) recommended a 6.5mm cube or a cylinder with a diameter of 7.5mm and a length of 6.5mm; after extensive testing with a number of different sample designs (Table 3.2). T.M. Keaveny et al. (1993) recommended a cylindrical specimen design but with a length to diameter ratio of 2:1. The design of the samples from previous studies is, however, variable as certain sample designs and sizes are restricted by the bone source.

Testing Errors

As the testing rigs have advanced in design and new miniature extensometers have become available, the output from compression tests has come under scrutiny and the reasons behind experimental error have been investigated.

Testing Machine Compliance

The original method for performing a compression test involved the insertion of a sample between two loading platens and the subsequent applied load and deflection of the sample recorded via the testing machine. It was, however, noted early on that the testing machine had a compliance of its own, which was corrected initially by simply compressing the loading platens together and adjusting the results accordingly. With the advent of new extensometers, it is now possible to either monitor the exact position of the platens, or to attach them directly to the sample removing the problems of testing machine compliance. The use of a contact or optical extensometer, which removes the testing machine compliance, provided significantly greater values for the Young's modulus and in many cases reduced yield and ultimate strain values, over and above the errors of the machine compliance (A. Odgaard and F. Linde, 1991; T.M. Keaveny et al., 1997)

End-Artifacts

Sources of difference come from what are now commonly known as 'end-artifacts', which were reviewed and investigated by T.M. Keaveny et al. (1997). End-artifacts are related to the interaction between the ends of the compression sample and the loading platens. Most compression testing is performed on samples removed from

within a larger bone network and as such the outer trabeculae may have lost a number of supporting network links. These weaker outer trabeculae will deform more easily than would normally be expected and can lead to irregular loading of the sample between the platens. The solution to the problem was to immobilise the end of the sample, F. Linde and I. Hvid (1989) investigated a number of different methods including cementing the sample ends to immobilise the loose trabeculae and even cementing the samples to the loading platens. Both methods had dramatic effects on the mechanical properties, with increases up to 40% in the stiffness and a reduction in energy dissipation of 67% relative to the unconstrained conditions.

One of the most commonly used methods involves the gluing of the ends of cylindrical samples into brass end-caps, so as to provide not only mechanical support for the loose trabeculae, but also a solid point for the loading of the sample (T.M. Keaveny et al. 1997, D.L. Kopperdahl & T.M. Keaveny, 1998, E.F. Morgan et al., 2003). This technique is, however, time consuming and expensive as each sample must be individually set into the end-caps, so much testing is still performed directly between the platens. F. Linde and I. Hvid, (1989) also investigated the interaction between the platens and the sample ends, in order to increase the sample ends' freedom to move relative to the platens during loading. The study demonstrated that samples with the freedom move beneath the platens, due to either polishing or the addition of a lubricant, exhibited a significantly reduced stiffness and energy dissipation compared with unpolished platens.

The best method to avoid all these possible experimental sources of error is to use a contact extensometer, which will exclude these end effects as only the portion within the gauge length of the extensometer will be assessed for deflection.

Loading Rate or Testing Conditions

The strain rate to which a sample is subjected is an important consideration in testing as it can affect both the Young's modulus and strength of the sample. There are two main studies within the literature which have investigated the effects of strain rate. The first was by D.R. Carter and W.C. Hayes (1977) who demonstrated that both strength and modulus were affected by strain rate raised to the power 0.06. The testing was, however, performed on bone samples measuring 5mm in length and 20mm in diameter (a length to diameter ratio of 0.25), dramatically different to any sample design used in Table 3.2 to Table 3.7 or that which was recommended by F. Linde et al. (1992) or T.M. Keaveny et al. (1993). The more recent study was performed by F. Linde et al. (1991) used 8.25mm long and 5.5mm diameter bone cores (L / D ratio 1.5:1), which were destructively tested at 6 different strain rates. Due to the significant effects that apparent density has, the resultant equations included both density and strain rate and, despite using a better recognised sample design and a more up to date testing rig, the resultant powers were 0.07 for strength and 0.05 for Young's modulus, showing very little difference to the earlier work. The authors were, however, quick to note that the strain rate effects seen were over a wide range, and that the normal range of strain rates between 10^{-3} and 10^{-2} provide very little variation in the results compared to other factors, but is an important consideration when comparing studies and when planning a testing regime.

3.2.2 Tensile Testing

Despite the tensile test being the industry preferred method for the determination of materials' properties, the nature of human cancellous bone makes the preparation and testing of standard test samples difficult. That said, a number of different research methods have been developed to investigate the tensile properties. S.L. Kaplan et al. (1985) used individually lathed cylindrical cores and specialised grips, while R.B. Ashman et al. (1989) glued rectangular samples to the loading grips; L. Røhl et al. (1991) impregnated the sample ends with resin to provide a more solid structure for the test rig to grip, or by using the same technique as in the compression testing, of gluing the sample ends into specially made brass end-caps (D.L. Kopperdahl and T.M. Keaveny, 1998, E.F. Morgan and T.M. Keaveny, 2001).

The results of the studies that used tensile testing demonstrated that the tensile mechanical parameters were affected by many of the same variables as the compression testing parameters, although the volume of studies to draw information from is reduced. The results of the studies that are available with relation to the density are shown in Table 3.8.

Table 3.8 Tensile mechanical properties and their relationships with density from within the literature

Reference	Type of Bone	Sample Design	Testing Conditions	A	B	r or r^2 value	A	B	r or r^2 value
				Linear Relationship			Power Function		
Young's Modulus									
R.B. Ashman et al. 1987 **Units**: E: MPa ρ: kg m^{-3}	Bovine Femora	Column Specimens 5mm x 5mm x 20mm Sample ends impregnated with PMMA for mechanical support	8mm gauge length contact extensometer, testing performed at a strain rate of 10^{-4} s^{-1}	6.31	-1647	$r^2 = 0.42$	0.00002	2.91	$r^2 = 0.66$
L. Røhl et al. (1991) **Units:** E : MPa, ρ: r_o*	Human Proximal Tibia	Column Specimens 9mm x 9mm x 20mm Sample ends impregnated with epoxy resin for mechanical support	QCT determined density (BMD) 9mm gauge length contact extensometer, testing performed at 0.005 s^{-1}	-	-	-	228	11.1	r = 0.80
Yield Stress									
T.M. Keaveny et al. (1994b) **Units**: σ_Y: MPa ρ: gm cm^{-3} $	Bovine Proximal Tibia	Cylindrical Cores: L = 40mm, D = 8mm Sample ends glued into Brass End-caps Reduced gauge length: L = 8mm, D = 6mm	QCT determined density (BMD) 5mm gauge length contact extensometer Tested to failure at 0.005 s^{-1}	78.9	-78.8	$r^2 = 0.71$	-	-	-
D.L. Kopperdahl & T.M. Keaveny (1998) **Units**: σ_Y: MPa ρ: g cm^{-3}	Human Lumbar Spine	Cylindrical Cores L = 25mm, D = 8mm Brass End-Caps	5mm gauge length contact extensometer Non-destructively tested between ±0.1% strain at 0.005 s^{-1} Tested to failure at 0.005 s^{-1}	10.1	-	$r^2 = 0.51$	10	1.04	$r^2 = 0.51$
E.F, Morgan & T.M. Keaveny, (2001) **Units**: σ_Y: MPa ρ: g cm^{-3}	Vertebra (T10 – L5)	Human Tissue Cylindrical Cores L = 25mm, D = 8mm Sample Ends glued into Brass end-caps	Platens extensometer and a 5mm gauge length contact extensometer Conditioned for 3 cycles to 0.1% strain Non-destructively tested at 0.005 s^{-1} tested to the yield point	-	-	-	21.7	1.52	$r^2 = 0.53$
	Prox. Tibia			-	-	-	52.9	1.77	$r^2 = 0.81$
	Greater Trochanter			-	-	-	50.1	2.04	$r^2 = 0.60$
	Femoral Neck			-	-	-	22.6	1.26	$r^2 = 0.84$

Table 3.8 Continued

Reference	Type of Bone	Sample Design	Testing Conditions	A	B	r or r^2 value	A	B	r or r^2 value
				Linear Relationship			Power Function		
Strength									
L. Røhl et al. (1991) **Units:** σ_{Ult} : MPa, ρ: r_o *	Human Proximal Tibia	Column Specimens 9mm x 9mm x 20mm Sample ends impregnated with epoxy resin for mechanical support	QCT determined density (BMD) 9mm gauge length contact extensometer, testing performed at 0.005 s^{-1}	-	-	-	1.6	10.7	r = 0.78
S.J. Kaplan et al. (1985) **Units**: σ_{Ult} : MPa, ρ: g cm^{-3}	Bovine Humeri	Cylindrical Cores: L = 30mm, D =14mm Reduced Gauge length L = 7mm, D = 5mm	Tested to failure at 0.01 s^{-1}	-	-	-	14.5	1.71	r^2 = 0.68
T.M. Keaveny et al. (1994b) **Units**: $\sigma_{Ult.}$: MPa ρ: gm cm^{-3} $	Bovine Proximal Tibia	Cylindrical Cores: L = 40mm, D = 8mm Sample ends glued into Brass End-caps Reduced gauge length L = 8mm, D = 6mm	QCT determined density (BMD) 5mm gauge length contact extensometer Tested to failure at 0.005 s^{-1}	76.9	-77.8	r^2 = 0.66	-	-	-
D.L. Kopperdahl & T.M. Keaveny (1998) **Units**: σ_Y: MPa ρ: g cm^{-3}	Human Lumbar Spine	Cylindrical Cores L = 25mm, D = 8mm Brass End-Caps	5mm gauge length contact extensometer Non-destructively tested between ±0.1% strain at 0.005 s^{-1} Tested to failure at 0.005 s^{-1}	13.2	-	r^2 = 0.47	13.3	1.07	r^2 = 0.47
Energy Absorption to Failure									
L. Røhl et al. (1991) **Units**: EA: kJ m^{-3} ρ: r_o *	Human Proximal Tibia	Column Specimens 9mm x 9mm x 20mm Sample ends impregnated with epoxy resin for mechanical support	9mm gauge length contact extensometer, testing performed at 0.005 s^{-1}	-	-	-	23.6	9.0	r = 0.58

$ gm cm^{-3} converted from g ml^{-1} of $K_2 PO_4$ * r_o is the relative linear attenuation coefficient

3.2.3 Compression vs. Tension

A number of comparative studies have been performed to investigate the relationship between the tensile and compressive properties of cancellous bone. In four (L. Røhl et al., 1991; T.M. Keaveny et al., 1994b; D.L. Kopperdahl & T.M. Keaveny, 1998; E.F. Morgan & T.M. Keaveny, 2001) studies, the Young's modulus in tension was not significantly different from the compressive modulus, although a study by T.M. Keaveny et al. (1994a) showed a significantly reduced modulus in tension, but only after a number of non-destructive tests; the modulus was not significantly different during the early stages of the test cycles.

Results in relation to the yield and ultimate stress are mixed although the study by L. Røhl et al., (1991) found that the tensile strength was significantly higher than the corresponding compressive results. Two of the studies (D.L. Kopperdahl & T.M. Keaveny, 1998; E.F. Morgan & T.M. Keaveny, 2001) were unable to find any statistically significant differences between the results in either loading mode. Whilst the study by E.F. Morgan & T.M. Keaveny, (2001) tested a number of different sites, and samples from the femoral neck did display a significant difference with the tensile yield strength being lower in tension than compression, the trend seen in the other sites failed to reach significance. This trend of the yield and ultimate strength being lower in tension than in compression was statistically significant in the studies by S.J. Kaplan et al. (1985) and T.M. Keaveny et al., (1994a,b) with, in most cases, the tensile yield and ultimate strengths being in the region of 70% of the compressive ones.

Yield and ultimate strains were also investigated; the study by L. Røhl et al., (1991) indicates a higher ultimate strain in tension than in compression, but the larger volume of studies (T.M. Keaveny et al., 1994b; D.L. Kopperdahl & T.M. Keaveny,

1998; E.F. Morgan & T.M. Keaveny, 2001) demonstrated that the yield strains in tension were significantly lower in compression, with the strains mimicking the stress values and being 70% of the compressive values.

The majority of the comparative studies suggest that the mechanical properties of cancellous bone are significantly better in compression than in tension, as would be expected due to the natural physiological loading conditions to which bone is subjected. These results will be important later in this thesis when the validity of the fracture toughness results are investigated (section 6.3.2.1 and 8.7.2.1).

3.2.4 Fracture Toughness Testing

The fracture toughness of bone has only been investigated in relation to cortical bone, and in this respect the subject has been extensively researched. There is, however, no data within the literature for any aspects of the fracture toughness of cancellous bone, and with this in mind it highlights the novel aspects of the present study.

Although investigation of the fracture toughness of cancellous bone has not been performed, it is a cellular solid and fracture toughness testing has been performed on other cellular solids or, in some cases, the effects have been investigated using computer modelling and simulations.

3.2.4.1 Fracture toughness simulations

The first problem with performing any simulation is one that was presented as a confounding factor for the testing of cancellous bone (section 3.2.1), and that is the different structures, either closed or open cell foams, deform differently. For example,

in compression the closed cell foam with planar walls would be expected to adhere to equation 3.3 for modulus and equation 3.4 for yield strength; in contrast an open cell foam would be more likely to adhere to equation 3.5 for modulus and equation 3.6 for yield strength. (S.K. Maiti et al. 1984; L.J. Gibson and M.F. Ashby, 1997b; H. Bart-Smith et al., 1998; E. Andrews et al. 1999; L.J. Gibson, 2005)

$$E^*/E_S = 0.35\rho$$ **Equation 3.3** Modulus prediction for closed cell foams

$$\sigma^*/\sigma_{YS} \approx 0.3\rho$$ **Equation 3.4** Yield strength prediction for closed cell foams

$$\frac{E^*}{E_S} = \left(\frac{\rho^*}{\rho_S}\right)^2$$ **Equation 3.5** Modulus prediction for open cell foams

$$\frac{\sigma^*_{pl}}{\sigma_{ys}} = C_2\left(\frac{\rho^*}{\rho_S}\right)^{3/2}$$ **Equation 3.6** Yield strength prediction for open cell foams

Where E is the Young's modulus, σ^*_{PL} is the yield strength, ρ^* is the density of the cellular solid, E_S is the modulus, σ_{YS} the yield strength and ρ_S is the density of the cell wall material.

For the determination of fracture toughness the modelling becomes far more complex, especially when considered in 3D. Although some studies which mechanically tested the fracture toughness of cellular solids preceded the paper by S.K. Maiti et al. (1984), it was the first within the literature to characterise the effects of loading on a cellular solid with respect to the fracture toughness and its relationship with density. The paper provided full derivations of the resultant equations for the effects of density on an open cell (equation 3.7) and a closed cell (equation 3.8) brittle cellular solid.

$$K_{IC} \propto \left(\frac{\rho}{\rho_S}\right)^{3/2}$$ **Equation 3.7** Fracture toughness of an open cell cellular solid

$$K_{IC} = \left(\frac{\rho}{\rho_S}\right)^2$$ **Equation 3.8** Fracture Toughness of a closed cell cellular solid

The study does, however, point out that the nature of the closed cell foam means that it is more likely to behave like an open cell foam as most of the material is found not in the cell walls but at the cell edges as in an open cell foam. With this in mind, the authors remodelled the relationship between the fracture toughness and density to provide equation 3.9.

$$K_{IC} = c\sigma_f \sqrt{\pi l}\left(\frac{\rho}{\rho_S}\right)^{3/2} \qquad \textbf{Equation 3.9}$$

Where c is a constant, given in the study as 0.65, σ_f is the tensile fracture stress of the cell wall material and l is the cell size. This equation provides an insight into the potential fracture toughness values of a brittle cellular solid, but in doing so it has an inherent problem when being applied to the fracture toughness of a natural cellular solid such as cancellous bone. The equation includes the parameter 'l' which relates to the cell size of the uniform structure of the cellular solid, a parameter which in cancellous bone will vary substantially within the same sample, regardless of the density, although clearly increasing as the porosity increases.

Having noted that the cell size of the cellular solid is a confounding factor, the study by R. Benzy and D.J. Green (1990), found that the fracture toughness of a cellular solid was in fact not affected by the cell size but by the struts which made up the cell walls, and the effect came from the reduction in the toughness and geometry of the cell wall struts with increasing cell size rather than the cell sizes themselves. However by viewing figure 2.2b it can be seen that the cell wall struts and the cell size both vary within cancellous bone. The second confounding factor in using these previous equations is that they were modelled on a brittle cellular solid, and cancellous bone is somewhat viscoelastic (F. Linde, 1994), which certainly affects the mode of

deformation seen in the cell wall struts, and therefore the fracture mechanics of the solid, rendering these previous equations mere guidelines for what might occur when testing cancellous bone.

The determination of the fracture toughness of cellular solids has been performed previously on metallic foams and a naturally occurring cellular solid, wood. In each case the determination of K_{IC} followed the guidelines laid out in ASTM Standard E 399-90 which are shown in section 6.2.1 of this study, but in a number of studies (J.S Huang and L.J. Gibson, 1991a,b; J.S. Huang and M.S. Chiang, 1996) one crucial difference was inserted. The ASTM standard recommends the selection of a point (P_Q) from the load deformation curve using the intersection between a 95% secant line to the linear portion of the loading curve and the original loading curve; the studies in question did not use this point, instead they opted for the critical load.

The results within the literature for the relationships between the relative density of the cellular solids and their fracture toughness are few and far between as the metallic foams, on which a number of the studies were performed, are reproducible engineering materials; they have a fixed density and pore size and as such the studies provide a single K_{IC} result for the material. Of the studies which have presented their results with respect to relative density, K.Y.G. McCullough et al. (1999) provided two separate equations for both the J-Integral and the K_{IC} of an aluminium foam (equations 2.10 to 2.13).

	K_{IC}	Equation No.	J-Integral	Equation No.
Inferred Crack Length	$K_{IC} = 22\overline{\rho}^{-1.69}$	**Equation 3. 10**	$J_{IC} = 10\overline{\rho}^{-1.60}$	**Equation 3.11**
Zero Traction Crack Length	$K_{IC} = 41\overline{\rho}^{-1.65}$	**Equation 3.12**	$J_{IC} = 37\overline{\rho}^{-1.52}$	**Equation 3.13**

The inferred crack length refers to the crack length measured using a travelling microscope as the point where the crack tip can be seen. The zero traction crack tip refers to the point where the two sides of the crack are no longer bridged or connected by any material. In both cases the power function of the relationships is between 1.5 and 1.7. The results of the fracture toughness testing on wood were presented by L.J. Gibson and M.F. Ashby, (1997c), but with wood being anisotropic like cancellous bone, the equations are provided for two different loading directions (equations 3.14 and 3.15)

$$K_{IC} = 1.8\left(\frac{\rho^*}{\rho_S}\right)^{3/2}$$ **Equation 3.14** The fracture toughness of wood along the grain

$$K_{IC} = 20\left(\frac{\rho^*}{\rho_S}\right)^{3/2}$$ **Equation 3.15** The fracture toughness of wood across the grain

In both cases it is only the initial value which changes, not the power function, which stands at 3/2 or 1.5, similar to that of the metallic foam. The relationships for K_{IC} and what is seen for the compressive mechanical properties are not strictly comparable, as the density used in these equations is the relative density and not the apparent density used in compressive studies. As mentioned previously, however, the fracture toughness of cancellous bone has never been previously published, although L.J. Gibson and M.F. Ashby (1997a) stated that:

'Work is needed to elucidate the way in which fracture toughness varies with structure and density (experience with foams suggests a dependence on density to a power of between 1 and 2).'

As such, this study has set out to test this hypothesis. Although the dependence of the fracture toughness of cancellous bone would appear to be focused on the relationship with density, testing of cortical bone has highlighted the importance of the composition (mineral content) of the bone with respect to its toughness. J.D. Currey et

al. (1996) demonstrated that the impact energy and the work of fracture were both significantly related to the ash content (%) with the higher ash contents reducing both of the energy values, and explaining as much as 53% of the variation in work of fracture and 52 % of the impact energy. The studies which have investigated the effects of collagen cross-linking on the fracture toughness of cortical bone, demonstrated that the levels of pentosidine were negatively correlated ($r = -0.48$) with K_{IC} (X. Wang et al., 2002), but the levels of pyridinoline were positively but not significantly linked to K_{IC}, the J-Integral and the work of fracture (P. Zioupos et al. 1999). The actual structural integrity of the collagen network was, however, of significant note with highly significant correlations with K_{IC} ($r = 0.65$), the J-Integral ($r = 0.86$) and the work of fracture ($r = 0.83$) (P. Zioupos et al. 1999). This is important with respect to this study as one of the bone sources is from individuals with osteoarthritis, which is a condition known to affect the mineralization of the bone (section 4.3).

With there being no work within the literature on the fracture toughness of cancellous bone, it is clearly of interest to know how K_{IC}, the J-integral and G_{IC} will change with density and mineral content in relation to some rudimentary conditions. Osteoporosis is our main interest, but normal cancellous bone and osteoarthritic bone provide the opportunity to see the effects of a range of variables with relation to the fracture toughness of cancellous bone, and will enable a better understanding of the mechanical failures seen in osteoporotic cancellous bone.

Concluding Remarks

This literature review on the biomechanics of cancellous bone has demonstrated that the compressive biomechanical properties of cancellous bone have been extensively researched, together with possible error sources and specific aspects of the compressive behaviour of cancellous bone. It also shows that the vast majority of the work is based on the study of cancellous bone which, for all intents and purposes, can be considered 'normal', or more specifically free from any conditions which might have affected the results. One of the aspects of this study is the investigation of bone from osteoporotic and osteoarthritic individuals whose cancellous bone can be considered to have apparent densities and compositions that are at opposite ends of the ranges for human cancellous bone tissue.

In addition to the compressive mechanical properties, this chapter also highlights the hole within the literature which is the lack of fracture toughness testing of cancellous bone. Cellular solids like cancellous bone, namely wood and engineering metallic foams, have been researched and their properties modelled in previous studies. However, only assumptions have been provided as to the nature of the fracture toughness properties of cancellous bone. The most important hypothesis, the proving of which forms one of the study aims, is the L.J. Gibson and M.F. Ashby (1997a) statement that the fracture toughness will be dependent on apparent density to the power of between 1 and 2. However, seeing as the literature contains no information at all on the fracture toughness of cancellous bone, it is of interest to investigate as many as possible of the independent variables for the fracture toughness of cancellous bone.

As the only sources of human bone within the study will be from osteoarthritic and osteoporotic fractured neck of femur individuals, it is important to review and understand the effects these conditions are known to have on the cancellous bone material, and to review the modes of diagnosis with respect to their determination of the biomechanics of the bone.

Chapter 4: Bone Conditions

4.1 Osteoporosis

4.1.1 Incidence and Scale of the Problem

Osteoporosis is a condition that affects millions of people world wide. The National Osteoporosis Society (NOS) estimates that in the UK alone 3 million people suffer from osteoporosis, couple this with the National Osteoporosis Foundation figures of 7.8 million people living in America suffering from osteoporosis and the prevalence of the disease is startling.

The burden of the disease is also vast; the NOS currently reports that 1 in 3 women and 1 in 12 men will suffer from a fracture over the age of 50, which is not only traumatic and debilitating for the individual, but the cost of treatment and care in the UK, because of osteoporosis, is estimated at over £1.7 billion each year. The incidence and impact of osteoporosis varies depending on factors such as race and geographic origin, with members of the Scandinavian population showing a significantly higher rate of fracture than individuals from other areas of Europe (A.A. Ismail et al., 2002) and around the world. (J. Chalmers and K.C. Ho, 1970)

4.1.2 Definition

Osteoporosis is characterised by a loss in the density and structural integrity of the cancellous bone, a thinning of the trabeculae and an increase in the porosity of the cortical bone. The result of these changes is a reduction in the mechanical competence of the remaining bone structure, leading to an increased risk of low trauma fracture, or

fragility fractures, which generally occur in areas of load bearing cancellous bone such as the spine or the proximal femur.

Osteoporosis can be split into two categories, primary or secondary osteoporosis. Primary osteoporosis relates to osteoporosis that is caused by natural occurrences such as aging and the menopause, and is divided into type I, type II or idiopathic osteoporosis.

4.1.3 Primary Osteoporosis

Type I or Postmenopausal Osteoporosis

Type I primary osteoporosis occurs in women during and after the menopause. The rate of bone loss in women is roughly 0.5% per year, after the achievement of peak bone mass (C.M. Bono and T.A. Einhorn, 2003). However the onset of the menopause and the cessation of oestrogen production causes a dramatic imbalance, over and above that already occurring because of age, and bone loss post menopause can be at a rate of up to 6%, (B.L. Riggs and L.J. Melton, 1986, 1992), although is on average 2% per year (C. Christiansen, 1995). This is of particular importance in those individuals that failed to achieve a high peak bone mass, where a small loss of bone constitutes a large percentage of their skeletal tissue, and can result in an individual suffering from osteoporosis at a younger age than they previously might.

Type II or Age-Related Osteoporosis

This relates to the natural loss of bone tissue that occurs with age. With women loosing bone at an average rate of 2% per year (C. Christiansen, 1995), and men at a rate of 0.3% per year (C.M. Bono and T.A. Einhorn, 2003), by the age of 70 the scale of skeletal tissue lost is considerable. Females are estimated to loose 25-30% of cortical

bone and 35-50% of trabecular bone during their life, with males losing 5-15% and 15-45% respectively (G.D. Summers, 2001). With this rate and degree of loss occurring, the percentage of the elderly population with low bone mass is increased. J.A. Kanis (2005) reports that in a Swedish population aged between 75 and 79, 37.5% of women and 10.3% of men were osteoporotic rising to 47.2% and 16.6% respectively by the age of 80.

Idiopathic Osteoporosis

Idiopathic Osteoporosis is characterised by the presence of osteoporosis but with no discernable risk factors or cause. Approximately 40% of male osteoporosis cases can be classified as being of idiopathic origin (D. Vanderschueren et al., 2000, G.D. Summers, 2001).

4.1.4 Secondary Osteoporosis

'Secondary osteoporosis is defined as bone loss that results from specific, well-defined clinical disorders.' (L.A.Fitzpatrick, 2002)

The causes of secondary osteoporosis are listed in Table 4.1 and include disorders of the endocrine system, gastrointestinal system, side effects of drug therapies and other conditions that have detrimental effects on the skeleton.

Table 4.1 Diseases, and drug therapies linked to secondary osteoporosis, adapted from L.A. Fitzpatrick, 2002; D.M. Reid and J. Harvie, 1997; NOF, 2003.

Endocrine / Metabolic Disorders	Nutritional / Gastrointestinal	Drug Therapies	Other
• Acromegaly • Cushing's Syndrome • Congenital Porphyria • Endometriosis • Hypercalciuria • Hyperparathyroidsim • Hyperprolactinemia • Hyperthyroidism • Hypogonadsim • Hypophosphatasia • Type 1 Diabetes Mellitus	• Anorexia Nervosa • Celiac Disease • Crohn's Disease • Gastrectomy • Inflammatory Bowel Disease • Liver Disease • Malnutrition – Vitamin D and Calcium Deficiency • Primary Biliary Cirrhosis	• Aluminium • Anticonvulsants • Cytotoxic Drugs • Glucocorticoids and Adrenocorticotropin • Gonadotropin-releasing hormone agonists • Heparin • Immunosuppressants • Lithium • Progesterone • Supraphysiological Thyroxine doses • Tamoxifen (premenopausal use)	• AIDS / HIV • Alcoholism • Amyloidosis • Ankylosing Spondylitis • Chronic Obstructive Pulmonary Disease • Hemophilia • Immobilization • Leukemia • Mastocytosis • Multiple Sclerosis • Myeloma • Organ Transplantation • Pregnancy • Rheumatoid Arthritis • Stroke

One of the main differences between the different types of osteoporosis is in the types of bone which are affected by the conditions. In Type II primary osteoporosis the loss of bone is universal, with a progressive loss of both cortical and trabecular tissue with age; however, in the case of Type I primary osteoporosis and secondary osteoporosis the bone lost is predominantly cancellous (B.L. Riggs and L.J. Melton, 1992). A proposed reason behind this relates to the degree of vascularity of the tissue, with cancellous bone showing a far higher degree of vascularity than cortical bone and, as such, is more prone to drug, endocrine and metabolic related causes (C.M. Bono and T.A. Einhorn, 2003).

4.2 Osteoarthritis (OA)

4.2.1 Definition and Incidence

Osteoarthritis (OA) is not recognised as a condition of the bone, but as a degenerative condition which affects the articular cartilage of the synovial joints. However the effects of the condition and the loss of the articular cartilage cause changes in the subchondral bone, and can lead to the formation of new bony processes (osteophytosis). OA is classified as the eighth largest cause of disability in the world, and in the US it is predicted that some 43 million individuals are affected by the condition, with an estimated cost to the government of $65 billion a year.

The causes of OA can be divided into two classes, either primary (idiopathic) or secondary.

4.2.2 Primary OA

The primary form of the condition has no specific identifiable cause, and is related to aging, ethnicity and hereditary factors. The condition as a whole has been shown to affect about 50% of people aged over 65 with the number increasing further to 85% in the over 75 age group (J.M. Jordan et al., 1997). The Framingham OA study (D.T. Felson et al., 1987) focused solely on knee OA, but showed that the prevalence of the condition increased from ~27% in people aged 63 – 70 to ~44% in those aged over 80. Gender and ethnicity do not affect the prevalence of the condition within the populations, but the prevalence of the condition at different sites, with males more susceptible to OA of the hip and females OA of the knee (J.M. Jordan et al. 1996; M.A. Cimmino and M. Parodi, 2005). The hereditary link is widely accepted, but most work in the field is focused on the specific genetic factors related to the condition.

4.2.3 Secondary OA

The secondary form of the condition is related to lifestyle and environmental factors. Cartilage contains chondrocyte cells which maintain and produce the extracellular matrix which makes up the cartilage, but cartilage tissue is avascular and all the nourishment and materials required by the cells must be gleamed from the synovial fluid of the joint (P. Ghosh, 2003). This means that the ability of the cartilage tissue to repair it-self is a slow and time consuming process, so high intensity sports, trauma or occupations that impart excessive and repetitive stresses on the cartilage can cause the accumulation of collagen damage and a predisposition to OA.

Other factors that can cause a predisposition to OA include diet and obesity. As mentioned previously, the nourishment of the cartilage tissue is important for its maintenance and condition, so dietary intake of the required vitamins and nutrients such as Vitamin D (C.K. Kee, 2000) are important. In the case of obesity, a number of studies (C.K. Kee, 2000; D. Coggon et al., 2001; A.M. Lievense et al., 2002) have shown the condition to predispose individuals to OA, although the most comprehensive study on the topic (T. Stürmer et al., 2000) found that is was a mechanical effect due to the increased loading on the joints, with the knee joint being most at risk.

4.3 The Effects of Osteoporosis and Osteoarthritis on Bone

4.3.1 Composition

In section 2.2 the composition of normal human bone was presented in relation to its mineral, organic and water content, from three papers by B. Li and R.M. Aspen, (1997a,b,c). These same papers also reviewed the effects of both osteoarthritis and osteoporosis on the compositional makeup of the bone, although some of the results

were conflicting. In all three studies the mineral content of the osteoarthritic bone was significantly lower than the bone of the normal subjects, with the net gain being seen in the water content of the bone and not in the organic content. However the effects of osteoporosis on the composition of the bone was mixed, with two studies (B. Li and R.M. Aspen, 1997a,c) showing no significant difference between the osteoporotic bone and the normals, but both indicated a reduction in the mineral content and an increase in the organic content of the osteoporotic trabecular bone in relation to the control. The third study (B. Li and R.M. Aspen, 1997b) showed this same relationship, only the increase in the organic content and corresponding drop in the mineral content was significant.

M.A. Rubin et al. (2003) performed an in-depth study into the nanostructure of osteoporotic bone in relation to normal trabecular bone, using transmission electron microscopy (TEM) analysis. The results showed that, despite the variation in the mineral content seen in the osteoporotic condition, the nature of the apatite crystals in both the normal and osteoporotic bone were identical both in their alignment in the collagen fibrils and geometry.

The levels and occurrence of the collagen cross-links within the different conditions are variable but can be explained by the nature of the conditions. In osteoporosis the equilibrium between the resorption and deposition are unbalanced with the resorption of the bone being preferential to the deposition. However, the metabolism of collagen is higher in osteoporotic subjects than in normals (A.J. Bailey et al, 1993), with the deposition phase of the bone metabolism producing ‘lower quality collagen’. This is adversely affecting the aggregation of the collagen fibrils producing lower numbers of immature cross-links such as HLNL and HLKNL (20-40% reduction, A.J.

Bailey et al., 1992) and, due to the over hydroxylation of lysine within the tissue, increased levels of hydroxylysine (20-50% increases, J.P. Mansell and A.J. Bailey 2003), all of which adversely affect the skeletal tissues mechanical properties (A.J. Bailey et al, 1993; A.J. Bailey and L. Knott 1999; J.P. Mansell and A.J. Bailey, 2003). The levels of cross-linking within normal tissue of the femoral head were demonstrated by A.J. Bailey et al., 1992; A.J. Bailey et al, 1993; J.P. Mansell and A.J. Bailey (2003) Table 4.2.

Table 4.2 Expected levels (mol/mol) of collagen cross-links with the tissues of normal osteoporotic and osteoarthritic individuals

Cross-link	Normal	Osteoporotic	Osteoarthritic
OHPyr	0.21 – 0.9	0.27 – 0.8	0.22 – 0.25
Lys-Pyr	0.07 – 0.09	0.11 – 0.12	0.07 – 0.08
HLNL	0.11 – 0.14	0.03 – 0.13	0.13 – 0.18
HLKNL	0.20 – 0.26	0.06 – 0.15	0.17 – 0.37

As with the biomechanics in section 3.2.1.5, the levels of collagen cross-linking varies between skeletal sites, with A.J. Bailey et al. (1992) demonstrating that the levels of HLKNL and OH-Pyr were increased in the femoral head region compared with the femoral neck, a trend supported by A.J. Bailey et al. (1993).

As with osteoporosis, osteoarthritis increases the rate of collagen metabolism and deposition within the cancellous bone, in relation to age matched controls (J.P. Mansell and A.J. Bailey, 1998). The increased deposition is, however, not of normal collagen, with the collagen molecules themselves being affected and increased levels of type III and V collagen being present in the tissue (A.J. Bailey and L. Knott 1999). The resultant effects on the cross-linking are mixed; the number of immature cross-links within the tissue, and more specifically HLKNL, have been shown to increase (J.P.

Mansell and A.J. Bailey, 1998), but the numbers of the other mature and immature cross-links vary very little between the normal bone and the osteoarthritic tissue.

4.3.2 Material Properties and Structure

The definition of osteoporosis (section 4.2) provides an indication of the effects it has on the material properties of the trabecular bone; however, for the osteoarthritic bone the effects of the condition are almost the inverse. The studies by B. Li and R.M. Aspen, (1997a,b) and S.J. Brown et al. (2002) provide a comparison between samples of osteoporotic, osteoarthritic and normal bone in relation to their apparent densities. The apparent density of the osteoporotic bone was found to be significantly reduced in comparison to the control bone, with the osteoarthritic bone being significantly higher than the control. The material density of the three groups has also been shown to be different with both the osteoarthritic and osteoporotic having lower material densities than the control bone, although only the osteoarthritic bone was significantly so (B. Li and R.M. Aspen, 1997a,b,c).

For both osteoarthritis and osteoporosis, the structure of the bone is affected, albeit in opposing fashions. In osteoarthritis the remodelling process is unbalanced with an increased quantity of less mineralised bone being deposited (B. Li et al., 1999); however, this imbalance affects the overall structure of the bone. C.D. Papaloucas et al. (2005) demonstrated that the larger trabeculae within the femoral head increase in size at the expense of the lesser trabeculae, with an overall increase in the volume of bone, but a reduction in the trabecular number and connectivity. In osteoporosis the loss in trabecular number and connectivity is also seen, but in this incidence the imbalance within the remodelling process means a reduction in the overall bone mass present. Figure 4.1 shows a comparison between two bone samples demonstrating not only the

loss in density, but also the loss in connectivity and the change in structure of the trabecular network that occurs in osteoporosis.

It is worth noting that the mechanisms behind the bone loss in osteoporosis are gender specific; E. Seeman (1999) reports that the method of bone loss in females is by the selective thinning of certain trabeculae which results in a loss of connectivity and structure, whereas in men the loss is more uniform, maintaining the structure. The selective loss means that a sample of female bone of equal density to a sample of male bone will have reduced mechanical properties due to its poor structure.

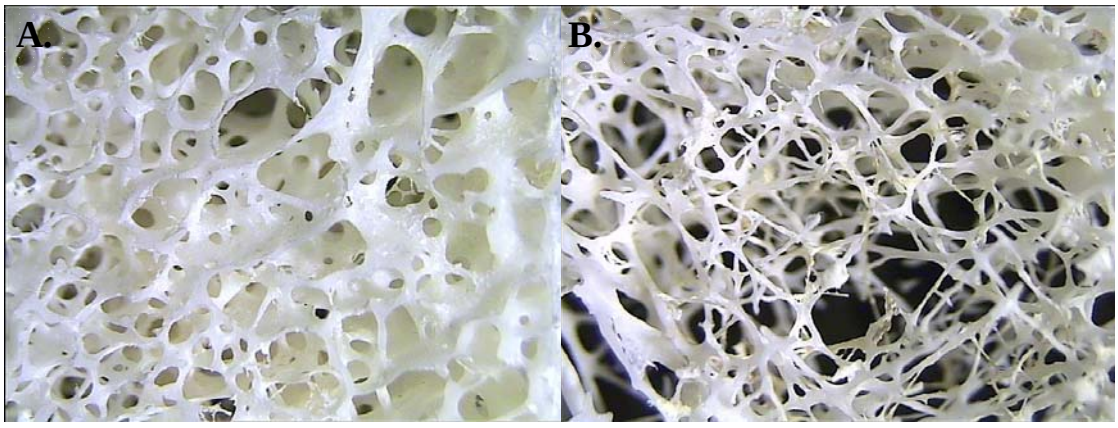

Figure 4.1 Cancellous bone samples from the neck of the femur of (A) a 54 year old female and (B) a 74 year old female.

4.4 Densitometry Assessment

The favoured method for the diagnosis of osteoporosis and low bone density is the use of X-ray based densitometry techniques such as dual energy X-ray absorptiometry (DXA) and quantitative computed tomography (QCT). Densitometry techniques allow for the assessment of the axial and peripheral skeleton, providing measurements of either Bone Mineral Content (BMC) or more commonly Bone Mineral Density (BMD) in g cm^{-2}; however the two are closely related (Equation 4.1).

$$BMC = BMD \times Area$$ **Equation 4.1** (G.M. Blake et al., 1997)

The results of the densitometry scan give the clinician the opportunity to visualise the scale of an individual's bone loss and skeletal condition, so that suitable therapies for the prevention of further skeletal tissue loss, and advice on lifestyle alterations, can be provided to the patient.

4.4.1 Dual Energy X-ray Absorptiometry (DXA)

Of the techniques available, DXA is recognised as the 'Gold Standard' technique for the diagnosis of osteoporosis and low bone density. The technique uses X-rays at two effective discrete energies, each of which interacts differently with the skeletal and soft tissue, with the different levels of attenuation of the X-rays allowing for differentiation between the two (skeletal tissue and the soft tissue). The resultant degree of attenuation for the two different energies by the skeletal tissue, allows for the quantitative determination of the density of the bone. (S. Grampp et al., 1993; G.M. Blake et al., 1997; N.A. Pocock, 1998).

DXA allows for the measurement of a number of skeletal sites, with the main two being the lumbar spine, vertebra L1-L4, and the proximal femur, with assessment of a number of sites such as the femoral neck, trochanter, the intertrochanteric region and Ward's triangle. The lumbar spine and proximal femur are of particular interest as they are areas of load bearing cancellous bone and, as such, are prone to fracture due to osteoporosis.

The advantage of DXA over other systems is the comparatively low precision error of the technique (Table 4.3), as the precision of a technique is important if the longitudinal changes occurring to an individual's skeleton are to be monitored. The low precision error of DXA enables it to monitor the effects of drug therapies and, with

normal annual changes in skeletal density of 2% in women and 0.3% in men, the technique requires a high level of precision if measured changes are to be considered significant, and not a result of measurement error. (C. Christiansen, 1995, C.M. Bono and T.A. Einhorn, 2003)

Table 4.3 Adapted from (S. Grampp et al., 1993; M. Jergas and H.K. Genant, 1993; C. Christiansen, 1995; D.T. Baran et al., 1997)

Technique	Measurement Site	Precision Error (%)
Radiographic Absorptiometry. (RA)	Phalanx / Metacarpal	1-2
Single-Photon Absorptiometry. (SPA) **Single X-ray Absorptiometry**. (SXA)	Radius / Calcaneus	1-2
Dual-Photon Absorptiometry. (DPA)	Lumbar Spine Proximal Femur	2-4 3-5
Dual Energy X-Ray Absorptiometry (DXA)	AP* Spine Lat$^{\curlyvee}$ Spine Forearm Proximal Femur Whole Body	1-1.5 2-3 ~1 1.5 - 3 ~1
Quantitative Computed Tomography (QCT)	Spine Trabecular Spine Integral	2-4 2-4
Peripheral Quantitative Computed Tomography (pQCT)	Forearm	0.5-3
Quantitative Ultrasound. (QUS) Broadband Ultrasound Attenuation (BUA) Speed of Sound (SOS)	BUA Calcaneus SOS Calcaneus SOS Radius / Phalanx / Tibia	0.4-4.0 0.15-1.9 0.5-8.9
Magnetic Resonance Imaging (MRI)		3.9-4.8

*Anteroposterior, ϒ Lateral

4.5 Diagnosis of Osteoporosis and Low Bone Density

In 1994 a group of leading experts was gathered together by the World Health Organisation (WHO) to produce specific guidelines for the diagnosis of conditions

relating to low bone density (WHO, 1994; J.A.Kanis et al., 1994). The resultant guidelines were designed for BMD results obtained from the axial skeleton of females, using DXA.

The guidelines relied on the production of a value known as a T-score (Equation 4.2). The T-score refers to the number of standard deviations above or below the mean peak value for young adults of the same gender and race, in which a measurement result falls.

$$T-score = \frac{Patients\ Measurement - Mean\ Peak\ Value\ For\ Normal\ Young\ Adults}{The\ Standard\ Deviation\ of\ the\ Peak\ Value\ For\ Normal\ Young\ Adults}$$

Equation 4.2 Equation for the calculation of T-scores

The guidelines defined specific thresholds, which enabled the classification of measurement results into four distinct groups.

1. Normal: A value for BMD greater than 1 SD below the peak value for normal young adults. A T-score of greater than -1.
2. Osteopenia: A value for BMD not greater than 1 SD below the young adult average but not less than 2.5 SD below. A T-score between -1 and -2.5.
3. Osteoporosis: A value for BMD more than 2.5 SD below the peak value for normal young adults. A T-score of less than -2.5.
4. Severe Osteoporosis: A value for BMD more than 2.5 SD below the peak value for normal young adults with the presence of one or more fragility fractures. A T-score of less than -2.5 with the presence of a fragility fracture.

Coupled to this, an additional value know as the Z-score was developed for the comparison of individuals of the same age (Equation 4.3). The Z-score refers to the number of standard deviations below or above the mean value of age matched individuals a result falls.

$$Z-score = \frac{Patients\ Result\ -\ Mean\ Value\ for\ Age.}{Standard\ Deviation\ of\ the\ Age\ Matched\ Mean}$$

Equation 4.3 Equation for the calculation of the Z-score

Since 1994, this diagnostic criterion has become widely accepted as the threshold for Osteopenia and Osteoporosis diagnosis when using BMD of the axial skeleton. However, the diagnosis and assessment of low bone density has developed and matured, with a number of different systems and techniques from different manufacturers becoming available to the clinician, while existing techniques have been improved and updated. This advance and proliferation in the technique has led to discrepancies within the field, as each system has a different normative database from which the T-score is calculated, derived from the manufacturers' chosen study population, which may not be suitable for the area and population the system is being used to assess, and may not provide results which would be comparable with those of another system.

In order to prevent misdiagnosis, and abuse of the WHO definition, societies such as the National Osteoporosis Foundation (NOF, 2003), The National Osteoporosis Society (NOS, 2002), The International Society for Clinical Densitometry (ISCD) (E.M. Lewiecki et al., 2004) and The Osteoporosis Society of Canada (OSC) (J.P. Brown and R.G. Josse, 2002) review the literature and provide position papers outlining the correct and proper use of the T-score system with respect to differing aspects related to age, gender, measurement site and technique. The definition of osteoporosis using the T-score system remains unchanged, only the groups for which the classification is true has been reduced to the postmenopausal women assessed at the axial skeleton as was used for the levels' initial definition. For any other groups such as the male population and

the pre- and perimenopausal females the different groups vary on their opinions, as the paper by J.A. Kanis et al. (2005) shows; however, whilst the use of the T-score and the previous thresholds still hold true, they cannot be considered a definitive diagnosis.

Not only have the methods of diagnosis developed and matured, but the demand for densitometry services, especially the hospital densitometry techniques such as DXA, has also increased, and it has become recognised that large scale population screening with DXA is not a cost effective approach for the management of osteoporosis (C.M. Langton et al. 1997, 1999, F. Marín et al., 2004). It is therefore important that referral criteria are produced that enable the accurate discrimination of individuals into those requiring densitometry, and those who do not, so as to reduce the demands and expense on the hospital services. The most readily available method is for a clinician to review the medical history of an individual and to make a referral based on the presence of one or more clinical risk factors.

4.6 Clinical Risk Factors

The medical conditions and medications which are risk factors for bone densitometry referral have been reviewed previously in section 4.2.4 as to their potential causes of secondary osteoporosis. In addition to these, certain anthropometrical values, lifestyle factors and information on personal and family medical history are included.

- A history of low-trauma fracture in a first-degree relative
- A history of fracture in adult life
- Low body weight or body-mass index (BMI)
- Low lifetime calcium intake

- Loss of height after menopause
- Tobacco smoking
- Radiological evidence of osteopenia or vertebral deformity or both

The different groups associated with Osteoporosis provide referral criteria for DXA assessment (NOF, 2003; NOS, 2001; OSC, (J.P. Brown and R.G. Josse, 2002) (Table 4.4). In addition to these organisations, specific osteoporosis centres have outlined their referral criteria (C.M. Langton et al., 1997, 1999), alongside a number of review papers on Osteoporosis, (J.E. Compston et al., 1995; P.A. Ballard et al., 1998; J.A. Kanis, 2002; L.K.H. Koh and D.C.E. Ng, 2002; E.M. Lewiecki et al., 2004).

The clinical risk factors offer the clinician a simple, accepted and officially endorsed method of determining those at risk of osteoporosis who require densitometry investigation. However, with referral criteria including all women over 65 (NOF, 2003; OSC, (J.P.Brown and R.G.Josse, 2002)) the number of unnecessary referrals that arise from the use of clinical risk factors has lead to the investigation and advent of other referral methods. In particular, the risk factors have been utilised and formed into questionnaires in an attempt to provide a cost effective method for the differentiation of individuals requiring densitometry investigations.

Table 4.4 Clinical referral criteria provided by the official groups related to osteoporosis and specialised centres for the study of Osteoporosis.

Royal College of Physicians, 1999 **National Osteoporosis Society, 2002**	**National Osteoporosis Foundation, 2003**	**Osteoporosis Society of Canada, 2002**
• Premature menopause or Oestrogen deficiency at an early age (<45 years) • Long-term secondary amenorrhoea. (>1 year) • Primary hypogonadism • Corticosteroid therapy, Prednisolone > 7.5mg/day for 1 year or more • Maternal history of hip fracture • Low Body Mass Index (<19kg/m^2) • Disorders Associated with Secondary Osteoporosis. • Anorexia Nervosa • Malabsorption Syndrome • Primary Hyperparathyroidism • Post-transplantation • Chronic Renal Failure • Hyperthyroidism • Prolonged Immobilisation • Cushing's Syndrome • Radiographic evidence of osteopenia and / or vertebral deformity. • Previous Fragility Fracture, especially of the hip, spine or wrist • Loss of Height, Thoracic Kyphosis (after radiographic confirmation of vertebral deformities)	• All women aged 65 and older regardless of risk factors • Younger Postmenopausal Women with one or more risk factors. (other than being white, postmenopausal and female) • Postmenopausal Women who present with fractures. (To confirm diagnosis and determine disease severity)	• BMD Assessment recommended in any individual with one major risk factor or two minor risk factors **Major Risk Factors** • Age >65 • Vertebral Compression Fracture • Fragility fracture after the age 40 • Family history of osteoporotic fracture • Systemic Glucocorticoid therapy for > 3 months duration • Malabsorption Syndrome • Primary Hyperparathyroidism • Propensity to fall • Osteopenia apparent on X-ray film • Hypogonadism • Early Menopause (before age 45) **Minor Risk Factors** • Rheumatoid Arthritis • Past history of clinical hyperthyroidism • Chronic Anticonvulsant therapy • Low dietary Calcium intake • Smoking • Excessive alcohol intake • Excessive caffeine intake • Weight <57kg • Weight loss >10% of weight at age 25 • Chronic Heparin therapy

Table 4.4 Continued

Centre for Metabolic Bone Disease, Hull C.M. Langton et al., 1997, 1999	The European Foundation For Osteoporosis and Bone Disease. J.A. Kanis et al., 1997	European Commission, 1998
• Any oestrogen deficient women who would want to be treated or would want to continue treatment if found to be osteopenic or osteoporotic. • Patients suspected to be osteoporotic from radiological or clinical findings • Patients who have a medical condition predisposing to osteoporosis if effective treatment is available. E.g. o Metabolic bone disease o Liver Disease o Anorexia Nervosa o Malabsorption Syndromes o And other rarer causes of osteoporosis • Patients receiving corticosteroid at a dose of ≥5mg Prednisolone or equivalent • Women who experience primary or secondary amenorrhoea (including hysterectomy) below the age of 45 years. • Patients with a positive family history of osteoporosis in at least one first degree relative.	• Presence of Strong Risk Factors: • Oestrogen Deficiency o Premature Menopause (<45 years) o Prolonged Secondary Amenorrhoea (>1 year) o Primary Hypogonadism • Corticosteroid Therapy o (>7.5 mg/day for 1 year or more) • Maternal Family History of Hip Fracture • Low Body Mass Index (<19 kg/m^2) • Other Disorders associated with Osteoporosis: o Anorexia nervosa o Malabsorption o Primary hyperparathyroidism o Post-Transplantation o Chronic Renal Failure o Hyperthyroidism o Prolonged Immobilization o Cushing's Syndrome • Radiological evidence of osteopenia and/or vertebral deformity • Previous fragility fracture particularly of the hip, spine or wrist • Loss of height, thoracic kyphosis	• Presence of strong risk factors o Premature menopause (<45 years) o Prolonged secondary amenorrhoea o Primary hypogonadism o Glucocorticoid therapy (>7.5 mg/day oral prednisolone or equivalent for six months or more) o Anorexia nervosa o Inflammatory bowel disease/malabsorption o Primary hyperparathyroidism o Organ transplantation o Chronic renal failure o Chronic liver disease o Hyperthyroidism o Prolonged immobilization o Maternal history of hip fracture o Long-term heparin therapy • Radiological evidence of osteopenia and/or vertebral deformity • Previous fragility fracture • Height loss • Monitoring of therapy
Monitoring • Patients prior to starting management with corticosteroids of a prolonged duration of 6 months or more. • To monitor response to treatment in patients with established osteopenia and osteoporosis.		

4.7 Questionnaire Systems

Questionnaires rely on different risk factors and anthropometrical values being weighted according to their significance so as to provide a numerical value. The numerical value can then be used in combination with the values of any other significant factors to provide a quantitative scale upon which definite thresholds, indicating different degrees of risk, can be applied. Within the literature, there are 8 questionnaire systems (Table 4.5) that have been developed and validated by different study groups for the prediction of the status of the axial skeleton.

Table 4.5 Previously developed and validated questionnaire systems from within the literature, with their modes of calculation.

Reference	Method of Calculation	Risk Index or Cut-off
Age, Bulk and No Estrogen Use (ABONE)		
L. Weinstein and B. Ullery (2000) S.M. Cadarette et al. (2001) L.S. Wallace et al. (2004)	Age >65 years = +1 Weight <140lbs = +1 Estrogen use >6 months = +1	Threshold ≥1
Osteoporosis Prescreening Risk Assessment (OPERA)		
F. Salaffi et al. (2005)	Age ≥65 years = +1 Weight <57kg = +1 History of low trauma fracture after age 45 = +1 Early Menopause (before age 45) = +1 Steroid Use > 6 months (>5mg/day) = +1	Threshold ≥ 2
Osteoporosis Risk Assessment Instrument (ORAI)		
S.M. Cadarette et al. (2000, 2001) S. Fujiwara et al. (2001) L.S. Wallace et al. (2004)	Age 75+years = +15, Age 65-74 years = +9, Age 55-64 years = +5, Age <55 years = 0 Weight <60kg = +9, Weight 60 – 70kg = +3, Weight >70kg = 0 Not currently using oestrogen = +2	<9 low risk 9 to 17 moderate risk >17 high risk
Osteoporosis Index of Risk (OSIRIS)		
W.B. Sedrine et al. (2002) J.Y. Reginster et al. (2004)	Age (years): x -2 and remove last digit Weight (kg): x 2 and remove last digit Current HRT Use = +2 Incidence of prior low trauma fracture = -2	>+1 low risk 1 to -3 moderate risk <-3 high risk

Table 4.5 Continued

Osteoporosis Self-assessment Tool (OST) For an Asian Population (OSTA) For a Female Asian Population (FOSTA)		
S. Fujiwara et al. (2001) L.K.H. Koh et al. (2001) P. Geusens et al. (2002) R.A. Adler et al. (2003) A.W.C. Kung et al. (2003) H.M. Park et al. (2003) F. Richy et al. (2004) L.S. Wallace et al. (2004)	• OST 0.2(weight (kg)) – 0.2 (age (years)) The last digit is dropped from each to give an integer, and the resulting values added together. • OSTA, FOSTA (weight (kg) – age (years)) × 0.2 The resultant value is truncated to give an integer	>2 low risk, 2 to -3 moderate risk <-3 denotes high risk
Patient Body Weight (pBW)		
K. Michaëlsson et al. (1996a, 1996b) S.M. Cadarette et al. (2001, 2004) L.S. Wallace et al. (2004)		Weight <70kg
Simple Calculated Osteoporosis Risk Estimation (SCORE)		
S.M. Cadarette et al. (1999, 2001) D. Von Mühlen et al. (1999) W.J. Ungar et al. (2000) S. Fujiwara et al. (2001) A.S. Russell and R.T. Morrison (2001) W.B. Sedrine et al. (2001) G.F. Falasca et al. (2003) L.S. Wallace et al. (2004)	Age: 3 x first digit of age Weight: -1 x Weight (lbs) / 10 (truncate to integer.) Race other than Black = +5 Rheumatoid Arthritis Sufferer = +4 History of fracture at wrist, hip or rib = +4 for each fracture Never used HRT = +1	<7 low risk 7 to 15 moderate risk >15 high risk
Study of Osteoporotic Fractures (SOFSURF)		
D.M. Black et al. (1998) S. Fujiwara et al. (2001)	Age over 65: +0.2 every year Age under 65: -0.2 every year Weight < 130lbs (59kg) = +3 Weight 130lbs – 150lbs (59kg - 68kg) = +1 Weight > 150lbs (68kg) = 0 Current Smoker = +1 History of Post-menopausal Fracture = +1	<0 low risk 0 to 4 moderate risk >4 high risk

The number of risk factors and anthropometrical values utilised to produce the questionnaire systems varies from just 1 in the case of patient body weight (pBW) to 6 (age, weight, race, arthritis sufferer, oestrogen usage and fracture history) for the Simple Calculated Osteoporosis Risk Estimation (SCORE)). The risk factors utilised in the questionnaire systems are only the most significant and predictive, the validation studies start with far more risk factors and anthropometrical values and, by factor and regression analysis, the most significant values and their corresponding weighting values are ascertained. ABONE: L. Weinstein and B. Ullery (2000) (18 variables),

OPERA: F. Salaffi et al. (2005), ORAI: S.M. Cadarette et al. (2000), OSIRIS: W.B. Sedrine et al. (2002), OST: L.K.H. Koh et al. (2001), pBW: K. Michaëlsson et al. (1996a), SCORE: E. Lydick et al. (1998), SOFSURF: D.M. Black et al. (1998). It is worth noting that of all the significant risk factors utilised in the production of these questionnaire systems, none of them contain any of the risk factors for secondary osteoporosis from Table 4.1, and many of the factors from within the referral guidelines in table 4.4 are also omitted.

In order to validate the questionnaires, the authors have all utilised population based studies involving large numbers of volunteers, independent of the study cohort which was use develop the questionnaire. The studies all report the abilities of their studies in the form of receiver operator characteristic (ROC) curves, and in particular the area under the curve (AUC) values from a sensitivity and specificity study.

Tables 4.5 to 4.9 show the area (AUC) from under the ROC curves, which provide a quantitative insight into the questionnaires' diagnostic ability and, if performed as part of the same study, enable a direct comparison of different techniques. R. Kent and J. Patrie (2005) supply guidelines for the interpretation of AUC values, with values greater than 0.9 indicating an 'excellent' level of diagnostic accuracy, 0.7 to 0.9 showing a 'good' diagnostic accuracy, 0.6-0.7 a 'moderate' ability and between 0.5 and 0.6 indicating the technique as having 'poor' ability.

Table 4.6 AUC values for the performance of the OST / OSTA / FOSTA questionnaire system to screen individuals based on their DXA derived T-score.

Reference Study Group Demographics	Predicted Site DXA T-Score Level	AUC
OST / OSTA / FOSTA		
R.A. Adler et al. (2003), F. Richy et al. (2004)	LS (L1-L4) DXA T-score ≤-2.5	0.686 - 0.845
R.A. Adler et al. (2003), F. Richy et al. (2004)	LS (L1-L4) DXA T-score ≤-2	0.761 - 0.663
R.A. Adler et al. (2003), A.W.C. Kung et al. (2003), H.M. Park et al. (2003), F. Richy et al. (2004)	FN DXA T-score ≤-2.5	0.814 0.768 - 0.873
R.A. Adler et al. (2003), H.M. Park et al. (2003) F. Richy et al. (2004)	FN DXA T-score ≤-2	0.821 0.751 - 0.861
R.A. Adler et al. (2003), F. Richy et al. (2004)	TH DXA T-score ≤-2.5	0.813 - 0.866
R.A. Adler et al. (2003), F. Richy et al. (2004)	TH DXA T-score ≤-2	0.787 - 0.826
A.W.C. Kung et al. (2003), S.M. Cadarette et al. (2004)	FN + LS (L1-L4) DXA T-score ≤-2.5	0.75 - 0.822
S.M. Cadarette et al. (2004) OST Chart	FN + LS (L1-L4) DXA T-score ≤-2.5	0.818
R.A. Adler et al. (2003), F. Richy et al. (2004)	Any Site DXA T-score ≤-2.5	0.803 0.726 - 0.848
R.A. Adler et al. (2003), F. Richy et al. (2004)	Any Site DXA T-score ≤-2	0.713 - 0.815

Table 4.7 AUC values for the performance of the ORAI questionnaire system to screen individuals based on their DXA derived T-score.

Reference Study Group Demographics	Predicted Site DXA T-Score Level	AUC
ORAI		
S.M. Cadarette et al. (2001) F. Richy et al. (2004)	FN DXA T-score ≤-2.5	0.706 - 0.79
S.M. Cadarette et al. (2001) F. Richy et al. (2004)	FN DXA T-score <-2	0.692 - 0.76
S.M. Cadarette et al. (2001)	FN DXA T-score <1	0.71
F. Richy et al. (2004)	TH DXA T-score ≤-2.5	0.741
F. Richy et al. (2004)	TH DXA T-score ≤-2	0.718
F. Richy et al. (2004)	LS (L2-L4) DXA T-score ≤-2.5	0.644
F. Richy et al. (2004)	LS (L2-L4) DXA T-score ≤-2	0.627
S.M. Cadarette et al. (2004)	LS (L1-L4) + FN DXA T-score ≤-2.5	0.802
F. Richy et al. (2004)	Any Site DXA T-score ≤-2.5	0.67
F. Richy et al. (2004)	Any Site DXA T-score ≤-2	0.668

Table 4.8 AUC values for the performance of the SCORE questionnaire system to screen individuals based on their DXA derived T-score.

Reference Study Group Demographics	Predicted Site DXA T-Score Level	AUC
SCORE		
S.M. Cadarette et al. (2001) W.B. Sedrine et al. (2001), F. Richy et al. (2004)	FN DXA T-score ≤-2.5	0.766 0.749 - 0.80
S.M. Cadarette et al. (1999), D. Von Mühlen et al. (1999), S.M. Cadarette et al. (2001), W.B. Sedrine et al. (2001), G.F. Falasca et al. (2003), F. Richy et al. (2004)	FN DXA T-score ≤-2	0.746 0.696 - 0.80
S.M. Cadarette et al. (2001), W.B. Sedrine et al. (2001)	FN DXA T-score <1	0.72
W.B. Sedrine et al. (2001), F. Richy et al. (2004)	LS (L2-L4) DXA T-score ≤-2.5	0.66 – 0.67
S.M. Cadarette et al. (1999), W.B. Sedrine et al. (2001), G.F. Falasca et al. (2003), F. Richy et al. (2004)	LS (L1-L4) DXA T-score ≤-2	0.664 0.647 - 0.69
W.B. Sedrine et al. (2001)	LS (L2-L4) DXA T-score ≤-1	0.64
W.B. Sedrine et al. (2001), G.F. Falasca et al. (2003), F. Richy et al. (2004)	TH DXA T-score ≤-2.5	0.802 0.78 - 0.84
W.B. Sedrine et al. (2001), G.F. Falasca et al. (2003), F. Richy et al. (2004)	TH DXA T-score ≤-2	0.763 0.76 - 0.77
W.B. Sedrine et al. (2001)	TH DXA T-score ≤-1	0.73
S.M. Cadarette et al. (1999), W.J. Ungar et al. (2000)	LS (L1-L4) + FN DXA T-score ≤-2	0.692 0.594 - 0.732
W.B. Sedrine et al. (2001), G.F. Falasca et al. (2003), F. Richy et al. (2004)	Any Site DXA T-score ≤-2.5	0.726 0.708 - 0.76
W.B. Sedrine et al. (2001), G.F. Falasca et al. (2003), F. Richy et al. (2004)	Any Site DXA T-score ≤-2	0.71 0.70 - 0.73
W.B. Sedrine et al. (2001)	Any Site DXA T-score ≤-1	0.69

Table 4.9 AUC values for the performance of the SOFSURF, OPERA and ABONE questionnaire systems to screen individuals based on their DXA derived T-score.

Reference Study Group Demographics	Predicted Site DXA T-Score Level	AUC
SOFSURF		
D.M. Black et al. (1998)	TH DXA T-score ≤-2.5	0.75
OPERA		
F. Salaffi et al. (2005)	LS (L1-L4) DXA T-score ≤-2.5	0.866
	FN DXA T-score ≤-2.5	0.814
ABONE		
S.M. Cadarette et al. (2001)	FN DXA T-score ≤-2.5	0.67
	FN DXA T-score <-2	0.71
	FN DXA T-score <1	0.72

Table 4.10 AUC values for the performance of the OSIRIS and pBW questionnaire systems to screen individuals based on their DXA derived T-score.

Reference **Study Group Demographics**	**Predicted Site** **DXA T-Score Level**	**AUC**
OSIRIS		
F. Richy et al. (2004)	TH DXA T-score ≤-2.5	0.817
F. Richy et al. (2004)	TH DXA T-score ≤-2	0.791
F. Richy et al. (2004)	FN DXA T-score ≤-2.5	0.772
F. Richy et al. (2004)	FN DXA T-score ≤-2	0.755
F. Richy et al. (2004)	LS (L1-L4) DXA T-score ≤-2.5	0.69
F. Richy et al. (2004)	LS (L1-L4) DXA T-score ≤-2	0.666
W.B. Sedrine et al. (2002), F. Richy et al. (2004)	Any Site DXA T-score ≤-2.5	0.71 - 0.73
F. Richy et al. (2004)	Any Site DXA T-score ≤-2	0.717
pBW		
S.M. Cadarette et al. (2001) 2365 menopausal women of mixed race aged 45 years and over (mean 66.4 ± 8.8)	FN DXA T-score ≤-2.5	0.68
	FN DXA T-score <-2	0.74
	FN DXA T-score <1	0.79
S.M. Cadarette et al. (2004)	LS (L1-L4) + FN DXA T-score ≤-2.5	0.733

The performance of the questionnaire systems varied in ability depending on the skeletal site they were predicting the status of, the DXA T-score level the questionnaire was predicting and the demographics of the study population. The threshold values for the different questionnaires were set during the validation stages of the studies, by distinctly different methods. The first method used by L.K.H. Koh et al. (2001) and W.B. Sedrine et al. (2002) was purely arbitrary, with the two thresholds for the division of the risk groups placed at positions within the range to suitably divide the population; however, for L.K.H. Koh et al. (2001) the lower threshold indicating high risk was set at a level which achieved a sensitivity of 90%. This is of note as the studies

by K. Michaëlsson et al. (1996a), E. Lydick et al. (1998), S.M. Cadarette et al. (2000), F. Salaffi et al. (2005), which all only produced single cut off values rather than risk indices, all based the cut off value at a point which ensured a 90% sensitivity from the resultant division of the population. The other two studies by D.M. Black et al. (1998), and L. Weinstein and B. Ullery (2000) used different methods with the first using the median value of the range as the cut-off point, and the second recommending that the presence of one or more of the risk factors constituted a requirement for further investigation. The production of the risk indices shown within Table 4.5 for the different questionnaires was developed in later studies which attempted to further validate the questionnaires.

The threshold levels for the different questionnaires have been investigated with relation adjustments that might be required for different populations; for example the OSTA index was developed on individuals of Asian origin, and the threshold was set at ≤-1 indicating high risk (L.K.H. Koh et al., 2001), but subsequently adjusted to <-3 for a Caucasian population (P. Geusens et al., 2002).

Although the sensitivity and specificity analysis, in the form of the ROC curve and the corresponding AUC analysis, provide the main source of information on the abilities of the questionnaire techniques, two studies by M. Ayers et al., (2000) and A.W.C. Kung et al., (2003) both presented Pearson's correlation coefficients between the questionnaire systems' skeletal assessments. M. Ayers et al., (2000) compared the SCORE questionnaire result with the DXA T-score results from the lumbar spine, total hip and femoral neck, along with the combined results from a Sahara ultrasound system; the resultant correlations were -0.33, -0.52, -0.51 and -0.21 respectively, all of which were statistically significant ($p<0.001$). A.W.C. Kung et al., (2003) demonstrated that

there were moderate correlations between OST and BMD of the femoral neck and Lumbar spine of 0.62 and 0.49 respectively ($p<0.0001$).

The questionnaires offer the clinician a valuable tool to help in the identification of individuals at high risk of having low BMD, and in the identification of those individuals at low risk, who could be safely excluded from having more expensive investigations such as DXA. The questionnaires are only designed to be an aid to diagnosis and an individual with additional risk factors, outside those utilised by a questionnaire system, should not be ignored. The difficulty for the clinician is that there are eight different questionnaires on offer, all of which are very similar in nature, and provide a moderate to good level of diagnostic ability, but which provides the best diagnostic ability and should be used?

Despite the large volume of research into the risk factor questionnaires, most of the information is related to the individual techniques' abilities, and their validation within different study groups, ethnic origins and ages. Only four of the studies reviewed performed any form of comparison between the different systems' abilities. L.S. Wallace et al. (2004) provided ROC curves for comparison of pBW, SCORE, OST, ABONE and ORAI, but plotted the curves using only three points, and failed to provide any AUC values for direct comparison. A.W.C. Kung et al. (2003) provided a comparison between the OST questionnaire system and a Calcaneal QUS system. The study found no statistically significant difference between the abilities of the two techniques, for the prediction of low BMD at the axial skeleton, although an additional finding indicated that a combination of the results from both systems provided a greater predictive ability. F. Richy et al. (2004) provided a direct comparison between four questionnaire systems, OST, ORAI, SCORE and OSIRIS. For prediction of individuals

with low BMD at the axial skeleton, the report states that all four techniques' performances were similar. Review of the AUC values provided indicated that in order of performance, ORAI showed the least predictive ability, followed by SCORE, then OST, and with OSIRIS displaying the highest level of performance. The final study S.M. Cadarette et al. (2001) compared the NOF guidelines, SCORE, ORAI, ABONE and pBW for the prediction of femoral neck BMD. The results showed that ABONE and pBW performed poorly and have limited utility, whereas SCORE and ORAI both performed better than the NOF guidelines for the selection of patients requiring DXA referral.

It is clear from this review of the literature that clinical questionnaire systems based on anthropometrical, medical history and lifestyle factors have the ability to differentiate individuals within a population according their risk of suffering from osteoporosis. However with 8 questionnaires all having proven abilities, and very few studies performing comparisons between the questionnaires, it is unclear as to which questionnaire system provides the best levels of ability. It is therefore justifiable to perform a study using as many of the questionnaires as possible within the same study group in order to obtain the performances of the questionnaires in relation to each other, so as to find the best questionnaire for clinical usage.

4.8 Quantitative Ultrasound (QUS)

The use of QUS in the assessment of bone is a relatively new assessment method. The technique's ability to perform quantitative assessment of the skeleton was originally published by C.M. Langton et al (1984), and since then the technique has

been researched and developed, with a number of different systems appearing, with most still based around this original principle.

J.J. Kaufman and T.A. Einhorn, 1993 and P. Laugier, 2004, highlight the key difference between ultrasound and densitometry being the method of interaction the technique has with the bone. Ultrasound is a mechanical wave, and as such interacts directly with the skeletal tissue during its transmission. This direct interaction means that properties of the bone such as density, composition and structure all have an effect, and the resultant value will contain information above and beyond that which can be gained by the assessment of pure density.

4.8.1 Ultrasound Parameters

The measurement values provided by QUS are different from the BMD and BMC values provided by densitometry assessment, and reflect an effect on the ultrasound wave that has occurred during its transmission through the bone, or is a combination of the ultrasound parameters obtained.

4.8.1.1 Broad-band Ultrasound Attenuation (BUA)

BUA is, as its name suggests, due to the attenuation of a number of ultrasound waveforms of different frequencies as they propagate through the bone. The ultrasound wave is a mechanical wave and is open to scattering and absorption of its energy as it passes through the bone. Normal bone has a greater density and structural integrity in comparison to osteoporotic bone, and as such will exhibit a significantly higher attenuation. The resultant attenuated waveforms can be compared against the original transmitted waveform and a quantitative measure of the attenuation calculated.

4.8.1.2 Velocity / Speed of Sound (VOS / SOS)

VOS or SOS are, as their names suggest, a measure of the speed of transmission, or the time-of-flight, an ultrasound pulse exhibits when passing through bone after normalisation against the distance travelled. Once again the ultrasound pulse will be affected by the nature of the bone, with the higher density and structural integrity of normal bone enabling a discernibly faster transmission of the ultrasound pulse. Ultrasound velocity has an important property related to it, in that it is closely related to elastic modulus or stiffness of the material, and has been used in a number of studies for the investigation of bone properties in-vitro (section 4.9).

Both of the above parameters are better explained and in more depth within two papers, C.M. Langton et al. (1984) and C.M. Langton and C.F. Njeh (1999).

4.8.1.3 Stiffness Index, Quantitative Ultrasound Index, Estimated Heel BMD

Three manufacturers of calcaneal ultrasound devices have developed additional parameters which can be outputted from their QUS systems.

The Lunar Corporation developed the stiffness index as an additional parameter for their system called the Achilles. The stiffness index is derived from a combination of BUA and SOS:

$$\text{Stiffness} = (0.67 \text{ x BUA}) + (0.28 \text{ x SOS}) - 420 \qquad \textbf{Equation 4.4}$$

Hologic have developed two parameters for use with their Sahara QUS machine, the Quantitative Ultrasound Index (QUI) and the Estimated Heel BMD, both derived from combinations of the BUA and SOS results.

$$\text{QUI} = 0.41 * (\text{BUA} + \text{SOS}) - 571 \qquad \textbf{Equation 4.5}$$

$$\text{Estimated Heel BMD} = 0.002592 * (\text{BUA} + \text{SOS}) - 3.687 \qquad \textbf{Equation 4.6}$$

Aloka Co. Ltd. have used the outputs of their Acoustic Osteo-Screener (AOS-100) calcaneal QUS system to develop a new parameter called the osteosono-assessment index (QSI). QSI is a relationship between the SOS and Transmission Index, equation 4.7

$$\text{OSI} = \text{TI} \times \text{SOS}^2 \qquad \textbf{Equation 4.7} \text{ (E. Tsuda-Futami et al., 1999)}$$

where transmission index is closely related to BUA, but is defined as the full-width-half-maximum (FWHM) of the first positive peak of the received waveform. (E. Tsuda-Futami et al., 1999)

4.8.2 The Utility of QUS

The guidelines for the diagnosis of osteoporosis were outlined in section 4.5 and were based around densitometry of the axial skeleton. Because of this, and ultrasound's inability to assess the axial skeleton, the official position of the NOF, NOS, and ISCD is that QUS should not be used to diagnose osteoporosis. However QUS is not a redundant technique as it has been proven to provide quantitative assessments of bone and as such has utility as a diagnostic investigation. The following section aims to highlight and investigate the ability and use of QUS from within the literature.

4.8.2.1 Precision

'Precision is an attribute of a quantitative measurement technique such as bone densitometry and refers to the ability to reproduce the same numerical result in

the setting of no real biological change when the test is repeatedly performed in an identical fashion.' S.L. Bonnick et al. (2001)

As mentioned previously in 4.4.1 the measurement of precision is especially important if the technique is to be used for the monitoring of skeletal change. Most studies that have utilised QUS or other quantitative systems for the assessment of bone quality report their precision, and even the manufacturers provide guidelines for the precision achievable with their systems (Table 4.11)

Table 4.11 The manufacturers' published precisions. Adapted from C.F. Njeh et al. (1997).

Systems	Parameter Measured	Site	Precision ($_{RMS}$CV%)
Lunar Achilles (Lunar corporation, Madison, WI, USA)	BUA and TOF Velocity.	Calcaneus.	BUA 2.0% Velocity 0.5%
CUBA Clinical (McCue, Winchester, UK)	BUA and Limb Velocity.	Calcaneus	BUA 1.3% Velocity 0.3%
DBM Sonic (IGEA, Carpi, Italy)	Limb Velocity	Proximal Phalanges	Velocity 0.5%
SoundScan 2000 (Myriad Ultrasound Systems, Revohot, Israel)	Bone Velocity	Tibial Cortex.	Velocity 0.3%
UBA575+ Hologic Inc. (Waltham, MA, USA)	BUA and Bone Velocity.	Calcaneus	BUA 2.0-4.0% Velocity 0.5%
Sunlight Omnisense (Sunlight Ultrasound Technologies Ltd., Rehovot, Israel.).	SOS	Radius, Proximal Phalanx, Metatarsal, Tibia.	Radius: 0.40% Proximal Phalanx: 0.81% Metatarsal: 0.66% Tibia: 0.45%

The precision of QUS techniques is variable and dependent on the parameter being measured (BUA, VOS, SOS or one of the combined parameters). It is also dependent on the system used, as certain calcaneal QUS systems have the ability to image the calcaneus and, as will be discussed later, this enhances the precision. The

other potential variable is which of the three types of precision is used; the coefficient of variation (CV%), the root mean square coefficient of variation ($_{RMS}$CV%) (C.-C. Glüer et al., 1995) or the standardised coefficient of variation ($_{S}$CV%) (C.F. Njeh et al. 2000, C. Chappard et al. 1999). The method of calculation for these three precisions can be found in section 5.4.1.1. Tables 4.11 to 4.16 show the range and average precision that has been achieved by different study groups using clinically available QUS systems.

Table 4.12 Precision of BUA assessment determined using calcaneal QUS machines. (Mean, Range).

Reference BUA Calcaneus	CV	$_{RMS}$CV	$_{S}$CV
Achilles + (Lunar, Madison, WI, USA)			
L. Rosenthall et al. (1996), F. Blanckaert et al. (1999), P. Hadji et al. (1999), M. Iki et al. (1999), C.H.M. Castro et al. (2000), C.F. Njeh et al. (2000), A. Stewart and D.M. Reid (2000a), A. Ekman et al. (2001), M.K. Karlsson et al. (2001), H.A. Sørensen et al. (2001), F. Hartl et al. (2002), M. Ito et al. (2003), M.A. Krieg et al. (2003)	1.72% 1% - 2.6%	2.17%	4.09% 1.5% - 6.19%
AOS-100 (Aloka Co. Ltd, Tokyo, Japan)			
E. Tsuda-Futami et al. (1999)		1.66%	2.70%
CUBA Clinical (McCue Plc., Hampshire, UK)			
W.C. Graafmans et al. (1996), J.C. Martin and D.M. Reid (1996), S.L. Greenspan et al. (1997), C.F. Njeh et al. (2000), A. Stewart and D.M. Reid (2000a)	5.52% 2.07 - 12.74%	4.52%	4.62% 2.92% - 8.04%
DTU-One (Osteometer, Rodovre, Denmark)			
H.L. Jørgensen and C. Hassager (1997), A. Stewart and D.M. Reid (2000a), G. Falgarone et al. (2004)	4.74% 1.20 - 10.62%		6.77% 4.74 – 9.23%
Osteospace (Medilink, Montpellier, France)			
C.F. Njeh et al. (2001)	1.72%	2.90%	6.09%
QUS-2 (Metra Biosystems, Mountain View, CA, USA)			
S. Cheng et al. (1999), S.L. Greenspan et al. (2001)	2.14% 1.32% - 2.6%		2.56% 1.87% - 2.9%
Sahara (Hologic, Bedford, MA, USA)			
M.L. Frost et al. (1999), Y.Q. He et al. (2000), C.F. Njeh et al. (2000), E.F.L. Dubois et al. (2001), F. Hartl et al. (2002), M. Sosa et al. (2002), M.A. Krieg et al. (2003), F. López-Rodríguez et al. (2003), G. Falgarone et al. (2004)	4.48% 2.72% - 8.17%	2.55% 0.27% -4.83%	4.09% 3.43% - 4.6%
UBA 575X, UBA 575+ (Walker Sonix / Hologic, Waltham, MA, USA)			
M. Agren et al. (1991), J.E. Damilakis et al. (1992), A. Stewart et al. (1994), Funke et al. (1995), H. Kröger et al. (1995), A. Stewart et al. (1996), D.C. Bauer et al. (1997), E. Tsuda-Futami et al. (1999), S.L. Greenspan et al. (1997), C.F. Njeh et al. (2000), Y.Q. He et al. (2000)	3.51% 2.01% - 5%	5.29% 4.27% - 6.3%	4.18% 1.61% - 6.4%
UBIS 3000 / Research System (DMS, France)			
J. Damilakis et al. (1998), C.F. Njeh et al. (2000), C. Chappard et al. (1999) (UBIS Research System)	1.92% 1.35% - 2.49%	1.62% 1.1% - 2.66%	1.76% 1.45% - 2.45%

Table 4.13 Precision of SOS assessment determined using calcaneal QUS machines. (Mean, Range).

Reference SOS Calcaneus	CV	$_{RMS}$CV	$_{S}$CV
Achilles + (Lunar, Madison, WI)			
L. Rosenthall et al. (1996), F. Blanckaert et al. (1999), P. Hadji et al. (1999), M. Iki et al. (1999), C.H.M. Castro et al. (2000), C.F. Njeh et al. (2000), A. Stewart and D.M. Reid (2000a), A. Ekman et al. (2001), M.K. Karlsson et al. (2001), H.A. Sørensen et al. (2001), F. Hartl et al. (2002), M. Ito et al. (2003), M.A. Krieg et al. (2003)	0.27% 0.2% - 0.5%	0.33%	3.23 1.6% - 4.6%
AOS-100 (Aloka Co. Ltd, Tokyo, Japan)			
C.F. Njeh et al. (2000), E. Tsuda-Futami et al. (1999)		0.175% 0.15% - 0.20%	2.44% 1.74% - 3.14%
CUBA Clinical (McCue Plc., Hampshire, UK)			
W.C. Graafmans et al. (1996), J.C. Martin and D.M. Reid (1996), C.F. Njeh et al. (2000), A. Stewart and D.M. Reid (2000a)	0.75% 0.28% - 1.4%	0.42%	4.34% 2.81% - 5.05%
DTU-One (Osteometer, Rodovre, Denmark)			
A. Stewart and D.M. Reid (2000a) G. Falgarone et al. (2004)	0.89% 0.08% - 3.94%		5.97% 4.47% - 6.94%
Osteospace (Medilink, Montpellier, France)			
C.F.Njeh et al. (2001)	0.64%	0.8%	3.87%
Sahara (Hologic, Bedford, MA, USA)			
M.L. Frost et al. (1999), Y.Q. He et al. (2000), C.F. Njeh et al. (2000), F. Hartl et al. (2002), M. Sosa et al. (2002), M.A. Krieg et al. (2003), F. López-Rodríguez et al. (2003), G. Falgarone et al. (2004)	0.3% 0.22% - 0.4%	0.17% 0.02% - 0.32%	3.94% 3.2% - 4.67%
UBA 575+ (Walker Sonix / Hologic, Waltham, MA, USA)			
E. Tsuda-Futami et al. (1999), Y.Q. He et al. (2000), C.F. Njeh et al. (2000)	0.61%	0.13% 0.11% - 0.15%	5.78% 5.13% - 6.1%
UBIS 3000 / Research System (DMS, France)			
J. Damilakis et al. (1998), C.F. Njeh et al. (2000), C. Chappard et al. (1999) (UBIS Research System)	0.27% 0.24% – 0.30%	0.16% 0.1% - 0.3%	2.16% 1.17% - 4.02%

Table 4.14 Precision of Manufacturer derived combination parameters, (Stiffness index, QUI, Est. Heel BMD, OSI) determined using calcaneal QUS machines. (Mean, Range).

Reference Stiffness / QUI / Est. Heel BMD	CV	$_{RMS}$CV	$_{S}$CV
Achilles + (Lunar, Madison, WI) Stiffness Index			
L. Rosenthall et al. (1996), S.L. Greenspan et al. (1997), F. Blanckaert et al. (1999), P. Hadji et al. (1999), M. Iki et al. (1999), C.H.M. Castro et al. (2000), A. Stewart and D.M. Reid (2000a), A. Ekman et al. (2001), M.K. Karlsson et al. (2001), H.A. Sørensen et al. (2001), F. Hartl et al. (2002), M. Ito et al. (2003), M.A. Krieg et al. (2003)	2.08% 1.25% - 4.38%		2.83% 1.6% - 4.7%
AOS-100 (Aloka Co. Ltd, Tokyo, Japan) Osteo Sono-assessment Index (OSI)			
E.Tsuda-Futami et al. (1999)		2.16%	2.66%
Sahara (Hologic, Bedford, MA, USA) Est. heel BMD, Quantitative Ultrasound Index (QUI)			
(Est. Heel BMD) M.L.Frost et al. (1999) (QUI) Y.Q.He et al. (2000), F.Hartl et al. (2002), M.Sosa et al. (2002), M.A.Krieg et al. (2003), F.López-Rodríguez et al. (2003)	2.96% 1.64% - 4.15%	0.09%	2.96% 2.2% - 3.8%

Table 4.15 Precision of Distal Radius SOS assessment determined using the Sunlight Omnisense QUS machine. (Mean, Range).

Reference	CV	$_{RMS}$CV	$_{S}$CV
Sunlight Omnisense (Sunlight Omnisense Technologies Ltd., Rehovot, Israel)			
D. Hans et al. (1999), R. Barkmann et al. (2000), M. Weiss et al. (2000), W.M. Drake et al. (2001), K.M. Knapp et al. (2001), J. Damilakis et al. (2003a), K.M. Knapp et al. (2004)	0.61% 0.4% - 0.87%	0.6% 0.2% - 1.01%	2.78% 1.4% - 4.4%

Table 4.16 Precision of Proximal Phalanx SOS assessment determined using either the DBM Sonic 1200, the IGEA Bone Profiler or the Sunlight Omnisense QUS systems. (Mean, Range).

Reference	CV	$_{RMS}$CV	$_{S}$CV
DBM Sonic 1200 (IGEA, Carpi, Italy)			
F.E. Alenfeld et al. (1998), J.Y Reginster et al. (1998), F. Blanckaert et al. (1999), J. Joly et al. (1999), A. Montagnani et al. (2000), C. Wüster et al. (2000), A. Ekman et al. (2001), P. Gerdham et al. (2002), H. Rico et al. (2002), B. Drozdzowska et al. (2003), M.A. Krieg et al. (2003)	1.12% 0.5% - 2.8%	0.77% 0.38% - 1.13%	5.67% 3.62% - 9.47%
IGEA Bone Profiler (IGEA, Carpi, Italy)			
R. Giardino et al. (2002), F. Hartl et al. (2002)	0.6%	0.64%	4.5%
Sunlight Omnisense (Sunlight Omnisense Technologies Ltd., Rehovot, Israel)			
D. Hans et al. (1999), R. Barkmann et al. (2000), M. Weiss et al. (2000), W.M. Drake et al. (2001), K.M. Knapp et al. (2001), J. Damilakis et al. (2003a), K.M. Knapp et al. (2004)	1.28% 0.81% - 2.04%	0.8% 0.2% - 1.22%	3.5% 1.8% - 5%

Table 4.17 Precision of Mid-Shaft Tibia SOS assessment determined using the SoundScan 2000 or the Sunlight Omnisense QUS machines. (Mean, Range).

Reference Mid-Shaft Tibia SOS	CV	$_{RMS}$CV	$_{S}$CV
SoundScan 2000 (Myriad Ultrasound Systems, Rehovot, Israel)			
L. Rosenthall et al. (1996), S.F. Wang et al. (1997), A.M. Tromp et al. (1999)	0.29% 0.2% - 0.4%		2.9% 1.39% - 4.4%
Sunlight Omnisense (Sunlight Omnisense Technologies Ltd., Rehovot, Israel)			
M. Weiss et al. (2000), W.M. Drake et al. (2001), K.M. Knapp et al. (2001), J. Damilakis et al. (2003a), K.M. Knapp et al. (2004)	0.5% 0.32% - 0.66%	0.49% 0.43% - 0.58%	2.3% 1.3% - 3.5%

The assessment of SOS appears to have a superior level of CV% and $_{RMS}$CV % precision in comparison to BUA and the combined parameters; this is due to the nature of the measurement results. SOS is in values of m/s which registers in values of 1400+m/s and in the case of the Sunlight system 4000+m/s; however, the actual range of measurement values is within ± 400m/s. In order to account for this, the most reliable comparison of the precision of the different techniques is to use the sCV%. This takes into account the magnitude of the measurement values and normalises it against the standard deviation of the population (C.F.Njeh et al., 2000). From tables 4.11 to 4.16, no system attained precision that was better than 2%, double that of the reported precision for DXA (Table 4.3) with the average sCV% of 4.41%, 3.87%, 2.85%, for BUA, SOS and the Combined parameters from measurement of the Calcaneus, and 2.78%, 4.85% and 2.54% of the SOS measured at the Distal Radius, Proximal Phalanx and Mid-shaft Tibia respectively.

Factors Affecting Precision

The level of precision error is one of the main reasons the use of QUS as a technique to monitor skeletal change is not feasible; however, the precision error is not a fault of the machine itself, but is caused by a number of different factors which combine to produce the error. The two most significant causes of error come from repositioning and either oedema or excess soft tissue.

Repositioning

A QUS investigation is performed on a region of interest (ROI) specific to the measurement site and the QUS system. If the repositioning of the patient causes an adjustment in the ROI with respect to the measurement site, then the resultant scan will be performed on a distinctly different area of bone, with the resultant difference between the two measurements considered to be the precision error. The effect of repositioning on ultrasound in transmission, or as used in the calcaneal assessments has been investigated specifically in two different studies. The first, by W.D. Evans et al. (1995), used a water based calcaneal system to investigate the effect that movement of the foot had in relation to the measurement results. Table 4.18 shows the results from the study and demonstrates that even small movements and rotation of the foot can provide precision errors of up to 9%. The advantage of having a fixed ROI, or the ability to ensure the ROI is correctly selected was highlighted in the second study, by H.L. Jørgensen et al. (1997), which used a calcaneal assessment device called the DTU-One (Osteometer, Rodovre, Denmark). The advantage of this system over other calcaneal systems is that it allows for the imaging of the calcaneus and a more precise

selection of the ROI which, in this study, reduced the precision from 3.87% to 1.20%, a clear indication of the importance of repositioning between scans.

Table 4.18 The potential repercussions of repositioning on the precision error (adapted from W.D. Evans et al., 1995).

Variable	Normal Value	Maximum likely variation	Maximum % BUA error
Rotation about long axis of leg.	0^o	5^o	9.2
Rotation about long axis of foot.	0^o	1^o	1.5
Translation across tank.	centre	1cm	2.0
Translation heel-toe.	7.5mm	2mm	9.2
Translation dorsal-plantar.	7.5mm	1mm	1.8

There are no studies into the effects of repositioning errors for the axial method of ultrasound transmission used in the Sunlight Omnisense system, but it is clear that any movement of the ROI will affect the measurement result and thus provide a precision error.

Oedema or Excess Soft Tissue

Both oedema and excess soft tissue affect the measurement in transmission in the same way and, with transmission having to pass through soft tissue on both sides of the site of measurement, the potential for it to affect both the attenuation and the velocity of the ultrasound is high. A. Johansen et al. (1997) investigated the effects of oedema and found that the potential effects could be up to 1.4% difference in the VOS results, and 14.2% difference in the BUA results. Once again the effects of oedema and excess soft tissue have not been investigated with relation to the axial mode of ultrasound transmission, but the ability of the technique to work requires the distance

between the ultrasound transducer and the bone to be as small as possible, a factor which will be adversely affected if either of the above conditions are present.

4.8.2.2 Inter-site Correlations

The correlations between the measurement values obtained from QUS investigations of the peripheral skeleton and densitometry investigations of the axial skeleton have been extensively investigated, and have provided a broad range of correlations which vary in both magnitude and significance. Tables 4.18 to 4.21 show the correlations that have been achieved previously by the different QUS investigations.

Table 4.19 The range and mean Pearson's correlations for the QUS systems prediction of BMD at the forearm.

QUS Assessment	References		Correlations (r)
BMC / BMD Forearm			
BUA Calcaneus	V. Poll et al. (1986), C.J. Hosie et al. (1987), P. Rossman et al. (1989), E.V. McCloskey et al. (1990), J.G. Truscott et al. (1992), H. Kröger et al. (1995), S. Minisola et al. (1995), P. Ross et al. (1995), S.H. Prinns et al. (1999), H.A. Sørensen et al. (2001), M.M.M. Saleh et al. (2002)	Female	Range: 0.25 – 0.85 Average: 0.533 St.Dev: 0.17
		Male + Female Combined	Range: 0.29 – 0.80 Average: 0.546 St.Dev: 0.24
		Male	r = 0.30
VOS Calcaneus	P. Rossman et al. (1989), S. Minisola et al. (1995), H.A. Sørensen et al. (2001), M.M.M. Saleh et al. (2002)	Female	Range: 0.49 – 0.66 Average: 0.574 St.Dev: 0.06
		Male + Female Combined	r = 0.68

Table 4.20 The range and mean Pearson's correlations for the QUS systems prediction of BMD at the forearm.

QUS Assessment	References		Correlations (r)
BMC / BMD Lumbar Spine			
BUA Calcaneus	D.T. Baran et al. (1988), P. Rossman et al. (1989), E.V. McCloskey et al. (1990), H. Resch et al. (1990), M. Agren et al. (1991), D.T. Baran et al. (1991), B. Lees and J.C. Stevenson (1993), J.G. Truscott et al. (1992), A. Massie et al. (1993), S. Palacios et al. (1993), H. Young et al. (1993), K.G. Faulkner et al. (1994), R.J.M. Herd et al. (1994), L.M. Salamone et al. (1994), K. Brooke-Wavell et al. (1995), M. Funke et al. (1995), H. Kröger et al. (1995), S. Minisola et al. (1995), M. Moris et al. (1995), L. Rosenthall et al. (1995), P. Ross et al. (1995), C.H. Turner et al. (1995), J.L. Cunningham et al. (1996), W.C. Graafmans et al. (1996), J.C. Martin and D.M. Reid (1996), P.L.A. Van Daele et al. (1996), C. Cepollaro et al. (1997), S.L. Greenspan et al. (1997), J. Damilakis et al. (1998), A. Johansen et al. (1999), A.M. Tromp et al. (1999), A. Çetin et al. (2001), E.F.L. Dubois et al. (2001), S.L. Greenspan et al. (2001), H.L. Jørgensen et al (2001), C.F. Njeh et al. (2001), H.A. Sørensen et al. (2001), P. Gerdhem et al. (2002), G. Falgarone et al. (2004)	Female	Range: 0.26 – 0.83 Average: 0.48 St.Dev: 0.12
		Male + Female Combined	Range: 0.34 – 0.81 Average: 0.51 St.Dev: 0.16
		Male	Range: 0.28 – 0.32 Average: 0.3 St.Dev: 0.03
VOS Calcaneus	P. Rossman et al. (1989), B. Lees and J.C. Stevenson (1993), R.J.M. Herd et al. (1994), K.G. Faulkner et al. (1994), S. Minisola et al. (1995), M. Moris et al. (1995), L. Rosenthall et al. (1995), J.L. Cunningham et al. (1996), W.C. Graafmans et al. (1996), C. Cepollaro et al. (1997), J. Damilakis et al. (1998), A. Johansen et al. (1999), A.M. Tromp et al. (1999), A. Çetin et al. (2001), H.L. Jørgensen et al (2001), C.F. Njeh et al. (2001), H.A. Sørensen et al. (2001), P. Gerdhem et al. (2002), G. Falgarone et al. (2004), J. Schneider et al. (2004)	Female	Range: 0.11 – 0.64 Average: 0.43 St.Dev: 0.12
		Male + Female Combined	Range: 0.49 – 0.67 Average: 0.58 St.Dev: 0.13
		Male	Range: 0.33 – 0.35 Average: 0.34 St.Dev: 0.01
SOS Radius	K.M. Knapp et al. (2001), J. Damilakis et al. (2003a)	Female	Range: 0.31 – 0.45 Average: 0.38 St.Dev: 0.1
SOS Phalanx	F.E. Alenfeld et al. (1998), F. Blanckaert et al. (1999), G.P. Feltrin et al. (2000), C. Wüster et al. (2000), K.M. Knapp et al. (2001), P. Gerdhem et al. (2002), J. Damilakis et al. (2003a), S. Gnudi and C. Ripamonti (2004), J. Schneider et al. (2004)	Female	Range: 0.1 – 0.52 Average: 0.35 St.Dev: 0.12
		Male	r = 0.179
SOS Tibia	J.L. Cunningham et al. (1996), A.M. Tromp et al. (1999), K.M. Knapp et al. (2001), J. Damilakis et al. (2003a)	Female	Range: 0.3 – 0.54 Average: 0.39 St.Dev: 0.1

Table 4.21 The range and mean Pearson's correlations for the QUS systems prediction of BMD at the Femoral Neck.

QUS Assessment	References		Correlations (r)
BMC / BMD Femoral Neck			
BUA Calcaneus	D.T. Baran et al. (1988), M. Agren et al. (1991), D.T. Baran et al. (1991), A. Massie et al. (1993), R.J.M. Herd et al. (1994), M. Funke et al. (1995), H. Kröger et al. (1995), L. Rosenthall et al. (1995), J.L. Cunningham et al. (1996), W.C. Graafmans et al. (1996), J.C. Martin and D.M. Reid (1996), S.L. Greenspan et al. (1997), H.L. Jørgensen and C. Hassager (1997), J. Damilakis et al. (1998), A. Johansen et al. (1999), A.M. Tromp et al. (1999), Y.Q. He et al. (2000), C.F. Njeh et al. (2000), A. Çetin et al. (2001), J. Damilakis et al. (2001), E.F.L. Dubois et al. (2001), A. Ekman et al. (2001), S.L. Greenspan et al. (2001), H.L. Jørgensen et al (2001), C.F. Njeh et al. (2001), H.A. Sørensen et al. (2001), P. Gerdhem et al. (2002), M.D. Stefano and G.C. Isaia (2002), J. Damilakis et al. (2004), G. Falgarone et al. (2004)	Female	Range: 0.24 – 0.87 Average: 0.483 St.Dev: 0.143
		Male + Female Combined	r = 0.43
		Male	r = 0.37
VOS Calcaneus	R.J.M. Herd et al. (1994), L. Rosenthall et al. (1995), J.L. Cunningham et al. (1996), W.C. Graafmans et al. (1996), J.C. Martin and D.M. Reid (1996), J. Damilakis et al. (1998), A. Johansen et al. (1999), A.M. Tromp et al. (1999), Y.Q. He et al. (2000), C.F. Njeh et al. (2000), J. Damilakis et al. (2001), A. Çetin et al. (2001), H.L. Jørgensen et al (2001), C.F. Njeh et al. (2001), H.A. Sørensen et al. (2001), P. Gerdhem et al. (2002), J. Damilakis et al. (2004), G. Falgarone et al. (2004), J. Schneider et al. (2004)	Female	Range: 0.14 – 0.59 Average: 0.394 St.Dev: 0.1
		Male	r = 0.29
SOS Radius	K.M. Knapp et al. (2001), J. Damilakis et al. (2003a), T.V. Nguyen et al. (2004)	Female	Range: 0.21 – 0.43 Average: 0.29 St.Dev: 0.12
SOS Phalanx	F.E. Alenfeld et al. (1998), F. Blanckaert et al. (1999), A. Ekman et al. (2001), K.M. Knapp et al. (2001), P. Gerdhem et al. (2002), J. Damilakis et al. (2003a), J. Damilakis et al. (2004), S. Gnudi and C. Ripamonti (2004), T.V. Nguyen et al. (2004), J. Schneider et al. (2004)	Female	Range: 0.09 – 0.48 Average: 0.315 St.Dev: 0.1
		Male	r = 0.034
SOS Tibia	A.M. Tromp et al. (1999), K.M. Knapp et al. (2001), J. Damilakis et al. (2003a), T.V. Nguyen et al. (2004)	Female	Range: 0.07 – 0.35 Average: 0.252 St.Dev: 0.11

Table 4.22 The range and mean Pearson's correlations for the QUS systems prediction of BMD at the Total Hip.

QUS Assessment	References		Correlations (r)
BMC / BMD Total Hip			
BUA Calcaneus	P. Rossman et al. (1989), B. Lees and J.C. Stevenson (1993), J.G. Truscott et al. (1992), S. Palacios et al. (1993), H. Young et al. (1993), K.G. Faulkner et al. (1994), L.M. Salamone et al. (1994), K. Brooke-Wavell et al. (1995), S. Minisola et al. (1995), C.H. Turner et al. (1995), H.L. Jørgensen and C. Hassager (1997), A. Johansen et al. (1999), S.H. Prinns et al. (1999), Y.Q. He et al. (2000), C.F. Njeh et al. (2000), E.F.L. Dubois et al. (2001), H.L. Jørgensen et al (2001), C.F. Njeh et al. (2001), H.A. Sørensen et al. (2001), G. Falgarone et al. (2004)	Female	Range: 0.31 – 0.68 Average: 0.48 St.Dev: 0.1
		Male + Female Combined	Range: 0.43 – 0.5 Average: 0.47 St.Dev: 0.05
		Male	r = 0.34
VOS Calcaneus	P. Rossman et al. (1989), B. Lees and J.C. Stevenson (1993), K.G. Faulkner et al. (1994), S. Minisola et al. (1995), A. Johansen et al. (1999), S.H. Prinns et al. (1999), Y.Q. He et al. (2000), C.F. Njeh et al. (2000), H.L. Jørgensen et al (2001), C.F. Njeh et al. (2001), H.A. Sørensen et al. (2001), G. Falgarone et al. (2004), J. Schneider et al. (2004)	Female	Range: 0.3 – 0.62 Average: 0.44 St.Dev: 0.1
		Male + Female Combined	r = 0.56
		Male	Range: 0.37 – 0.5 Average: 0.43 St.Dev: 0.09
SOS Radius	K.M. Knapp et al. (2001), J. Damilakis et al. (2003a)	Female	Range: 0.25 – 0.47 Average: 0.36 St.Dev: 0.16
SOS Phalanx	F.E. Alenfeld et al. (1998), F. Blanckaert et al. (1999), A. Ekman et al. (2001), K.M. Knapp et al. (2001), P. Gerdhem et al. (2002), J. Damilakis et al. (2003a), J. Damilakis et al. (2004), S. Gnudi and C. Ripamonti (2004), T.V. Nguyen et al. (2004), J. Schneider et al. (2004)	Female	Range: 0.31 – 0.48 Average: 0.375 St.Dev: 0.08
		Male	r = 0.058
SOS Tibia	K.M. Knapp et al. (2001), J. Damilakis et al. (2003a)	Female	Range: 0.27 – 0.3 Average: 0.29 St.Dev: 0.021

Within the female study cohorts the average correlations between the QUS investigations of the calcaneus and the axial skeleton were found to be between 0.40 and 0.60, which indicates a moderate to good level of agreement. The peripheral sites such as the distal radius, the proximal phalanx and mid-shaft tibia failed to provide correlations that were of the same magnitude, with the averages between 0.3 and 0.4. The differences in the correlations between the genders were minor, with the males

displaying a slightly lower level of correlation between sites. There is, however, a marked reduction in the number of studies which have investigated males, in comparison to studies which have investigated females; this is mainly due to the increased prevalence of osteoporosis within the female population. This is slowly changing as male osteoporosis has recently started to be thoroughly investigated.

Although the correlations are only moderate and good at best, they are mostly statistically significant and show that there is a link between the condition of one skeletal site and another. This finding opened the possibility that QUS at one site could be used to predict the skeletal status of other skeletal sites, and in particular identify patients with osteoporosis or low bone density of the axial skeleton.

4.8.2.3 Discriminatory Ability

The discriminatory ability of a technique refers to its ability to correctly diagnose an individual in relation to his or her skeletal condition. In most studies the definitive skeletal condition is taken to be the results of a DXA scan, and a number of studies have shown that the measurement results from QUS techniques were significantly lower in individuals that have DXA diagnosed osteoporosis of their axial skeleton, than in individuals considered normal (Table 4.23). The ability of the two techniques to agree on the condition of the skeleton opens the opportunity that the peripheral QUS systems have the ability to correctly classify individuals with relation to their DXA results.

Table 4.23 Previous studies and QUS systems utilised, that have shown a significant difference in QUS measurement results between DXA confirmed osteoporotic individuals and normal individuals.

Ultrasound System	References
BUA Calcaneus	
Achilles (Lunar Corporation, Madison, WI, USA)	P. Hadji et al. (1999), J.L. Cunningham et al. (1996)
CUBA Clinical (McCue Plc., Hampshire, UK)	W.C. Graafmans et al. (1996), S.L. Greenspan et al. (1997), A.M. Tromp et al. (1999)
Sahara (Hologic Inc. Bedford, MA, USA)	A. Çetin et al. (2001), A. Díez-Pérez et al. (2003)
UBA 575+ or UBA 575X (Hologic Inc., Waltham, MA, USA)	S.L. Greenspan et al. (1997), M. Agren et al. (1991)
UBIS 3000 (DMS, France)	J. Damilakis et al. (1998)
SOS Calcaneus	
Achilles (Lunar Corporation, Madison, WI, USA)	J.L. Cunningham et al. (1996)
CUBA Clinical (McCue Plc., Hampshire, UK)	A.M. Tromp et al. (1999)
Sahara (Hologic Inc. Bedford, MA, USA)	A. Díez-Pérez et al. (2003)
UBIS 3000 (DMS, France)	J. Damilakis et al. (1998)
Stiffness / QUI/ Est. Heel BMD	
Achilles (Lunar Corporation, Madison, WI, USA)	S.L. Greenspan et al. (1997), P. Hadji et al. (1999)
Sahara (Hologic Inc. Bedford, MA, USA)	A. Çetin et al. (2001), A. Díez-Pérez et al. (2003)
SOS Phalanx	
DBMSonic 1200 (IGEA, Carpi, Italy)	J.Y. Reginster et al. (1998), J. Joly et al. (1999)
SOS Tibia	
SoundScan 2000 (Myriad Ultrasound System, Rehovot, Israel)	A.M. Tromp et al. (1999)

Only a few studies have attempted to review the agreement between the diagnostic classifications of a QUS system in relation to the DXA, within the same study population. The studies all used the Kappa index, an index which provides a quantitative value for the agreement between the diagnoses of two different systems. The results of the five studies which used the technique are shown in Table 4.24. The results of these studies demonstrated a level of agreement that could only be described as fair although the study by I. Lernbass et al. (2002) demonstrated a moderate

agreement between both BUA and VOS diagnoses in comparison to the DXA determined femoral neck diagnoses.

Table 4.24 Kappa indices for the comparison between QUS diagnoses and DXA diagnoses.

Authors	QUS Sytems	DXA Measurement Site	QUS Parameter	
Calcaneal QUS			BUA	VOS
A. Stewart and D.M. Reid (2000)	CUBA Clinical + DTU-One	Spine	CUBA: 0.19 DTU-One: 0.23	DTU-One: 0.05
		Femoral Neck	CUBA: 0.31 DTU-One: 0.21	DTU-One: 0.13
C.R. Krestan et al. (2001)	DTU-One	Spine	0.28	n.s.
		Total Hip	0.37	n.s.
I. Lernbass et al. (2002)	DTU-One	Lumbar Spine	0.28	0.28
		Femoral Neck	0.46	0.46
S.Grampp et al. (1997)	Walker Sonix: WS Luner Achilles: LA	Femoral Neck	WS: n.s. LA: 0.17	WS: 0.25 LA: 0.28
		Trochanter	WS: 0.33 LA: 0.07	WS: 0.33 LA: 0.37
Tibial QUS			Tibial SOS	
K.I.I. Kim et al. (2001)	SoundScan Compact	Spine	0.35	
		Femoral Neck	0.33	

The difference seen in the indices can be viewed in two different ways, either optimistic or pessimistic; the optimistic trend refers to the QUS technique as having underestimated the number of osteoporotic individuals, while the pessimistic trend refers to the opposite, i.e. that the QUS investigation has over diagnosed the number of osteoporotic individuals with relation to DXA. Of the studies that presented the breakdowns of the study populations in relation to calcaneal assessment, the results were mixed; I. Lernbass et al. (2002) showed the BUA results to have a pessimistic view, but A. Stewart and D.M. Reid (2000) and V. Naganathan et al. (1999) both showed BUA to be slightly over optimistic. The VOS results were also mixed with I. Lernbass et al. (2002) and A. Stewart and D.M. Reid (2000) both showing a highly optimistic view of the results, but with V. Naganathan et al. (1999) showing a slightly pessimistic view.

The results of the studies (K.I.I. Kim et al., 2001, J. Damilakis et al., 2003b) which used alternative techniques for assessment of the peripheral skeletal sites such as the radius, phalanges and tibia all showed an optimistic trend in relation to DXA. The level of disagreement between the studies is most likely due to the nature of the skeletal sites with both measurement values providing the correct diagnoses for the specific site but there being an inhomogeneity in the condition at different skeletal sites.

The significant correlations provide proof that there is a relationship between one skeletal site and another and the fact that individuals with osteoporosis at the axial skeleton can be seen to have low bone quality when assessed with QUS shows that QUS has a good degree of discriminatory ability. The level of discriminatory ability of the QUS techniques gives rise to the opportunity of using QUS as a tool for the differentiation of individuals with low axial BMD from normals, so as to pre-screen large populations to reduce the number of referrals for densitometry investigations.

4.8.2.4 Predictive Ability

Tables 4.24 to 4.27 show the area (AUC) from under the receiver operator characteristic curves (ROC), which can be interpreted using the guidelines laid out by R.Kent and J.Patrie (2005) (sections 4.7 and 5.4.2.3)

Table 4.25 Area Under (AUC) Receiver Operating Characteristic (ROC) Curves for the prediction of T-scores ≤ -2.5, or T-scores ≤ -1, using BUA assessment of the Calcaneus.

References BUA Calcaneus	Prediction of Osteoporosis AUC	Prediction of Osteoporosis + Osteopenia AUC
Achilles (Lunar Corporation, Madison, WI, USA)		
P. Hadji et al. (1999)	0.83	
H.A. Sørensen et al. (2001)	LS = 0.69 FN = 0.81	
CUBA Clinical (McCue Plc., Hampshire, UK)		
R.J.M. Herd et al. (1994)		LS = 0.75 FN = 0.72
S.L. Greenspan et al. (1997)	0.90	
C.M. Langton et al. (1999)	0.76	0.688
C.M. Langton and D.K. Langton (2000)	0.791	0.773
A. Stewart and D.M. Reid (2000b)	Hip = 0.856 Spine = 0.816	0.768
DTU-one (Osteometer MediTech, Hawthorne, CA, USA)		
A. Stewart and D.M. Reid (2000b)	Hip = 0.847 Spine = 0.888	0.799
G.Falgarone et al. (2004)	0.712	
Sahara (Hologic Inc. Bedford, MA, USA)		
A. Çetin et al. (2001)	0.751	
A. Díez-Pérez et al. (2003)	0.678	
F. López-Rodríguez et al. (2003)	0.75	
G. Falgarone et al. (2004)	0.697	
UBA 575X (Hologic Inc., Waltham, MA, USA)		
M. Agren et al. (1991)	0.84	
S.L. Greenspan et al. (1997)	0.88	
UBIS 3000 (DMS, France)		
J. Damilakis et al. (1998)	0.87	

Table 4.26 Area Under (AUC) Receiver Operating Characteristic (ROC) Curves for the prediction of T-scores ≤ -2.5, or T-scores ≤ -1, using SOS assessment of the Calcaneus.

References SOS Calcaneus	Prediction of Osteoporosis AUC	Prediction of Osteoporosis + Osteopenia AUC
Achilles (Lunar Corporation, Madison, WI, USA)		
P.Hadji et al. (1999)	0.84	
H.A.Sørensen et al. (2001)	LS = 0.68 FN = 0.78	
CUBA Clinical (McCue Plc., Hampshire, UK)		
R.J.M.Herd et al. (1994)		LS = 0.72 FN = 0.68
C.M.Langton and D.K.Langton (2000)	0.717	0.783
A. Stewart and D.M. Reid (2000b)	Hip = 0.871 Spine = 0.820	0.739
DTU-one (Osteometer MediTech, Hawthorne, CA, USA)		
G.Falgarone et al. (2004)	0.703	
A. Stewart and D.M. Reid (2000b)	Hip = 0.842 Spine = 0.871	0.779
Sahara (Hologic Inc. Bedford, MA, USA)		
A.Çetin et al. (2001)	0.722	
A.Díez-Pérez et al. (2003)	0.662	
F.López-Rodríguez et al. (2003)	0.754	
G.Falgarone et al. (2004)	0.735	
UBIS 3000 (DMS, France)		
J.Damilakis et al. (1998)	0.85	
J.Damilakis et al. (2001)	0.82	
J.Damilakis et al. (2001)	0.75	

Table 4.27 Area under (AUC) Receiver Operating Characteristic (ROC) Curves for the prediction of T-scores ≤ -2.5, or T-scores ≤ -1, using manufacturer derived combination parameters from the assessment of the Calcaneus.

References Stiffness / QUI/ Est. Heel BMD	Prediction of Osteoporosis AUC	Prediction of Osteoporosis + Osteopenia AUC
Achilles (Lunar Corporation, Madison, WI, USA)		
S.L.Greenspan et al. (1997)	0.93	
P.Hadji et al. (1999)	0.88	
H.A.Sørensen et al. (2001)	LS = 0.71 FN = 0.82	
Sahara (Hologic Inc. Bedford, MA, USA)		
A.Díez-Pérez et al. (2003) A. QUI B. Est. Heel BMD	A. 0.67 B. 0.67	
F.López-Rodríguez et al. (2003)	0.76	

Table 4.28 Area under (AUC) Receiver Operating Characteristic (ROC) Curves for the prediction of T-scores ≤ -2.5, or T-scores ≤ -1 using SOS assessment of the Distal Radius, Proximal Phalanx or Mid-Shaft Tibia.

References	Prediction of Osteoporosis AUC	Prediction of Osteoporosis + Osteopenia AUC
SOS Distal Radius Sunlight Omnisense 7000S (Sunlight Technologies, Rehovot, Israel)		
J.Damilakis et al. (2003b)	0.659	0.609
SOS Proximal Phalanx DBMSonic 1200 (IGEA, Carpi, Italy)		
J.Joly et al. (1999)	0.803	
J.Y.Reginster et al. (1998)	0.82	
SOS Proximal Phalanx Sunlight Omnisense 7000S (Sunlight Technologies, Rehovot, Israel)		
J.Damilakis et al. (2003b)	0.709	0.69

Tables 4.24 to 4.27 show that for the prediction of osteoporosis at the axial skeleton, the ability of quantitative ultrasound is 'good'. (Averages, all AUC values = 0.783, BUA Calcaneus = 0.798, SOS Calcaneus = 0.774, Combined parameters = 0.777.) However, for the prediction of low BMD (T-score ≤ -1) the ability was reduced, although could still be considered 'good' (Average, all AUC values = 0.73, BUA Calcaneus = 0.75, SOS Calcaneus = 0.74).

The investigation into the diagnostic abilities of the QUS techniques enabled a review of the threshold values that were applied to the different systems, and was of particular interest bearing in mind the governing bodies mentioned previously in section 4.5, considered the use of the WHO threshold values for QUS investigations as unsuitable. The only paper known to the author for the variation of the thresholds of the Sunlight Omnisense system was performed by K.M. Knapp et al. (2004), in which the authors recommend that, for the diagnosis of osteoporosis, the T-scores that should be used are -2.6, -3.0 and -3.0 for the distal radius, proximal phalanx and mid-shaft tibia respectively, and for osteopenia -1.4, -1.6 and -2.3 respectively.

A number of different studies have presented T-score thresholds for use with calcaneal QUS investigations, although only two studies were specifically investigating

the T-score threshold levels. The first study by M.L. Frost et al. (2000) investigated three calcaneal devices, the Sahara (Hologic Inc. Bedford, MA, USA), the DTU-one (Osteometer MediTech, Hawthorne, CA, USA) and the UBA 575+ (Hologic Inc., Waltham, MA, USA) although the latter is now obsolete. For the three devices in unison the recommended T-score threshold for the diagnosis of osteoporosis was -1.80 for both BUA and VOS; however, for the Sahara system a T-score of -1.61 and -1.94 for BUA and VOS respectively were recommended, and for the DTU-One system these would be adjusted to -1.45 and -2.10 respectively. The second study by J. Damilakis et al. (2001) focused solely on the UBIS 3000 system (UBIS, DMS, France) and concluded that a T-score of -1.3 for BUA and -1.5 for SOS were optimum for the discrimination of osteoporosis.

The only study which presents results based on the CUBA Clinical was by C.M. Langton et al. (1999), in which the recommended threshold for the discrimination of osteoporotic individuals was set at 63 dB MHz^{-1}, which equates to a T-score of between -1.58 and -1.64.

The only other thresholds that have been suggested both come from studies in which the authors are using QUS for the preparation of a screening strategy. The first study by M. Gambacciani et al. (2004) reviewed the abilities of a DBM Sonic phalangeal QUS system, and recommended the use of a QUS T-score of -2 as a threshold to distinguish between individuals with moderate and high risk of osteoporosis, with the high risk category falling <-3.2. The screening strategy developed in the study utilised both phalangeal QUS and a fracture risk assessment based on a questionnaire and, dependent on the results of both the investigations, the patients' management was planned. Any individuals obtaining a T-score within the high risk

category bypassed both the questionnaire and the need for a DXA and were placed straight into a suitable course of treatment.

The second study was by P. Dargent-Molina et al. (2003) who developed a screening strategy based on BUA and weight prior to any DXA investigation. The weight limit was set at <59kg which is discernibly lower than that of the pBW technique used in section 4.7, but more importantly the BUA was subdivided to produce three groupings, high, low and very low. The problem is that the thresholds are BUA values in dB MHz^{-1}, and the threshold values are based on a Lunar Achilles (Lunar Corporation, Madison, WI, USA) QUS system and as such the author is unable to convert the results into T-scores.

The 'good' ability of QUS for the prediction of the condition of the axial skeleton enabled the technique to be utilised as a method of screening individuals. The cost effectiveness of this approach has been investigated, C.M. Langton et al. (1997, 1999) suggests that the use of BUA for calcaneal measurements is both a cost effective and improved method for the accurate referral of individuals for DXA; however, M.F.V. Sim et al. (2005) and F. Marín et al. (2004), found that the use of QUS was not a cost effective method of screening, despite its ability as an improved referral procedure.

4.8.2.5 Fracture Prediction and Fracture Risk

Despite this restriction, the research into the abilities of QUS continued, and a large volume of evidence emerged that the utility of QUS does not appear to lie in the diagnosis of Osteoporosis, but in the prediction of an individual's fracture risk. The results within the literature (Tables 4.28 to 4.31) show, on the most part, that individuals

who had sustained fractures displayed significantly lower QUS values in comparison to control subjects.

This finding lead to interest into whether or not QUS had the ability to differentiate individuals that had sustained fractures, from an age matched population. The QUS assessments were being analysed so as to produce odds ratios (OR) relating to the increased probability of an individual sustaining a fracture, for every standard deviation reduction in QUS value. In addition to this, the abilities of the QUS results to correctly diagnose individuals at risk of fracture were made using ROC curves and subsequent calculation of AUC (tables 4.28 to 4.31)

The ORs varied depending on the fracture being predicted, the system performing the prediction, and the number of variables the OR were normalised against. In every study which reported ORs there was a significant increase in risk for every standard deviation reduction in the QUS T-score value.

Not every study agreed that QUS was capable of predicting fracture risk. A. Stewart et al. (1996), M.K. Karlsson et al. (2001) and A. Ekman et al. (2001), found that neither BUA assessment of the Calcaneus, or SOS measured at the Calcaneus, or SOS determined at the proximal Phalanx, were able to differentiate between individuals who had sustained fractures from the control individuals, and studies by F. Blanckaert et al. (1999), M.A. Krieg et al (2003) and J. Schneider et al. (2004) provide AUC values below 0.6, which would indicate the investigations had no diagnostic ability in relation to fracture risk.

Table 4.29 Table showing the studies in which the BUA results at the calcaneus were lower in individuals with fractures and the studies which provided OR and AUC values for the prediction fractures.

Fracture Site	**QUS System**	References	Unadj. OR	Age Adj. OR	Age / Weight / BMI Adj. OR	Multiple Adj. OR	Age / BMD Adj OR	AUC
BUA (dB/MHz) measured at the Calcaneus								
Forearm Fracture	Achilles	M.A. Krieg et al. (2003)			1.5			0.61
	Sahara	M.A. Krieg et al. (2003)			1.7			0.63
	DTU-One	M.M.M. Saleh (2002)	3.1					
	UBA 575	H. Kröger et al. (1995)						
Hip Fracture	Achilles	A.M. Schott et al. (1995), C.H. Turner et al. (1995), D. Hans et al. (1996), C.F. Njeh et al. (2000a), A. Ekman et al. (2001), A. Ekman et al. (2002), D. Hans et al. (2003), M.A. Krieg et al. (2003)	1.9 - 4.70	3.0	1.9 - 3.62	3.7		0.68 - 0.83
	Sahara	Y.Q. He et al. (2000), C.F. Njeh et al. (2000a), D. Hans et al. (2003), M.A. Krieg et al. (2003)	2.7 - 5.18		2.1 - 4.1		2.3	0.71 - 0.84
	UBA 575+	M. Agren et al. (1991), A. Stewart et al. (1994), D.C. Bauer et al. (1997), Y.Q. He et al. (2000), C.F. Njeh et al. (2000a)	3.0	2.0	2.5	1.5	1.3 - 2.6	0.65 - 0.77
	Walker Sonix	D.T.Baran et al. (1988)						
	DTU-One	S.H. Prins et al. (1999), M.M.M. Saleh (2002)						
	UBIS 3000	C.F. Njeh et al. (2000a), J. Damilakis et al. (2004)	2.18		3.4			0.70 - 0.71
	CUBA Clinical	S.M.F. Pluijm et al. (1999), C.F. Njeh et al. (2000a), K.-T. Khaw et al. (2004)	2.3	2.3	2.5	2.22		0.62
	AOS - 100	E. Tsuda-Futami et al. (1999), C.F. Njeh et al. (2000a)			2.4			0.67
Vertebral fracture	Achilles	S. Gonnelli et al. (1995), C.H. Turner et al. (1995), C. Cepollaro et al. (1997), F. Hartl et al. (2002), C.-C. Glüer et al. (2004)	1.56 - 3.9	1.26 - 2.7			2.8	0.65 - 0.79
	Sahara	M.L. Frost et al. (1999), F. Hartl et al. (2002), F. López-Rodríguez et al. (2003)		3.6				0.79 - 0.87
	UBA 575	M. Agren et al. (1991), D.C. Bauer et al. (1995), P. Ross et al. (1995)	1.6		1.8	1.5 - 1.6		
	Osteospace	C.F. Njeh et al. (2001)	2.08		1.62			0.76
	CUBA Clinical	R.J.M. Herd et al. (1993),						
	QUS-2	S.L. Greenspan et al. (2001), C.-C. Glüer et al. (2004)	1.61	1.31 - 2.68				0.65
	UBIS 5000	C.-C. Glüer et al. (2004)	1.56	1.29 - 1.40				0.65
	DTU-One	C.-C. Glüer et al. (2004)	1.45	1.23 - 1.30				0.65

Table 4.29 Continued

Fracture Site	QUS System	References	Unadj. OR	Age Adj. OR	Age / Weight / BMI Adj. OR	Multiple Adj. OR	Age / BMD Adj OR	AUC
BUA (dB/MHz) measured at the Calcaneus Continued								
Mixed Fracture	Achilles	F. Blanckaert et al. (1999), P. Hadji et al. (1999), M.K. Karlsson et al. (2001), P. Gerdhem et al. (2002), M.A. Krieg et al. (2003), M.M. Pinheiro et al. (2003), J. Huopio et al. (2004), A. Devine et al. (2005)	13.5 - 6.0		1.1	1.29 - 1.53		0.53 - 0.89
	Sahara	M.A. Krieg et al. (2003), F. López-Rodríguez et al. (2003), G. Falgarone et al. (2004), J.L. Hernández et al. (2004)		1.48 - 1.58	1.1		1.43	0.54 - 0.69
	UBA 575	M. Funke et al. (1995), D.C. Bauer et al. (1997), S.L. Greenspan et al. (1997),		1.3		1.2	1.1	0.88
	CUBA Clinical	S.L. Greenspan et al. (1997), S.M.F. Pluijm et al. (1999), K.-T. Khaw et al. (2004)	1.8 - 1.95	1.6		1.87 - 1.90		
	DTU-One	M.M.M. Saleh (2002), G. Falgarone et al. (2004)	3.6	2.79			2.49	0.774
	UBIS 3000	J. Damilakis et al. (1998)						
	Osteospace	C.F. Njeh et al. (2001)	2.43		1.79			0.77
	QUS-2	S.L. Greenspan et al. (2001)		2.35				0.623

Table 4.30 Table showing the studies in which the VOS results at the calcaneus were lower in individuals with fractures and the studies which provided OR and AUC values for the prediction fractures.

Fracture Site	QUS System	References	Unadj. OR	Age Adj. OR	Age / Weight / BMI Adj. OR	Multiple Adj. OR	Age / BMD Adj OR	AUC
SOS / VOS (m/s) measured at the Calcaneus								
Forearm Fracture	Achilles	M.A. Krieg et al. (2003)			1.6			0.62
	Sahara	M.A. Krieg et al. (2003)			1.7			0.64
	DTU-One	M.M.M. Saleh (2002)	4.1					
Hip Fracture	Achilles	A.M. Schott et al. (1995), C.H. Turner et al. (1995), D. Hans et al. (1996), C.F. Njeh et al. (2000a), A. Ekman et al. (2001), A. Ekman et al. (2002), D. Hans et al. (2003), M.A. Krieg et al. (2003)	1.9 – 3.97		1.7 – 3.1	2.7		0.70 – 0.80
	Sahara	Y.Q. He et al. (2000), C.F. Njeh et al. (2000a), D. Hans et al. (2003), M.A. Krieg et al. (2003)	2.7 – 5.65		2.3 – 4.54		2.2 – 2.4	0.65 – 0.83
	UBA 575+	Y.Q. He et al. (2000), C.F. Njeh et al. (2000a)	3.2		2.9		2.5 – 2.7	0.71 – 0.78
	DTU-One	S.H. Prins et al. (1999), M.M.M. Saleh (2002)						
	UBIS 3000	C.F. Njeh et al. (2000a), J. Damilakis et al. (2004)	1.88		2.8			0.66 – 0.68
	CUBA Clinical	S.M.F. Pluijm et al. (1999), C.F. Njeh et al. (2000a), K.-T. Khaw et al. (2004)	1.8	1.6	2.1	1.99		0.68
	AOS - 100	E. Tsuda-Futami et al. (1999), C.F. Njeh et al. (2000a)			2.5			0.65
Vertebral fracture	Achilles	S. Gonnelli et al. (1995), C.H. Turner et al. (1995), C. Cepollaro et al. (1997), A. Ekman et al. (2001), F. Hartl et al. (2002), C.-C. Glüer et al. (2004)	1.72 – 4.9	1.49 – 2.8	2.7		3.1	0.67 – 0.80
	Sahara	M.L. Frost et al. (1999), F. Hartl et al. (2002)		3.5 – 5.3				0.761 – 0.89
	Osteospace	C.F. Njeh et al. (2001)	1.71	1.58				0.76
	CUBA Clinical	R.J.M. Herd et al. (1993)						
	DTU-One	C.-C. Glüer et al. (2004)	1.55	1.37 – 1.45				0.66
	UBIS 5000	C.-C. Glüer et al. (2004)	1.65	1.46 – 1.47				0.67
Mixed Fracture	Achilles	F. Blanckaert et al. (1999), P. Hadji et al. (1999), P. Gerdhem et al. (2002), M.A. Krieg et al. (2003), M.M. Pinheiro et al. (2003), J. Huopio et al. (2004), A. Devine et al. (2005)	1.80 – 4.4		1.1	1.39 – 1.80		0.53 – 0.86
	Sahara	M.A. Krieg et al. (2003), F. López-Rodríguez et al. (2003), J.L. Hernández et al. (2004)		1.54 – 2.28			2.02	0.54 – 0.742
	CUBA Clinical	S.M.F. Pluijm et al. (1999), K.-T. Khaw et al. (2004)	1.4 – 1.63	1.3		1.62 - 1.65		
	UBIS 3000	J. Damilakis et al. (1998)						
	Osteospace	C.F. Njeh et al. (2001)	2.0		1.83			0.76
	DTU-One	M.M.M. Saleh (2002), G. Falgarone et al. (2004)	4.7	2.33			2.09	0.74

Table 4.31 Table showing the studies in which the manufacturers combination parameter results from the calcaneus were lower in individuals with fractures and the studies which provided OR and AUC values for the prediction fractures.

Fracture Site	**QUS System**	References	Unadj. OR	Age Adj. OR	Age / Weight / BMI Adj. OR	Multiple Adj. OR	Age / BMD Adj OR	AUC
Stiffness Index / QUI / Est. Heel BMD / OSI								
Forearm Fracture	Achilles	M.A. Krieg et al. (2003)		1.6				0.63
	Sahara	M.A. Krieg et al. (2003)		1.7				0.64
Hip Fracture	Achilles	A.M. Schott et al. (1995), C.H. Turner et al. (1995), C.F. Njeh et al. (2000a), A. Ekman et al. (2001), A. Ekman et al. (2002), D. Hans et al. (2003), M.A. Krieg et al. (2003)	2.2 – 4.51		2.2 – 3.50	3.5		0.69 – 0.82
	Sahara	C.F. Njeh et al. (2000a), Y.Q. He et al. (2000), D. Hans et al. (2003), M.A. Krieg et al. (2003)	5.93		2.4 – 4.76			0.65 – 0.84
	AOS - 100	E. Tsuda-Futami et al. (1999), C.F. Njeh et al. (2000)			2.4			0.69
Vertebral Fracture	Achilles	S. Gonnelli et al. (1995), C.H. Turner et al. (1995), C. Cepollaro et al. (1997), F. Hartl et al. (2002), C.-C. Glüer et al. (2004), J. Schneider et al. (2004)	1.71 - 6.3	1.44 – 3.0			4.1	0.55 – 0.81
	Sahara	M.L. Frost et al. (1999), F. Hartl et al. (2002)		3.8 – 4.8				0.78 – 0.89
Mixed Fracture	Achilles	S.L. Greenspan et al. (1997), F. Blanckaert et al. (1999), P. Hadji et al. (1999), M.K. Karlsson et al. (2001), P. Gerdhem et al. (2002), M.A. Krieg et al. (2003), M.M. Pinheiro et al. (2003), J. Huopio et al. (2004), J. Schneider et al. (2004), A. Devine et al. (2005)	1.72 – 10.8	2.8	1.1	1.76 – 1.90		0.54 – 0.92
	Sahara	M.A. Krieg et al. (2003), F. López-Rodríguez et al. (2003), J.L. Hernández et al. (2004)		1.55	1.2			0.54 – 0.718

Table 4.32 Table showing the studies in which the SOS from peripheral sites other than the calcaneus were lower in individuals with fractures and the studies which provided OR and AUC values for the prediction fractures.

Fracture Site	**QUS System**	References	Unadj. OR	Age Adj. OR	Age / Weight / BMI Adj. OR	Multiple Adj. OR	Age / BMD Adj OR	AUC
Ad-SOS or SOS (m/s) measured at the Proximal Phalanx								
Forearm Fracture	Sunlight Omnisense	K.M. Knapp et al. (2002)	1.85					0.64
	DBM Sonic 1200	R. Giardino et al. (2002), B. Drozdzowska et al. (2003), M.A. Krieg et al. (2003)	0.99	12.03	1.2 – 2.24			0.55 – 0.783
Hip Fracture	Sunlight Omnisense	D. Hans et al. (1999a), J. Damilakis et al. (2004)	2.63 - 2.7	2.0	2.0			0.74 - 0.82
	DBM Sonic 1200	F.E. Alenfeld et al. (1998), A. Ekman et al. (2001), A. Ekman et al. (2002), B. Drozdzowska et al. (2003), M.A. Krieg et al. (2003)	2.0	0.9	1.0 – 3.49			0.52 – 0.91
Vertebral Fracture	Sunlight Omnisense	K.M. Knapp et al. (2001), K.M. Knapp et al. (2004)		2.0				0.60
	DBM Sonic 1200	J.Y. Reginster et al. (1998), B. Drozdzowska et al. (2003), G. Guglielmi et al. (2003)	1.44	1.22 – 2.1	2.51 – 3.25			0.52 – 0.89
Any Site	Sunlight Omnisense	R. Barkmann et al. (2000), J. Damilakis et al. (2003a), T.V. Nguyen et al. (2004)	1.83 – 2.69	4.1				0.67 – 0.89
	DBM Sonic 1200	F.E. Alenfeld et al. (1998), F. Blanckaert et al. (1999), C. Wüster et al. (2000), A. Montagnani et al. (2001), B. Drozdzowska et al. (2003), M.A. Krieg et al. (2003)	1.8		1.0 – 1.81			0.51 – 0.83
SOS (m/s) Measured at the Distal Radius								
Forearm Fracture	Sunlight Omnisense	K.M. Knapp et al. (2002)		1.5				0.61
Vertebral Fracture	Sunlight Omnisense	K.M. Knapp et al. (2001), K.M. Knapp et al. (2004)		1.4				0.60
Hip Fracture	Sunlight Omnisense	D. Hans et al. (1999a), M. Weiss et al. (2000), D. Hans et al. (2003)	2.16 – 3.2	2.4	1.92 – 2.72			0.69 – 0.92
Mixed Site	Sunlight Omnisense	R. Barkmann et al. (2000), J. Damilakis et al. (2003a), T.V. Nguyen et al. (2004)	1.69 – 2.23	4.5				0.69 – 0.89
SOS (m/s) Measured at the Mid-Shaft Tibia								
Forearm Fracture	Sunlight Omnisense	K.M. Knapp et al. (2002)						
Vertebral Fracture	Sunlight Omnisense	K.M. Knapp et al. (2001), K.M. Knapp et al. (2004)		1.2				0.60
Mixed Site	Sunlight Omnisense	J. Damilakis et al. (2003a), T.V. Nguyen et al. (2004)	1.47 – 1.75					0.61 – 0.66

The AUC results reflect these abilities; for assessments of the calcaneus, the AUC values from all of the studies reported for BUA measurements ranged from 0.53 – 0.89 (average = 0.71, SD = 0.09), for SOS they also ranged from 0.53 – 0.89 (average = 0.71, SD = 0.08) and for the manufacturers combined parameters 0.54 – 0.92 (average = 0.72, SD = 0.11). The measurement results from the peripheral sites provided similar values with the proximal phalanx ranging from 0.51 – 0.91 (average = 0.7, SD = 0.12), the distal radius ranging from 0.6 – 0.92 (average = 0.75, SD = 0.12) and for the mid-shaft tibia it ranged from 0.6 – 0.66 (average = 0.62, SD = 0.03). Once again the guidelines laid out by R. Kent and J. Patrie (2005) (section 4.7 and 5.4.1.2) provide an understanding of the AUC results. For assessment of the calcaneus, the range of AUC results spans from no ability to good ability, with the distal radius and Proximal phalanx spanning the full range from no ability to excellent ability, while the mid-shaft tibia only managed a poor level of ability.

If the averages for each of the investigations are compared, even the highest average of 0.75 achieved for the distal radius can only be considered to have a moderate level of ability. If these results are compared to those of the previous section they are found to be slightly lower than those for the ability of QUS to predict the density of the axial skeleton, although they both fall within the boundaries of having moderate ability. These results are, however, slightly biased and it would appear that QUS results are slightly better at predicting fractures of the hip and of the spine than predicting mixed fracture from any site of the body.

The predisposition of the osteoporotic bone to fracture would appear to indicate that the mechanical properties of the bone at the fracture site could be considered impaired compared to the bone of a normal individual. If this was the case

then the biomechanics of the skeletal tissue could be related to the QUS results either from the site of assessment, or from another site within the same skeleton.

4.9 Biomechanics vs. Quantitative Ultrasound

One of the aspects of the work within this study is to investigate the ability of the clinical QUS systems to predict the mechanical properties of cancellous bone samples removed from the femoral head.

4.9.1 QUS for the Determination of Modulus

Ultrasound has been used for a number of years for the determination of the Young's modulus of a material, and the basic principle is outlined by C.H. Turner and D.B. Burr (1993). As mentioned in section 4.8.1 ultrasound is a mechanical wave, and is therefore affected by the nature of the material and in particular its density and Young's modulus. The equations relating the variables have been presented in a number of different studies (R.B. Ashman et al. 1987, R.B. Ashman and J.Y. Rho, 1988, C.H. Turner and D.B. Burr, 1993, B. Li and R.M. Aspden, 1997a,b, C.M. Langton and C.F. Njeh, 1999):

$$\nu = \sqrt{\frac{E}{\rho}} \qquad \textbf{Equation 4.8}$$

$$E = \rho \nu^2 \qquad \textbf{Equation 4.9}$$

where ν is velocity, ρ is the density, and E is the Young's Modulus. However the propagation of US through a material occurs at two different velocities referred to as

bulk and bar which interact differently with the material. The bar velocities correspond to equations 4.8 and 4.9, while the bulk velocities adhere to equation 4.10 (R.B. Ashman et al. 1984):

$$v = \sqrt{\frac{c}{\rho}} \qquad \textbf{Equation 4.10}$$

where c is an elastic coefficient that is a combination of Young's Modulus and Poisson's ratio (C.H. Turner and D.B. Burr, 1993). Of the 7 studies presented in this section that have utilised QUS for the determination of the modulus of cancellous bone, all without exception used equations 4.8 and 4.9, for bar wave velocities.

A number of previous studies have provided comparisons between the modulus determined by QUS and the compressive modulus. One example is the study by R.B. Ashman et al., 1987 which was performed using bovine bone, but can be assumed to mimic the effects that would be seen in human tissue, and demonstrated a strongly correlated relationship ($r^2 = 0.935$).

The relationship between the Young's modulus and the apparent density was once again the most investigated of the relationships (Table 4.33), with power functions providing the superior relationships ($r^2 = 0.648 – 0.96$) in comparison to their linear counterparts ($r^2 = 0.24 – 0.96$). The powers ranged from 1.27 to 2.82, showing little difference to the relationships seen for the mechanical testing parameters and their relationship with apparent density.

The advantage of ultrasonic testing is that it provides a 100% non-destructive method of determining the modulus of a bone sample; the down side is that it can only be used for the determination of modulus, and through mechanical testing a number of

other important parameters can be obtained. The non-destructive nature of the testing has, however, highlighted a key issue which must be considered when performing any ultrasonic testing, and is one that has been much discussed, namely considering what information is contained within an ultrasound result in comparison to a densitometry result.

The correlations between the QUS investigations and the densitometry investigations are not comparisons between similar parameters, although QUS is strongly affected by density, with it explaining 88 – 93% of the variance in SOS (D. Hans et al., 1999b). Density alone cannot explain the entire variation in ultrasound results, and when density is ignored the structural variables such as trabecular number, spacing, thickness and apparent volume fraction can explain up to 60% of the variance in the ultrasound results (D. Hans et al., 1999b). The effects of structural variation were investigated further for both cortical (B. Li and R.M. Aspden, 1997c) and cancellous bone (C.-C. Glüer et al., 1993). In both cases the anisotropy seen in the non-destructive mechanical testing (section 3.2.1.5) was also seen in both BUA and SOS ultrasound results, with both cortical and cancellous bone demonstrating an increased stiffness in the axial direction of loading compared to the other two orthogonal directions. In the case of the cancellous bone, C.-C. Glüer et al. (1993) reports the difference for BUA to be as much as 36.1 dB MHz^{-1}, equal to the difference between an osteoporotic and a normal individual within a clinical setting!

Table 4.33 Modulus vs. Density relationships, determined from the ultrasonic determination of modulus

Study	Bone Source	Ultrasound Sample Design	Linear Function	r^2 values	Power Functions	r^2 values
R.B. Ashman et al. (1987) E = MPa $\rho = (kg\ m^{-3})$	Prox. and dist. bovine femoral cancellous bone.	Transducer freq. : 50kHz Wavelength: 1-2cm Samples: 5 x 5 x 10mm	-	-	$E_{Ultrasound} = 3.2\ (10^{-5})\rho^{2.82}$	r2 = 0.648
R.B. Ashman and J.Y. Rho (1988) E = GPa $\rho = (kg\ m^{-3})$	Human Femora	Transducer freq. : 50kHz Wavelength: 20mm Velocities: 1000-1600 ms^{-1} Cylindrical Specimens L = 15mm D = 5mm	$E_{Ultrasound} = 0.0094\rho - 1.48$	$r^2 = 0.93$	$E_{Ultrasound} = 2.73\ (10^{-5})\rho^{1.88}$	$r^2 = 0.95$
	Bovine Femora		$E_{Ultrasound} = 0.0058\rho - 1.34$	$r^2 = 0.92$	$E_{Ultrasound} = 9.23\ (10^{-5})\rho^{1.57}$	$r^2 = 0.87$
M.-C. Hobatho et al. (1997) E = MPa $\rho = (kg\ m^{-3})$	Human Prox. Tibia	Transducer freq. : 50kHz	$E_{Ultrasound} = 5.54\rho - 326$	$r^2 = 0.95$	$E_{Ultrasound} = 0.51\rho^{1.37}$	$r^2 = 0.96$
	Human Prox. Femur		$E_{Ultrasound} = 4.56\rho - 331$	$r^2 = 0.95$	$E_{Ultrasound} = 0.58\rho^{1.30}$	$r^2 = 0.94$
	Human Dist. Femur		$E_{Ultrasound} = 5.27\rho - 384$	$r^2 = 0.91$	$E_{Ultrasound} = 0.82\rho^{1.27}$	$r^2 = 0.95$
	Human Prox. Humerus		$E_{Ultrasound} = 4.25\rho - 270$	$r^2 = 0.92$	$E_{Ultrasound} = 0.32\rho^{1.41}$	$r^2 = 0.92$
	Human Patella		$E_{Ultrasound} = 5.65\rho - 1327$	$r^2 = 0.85$	$E_{Ultrasound} = 0.04\rho^{1.68}$	$r^2 = 0.87$
	Human Lumbar Spine		$E_{Ultrasound} = 5.82\rho - 349$	$r^2 = 0.96$	$E_{Ultrasound} = 0.63\rho^{1.35}$	$r^2 = 0.94$
B. Li and R.M. Aspden (1997a) E = GPa $\rho = (g\ cm^{-3})$	Normal Femoral Heads	Transducer freq. : 10MHz Cylindrical Cores L = ~1mm, D = 9mm	$E_{Ultrasound} = 16.6\rho - 10.5$	$r^2_{Adj.} = 0.24$	-	-
	OA Femoral Heads		$E_{Ultrasound} = 17.4\rho - 13.1$	$r^2_{Adj.} = 0.39$	-	-
	OP Femoral Heads		$E_{Ultrasound} = 22.1\rho - 21.4$	$r^2_{Adj.} = 0.40$	-	-

4.9.2 Biomechanics vs. Clinical QUS

In this section the aim is to review the 14 studies that have been performed previously in humans to investigate the relationships between clinical QUS investigations and the biomechanics of human bone. A brief review of each study, including the test methods, QUS system and results is shown in Table 4.34.

The studies had all sourced their bone from five different sites, either the tibia (S. Han et al., 1996; S. Han et al., 1997; S.C. Lee et al., 1997), femur (M.L. Bouxsein et al., 1999; C.F. Njeh et al., 1997), calcaneus (C.M. Langton et al., 1996; M.L. Bouxsein and S.E. Radloff 1997; R. Hodgskinson et al., 1997), spine (E.-M.Lochmüller et al., 1998, D.Hans et al., 1999), the forearm (C. Wu et al., 2000; C.F. Njeh et al., 2000) or a mixture of the sites (E.-M. Lochmüller et al., 2003; M.A. Kakulinen et al., 2005), with all bar one of the studies (C.F. Njeh et al., 1997) using cadaveric tissue. In the case of the study by C.F. Njeh et al. (1997) the authors used the femoral heads of individuals undergoing hip replacement surgery due to osteoarthritis, but fixed the bone samples in formalin prior to any testing, a process which has been shown to affect the bone collagen, and therefore the bone mechanical properties, when tested.

The nature of the testing that was performed was dramatically different between the studies, with the studies on the forearm and more specifically the radiocarpal joint testing the whole skeletal unit in relation to QUS measurements. Other studies tested intact femurs to determine the load required to fracture the proximal femur, while the most common test was that performed on small samples of bone either cores or cubes, which could be tested in compression to produce the biomechanical properties.

Table 4.34 Relationships between clinical QUS measurements and the biomechanics of human skeletal tissue from within the literature.

Reference	Study Design	Results
S.Han et al. 1996	**Bone Source**: Human cadaveric Tibia; 5 Females (aged 69 ± 4) **QUS**: Direct measurement of the bone cubes (9.5 ± 0.1mm) Panametrics V101 and V301 (Panametrics, Waltham, MA, USA) **Test Method**: Bone cubes were removed from the proximal tibia an cleaned prior to QUS testing in three orthongonal directions. Each bone cube was then destructively tested in either the superior-inferior or the anterior-posterior directions.	Pearson's Correlations (p-value) $\sigma_{Ultimate}$ AP: BUA 0.724 (<0.001); nBUA 0.820 (<0.001); UV 0.723 (<0.001) $\sigma_{Ultimate}$ SI: BUA 0.561 (<0.001); nBUA 0.462 (<0.001); UV 0.659 (<0.001)
C.M.Langton et al. 1996	**Bone Source**: Human cadaveric Calcanei; 10 Males and 10 Females (aged 59-90) **QUS**: Contact Ultrasonic Bone Analyzer (CUBA) (McCue Plc., Winchester, UK) **Test Method**: QUS investigations were performed on a number of occasions on the same samples. 1. Whole calcanei without soft tissue (Whole) 2. 21mm diameter core removed in mediolateral direction and scanned (Core) 3. Any cortical end surfaces were removed from the core and rescanned (Can) 4. The sample was cleaned of any fat and rescanned (Def) The defatted cylinders were tested in compression to determine the modulus and strength	Linear Pearson's Correlations (r) nBUA Whole: Elasticity (MPa) 0.85; Strength (MPa) 0.83 nBUA Core: 0.83; 0.80 nBUA Can: 0.89; 0.87 nBUA Def: 0.88; 0.84 Logarithmic Regressions r^2 values nBUA Whole: Elasticity (MPa) 72.2; Strength (MPa) 69.3 nBUA Core: 64.8; 62.1 nBUA Can: 75.7; 73.6 nBUA Def: 76.5; 72.7
M.L.Bouxsein and S.E.Radloff 1997	**Bone Source:** Human Calcanei; 31 Pairs of cadaveric feet. 13 male and 18 female (mean age 77 years) **QUS:** Calcaneus; UBA575+ (Hologic, Waltham, MA, USA) **Test Method:** The intact cadaveric feet were assessed using the QUS system to mimic clinical investigation conditions. The calcanei were then dissected from the foot and 15mm cubes of trabecular bone were removed from the point matching the position of the QUS scan. The cubes were non-destructively tested (strain rate: 0.005 s^{-1}) in the three orthogonal directions prior to destructive testing in the mediolateral direction, as this was the direction the QUS pulse was transmitted. The extensometer monitored the platens, and the morrow was in-situ during testing.	r^2 (p-value) Modulus (MPa): BUA (dB MHz^{-1}) 0.64 (p<0.001); SOS (m s^{-1}) 0.41* (p<0.001) Strength (MPa): 0.44 (p<0.001); 0.53 (p<0.001) *1 outlier which on removal r^2 increase to 0.57
R.Hodgskinson et al. 1997	**Bone Source**: Human cadaveric calcanei; 10 male 10 female (aged 59-90) **QUS**: Performed directly on bone cores Contact Ultrasonic Bone Analyzer (CUBA) (McCue Plc., Winchester, UK) **Test Method**: 21mm bone cores the width of the calcaneus it was taken from, orientated in the mediolateral direction. QUS performed directly on the cubes submerged in water. The Young's Modulus was determined from an unconstrained compression test.	Human Calcaneal E = -46.9 + 15.1Velocity r^2 = 71.6

Table 4.34 Continued

Reference	Study Design	Results			
S.Han et al. 1997	**Bone Source**: Proximal Tibia; 8 cadaveric tibiae (aged 66 years ± 7) **QUS**: Individual cores of tibial trabecular bone. Panametrics V101 and V301 (Panametrics, Waltham, MA, USA) **Test Method**: The cores (10mm dia. x 14.5mm length) were prepared in the superior-inferior direction, and tested for their BUA and UV in this direction. The core were divided into two groups and each was tested at different loading rates A: 0.0004s-1 and B: 0.08 s-1 (200x faster)	Pearson's Correlations (p-value)			
				Slow Loading	Fast Loading
		$\sigma_{Ultimate}$	BUA	0.628 (<0.001)	0.502 (0.005)
			UV	0.712 (<0.001)	0.728 (<0.001)
		E	BUA	0.634 (<0.001)	0.281 (n.s.)
			UV	0.646 (<0.001)	0.775 (<0.001)
		Energy	BUA	0.572 (<0.001)	0.695 (<0.001)
			UV	0.655 (<0.001	0.396 (0.035)
S.C.Lee et al. 1997	**Bone Source**: Human cadaveric Tibia; 10 men and 16 women (aged 81 ± 12 years) **QUS**: Mid-Shaft Tibia; SoundScan 2000 system (Myriad Ultrasound Systems, Rehovot, Israel) **Test Method**: The QUS scan was performed on the midpoint of the tibial shaft with soft tissues intact. The mid-section 20mm distal and 20mm proximal to the tibial mid-diaphysis was removed and bone cores 4.5mm in diameter removed from the anterior cortical bone and prepared as tensile specimens. The samples were tested at 0.025 mm s^{-1} (0.5 s^{-1}) with a contact extensometer.	Regression analysis (p-value)			
			tUV		
			r	r2	95% CI
		E	0.92 (p<0.001)	0.84	0.70-0.98
		$\sigma_{Ultimate}$	0.87 (p<0.001)	0.75	0.55-0.97
		σ_{Yield}	0.83 (p<0.005)	0.69	0.43-0.96
		$\varepsilon_{Ultimate}$	0.56 (n.s.)	0.31	-0.06-0.87
		ε_{Yield}	0.53 (n.s.)	0.28	-0.15-0.87
C.F.Njeh et al. 1997	**Bone Source**: Fresh Femoral Heads; Osteoarthritic Individuals 20 Females and 3 Males (aged 68.3 ± 11.5 years) **QUS**: Direct contact with the bone cubes in three orthogonal directions CUBA Research (McCue Plc., Winchester, UK) **Test Method**: The Femoral heads were formalin fixed, then cubes 20 ± 1mm were removed from the centre of each head. QUS investigations were performed by placing the cubes in direct contact with the QUS transducers. The cubes were then non-destructively testing in three orthogonal directions then destructively tested in the PD direction.	Pearson's Correlations (p-value)			
			Ultrasound Velocity		
			PD Direction	ML Direction	AP Direction
		E	0.83 (<0.0001)	0.81 (<0.0001)	0.79 (<0.0001)
		$\sigma_{Ultimate}$	0.76 (<0.0001)		

Table 4.34 Continued

Reference	Study Design	Results
E.-M.Lochmüller et al. 1998	**Bone Source**: Lumbar Vertebral bodies (L4); 49 cadaveric spines 32 men (aged 82.1± 9.0years)17 women (aged 83.1± 10.1 years) **QUS**: Calcaneus; Achilles (Lunar, Madison, WI) **Test Method**: The QUS assessments were performed on the calcaneus of each of the cadavers, with all soft tissues intact. The L4 vertebrae were removed with the vertebral disks on either side intact. The vertebral body was tested as an intact unit, and was cyclically tested with increasing loads until failure. The peak load achieved was taken as the failure load.	Pearson's Correlations (p-value) BUA (dB MHz^{-1}) / SOS (m s^{-1}) / Stiff. Index Fail. Load All: 0.27 (n.s) / 0.48 (p<0.001) / 0.40 (p<0.01) Fail. Load Male: 0.16 (n.s.) / 0.36 (p<0.05) / 0.28 (n.s.) Fail. Load Female: -0.22 (n.s.) / 0.41 (n.s.) / 0.15 (n.s.)
M.L.Bouxsein et al. 1999	**Bone Source**: 26 Human cadaveric Proximal Femurs and Lower limbs 16 Females and 10 Males (aged 81 ± 12 years) **QUS**: Tibia: SoundScan 2000 system (Myriad Ultrasound Systems, Rehovot, Israel) Calcaneus: UBA575+ (Hologic, Waltham, MA, USA) **Test Method**: QUS investigations performed on the relevant site of the cadaveric tissue with all soft tissue in place. The strength of the proximal femur was determined from impact (100mm s^{-1}) on the greater trochanter to mimic a sideway fall, and the point taken as the maximum load.	All Fractures Site / r / r2 / p-value Tibial SOS: 0.44 / 0.19 / 0.03 Heel SOS: 0.82 / 0.67 / <0.0001 Heel BUA: 0.83 / 0.70 / <0.0001 Clinically Representative Fracture Site / r / r2 / p-value Tibial SOS: 0.55 / 0.31 / 0.01 Heel SOS: 0.80 / 0.64 / <0.0001 Heel BUA: 0.84 / 0.72 / <0.0001
D.Hans et al. 1999	**Bone Source**: Lumbar Spine; 7 cadaveric spines (aged 55 ± 15 years) **QUS**: Individual cubes of vertebral trabecular bone; DBM Sonic 1200 (IGEA, Carpi, Italy) **Test Method**: Bone Cubes of 1.2 mm in length were removed from the vertebrae, and tested ultrasonically while submerged in water. The cubes were the non-destructively tested in the three orthogonal directions, before being destructively tested in the axial plane.	Spearman Correlation Coefficients (p-value) Sagittal / Coronal / Axial E Axial: 0.65 (p<0.05) / 0.6 (p<0.05) / 0.58 (p<0.05) E Coronal: 0.87 (p<0.05) / 0.77 (p<0.05) / 0.80 (p<0.05) E Sagittal: 0.44 (n.s.) / 0.30 (n.s.) / 0.45 (n.s.) Axial Strength: 0.71 (p<0.05) / 0.77 (p<0.05) / 0.64 (p<0.05)
C.Wu et al. 2000	**Bone Source**: Forearm / Wrist; 13 human cadaveric forearms. (mean age 63.9 ± 15.5) **QUS**: Proximal Phalanges of the index, middle and ring fingers. DBM Sonic 1200 (IGEA, Carpi, Italy) **Test Method**: The testing was set up and performed using the same methods as in the paper by C.F.Njeh et al. 2000, but only the fracture load was considered.	Pearson's Correlations (p-value) $SOS_{Phalanx}$ Index / Middle / Ring / Average Fracture Load: 0.63 / 0.72 / 0.64 / 0.71

Table 4.34 Continued

<table>
<tr><th>Reference</th><th></th><th></th></tr>
<tr><td>C.F.Njeh et al. 2000</td><td>Bone Source: Forearm / Wrist; 14 Cadaveric forearms.
4 women and 10 men (mean age 68.6 years)
QUS: Proximal Phalanx; The Sunlight Omnisense System
(Sunlight Ultrasound Technologies Ltd., Rehovot, Israel)
Test Method: The radiocarpal joint was maintained intact, but the ulna was sectioned to ensure all loading was passed through the radius. The whole wrist complex was tested in compression, with a cross-head speed of 75mm/s to mimic a fall situation. The fracture load was defined as the maximum load on the load displacement curve, with the fracture stress representing the ratio of the fracture load to the total area at 15% the length of the radius.</td><td>Pearson’s Correlations (p-value)
<table><tr><td></td><td>$SOS_{Phalanx}$</td></tr><tr><td>Fracture Load</td><td>0.60 (0.03)</td></tr><tr><td>Fracture Stress</td><td>0.74 (0.004)</td></tr></table></td></tr>
<tr><td>E.-M. Lochmüller et al. 2003</td><td>Bone Source: 126 Formalin Fixed cadavers: Femora, Thoracic and Lumbar Vertebrae, Forearms
46 Male (aged 76.4 ± 11.4) 80 Females (aged 82.2 ± 9.0 years)
QUS: Excised Calcanei from matched cadavers: Achilles + (Lunar, Madison, WI)
Test Method: Femora – 1. Side impact loading on the trochanter to mimic a fall.
2. Vertical loading through the femoral head.
Vertebra: Tested in axial compression in functional units (T5-T7, T8-T11, L2-L4)
Forearms: Tested with the hand in 70^{o} dorsifelxion and 10^{o} radial abduction to mimic a fall onto an outstretched hand</td><td><table><tr><td></td><td colspan="2">Femora</td><td colspan="2">Spine T6/T10/L3 Forearm</td></tr><tr><td></td><td>Vertical loading</td><td>Side-Impact</td><td colspan="2"></td></tr><tr><td>SOS</td><td>0.34 (<0.01)</td><td>0.46 (<0.01)</td><td>0.41 (<0.01)</td><td>0.35 (<0.01)</td></tr><tr><td>BUA</td><td>0.45 (<0.01)</td><td>0.53 (<0.05)</td><td>0.51 (<0.01)</td><td>0.40 (<0.01)</td></tr><tr><td>Stiff. Index</td><td>0.42 (<0.01)</td><td>0.52 (<0.05)</td><td>0.49 (<0.01)</td><td>0.40 (<0.01)</td></tr></table></td></tr>
<tr><td>M.A.Kakulinen et al. (2005)</td><td>Bone Source: 11 mixed femurs and tibias; 10 Male, 1 Female (aged 60 ± 18 years)
QUS: Performed directly on the 16mm diameter x 8mm thick trabecular bone cyclinders
2 systems using either UltraPAC (Physical Acoustics Co., Nj, USA) or Panametrics V301, V302, V304, V380 and V307 (Panametrics Inc., Waltham, MA, USA)
Test Method: The bone cores were removed from either the femurs or tibias and then tested ultrasonically while submerged in water. The cubes were then destructively tested in compression, to provide modulus (E) values, strength ($\sigma_{Ultimate}$) and resilience to the yield point.</td><td><table><tr><td></td><td></td><td colspan="5">Transducer Centre Frequency</td></tr><tr><td></td><td></td><td>0.5 MHz</td><td>1 MHz</td><td>2.25 MHz</td><td>3.5 MHz</td><td>5 MHz</td></tr><tr><td>E</td><td>Avg. Att.</td><td>0.20</td><td>0.33</td><td>0.51^{+}</td><td>0.44</td><td>0.56^{+}</td></tr><tr><td></td><td>nBUA</td><td>0.05</td><td>0.56*</td><td>0.44</td><td>0.29</td><td>0.41</td></tr><tr><td></td><td>SOS</td><td>0.57*</td><td>0.58*</td><td>0.67*</td><td>0.65*</td><td>0.71*</td></tr><tr><td>$\sigma_{Ultimate}$</td><td>Avg. Att.</td><td>0.20</td><td>0.50^{+}</td><td>0.68*</td><td>0.59*</td><td>0.70*</td></tr><tr><td></td><td>nBUA</td><td>0.03</td><td>0.71*</td><td>0.53^{+}</td><td>0.31</td><td>0.45</td></tr><tr><td></td><td>SOS</td><td>0.60*</td><td>0.68*</td><td>0.75*</td><td>0.76*</td><td>0.82*</td></tr><tr><td>Resiliance</td><td>Avg. Att.</td><td>0.12</td><td>0.54^{+}</td><td>0.68*</td><td>0.60*</td><td>0.68*</td></tr><tr><td></td><td>nBUA</td><td>0.01</td><td>0.73*</td><td>0.46^{+}</td><td>0.25</td><td>0.38</td></tr><tr><td></td><td>SOS</td><td>0.51^{+}</td><td>0.61*</td><td>0.68*</td><td>0.70*</td><td>0.75*</td></tr></table>$^{+}$ p<0.05, * p<0.01</td></tr>
</table>

4.9.2.1 The Forearm

The three studies which investigated the forearm each used different QUS systems to attempt to predict the fracture load, C.F.Njeh et al. (2000) used the Sunlight Omnisense system to investigate the proximal phalanx of the middle finger, C.Wu et al. (2000) used the DBM Sonic 1200 system to assess the index, middle and ring fingers, while E.-M.Lochmüller et al. (2003) used the Achilles + system to assess the calcaneus of the donor cadaver. All three tests provided significant correlations between the QUS investigations and either the fracture load or the fracture stress of the forearm, with the assessments of the phalanges by the two different systems providing equal correlations ($r = 0.60 – 0.74$), which were superior to that provided by the calcaneal assessment ($r = 0.35 – 0.40$).

4.9.2.2 Intact Femurs

The testing of the intact femurs was performed by attempting to simulate either a sideways fall onto the trochanter, or a vertical impact onto the femoral head. As with the study of the forearm, different QUS systems were utilised, M.L.Bouxsein et al. (1999) utilised two systems, a SoundScan 2000 system for the assessment of the tibia, and an UBA575+ system to assess the calcaneus. E.-M.Lochmüller et al. (2003) only used one QUS system, the Achilles + for the assessment of the calcaneus. The results found by M.L.Bouxsein et al. (1999) were on the whole superior to those of E.-M.Lochmüller et al. (2003), with correlations between 0.80 to 0.84 and 0.34 to 0.53 respectively for the calcaneal assessments. The correlations between the tibial assessment and the fracture load were below those of the calcaneal results for the same study, but were comparable to those of the E.-M.Lochmüller et al. (2003) study (0.44

and 0.55). One noticeable feature of both studies and in particular the M.L.Bouxsein et al. (1999) study, was the predictive abilities of the QUS systems in relation to the fracture load, as this work clearly supports the clinical findings of clinical based studies which have shown the ability of QUS to predict fracture risk.

4.9.2.3 Vertebral Bodies

The two studies which investigated the biomechanics of vertebrae were performed by the same study group, (E.-M.Lochmüller et al., 1998, 2003) The studies were similar in their methodologies, using the same Achilles QUS system for the assessment of the calcaneus, and testing the vertebrae as functional units, with either the intervertebral discs on either side intact or, in the case of the 2003 study, as 3 vertebra units. The results of the two studies differed slightly, with the larger sample numbers of the 2003 study providing stronger and more significant correlations for BUA 0.51 compared to 0.27 and the stiffness index 0.49 compared to 0.40, but with the SOS results being similar, 0.41 compared to 0.48.

4.9.2.4 Sample Specific Testing

The final mode of testing which was used in most of the studies, involved the preparation of either cylindrical cores, or cubic compression testing samples of trabecular bone. The test samples had either been tested by QUS in-situ prior to sample preparation, or the sample was prepared and tested by QUS prior to any mechanical testing. The study by C.M.Langton et al. (1996) was an exception to both of these study designs, and performed QUS investigations prior to and throughout the sample preparation procedure. The nBUA results that were achieved for before, during and after

sample preparation varied very little in their relationship to either strength or Young's modulus. For modulus and strength the linear relationship to the nBUA value was significant with values ranging between 0.83-0.89 and 0.80-0.87, relationships which were of the same order of magnitude when viewed in a logarithmic form. The results of this study were important in showing that the results achieved for this type of testing were independent of the condition of the core, and enabled a more direct comparison to be made between different studies.

The results seen within the other studies on cancellous bone provide a range of correlations depending on the QUS parameter and the mechanical parameter. For the Young's modulus the relationship with nBUA or BUA ranged between 0.44 (M.L.Bouxsein and S.E.Radloff 1997) to 0.634 (S.Han et al. 1997), for SOS, VOS or tUV the correlations were between 0.30 (D.Hans et al., 1999) and 0.85 (R.Hodgskinson et al., 1997). The relationships between the QUS parameters and strength were of the same order of magnitude, with BUA and nBUA ranging from 0.20 (M.A.Kakulinen et al., 2005) to 0.87 (C.M.Langton et al., 1996).

The study by S.C.Lee et al. (1997) was different to other studies in that it assessed the relationship between QUS investigation results and the tensile properties of cortical bone from the tibia. The correlations that were achieved between the ultrasound velocity, the modulus and the yield and ultimate strength were excellent (0.92, 0.83 and 0.87 respectively), but no significant relationship was found with the strain values.

The previous studies provide proof of the abilities of QUS to predict the biomechanics of both cortical and cancellous bone material, and provide support for the statement that QUS is important in the prediction of fracture risk. However, all the work performed in these studies was on cadaveric tissue, or the QUS investigation was

performed in vitro. One of the novel aspects of this study is to perform a comparison between the biomechanics of cancellous bone in vitro vs. the QUS investigation results obtained in-vivo from the donor patient.

Concluding Remarks

The literature within this chapter demonstrates that the effects of the bone conditions osteoporosis and osteoarthritis are not restricted to the density of the bone alone, and that the effects of the conditions are also seen on the cancellous bone composition and structural integrity and the cancellous bone collagen network integrity.

The diagnosis of osteoporosis is an extensively researched field with a number of options being available to the clinician. However, the poor precision error of QUS has meant that only DXA of the axial skeleton has any official guidelines for the diagnosis of osteoporosis and is the technique of choice for the monitoring of either bone loss or pharmaceutical therapies. Since official referral criteria for individuals requiring DXA are poor, there has been a rise in the number of studies trying to find new methods for the screening of individuals to ensure the demands on DXA services are minimised.

The two feasible options are either quantitative ultrasound or questionnaires based on specific anthropometrical measures and certain aspects of an individual's medical history. For both QUS and the questionnaires their abilities have been widely investigated; however, never has a widescale study been performed to directly compare the various different techniques. The novel aspect of the clinical research in this study is the comparison between six different osteoporotic risk factor questionnaires from within

the literature with a further two QUS systems, the Sunlight Omnisense and the CUBA Clinical.

Chapter 5 Materials and Methods: Clinical Studies

5.1 Ethical Approval

This study was approved by the ethical research committee of Swindon and Marlborough NHS Trust.

5.2 Quantitative Ultrasound Systems

Two commercially available QUS systems were utilised in the study, the CUBA Clinical system (McCue Plc., Hampshire, UK) and the Sunlight Omnisense 7000S system (Sunlight Omnisense Technologies Ltd., Rehovot, Israel).

5.2.1 CUBA Clinical

The CUBA is a calcaneal assessment device, which provides both BUA and VOS results. The system is a dry ultrasound system which does not require the subject's foot to be immersed in a water bath, but instead uses patented silicone pads on the transducers, which are brought into contact with the heel during the measurement process. Transmission of the ultrasound pulse is ensured by the addition of a coupling gel between the transducers and the skin, so as to provide an air free contact with the subject's skin. The region of interest selection for the system is based on the size of the individual's foot, with smaller feet requiring the insertion of one of two different inserts, that repositions the subject's heel by a fixed amount in relation to the base of the footwell and the transducers. Each assessment takes about a minute to

perform, with an initial 30s settling period prior to assessment to allow the light pressure imparted by the transducers to remove any air from the coupling gel, and to compress any excess soft tissue at the measurement site.

The system was controlled via a laptop and the CUBA^{PLUS} software version 4.

5.2.2 Sunlight Omnisense

The Sunlight system enables the assessment of three different measurement sites, the distal Radius, proximal phalanx of the third digit, and the mid-shaft Tibia. The system relies on the patented Omnipath technology, which enables the measurement of the SOS through the bone's outer cortex at the measurement site. The region of interest selection is determined as preset points related to the measurement of distances between anatomical sites. For the distal Radius this was half the distance between the elbow (olecranon) and the tip of the middle finger. For the proximal phalanx it was the length of the middle phalanx measured back from the interphalangeal joint towards the metacarpophalangeal joint of the middle finger. For the mid-shaft Tibia the region of interest is half the distance between the base of the heel and the top of the knee joint when flexed at 90^{o}. Measurements are performed by passing the probe across or around the measurement site, with the coupling between the transducer and the skin ensured by a layer of ultrasound coupling gel. Each assessment takes between 2 and 3 minutes, with each complete measurement requiring the collection of 3 sets of 300 points, with a result supplied if the three sets are considered the same; if not a fourth and fifth set of 300 points are required until three matching sets are obtained.

In this study, all QUS assessments were performed by the same operator, using the same two systems throughout the study, and the same Parker ultrasound gel (Parker Laboratories Inc., Fairfield, New Jersey, U.S.A.) as the coupling gel. All assessments were performed on the non-dominant side of the subject, with dominance determined by asking the subject, or in the case of any uncertainty, by the asking of simple questions designed to indicate dominance. Both ultrasound systems were supplied with device specific phantoms, which ensured the quality assurance of the systems; the phantoms of both systems were assessed prior to any measurement session.

5.2.3 Dual-Energy X-ray Absorptiometry (DXA)

The DXA system utilised in this study was a Hologic QDR-4500C (Hologic Inc., Bedford, MA, USA), which enabled the assessment of the lumbar spine (L1-L4) and four sites around the proximal femur (Trochanter, Femoral Neck, Intertrochanteric region and Ward's Triangle). The DXA investigations were performed by four skilled radiographers from the radiography department of the Great Western Hospital, Swindon. Quality assurance checks were performed prior to every scanning session using the phantoms provided by the manufacturer.

5.3 Study Groups and Anthropometric data

Group 1: 16 individuals considered to be healthy controls, 10 males and 6 females.

Groups 2 and 3 consisted of subgroups from a total population cohort of 424 volunteers (58 males and 366 females) recruited from the catchment area of the Great Western Hospital, Swindon. All volunteers were attending prearranged appointments at the DXA scanning Clinic at the Great Western Hospital, Swindon and were provided with an information pamphlet containing the outline, aims and requirements of the study (Appendix 1) with their appointment letter. Upon arrival at the hospital the patients underwent their scheduled DXA scan, and were asked by the radiographer if they wished to partake in the study; any volunteers were taken into an additional room and introduced to the researcher. The researcher double checked the volunteer was happy to partake in the study and understood the requirements, and answered any queries that they had. Every volunteer provided informed consent to partake in the study by signing a consent form (Appendix 2) prior to inclusion within the study. Each individual was investigated using both QUS systems and completed a questionnaire designed to highlight nutritional, lifestyle and clinical risk factors which are associated with osteoporosis (Appendix 3).

Group 2: 268 Caucasian women of pre- peri- and postmenopausal status,

Group 3: This group was a subset of group 2, which contained 208 women considered to be postmenopausal through natural or unnatural causes, all of whom had a full complement of scans and a correctly filled out questionnaire.

The anthropometrical data for the three study groups can be found in Table 5.1.

The groupings within this thesis and the methods and results from this point forward were determined and developed for publication purposes and can be found in a number of sources. The methods used and the representation of the results are on the whole the same for the different study groups, but any difference in presentation of the results is due to the peer review process of the separate journals, and as such the results have remained in their published form.

Table 5.1 Anthropometric data for the study groups.

	Group 1	Group 2	Group 3
Age (years)	25 - 58 37.6 (12.2)	18 - 87 56.7 (12.6)	29 - 87 59.7 (11)
BMI (kg/m^2)	n/a	15.7 - 45.8 25.4 (4.6)	15.7 - 43 25.4 (4.6)
Height (cm)	n/a	137.2 - 195 164.4 (9.2)	137 - 182 161.1 (7.1)
Weight (kg)	n/a	41.3 - 160 68.5 (15.6)	41.3 - 104.8 65.6 (12.6)
Years Since Menopause	n/a	n/a	0 - 54 15.4 (11)
No. of Osteoporotic Subjects (% of group)	n/a	47 (19.1%)	45 (21.6%)
No. of Osteopenic Subjects (%of group)	n/a	113 (45.94%)	99 (47.6%)
No. of Normal Subjects (% of group)	n/a	86 (34.96)	64 (30.8%)

5.4 Study Designs

5.4.1 Precision Study

The precision study was performed separately on groups 1 and 2.

Group 1 received quadruple measurements of the Calcaneus using the CUBA Clinical system, with repositioning between the measurements. Quadruple measurements were also performed on both the distal radius and the proximal phalanx using the Sunlight Omnisense system.

Group 2 received paired measurements on the Calcaneus using the CUBA Clinical system, with repositioning and flexion of the foot between the measurements. Paired measurements were also performed on the distal radius, proximal phalanx and the mid-shaft tibia using the Sunlight Omnisense system.

5.4.1.1 Precision Calculation

For both groups three different short-term precisions were calculated, average percentage coefficient of variation (CV%) (S.L. Bonnick et al, 2001), root mean squared average of the precision errors ($_{RMS}$CV%) (C.-C. Glüer et al., 1995, C.F. Njeh et al., 2000) and the standardized coefficient of variation ($_{S}$CV%) (C. Chappard et al., 1999; C.F. Njeh et al., 2000).

CV%

This is the most simplistic method for the calculation of the precision error of a quantitative system. The standard deviation of the measurements made on an

individual are compared against the mean of the measurements, and the percentage of the mean which 1 standard deviation represents is considered to be the precision.

$$CV\% = \frac{SD}{\overline{X}}(100) \qquad \textbf{Equation 5.1} \text{ (S.L. Bonnick et al., 2001)}$$

where SD is the standard deviation, and $\overline{X}$ is the mean of the measurement values obtained from an individual. The precision of the technique is considered to be the average of the CV% attained from the individuals.

$_{RMS}$CV%

C.-C. Glüer et al. (1995) published guidelines for the calculation and determination of the precision errors of quantitative bone densitometry techniques. The study reports that the precision of a technique is not given by the average of the individual's precision errors, but by the root-mean square (RMS) average of the precision error.

Slightly different equations have been provided for the calculation of $_{RMS}$CV, with C.F. Njeh et al. (2000) providing equation 5.2 which enables the calculation based on paired measurements.

$$_{RMS}CV\% = \frac{\sqrt{\sum_{j=1}^{m} d_j^2 / 2m}}{\sum_{j=1}^{m} \overline{x}_j / m}.100 \qquad \textbf{Equation 5.2}$$

where d_j is the difference between the two measurements for individual j, m is the number of paired measurements, $\overline{x}_j$ is the mean of the paired measurements for individual j. The original paper by C.-C. Glüer et al. (1995) provides a series of equations which allow for the inclusion of a greater number of repeat measurements on a single individual (equations 5.3 to 5.5)

$$SD_j = \sqrt{\sum_{i=1}^{n_j} \frac{(x_{ij} - \bar{x}_j)^2}{n_j - 1}} \qquad \textbf{Equation 5.3}$$

Equation 5.3 relates to the precision error of an individual, where x_{ij} is the *i*th measurement on individual j, $\bar{x}_j$ is the average of all the measurements performed on individual j, and n_j is the number of repeated measurements performed.

$$SD = \sqrt{\sum_{j=1}^{m} SD_j^2 / m} \qquad \textbf{Equation 5.4}$$

Equation 5.4 is the precision error of the technique, where m is the number of individuals investigated, and equation 5.5 relates to the conversion of the technique's precision error into a percentage.

$$_{\text{RMS}}\text{CV}\% = \left(SD \Big/ \sum_{j=1}^{m} \bar{x}_j / m \right).100\% \qquad \textbf{Equation 5.5}$$

In addition to the equations for the determination of the precision error C.-C. Glüer et al. (1995) provide guidelines for the determination of the confidence intervals for the precision errors, using the chi-square (χ^2) distribution (Equation 5.6).

$$\frac{df}{\chi^2_{1-\frac{\alpha}{2},df}} SD^2 < \sigma^2 < \frac{df}{\chi^2_{\frac{\alpha}{2},df}} SD^2 \qquad \textbf{Equation 5.6}$$

Where χ^2(df) is the chi-square distribution, and df is the degrees of freedom calculated using equation 5.7

$$df = \sum_{j=1}^{m} df_j = \sum_{j=1}^{m} (n_j - 1) \qquad \textbf{Equation 5.7}$$

sCV%

The sCV% is calculated to account for the variation in the magnitude of the measurement result value that is provided, as it compares the $_{RMS}$CV% with the standard deviation and mean of the study population (Equation 5.8).

$$sCV\% = \frac{_{RMS}CV\%}{4SD/Mean_{pop}}$$

Equation 5.8 (C.F. Njeh et al. 2000, C. Chappard et al. 1999)

where SD is the standard deviation for the population and $mean_{pop}$ is the average of the population.

5.4.2 Sensitivity and Specificity Study

The sensitivity and specificity study was performed on groups 2 and 3 separately.

Group 2: Each volunteer received their scheduled DXA assessments, which were single assessments of the investigation sites. Paired measurements were performed on the Calcaneus using the CUBA Clinical system, with repositioning, flexion and rotation of the foot between scans. Paired measurements were also performed on the Distal Radius, Proximal Phalanx and Mid-Shaft Tibia using the Sunlight Omnisense system. Of the 268 women within the study, 22 individuals were removed from the final analysis due to incomplete sets of scan data.

Group 3: Each volunteer within group 3 received the same assessments as those in group 2, but in addition to the quantitative assessments, each volunteer answered a questionnaire containing 30 questions relating to medical history, lifestyle and diet, designed to highlight any risk factors the individual had, and to enable the calculation of the existing questionnaire systems from the literature (Table 4.4).

5.4.2.1 Discriminatory Ability

The discriminatory ability of a technique relates to its capability to correctly diagnose an individual's skeletal condition. For the purposes of this study the diagnostic ability related to the QUS systems ability to produce a T-score that was in agreement with the DXA T-score.

Groups 2 and 3 were split according to their T-score result using two threshold levels that provided three distinct groups. The thresholds were set at a T-score of -1, and -2.5, so as to provide the same grouping as defined and outlined by the WHO (Section 4.5).

Due to the recognised incompatibility between QUS and the WHO thresholds, the analysis was repeated a second time using a different set of threshold levels that related to the manufacturer's guidelines. For the Sunlight Omnisense system this required no adjustment, as the recommended guidelines adhere to the WHO definition; in the absence of official guidelines relating to the T-score values from VOS assessment using the CUBA clinical system, the WHO definition was also applied. The one change that was implemented was a threshold change for BUA assessment using the CUBA clinical where T-score of -2.5 was raised to -2.

In order to obtain a formal comparison of the technique's discriminatory abilities, the Kappa index was calculated following the guidelines laid out by R.F. Mould (1998). The Kappa index is based on a technique's ability to provide the same diagnostic outcome; in this study this refers to the grouping, either normal, osteopenic or osteoporotic, as another technique. The meaning of the values obtained from the Kappa index ranges are explained by R.F. Mould (1998) (Table 5.2).

Table 5.2 Meaning of the Kappa indices taken from R.F. Mould (1998)

Kappa index value	Degree of Agreement
<0.2	Poor
0.21 – 0.40	Fair
0.41 – 0.60	Moderate
0.61 – 0.80	Good
0.81 – 1.00	Very good

5.4.2.2 Inter-site correlation

The Kappa indices allowed for a direct comparison between the groupings that the systems placed people into; the inter-site correlation study was performed to investigate the comparison between the different techniques measurement results as a whole. The inter-site correlation study was performed for both groups 2 and 3 using Minitab version 13 statistical software.

5.4.2.3 Diagnostic Ability Investigation

The STARD initiative has produced reports on the methods for the complete and accurate reporting of studies of diagnostic accuracy (P.M. Bossuyt et al., 2003). Further papers (T. Greenhalgh, 1997, A.S. Glas et al., 2003, D.A. Grimes and K.F. Schulz, 2002, B.J. Biggerstaff, 2000) report the correct method for calculation of factors, which allows for the comparison of the diagnostic ability of different techniques.

The basis of the calculations is the 2 x 2 table (Table 5.3), into which four different numbers are placed; the true positive results (TP), or the number of correctly diagnosed diseased people, the false negative results (FN), or the number of

undiagnosed diseased people, the false positive results (FP), or the number of incorrectly diagnosed normal people, and the true negative results (TN), or the number of people correctly diagnosed without the disease.

Table 5.3 Demonstration 2x2 table

Diagnostic Tool Test Result	Gold Standard Test Result		
	With Disease	Without Disease	
Positive	TP	FP	TP + FP
Negative	FN	TN	FN + TN
	TP + FN	FP + TN	TP+FP+FN+TN

The table enables the calculation of a number of different parameters at the recommended threshold levels, such as the sensitivity, specificity, positive and negative predictive values. The *sensitivity* is a measure of how good a test is at picking up people who have the condition and is calculated as TP/ (TP + FN). The *specificity* is a measure of how well a test correctly excludes people without the condition calculated as TN/ (FP + TN).

In addition the table enables the adjustment of the threshold level of the diagnostic tool from one extreme to another, and also the adjustment of the threshold of the standard test in this case DXA.

For group 2, four different levels, and for group 3 three different levels, for the DXA assessments were used. For the diagnostic tools, group 2 (QUS) and group 3 (questionnaires and QUS) a range of *sensitivity* values from 0% to 100% were calculated with corresponding *specificity* values. Using SigmaPlot® version 8.06, the results were plotted as *sensitivity* vs. *1-specificity*, to provide a range of receiver operator characteristic curves (ROC curves), which provided an initial qualitative

comparison between the different techniques, with the curve closest to the top left hand corner of the graph indicating a superior diagnostic ability in relation to a curve which passed closer to the mid line. A formal quantitative comparison was then performed by comparing of the areas under the curves (AUC), with areas between 0.5 and 1. R. Kent and J. Patrie (2005) give practical guidelines for the understanding of the resultant AUC value reproduced in Table 5.4.

Table 5.4 Table representing the meaning of an AUC value for a diagnostic technique

AUC	Considered Ability
0.50	The technique has no diagnostic ability, the result is perfectly 50:50
0.50 – 0.60	The technique can be considered to have little or no diagnostic ability
0.60 – 0.70	The technique has only poor diagnostic ability
0.70 – 0.80	The technique has a moderate degree of ability
0.80 – 0.90	The technique has a good level of diagnostic ability
0.90 – 1.0	The technique has an excellent level of diagnostic ability

5.4.2.4 Cut-off / Threshold Selection

With QUS investigations on the whole being thought not to agree with the WHO definition of osteoporosis, it was decided to investigate the potential threshold values for all the potential screening techniques within the same study population so as to maximise the efficiency.

The purpose of a screening tool is to select correctly those patients that have, or are at risk of having, low BMD and to exclude those patients who are subsequently found to have normal BMD levels. The optimum screening tool would provide a cut-off point that could be used to provide the correct diagnosis of every individual's bone status and provide no false positives or false negatives. It is therefore important that a point be selected above which patients are considered to be normal, and below which they are deemed to need a further investigation.

The selection of the cut-off values or threshold values within this study, were determined using three different methods for groups 2 and 3.

1. Best Sensitivity and Specificity Cut-off

The sensitivity and specificity analysis that was performed in the diagnostic abilities section of this study provided a range of values of sensitivity, with their corresponding specificity values, which ranged from 0 to 1 or 0% to 100%. Sensitivity and specificity both provide information on the techniques' abilities to correctly diagnose individuals with and without the condition. This technique was used for both groups 2 and 3, with the threshold level determined by adding the % sensitivity and % specificity together at each point, and setting the threshold at the point where the resultant value was maximum.

2. Best Accuracy

Using the analysis from the diagnostic abilities section once again, a new parameter referred to as the *accuracy* was determined from the 2 x 2 table, calculated as (TP + TN) / (TP + TN + FP + FN) or the number of correct results divided by the number of study participants. For group 2 the best accuracy threshold was determined as the point at which the accuracy was the greatest.

3. 90% Sensitivity

Previous studies performing validation of screening tools, and in particular the questionnaire systems (L.K.H. Koh et al., 2001; S.M. Cadarette et al., 2000) used cut-offs which supply a sensitivity of 90%, regardless of the specificity. So for group 3 the threshold was set at the point where the technique first achieved ≤ 90% sensitivity.

In order to provide additional information for the threshold values, the positive and negative predictive values were determined from the 2 x 2 tables. The positive and negative predictive values are measures of probability, with the positive

referring to the probability of the individual having the condition if they test positive, and the negative to the probability of an individual not having a condition, should they test negative, and are calculated as TP/ (TP + FP) and TN/ (FN + TN) respectively.

5.4.2.5 Screening Strategy

The determination of a potential screening strategy was something that was requested by the reviewers during the peer review process during the publication of the Osteoporosis International paper (R.B. Cook et al., 2005). The analysis was duly performed but only on the subjects within group 3.

The development of the potential screening strategies involved stepwise regression analysis to predict the minimum of the two T-scores for hip and spine (worst case scenario) by using the raw data output of the QUS systems and questionnaires. The analysis considered three likely situations:

1. A situation where the clinician possesses no instruments and could only apply questionnaires.
2. A case where the QUS instruments are available, but not the questionnaires.
3. A situation where both QUS scanners and questionnaires are available for full use by the clinician.

The resultant stepwise regression provides equations from which the minimum T-score of any DXA investigation of the total hip or lumbar spine an individual is likely to receive can be determined.

Concluding Remarks

The methods in this chapter outline the three cohorts which were investigated as part of this study, which included in the analysis a total 268 women. They further allow for the calculation of three different types of precision for QUS systems, all three of which were used in this study on two distinctly different study cohorts and using two different QUS machines.

The methods also outline the modes of analysis used for both the discriminatory and diagnostic abilities of 6 different questionnaire systems in relation to two clinically available QUS devices for the prediction of the DXA derived density of the axial skeleton. From the resultant analysis of the diagnostic accuracy, the methods are then outlined for how the results were used to provide potential cut-off thresholds for using the systems as screening tools, and in addition the best screening tool that could be devised if all the systems were used in unison.

Chapter 6: Materials and Methods: In-Vitro Testing

6.1 Compression Testing Parameters

The aim of the compression testing was to provide information on the Young's modulus, strength, yield strength, ultimate strain, yield strain and work to failure (defined in this test as the energy absorption at the maximum load) of the cancellous bone material (Figure 6.1).

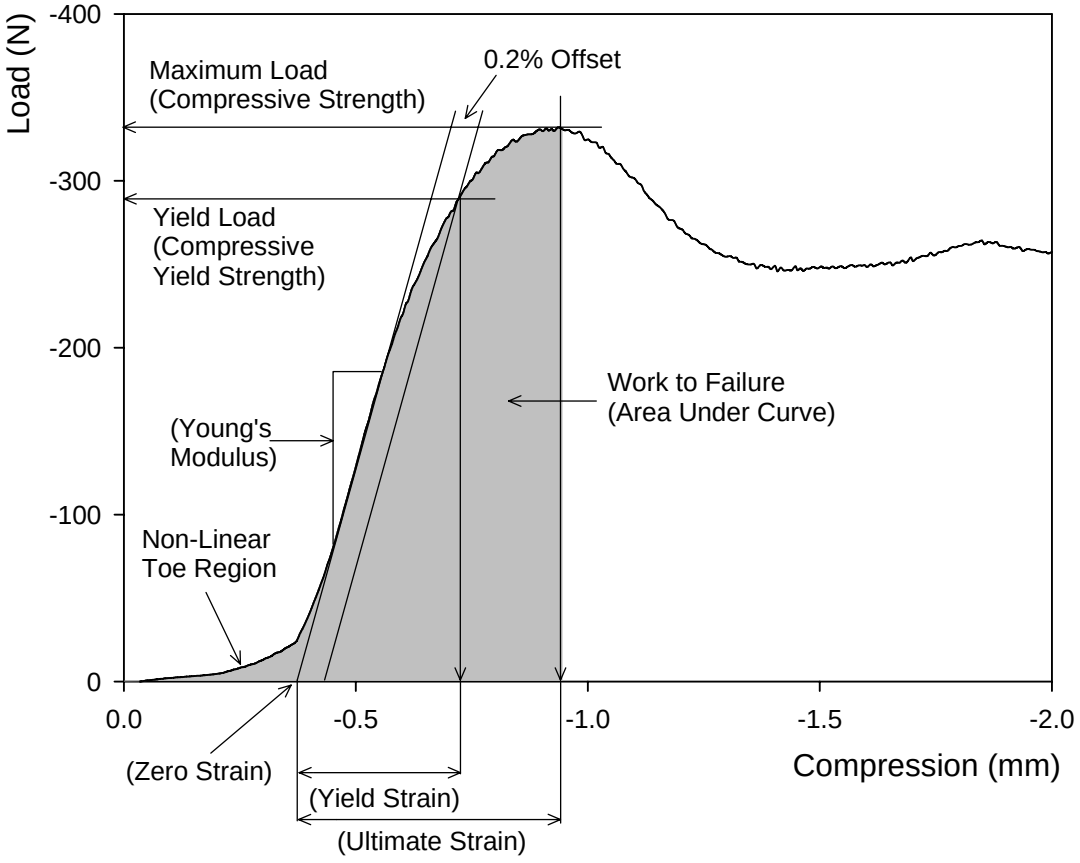

Figure 6.1 Load deformation curve demonstrating the points from which the compressive mechanical parameters are determined

The Young's modulus (MPa) was determined from the slope of a best fit line, fitted to the linear portion of the loading curve, and by extrapolating the best fit line to provide an intersection with the X-axis provided the point of zero strain. The

yield point was determined by plotting a line of equal gradient to the linear portion of the loading curve, but at 0.2% strain (0.2% = the sample gauge length* 0.002 (in mm)), with the yield point defined as the intersection between this line and the loading curve. The yield point then enabled the calculation of the compressive yield strength (MPa) and the yield strain (%). The compressive strength (MPa) and ultimate strain (%) were calculated using the maximum load. The work to failure of the material was determined from the area under the curve up to the maximum load.

6.2 Fracture Toughness Parameters

The aim of the fracture toughness tests is to enable the determination of three parameters related to the fracture toughness of cancellous bone.

6.2.1 K_{IC}

K_{IC} is the plane strain fracture toughness of a material, or '*the critical value of the stress intensity factor (i.e. at which crack propagation occurs) for the condition of plane strain*' W.D. Callister (2000). The fracture toughness of a material (K_C) depends on the thickness (B) of the sample; however, this is only true to a point, as eventually the K_C becomes independent of B, with any increase in B having no effect on the K_C value. The value of K_C at and beyond this point is the plane strain fracture toughness (K_{IC}) of the material in MPa $m^{-1/2}$. (W.D. Callister, 2000; R.W. Hertzberg, 1996; J.C. Anderson et al., 1990).

6.2.2 G_{IC}

G is the strain energy release rate at which, when it reaches a critical value (the critical strain energy release rate G_{IC}), a crack will propagate through the material. (J.C. Anderson et al., 1990).

6.2.3 J-Integral

The J integral was first proposed by J.R. Rice (1968), in relation to the fracture mechanics of a material undergoing elastic and plastic deformation. It is a measure of the energy within the vicinity of the crack tip which, upon the onset of crack initiation or failure, reaches a critical value J (R.W. Hertzberg, 1996; P. Zioupos and J.D. Currey, 1998).

6.3 Fracture Toughness Sample Design and Calculation

The guidelines for the calculation of K_{IC} are outlined in ASTM standard E399-90 Standard Test Method for Plane-Strain Fracture Toughness of Metallic Materials. Although these have not been produced specifically for cancellous bone, they are the standard method, along with their precursors, most utilised by previous studies (T.L. Norman et al., 1992; X. Wang et al., 1994; T.L. Norman et al., 1996; X. Wang and C.M. Agrawal, 1996; P. Zioupos and J.D. Currey, 1998; Y. Tanabe and W. Bonfield, 1999; O. Akkus et al., 2000; C.U. Brown et al., 2000; Z. Feng et al. 2000; J.B. Phelps et al., 2000; C.L. Malik et al., 2003; H. Kikugawa and T. Asaka, 2004; R.K. Nalla et al., 2004; D. Vashishth, 2004) into the fracture toughness of cortical bone material. The standard provides guidelines for the production of test specimens, test rigs and provides the equations and guidelines for the calculation and verification of fracture toughness tests.

6.3.1 Sample Design

ASTM standard E399-90 provides schematics for a number of different sample designs and test rig set-ups from which the assessment of fracture toughness can be performed. The specific use of a standard for any material is implemented by three specific rationales: 1. provides determination of the geometric scaling factor

(section 3.6.2.1) 2. provides methods for validation of the K_{IC} values achieved during testing (section 6.3.2.1) 3. determination of the minimum sample thickness requirements through knowledge of the K_{IC} and σ_y (yield strength). Not being able to develop a new standard from scratch, it was decided to assess and validate 2 different standard sample geometry configurations to eventually derive the optimum. The two sample designs were the disk-shaped compact specimen and the beam specimen, both taken from the ASTM standard E399-90.

6.3.1.1 Disk-Shaped Compact Specimen

The disk-shaped specimen was adjusted only slightly from that which is provided by the ASTM standard, and this was that the area around the mouth of the notch was left intact and not made flat by cutting along the line denoted by measurement *C (Figure 6.2) as is usual for the sample. This adjustment provided an area of bone which was required for the fixation of the extensometer for the monitoring of the crack mouth opening.

The diameter of the disks was set at 2cm, which provided a W value of roughly 15mm, which in turn dictated that the thickness of each sample was required to be 7.5mm. (Figure 6.2)

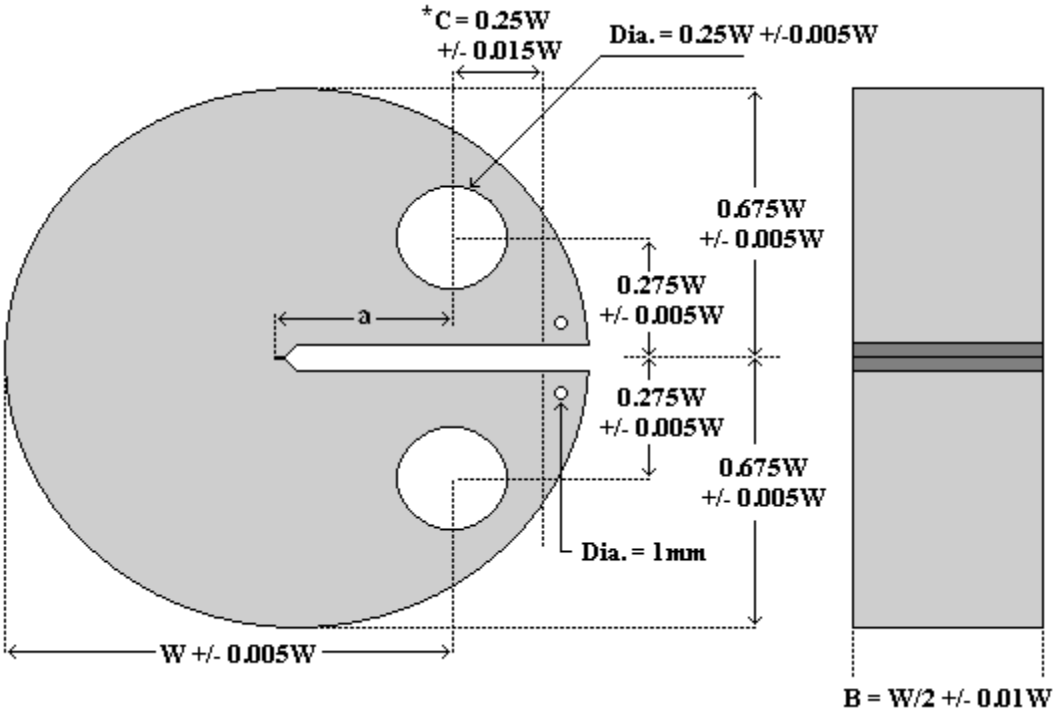

Figure 6.2 Disk-shaped compact specimen adapted from ASTM standard E399-90, *C section was not removed leaving an area for the extensometer attachment.

6.3.1.2 Beam Specimens

The beam sample design adhered to the specifications of ASTM standard E399-90, with W = 6mm, B = 3mm, and the length of the sample set at 30mm to ensure it was greater than 4.2W (Figure 6.3).

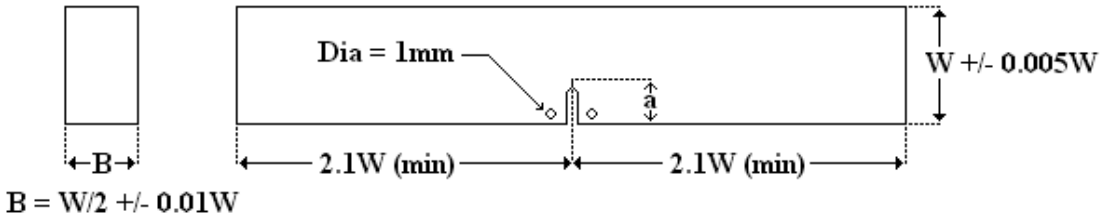

Figure 6.3 Three point bending specimen adapted from ASTM standard E399-90

The preparation and notching procedures for both of the sample designs are explained in full in sections 6.5 (sample manufacture) and 6.7 (sample preparation).

6.3.2 Fracture Toughness Calculation

(Section 9 ASTM Standard E399-90)

The determination of K_{IC} is derived from the load displacement curve (applied load vs. crack opening displacement), and the presence of 3 points P_Q, P_{max} and P_5 on the resultant trace (Figure 6.4). P_5 is determined by plotting a secant line at 95% the gradient of the initial linear portion of the loading trace, with P_5 referring to the point where the secant line and the loading curve intersect. The Point P_Q is dependant on the position of P_5 in relation to the nature of the loading curve, with the three most common occurrences displayed in Figure 6.4 from ASTM standard E399-90. In linear elastic/brittle materials (Trace type III, Figure 6.4) the load point can be considered to be P_{max}, as the P_5 and P_Q are both beyond the P_{max} point when crack growth occurs.

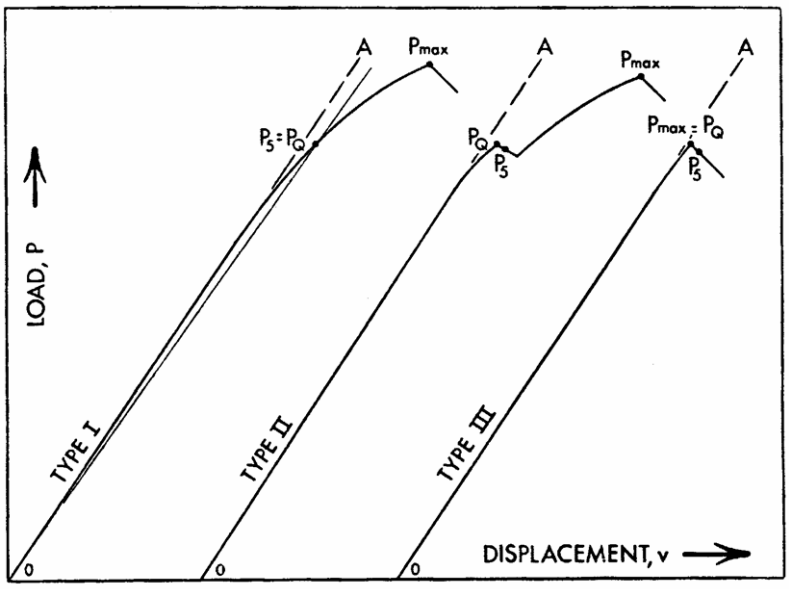

Figure 6.4 Principle types of load-displacement curves for the determination of P_5, P_Q and P_{max}. (Taken from ASTM standard E399-90).

6.3.2.1 K_Q

K_Q is a precursor to K_{IC}, which under certain situations and through ensuring the validation of the test procedure, can equal to K_{IC}. The calculation of K_Q is based on equations which are combinations of specimen and test rig dimensions combined with the P_Q value. The equations are provided by the standard and vary depending on the sample design being utilised.

Disk Samples (Section A6.5 ASTM Standard E399-90):

$$K_Q = \left(P_Q / BW^{1/2}\right) f\left(a/W\right) \quad \textbf{Equation 6.1}$$

Equation 6.1 is used for the calculation of K_Q for the disk samples, where P_Q (kN) is the load as explained above (Figure 6.4), B (cm) is the specimen thickness, W(cm) is the specimen height (Figure 6.2), and f(a/W) is a function of the initial crack length in relation to the specimen's height, given by an additional equation 6.2.

$$f\left(a/W\right) = \frac{\left(2 + a/W\right)\left(0.76 + 4.8\,a/W - 11.58\left(a/W\right)^2 + 11.43\left(a/W\right)^3 - 4.08\left(a/W\right)^4\right)}{\left(1 - a/W\right)^{3/2}}$$

Equation 6.2

Beam Samples (Section A3.5 ASTM Standard E399-90):

$$K_Q = \left(P_Q S / BW^{3/2}\right) f\left(a/W\right) \qquad \textbf{Equation 6.3}$$

The determination of K_Q is performed using equation 6.3, where P_Q (kN) is the load as explained above, S (cm) is the span of the test rig, B (cm) is the specimen thickness, W(cm) is the specimen height (Figure 6.3), and f(a/W) is a function of the initial crack length in relation to the specimen's height, given by an additional equation 6.4.

$$f(a/W) = \frac{3(a/W)^{1/2}\left[1.99 - (a/W)(1-a/W)(2.15 - 3.93\,a/W + 2.7\,a^2/W^2)\right]}{2(1+2\,a/W)(1-a/W)^{3/2}}$$

Equation 6.4

Validation

(Section 9 ASTM Standard E399-90 for plane-strain fracture toughness)

The validation process is performed in order to ascertain if the K_Q value bears any relation to K_{IC}, and if so if the test was valid. The first step is to calculate the ratio P_{max} / P_Q, where P_{max} is the maximum load sustained by the sample prior to fracture (Figure 6.4). If the resultant value is greater than 1.10 then $K_Q \neq K_{IC}$ and there can be considered to be a large elastic/plastic deformation beyond P_Q and before P_{max}, uncharacteristic of a linear elastic brittle material. In this situation the thickness requirement ('specimen strength ratio') is calculated (Equation 6.5).

$$2.5(K_Q/\sigma_{YS})^2 \qquad \textbf{Equation 6.5}$$

Where σ_{YS} is the 0.2% offset yield strength in tension of the material. If the resultant value is less than the specimen thickness and the initial notch length a_o, then $K_Q = K_{IC}$. In the eventuality that the test fails to meet this criterion, the specimen size used in the test must be increased, with specimens at least 1.5 times the size of the original specimen generally required, in order to achieve plane-strain test conditions.

6.3.2.2 G_{IC} Determination

G_{IC} was determined not from direct measurement but using the relationship between either the K_Q or the K_C result from the fracture toughness testing, the Young's modulus from compression testing and the Poisson's ratio (ν) (equation 6.6).

$$G_{IC} = \frac{K_c^2}{E}\left(1-\nu^2\right)$$ **Equation 6.6** (J.C.Anderson et al., 1990)

In order to gain modulus values for the calculation of $G_{IC,}$ the logarithmic relationship between the apparent density of the compression cores and modulus was determined for both the osteoporotic subjects and the osteoarthritic subjects. Using this relationship, the moduli of the fracture toughness samples were determined from the apparent density. No compression cores were taken from the equine material, so in order to calculate the G_{IC} values for this group the relationship determined for the osteoporotic samples was utilised. The osteoporotic relationship was used over the osteoarthritic group as the nature of the bone within osteoporotic subject can be considered normal but of low apparent density and high porosity, whereas the material within the osteoarthritic samples has variation in composition, both in the mineral and organic fraction contents. The resultant values for the G fracture toughness values were N m^{-1}.

6.3.2.3 J-Integral Determination

The determination of the J-integral followed the same method as was used in the study by P.Zioupos and J.D.Currey (1998). The load displacement curve was divided into a number of areas (N mm) with set and equal displacements; for the beam samples areas were taken 0.05mm of crack opening displacement (COD). This

was doubled for the disk shaped compact specimens and areas were taken every 0.1mm of COD. The number of areas assessed varied between the sample designs; for each disk sample a total of 12 areas and for each beam sample 13 areas were taken. The high number of areas taken ensured that the critical displacement was within one of the areas taken for every sample.

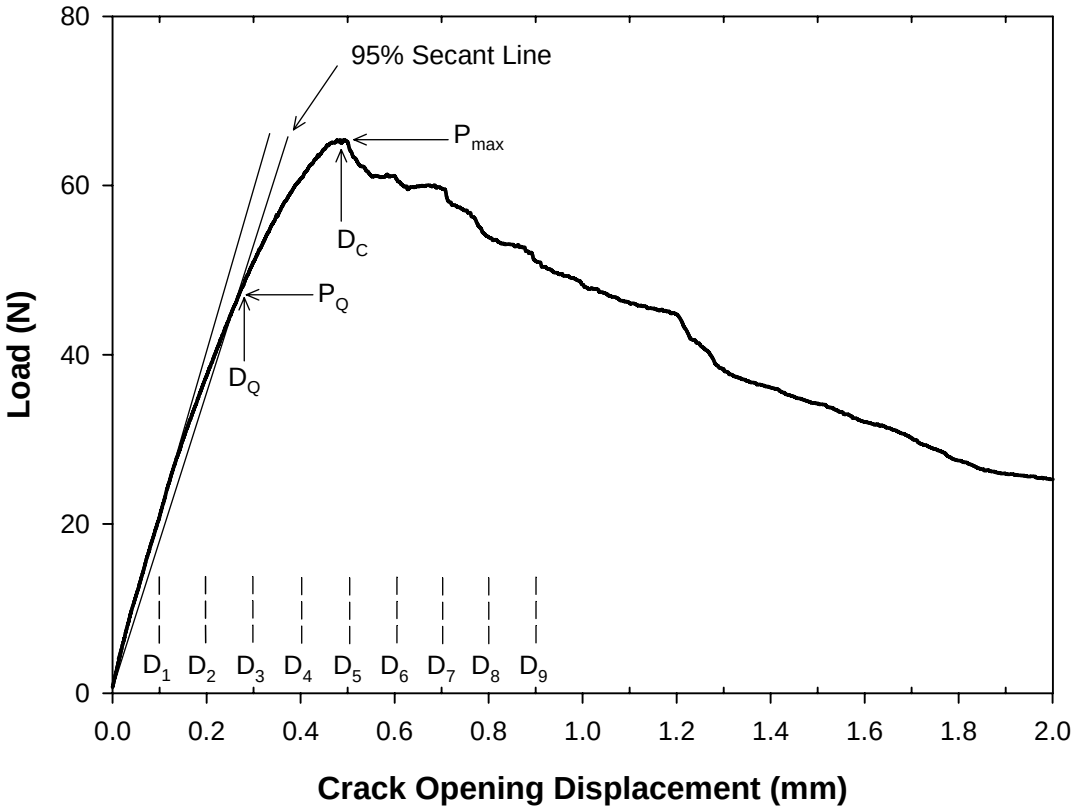

Figure 6.5 Load vs. crack opening displacement curve from an osteoporotic disc sample, with the notch orientated to travel across the trabecular structure. Demonstrating the points P_Q and P_{max} with their corresponding displacements D_Q and D_C, as well as the fixed displacements (D_1-D_9).

The calculation of the J-integral values was performed using Minitab version 13 statistical software. Each area was normalised with respect to the thickness of the specimen, and then regressed against the initial crack length of the sample. This provided either 12 (disk samples) or 13 (beam samples) regression equations each specific to a displacement, from which the slope was noted (Figure 6.6).

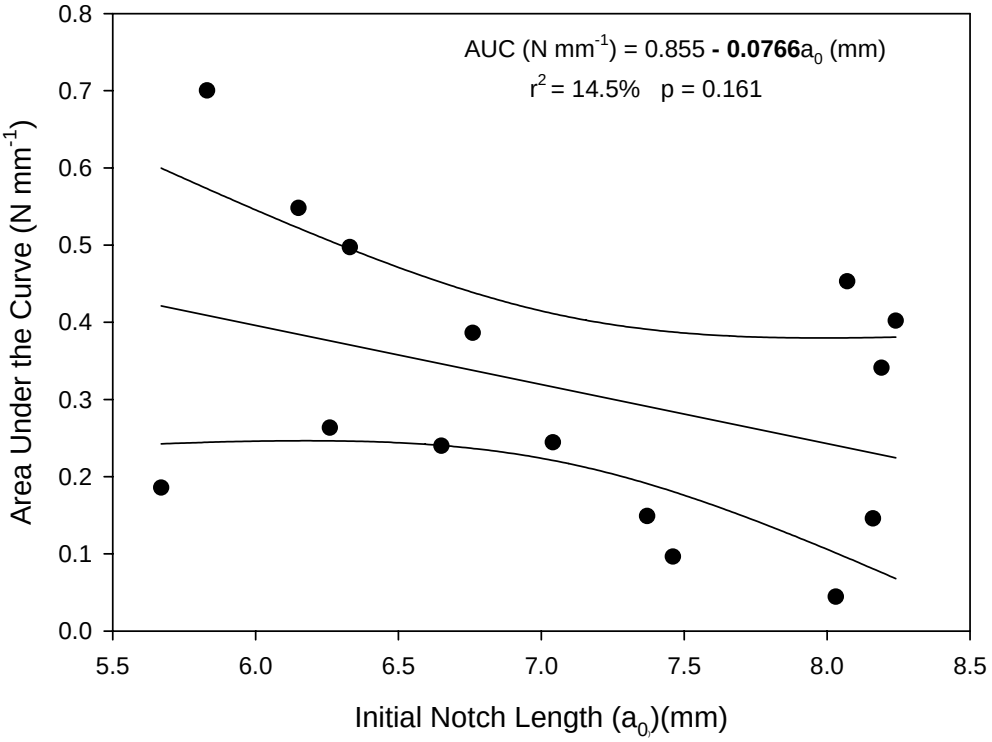

Figure 6.6 Regression plot of the AUC values for displacement 1 vs. the initial notch length, taken from the OP+ scan groups disc samples orientated in the Ac direction, where the slope that was required is in bold (-0.0766).

Each displacement was then squared and cubed, and the normal squared and cubed values were regressed together against the slopes of the previous regression. This provided one regression equation of the slopes vs. the displacements. From the resultant regression analysis the level of significance of the displacements (either original, squared, cubic) was viewed and if any had failed to achieve significance they were removed from the model and the regression rerun to provide a new model where each displacement was significant. The resultant equation can be plotted as shown in Figure 6.7

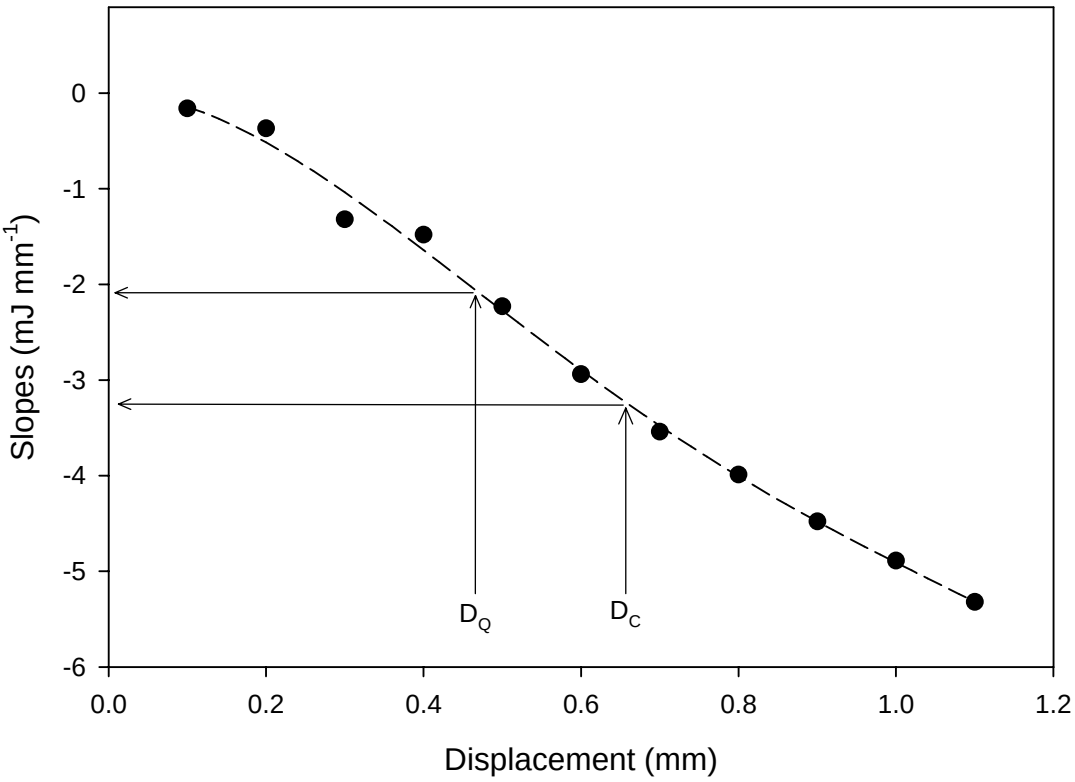

Figure 6.7 Plot of the slopes vs displacements (the J-integral calibration curve), using the best regression equation, and demonstrating the methods for the insertion of D_Q and D_C.

The displacements in the regressions were then replaced by the displacements at which both P_Q or P_{max} occurred (D_Q and D_C), and the result of the equation (shown graphically in Figure 6.7) was divided by the mean specimen thickness and rescaled to provide either J_Q or J_C in J m^{-2}.

6.4 Subjects and Materials

6.4.1 Equine Material

19 vertebrae were harvested from the thoracic spine of two horses, supplied by the Cotswold hunt from 'fallen stock', with both animals having died naturally of old age. The vertebrae were prepared by separating the spines into individual vertebra, by cutting through the intervertebral disks using a hack saw. The vertebral bodies were then separated from the spinal processes by cutting through the pedicle with a carpenter's bandsaw (360mm bandsaw, Draper Tools Ltd., Hants, UK). The individual vertebrae were then cleaned of any soft tissue using a scalpel and scissors and were frozen individually at -20^{o}C until ready for sample preparation.

6.4.2 Human Tissue

Ethical approval for the collection, and use of, the human tissue was provided by the Gloucestershire NHS trust Ethics Committee. Each individual was provided with an information sheet (Appendix 4) outlining the aims and requirements of the study, and had the opportunity to talk through any queries with an experienced nurse practitioner. Informed consent was obtained from each donor by them signing a consent form (Appendix 5) prior to the operation and collection of the tissue by a nurse practitioner. The orthopaedic departments of three different hospitals, Gloucester Royal Hospital, Standish Hospital and Aberdeen Hospital, provided the human femoral head tissue used in this study. The femoral heads were divided into three distinct groups.

6.4.2.1 Osteoporotic + Scan Data (OP+): Gloucester Royal Hospital

Femoral heads were collected from 20 osteoporotic individuals who had suffered low trauma fractures of the femoral neck and required hip replacement surgery. Each individual was scanned using the two quantitative ultrasound machines (CUBA Clinical and Sunlight Omnisense) at four body sites (distal radius, proximal phalanx, mid-shaft tibia and calcaneus).

6.4.2.2 Osteoporotic No Scan Data (OP-): Gloucester and Aberdeen

Femoral heads were collected from 17 osteoporotic individuals who had suffered low trauma fractures of the femoral neck and required hip replacement surgery. The subjects were not investigated with either of the available QUS systems, and only age and gender information was provided with the heads.

6.4.2.3 Osteoarthritic (OA): Standish Hospital

Femoral heads were taken from 8 osteoarthritic individuals who were undergoing elective surgery. Each individual was scanned using the two quantitative ultrasound machines (CUBA Clinical and Sunlight Omnisense) at four body sites (Distal Radius, Proximal Phalanx, Mid-shaft Tibia, Calcaneus)

Table 6.1 Study Group Demographics

	OP+	OP-	OA
No. Subjects	20	17	8
Male/Female	4 / 16	3 / 14	5 / 3
Age (years)			
Range	59 - 90	75 - 96	53 - 76
Mean	80.1	84.4	66
St. Dev	6.6	6.1	7.3
Weight (kg)			
Range	41.3 – 82.6	n/a	68 – 108
Mean	64.16	n/a	84.5
St. Dev	10.47	n/a	12.96
Height (m)			
Range	1.55 – 1.80	n/a	1.65 – 1.83
Mean	1.67	n/a	1.76
St. Dev	0.076	n/a	0.074

The surgeons performing the operations took care to ensure that the use of the 'screw', normally utilised for the removal of the femoral head from the hip joint, was not used, as this enabled the head to be removed intact without damage to the cancellous bone. This was not always feasible and two femoral heads from group 1 had screw damage at their centre. Each femoral head was frozen at -20^{o}C within 10 minutes of extraction from the patient.

QUS investigations were performed on the donors within three days after the operation, as this ensured that any skeletal change that might have occurred between the extraction of the bone and the QUS assessment was minimised. All QUS measurements were performed in triplicate to ensure the no measurement error occurred.

6.5 Sample Manufacture

6.5.1 Equine Vertebra Preparation

The individual vertebrae were allowed to defrost at room temperature prior to sample preparation. The intervertebral disk and endplates were removed from either end of the vertebral bodies using the bandsaw. The vertebral bodies were sectioned into four slices in the caudal – cranial (CC) direction, ensuring that the two central slices of the four were ~1cm in thickness (Figure 6.8).

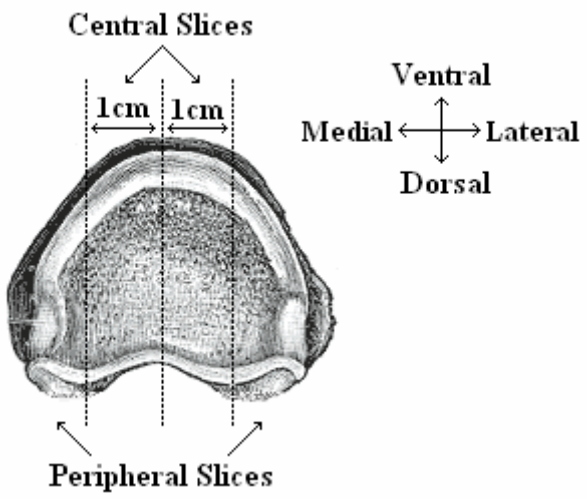

Figure 6.8 Diagrammatic representation of the sectioning of the equine thoracic vertebrae

The four slices of each vertebra were half submerged in Fuschin solution and allowed to stand for 1 minute, before being removed from the solution and rinsed beneath running water to remove any excess dye. This enabled the identification of the CC direction later in the sample preparation process.

6.5.1.1 Central Slices.

Using a 2cm internal diameter diamond edged grinding core drill (D.K.Holdings Ltd., Kent, UK), disk samples of 2cm in diameter were removed from each of the central slices. The samples were kept under constant irrigation with water to prevent any excessive heating of the bone during drilling. From the remaining section of the vertebra, oblong blocks were removed using the bandsaw and cutting in the dorsal ventral direction (DV), from which the beam samples were to be prepared (Figure 6.9 and Figure 6.10).

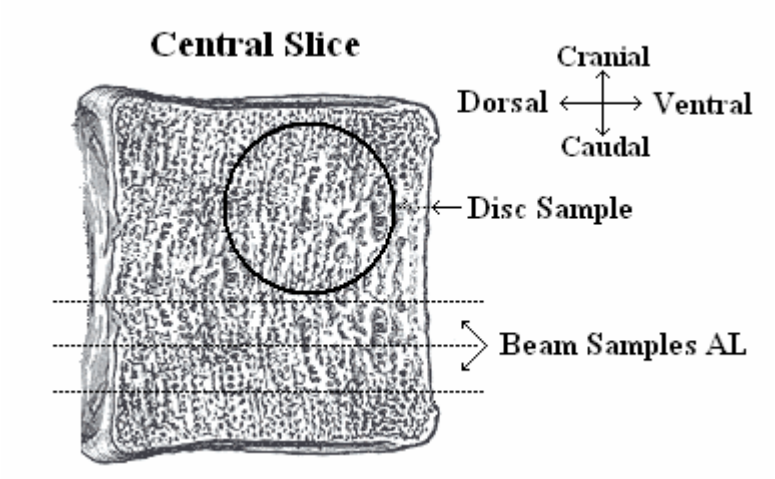

Figure 6.9 Diagrammatic representation of the sample manufacture from the central slice of the equine vertebrae

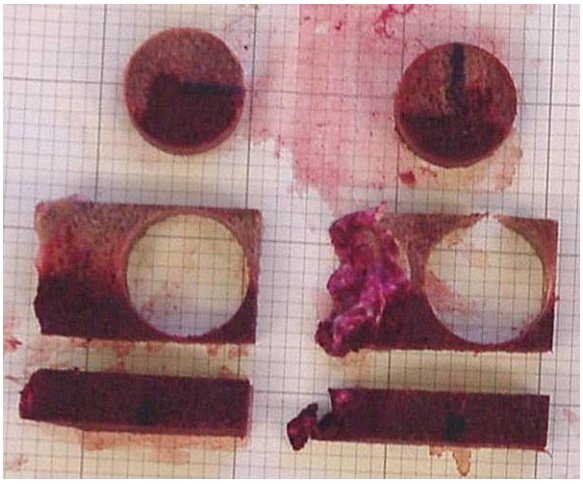

Figure 6.10 Central slices of an equine vertebra with two disk samples and two oblong blocks removed.

6.5.1.2 Peripheral Slices

The tissue from the outer slices of the vertebra was insufficient to enable the production of compact disk shaped specimens; however using the bandsaw it was possible to section the outer slices in the CC direction and produce beam specimens, orientated in the CC direction (Figure 6.11 and Figure 6.12).

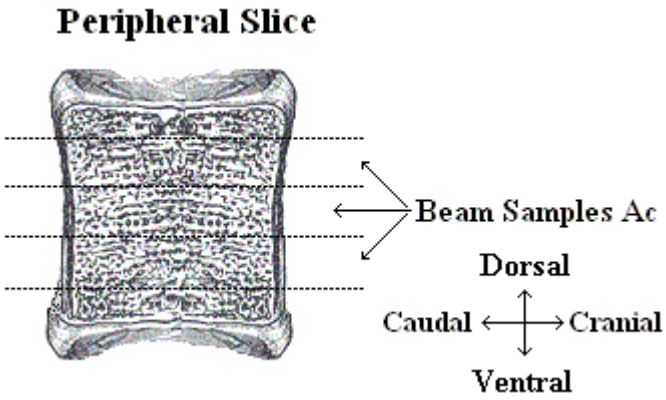

Figure 6.11 Diagrammatic representation of the sample manufacture from the peripheral slice of the equine vertebrae

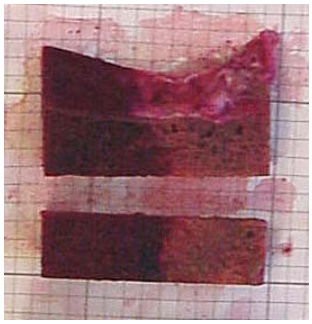

Figure 6.12 Sectioning of the outer slice in the CC direction.

6.5.2 Human Femoral Head Preparation

The femoral heads were prepared in a frozen condition; this allowed not only the marrow tissue to provide support to the surrounding cancellous network, but also aided in the prevention of any thermal damage to the tissue during the sectioning and coring processes.

The femoral heads were sectioned in the medial lateral direction into slices of approximately 9mm thickness. The sizes of the femoral heads from the different groups varied with the osteoarthritic heads from group 2 being generally larger than those obtained from the osteoporotic individuals of groups 1 and 3. This meant the number of slices obtained from each head differed; however, on average 4 slices were produced, two edge slices and two central slices (Figure 6.13).

6.5.2.1 Central Slices

Immediately after sectioning, small samples were cut from the edge of each central slice, refrozen, packed in dry ice and sent to the Department of Molecular Biology at the University of Bristol for collagen analysis (section 6.7). When three central slices were available, only two were sampled, and in the case of less than four slices being available then a sample was removed from a peripheral slice, this ensured that each femoral head had two samples for collagen analysis.

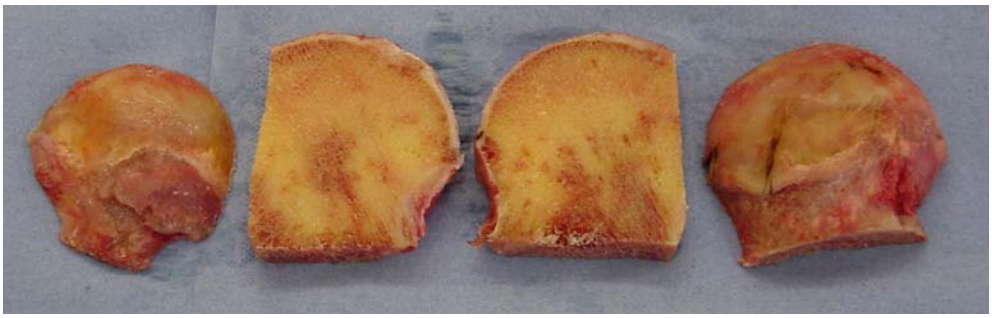

Figure 6.13 Osteoarthritic femoral head sectioned into 4 slices in the medial-lateral direction, showing the sections of tissue removed from the central slices for collagen analysis.

From the remaining tissue the samples were prepared in same manner as section 6.5.1.1, 2cm disks were removed from each of the central slices using the 2cm internal diameter diamond edged grinding core drill (D.K.Holdings Ltd., Kent, UK).

Due to the nature of the trabecular structure of the femoral head, but also to ensure that the maximum amount of beam samples were obtained, it was not feasible to orientate the beams exactly along the main trabecular orientation; however, the beam samples were cut using the bandsaw so as to provide samples in which the crack propagation would be forced in two different directions in relation to the trabecular orientation, across (AC) and along (AL) (Figure 6.14 and Figure 6.15).

Figure 6.14 Central slice of an osteoarthritic femoral head, with a disk sample and three beam samples taken in the AC direction (Ac: Notch across the trabecular structure)

Figure 6.15 Central slice of an osteoarthritic femoral head, with a disk sample and two beam samples taken in the AL direction. (AL: Notch along the trabecular structure).

6.5.3 Sample Sizing

Both equine and human disk and beam samples were prepared so that they were oversized, so as to allow the samples to be resized reducing any damage to the outer trabeculae which might have occurred while using the bandsaw. In addition to this it also enabled the samples to be more accurately sized to the required dimensions for the standard samples. The oversized samples were polished down to size using a rotary grinding / polishing system (Metaserv Rotary Pregrinder, Metallurgical Services, Surrey, UK) (Figure 6.16) with 800 grit wet and dry SiC paper (Buehler Ltd, Lake Bluff, Illinois, USA), ensuring that the sample was constantly being washed with cold water.

Figure 6.16 The rotary pregrinder used for the grinding of samples to the correct size.

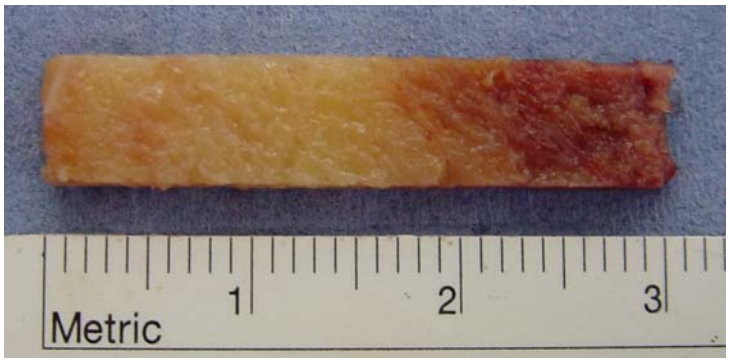

Figure 6.17 Beam sample from an osteoarthritic femoral head central slice, after polishing to size.

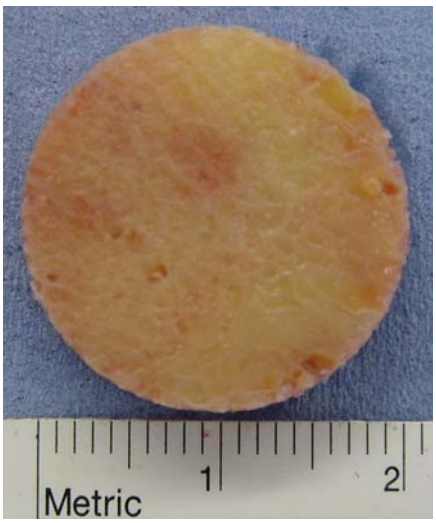

Figure 6.18 Disk sample from osteoarthritic femoral head central slice, after polishing to size.

The average and standard deviation for the equine sample sizes is shown in Table 6.2, with all samples being within 0.2mm of the required dimensions, except the disk samples where the thickness was increased from 7.5mm to 8mm. This was necessary due to the cellular nature of the test samples and the loading mode. The extra thickness was implemented to provide a greater loading area so as to prevent pull out of the loading pins through the side of the sample during testing.

Table 6.2 Average (Standard deviation) of the sample sizes for the equine vertebral disk and beam test samples.

Beam		Disk	
Length	29.99mm (0.53)	Diameter	19.99mm (0.07m)
Width (W)	6.15mm (0.15)	Thickness (B)	8.03mm (0.04m)
Thickness (B)	3.13mm (0.08m)		

For the human tissue the size of the femoral heads prevented the manufacture of some of the specimens from adhering to the uniform size, and this is reflected in table 6.3. The main effects were seen in the lengths of the beam samples, which in the OP groups averaged less than 30mm; however this is of no consequence, as all samples were longer than the required span for the three point bending rig. The disks of the OA group showed a reduced average, and an increased standard deviation, due to 7 samples that were under thickness, four measured 7mm and three 6.5mm. This was due to errors in the sectioning and resizing of the heads and samples, but the thickness (B) is one of the variables in the equations for the calculation of all the fracture toughness parameters (Equation 6.1) and therefore the thickness was accounted for in the later calculations.

Table 6.3 Average (Standard deviation) of the sample sizes for the human femoral disk and beam test samples

Beam	OP+	OA	OP-
Length	29.63 (1.06)	29.99 (0.52)	29.91 (0.61)
Width (W)	6.05 (0.44)	6.08 (0.040)	6.1 (0.06)
Thickness (B)	3.11 (0.05)	3.08 (0.03)	3.08 (0.048)
Disk	OP+	OA	OP-
Diameter	19.97 (0.036)	19.98 (0.1)	20.01 (0.032)
Thickness (B)	7.49 (0.2)	7.31 (0.37)	7.51 (0.94)

6.5.4 Cleaning

In order to test the material properties of the cancellous bone, the bone marrow and fat in between the trabecular struts was removed. The method used within this study for the cleaning of cancellous bone samples was similar to that of T.S.Keller, (1994) and C.H.Turner, (1989) where a high pressure water jet was used to remove the marrow from the pores of the samples, before being submerged in a chemical solution for the dissolution of the remaining fat within the network.

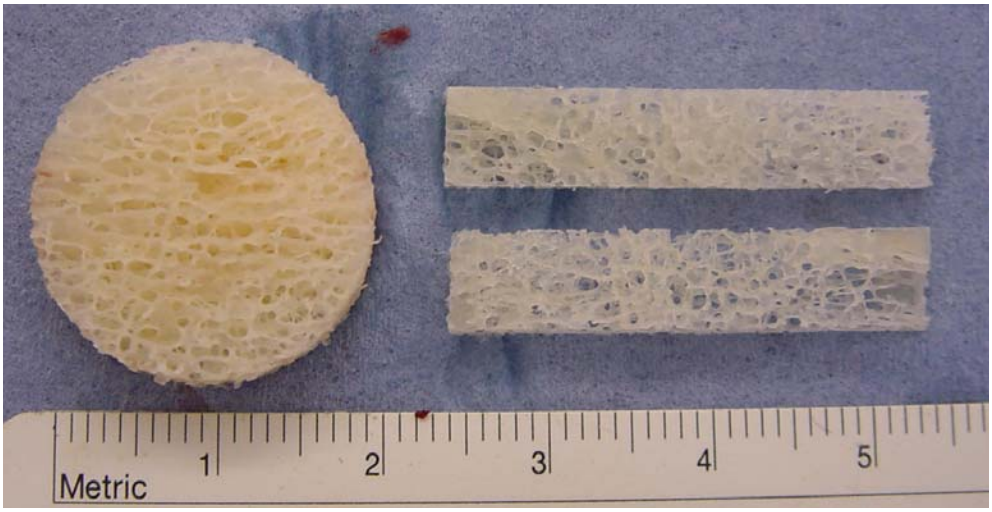

Figure 6.19 Disk and beam samples from group 2 after the cleaning process, showing the cancellous bone structure free of marrow.

The solution used within this study was a 1:1 mix of Chloroform and Methanol. The samples were left submerged in the solution and continuously agitated for 72 hours to ensure all the remaining fat was removed from the samples. After 72 hours, the chloroform methanol solution was removed and the samples were washed and then submerged in methanol for a further 24 hours, to remove any remaining chloroform. The samples were then rewashed using the high pressure water jet, to remove any methanol, and were submerged in Ringer's solution to reconstitute them to their normal physiological status.

6.6 Density Determination

Once the samples were free of any marrow and fat, so only the cancellous bone structure remained, the samples were assessed for density, by utilising a set of Mettler-Tolledo College B154 scales (Figure 6.20a) (Mettler-Tolledo Inc., Columbus, OH, USA), which have an accuracy of 0.0001g. The scales were fitted with a density determination equipment (Figure 6.20b), which enabled the determination of apparent density, material density and porosity based on the Archimedes principle.

Each sample was submerged in distilled water and centrifuged (Mistral 1000, MSE) at 3000rpm for 3 minutes, to remove all air from the bone samples. The fully hydrated samples were then placed on the small wire platform 1, of the density determination equipment (Figure 6.20b) and weighed while submerged in distilled water to give the submerged wet weight (W_{SUB}). The samples were removed from the water wrapped in blotting paper and centrifuged again to remove any excess water from the surface and pores. The hydrated samples were placed onto platform 2

(Figure 6.20b) above the water beaker and reweighed in a hydrated state to give the wet weight (WW).

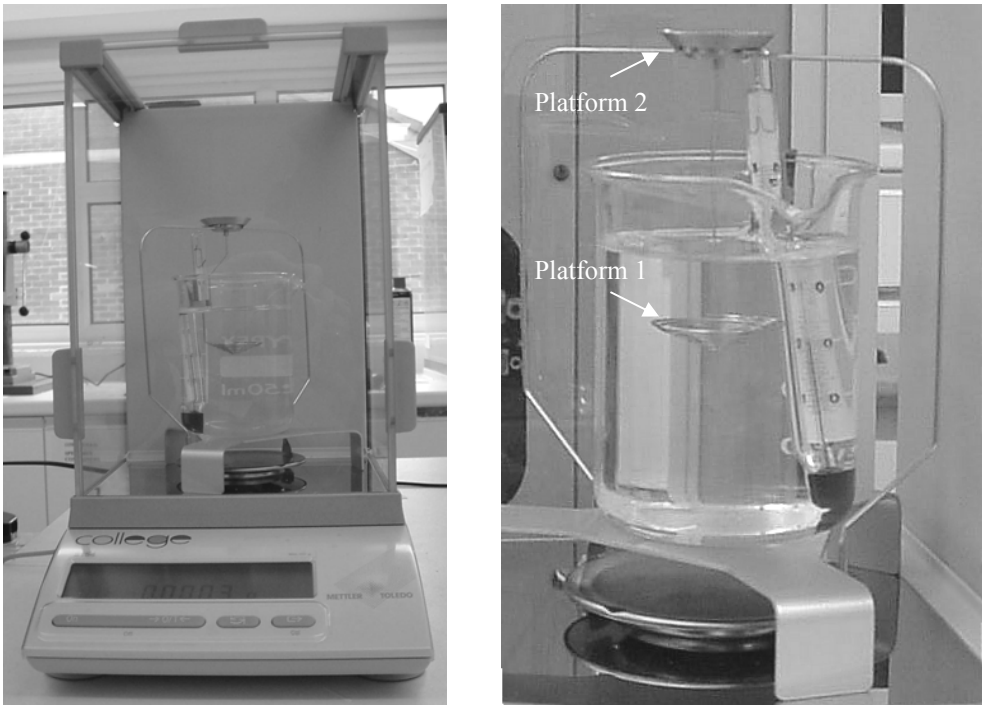

Figure 6.20 a Mettler-Tolledo College B154 scales
b. Density determination equipment

The samples' dimensions were determined using a digital vernier calliper with an accuracy 0.01mm (Absolute Digimatic, Mitutoyo UK Ltd., Andover, Hampshire, UK), and used to calculate the volume (V_0) of the specimen sample. The densities of the cancellous bone samples were calculated according to equations 6.7 and 6.8.

$$\text{Apparent Density } (\rho_{App.}) = \frac{WW}{V_0} \qquad \textbf{Equation 6.7}$$

$$\text{Matrix Density } (\rho_{Mat.}) = \left(\frac{WW}{WW - W_{SUB}} \right) D_0 \qquad \textbf{Equation 6.8}$$

where D_0 is the density of the liquid in which the sample is submerged. In this study the liquid used was distilled water which has a density of 1. The porosity and the relative density were calculated using the results of the apparent density and matrix density calculations, the equations for the determination of porosity and relative density are shown in equations 6.9 and 6.10 respectively.

$$\text{Porosity} = 1 - \left(\rho_{\text{App.}} / \rho_{\text{Mat.}}\right) \qquad \textbf{Equation 6.9}$$

$$\text{Relative Density}\ (\rho_{\text{Rel.}}) = \rho_{\text{App.}} / \rho_{\text{Mat.}} \qquad \textbf{Equation 6.10}$$

6.7 Collagen Cross-Linking Analysis

The collagen cross-link analysis was performed by the collagen research group, the division of molecular and cellular biology at the University of Bristol, and the following methods were provided by the group and are the same as the techniques laid out in T.J. Sims et al. (2000).

6.7.1 Sample Preparation

The total wet weight of each sample was determined by weighing. They were then frozen in liquid nitrogen and powdered using a steel pestle and mortar at the same temperature. The powder was recovered into plastic vessels and between 1 and 2 mls of a Brij 35 / triethanolamine extraction buffer was added according to the calculated dry weight of each sample. The samples were left to extract overnight at +4˚C with constant agitation. Insoluble material was recovered next day by centrifugation and the supernatant stored at -20˚C until required for substrate linked sodium dodecyl sulphate polyacrylamide gel electrophoresis (substrate zymography SDS PAGE).

6.7.2 Decalcification

The insoluble material was decalcified by extraction at room temperature with two changes of 0.5M tetra-sodium ethylenediamine tetra-acetic acid pH 7.5 (EDTA) initially after 8 hours and then after overnight for a further 8 hours with constant agitation throughout. The supernatants were discarded after each centrifugation.

6.7.3 Borohydride Reduction

The pelleted material was twice washed with distilled water, centrifuged and then suspended in phosphate buffered saline prior to reduction with sodium borohydride at room temperature for 1 hour. The reduction was stopped by adjusting the pH to approximately 3.0 with acetic acid and the reagents discarded after centrifugation. The pellet was finally washed with distilled water prior to freeze-drying and final weighing.

6.7.4 Hydrolysis

The dry material was placed in glass hydrolysis tubes with 6N hydrochloric acid, sealed and then hydrolysed at 115˚C for 24 hours. After that period they were cooled to -80˚C and the acid removed by freeze-drying. The hydrolysates were now re-hydrated with 0.5ml of water and a 100µl aliquot stored frozen for subsequent hydroxyproline determination and high performance liquid chromatography (HPLC). The collagen cross-links in the remaining 400µl were concentrated using fibrous cellulose (CF1) columns.

6.7.5 Cross-link Analysis

After CF1 chromatography the samples were vacuum concentrated, re-hydrated with 200µl of 0.01N hydrochloric acid and 0.2µm filtered prior to analysis using an Alpha Plus amino acid analyser (Pharmacia) configured for cross-link analysis.

6.7.6 Hydroxyproline Analysis

Aliquots equal to 0.5µl of each original hydrolysate were analysed in duplicate using a Chembase 2000 autoanalyser (Burkard Scientific) configured for hydroxyproline analysis.

6.7.7 Glycated Cross-link Analysis

Duplicate aliquots of the original hydrolysates equal to 90µg of collagen were analysed by HPLC (Waters), after 0.2µm filtration, using a Hypercarb S column (Shandon Scientific) and fluorescence detection (Perkin Elmer).

6.7.8 Substrate Zymography

SDS PAGE gels containing gelatin as substrate were prepared and 10µl aliquots of the Brij 35 / triethanolamine extract from each sample electrophoresed. After incubation overnight at 37˚C the gels were stained with PAGE blue and the zones of clarity due to protease activity were quantified by scanning.

6.8 Sample Testing Preparation

After density determination had been performed, the samples required an additional stage of preparation which involved the introduction of a notch, extensometer attachment holes and, for each disk specimen, a pair of holes for the loading pins. In order to ensure the uniformity of preparation between samples, two specimen specific jigs were manufactured Figure 6.21 and Figure 6.22

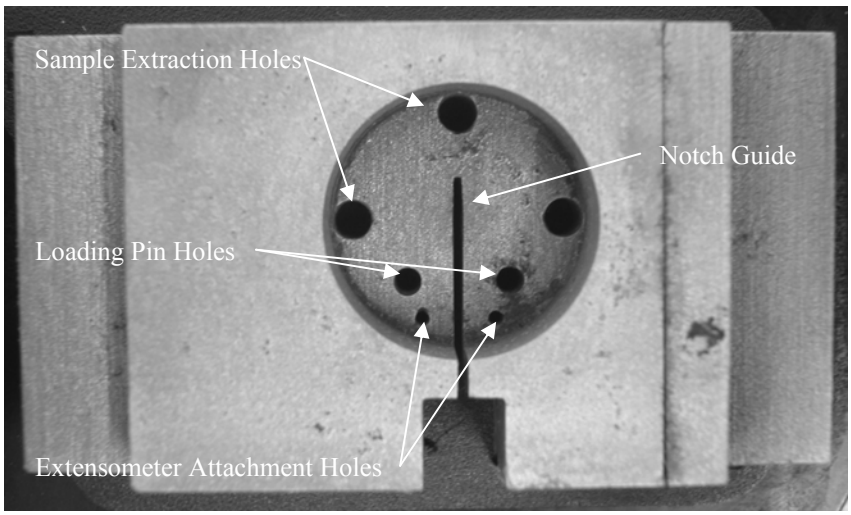

Figure 6.21 Jig for the preparation of disk-shaped compact specimens.

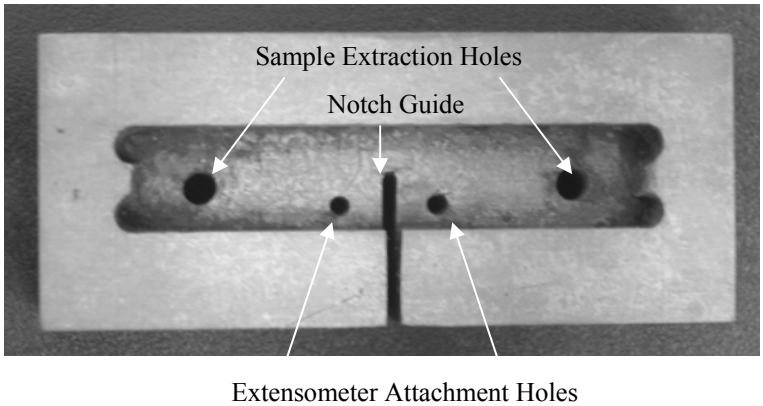

Figure 6.22 Jig for the preparation of beam samples.

6.8.1 Notching

ASTM standard E399-90 provides three different designs of starter notch, which are intended to undergo a process of fatigue to introduce a crack of specific length at the tip of the notch. For this study however the notch did not adhere to the recommended designs and neither were they fatigue crack prior to testing.

The notches inserted were straight notches with a blunt unsharpened end, inserted into each specimen using a Struers® Accutom 2 wafering saw (Struers A/S, Rodovre, Denmark) with a 300µm thick diamond impregnated circular blade (Figure 6.23), while being constantly irrigated with water. The resultant notch was therefore 300µm wide with a root tip radius of 150µm.

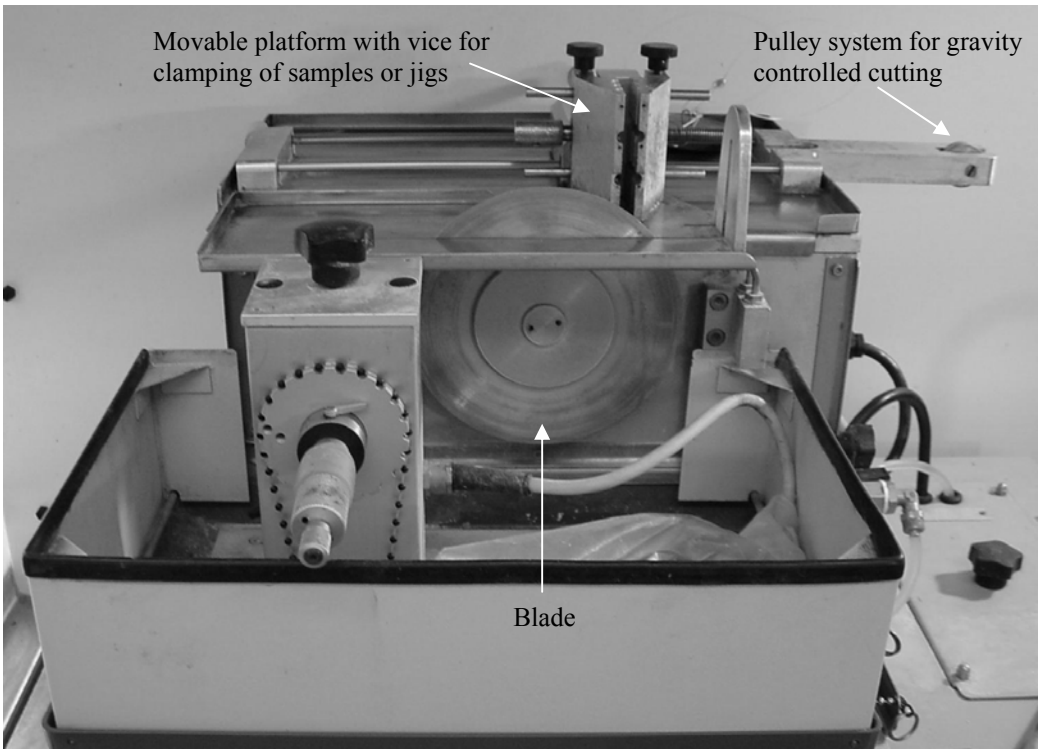

Figure 6.23 Struers® Accutom 2 wafering saw with a 300µm thick diamond impregnated circular blade

The tip of the notch was not sharpened by a scalpel blade and nor were the samples pre-fatigued as in cortical or compact bone applications. This was deemed unnecessary, as the crack tip consisted of only a few trabeculae to sustain/prevent the subsequent fracture. The act of sharpening the crack tip would not have made any difference to the resultant value and would only have served to increase the length of the initial notch. This peculiarity is one of many arising from the cellular nature of this solid, and may go some way to explaining why fracture toughness tests on cancellous bone have never previously been performed.

In order to provide the information required for the calculation of the J-integral (section 6.3.2.3) it was necessary to vary the length of the initial notch(a_o), so as to provide a range of values related to a_o/W, or initial crack length / specimen width. The disk specimens were divided into four groups, with each group having a different notch length introduced by the addition of blocks beneath the specimen jig to raise the sample a set distance. Due to the small size of the beam samples under investigation it was not feasible to introduce a set range of notches, however during the notching process the notch length was varied between samples to provide a range of lengths.

The notch length of each specimen was determined using a travelling microscope (Figure 6.24) (W.G.Pye and Co. Ltd., Cambridge, UK), which enabled the determination of a_o and W with an accuracy of 0.01mm. The length of the notches for the equine specimens and the different human groups are shown in Table 6.4, Table 6.5 and Table 6.6.

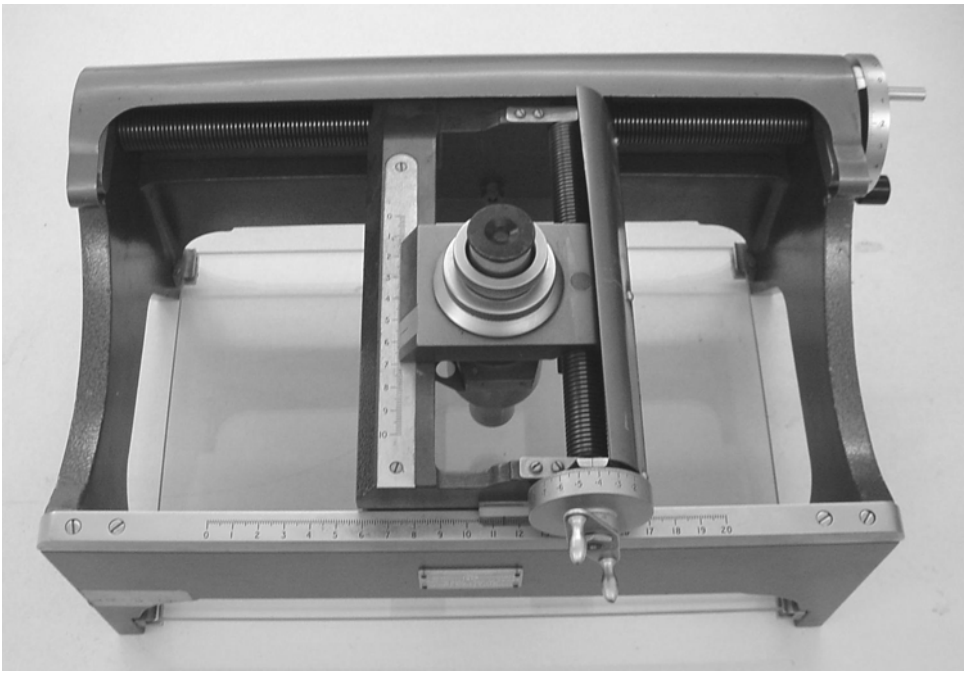

Figure 6.24 Travelling microscope (W.G.Pye and Co. Ltd., Cambridge, UK)

Table 6.4 a_o and a_o/W ratios for the equine disk and beam specimens

Disk Specimens			Beam Specimens		
Length	a_o (mm)	a_o/W		a_o (mm)	a_o/W
1	5.87 (0.150)	0.391 (0.0099)	Range	2.26 – 3.39	0.372 – 0.545
2	6.96 (0.071)	0.464 (0.0042)	Average	2.85	0.464
3	7.57 (0.096)	0.506 (0.0046)	St. Dev.	0.206	0.0348
4	8.18 (0.085)	0.546 (0.0063)			

Table 6.5 Average (standard deviation) for the a_o and a_o/W ratios for the human disk specimens from the 4 different lengths.

Length	OP+		OA		OP-	
	a_o (mm)	a_o/W	a_o (mm)	a_o/W	a_o (mm)	a_o/W
1	5.62 (0.290)	0.373 (0.022)	5.66 (0.18)	0.377 (0.001)	5.82 (0.23)	0.388 (0.015)
2	6.43 (0.245)	0.427 (0.016)	6.28 (0.22)	0.418 (0.015)	6.94 (0.067)	0.462 (0.005)
3	7.33 (0.184)	0.486 (0.012)	7.3 (0.18)	0.485 (0.011)	7.46 (0.15)	0.497 (0.01)
4	8.07 (0.144)	0.535 (0.001)	8.09 (0.091)	0.539 (0.009)	8.23 (0.17)	0.549 (0.01)

Table 6.6 a_o and a_o/W ratios for the human beam specimens

Length	OP+		OA		OP-	
	a_o (mm)	a_o/W	a_o (mm)	a_o/W	a_o (mm)	a_o/W
Range	2.32 - 3.29	0.381 - 0.542	2.52 – 3.52	0.417 – 0.576	2.43 - 3.27	0.402 - 0.527
Average	2.9	0.474	2.92	0.48	2.85	0.467
St. Dev.	0.161	0.0261	0.241	0.0395	0.176	0.0286

6.8.2 Loading and Extensometer Holes

The holes for the loading pins were inserted by passing a 2mm diameter drill bit through the corresponding hole in the disk specimen's jig. The Extensometer attachment holes were inserted using a 1mm drill bit passed through the relevant holes in the specimen specific jig. The resultant samples ready for testing are shown in Figure 6.25 and Figure 6.26

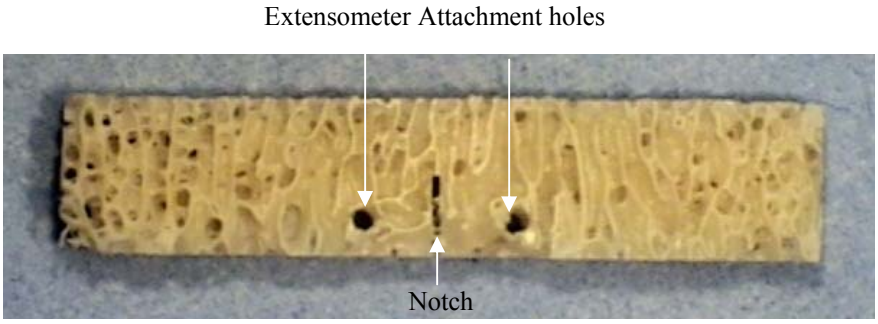

Figure 6.25 Equine AC Beam sample with extensometer attachment holes and notch.

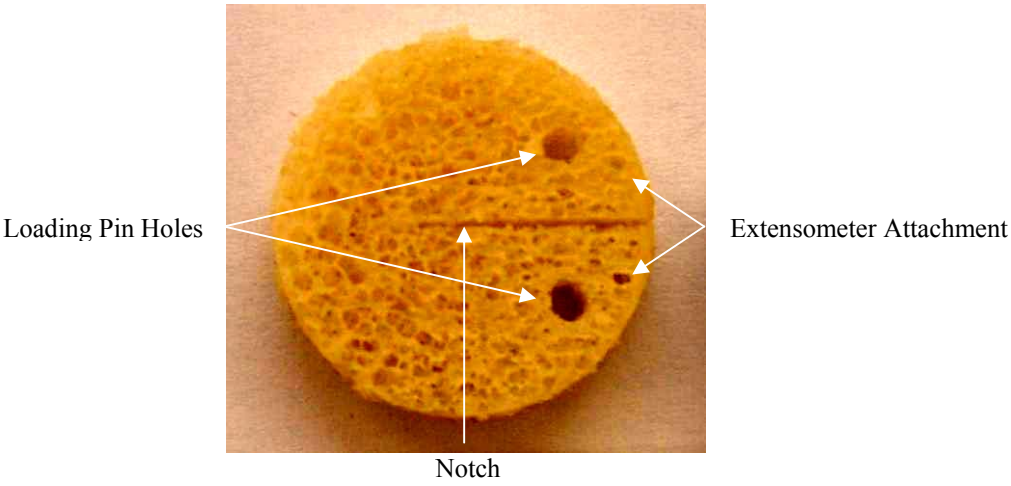

Figure 6.26 Equine AL disk with loading holes, extensometer attachment holes and notch.

6.9 Compression Testing Samples

Compression testing was performed on the human femoral heads from all three groups, but not on the equine vertebra. Cores were cut from the external slices of the femoral heads using a diamond edged grinding core drill (D.K.Holdings Ltd., Kent, UK) with an internal diameter of 9mm. In order to remove the articular cartilage from the core, the specimens were gripped in a polycarbonate jig within the vice system of the Struers® Accutom 2 wafering saw (Figure 6.23); this jig not only provided a means of mechanical support but also ensured that the sample ends remained parallel.

The compression cores underwent the same cleaning and density determination process as was performed on the fracture toughness samples (section 6.5.4), to provide cores free of any marrow or fat (Figure 6.27).

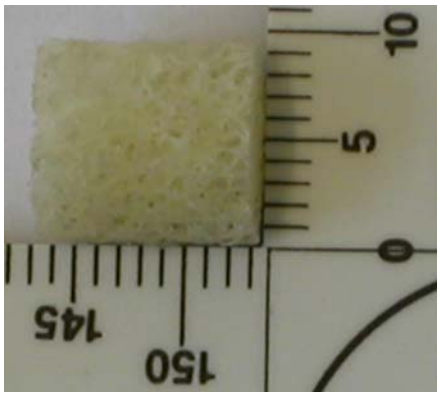

Figure 6.27 Cleaned compression core from OP+

Due to the nature of the external slices, the lengths of the compression cores were restricted by the size of the external slice, with the average length of the cores being 11.35mm (Table 6.7).

Table 6.7 Range, average and standard deviation of the diameter and length of the compression cores, taken from the femoral heads of all groups.

	OP+		OA		OP-		Average	
	Diameter (mm)	Length (mm)	Diameter (mm)	Length (mm)	Diameter (mm)	Length (mm)	Diameter (mm)	Length (mm)
Range	8.93 - 9.05	7.8 - 14.88	8.98 - 9.04	9.39 - 14.46	8.95 - 9.09	7.29 - 16.71	8.93 - 9.09	7.29 - 16.71
Average	9.02	10.44	9.01	11.55	9.03	12.21	9.03	11.35
St. Dev.	0.027	2.02	0.017	1.76	0.032	2.42	0.0282	2.26

The length of the compression cores presented a problem, due to the nature of the compression testing rig and the miniature extensometer attachment (section 6.11.2); a longer length sample was required to provide clearance for attaching the extensometer legs on the sample without touching the platens. The solution was the addition to either end of the sample of wooden spacers. The spacers were made from cores of teak, produced using the same 9mm diameter core drill used to produce the

compression cores, and were fixed to either end using cyanoacrylate super glue (Figure 6.28).

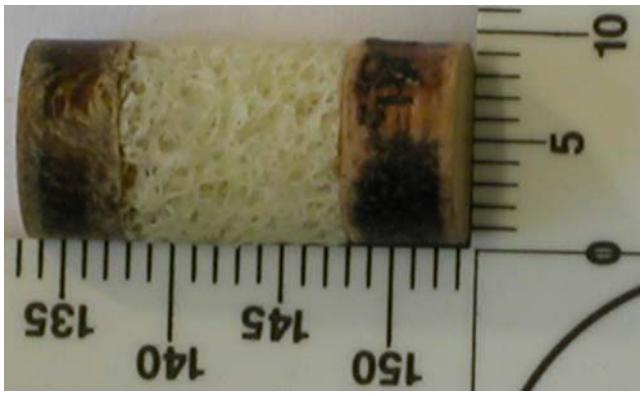

Figure 6.28 Compression core from OP+ with the addition of teak spacers to either end of the sample.

The addition of the teak spacers caused an increase in the gauge length of the samples (Table 6.8), but provided enough additional length to the samples for the miniature extensometer to be attached directly to the bone without interference with the loading platens.

Table 6.8 Range, standard deviation and average gauge lengths of the compression cores taken from the femoral heads of all groups after the addition of the teak spacers.

	OP+	OA	OP-	Average
Range	17.45 - 24	19.1 - 23.7	16.15 - 24.2	16.15 - 31.8
Average	20.05	20.71	20.92	20.71
St. Dev.	2.12	1.49	2.24	2.63

6.10 Testing Rigs

6.10.1 Three Point Bending Rig

The three point bending rig was designed and manufactured to adhere as closely to the guidelines laid out in ASTM Standard E399-90 as possible. The rig had

a span of 24mm with the loading points at the base of the rig having a diameter of 3mm, and the upper loading pin 6mm.

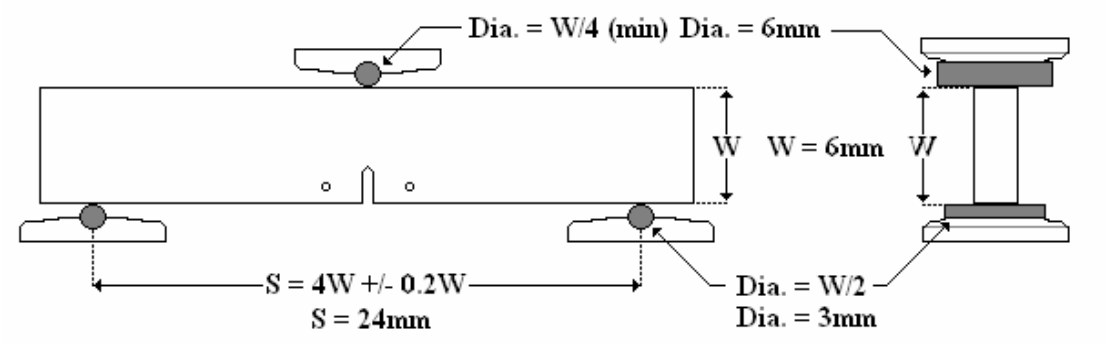

Figure 6.29 Schematic representation of the three-point bending rig.

It was not possible to provide an irrigation system for this test rig, so as to keep the specimen hydrated with physiological saline during testing, due to the positioning of the extensometer below the sample during testing. Samples were, however, saturated with physiological saline at 37^{o}C prior to testing and tested as quickly as possible to prevent the samples having time to dehydrate.

6.10.2 Disk-Shaped Compact Specimen Test Rig

Due to the small sample size it was not feasible to adhere to the standard for the test rig. The loading pin diameter was recommended at 0.24W, but the loading pins measured 2mm (~0.13W) in diameter, this ensured that there was as much bone as possible between the loading pins and the sample edge to prevent the loading pins pulling out of the sample sides during testing. The clevis into which the specimen fits was recommended to measure 0.5W, but in order for attachment of the extensometer this was increased to 12mm (~0.8W).

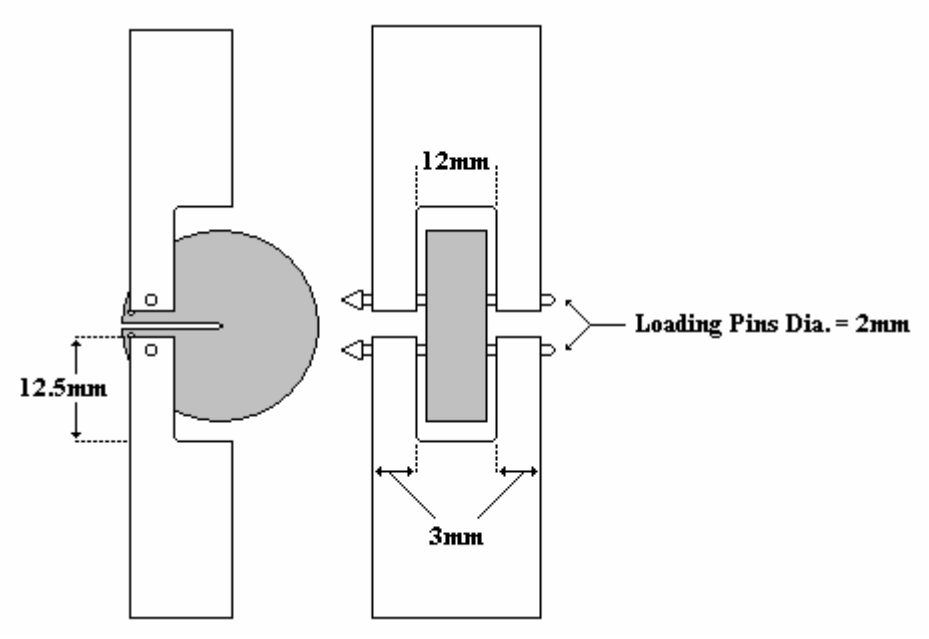

Figure 6.30 Schematic representation of the test rig for the compact disk-shaped specimens.

The samples were constantly irrigated with physiological saline during testing at 37^{o}C to mimic the in-vivo conditions.

6.10.3 Compression Testing Rig

The compression testing rig comprised of two loading platens 12.7mm in diameter, with each surface having a 9.2mm diameter wide and 1mm diameter deep depression into it. The depression was added to allow for the teak ends of the compression cores to be restrained, so as to ensure the linearity of the samples during testing. The upper loading platen was articulated on a spherical surface, so as to ensure that any slight nonlinearity in the test sample was accounted for. The test rig included an irrigation system so that the samples were constantly washed with physiological saline at 37^{o}C throughout testing.

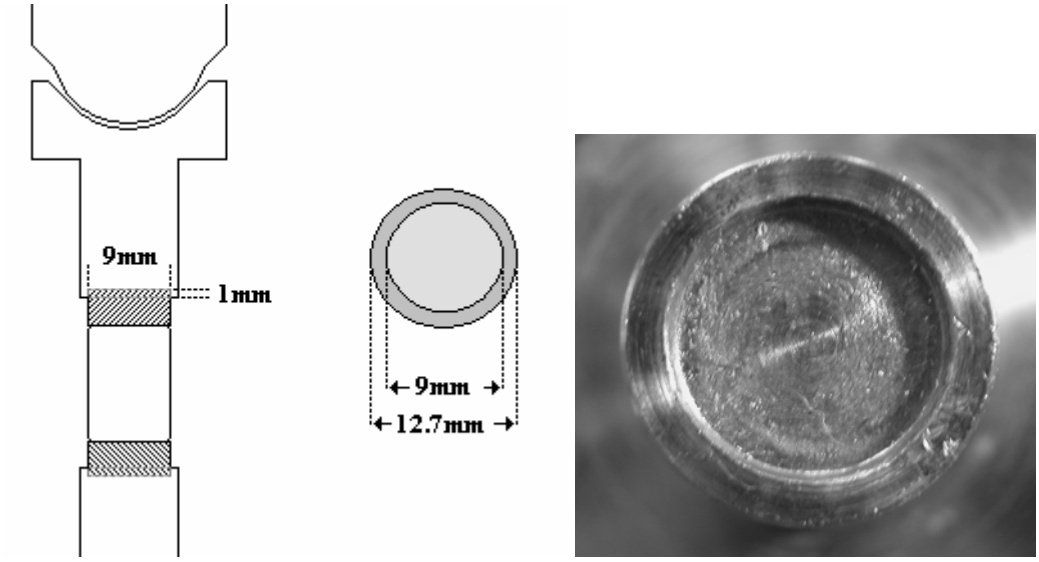

Figure 6. 31 a: Schematic of the compression testing rig, showing the articulated upper platen, an 1mm deep depressions on the loading platen surfaces. b: Image showing 1mm deep depressions on the loading platen.

6.11 Mechanical Testing

6.11.1 Fracture Toughness Testing

All fracture toughness testing was performed on a 'Dartec Series HC25' materials testing machine driven by a '9610 series controller' unit and operated via a PC interface using the 'Workshop 96' software. The load was monitored using a 500N load cell (Sensotec, RDP Electronics Ltd., Wolverhampton, UK). The crack mouth opening displacement (CMOD) was monitored using a miniature extensometer (Miniature Model 3442-006M-050ST, Epsilon Technology Corp., Jackson, WY, USA) (Figure 6.32a), which had a gauge length of 6mm, (+3mm, -6mm). The extensometer was fixed to the mouth of the notch by specially designed attachments (Figure 6.32b), with 1mm diameter pins which pass through the specimen.

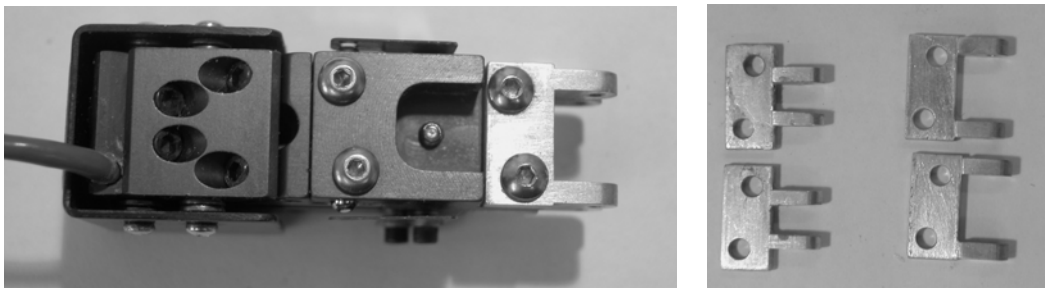

Figure 6.32 a Miniature extensometer (Miniature Model 3442-006M-050ST, Epsilon Technology Corp., Jackson, WY, USA). b. Extensometer attachments for connection of the extensometer to the mouth of the notch.

The loading rate for the disk-shaped compact specimens, and the beam specimens, was 0.05 mm/s (3mm/min), with the software set up to capture 1000 points per minute, with each test lasting a minute. The disk shaped compact specimens were tested in tension and the beam specimens in three point bending (Figures 6.33 and Figure 6.34).

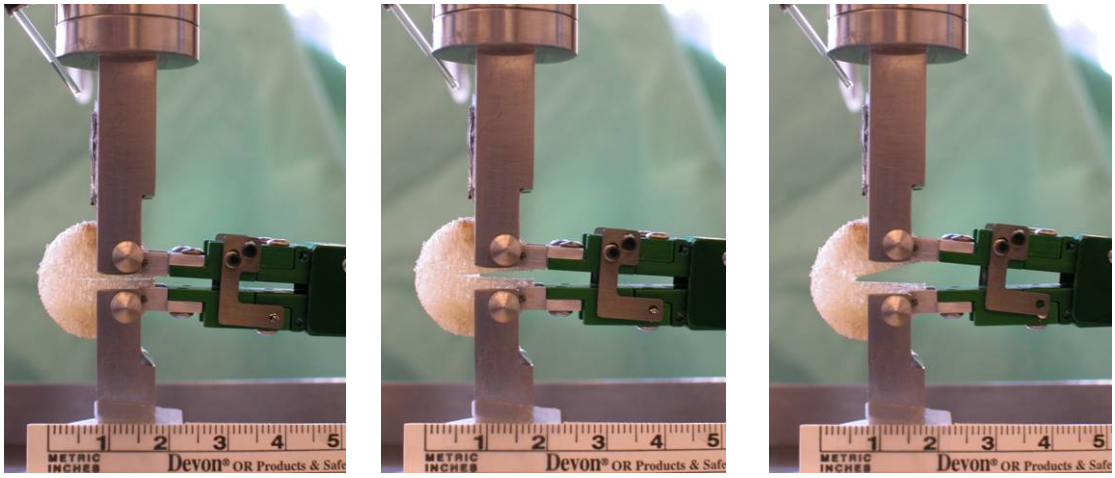

Figures 6.33 Tensile testing of the compact disk specimens showing the crack opening during testing

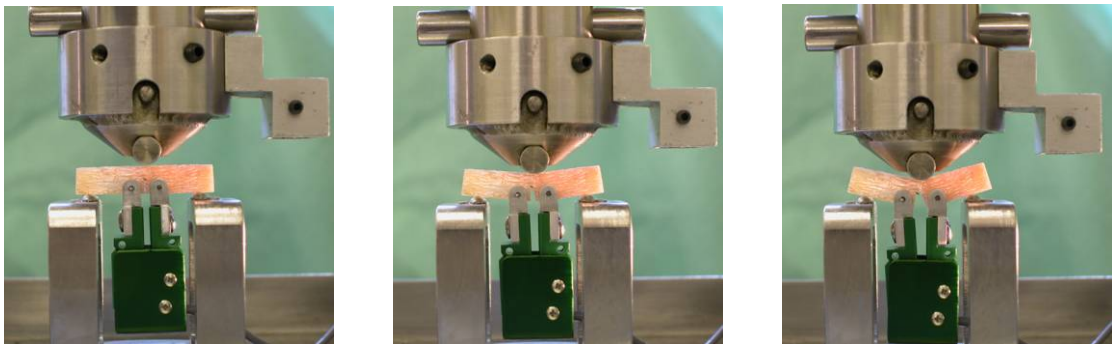

Figure 6.34 Three point bend testing of the beam specimens showing the crack opening during testing.

6.11.2 Compression Testing

The compression testing was performed on the same Dartec Series HC25 materials testing machine driven by a 9610 series controller unit and operated via a PC interface using the Workshop 96 software. The load was monitored using a 5kN load cell (Sensotec, RDP Electronics Ltd., Wolverhampton, UK), with the sample deflection monitored using two different extensometers.

- A miniature contact extensometer (Miniature Model 3442-006M-050ST, Epsilon Technology Corp., Jackson, WY, USA), which had a gauge length of 6mm, (+3mm, -6mm) (Figure 6.32a). The extensometer was fixed to the surface of the bone sample via knife edges and held in place using 8mm diameter orthodontic elastic bands (G&H Wire Company, Greenwood, In, USA).
- A LVDT with a 10mm gauge length (RDP Electronics Ltd., Wolverhampton, UK) was placed into contact with the loading platens on either side of the test sample to measure the displacement of the platen ends relative to each other.

Prior to compressive testing, each sample was preconditioned by cyclically compressing the samples 40 times at 1Hz. The loading rate for the compression testing was set at 0.15mm/s (9mm/min), which for the samples with the teak end caps equated to a strain rate of ~0.75%s^{-1}, and a strain rate of 2.5%s^{-1} for the contact

extensometer with a 6mm gauge length. The software was set-up to collect 2000 points per minute, with the average test lasting ~30 seconds.

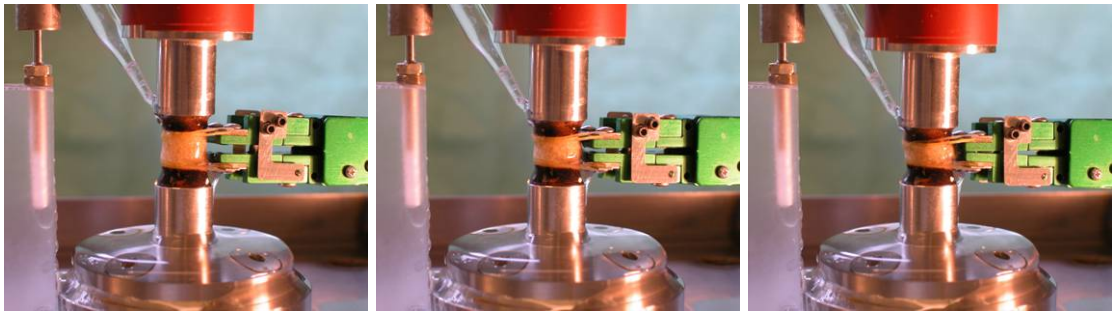

Figure 6.35 The compressive testing of a compression core, showing both the contact extensometer and the platens LVDT.

6.12 Compositional Testing

After the mechanical testing of the samples was completed, the composition in relation to the percentage mineral, organic and water of the samples was determined. This was a result of weight percentages and not a result of geometry or structure investigations.

From each beam sample, approximately 10mm was removed from its length, using the Struers® Accutom 2 wafering saw, leaving the fracture area and surface unaffected. For the disk samples a 5mm internal diameter diamond edged grinding core drill (D.K.Holdings Ltd., Kent, UK) was used to remove a core from the periphery of the sample, once again ensuring that the fracture area and surface were unaffected. Any excess water was removed from within the cancellous structure using blotting paper, and each sample was weighed in a hydrated state (WW_{ash}). The samples were then allowed to dry in a hot-box oven at 37^{o}C for a period of three days. After the three days the samples were placed into crucibles of known weight and reweighed in the dried state to provide the dry mineralised weight (DMW). The

samples contained within individual crucibles were then placed into a furnace (Monometer, MFG. Co. Ltd. Essex, UK) and ashed for 3 hours at 600^{o}C. The samples were then reweighed in the ashed state (W_{ashed}).

From these parameters it was then possible to calculate the percentage water fraction (Equation 6.11) the percentage hydrated mineral content (Equation 6.12) and the percentage hydrated organic content (Equation 6.13).

$$\%\ \text{Water Fraction} = \frac{\left(WW_{ash} - DMW\right)}{WW_{ash}} * 100 \qquad \textbf{Equation 6.11}$$

$$\%\ \text{Mineral Content} = \left(W_{ash} / WW_{ash}\right) * 100 \qquad \textbf{Equation 6.12}$$

$$\%\ \text{Organic Content} = 100 - (\%\ \text{Water Fraction} + \%\ \text{Mineral Content}) \qquad \textbf{Equation 6.13}$$

If the water content was excluded from the analysis and the cancellous bone material was considered alone then the percentage dry mineral content (Equation 6.14) could be calculated, with the remaining percentage representing the percentage dry organic content.

$$\%\ \text{Dry Mineral Content} = \left(W_{ash} / DMW\right) * 100 \qquad \textbf{Equation 6.14}$$

Concluding Remarks

The results of these methods provided 50 compression cores, (41 osteoporotic and 9 osteoarthritic), 293 beam fracture toughness samples (111 equine, 128 osteoporotic and 55 osteoarthritic) and 121 disk-shaped compact fracture toughness samples (39 equine, 61 osteoporotic and 21 osteoarthritic), with the fracture toughness samples being additionally split into two separated orientations either across the trabecular structure (Beams Ac: 170, Discs Ac: 61) or along it (Beams AL: 126, Discs: AL: 60). Each sample was tested with respect to its design; the compression cores provided 6 mechanical parameters, 4 of which were in duplicate

due to the different displacement measurement methods (platens vs. contact extensometers) and each of the fracture toughness samples provided 3 parameters which were calculated at both the yield point P_Q and the point at which crack growth occurred (P_{max}).

Each individual sample was assessed for apparent density, relative density, porosity and material density, as well as its mineral, organic and water fractions. Two samples were extracted from each of the femoral heads and analysed for the levels of 6 different collagen cross-links, 2 immature, 3 mature and one as the result of glycation. The last of the variables were 5 QUS investigations (measurement value, T-score and Z-score), performed on 4 different skeletal sites of the donors from which the femoral heads were obtained.

In conclusion these methods provide 16 dependent variables in the form of mechanical parameters, and an additional 23 independent variables including material, compositional and biochemical properties, as well as clinical QUS results. The study will assess both human and equine skeletal tissue, as well as encompassing two different human skeletal conditions known to affect the properties of the bone.

Chapter 7: Results: Clinical Studies

7.1 Precision Study

The first phase of the study was the undertaking of the precision investigation on the subjects within group 1. The aims and reasons behind performing the study were twofold; to enable the researcher to gain valuable experience in the functioning of the systems, but also to provide a quantitative value of the researcher's abilities with the two systems, prior to the onset of the clinical population based study.

The precision results obtained from the quadruple measurements on the 16 healthy individuals from group 1 are displayed in Table 7.1. The Sunlight Omnisense system demonstrated a level of precision superior to that provided by the manufacturer of the system (Table 4.10). The precision of the CUBA clinical system was, on the other hand, roughly 1.5% below that provided by the manufacturer.

Table 7.1 Short Term Precision of Group 1 (95% Confidence intervals)

System	Measurement Site	CV%	$_{RMS}$CV%	$_{s}$CV%
Sunlight Omnisense	Distal Radius	0.26 (0.258 - 0.263)	0.29 (0.24 – 0.36)	4.08 (4.04 - 4.11)
	Proximal Phalanx	0.47 (0.462 - 0.479)	0.54 (0.45 – 0.67)	3.52 (3.45 - 3.58)
CUBA Clinical	BUA Calcaneus	2.40 (2.208 - 2.715)	2.72 (3.4 – 2.27)	3.41 (3.08 - 3.75)
	VOS Calcaneus	0.23 (0.229 - 0.234)	0.26 (0.22 – 0.33)	2.96 (2.92 - 2.99)

The levels of precision were considered suitable for the undertaking of the population based study at the Great Western Hospital in Swindon. The precision of the

paired measurements from 268 caucasian women from group 2 are shown in Table 7.2. The results are comparable to the precision achieved previously from group 1 and, in the case of the Sunlight Omnisense system, they were comparable but slightly worse than the manufacturer's guidelines. The CUBA Clinical results were, however, roughly 2% below the level of precision which the manufacturer's had provided, a further 0.5% over that which was obtained in group 1.

Table 7.2 Short-Term Precision of Group 2 (95% Confidence intervals)

System	Measurement Site	CV%	$_{RMS}$CV%	$_{s}$CV%
Sunlight Omnisense	Distal Radius	0.360 (0.359 - 0.361)	0.48 (0.44 – 0.53)	3.51 (3.50 - 3.52)
	Proximal Phalanx	0.795 (0.791 - 0.799)	1.06 (0.98 – 1.16)	4.55 (4.53 - 4.57)
	Mid-Shaft Tibia	0.363 (0.362 - 0.364)	0.74 (0.68 – 0.81)	5.20 (5.19 - 5.22)
CUBA Clinical	BUA Calcaneus	2.67 (2.6 - 2.75)	3.54 (3.27 – 3.87)	3.15 (3.07 - 3.22)
	VOS Calcaneus	0.248 (0.247 – 0.249)	0.36 (0.33 – 0.389)	3.61 (3.60 – 3.62)

7.2 Discriminatory Ability

The discriminatory ability of the systems refers to the capability of the systems to agree on the classification of an individual's skeletal status, by providing similar T-score results. The analysis was performed on both groups 2 and 3 using the T-score and threshold levels provided by the manufacturers of the QUS and the designers of the questionnaire systems.

7.2.1 Graphical Representation

The initial results are provided in graphical form for Group 2 (Figure 7.1) and demonstrate that, for the most part, the systems show wide variations when asked to classify individuals within the three different classification levels.

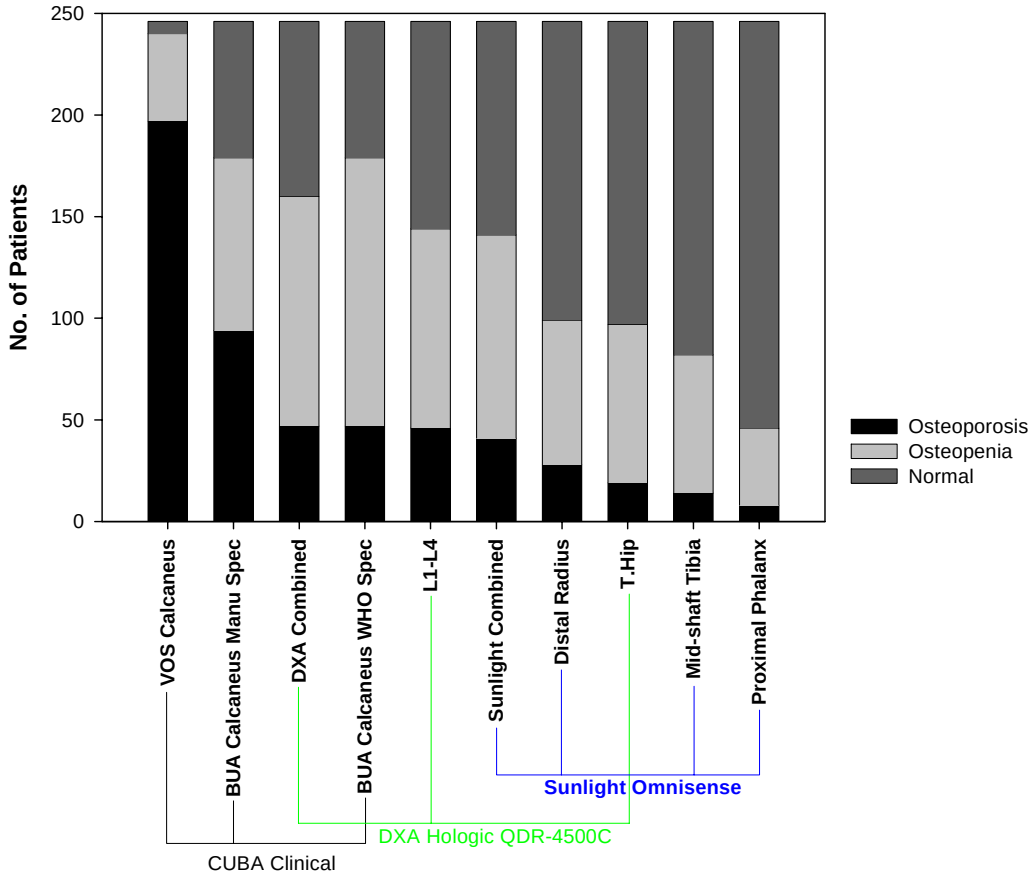

Figure 7.1 Group 2 Discriminatory abilities.

Certain techniques display either an over pessimistic view (VOS calcaneus, and BUA using the manufacturer's threshold) and others display an over optimistic view (Proximal Phalanx). These trends are also seen when the same graphical analysis is performed on group 3 (Figure 7.2)

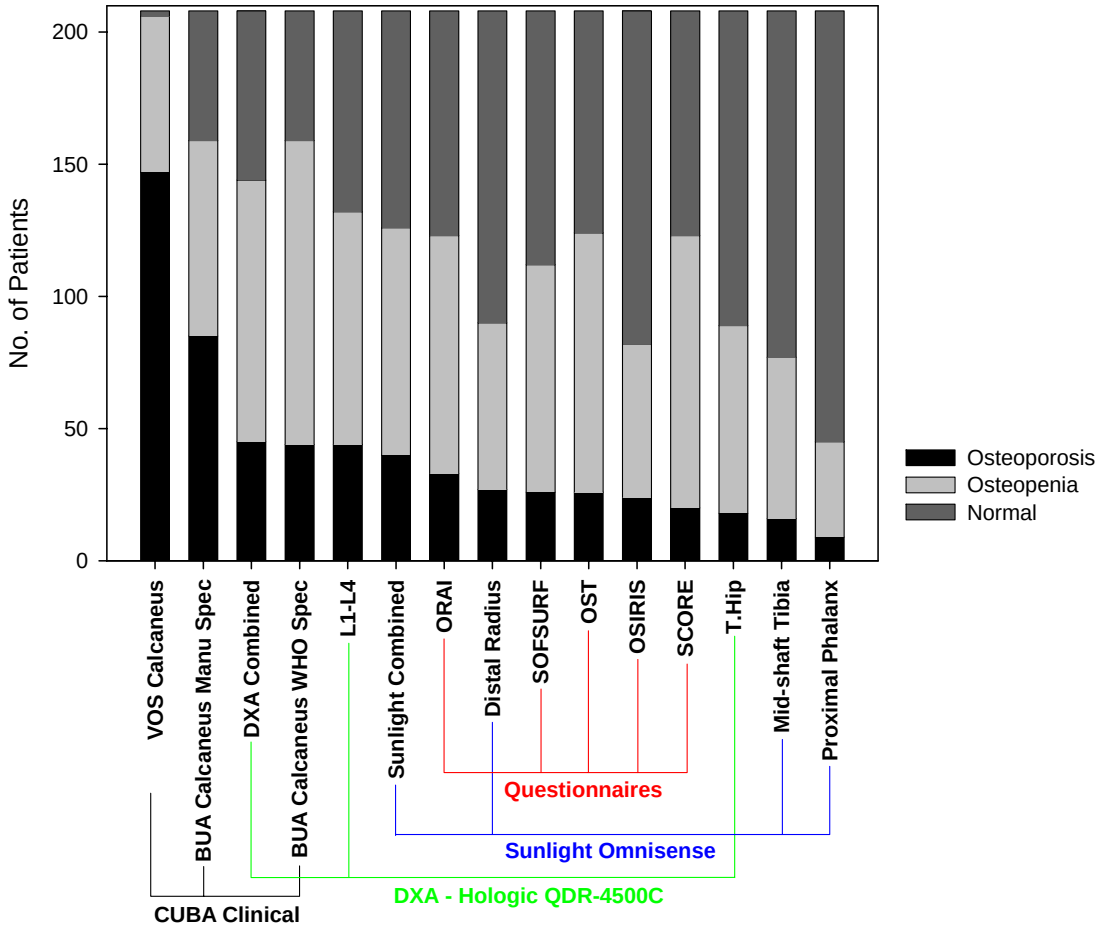

Figure 7.2 Group 3 Discriminatory abilities.

The graphical evaluation provides an informative comparison between the different systems on the population as a whole, but in order to compare the results between each site within the same individual, a quantitative approach utilising the Kappa indices is necessary.

7.2.2 Kappa Indices

The Kappa indices provide a value which denotes the degree of agreement between measurement values with 1 equating to a perfect agreement and 0 no agreement at all. For group 2 the analysis was performed between all the individual sites

(Table 7.3) and demonstrated that, although the numbers within each category were similar, the individuals within each classification varied depending on the techniques. This finding is further supported by the relationships found between the scanning techniques in group 3 (Table 7.4) where, within a postmenopausal population, the agreement between the measurement techniques was also poor. The performance of the questionnaire techniques to correctly classify individuals, in relation to their DXA result, was superior to that of the scanning techniques, although with values in the region of 0.2-0.4 the level of agreement can still be considered to be comparatively low.

The lack of agreement between the QUS techniques is not the technique's fault but is due to the nature of the human skeleton. Within the human skeleton, it is possible to have one skeletal site which can be considered osteoporotic and another site within the same skeleton considered normal. The same cannot be said for the questionnaire techniques which, despite performing better than the ultrasound techniques, were designed specifically for the prediction of the DXA result of an individual, and one would have hoped for them to have shown higher Kappa indices. This would indicate that despite the usage of the anthropometrical and other risk factors, proven to provide a high level of diagnostic ability, there are other variables which have a bearing on the skeleton which are not considered by the questionnaire systems.

Table 7.3 Kappa scores for the comparison between group 2 measurement results

Kappa Group 2	Distal Radius	Proximal Phalanx	Mid-Shaft Tibia	Sunlight Combined	BUA Calcaneus (Manufacturers Threshold)	BUA Calcaneus (WHO Threshold)	VOS Calcaneus
Proximal Phalanx	0.19						
Mid-shaft Tibia	0.12	0.14					
Sunlight Combined	0.68	0.24	0.5				
BUA Calcaneus (Manufacturers Threshold)	0.12	0.03	0.08	0.16			
BUA Calcaneus (WHO Threshold)	0.14	0.04	0.1	0.18	-		
VOS Calcaneus	0	0	0	0.02	0.18	0.001	
L1-L4 BMD	0.14	0.09	0.02	0.15	0.20	0.24	0.07
T. Hip BMD	0.14	0.18	0.08	0.11	0.14	0.24	0
DXA Combined	0.14	0.07	0.11	0.14	0.22	0.25	0.07

Table 7.4 Kappa scores for the comparison between group 3 assessment measures and DXA

Kappa Group 3	L1-L4	T.Hip	Distal Radius	Proximal Phalanx	Mid-Shaft Tibia	Sunlight Combined	BUA Calcaneus (WHO Threshold)	BUA Calcaneus (Manufacturers Threshold)	VOS Calcaneus	SOFSURF	SCORE	OST	OSIRIS	ORAI
L1-L4		0.317	0.102	0.056	0.075	0.099	0.16	0.148	0.068	0.321	0.311	0.279	0.26	0.295
T.Hip	0.327		0.134	0.174	0.075	0.119	0.208	0.131	0	0.325	0.356	0.332	0.342	0.38
DXA Combined			0.102	0.027	0.067	0.091	0.192	0.182	0.049	0.287	0.3	0.299	0.201	0.295

7.3 Inter-site Correlation

In addition to the Kappa indices, and in keeping with other studies on the relationship between QUS, questionnaires and DXA assessment of the axial skeleton, the inter-site Pearson's correlations were determined. This analysis provided a quantitative representation of the relationship between all the assessment techniques, from both group 2 (Table 7.5) and group 3 (Table 7.6).

Table 7.5 Pearson's correlations between the different techniques for group 2

Group 2		Sunlight Omnisense			CUBA Clinical		Hologic QDR-4500C
		Distal Radius	Proximal Phalanx	Mid-shaft Tibia	BUA Calcaneus	VOS Calcaneus	L1-L4 BMD
Sunlight Omnisense	Proximal Phalanx	0.492 (<0.001)					
	Mid-Shaft Tibia	0.307 (<0.001)	0.215 (<0.001)				
CUBA Clinical	BUA Calcaneus	0.349 (<0.001)	0.360 (<0.001)	0.231 (<0.001)			
	VOS Calcaneus	0.294 (<0.001)	0.322 (<0.001)	0.270 (<0.001)	0.780 (<0.001)		
Hologic QDR-4500C	L1-L4 BMD	0.305 (<0.001)	0.309 (<0.001)	0.228 (<0.001)	0.527 (<0.001)	0.481 (<0.001)	
	T.Hip BMD	0.240 (<0.001)	0.305 (<0.001)	0.161 (<0.001)	0.637 (<0.001)	0.535 (<0.001)	0.712 (<0.001)

Cells: Correlation Coefficient (p-value)

The analysis of both groups 2 and 3 provided correlations superior to that which might have been suspected from the Kappa indices, with moderate to good correlations seen between most techniques and, in all bar the mid-shaft tibia, a high degree of statistical significance.

Table 7.6 Pearson's correlations between the different techniques for group 3

Group 3		Questionnaires						Sunlight Omnisense			CUBA Clinical		Hologic QDR-4500C
		Weight	SOFSURF	SCORE	OST	OSIRIS	ORAI	Distal Radius	Proximal Phalanx	Mid-shaft Tibia	BUA Calcaneus	VOS Calcaneus	BMD L1-L4
Questionnaires	SOFSURF	–0.460 (<0.001)											
	SCORE	–0.536 (<0.001)	0.897 (<0.001)										
	OST	0.774 (<0.001)	–0.883 (<0.001)	–0.878 (<0.001)									
	OSIRIS	0.666 (<0.001)	–0.904 (<0.001)	–0.927 (<0.001)	0.945 (<0.001)								
	ORAI	–0.469 (<0.001)	0.880 (<0.001)	0.778 (<0.001)	–0.819 (<0.001)	–0.839 (<0.001)							
Sunlight Omnisense	Distal Radius	0.112 (0.113)	–0.474 (<0.001)	–0.453 (<0.001)	0.400 (<0.001)	0.457 (<0.001)	–0.402 (<0.001)						
	Proximal Phalanx	0.220 (0.001)	–0.574 (<0.001)	–0.558 (<0.001)	0.512 (<0.001)	0.543 (<0.001)	–0.479 (<0.001)	0.485 (<0.001)					
	Mid-shaft Tibia	–0.087 (0.219)	–0.143 (0.042)	–0.157 (0.025)	0.092 (0.191)	0.136 (0.053)	–0.132 (0.060)	0.262 (<0.001)	0.183 (0.009)				
CUBA Clinical	BUA Calcaneus	0.233 (0.001)	–0.590 (<0.001)	–0.560 (<0.001)	0.515 (<0.001)	0.594 (<0.001)	–0.507 (<0.001)	0.362 (<0.001)	0.383 (<0.001)	0.244 (<0.001)			
	VOS Calcaneus	–0.028 (0.689)	–0.438 (<0.001)	–0.391 (<0.001)	0.299 (<0.001)	0.379 (<0.001)	–0.367 (<0.001)	0.312 (<0.001)	0.323 (<0.001)	0.294 (<0.001)	0.792 (<0.001)		
Hologic QDR-4500C	BMD L1-L4	0.330 (<0.001)	–0.463 (<0.001)	–0.460 (<0.001)	0.451 (<0.001)	0.508 (<0.001)	–0.417 (<0.001)	0.295 (<0.001)	0.318 (<0.001)	0.225 (0.001)	0.568 (<0.001)	0.473 (<0.001)	
	BMD Total Hip	0.492 (<0.001)	–0.599 (<0.001)	–0.598 (<0.001)	0.633 (<0.001)	0.658 (<0.001)	–0.558 (<0.001)	0.275 (<0.001)	0.340 (<0.001)	0.127 (0.070)	0.650 (<0.001)	0.519 (<0.001)	0.717 (<0.001)

Cells: Correlation Coefficient (p-value)

7.4 Diagnostic Ability

Despite the Kappa indices results which indicated a poor relationship between individual measurements taken on the same skeleton, the Pearson's correlation coefficients demonstrated that there was a statistically significant link between the results obtained from one assessment technique and another. This significant relationship provides evidence that the quantitative results from one technique have the ability to provide a significant indication of the skeletal status of another site within the same skeleton. In order to assess this diagnostic ability the sensitivity and specificity of the techniques in relation to the DXA results were assessed.

7.4.1 ROC Curve Analysis

The analysis was performed for both groups 2 and 3 due to the different nature of the study cohort make ups, with the initial phase of the results consisting of receiver operator characteristic (ROC) curves production. Each curve was produced by calculating the full range of sensitivity values from 1 to 0 for each technique, along with their corresponding specificity values, and plotting 1-specificity against the sensitivity. The resultant curves allow for the qualitative comparison of the technique's abilities, with a curve extending close to the top left corner of the graph being considered to have a greater degree of diagnostic ability than one which is closer to the mid-line.

The ROC curves for group 2 are shown in Figure 7.3 to Figure 7.6, and show the different QUS techniques' (The CUBA Clinical and The Sunlight Omnisense) abilities to correctly predict four different levels of DXA T-scores.

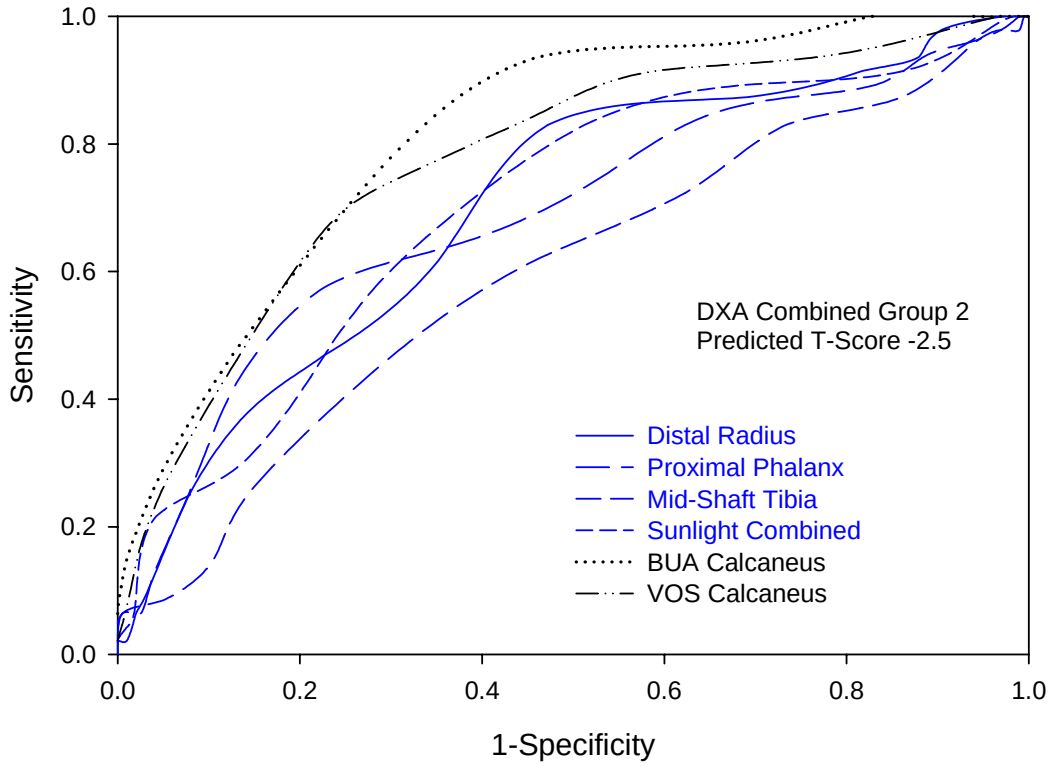

Figure 7.3 ROC Curves for the Group 2 QUS results prediction of DXA Combined at a T-score of -2.5.

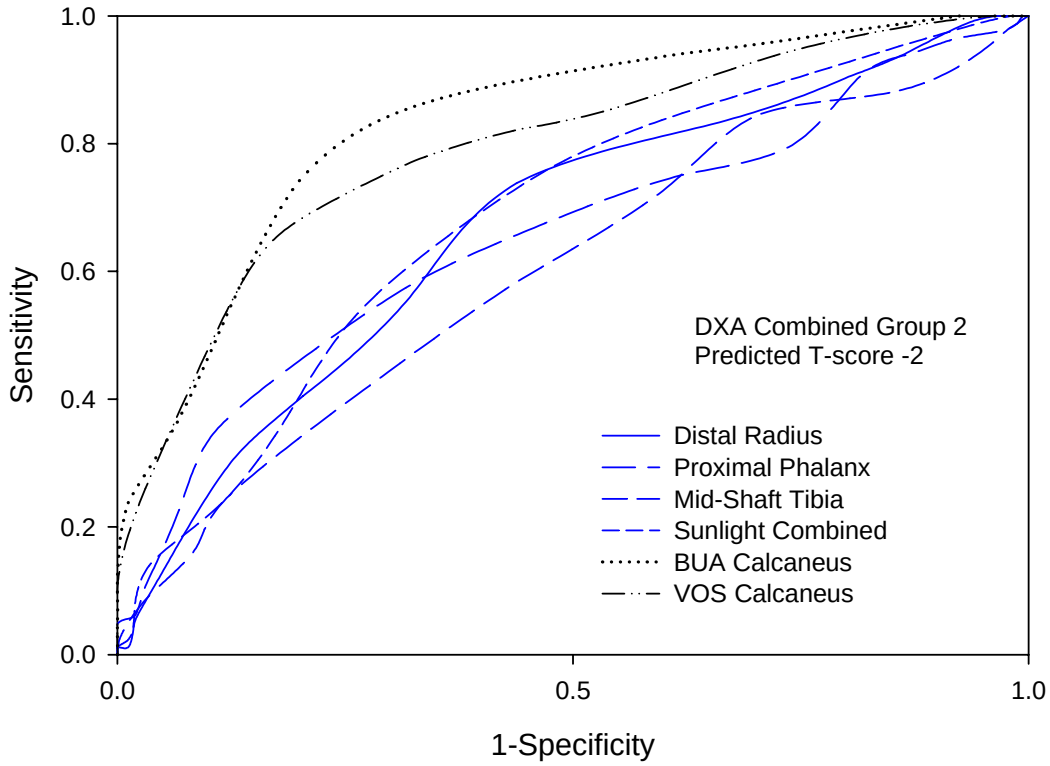

Figure 7.4 ROC Curves for the Group 2 QUS results predictions of DXA Combined at a T-score of -2.

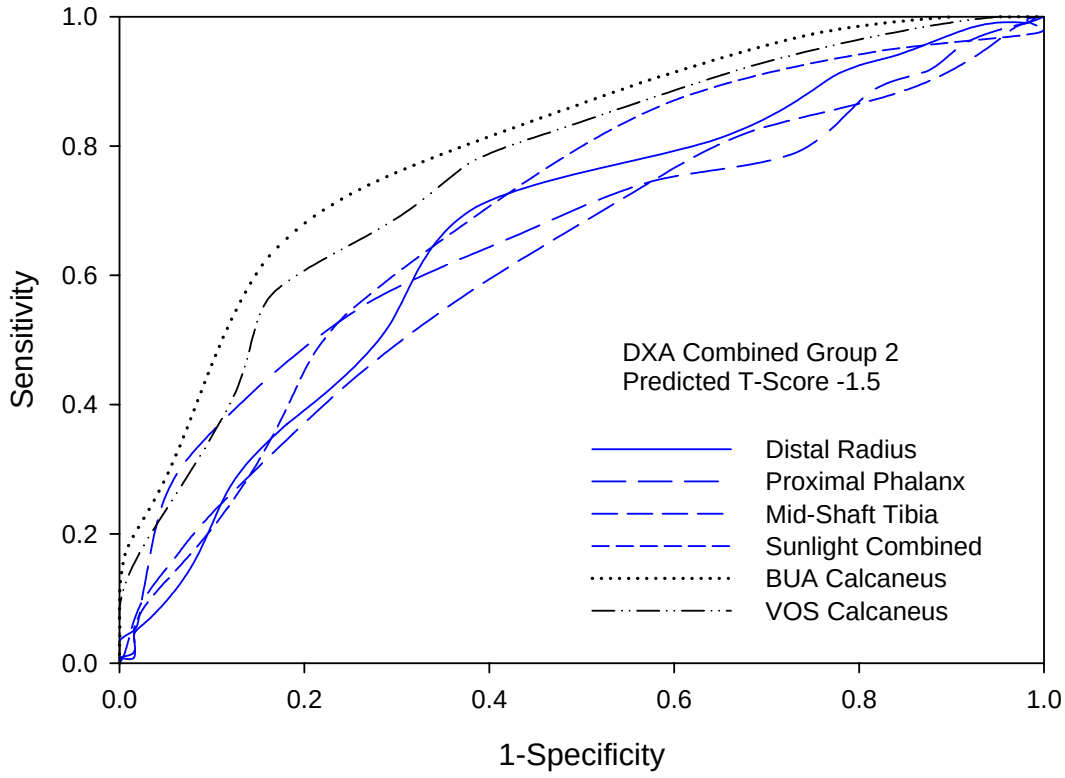

Figure 7.5 ROC Curves for the Group 2 QUS results prediction of DXA Combined at a T-score of -1.5.

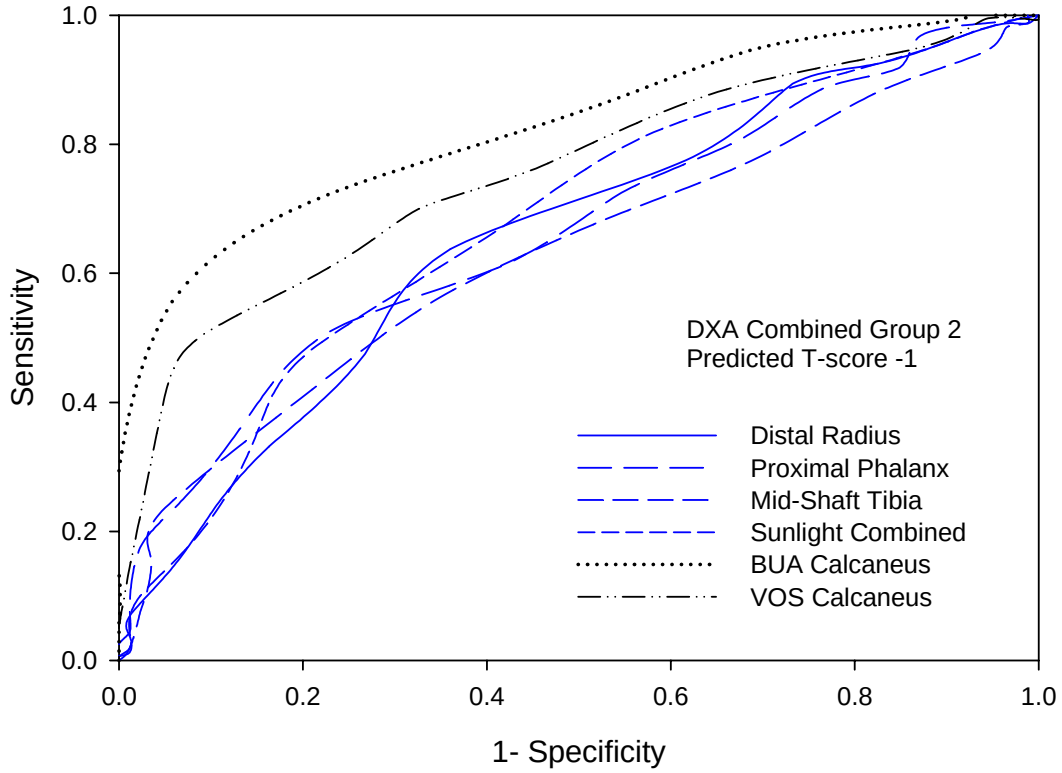

Figure 7.6 ROC Curves for the Group 2 QUS results prediction of DXA Combined at a T-score of -1.

The ROC curves for group 3, both for the QUS systems (the CUBA Clinical and the Sunlight Omnisense) and the Questionnaire systems (pBW, SOFSURF, SCORE, OST, OSIRIS, ORAI) in comparison to the DXA combined results at three different T-score thresholds, are shown in Figure 7.7 to Figure 7.9. The results for the prediction of the individual DXA assessment sites are shown in Figure 7.10 to Figure 7.15 and included the additional line of the other DXA investigation (Total Hip or Lumbar Spine).

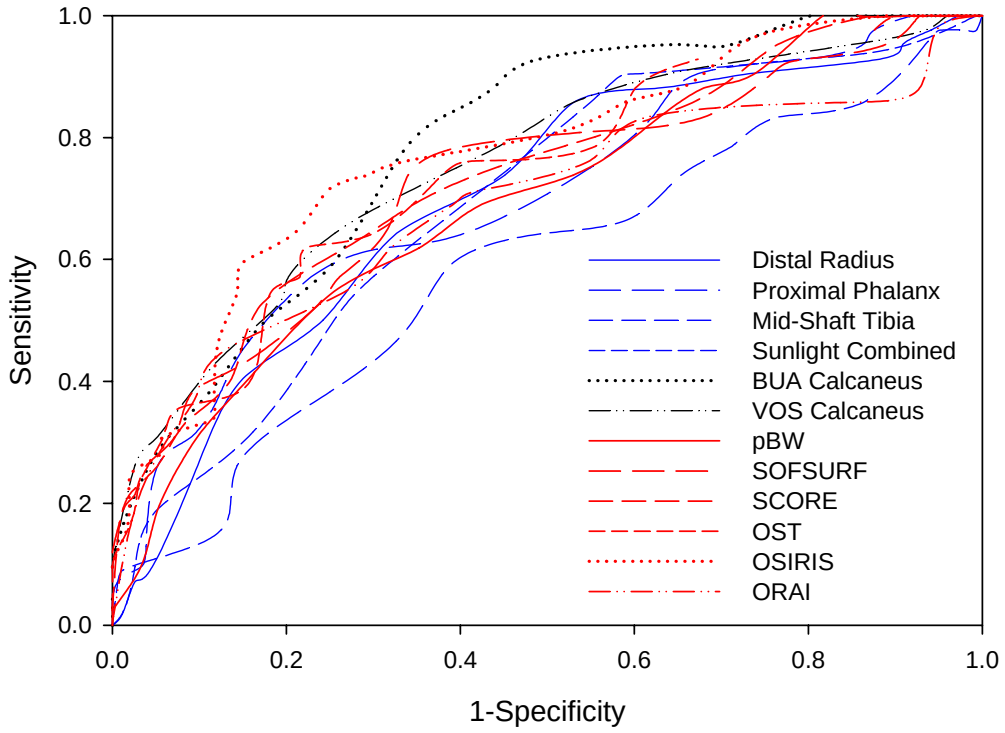

Figure 7.7 ROC Curves for the Group 3 QUS and questionnaire results prediction of DXA Combined at a T-score of -2.5.

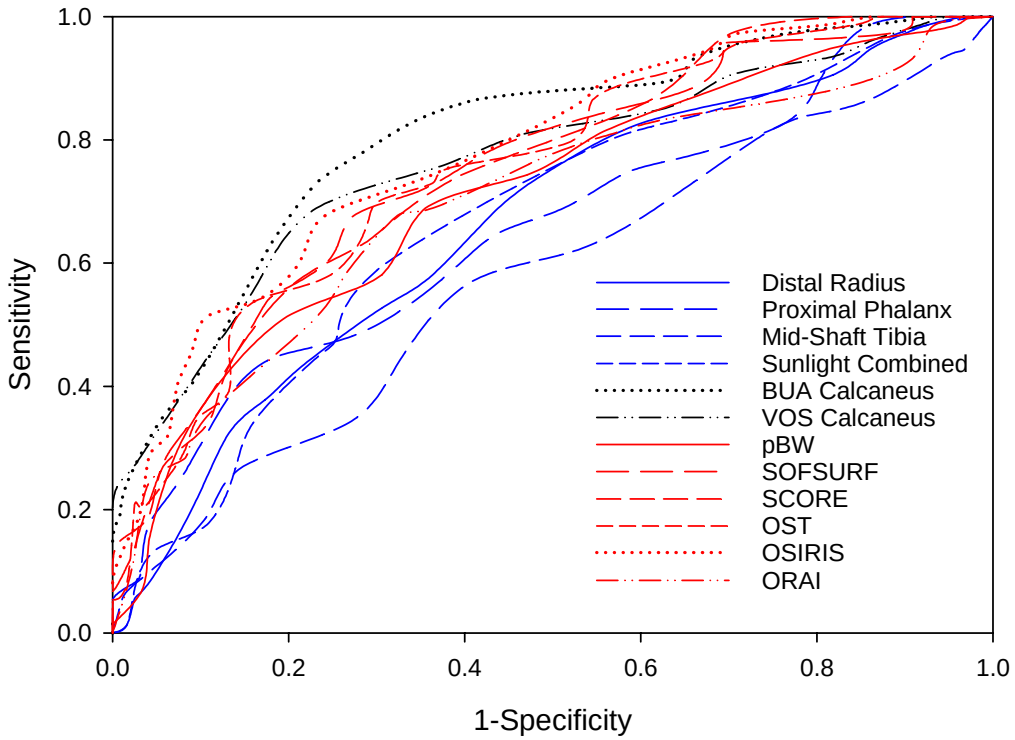

Figure 7.8 ROC Curves for the Group 3 QUS and questionnaire results prediction of DXA Combined at a T-score of -2.

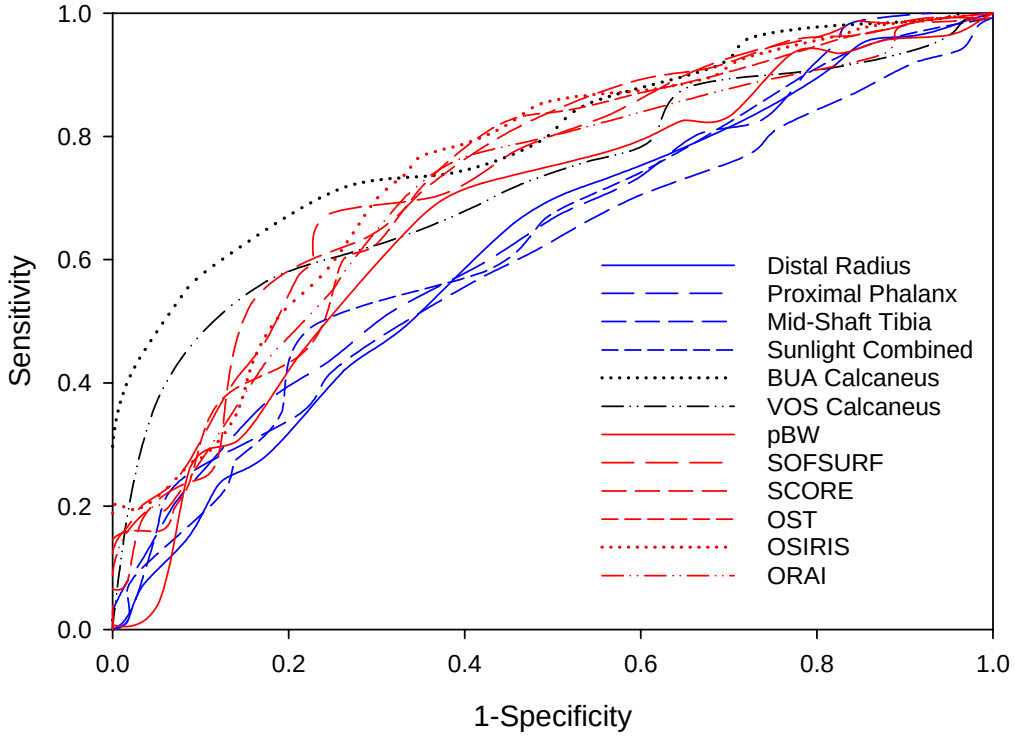

Figure 7.9 ROC Curves for the Group 3 QUS and questionnaire results prediction of DXA Combined at a T-score of -1.

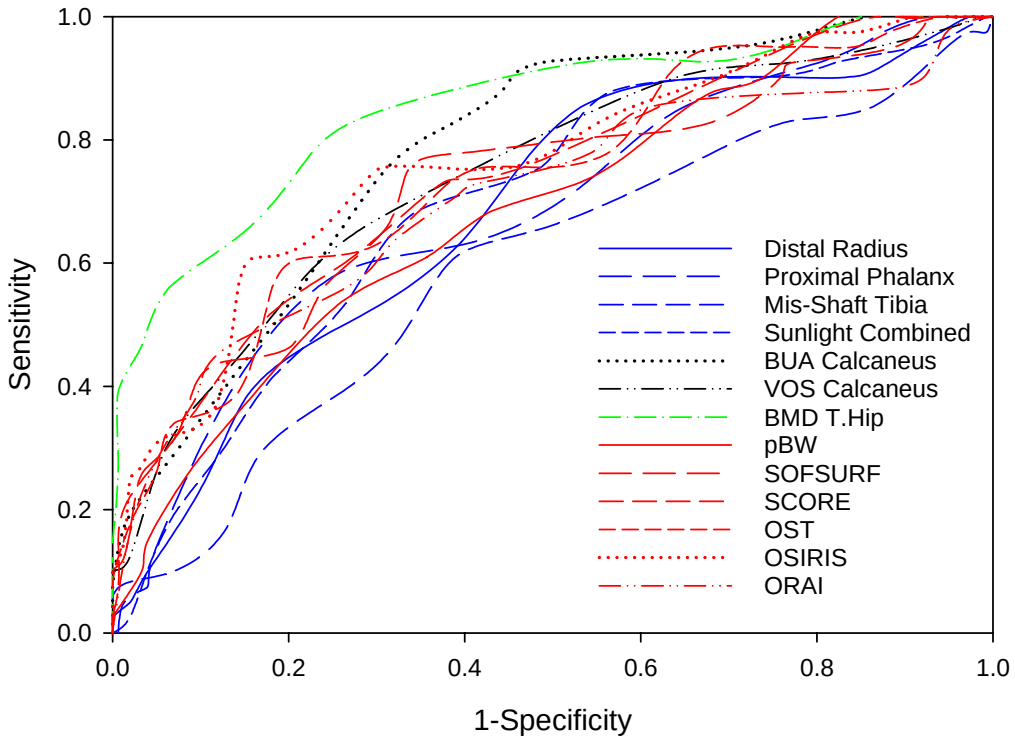

Figure 7.10 ROC Curves for the Group 3 QUS and questionnaire results prediction of Lumbar Spine DXA at a T-score of -2.5

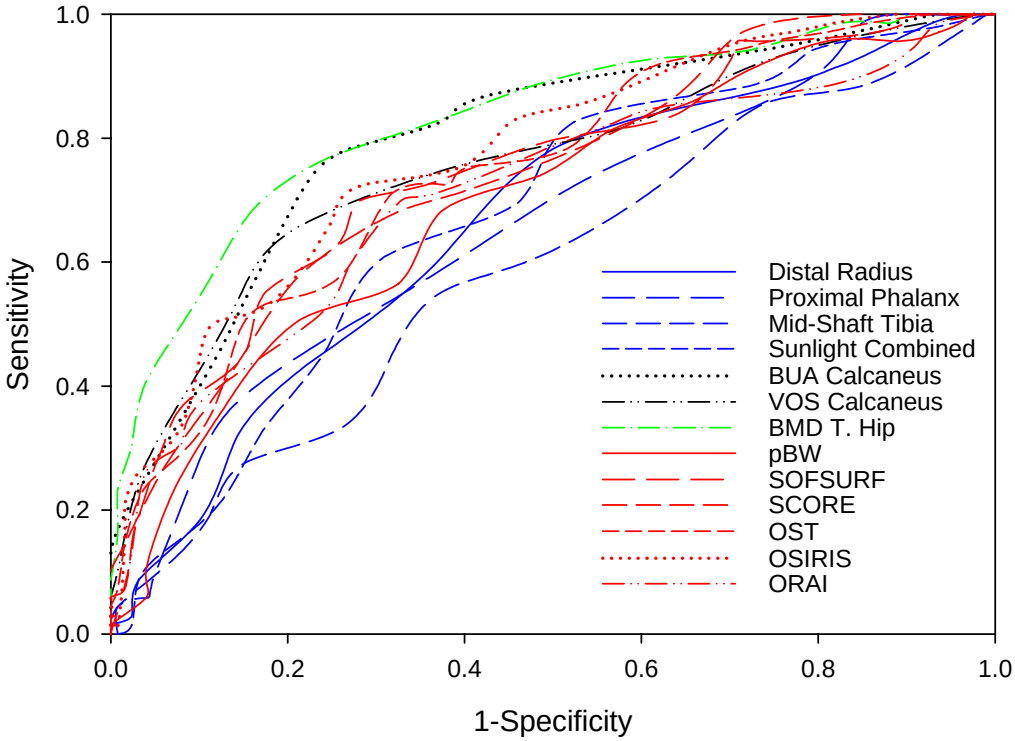

Figure 7.11 ROC Curves for the Group 3 QUS and questionnaire results prediction of Lumbar Spine DXA at a T-score of -2.

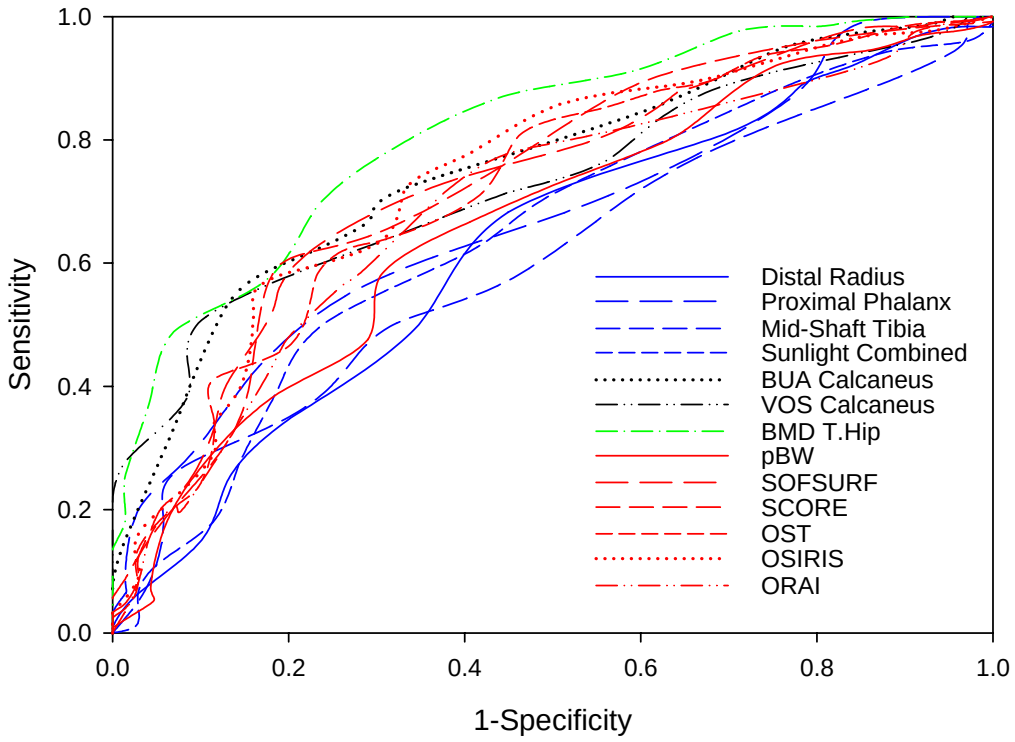

Figure 7.12 ROC Curves for the Group 3 QUS and questionnaire results prediction of Lumbar Spine DXA at a T-score of -1.

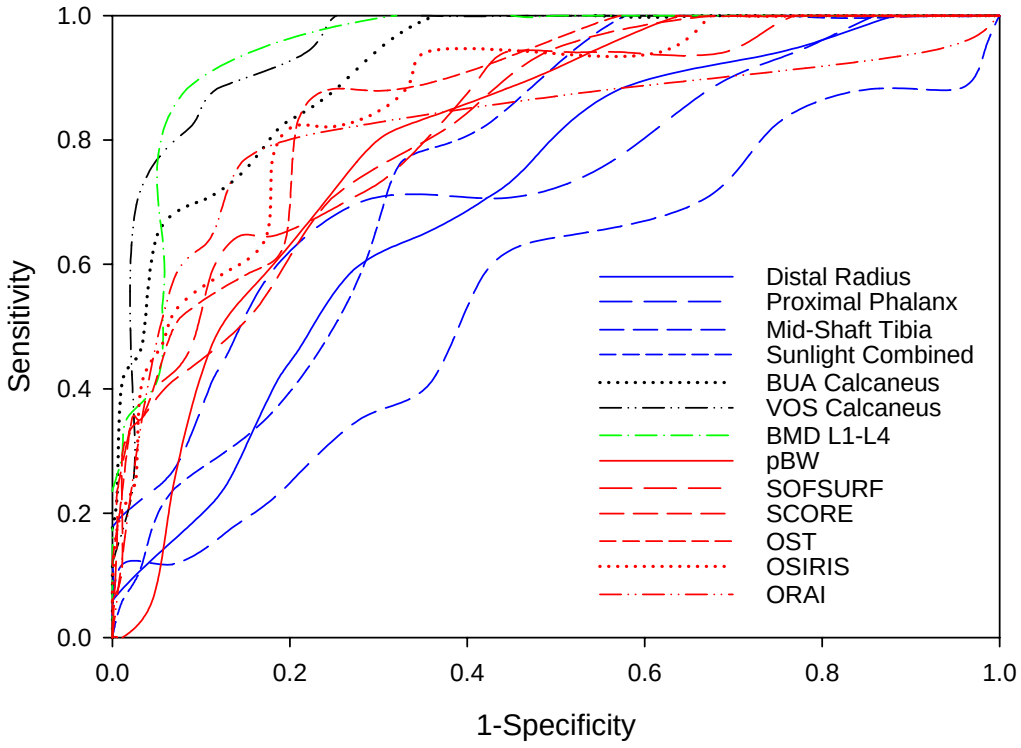

Figure 7.13 ROC Curves for the Group 3 QUS and questionnaire results prediction of Total Hip DXA at a T-score of -2.5.

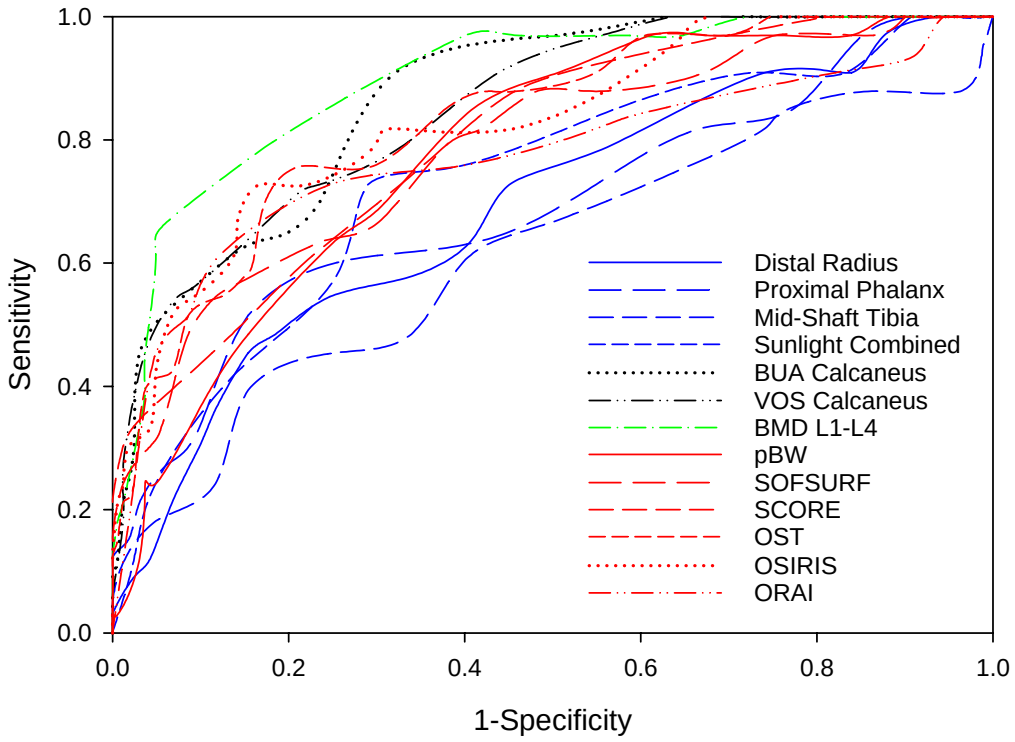

Figure 7.14 ROC Curves for the Group 3 QUS and questionnaire results prediction of Total Hip DXA at a T-score of -2.

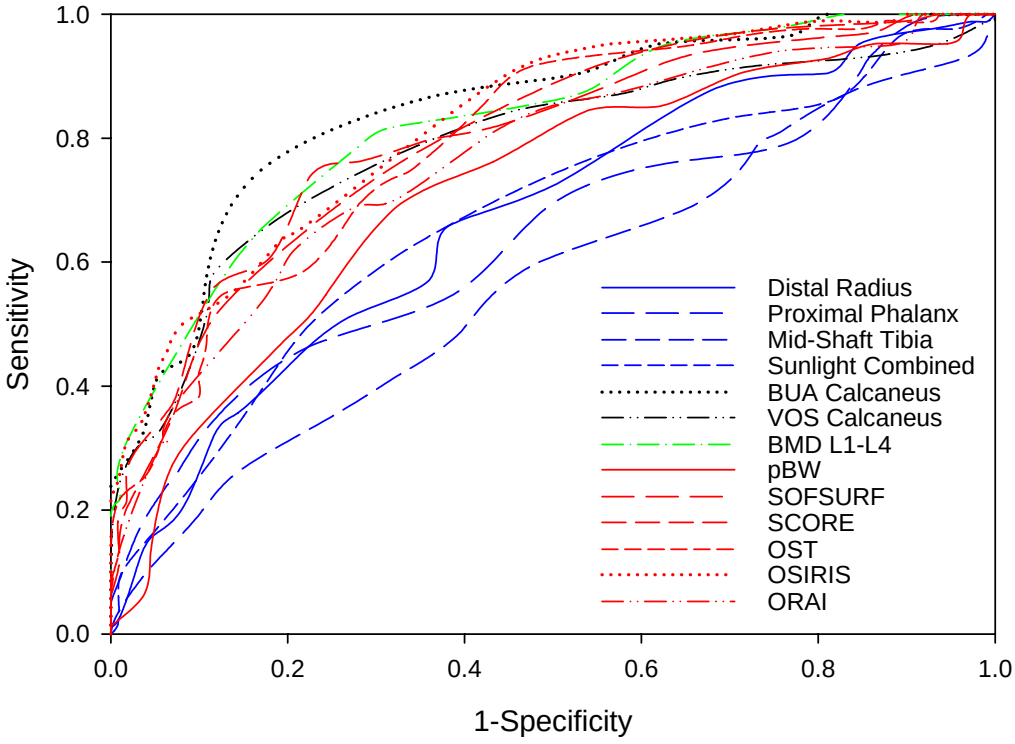

Figure 7.15 ROC Curves for the Group 3 QUS and questionnaire results prediction of Total Hip DXA at a T-score of -1.

In order to gain a direct quantitative comparison between the different techniques it is necessary to measure the area beneath the ROC curves (AUC). As mentioned previously, the greater the technique's ability, the closer the curve will pass to top left corner of the graph, which in turn provides a superior AUC indicating a high degree of diagnostic ability.

7.4.2 AUC Analysis

The AUC results for group 2 are shown in table 7.7. The results show that for a mixed population of pre-, peri- and postmenopausal women, the system best suited for the prediction of skeletal status at the axial skeleton is the CUBA clinical. The AUC results achieved by the CUBA Clinical were consistently higher than those achieved by any of the sites assessed by the Sunlight Omnisense, both individually and when combined, and provided the greatest diagnostic ability for each DXA T-score level that was predicted. According to the guidelines set out by R. Kent and J. Patrie (2005) (Table 5.4) the AUC values obtained for the techniques showed the BUA Calcaneus to have a 'good' diagnostic ability, with the VOS Calcaneus results showing a 'moderate' diagnostic ability, and with the results from the Sunlight Combined, Distal radius and Proximal Phalanx showing only a poor diagnostic ability, with the Mid-shaft Tibia displaying no diagnostic ability.

Table 7.7 AUC Results for Group 2

Measurement site	DXA Combined –2.5 AUC	DXA Combined –2 AUC	DXA Combined –1.5 AUC	DXA Combined -1 AUC
BUA calcaneus	**0.809 (0.847 – 0.787)**	**0.828 (0.851 – 0.817)**	*0.798 (0.806 – 0.790)*	**0.821 (0.831 – 0.820)**
VOS calcaneus	*0.773 (0.826 – 0.731)*	*0.791 (0.822 – 0.771)*	*0.762 (0.770 – 0.759)*	*0.754 (0.762 – 0.751)*
Sunlight combined	0.696 (0.755 – 0.645)	0.682 (0.704 – 0.663)	0.693 (0.697 – 0.695)	0.676 (0.698 – 0.66)
Proximal phalanx	0.688 (0.755 – 0.628)	0.654 (0.69 – 0.623)	0.665 (0.684 – 0.652)	0.663 (0.678 – 0.655)
Distal radius	0.696 (0.751 – 0.649)	0.668 (0.692 – 0.651)	0.666 (0.669 – 0.668)	0.655 (0.677 – 0.638)
Mid-shaft tibia	0.595 (0.659 – 0.536)	0.603 (0.632 – 0.576)	0.627 (0.637 – 0.621)	0.631 (0.641 – 0.624)

Excellent Ability **Good Ability** *Moderate Ability* Little or Poor Ability

The results for the AUC analysis of group 3 (Table 7.8) once again provided a range of abilities for the different systems. Of the scanning systems available the DXA consistently provided the greatest degree of diagnostic ability, when predicting the alternative DXA assessment; of the QUS systems, the CUBA Clinical provided the greatest degree of diagnostic ability. Both BUA and VOS consistently provided moderate or good levels of diagnostic ability, with BUA achieving the greatest AUC (0.95) of any test performed for the prediction of osteoporosis at the hip. The Sunlight Omnisense system performed poorly for the most part, but when utilised in combination to predict the total hip DXA results, the diagnostic ability could be considered either good or excellent, and out performed both the CUBA Clinical system and questionnaire systems in two out of three DXA T-score threshold levels.

The performance of the questionnaire systems was consistently moderate, but as with the QUS systems, their ability to predict the condition of the total hip was superior to their abilities to predict the lumbar spine and DXA combined, with most questionnaire systems displaying a good level of diagnostic ability. Of the questionnaire

systems investigated, OSIRIS consistently performed the best with SOFSURF, SCORE and OST displaying a similar degree of ability, closely followed by ORAI then pBW.

When comparing between the QUS systems and the questionnaire systems, the BUA assessments performed using the CUBA Clinical system proved to be the best of the investigations performed, with questionnaire systems like OSIRIS only marginally behind.

Table 7.8 AUC results for Group 3 for the different diagnostic abilities of the systems in relation to DXA

	DXA Combined -2.5 AUC	DXA Combined -2 AUC	DXA Combined -1 AUC	DXA L1-L4 -2.5 AUC	DXA L1-L4 -2 AUC	DXA L1-L4 -1 AUC	DXA T.Hip -2.5 AUC	DXA T.Hip -2 AUC	DXA T.Hip -1 AUC
Distal Radius	0.698 (0.75 - 0.654)	0.662 (0.680 - 0.651)	0.619 (0.584 - 0.658)	0.681 (0.736 - 0.633)	0.663 (0.684 - 0.648)	0.621 (0.598 - 0.647)	*0.7 (0.79 - 0.616)*	0.689 (0.761 - 0.627)	0.672 (0.688 - 0.662)
Proximal Phalanx	*0.702 (0.760 - 0.655)*	0.654 (0.682 - 0.636)	0.639 (0.611 - 0.678)	0.684 (0.739 - 0.638)	0.658 (0.68 - 0.643)	0.668 (0.659 - 0.688)	*0.737 (0.856 - 0.636)*	0.689 (0.776 - 0.617)	0.64 (0.666 - 0.622)
Mid-Shaft Tibia	0.589 (0.655 - 0.527)	0.574 (0.604 - 0.548)	0.598 (0.577 - 0.620)	0.595 (0.660 - 0.532)	0.591 (0.62 - 0.567)	0.604 (0.594 - 0.619)	0.562 (0.697 - 0.426)	0.617 (0.712 - 0.525)	0.566 (0.588 - 0.545)
Sunlight Combined	0.692 (0.743 - 0.649)	0.666 (0.688 - 0.651)	0.631 (0.612 - 0.654)	0.6955 (0.749 - 0.648)	0.673 (0.690 - 0.662)	0.644 (0.624 - 0.667)	**0.918 (0.961 - 0.9)**	**0.864 (0.897 - 0.847)**	**0.843 (0.861 - 0.840)**
BUA Calcaneus	*0.785 (0.822 - 0.763)*	**0.806 (0.829 - 0.794)**	*0.799 (0.777 - 0.81)*	*0.783 (0.822 - 0.758)*	*0.799 (0.825 - 0.785)*	*0.755 (0.75 - 0.772)*	**0.950 (0.973 - 0.949)**	**0.849 (0.897 - 0.825)**	*0.787 (0.819 - 0.764)*
VOS Calcaneus	*0.754 (0.816 - 0.705)*	*0.766 (0.803 - 0.742)*	*0.719 (0.713 - 0.734)*	*0.74 (0.801 - 0.689)*	*0.755 (0.791 - 0.731)*	*0.729 (0.737 - 0.734)*	*0.761 (0.818 - 0.728)*	*0.733 (0.802 - 0.676)*	0.668 (0.689 - 0.654)
BMD Total Hip	-	-	-	**0.851 (0.906 - 0.809)**	**0.828 (0.858 - 0.810)**	**0.813 (0.806 - 0.833)**	-	-	-
BMD L1-L4	-	-	-	-	-	-	**0.947 (0.96 - 0.945)**	**0.896 (0.929 - 0.874)**	**0.825 (0.845 - 0.82)**
pBW	0.695 (0.745 - 0.659)	*0.709 (0.733 - 0.694)*	0.674 (0.642 - 0.711)	0.685 (0.737 - 0.649)	0.693 (0.717 - 0.676)	0.662 (0.642 - 0.687)	**0.808 (0.858 - 0.768)**	*0.780 (0.823 - 0.745)*	*0.715 (0.729 - 0.707)*
SOFSURF	*0.725 (0.791 - 0.672)*	*0.751 (0.772 - 0.741)*	*0.739 (0.718 - 0.773)*	*0.726 (0.793 - 0.672)*	*0.746 (0.773 - 0.73)*	*0.73 (0.713 - 0.755)*	**0.831 (0.911 - 0.76)**	*0.787 (0.857 - 0.731)*	**0.8 (0.82 - 0.792)**
SCORE	*0.733 (0.790 - 0.691)*	*0.748 (0.765 - 0.745)*	*0.74 (0.713 - 0.775)*	*0.738 (0.792 - 0.696)*	*0.74 (0.763 - 0.731)*	*0.732 (0.714 - 0.759)*	**0.821 (0.894 - 0.769)**	*0.798 (0.856 - 0.758)*	*0.796 (0.808 - 0.795)*
OST	*0.744 (0.797 - 0.703)*	*0.752 (0.770 - 0.747)*	*0.726 (0.701 - 0.763)*	*0.737 (0.795 - 0.691)*	*0.746 (0.77 - 0.734)*	*0.722 (0.702 - 0.749)*	**0.868 (0.922 - 0.829)**	**0.832 (0.884 - 0.797)**	*0.795 (0.809 - 0.794)*
OSIRIS	*0.774 (0.828 - 0.736)*	*0.781 (0.801 - 0.775)*	*0.746 (0.725 - 0.78)*	*0.763 (0.822 - 0.718)*	*0.775 (0.797 - 0.763)*	*0.74 (0.723 - 0.764)*	**0.866 (0.927 - 0.814)**	**0.830 (0.927 - 0.814)**	**0.824 (0.840 - 0.821)**
ORAI	0.688 (0.764 - 0.619)	0.698 (0.729 - 0.673)	*0.712 (0.692 - 0.742)*	*0.704 (0.779 - 0.638)*	*0.71 (0.745 - 0.682)*	0.694 (0.678 - 0.716)	**0.825 (0.950 - 0.715)**	*0.772 (0.860 - 0.696)*	*0.765 (0.786 - 0.756)*

Excellent Ability **Good Ability** *Moderate Ability* Little or Poor Ability

7.5 Threshold Selection

7.5.1 The Best Accuracy Method (Table 7.9)

The trend within the results suggests that as the T-score level increases away from -2.5 towards -1, the number of individuals that are misdiagnosed also increases. However the misdiagnoses that are made are mostly within the false negatives at a T-score of -2.5 and in the false positives at a T-score of -1. This calls into question what is required of the screening tool. In the case of the DXA -2.5 T-score prediction, the numbers of individuals misdiagnosed are relatively few but even at best the number of false negatives was 34, and considering there were only 47 individuals within the entire group actually being osteoporotic at the axial skeleton, a large percentage of the osteoporotic individuals would have been incorrectly classified. However, for the prediction of a DXA T-score of -1 the threshold of the sunlight systems provide very low numbers of false negative, although the CUBA system does not perform so well.

7.5.2 The Best Sensitivity and Specificity Method (Table 7.9 / Table 7.10)

The results of the best sensitivity and specificity method were determined on both groups 2 and 3, and produced results which were closely related although the threshold values and the numbers of misdiagnoses varied. In contrast to the best accuracy threshold selection method the number of patients misdiagnosed when predicting for a DXA T-score of -2.5 was not surprisingly higher in number, but the number of false negatives from group 2, and the higher sensitivity values from group 3, both indicate a reduction in the number of osteoporotic subjects that were misclassified.

However the number of misdiagnoses increases with the higher DXA T-scores to a level that could be considered to be unacceptable.

7.5.3 The 90% Sensitivity Method (Table 7.11)

As mentioned previously it is important to decide on what is required from a screening technique. In the case of the 90% sensitivity method, the aim is to correctly diagnose as many individuals with the condition as possible. The overall level of misdiagnoses is the highest of any of the results of the three methods for the DXA T-score levels of -2 and -2.5, but the high sensitivity ensures the number of false negatives is minimal. In contrast, the number of misdiagnoses at a DXA T-score of -1 is almost identical to, and in many cases superior to, the number seen using the best accuracy method. However, the negative predictive values show at best only a 75% certainty that a negative result for the QUS will correspond to a negative result from the DXA, in contrast to the -2.5 T-score DXA prediction where the negative predictive value can at best ensure a 95% certainty in the diagnosis.

Table 7.9 Group 2: Potential cut-off values for prediction of DXA and their associated numbers of false-positive and false-negative results

Site	DXA	Best Sens. + Spec. Threshold Value	False Negatives	False Positives	Total Patients Misdiagnosed (% Of Group)	Best Accuracy Threshold Value	False Negatives	False Positives	Total Patients Misdiagnosed (% Of Group)
Distal Radius	-2.5	-0.5	8	94	102 (41.5)	-4.5	46	0	46 (18.7)
Proximal Phalanx	-2.5	-0.5	20	45	65 (26.4)	-3	44	1	45 (18.3)
Mid-Shaft Tibia	-2.5	-1	25	60	85 (34.6)	-3	44	1	45 (18.3)
Sun Combined	-2.5	-1	8	102	110 (44.7)	-3	37	8	45 (18.3)
BUA Calcaneus	-2.5	-2	11	58	69 (28.0)	-3.5	40	2	42 (17.1)
VOS Calcaneus	-2.5	-3.25	13	55	68 (27.6)	-4	34	11	45 (18.3)
Distal Radius	-2	-0.5	22	71	93 (37.8)	-2	58	21	79 (32.1)
Proximal Phalanx	-2	-0.5	45	33	78 (31.7)	-1	55	17	72 (29.3)
Mid-Shaft Tibia	-2	-0.5	35	71	106 (43.1)	-2.5	76	6	82 (33.3)
Sun Combined	-2	-1	20	77	97 (39.4)	-2	48	34	82 (33.3)
BUA Calcaneus	-2	-2	22	32	54 (22.0)	-2	22	32	54 (22.0)
VOS Calcaneus	-2	-3.25	27	32	59 (24.0)	-3.5	38	20	58 (23.6)
Distal Radius	-1.5	-0.5	35	49	84 (34.1)	-0.5	35	49	84 (34.1)
Proximal Phalanx	-1.5	0	52	35	87 (35.4)	0	52	35	87 (35.4)
Mid-Shaft Tibia	-1.5	-0.5	49	50	99 (40.2)	-0.5	49	50	99 (40.2)
Sun Combined	-1.5	-1	32	54	86 (35.0)	-1	32	54	86 (35.0)
BUA Calcaneus	-1.5	-2	45	20	65 (26.4)	-2	45	20	65 (26.4)
VOS Calcaneus	-1.5	-3.25	51	21	71 (28.9)	-3.25	51	21	72 (29.3)
Distal Radius	-1	-0.5	58	31	89 (36.2)	0.5	17	63	80 (32.5)
Proximal Phalanx	-1	0	78	20	98 (39.8)	3	5	75	80 (32.5)
Mid-Shaft Tibia	-1	-0.5	70	30	100 (40.7)	3	0	85	85 (34.6)
Sun Combined	-1	-1.5	83	18	101 (41.1)	-0.5	29	50	79 (32.1)
BUA Calcaneus	-1	-2	71	5	76 (30.9)	-1.5	44	20	64 (26.0)
VOS Calcaneus	-1	-3.25	79	8	87 (35.4)	-2.75	48	28	76 (30.9)

Table 7.10 The suggested cut-off points that allow for the best sensitivity and specificity balance within study group 3

Site	Sens + Spec Threshold	Sensitivity	Specificity	PPV	NPV	% Of Group (Total FN +FP)
DXA T-score Level: -2.5						
OSIRIS"	0	0.7	0.73	0.42	0.89	27.9% (58)
SOFSURF*	1	0.72	0.67	0.38	0.89	32.2% (67)
ORAI*	14	0.43	0.86	0.48	0.84	23.1% (48)
OST"	-1	0.52	0.82	0.44	0.56	25% (52)
SCORE*	12	0.5	0.83	0.46	0.85	24% (50)
Distal Radius	-0.5	0.84	0.47	0.30	0.91	43.3% (90)
Proximal Phalanx	-0.5	0.56	0.75	0.38	0.86	29.3% (61)
Mid-Shaft Tibia	-0.5	0.64	0.51	0.26	0.84	45.2% (94)
Sun Combined	-1.5	0.69	0.66	0.35	0.89	32.2% (67)
BUA Calcaneus	-1.5	0.91	0.51	0.34	0.95	40.4% (84)
VOS Calcaneus	-3.5	0.53	0.8	0.42	0.86	26% (54)
Weight	60kg	0.56	0.7	0.34	0.85	33.2% (69)
DXA T-score Level: -2						
OSIRIS"	1	0.7	0.74	0.63	0.80	27.4% (57)
SOFSURF*	1	0.68	0.74	0.62	0.79	28.4% (59)
ORAI*	10	0.68	0.68	0.57	0.77	32.2% (67)
OST"	1	0.71	0.65	0.56	0.79	32.7% (68)
SCORE*	8	0.68	0.71	0.59	0.78	30.3% (63)
Distal Radius	-0.5	0.73	0.5	0.48	0.74	39.9% (83)
Proximal Phalanx	-1	0.37	0.88	0.64	0.70	31.3% (65)
Mid-Shaft Tibia	-1.5	0.27	0.85	0.53	0.65	36.5% (76)
Sun Combined	-1.5	0.59	0.68	0.53	0.73	33.2% (69)
BUA Calcaneus	-2	0.71	0.76	0.61	0.83	26% (54)
VOS Calcaneus	-3.5	0.51	0.88	0.72	0.74	26.4% (55)
Weight	55kg	0.36	0.9	0.69	0.69	30.8% (64)
DXA T-score Level: -1						
OSIRIS"	2	0.7	0.73	0.86	0.52	28.8% (60)
SOFSURF*	0	0.63	0.8	0.87	0.49	32.2% (67)
ORAI*	8	0.71	0.67	0.83	0.51	30.3% (63)
OST"	2	0.72	0.67	0.83	0.51	29.8% (62)
SCORE*	8	0.56	0.84	0.98	0.46	35.1% (73)
Distal Radius	-0.5	0.65	0.54	0.77	0.39	37% (77)
Proximal Phalanx	0	0.51	0.7	0.79	0.39	42.3% (88)
Mid-Shaft Tibia	-1.5	0.25	0.93	0.90	0.35	52.9% (110)
Sun Combined	-1.5	0.51	0.77	0.84	0.39	38.9% (81)
BUA Calcaneus	-2	0.56	0.92	0.94	0.48	33.2% (69)
VOS Calcaneus	-3	0.61	0.72	0.85	0.45	35.6% (74)
Weight	65kg	0.71	0.55	0.82	0.46	34.1% (71)

* Less than the threshold = requires DXA
"Greater than the threshold = requires DXA

Table 7.11 The suggested cut-off points that allow for a guaranteed 90% sensitivity level within study group 3

Site	90% Sensitivity Threshold	Sensitivity	Specificity	PPV	NPV	% Of Group (Total FN +FP)
DXA T-score Level: -2.5						
OSIRIS”	5	0.96	0.22	0.26	0.95	61.5% (128)
SOFSURF*	-2	0.91	0.22	0.25	0.9	63% (131)
ORAI*	0	0.96	0.056	0.22	0.82	74.5% (155)
OST”	3	0.91	0.33	0.28	0.93	53.8% (112)
SCORE”	4	0.93	0.26	0.26	0.93	59.1% (123)
Distal Radius	1	0.93	0.12	0.22	0.86	68.3% (142)
Proximal Phalanx	2	0.91	0.15	0.23	0.86	67.8% (141)
Mid-Shaft Tibia	1.25	0.93	0.1	0.22	0.84	70.2% (146)
Sun Combined	-0.5	0.93	0.24	0.25	0.92	57.7% (120)
BUA Calcaneus	-1.5	0.91	0.51	0.34	0.95	40.4% (84)
VOS Calcaneus	-2.5	0.91	0.35	0.28	0.93	52.9% (110)
Weight*	80kg	0.96	0.15	0.24	0.92	67.8% (141)
DXA T-score Level: -2						
OSIRIS”	4	0.91	0.41	0.49	0.88	39.9% (83)
SOFSURF*	-2	0.95	0.27	0.46	0.9	46.6% (97)
ORAI*	2	0.925	0.1	0.39	0.68	58.2% (121)
OST”	3	0.9	0.39	0.48	0.86	41.3% (86)
SCORE”	4	0.96	0.33	0.47	0.93	42.8% (89)
Distal Radius	0.5	0.9	0.19	0.41	0.74	51.9% (108)
Proximal Phalanx	2	0.94	0.18	0.41	0.82	52.9% (110)
Mid-Shaft Tibia	1.25	0.92	0.1	0.39	0.68	56.7% (118)
Sun Combined	0	0.97	0.091	0.4	0.85	53.8% (112)
BUA Calcaneus	-1	0.93	0.33	0.43	0.90	46.2% (96)
VOS Calcaneus	-2	0.94	0.26	0.44	0.87	48.1% (100)
Weight*	80kg	0.94	0.16	0.41	0.81	53.8% (112)
DXA T-score Level: -1						
OSIRIS”	5	0.9	0.36	0.76	0.61	26.9% (56)
SOFSURF*	-2	0.9	0.38	0.76	0.62	26.4% (55)
ORAI*	2	0.93	0.14	0.71	0.47	31.3% (65)
OST”	5	0.94	0.25	0.74	0.64	27.4% (57)
SCORE”	3	0.91	0.36	0.76	0.64	26% (54)
Distal Radius	1	0.92	0.19	0.73	0.5	28.4% (59)
Proximal Phalanx	2	0.9	0.22	0.72	0.5	30.8% (64)
Mid-Shaft Tibia	1.5	0.94	0.033	0.69	0.2	31.7% (66)
Sun Combined	0	0.95	0.11	0.72	0.46	27.9% (58)
BUA Calcaneus	-0.5	0.96	0.27	0.75	0.74	25.5% (53)
VOS Calcaneus	-1.5	0.95	0.063	0.695	0.36	32.2% (67)
Weight*	80kg	0.92	0.23	0.73	0.58	28.8% (60)

* Less than the threshold = requires DXA

“Greater than the threshold = requires DXA

It is clear that the optimal screening tool would ensure that the diagnosis of the individuals with the condition would be preferential to the exclusion of individuals without the condition, and as such the use of the thresholds determined using the 90% sensitivity method will provide the most desirable results. It is worthy of note that in all three methods for the selection of threshold values, and at all of the DXA T-score levels bar one, that were investigated, the BUA results from the calcaneal investigations consistently provided the lowest number of misdiagnoses. In addition to this, of all the QUS systems where threshold values were provided by the manufacturers, it was the BUA results from the CUBA clinical system which adhered to them most closely.

7.6 Screening Strategy

The aim of the screening strategy was to use the questionnaires in combination or alone to provide the best possible prediction of what the minimum T-score an individual was likely to have would be. The stepwise regression analysis provided 10 equations based on the variables that were entered with a range of r^2 values from 31.0 to 46.8. The first thing of note is that the three equations provided for strategy 2, are identical to the first three equations provided in strategy 3. The second thing to note is that by using stepwise regression, the factor which provides the strongest predictive value will be alone in an equation and the subsequent variables are added in order of their predictive ability.

Table 7.12 Stepwise regression analysis for the three scenarios presented in section 5.4.2.5

Strategy	Parameters	Equation	r^2	Equation No.
1	Weight (kg), Age (years), OSIRIS, OST, SOFSURF, SCORE, ORAI	Min. DXA T-score = 0.178 OSIRIS – 1.915	31.0	**Equation 7.1**
2	Weight (kg), Age (years), Distal Radius, Proximal Phalanx, Mid-Shaft Tibia, BUA Calcaneus, VOS Calcaneus	Min. DXA T-score = 0.0472 BUA – 4.471	37.7	**Equation 7.2**
		Min. DXA T-score = 0.0431 BUA + 0.0249 weight (kg) – 5.84	43.0	**Equation 7.3**
		Min. DXA T-score = 0.0259 BUA + 0.0308 weight (kg) + 0.009 VOS -18.51	44.6	**Equation 7.4**
3	Weight (kg), Age (years), OSIRIS, OST, SOFSURF, SCORE, ORAI, Distal Radius, Proximal Phalanx, Mid-Shaft Tibia, BUA Calcaneus, VOS Calcaneus	Min. DXA T-score = 0.0472 BUA – 4.471	37.7	**Equation 7.5**
		Min. DXA T-score = 0.0431 BUA + 0.0249 weight (kg) – 5.84	43.0	**Equation 7.6**
		Min. DXA T-score = 0.0259 BUA + 0.0308 weight (kg) + 0.009 VOS -18.51	44.6	**Equation 7.7**
		Min. DXA T-score = 0.0215 BUA + 0.022 weight (kg) + 0.008 VOS + 0.047 OSIRIS – 17.0	45.3	**Equation 7.8**
		Min. DXA T-score = 0.0208 BUA + 0.0304 weight (kg) + 0.0085 VOS + 0.12 OSIRIS – 0.112 OST -18.29	46.0	**Equation 7.9**
		Min. DXA T-score = 0.0198 BUA + 0.046 weight (kg) + 0.0087 VOS + 0.088 OSIRIS – 0.22 OST – 0.144 SOFSURF – 19.29	46.8	**Equation 7.10**

N.B. Equations 7.2 to 7.4 are identical to equations 7.5 to 7.7

For strategy 1, only one equation (Equation 7.1) is provided, with the questionnaire that supplied the best level of predictive ability (r^2 = 31.0%) being OSIRIS.

For strategy 2 the number of equations provided increased to three, with BUA, weight and VOS all supplying a level of predictive ability, and enabling an r^2 that ranged from 37.7% for BUA alone to 44.6% for the combined variables. As mentioned previously the first three equations of strategy 3 were identical to those of strategy 2, which indicates that the QUS variables and weight provide a better level of predictive value than the questionnaires, as can be seen by the higher r^2 values of equation 7.3 compared to equation 7.1. With regard to the order of appearance, OSIRIS shows up first (equation 7.8), followed by OST and SOFSURF to provide a relationship with an r^2 of 46.8%.

Concluding Remarks

This study was performed on a relatively small study population, although one which could be considered to be characteristic of the British Caucasian female population. The precision study lends further support to the previous statements that the precision of the QUS systems is the primary source of restriction on the widespread use of QUS for the monitoring of bone loss and therapies related to the skeleton.

With the Kappa scores demonstrating at best, a relationship of 0.4, the results of this study demonstrate that no single QUS system or questionnaire provides a 100% satisfactory screening tool. However, there are significant links between the QUS and questionnaire results in relation to the condition of the axial skeleton, which when

assessed in terms of diagnostic ability, provided a number of good and excellent levels of ability. However, the relationships of a number of the techniques, especially the BUA results from the CUBA clinical system, were highly predictive of the condition of the total hip region. When the abilities of QUS to predict fracture risk are taken into consideration, no QUS result can confidently be referred to as a false positive.

When using the different techniques as a screening tool, it is important to consider what outcome of the system is preferable; in most cases this will be the assurance that as many as possible of the sufferers are correctly diagnosed. With sensitivity and specificity being inversely related, the higher the sensitivity the system provides, the more likely there are to be high number of individuals undergoing further unnecessary investigations. The combination of the techniques to provide a screening system for the prediction of the lowest DXA T-score from either of the axial skeletal sites provided an equation that included one QUS system, the weight of the subject and a number of questionnaires provided an r^2 value of 46.8%. It is clear that both the CUBA clinical system and the questionnaire systems have the potential to be useful aids to the clinician, but a large percentage of the skeleton status remains unexplained and clinicians will still have to rely on their judgement for the referral of individuals.

Chapter 8: Results: In-Vitro Testing

The in-vitro testing comprised both compressive testing and fracture toughness testing of the cancellous bone samples, each of which was individually tested to obtain material properties such as the apparent density, material density and porosity, as well as compositional properties such as the percentage water, mineral and organic contents. Additional investigations were also undertaken in the form of collagen cross-link analysis of samples from the femoral heads and clinical QUS investigations on the donor of the femoral head on both the osteoporotic and osteoarthritic groups.

In this section, the aim is to compare and contrast the results from the different study groups in order to highlight how any effects the conditions the donors may have had have affected the mechanical properties of the bone. It is also to investigate the relationships between the mechanical parameters from both the compression testing and the fracture toughness testing with respect to the material and compositional properties of the bone.

8.1 Compression Testing

Of the 50 compression cores that were manufactured, one of the osteoarthritic cores was lost during testing, a further 3 osteoporotic samples and 1 osteoarthritic sample failed outside the gauge length of the contact extensometer and so only provided information from the platens extensometer. The compression testing was only performed on the osteoarthritic and osteoporotic groups; however for each compression core ten dependent variables (mechanical properties) were determined.

8.1.1 Extensometer and Group Comparisons

The differences between the two extensometers that were used to determine the deflection of the sample during testing have been demonstrated previously to provide different values for the mechanical properties of the test sample. (section 3.2.1.5). The results of this study support these findings; Figure 8.1 shows the loading curves obtained from an osteoporotic compression core using the contact and platens extensometers.

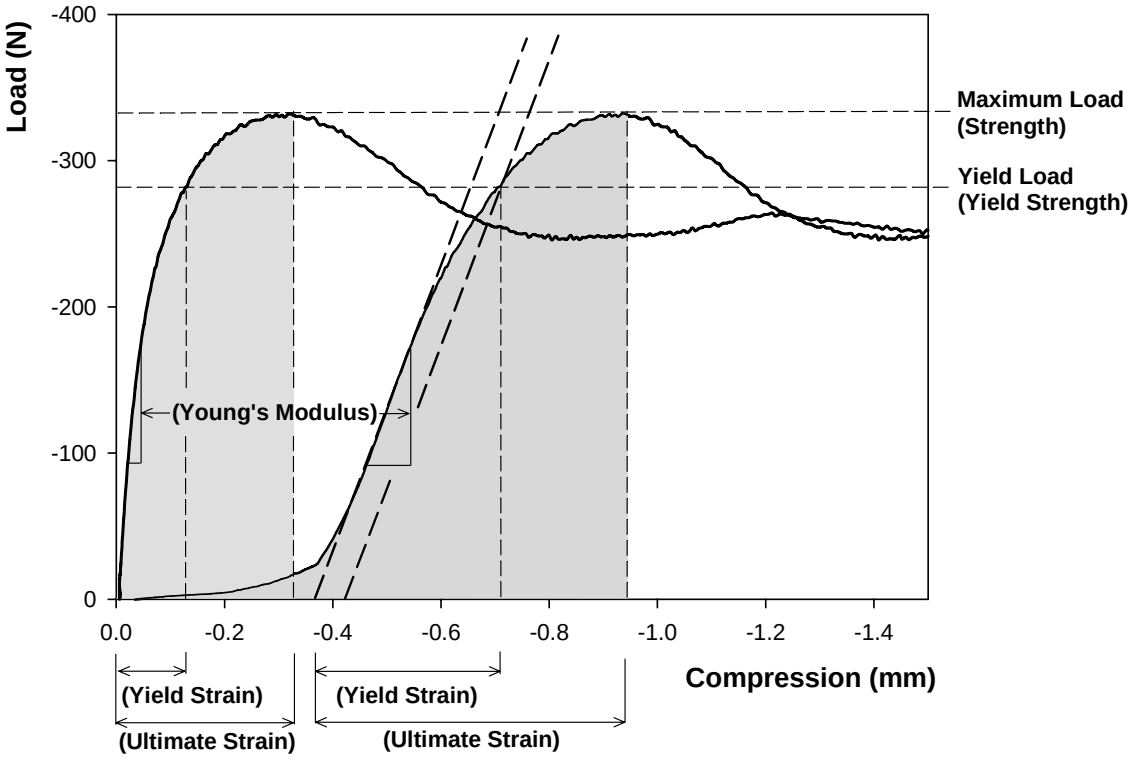

Figure 8.1 Loading curves obtained from the two different extension determining methods for the same osteoporotic compression core.

The results in Figure 8.1 and Table 8.1 both show differences in the mechanical properties obtained from the two different extensometers. The Young's modulus obtained from the contact extensometer was significantly higher than that

which was obtained from the platens extensometer ($p = 0.019$), the work to failure was significantly greater when assessed using the platens extensometer, but there were no significant differences between either of the strain values.

Table 8.1 ANOVA comparisons between the results of the two different extensometers.

Mechanical Parameters	ANOVA (Extensometers)
Young's Modulus	0.019
Yield Strain	0.057
Ultimate Strain	0.284
Work to Failure	<0.001

The results of the comparisons between the two different study groups are shown in table 8.2. Analysis of the strain results showed that neither the yield strain nor the ultimate strain of the samples from the two groups were statistically significantly different. In contrast, the yield stress, strength and work to failure of the osteoarthritic samples were all significantly ($p < 0.01$) greater than the results from the osteoporotic group. The Young's moduli of the two different study groups were in contrast depending on the extensometer used; the results of the Young's moduli obtained from the platens extensometer were significantly greater ($p = 0.043$) in the osteoarthritic group, whereas the contact extensometer showed no significant differences ($p = 0.553$) between the two groups.

Table 8.2 Comparison between the range, mean and standard deviations of the compressive mechanical properties of the two different study groups

Mechanical parameter	Osteoporotic	Osteoarthritic	ANOVA
$E_{Platens}$ (MPa)			
Range	41.7 – 927.9	188.2 – 799.6	
Mean	172.4	416.7	0.043
St Dev.	271.1	217.5	
$E_{Contact}$ (MPa)			
Range	43.9 – 1461.1	160 – 1285	
Mean	432.0	521	0.553
St Dev.	381.0	378	
$\varepsilon_{Yield\ Platens}$ (%)			
Range	-0.29 – -4.7	-1 – -2.1	
Mean	-1.47	-1.5	0.851
St Dev.	0.89	0.43	
$\varepsilon_{Ult.Platens}$ (%)			
Range	-0.46 – -7.98	-1.5 – -5.5	
Mean	-2.43	-2.85	0.471
St Dev.	1.47	1.59	
$\varepsilon_{Yield\ Contact}$ (%)			
Range	-0.18 – -4.44	-0.7 – -1.9	
Mean	-1.09	-1.38	0.359
St Dev.	0.82	0.39	
$\varepsilon_{Ult.Contact}$ (%)			
Range	-0.45 – -8.96	-1.98 – -7.6	
Mean	-2.87	-4.5	0.061
St Dev.	2.11	2.06	
σ_{Yield} (MPa)			
Range	0.297 – 8.307	2.40 – 10.09	
Mean	3.04	5.52	0.008
St Dev.	2.16	3.07	
$\sigma_{Ult.}$ (MPa)			
Range	0.359 – 10.24	2.78 – 15.29	
Mean	3.696	6.92	0.007
St Dev.	2.54	4.77	
Work to $Failure_{Platens}$ (Nmm^{-1})			
Range	1.03 – 119.4	20.2 – 344.2	
Mean	28.93	108.2	<0.001
St Dev.	24.45	118.8	
Work to $Failure_{Contact}$ (Nmm^{-1})			
Range	3.0 – 268	47 – 775	
Mean	79.2	236	0.003
St Dev.	63.8	289	

8.1.2 Dependent and Independent Variable Relationships

In addition to the ten dependant variables shown previously in Table 8.2, each sample had nine independent variables (3 material properties and 6 collagen cross-link). The relationships were investigated both in linear and logarithmic regressions, with the results in Table 8.3 to Table 8.4 displaying the Pearson's correlation coefficient from the most significant or best performing of the regressions. The degree of significance for the comparisons is also demonstrated in the form of a p-value which is classified as significant when it falls below 0.05. The full linear and logarithmic regression analyses can be found in appendix 6 for the osteoporotic group and appendix 7 for the osteoarthritic group. The results of the regression analysis provide an insight into the dominant variables which affect the compressive properties of cancellous bone but, in order to provide proof of the magnitude of their effects, it was necessary to perform step-wise regression analysis on the results.

8.1.2.1 Regression Analysis

Material Properties

The apparent densities from the osteoporotic and osteoarthritic groups correlate positively with all the compressive mechanical testing parameters, with an increase in the apparent density of the bone core resulting in superior compressive mechanical properties. The exception to the rule was the ultimate strain determined from the contact extensometer in the osteoporotic group, where the effect of apparent density was non-significant and negligible. The positive correlations that were achieved for the osteoporotic group could be considered to be good (r = 0.428 - 0.69), but the

correlations achieved for the osteoarthritic samples were superior to those of the osteoporotic group and could be considered to be excellent (r = 0.567 - 0.967).

As would be expected, the porosity of the samples displayed the inverse relationship to that seen for the apparent density when compared to the compressive mechanical testing parameters. The levels of correlation were also in agreement; although the osteoporotic correlations were more moderate than good (r = -0.314 – -0.589), the osteoarthritic were still excellent (r = -0.470 – -0.973).

The effect of the material density on the compressive mechanical testing parameters was in marked contrast between the two groups. For the osteoporotic samples the material density had little significant effect, except on the ultimate strain and work to failure from the platens extensometer, where it positively correlated, 0.483 and 0.358 respectively, but on the most part the correlations were positive. In contrast the correlations seen between the material density of the osteoarthritic samples and the compressive mechanical testing parameters were highly correlated (r = -0.348 – -0.900) mostly significant, but inversely related.

Table 8.3 Pearson's correlations between the compressive mechanical parameters and the material properties and composition for the osteoporotic group

	$E_{Platens}$ (MPa)	$E_{Contact}$ (MPa)	$\varepsilon_{Yield\ Platens}$ (%)	$\varepsilon_{Ult.Platens}$ (%)	$\varepsilon_{Yield\ Contact}$ (%)	$\varepsilon_{Ult.Contact}$ (%)	σ_{Yield} (MPa)	$\sigma_{Ult.}$ (MPa)	Work to $Failure_{Platens}$ (Nmm^{-1})	Work to $Failure_{Contact}$ (Nmm^{-1})
Osteoporotic										
$\rho_{App.}$	*0.536 (0.001)*	0.498 (0.002)	0.374 (0.029)	0.428 (0.012)	*-0.055 (0.747)*	*-0.055 (0.772)*	*0.680 (<0.001)*	0.69 (<0.001)	0.655 (<0.001)	0.552 (<0.001)
Porosity	*-0.475 (0.003)*	-0.436 (0.008)	-0.271 (0.122)	-0.314 (0.070)	*0 (0.916)*	*0.1 (0.562)*	-0.574 (<0.001)	-0.589 (<0.001)	-0.554 (<0.001)	-0.497 (0.002)
$\rho_{Mat.}$	-0.076 (0.649)	0.076 (0.658)	*0.448 (0.008)*	*0.483 (0.004)*	0.055 (0.754)	0.222 (0.193)	*0.207 (0.207)*	*0.207 (0.203)*	*0.358 (0.030)*	*0.155 (0.359)*
m/m HLNL	*0.095 (0.562)*	*0.182 (0.279)*	*-0.032 (0.841)*	0.086 (0.622)	-0.086 (0.617)	*-0.077 (0.653)*	*0.126 (0.435)*	*0.179 (0.269)*	-0.028 (0.868)	0.164 (0.326)
m/m HHL	*-0.173 (0.302)*	-0.078 (0.653)	-0.081 (0.649)	-0.119 (0.502)	*-0.232 (0.180)*	-0.134 (0.436)	-0.137 (0.406)	-0.164 (0.318)	*-0.195 (0.250)*	-0.203 (0.228)
m/m HLKNL	*-0.285 (0.083)*	-0.159 (0.349)	-0.165 (0.345)	*-0.158 (0.361)*	*-0.077 (0.655)*	*-0.063 (0.716)*	-0.205 (0.205)	-0.179 (0.268)	-0.219 (0.186)	*-0.205 (0.216)*
m/m OHPyr	-0.071 (0.668)	-0.243 (0.142)	-0.194 (0.258)	*-0.1 (0.553)*	*0.114 (0.501)*	0.236 (0.155)	*-0.212 (0.181)*	*-0.173 (0.278)*	*-0.055 (0.73)*	*-0.130 (0.434)*
m/m LysPyr	-0.062 (0.707)	-0.151 (0.365)	-0.173 (0.314)	*-0.055 (0.751)*	*0.077 (0.648)*	*0.152 (0.363)*	*-0.122 (0.449)*	*-0.071 (0.657)*	0.140 (0.394)	*-0.063 (0.702)*
fmoles Pentosidine / pmole collagen	-0.059 (0.730)	0 (0.983)	*-0.134 (0.444)*	*0.072 (0.704)*	-0.063 (0.726)	0.070 (0.683)	-0.088 (0.592)	*0.122 (0.455)*	*0.11 (0.510)*	*0.1 (0.565)*

Table 8.4 Pearson's correlations between the compressive mechanical parameters and the material properties and composition for the osteoarthritic group

	$E_{Platens}$ (MPa)	$E_{Contact}$ (MPa)	$\varepsilon_{Yield\ Platens}$ (%)	$\varepsilon_{Ult.Platens}$ (%)	$\varepsilon_{Yield\ Contact}$ (%)	$\varepsilon_{Ult.Contact}$ (%)	σ_{Yield} (MPa)	$\sigma_{Ult.}$ (MPa)	Work to $Failure_{Platens}$ (Nmm^{-1})	Work to $Failure_{Contact}$ (Nmm^{-1})
Osteoathritic										
$\rho_{App.}$	*0.613 (0.106)*	*0.567 (0.143)*	0.536 (0.17)	0.917 (0.01)	*0.509 (0.244)*	0.699 (0.081)	*0.928 (0.001)*	0.967 (<0.001)	0.964 (<0.001)	0.909 (0.005)
Porosity	*-0.55 (0.157)*	*-0.470 (0.239)*	-0.532 (0.174)	-0.927 (0.001)	-0.497 (0.257)	-0.712 (0.073)	-0.919 (0.001)	-0.968 (<0.001)	-0.973 (<0.001)	-0.921 (0.003)
$\rho_{Mat.}$	*-0.499 (0.208)*	*-0.348 (0.398)*	-0.461 (0.25)	-0.875 (0.004)	*-0.542 (0.209)*	-0.767 (0.044)	-0.82 (0.013)	-0.878 (0.004)	-0.900 (0.002)	-0.860 (0.013)
m/m HLNL	*-0.141 (0.741)*	*-0.1 (0.810)*	0.587 (0.126)	0.765 (0.027)	0.479 (0.277)	0.310 (0.499)	0.480 (0.228)	0.568 (0.142)	0.557 (0.194)	0.727 (0.041)
m/m HHL	*-0.224 (0.631)*	0.188 (0.656)	0.828 (0.011)	0.872 (0.005)	*0.205 (0.696)*	0.250 (0.588)	0.629 (0.095)	0.684 (0.062)	0.646 (0.117)	0.786 (0.021)
m/m HLKNL	*-0.245 (0.557)*	-0.143 (0.736)	0.687 (0.060)	0.663 (0.073)	0.404 (0.368)	*-0.118 (0.798)*	0.345 (0.403)	0.426 (0.293)	0.390 (0.387)	0.592 (0.122)
m/m OHPyr	0.65 (0.081)	0.876 (0.004)	*0.936 (0.002)*	*0.628 (0.13)*	*-0.270 (0.558)*	*-0.263 (0.57)*	*0.477 (0.279)*	*0.439 (0.323)*	0.294 (0.522)	*0.495 (0.259)*
m/m LysPyr	0.375 (0.360)	*0.768 (0.026)*	0.359 (0.382)	0.601 (0.115)	*-0.351 (0.441)*	0.214 (0.645)	0.606 (0.111)	0.613 (0.106)	0.547 (0.204)	0.628 (0.095)
fmoles Pentosidine / pmole collagen	-0.213 (0.613)	-0.404 (0.321)	-0.374 (0.361)	-0.173 (0.683)	-0.010 (0.984)	*0.341 (0.455)*	-0.302 (0.467)	-0.246 (0.558)	*0.134 (0.771)*	-0.194 (0.645)

Collagen Cross-linking Analysis

For the osteoporotic groups, the effects of variation in the levels of collagen cross-linking appeared to have no significant effect on the compressive mechanical properties of the tissues. It was noticeable, however, that the relationships between the parameters were negative in nature. In contrast, the osteoarthritic group provided a number of strong and significant correlations with the compressive mechanical properties. The immature Aldimine cross-link HLNL, and its corresponding mature cross-link (HHL), both significantly correlated with the strain and compressive toughness of the material. The mature Ketoimine cross-links OH-Pyr and Lys-Pyr both correlated significantly with the modulus and OH-Pyr, additionally, with the platens yield strain, with the related immature cross-link HLKNL also approaching significance for the platens yield strain. The difference between the groups and the reasons for the significant correlations are difficult to explain, and after personal communication with the collagen research group in Bristol, it was decided that although the collagen cross-links may be having an effect on the overall mechanics of the bone, is more likely that the effects are being overshadowed by the apparent density, and the high correlations and significance seen in the osteoarthritic group are more likely due to close adherence to the apparent density of the sample than actual effects.

Although there were a number of significant correlations between the different independent variables and the mechanical properties, it was not certain or clear which of the variables were providing effects that affected the compressive mechanics of the bone. In order to clarify the magnitudes of the effects and the order of dominance with respect to the independent variables, it was necessary to perform stepwise regression analysis.

8.1.2.2 Stepwise Regression Analysis

Each mechanical dependant variable was compared against the eight independent variables simultaneously, in order to determine the magnitudes of their effects and the order of dominance of the independent variables.

Table 8.5 Stepwise regression analysis of the Osteoporotic compression results vs. the 9 independent variables.

OP Group	$\rho_{App.}$ (g cm^{-3})	Porosity (%)	$\rho_{Mat.}$ (g cm^{-3})	OHPyr (m/m)	LysPyr (m/m)	HLKNL (m/m)	HLNL (m/m)	fmoles Pentosidine / pmole collagen	r^2 value
E Platens (MPa)	1 (0.003)	-	-	-	-	-	-	-	22.1
E Contact (MPa)	1 (0.002)	-	-	-	-	-	-	-	24.8
	1 (0.024)	2 (0.100)	-	-	-	-	-	-	30.8
ε_{Yield} Platens	-	-	-	-	-	-	-	1 (0.092)	7.9
	-	-	-	2 (0.093)	-	-	-	1 (0.049)	15.3
	-	-	3 (0.084)	2 (0.039)	-	-	-	1 (0.052)	22.7
$\varepsilon_{Ult.}$ Platens	-	-	1 (0.049)	-	-	-	-	-	10.7
ε_{Yield} Contact	-	-	-	-	-	-	-	1 (0.094)	8.0
	-	-	-	-	-	-	2 (0.094)	1 (0.040)	15.6
$\varepsilon_{Ult.}$ Contact	-	-	-	-	-	-	-	-	-
σ_{Yield} (MPa)	1 (<0.001)	-	-	-	-	-	-	-	45.6
	1 (<0.001)	2 (0.001)	-	-	-	-	-	-	59.7
	1 (<0.001)	2 (<0.001)	-	3 (0.147)	-	-	-	-	62.1
	1 (0.002)	2 (0.006)	4 (0.070)	3 (0.064)	-	-	-	-	65.6
	1 (0.001)	2 (0.003)	4 (0.034)	3 (0.206)	-	5 (0.142)	-	-	67.8
	1 (0.001)	2 (0.005)	3 (0.049)	-	-	4 (0.045)	-	-	66.2
$\sigma_{Ult.}$ (MPa)	1 (<0.001)	-	-	-	-	-	-	-	47.7
	1 (<0.001)	2 (0.001)	-	-	-	-	-	-	61.5
	1 (0.005)	2 (0.019)	3 (0.147)	-	-	-	-	-	63.8
Work to Failure Platens (Nmm^{-1})	1 (<0.001)	-	-	-	-	-	-	-	30.4
	1 (<0.001)	-	-	-	2 (0.141)	-	-	-	34.8
Work to Failure Contact (Nmm^{-1})	1 (<0.001)	-	-	-	-	-	-	-	42.9
	1 (<0.001)	2 (0.004)	-	-	-	-	-	-	55.6

For the Young's modulus, yield strength, ultimate strength, and work to failure for both the extensometers of the osteoporotic compression cores, the dominant independent variable was apparent density, with in most cases the porosity of the core providing an additional significant level of explanation. In addition to these two

variables, the yield strength and ultimate strength were both affected by the material density of the sample; with the yield strength also affected by the levels of HLKNL and OHPyr collagen cross-links, although the additional explanation these variables provided over and above that of the porosity and apparent density was not significant.

The ultimate and yield strains from both the extensometers differed from the other mechanical properties, in that they were predominantly affected by the levels of the pentosidine cross-link within the collagen molecules. Additional explanation came from two other cross-links, HLNL and OHPyr, and the material density of the samples; however, in very few cases were any of the explanatory variables significant.

The osteoarthritic group results were interesting, with r^2 values ranging between 42.3% and 99.5%, far higher than those seen for the osteoporotic group, but mimicking those seen in the normal regression analysis of the previous section. In contrast to the osteoporotic group the predominant factor appeared to be the porosity of the cores, with apparent density only affecting the yield strength and platens work to failure. The effects of the levels of the collagen cross-linking were pronounced, with each of the collagen cross-links investigated within the study affecting one or more of the mechanical variables, and on the most part significantly.

However, the number of samples included within the osteoarthritic analysis was only 8, with one additional core not providing any results for the contact extensometer, and the author believes that this may have affected the results. One crucial area of any future work would be to determine the compositional properties of the cores with respect to the mineral and organic contents, as for the osteoporotic samples in particular a large percentage of the different mechanical parameters remains unexplained.

Table 8.6 Stepwise regression analysis of the Osteoarthritic compression results vs. the 9 independent variables.

OA Group	$\rho_{App.}$ (g cm^{-3})	Porosity (%)	$\rho_{Mat.}$ (g cm^{-3})	OHPyr (m/m)	LysPyr (m/m)	HHL (m/m)	HLKNL (m/m)	HLNL (m/m)	fmoles Pentosidine / pmole collagen	r^2 value
E Platens (MPa)	-	-	-	1 (0.081)	-	-	-	-	-	42.3
E Contact (MPa)	-	-	-	1 (0.004)	-	-	-	-	-	76.8
ε_{Yield} Platens	-	-	-	-	-	1 (0.011)	-	-	-	68.5
	-	-	-	-	2 (0.053)	1 (0.004)	-	-	-	86.2
$\varepsilon_{Ult.}$ Platens	-	1 (0.001)	-	-	-	-	-	-	-	86.0
	-	1 (0.018)	-	-	-	2 (0.076)	-	-	-	93.0
	-	1 (0.013)	-	-	-	2 (0.030)	-	-	3 (0.119)	96.5
ε_{Yield} Contact	-	-	-	-	-	-	-	-	-	-
$\varepsilon_{Ult.}$ Contact	-	-	1 (0.044)	-	-	-	-	-	-	58.8
	-	-	1 (0.016)	-	-	-	2 (0.110)	-	-	79.9
	-	-	1 (0.020)	-	-	-	2 (0.022)	3 (0.047)	-	95.6
σ_{Yield} (MPa)	1 (0.001)	-	-	-	-	-	-	-	-	86.0
	1 (0.001)	-	-	-	-	-	2 (0.088)	-	-	92.6
$\sigma_{Ult.}$ (MPa)	-	1 (<0.001)	-	-	-	-	-	-	-	93.6
	-	1 (<0.001)	-	-	-	-	2 (0.031)	-	-	97.7
	-	1 (<0.001)	-	-	3 (0.131)	-	2 (0.022)	-	-	98.8
	-	1 (0.001)	-	-	3 (0.109)	-	2 (0.042)	4 (0.140)	-	99.5
Work to Failure Platens (Nmm^{-1})	-	1 (<0.001)	-	-	-	-	-	-	-	94.7
	2 (0.074)	1 (0.033)	-	-	-	-	-	-	-	97.4
Work to Failure Contact (Nmm^{-1})	-	1 (0.003)	-	-	-	-	-	-	-	84.8

8.1.2.3 Power Functions

The results within the literature all refer to the power function relationship between the apparent density and the Young's modulus or strength of the material, when tested in compression (section 3.2.1). The results of this study showed that the power function relationships were equally as well correlated to the results as the linear function relationships for a number of the parameters; however, for comparison purposes the powers of the relationships are shown in Table 8.7.

Table 8.7 The powers of the logarithmic relationships between the compressive mechanical parameters and apparent density

Mechanical Parameter	Power Function	
	Osteoporotic	Osteoarthritic
E- Platens (MPa)	1.215	0.663
E- Contact (MPa)	1.479	0.82
ε_{Yield} Platens (%)	0.58	0.313
$\varepsilon_{Ult.}$ Strain Platens (%)	0.57	0.828
ε_{Yield} Contact (%)	0.114	0.315
$\varepsilon_{Ult.}$ Contact (%)	-0.113	0.553
σ_{Yield} (MPa)	1.73	1.067
$\sigma_{Ult.}$ (MPa)	1.72	1.27
Work to Failure Platens (Nmm^{-1})	1.89	2.086
Work to Failure Contact (Nmm^{-1})	1.70	1.649

The powers of the logarithmic regressions are as would have been expected within the osteoporotic group, but are slightly lower than might have been expected in the osteoarthritic group; however the low numbers of cores within the osteoarthritic group may have adversely affected the significance of the final results.

.

8.2 Fracture Toughness Testing

The fracture toughness testing was performed on all three study groups, with each study group having samples manufactured in both designs, compact disk shaped specimen and beam specimens, and orientated in two directions either with the crack propagating across the trabecular structure or along the trabecular structure of the cancellous bone. For each sample the material and compositional properties were determined, with the collagen cross-linking analysis restricted to the osteoporotic and osteoarthritic groups and the clinical QUS investigations restricted to the osteoarthritic group and a section of the osteoporotic group.

Of the 294 beam samples which were manufactured, the resultant fracture toughness validation and comparisons were performed on 280 samples. 2 beams from the equine group (1 Ac, 1 AL), 10 beams from the osteoporotic group (5 Ac, 5 AL) and 2 beams from the osteoarthritic group (1 Ac, 1 AL) were lost during testing. Of the 121 disk-shaped compact specimens, the equine samples were all tested successfully, but with 8 disks (6 Ac, 2 AL) from the osteoporotic group and 4 disks (2 Ac, 2 AL) lost from the osteoarthritic group, this meant that the total number of disks included in the analysis was 109.

8.2.1 Fracture Toughness Validation

As introduced in section 6.3.2.1 the values for the fracture toughness tests require validation to ensure that the methods used fit the requirements for obtaining the correct values for K_{IC}. The initial stage of the process is to obtain the ratio between P_{max} and P_Q; in order for the value to be considered a valid K_{IC} value, the ratio must be below 1.10. The results of the ratios for the different groups are shown in Table 8.8.

Table 8.8 Validation P_{max} / P_Q ratio values

	Beams Ac	Beams AL	Disks Ac	Disks AL
Equine				
Range	1.27 – 1.66	1.22 – 1.78	1.3 – 1.49	1.17 – 1.41
Average	1.46	1.46	1.38	1.3
St.Dev	0.093	0.1	0.06	0.07
OP				
Range	1.08 – 2.25	1.16 – 2.54	1.23 – 1.94	1.16 – 1.82
Average	1.5	1.56	1.46	1.43
St.Dev	0.17	0.22	0.18	0.167
OA				
Range	1.31 – 3.28	1.32 – 1.93	1.34 – 1.47	1.36 – 1.56
Average	1.58	1.55	1.41	1.44
St.Dev	0.31	0.21	0.04	0.08

The results in Table 8.8 show that for all three study groups the ratio between P_{max} and P_Q is above the 1.10 threshold level, meaning that under this initial validation test the values calculated are not valid measures of K_{IC}.

The final method of validation is the calculation of the specimen strength ratio, by comparing the K_Q result that was achieved with the tensile yield strength of the material using equation 6.5 (section 6.3.2.1). The testing procedures that were undertaken as part of this study did not provide any values for the tensile yield strength as testing was performed in compression, but in order to achieve an assessment of the measurement validity the compressive yield strength was utilised. The compressive

yield strength was regressed against apparent density in order to provide a logarithmic relationship between the two variables. This relationship was then utilised to predict the yield strength of the material for the individual fracture toughness samples. The OP and the OA samples were analysed separately in order to obtain group specific relationships, but for the equine group the previous OP relationship was utilised.

Table 8.9 Average (Standard Deviation) specimen strength ratios

	Beams Ac		Beams AL		Disks Ac		Disks AL	
	K_Q	$K_{C\ Pop\text{-}Ins}$	K_Q	$K_{C\ Pop\text{-}Ins}$	K_Q	$K_{C\ Pop\text{-}Ins}$	K_Q	$K_{C\ Pop\text{-}Ins}$
Equine								
Ratio σ_{ys} Comp.	0.025 (0.018)	0.05 (0.039)	0.008 (0.005)	0.016 (0.011)	0.02 (0.009)	0.037 (0.019)	0.011 (0.005)	0.018 (0.01)
Ratio σ_{ys} 70% Comp.	0.05 (0.038)	0.1 (0.079)	0.016 (0.011)	0.033 (0.023)	0.041 (0.019)	0.076 (0.038)	0.021 (0.011)	0.037 (0.021)
B (cm)	3.13 (0.08)				8.03 (0.04)			
a_0 (cm)	0.285 (0.21)				0.587 (0.015)			
OP								
Ratio σ_{ys} Comp.	0.015 (0.012)	0.032 (0.023)	0.013 (0.014)	0.023 (0.02)	0.015 (0.01)	0.03 (0.022)	0.009 (0.0054)	0.017 (0.01)
Ratio σ_{ys} 70% Comp.	0.023 (0.016)	0.052 (0.031)	0.011 (0.009)	0.024 (0.017)	0.006 (0.004)	0.043 (0.033)	0.003 (0.003)	0.022 (0.014)
B (cm)	0.31 (0.0049)				0.75 (0.057)			
a_0 (cm)	0.29 (0.017)				0.572 (0.026)			
OA								
Ratio σ_{ys} Comp.	0.011 (0.008)	0.03 (0.02)	0.03 (0.002)	0.005 (0.004)	0.003 (0.002)	0.021 (0.016)	0.002 (0.002)	0.011 (0.007)
Ratio σ_{ys} 70% Comp.	0.03 (0.023)	0.065 (0.046)	0.027 (0.028)	0.046 (0.04)	0.03 (0.021)	0.061 (0.044)	0.018 (0.011)	0.035 (0.02)
B (cm)	0.308 (0.003)				0.731 (0.037)			
a_0 (cm)	0.292 (0.241)				0.566 (0.018)			

The standard states that if the resultant value is below both the sample thickness (B - cm) and the initial notch length (a_0 -cm) then the result is a valid measure of K_{IC}. The results of this analysis along with the B and a_0 values for the different study groups are shown in Table 8.9, for the disk samples the lowest of the a_0 values was used for comparison. The results of this validation would indicate that the results from all three study groups, both sample designs and orientations, and both P_Q and P_{max} related

values provide valid results of K_{IC}. The results were, however, calculated using the compressive yield strength, and previous studies which have compared the compressive yield strength with the tensile yield strength have demonstrated that the tensile yield strength of cancellous bone is approximately 70% of the compressive yield strength (Section 3.2.3). In order to take this difference into account the compressive yield strength was reduced to 70% of the value used in the first analysis and the specimen strength ratios were recalculated (Table 8.9).

The results of the specimen strength ratios, after the adjustment of the yield strengths to account for the difference between the tensile and compressive nature of the results, provided a new set of validity results all of which were greater in magnitude than the previous results, but still below both the specimen thickness values and the initial notch length values. The implication of these results is that the samples used for the testing have provided valid K_{IC} results.

The other validation assessment that was required was to investigate if the results of the test were dependant on sample thickness and displaying values of plane stress, or if they were independent of the specimen thickness in plane strain. The testing that was performed was designed to enable the calculation of the J-integral; as such the parameter which was changed was the initial notch length and other variables such as the specimen thickness were kept the same. This meant the variation in the specimen thickness was not wide enough to allow for any relationships with the K fracture toughness parameters to provide any indication of whether the tests represented plane strain or plane stress.

8.2.2 Study Group Comparisons

The results from the five different fracture toughness parameters for each of the groups and sample designs are displayed in Table 8.10 and Table 8.11, along with ANOVA comparison to highlight any statistically significant differences between the study groups.

If the results were based solely on the porosity and apparent density results displayed in Table 8.29, then the results of the analysis should suggest that the osteoarthritic samples would provide the best fracture toughness results followed by the equine material with the osteoporotic samples being the weakest. In all bar a couple of situations, the fracture toughness of the equine material is superior to that of the osteoporotic group, as would have been expected. The osteoarthritic group, however, did not perform as would have been expected, and despite having a mean apparent density (0.608 g cm^{-3}, ± 0.21) that was superior to the equine material (0.562 g cm^{-3}, ± 0.12), it was out performed on a number of occasions. In comparison to the osteoporotic group, the K_Q and K_C results, as well and the G_Q and G_C results with relation to the beam Ac results would seem to agree with the original hypothesis; however, the results of the beam AL samples and the disk samples differ, in that the mean K and G values for the osteoporotic samples are not significantly different from those of the osteoarthritic group.

The main difference, however, is observed in the J-integral results. The equine and osteoporotic samples are mixed with different results seen in the different samples groups; however the osteoarthritic disk Ac results are an exception and are highly significantly superior to any of the other sample groups.

Table 8.10 Comparison between the fracture toughness results of the beam samples from the different study groups

	OP	OA	EQ	ANOVA Comparison	p-value
Beams Ac					
K_Q (MPa $m^{-1/2}$)					
Range	0.040 - 0.486	0.08 - 0.76	0.069 - 0.817	Osteoporotic vs. Osteoarthritic	<0.001
Mean	0.207	0.343	0.316	Osteoporotic vs. Equine	<0.001
St. Dev.	0.125	0.176	0.165	Osteoarthritic vs. Equine	0.431
K_C (MPa $m^{-1/2}$)					
Range	0.062 - 0.697	0.112 - 1.08	0.106 - 1.169	Osteoporotic vs. Osteoarthritic	<0.001
Mean	0.301	0.517	0.449	Osteoporotic vs. Equine	<0.001
St. Dev.	0.173	0.244	0.240	Osteoarthritic vs. Equine	0.170
J_Q (j m^{-2})					
Range	22.15 - 106.9	70.27 - 291.3	57.1 - 207.6	Osteoporotic vs. Osteoarthritic	<0.001
Mean	51.95	172.7	107.9	Osteoporotic vs. Equine	<0.001
St. Dev.	17.6	50.3	34.3	Osteoarthritic vs. Equine	<0.001
J_C (j m^{-2})					
Range	49.02 - 308.3	210.7 - 1389.2	110.2 - 432.0	Osteoporotic vs. Osteoarthritic	<0.001
Mean	170.0	719.8	295.5	Osteoporotic vs. Equine	<0.001
St. Dev.	52.4	237.7	81.8	Osteoarthritic vs. Equine	<0.001
G_Q (N m^{-1})					
Range	8.1 - 569.0	24.9 - 1275.5	10.0 - 1321.6	Osteoporotic vs. Osteoarthritic	<0.001
Mean	143.3	284.9	285.3	Osteoporotic vs. Equine	<0.001
St. Dev.	138.1	254.6	251.2	Osteoarthritic vs. Equine	0.994
G_C (N m^{-1})					
Range	11.4 - 1172.1	55.7 - 2451.9	23.5 - 2703.2	Osteoporotic vs. Osteoarthritic	<0.001
Mean	298.2	622.2	579.8	Osteoporotic vs. Equine	<0.001
St. Dev.	271.5	494.2	529.6	Osteoarthritic vs. Equine	0.686
Beams AL					
K_Q (MPa $m^{-1/2}$)					
Range	0.024 - 0.603	0.057 - 0.771	0.060 - 0.467	Osteoporotic vs. Osteoarthritic	0.079
Mean	0.174	0.249	0.233	Osteoporotic vs. Equine	0.009
St. Dev.	0.118	0.205	0.108	Osteoarthritic vs. Equine	0.703
K_C (MPa $m^{-1/2}$)					
Range	0.039 - 0.825	0.091 - 1.097	0.095 - 0.66	Osteoporotic vs. Osteoarthritic	0.018
Mean	0.233	0.37	0.333	Osteoporotic vs. Equine	0.001
St. Dev.	0.154	0.287	0.153	Osteoarthritic vs. Equine	0.534
J_Q (j m^{-2})					
Range	30.7 - 156.6	236.3 - 533.1	10.23 - 57.76	Osteoporotic vs. Osteoarthritic	<0.001
Mean	90.52	365.2	31.96	Osteoporotic vs. Equine	<0.001
St. Dev.	32.93	104.1	9.93	Osteoarthritic vs. Equine	<0.001
J_C (j m^{-2})					
Range	79.0 - 713.2	785 - 3287	38.2 - 109.1	Osteoporotic vs. Osteoarthritic	<0.001
Mean	364.2	1596	85.52	Osteoporotic vs. Equine	<0.001
St. Dev.	149.1	745	17.87	Osteoarthritic vs. Equine	<0.001
G_Q (N m^{-1})					
Range	2.8 - 668.2	13.9 - 592.7	8 - 392	Osteoporotic vs. Osteoarthritic	0.656
Mean	114.8	140.3	124.2	Osteoporotic vs. Equine	0.695
St. Dev.	139.4	162.2	97.6	Osteoarthritic vs. Equine	0.652
G_C (N m^{-1})					
Range	7.8 - 1249.7	30.4 - 1199.1	18.7 - 822.9	Osteoporotic vs. Osteoarthritic	0.203
Mean	200.4	300.9	253.7	Osteoporotic vs. Equine	0.218
St. Dev.	236.9	324.3	197.8	Osteoarthritic vs. Equine	0.513

Table 8.11 Comparison between the fracture toughness results of the disk samples from the different study groups

	OP	OA	EQ	ANOVA Comparison	p-value
Disks Ac					
K_Q (MPa $m^{-1/2}$)					
Range	0.038 - 0.44	0.048 - 0.427	0.302 - 0.669	Osteoporotic vs. Osteoarthritic	0.310
Mean	0.241	0.194	0.489	Osteoporotic vs. Equine	<0.001
St. Dev.	0.116	0.127	0.126	Osteoarthritic vs. Equine	<0.001
K_C (MPa $m^{-1/2}$)					
Range	0.074 - 0.604	0.111 - 0.9	0.403 - 0.96	Osteoporotic vs. Osteoarthritic	0.046
Mean	0.335	0.492	0.669	Osteoporotic vs. Equine	<0.001
St. Dev.	0.152	0.286	0.182	Osteoarthritic vs. Equine	0.050
J_Q (j m^{-2})					
Range	103.0 - 540.5	88.6 - 204.2	188.6 - 596.2	Osteoporotic vs. Osteoarthritic	0.002
Mean	278.7	132.6	327.6	Osteoporotic vs. Equine	0.208
St. Dev.	129.4	39.3	128.9	Osteoarthritic vs. Equine	<0.001
J_C (j m^{-2})					
Range	309.5 – 1542	220.1 - 336.6	411.2 - 1318.1	Osteoporotic vs. Osteoarthritic	<0.001
Mean	723.7	296.4	874.1	Osteoporotic vs. Equine	0.087
St. Dev.	323.6	42.4	245.7	Osteoarthritic vs. Equine	<0.001
G_Q (N m^{-1})					
Range	6.3 - 261.7	5.1 - 172.5	184.2 - 766.6	Osteoporotic vs. Osteoarthritic	0.024
Mean	146.3	71.3	404.2	Osteoporotic vs. Equine	<0.001
St. Dev.	88.4	53.7	177.7	Osteoarthritic vs. Equine	<0.001
G_C (N m^{-1})					
Range	23.2 - 615.3	27 - 894	332.5 - 1577.2	Osteoporotic vs. Osteoarthritic	0.022
Mean	279.6	481	759.5	Osteoporotic vs. Equine	<0.001
St. Dev.	161.6	319	359.1	Osteoarthritic vs. Equine	0.054
Disks AL					
K_Q (MPa $m^{-1/2}$)					
Range	0.048 - 0.370	0.062 - 0.455	0.162 - 0.596	Osteoporotic vs. Osteoarthritic	0.348
Mean	0.194	0.155	0.334	Osteoporotic vs. Equine	<0.001
St. Dev.	0.096	0.127	0.108	Osteoarthritic vs. Equine	0.001
K_C (MPa $m^{-1/2}$)					
Range	0.077 - 0.497	0.164 - 0.976	0.204 - 0.841	Osteoporotic vs. Osteoarthritic	0.037
Mean	0.263	0.404	0.436	Osteoporotic vs. Equine	<0.001
St. Dev.	0.119	0.27	0.152	Osteoarthritic vs. Equine	0.689
J_Q (j m^{-2})					
Range	80.25 - 244.6	349.1 - 742.3	97.7 - 232.2	Osteoporotic vs. Osteoarthritic	<0.001
Mean	168.1	495.2	143.2	Osteoporotic vs. Equine	0.040
St. Dev.	45.01	148.9	36.8	Osteoarthritic vs. Equine	<0.001
J_C (j m^{-2})					
Range	245.4 - 419.3	908 - 2555	217.8 - 307.1	Osteoporotic vs. Osteoarthritic	<0.001
Mean	342.4	1499	276.2	Osteoporotic vs. Equine	<0.001
St. Dev.	42.66	536	24.8	Osteoarthritic vs. Equine	<0.001
G_Q (N m^{-1})					
Range	9.0 - 256.7	9.3 - 197.8	47.0 - 492.3	Osteoporotic vs. Osteoarthritic	0.065
Mean	100.5	47.2	188.7	Osteoporotic vs. Equine	0.001
St. Dev.	71.6	62.5	100.8	Osteoarthritic vs. Equine	0.001
G_C (N m^{-1})					
Range	17.0 419.6	64.2 - 911.7	74.6 - 981.9	Osteoporotic vs. Osteoarthritic	0.103
Mean	183.1	293.8	321.5	Osteoporotic vs. Equine	0.003
St. Dev.	119.4	277.6	190.7	Osteoarthritic vs. Equine	0.758

8.2.3 Linear and Logarithmic Regression Relationships

8.2.3.1 Material Properties

The results from the fracture toughness testing in comparison to the material and compositional properties of the test samples are shown in tables 8.17 to 8.22. The tables have been reduced from the full analysis, to the Pearson's correlations between the parameters, with the most significant of either the linear or logarithmic relationship being displayed. Full analysis can be seen in appendix 8 for the equine samples, appendix 9 for the osteoporotic samples and appendix 10 for the osteoarthritic samples.

Apparent Density

The relationship between the fracture toughness parameters and the apparent density consistently provided significant correlations within all three study groups, sample designs and orientations. The relationships between the parameters were on the whole equally significant when viewed as either a linear relationship or a logarithmic relationship, with the r and r^2 values varying little between the two.

For both the K values and the G values the relationship is positive with the increase in density resulting in an increase in the fracture toughness parameter. However the J-integral values were not in agreement, and showed an inverse relationship with in apparent density, in that an increase in the apparent density lead to a reduction in the J-integral for the sample tested. The reasoning behind this relationship will be investigated further later in this section.

Table 8.12 Pearson's correlations between the fracture toughness parameters from the equine beam samples, and the material and compositional properties

Equine Beams	Beams AC						Beams AL					
	K_Q	K_C	J_Q	J_C	G_Q	G_C	K_Q	K_C	J_Q	J_C	G_Q	G_C
$\rho_{App.}$	0.652 (<0.001)	0.652 (<0.001)	*-0.369 (0.003)*	*-0.197 (0.124)*	0.494 (<0.001)	0.502 (<0.001)	0.663 (<0.001)	0.645 (<0.001)	*-0.453 (0.001)*	-0.336 (0.020)	*0.532 (<0.001)*	*0.527 (<0.001)*
Porosity	*-0.645 (<0.001)*	*-0.644 (<0.001)*	*0.385 (0.002)*	*-0.192 (0.138)*	*-0.509 (<0.001)*	*-0.504 (<0.001)*	-0.587 (<0.001)	-0.562 (<0.001)	0.385 (0.007)	0.340 (0.018)	-0.451 (0.001)	-0.416 (0.003)
$\rho_{Mat.}$	0.327 (0.009)	0.313 (0.013)	*0.138 (0.285)*	*0.105 (0.427)*	0.344 (0.006)	0.321 (0.011)	-0.227 (0.120)	-0.197 (0.181)	0.137 (0.352)	*0.283 (0.052)*	-0.169 (0.252)	-0.134 (0.362)
$\rho_{Rel.}$	0.553 (<0.001)	0.537 (<0.001)	*-0.349 (0.005)*	*-0.182 (0.157)*	0.383 (0.002)	0.396 (0.001)	0.587 (<0.001)	0.563 (<0.001)	*-0.402 (0.005)*	-0.340 (0.018)	0.451 (0.001)	*0.440 (0.002)*
MC_{HYD}	0.09 (0.487)	0.078 (0.547)	*-0.063 (0.616)*	*-0.279 (0.03)*	0.146 (0.258)	0.119 (0.358)	-0.093 (0.529)	-0.087 (0.555)	0.397 (0.005)	*0.476 (0.001)*	-0.081 (0.583)	-0.080 (0.591)
OC_{HYD}	*-0.161 (0.213)*	*-0.145 (0.256)*	0.106 (0.411)	0.088 (0.498)	*-0.192 (0.136)*	*-0.176 (0.170)*	0.339 (0.019)	*0.307 (0.034)*	*-0.089 (0.553)*	-0.104 (0.480)	0.313 (0.03)	*0.293 (0.043)*
MC_{DEHYD}	*0.176 (0.168)*	*0.182 (0.158)*	-0.058 (0.655)	-0.109 (0.401)	*0.235 (0.067)*	*0.241 (0.06)*	-0.324 (0.025)	-0.291 (0.045)	0.370 (0.01)	0.433 (0.002)	-0.295 (0.042)	-0.248 (0.089)
OC_{DEHYD}	*-0.176 (0.171)*	*-0.179 (0.166)*	0.058 (0.665)	0.109 (0.401)	*-0.232 (0.069)*	*-0.235 (0.066)*	0.324 (0.025)	0.291 (0.045)	-0.370 (0.01)	-0.443 (0.002)	0.295 (0.042)	0.248 (0.089)

Table 8.13 Pearson's correlations between the fracture toughness parameters from the equine disk samples, and the material and compositional properties.

Equine Disks	Disks AC						Disks AL					
	K_Q	K_C	J_Q	J_C	G_Q	G_C	K_Q	K_C	J_Q	J_C	G_Q	G_C
$\rho_{App.}$	*0.625 (0.002)*	*0.611 (0.003)*	-0.411 (0.064)	-0.246 (0.283)	*0.292 (0.199)*	*0.293 (0.196)*	0.591 (0.003)	0.545 (0.007)	-0.481 (0.023)	-0.450 (0.04)	0.465 (0.029)	0.425 (0.048)
Porosity	*-0.440 (0.046)*	*-0.421 (0.058)*	0.338 (0.135)	0.268 (0.241)	*-0.084 (0.724)*	*-0.077 (0.732)*	*-0.396 (0.061)*	*-0.345 (0.106)*	*0.673 (0.001)*	*0.618 (0.003)*	-0.281 (0.205)	-0.255 (0.251)
$\rho_{Mat.}$	*-0.114 (0.629)*	*-0.095 (0.688)*	0.137 (0.552)	0.308 (0.175)	0.298 (0.19)	0.320 (0.158)	*0.141 (0.523)*	*0.195 (0.374)*	*0.871 (<0.001)*	0.780 (<0.001)	*0.283 (0.202)*	*0.332 (0.132)*
$\rho_{Rel.}$	*0.485 (0.026)*	*0.468 (0.032)*	-0.338 (0.135)	0.268 (0.241)	*0.126 (0.579)*	*0.130 (0.576)*	*0.394 (0.063)*	0.342 (0.111)	-0.672 (0.001)	-0.616 (0.003)	0.281 (0.205)	0.255 (0.251)
MC_{HYD}	0.245 (0.285)	0.267 (0.241)	0.220 (0.339)	0.323 (0.153)	0.460 (0.036)	0.477 (0.029)	-0.399 (0.066)	-0.450 (0.035)	-0.147 (0.524)	0.017 (0.943)	-0.468 (0.032)	-0.533 (0.013)
OC_{HYD}	*0.636 (0.002)*	*0.605 (0.004)*	-0.008 (0.973)	0.175 (0.448)	*0.592 (0.005)*	*0.555 (0.009)*	*0.324 (0.131)*	*0.363 (0.088)*	*0.268 (0.228)*	0.212 (0.357)	*0.332 (0.132)*	*0.373 (0.087)*
MC_{DEHYD}	*-0.356 (0.112)*	*-0.315 (0.164)*	0.196 (0.393)	0.119 (0.607)	*-0.161 (0.484)*	*-0.122 (0.595)*	-0.40 (0.059)	*-0.447 (0.032)*	*-0.297 (0.18)*	*-0.212 (0.358)*	-0.403 (0.063)	-0.452 (0.035)
OC_{DEHYD}	*0.359 (0.109)*	*0.318 (0.16)*	-0.196 (0.393)	-0.119 (0.607)	*0.161 (0.482)*	*0.122 (0.593)*	0.40 (0.059)	*0.454 (0.030)*	*0.305 (0.167)*	*0.215 (0.35)*	0.403 (0.063)	*0.466 (0.029)*

Table 8.14 Pearson's correlations between the fracture toughness parameters from the osteoporotic beam samples, the material and compositional properties and the collagen cross-linking analysis.

OP Beams	Beams AC						Beams AL					
	K_Q	K_C	J_Q	J_C	G_Q	G_C	K_Q	K_C	J_Q	J_C	G_Q	G_C
$\rho_{App.}$	*0.807 (<0.001)*	*0.781 (<0.001)*	-0.214 (0.110)	-0.271 (0.040)	*0.701 (<0.001)*	*0.655 (<0.001)*	*0.733 (<0.001)*	0.719 (<0.001)	*-0.516 (<0.001)*	-0.436 (0.001)	*0.631 (<0.001)*	0.595 (<0.001)
Porosity	*-0.782 (<0.001)*	-0.767 (<0.001)	0.161 (0.234)	0.240 (0.072)	*-0.685 (<0.001)*	*-0.648 (<0.001)*	-0.668 (<0.001)	-0.659 (<0.001)	0.494 (<0.001)	0.450 (0.001)	*-0.564 (<0.001)*	-0.531 (<0.001)
$\rho_{Mat.}$	-0.119 (0.384)	*-0.141 (0.299)*	-0.076 (0.585)	0.050 (0.719)	*-0.083 (0.539)*	*-0.11 (0.427)*	*-0.167 (0.223)*	-0.119 (0.387)	*0.164 (0.235)*	0.283 (0.037)	*-0.130 (0.338)*	*0.063 (0.641)*
$\rho_{Rel.}$	*0.801 (<0.001)*	0.790 (<0.001)	-0.218 (0.121)	-0.217 (0.118)	*0.704 (<0.001)*	*0.671 (<0.001)*	*0.719 (<0.001)*	*0.691 (<0.001)*	*-0.512 (<0.001)*	-0.448 (0.001)	*0.618 (<0.001)*	*0.569 (<0.001)*
MC_{HYD}	*0.134 (0.303)*	0.103 (0.429)	*-0.122 (0.362)*	-0.042 (0.749)	*0.126 (0.337)*	0.101 (0.438)	-0.178 (0.19)	-0.227 (0.092)	*0.212 (0.118)*	*0.187 (0.166)*	-0.181 (0.183)	-0.223 (0.099)
OC_{HYD}	-0.336 (0.009)	-0.315 (0.014)	*0.057 (0.678)*	*0.148 (0.261)*	-0.32 (0.013)	-0.293 (0.023)	*-0.114 (0.403)*	0.117 (0.398)	-0.30 (0.827)	*0.122 (0.376)*	*-0.11 (0.431)*	0.179 (0.195)
MC_{DEHYD}	0.389 (0.002)	0.355 (0.005)	*-0.105 (0.429)*	*-0.1 (0.457)*	0.391 (0.002)	0.357 (0.005)	*0.122 (0.368)*	*0.247 (0.067)*	*-0.245 (0.069)*	*-0.105 (0.435)*	*0.126 (0.357)*	*0.266 (0.047)*
OC_{DEHYD}	-0.410 (0.001)	-0.376 (0.003)	*0.17 (0.2)*	*0.17 (0.191)*	-0.404 (0.001)	-0.371 (0.003)	*-0.122 (0.364)*	*-0.245 (0.069)*	*0.249 (0.065)*	*0.122 (0.375)*	*-0.126 (0.353)*	*-0.265 (0.048)*
m/m HLNL	-0.075 (0.583)	-0.06 (0.661)	*0.205 (0.137)*	0.163 (0.234)	-0.160 (0.238)	-0.148 (0.276)	0.015 (0.913)	0.070 (0.603)	0.333 (0.011)	0.176 (0.191)	0.054 (0.692)	0.117 (0.385)
m/m HHL	*0.202 (0.164)*	*0.167 (0.252)*	*0.122 (0.404)*	-0.061 (0.681)	*0.122 (0.396)*	0.096 (0.512)	*0.1 (0.465)*	-0.063 (0.653)	*0.230 (0.095)*	*0.077 (0.593)*	*0.089 (0.524)*	-0.104 (0.456)
m/m HLKNL	-0.043 (0.747)	-0.023 (0.866)	*0.285 (0.033)*	0.337 (0.01)	-0.087 (0.514)	-0.066 (0.622)	0.126 (0.35)	0.066 (0.627)	0.216 (0.11)	*-0.045 (0.745)*	0.159 (0.238)	0.104 (0.440)
m/m OHPyr	*0.1 (0.439)*	-0.066 (0.612)	-0.047 (0.726)	*0.1 (0.454)*	-0.05 (0.704)	-0.024 (0.856)	*-0.263 (0.051)*	*-0.286 (0.033)*	*0.31 (0.02)*	0.191 (0.159)	*-0.23 (0.089)*	-0.268 (0.046)
m/m LysPyr	*-0.283 (0.032)*	*-0.288 (0.028)*	*0.19 (0.159)*	*0.1 (0.455)*	*-0.251 (0.057)*	*-0.255 (0.054)*	*-0.2 (0.140)*	*-0.221 (0.101)*	*0.395 (0.003)*	*0.19 (0.162)*	*-0.167 (0.218)*	*-0.187 (0.167)*
fmoles Pentosidine / pmole collagen	*0.170 (0.195)*	*0.164 (0.217)*	-0.085 (0.529)	-0.033 (0.809)	*0.179 (0.173)*	*0.167 (0.202)*	-0.434 (0.001)	-0.400 (0.002)	*0.1 (0.470)*	*0.214 (0.116)*	-0.420 (0.001)	-0.407 (0.002)

Table 8.15 Pearson's correlations between the fracture toughness parameters from the osteoporotic disk samples, the material and compositional properties and the collagen cross-linking analysis.

OP Disks	Disks AC						Disks AL					
	K_Q	K_C	J_Q	J_C	G_Q	G_C	K_Q	K_C	J_Q*	J_C*	G_Q	G_C
$\rho_{App.}$	0.746 (<0.001)	*0.712 (<0.001)*	*-0.005 (0.956)*	*-0.270 (0.323)*	*0.555 (0.005)*	*0.484 (0.017)*	0.819 (<0.001)	*0.775 (<0.001)*	-0.225 (0.250)	-0.220 (0.290)	*0.672 (<0.01)*	*0.596 (0.001)*
Porosity	-0.695 (<0.001)	-0.657 (<0.001)	*0.077 (0.709)*	*0.207 (0.317)*	*-0.434 (0.034)*	*-0.377 (0.069)*	-0.826 (<0.001)	-0.821 (<0.001)	0.062 (0.764)	0.059 (0.791)	-0.701 (<0.001)	-0.682 (<0.001)
$\rho_{Mat.}$	-0.459 (0.021)	-0.437 (0.029)	-0.285 (0.167)	-0.193 (0.355)	*-0.336 (0.108)*	*-0.297 (0.16)*	-0.319 (0.099)	-0.292 (0.131)	*0.297 (0.118)*	*0.114 (0.575)*	-0.09 (0.649)	-0.032 (0.870)
$\rho_{Rel.}$	*0.697 (<0.001)*	*0.666 (<0.001)*	*0.055 (0.807)*	*-0.141 (0.497)*	*0.532 (0.007)*	*0.465 (0.022)*	*0.741 (<0.001)*	*0.706 (<0.001)*	-0.251 (0.197)	-0.255 (0.218)	*0.558 (0.001)*	*0.514 (0.006)*
MC_{HYD}	0.095 (0.653)	0.053 (0.803)	0.208 (0.318)	0.175 (0.402)	*-0.045 (0.844)*	*-0.077 (0.727)*	*0.239 (0.220)*	*0.272 (0.162)*	-0.091 (0.640)	*0.138 (0.497)*	*0.2 (0.307)*	*0.232 (0.234)*
OC_{HYD}	*-0.126 (0.549)*	*-0.105 (0.614)*	-0.405 (0.044)	-0.316 (0.124)	*-0.152 (0.482)*	*-0.126 (0.556)*	0.050 (0.800)	*-0.014 (0.942)*	*0.155 (0.424)*	-0.148 (0.471)	0.159 (0.419)	0.111 (0.573)
MC_{DEHYD}	0.130 (0.553)	0.117 (0.596)	-0.513 (0.012)	-0.564 (0.005)	*0.118 (0.606)*	0.087 (0.699)	0.233 (0.251)	0.177 (0.338)	-0.006 (0.978)	0.014 (0.947)	0.221 (0.277)	0.141 (0.491)
OC_{DEHYD}	*-0.134 (0.546)*	-0.117 (0.596)	0.513 (0.012)	0.564 (0.005)	*-0.122 (0.583)*	*-0.089 (0.685)*	-0.233 (0.251)	-0.177 (0.388)	0.006 (0.949)	*-0.014 (0.947)*	-0.221 (0.277)	-0.141 (0.491)
m/m HLNL	0.067 (0.749)	0.09 (0.668)	-0.083 (0.694)	-0.119 (0.570)	0.291 (0.167)	0.325 (0.121)	*-0.355 (0.064)*	*-0.319 (0.098)*	0.399 (0.039)	*-0.084 (0.701)*	*-0.319 (0.097)*	*-0.265 (0.174)*
m/m HHL	*0.339 (0.123)*	0.243 (0.031)	*0.418 (0.053)*	0.301 (0.173)	0.472 (0.031)	*0.457 (0.037)*	*0.055 (0.804)*	*0.089 (0.674)*	*0.084 (0.695)*	*0.243 (0.302)*	*0.055 (0.801)*	*0.1 (0.638)*
m/m HLKNL	*0.089 (0.676)*	*0.084 (0.704)*	0.499 (0.013)	0.504 (0.012)	0.189 (0.387)	0.209 (0.338)	*-0.218 (0.275)*	*-0.168 (0.401)*	*0.330 (0.1)*	0.130 (0.538)	*-0.174 (0.386)*	*-0.088 (0.664)*
m/m OHPyr	*-0.055 (0.802)*	*-0.045 (0.853)*	0.111 (0.598)	*0.126 (0.551)*	0.327 (0.119)	0.333 (0.112)	*-0.285 (0.143)*	*-0.274 (0.159)*	0.421 (0.029)	*-0.055 (0.815)*	*-0.176 (0.369)*	*-0.148 (0.454)*
m/m LysPyr	*-0.155 (0.466)*	*-0.130 (0.541)*	*-0.016 (0.930)*	*0.141 (0.506)*	0.111 (0.616)	0.158 (0.472)	-0.168 (0.401)	*-0.148 (0.461)*	*0.315 (0.118)*	*-0.161 (0.451)*	*-0.118 (0.561)*	*-0.095 (0.640)*
fmoles Pentosidine / pmole collagen	*0.202 (0.330)*	*0.207 (0.321)*	-0.252 (0.224)	*-0.302 (0.142)*	*0.217 (0.309)*	*0.221 (0.298)*	*0.170 (0.407)*	*0.134 (0.515)*	*0.047 (0.839)*	*-0.130 (0.544)*	*0.192 (0.348)*	*0.145 (0.480)*

Table 8.16 Pearson's correlations between the fracture toughness parameters from the osteoarthritic beam samples, the material and compositional properties and the collagen cross-linking analysis.

OA Beams	Beams AC						Beams AL					
	K_Q	K_C	J_Q	J_C	G_Q	G_C	K_Q	K_C	J_Q	J_C	G_Q	G_C
$\rho_{App.}$	*0.769 (<0.001)*	*0.764 (<0.001)*	-0.450 (0.006)	*-0.432 (0.007)*	*0.616 (<0.001)*	*0.583 (<0.001)*	0.861 (<0.001)	0.849 (<0.001)	-0.401 (0.086)	-0.495 (0.175)	0.920 (<0.001)	0.906 (<0.001)
Porosity	-0.676 (<0.001)	-0.702 (<0.001)	*0.416 (0.012)*	*0.4 (0.014)*	*-0.473 (0.003)*	-0.474 (0.003)	-0.888 (<0.001)	-0.874 (<0.001)	*0.509 (0.076)*	0.478 (0.217)	-0.939 (<0.001)	-0.924 (<0.001)
$\rho_{Mat.}$	-0.341 (0.039)	-0.382 (0.02)	*0.084 (0.629)*	*0.118 (0.486)*	*0.221 (0.190)*	*0.241 (0.150)*	-0.806 (0.001)	-0.776 (0.001)	*0.187 (0.541)*	*-0.071 (0.818)*	-0.818 (0.002)	-0.794 (0.001)
$\rho_{Rel.}$	*0.798 (<0.001)*	*0.781 (<0.001)*	*-0.436 (0.009)*	*-0.415 (0.011)*	*0.664 (<0.001)*	*0.615 (<0.001)*	0.924 (<0.001)	0.939 (<0.001)	-0.478 (0.098)	-0.368 (0.217)	0.874 (<0.001)	0.888 (<0.001)
MC_{HYD}	-0.254 (0.130)	-0.338 (0.041)	0.197 (0.257)	*0.071 (0.679)*	-0.108 (0.526)	-0.195 (0.247)	-0.696 (0.013)	*-0.724 (0.008)*	*0.318 (0.315)*	*-0.1 (0.762)*	-0.721 (0.02)	*-0.704 (0.011)*
OC_{HYD}	*0.179 (0.282)*	*0.126 (0.456)*	-0.037 (0.828)	-0.202 (0.224)	*0.173 (0.3)*	*0.1 (0.542)*	-0.666 (0.084)	-0.558 (0.045)	*0.558 (0.074)*	0.521 (0.835)	-0.613 (0.075)	-0.543 (0.025)
MC_{DEHYD}	-0.340 (0.037)	-0.395 (0.014)	0.106 (0.54)	*0.072 (0.662)*	-0.193 (0.246)	*-0.249 (0.130)*	-0.351 (0.259)	-0.382 (0.286)	*-0.21 (0.513)*	*-0.045 (0.904)*	-0.336 (0.220)	0.354 (0.264)
OC_{DEHYD}	0.340 (0.037)	0.395 (0.014)	-0.106 (0.54)	-0.072 (0.668)	0.193 (0.246)	0.249 (0.131)	0.351 (0.259)	0.382 (0.286)	*0.219 (0.496)*	*0.055 (0.874)*	0.336 (0.220)	0.354 (0.264)
m/m HLNL	0.068 (0.693)	0.107 (0.534)	*0.167 (0.337)*	*0.195 (0.256)*	0.077 (0.652)	0.096 (0.573)	0.549 (0.034)	0.542 (0.034)	*0.130 (0.685)*	-0.007 (0.661)	0.612 (0.069)	0.614 (0.065)
m/m HHL	*-0.305 (0.158)*	*-0.253 (0.245)*	0.151 (0.472)	0.278 (0.189)	*-0.226 (0.301)*	*-0.148 (0.502)*	0.409 (0.169)	0.364 (0.157)	*-0.497 (0.10)*	*-0.303 (0.337)*	0.436 (0.245)	0.242 (0.187)
m/m HLKNL	0.245 (0.151)	0.330 (0.05)	-0.124 (0.477)	*0.089 (0.609)*	0.032 (0.849)	0.099 (0.559)	0.530 (0.045)	0.519 (0.046)	*0.141 (0.658)*	*0.11 (0.739)*	0.584 (0.084)	0.586 (0.076)
m/m OHPyr	*-0.032 (0.823)*	0.072 (0.673)	-0.012 (0.946)	-0.049 (0.774)	-0.111 (0.507)	-0.051 (0.763)	0.102 (0.586)	0.092 (0.601)	*-0.354 (0.260)*	*-0.321 (0.309)*	0.168 (0.777)	0.175 (0.753)
m/m LysPyr	*-0.19 (0.248)*	*-0.152 (0.358)*	-0.102 (0.544)	0.019 (0.91)	*-0.145 (0.372)*	*-0.095 (0.571)*	0.358 (0.395)	0.285 (0.346)	*-0.378 (0.225)*	-0.362 (0.737)	0.298 (0.368)	0.270 (0.253)
fmoles Pentosidine / pmole collagen	0.399 (0.032)	0.439 (0.017)	*-0.221 (0.238)*	*-0.158 (0.415)*	*0.389 (0.034)*	*0.4 (0.029)*	-0.203 (0.588)	-0.147 (0.552)	0.115 (0.094)	0.505 (0.722)	-0.191 (0.649)	-0.174 (0.528)

Table 8.17 Pearson's correlations between the fracture toughness parameters from the osteoarthritic disk samples, the material and compositional properties and the collagen cross-linking analysis.

OA Disks	Disks AC						Disks AL					
	K_Q	K_C	J_Q	J_C	G_Q	G_C	K_Q	K_C	J_Q	J_C	G_Q	G_C
$\rho_{App.}$	0.844 (0.004)	0.757 (0.018)	*-0.605 (0.084)*	-0.671 (0.048)	0.648 (0.059)	0.341 (0.369)	0.935 (0.006)	0.944 (0.005)	*-0.552 (0.256)*	*-0.649 (0.163)*	0.877 (0.022)	0.955 (0.003)
Porosity	-0.849 (0.004)	-0.753 (0.019)	0.554 (0.121)	0.647 (0.060)	-0.659 (0.054)	-0.339 (0.372)	-0.950 (0.004)	-0.956 (0.003)	*0.327 (0.527)*	*0.497 (0.316)*	-0.854 (0.031)	-0.946 (0.004)
$\rho_{Mat.}$	-0.537 (0.136)	-0.409 (0.274)	0.612 (0.08)	0.392 (0.297)	-0.430 (0.248)	-0.118 (0.762)	*-0.484 (0.331)*	*-0.436 (0.387)*	*-0.514 (0.298)*	-0.481 (0.334)	*-0.454 (0.365)*	*-0.416 (0.412)*
$\rho_{Rel.}$	0.849 (0.004)	0.753 (0.019)	*-0.619 (0.076)*	*-0.651 (0.057)*	0.659 (0.054)	0.339 (0.372)	0.995 (<0.001)	0.988 (<0.001)	*-0.387 (0.390)*	*-0.435 (0.329)*	0.987 (<0.001)	0.983 (<0.001)
MC_{HYD}	-0.539 (0.134)	-0.454 (0.219)	0.251 (0.515)	0.193 (0.619)	-0.340 (0.371)	*-0.122 (0.750)*	*-0.308 (0.553)*	*-0.253 (0.629)*	*-0.554 (0.254)*	-0.571 (0.236)	*-0.329 (0.524)*	*-0.276 (0.597)*
OC_{HYD}	*-0.122 (0.751)*	*-0.182 (0.639)*	*-0.245 (0.526)*	*-0.363 (0.336)*	0.208 (0.592)	*-0.176 (0.653)*	0.598 (0.210)	0.631 (0.179)	*-0.725 (0.103)*	*-0.828 (0.042)*	0.603 (0.205)	0.668 (0.147)
MC_{DeHyd}	-0.647 (0.060)	-0.466 (0.207)	*0.423 (0.257)*	*0.463 (0.209)*	-0.525 (0.147)	-0.114 (0.770)	*-0.489 (0.325)*	*-0.442 (0.381)*	*-0.439 (0.383)*	-0.444 (0.378)	*-0.495 (0.318)*	*-0.457 (0.362)*
OC_{DeHyd}	0.647 (0.060)	0.466 (0.207)	-0.419 (0.262)	-0.456 (0.217)	0.525 (0.147)	0.114 (0.770)	*0.5 (0.313)*	*0.451 (0.369)*	*0.432 (0.391)*	0.444 (0.378)	*0.506 (0.306)*	*0.467 (0.350)*
m/m HLNL	0.616 (0.077)	0.436 (0.241)	-0.319 (0.403)	-0.493 (0.177)	0.675 (0.046)	0.297 (0.437)	0.610 (0.146)	0.792 (0.034)	0.364 (0.422)	0.346 (0.446)	*0.138 (0.766)*	0.571 (0.181)
m/m HHL	0.567 (0.111)	0.397 (0.290)	-0.338 (0.373)	-0.585 (0.098)	0.569 (0.109)	*0.402 (0.322)*	0.804 (0.029)	0.879 (0.009)	*-0.217 (0.728)*	*-0.308 (0.614)*	0.480 (0.276)	0.800 (0.031)
m/m HLKNL	0.480 (0.191)	0.255 (0.509)	-0.416 (0.265)	-0.458 (0.215)	0.474 (0.198)	*-0.221 (0.568)*	0.758 (0.048)	0.820 (0.024)	0.480 (0.276)	0.435 (0.329)	0.367 (0.418)	0.662 (0.106)
m/m OHPyr	0.494 (0.176)	0.337 (0.375)	*-0.396 (0.291)*	-0.488 (0.183)	0.407 (0.277)	*0.176 (0.651)*	0.286 (0.535)	0.458 (0.302)	0.117 (0.803)	0.237 (0.610)	*-0.141 (0.762)*	0.171 (0.714)
m/m LysPyr	0.387 (0.304)	*0.3 (0.433)*	*-0.13 (0.741)*	-0.377 (0.318)	0.445 (0.230)	*0.348 (0.359)*	0.700 (0.08)	0.605 (0.150)	*-0.627 (0.132)*	*-0.597 (0.157)*	0.804 (0.029)	0.874 (0.010)
fmoles Pentosidine / pmole collagen	*0.709 (0.032)*	*0.801 (0.009)*	0.374 (0.321)	0.308 (0.419)	*0.789 (0.012)*	*0.852 (0.004)*	-0.050 (0.915)	*0.19 (0.686)*	*0.503 (0.249)*	*0.339 (0.457)*	-0.218 (0.639)	*0.077 (0.874)*

The hypothesis that was laid out in section 3.2.4.1 by L.J. Gibson and M.F. Ashby (1997a) predicted the relationship between the K_{IC} results and density would be a power function of between 1 and 2. The resultant powers for the relationships between the K, G and J-Integral values in relation to apparent and relative density are shown in Table 8.18 respectively.

For both the apparent and relative densities the majority of the power functions for the K_Q and K_C values fell within these guidelines; however, in certain groups of samples such as the equine disk samples, the power functions were discernibly lower with respect to relative density, while in other groups such as the osteoarthritic disks AL and the equine beams AL were both noticeably higher. The sample groups were also used in combination to investigate the relationship with density of the different sample designs, and provided results for K_Q and K_C which were strongly in agreement with the hypothesis, with all powers falling between 1 and 2.

It was noticeable that the disk samples all provided powers that were below those of the beam samples, and that the samples in the AL direction provided superior powers to the their corresponding Ac orientated counterparts, although the trend was not seen in the relationships with the sample groups combined.

The G_Q and G_C powers were all superior to that of the K_Q and K_C, and varied greatly between both the individual groups and sample designs. The combination of the samples from the three groups did, however, provide power functions which were on the most part in agreement with those of the hypothesis, although in each case still superior to the corresponding K values.

The J-Integral results were, however, dramatically different; the inverted nature of the relationships seen previously was demonstrated, with only the beam sample in the

AL direction obtaining powers relating to the hypothesis. The combining of the groups failed to assist in the analysis, although surprisingly the beams Ac samples reverted to a positive relationship.

Table 8.18 Power functions of the relationships between the apparent density and relative density with respect to the fracture toughness parameters

	Apparent Density				Relative Density			
	Beams Ac	Beams AL	Disks Ac	Disks AL	Beams Ac	Beams AL	Disks Ac	Disks AL
Osteoporotic								
K_Q	2.076	2.398	1.477	1.6997	2.171	2.21	1.022	1.29
K_C	1.92	2.092	1.257	1.487	2.04	1.917	0.876	1.129
J_Q	-0.248	-0.977	0.0166	-0.139	-0.272	-0.91	0.06	-0.133
J_C	-0.327	-0.938	-0.27	-0.094	-0.284	-0.915	-0.154	-0.087
G_Q	2.977	3.622	1.743	2.223	3.2	3.332	1.38	1.62
G_C	2.661	3.01	1.3	1.798	2.93	2.745	1.031	1.292
Osteoarthritic								
K_Q	1.68	1.785	1.134	2.51	1.57	1.684	1.01	1.94
K_C	1.496	1.71	0.993	2.69	1.399	1.619	0.862	1.73
J_Q	-0.511	-0.349	-0.405	-1.07	-0.468	-0.313	-0.374	-0.286
J_C	-0.578	-0.459	-0.238	-1.25	-0.511	-0.384	-0.211	-0.319
G_Q	2.184	2.395	1.09	4.123	2.07	2.284	0.952	2.876
G_C	1.815	2.25	0.81	4.479	1.721	2.153	0.665	2.45
Equine								
K_Q	1.852	2.326	0.95	1.233	1.48	1.686	0.527	0.631
K_C	1.81	2.322	0.978	1.169	1.44	1.663	0.537	0.560
J_Q	-0.575	-1.051	-0.767	-0.849	-0.52	-0.769	-0.438	-0.878
J_C	-0.321	-0.462	-0.33	-0.276	-0.283	-0.414	-0.26	-0.273
G_Q	2.528	3.477	7.24	1.244	1.852	2.43	0.228	0.484
G_C	2.448	3.468	0.779	1.112	1.786	2.381	0.246	0.352
All Samples								
K_Q	1.86	1.68	1.44	1.647	1.75	1.54	1.16	1.317
K_C	1.78	1.64	1.35	1.547	1.68	1.49	1.09	1.23
J_Q	0.44	-1.14	-0.103	-0.181	0.486	-1.01	-0.09	-0.193
J_C	0.6	-1.43	-0.132	-0.128	0.649	-1.28	-0.124	-0.1
G_Q	2.54	2.19	1.73	2.07	2.415	1.996	1.34	1.61
G_C	2.38	2.1	1.55	1.87	2.25	1.898	1.2	1.43

Porosity

The high correlations and level of significance for the apparent density is reflected in the correlations and significance seen in comparison to the porosity of the samples. As expected the relationship is the inverse of the apparent density relationship, with samples of higher porosity having reduced values for K and G. The difference

between the linear and logarithmic relationships was again minimal with both providing the same degree of correlation and significance. Once again the J-Integral is the inverse of the K and G values with samples of higher porosity displaying higher values.

Material Density

The correlations between the material density and compositional parameters in relation to the fracture toughness parameters were weaker and less significant than the corresponding relationships with the apparent density and porosity. The relationship with material density was negative in nature in comparison to the K and G values, with samples of higher material density providing lower values of K and G. The relationship to the J-integral values was mixed, with both positive an negative correlations being found; however, the greater number indicated a positive correlation, with all significant correlations between the parameters being positive in nature.

8.2.3.2 Compositional Properties

Hydrated and Dehydrated Mineral and Organic Content

With the exclusion of the equine beams Ac samples, the relationship between the fracture toughness parameters and the compositional parameters are the same for both the equine and osteoarthritic samples. The results show that in the balance between the organic and mineral content of the samples, an increase in the mineral content of the samples corresponds to a decrease in the K and G fracture toughness parameters. The J-Integral values show the inverse relationship seen previously, with the J-integral values increasing with increased mineral content.

The equine beam Ac samples display the inverse of the relationship produced by the other equine samples, and the relationship is in agreement with the osteoporotic samples. The reason for this discrepancy is due to the sampling site of the material used to manufacture the beams and the nature of the bone. The equine beams Ac were manufactured from the side slices taken from the vertebrae, whereas all the other samples were taken from the central slices. This in itself is not enough to provide the differences seen in the results, but the material properties of the different equine samples were investigated previously (Table 8.32) and the beam Ac samples were shown to have significantly ($p<0.001$) lower apparent density and higher porosity than the other samples from the equine group. The average apparent density and porosity of the samples was 0.479 g cm^{-3} and 74.0% respectively, which are closer to the density and porosity of the osteoporotic samples (0.435 g cm^{-3} and 75.7%) than the average for the equine (0.562 g cm^{-3} and 68.6%).

The relationship shown by the osteoporotic samples and the equine beams Ac show that for the low apparent density bone, the relationship between the mineral content and the mechanical parameters is positive with samples of higher mineral content displaying higher K and G value. Once again the J-integral is the inverse with higher J-integral values being seen in the samples with greater organic content.

Collagen Cross-Link Analysis

The effects of the collagen cross-linking on the fracture toughness of the cancellous bone is similar to that seen for the compression testing in that it is confusing. The osteoporotic beams appear to be in agreement with the compositional studies of the collagen content for the beam samples, in that the increased collagen content and cross-link volume causes a reduction in the initiation toughness K and G while the energy

absorption of the tissue (J-Integral) increases, and the osteoporotic disk samples provide some weak support of these findings as well, although the significant correlations for the initiation toughness of the disks Ac are positive. The osteoarthritic samples, however, display the inverse of this relationship with the increased collagen content and cross-link content seeming to increase the initiation toughness and reduce the J-Integral.

8.2.4 Step-Wise Regression Relationships

As with the compression testing which was performed previously, the six fracture toughness parameters were compared against the 13 independent variables simultaneously using stepwise regression. The analysis was performed for the three different groups, with the different sample designs and orientations treated separately and the collagen cross-linking analysis restricted to the osteoporotic and osteoarthritic groups.

The results for the equine group are shown in Table 8.19 and Table 8.20. In nearly all of the regressions that were performed the apparent density proved to be a significant predictive variable and on the most part was the dominant variable that provided the highest degree of explanation, as would have been expected from the individual regressions of the previous section. Although the other independent variables all provided highly significant degrees of explanation, and in some cases the material density, water fraction, hydrated mineral content and hydrated organic content all usurped the apparent density and were the dominant variables.

Table 8.19 Stepwise regression analysis of the equine fracture toughness results from the beam samples in relation to the 6 independent variables

Equine Beams Ac	$\rho_{App.}$ (g cm^{-3})	$\rho_{Mat.}$ (g cm^{-3})	OC_{HYD}	r^2 value
K_Q	1 (<0.001)	-	-	42.5
	1 (<0.001)	2 (<0.001)	-	57.3
	1 (<0.001)	2 (<0.001)	3 (0.122)	59.1
K_C	1 (<0.001)	-	-	42.5
	1 (<0.001)	2 (<0.001)	-	56.3
	1 (<0.001)	2 (<0.001)	3 (0.124)	58.0
J_Q	1 (0.004)	-	-	13.0
J_C	-	-	-	-
G_Q	1 (<0.001)	-	-	24.4
	1 (<0.001)	2 (<0.001)	-	39.5
G_C	1 (<0.001)	-	-	25.2
	1 (<0.001)	2 (0.001)	-	38.6
Equine Beams AL	$\rho_{App.}$ (g cm^{-3})	Porosity (%)	MC_{HYD}	r^2 value
K_Q	1 (<0.001)	-	-	44.0
	1 (<0.001)	2 (0.022)	-	50.2
K_C	1 (<0.001)	-	-	41.6
	1 (<0.001)	2 (0.012)	-	49.2
J_Q	1 (0.001)	-	-	20.4
	1 (0.009)	-	2 (0.038)	27.8
	1 (<0.001)	3 (0.002)	2 (0.001)	42.0
J_C	-	-	1 (0.001)	22.0
	2 (0.126)	-	1 (0.004)	26.0
G_Q	1 (<0.001)	-	-	27.0
	1 (0.007)	2 (0.066)	-	32.3
G_C	1 (<0.001)	-	-	23.9
	1 (0.006)	2 (0.049)	-	30.2

Table 8.20 Stepwise regression analysis of the equine fracture toughness results from the disk samples in relation to the 6 independent variables.

Equine Disks Ac	$\rho_{App.}$ (g cm^{-3})	Porosity (%)	$\rho_{Mat.}$ (g cm^{-3})	WF (%)	OC_{HYD}	r^2 value
K_Q	-	-	-	-	1 (0.004)	35.6
	2 (0.033)	-	-	-	1 (0.023)	50.3
	2 (<0.001)	2 (<0.001)	-	-	1 (0.083)	87.6
K_C	-	-	-	-	1 (0.008)	31.8
	2 (0.047)	-	-	-	1 (0.039)	45.6
	2 (<0.001)	3 (<0.001)	-	-	1 (0.185)	86.8
	1 (<0.001)	2 (<0.001)	-	-	-	85.3
	1 (<0.001)	2 (<0.001)	-	3 (0.108)	-	87.4
J_Q	1 (0.064)	-	-	-	-	16.9
	1 (0.018)	-	2 (0.098)	-	-	28.9
	1 (0.005)	-	2 (0.024)	3 (0.090)	-	40.3
J_C	-	-	-	-	-	-
G_Q	-	-	-	1 (0.005)	-	34.2
G_C	-	-	-	1 (0.006)	-	33.5
Equine Disks AL	$\rho_{App.}$ (g cm^{-3})	$\rho_{Mat.}$ (g cm^{-3})	WF (%)	MC_{HYD}	OC_{HYD}	r^2 value
K_Q	1 (0.003)	-	-	-	-	36.3
	1 (<0.001)	2 (<0.001)	-	-	-	72.3
	1 (<0.001)	2 (<0.001)	3 (0.082)	-	-	76.7
K_C	1 (0.007)	-	-	-	-	31.0
	1 (<0.001)	2 (<0.001)	-	-	-	67.6
	1 (<0.001)	2 (<0.001)	2 (0.061)	-	-	73.5
J_Q	-	1 (<0.001)	-	-	-	70.4
	-	1 (<0.001)	-	-	2 (0.087)	75.0
	3 (0.128)	1 (<0.001)	-	-	2 (0.026)	78.2
J_C	-	1 (<0.001)	-	-	-	64.9
G_Q	1 (0.029)	-	-	-	-	22.7
	1 (<0.001)	2 (0.001)	-	-	-	57.6
	1 (<0.001)	2 (0.001)	3 (0.056)	-	-	66.0
G_C	-	-	-	1 (0.013)	-	28.5
	-	-	2 (0.069)	1 (0.004)	-	40.8
	3 (0.105)	-	2 (0.083)	1 (0.008)	-	49.5
	3 (0.007)	4 (0.028)	2 (0.878)	1 (0.429)	-	62.9
	2 (0.001)	3 (0.004)	-	1 (0.029)	-	62.9

The results that were achieved for the osteoporotic group differed from those of the equine group due to the inclusion of the collagen cross-link analysis; however, the dominance of the apparent density over the fracture toughness of the bone was pronounced and for the K values it explained over 50% of the variance each time, and over 30% of the G values. The additional variables that were included in the analysis were predominantly from the collagen cross-linking analysis, which proved to be more significant than the overall compositional values such as % mineral and organic contents. Of the r^2 values for the different regressions none of them could explain the full variance within the results, with in most cases upwards of 25% of the results going unexplained.

The J-integral did not match the trends set by the K and G values and, with the exception of the beams AL, the dominant determining factors were the organic content and the levels of collagen cross-linking. The dominant collagen cross-links varied between the sample designs and orientations, with the stepwise regressions failing to provide r^2 values that were as strong as for the K and G values.

Table 8.21 Stepwise regression analysis of the osteoporotic fracture toughness results from the beam samples in the Ac direction in relation to the 12 independent variables.

OP Beams Ac	$\rho_{App.}$ (g cm^{-3})	$\rho_{Mat.}$ (g cm^{-3})	OC_{HYD} (%)	HLNL (m/m)	HLKNL (m/m)	OHPyr (m/m)	r^2 value (%)
K_Q	1 (<0.001)	-	-	-	-	-	62.6
	1 (<0.001)	-	-	2 (0.001)	-	-	72.6
	1 (<0.001)	-	-	2 (<0.001)	-	3 (0.117)	74.4
	1 (<0.001)	4 (0.115)	-	2 (<0.001)	-	3 (0.05)	76.1
K_C	1 (<0.001)	-	-	-	-	-	62.9
	1 (<0.001)	-	-	2 (0.001)	-	-	72.3
	1 (<0.001)	-	-	2 (<0.001)	-	3 (0.104)	74.2
J_Q	-	-	1 (0.056)	-	-	-	9.3
J_C	-	-	-	-	1 (0.091)	-	7.3
	2 (0.133)	-	-	-	1 (0.083)	-	12.9
G_Q	1 (<0.001)	-	-	-	-	-	42.0
	1 (<0.001)	-	-	2 (0.001)	-	-	56.4
	1 (<0.001)	-	3 (0.088)	2 (0.001)	-	-	59.8
	1 (<0.001)	-	3 (0.065)	2 (<0.001)	-	4 (0.147)	62.1
G_C	1 (<0.001)	-	-	-	-	-	42.1
	1 (<0.001)	-	-	2 (0.001)	-	-	55.9
	1 (<0.001)	-	3 (0.118)	2 (0.001)	-	-	58.8
	1 (<0.001)	-	3 (0.088)	2 (<0.001)	-	4 (0.147)	61.1

Table 8.22 Stepwise regression analysis of the osteoporotic fracture toughness results from the beam samples in the AL direction in relation to the 12 independent variables.

OP Beams AL	$\rho_{App.}$ (g cm^{-3})	Porosity (%)	WF (%)	MC_{HYD} (%)	OC_{HYD} (%)	HHL (m/m)	HLNL (m/m)	HLKNL (m/m)	OHPyr (m/m)	fmoles Pentosidine / pmole collagen	r^2 value (%)
K_Q	1 (<0.001)	-	-	-	-	-	-	-	-	-	52.4
	1 (<0.001)	-	-	-	-	-	-	-	-	2 (0.006)	60.0
	1 (0.008)	3 (0.080)	-	-	-	-	-	-	-	2 (0.007)	62.8
K_C	1 (<0.001)	-	-	-	-	-	-	-	-	-	53.0
	1 (<0.001)	-	-	-	-	-	-	-	-	2 (0.013)	59.3
	1 (<0.001)	-	3 (0.019)	-	-		-	-	-	2 (0.007)	64.2
	1 (<0.001)	-	3 (0.025)	-	-	4 (0.039)	-	-	-	2 (0.005)	67.7
J_Q	1 (<0.001)	-	-	-	-	-	-	-	-	-	29.4
	1 (<0.001)	-	-	-	-	-	2 (0.024)	-	-	-	37.2
	1 (<0.001)	-	-	-	-	-	2 (0.069)	-	-	3 (0.126)	40.5
	1 (<0.001)	-	-	4 (0.083)			2 (0.083)	-	-	3 (0.069)	44.7
J_C	1 (<0.001)	-	-	-	-	-	-	-	-	-	22.8
	1 (<0.001)	-	2 (0.076)	-	-	-	-	-	-	-	28.2
	1 (<0.001)	-	2 (0.016)	-	3 (0.091)	-	-	-	-	-	32.9
G_Q	1 (<0.001)	-	-	-	-	-	-	-	-	-	30.5
	1 (0.001)	-	-	-	-	-	-	-	-	2 (0.009)	40.5
	1 (<0.016)	3 (0.059)	-	-	-	-	-	-	-	2 (0.011)	45.3
G_C	1 (<0.001)	-	-	-	-	-	-	-	-	-	36.7
	1 (<0.001)	-	-	-	-	-	-	-	-	2 (0.012)	45.2
	1 (<0.001)	-	3 (0.014)	-	-	-	-	-	-	2 (0.006)	52.5
	1 (<0.001)	-	3 (0.018)	-	-	4 (0.043)	-	-	-	2 (0.004)	57.0
	1 (<0.001)	-	3 (0.010)	-	-	4 (0.012)	-	5 (0.112)	-	2 (0.034)	59.6
	1 (<0.001)	-	3 (0.009)	-	-	4 (0.040)	-	5 (0.032)	6 (0.143)	2 (0.185)	61.7
	1 (<0.001)	-	2 (0.009)	-	-	3 (0.041)	-	4 (0.001)	5 (0.027)	-	60.0

Table 8.23 Stepwise regression analysis of the osteoporotic fracture toughness results from the disk samples in the Ac direction in relation to the 12 independent variables.

OP Disks Ac	$\rho_{App.}$ (g cm^{-3})	HHL (m/m)	HLNL (m/m)	HLKNL (m/m)	OHPyr (m/m)	r^2 value (%)
K_Q	1 (<0.001)	-	-	-	-	54.9
	1 (<0.001)	-	2 (0.021)	-	-	67.4
K_C	1 (0.001)	-	-	-	-	46.9
	1 (<0.001)	-	2 (0.020)	-	-	61.7
J_Q	-	-	-	1 (0.018)	-	26.1
J_C	-	-	-	1 (0.020)	-	25.5
G_Q	1 (0.017)	-	-	-	-	27.6
	1 (0.002)	-	-	-	2 (0.015)	49.2
	1 (0.001)	-	-	3 (0.108)	2 (0.010)	57.0
G_C	1 (0.076)	-	-	-	-	16.5
	1 (0.008)	-	2 (0.019)	-	-	40.3
	1 (0.013)	3 (0.101)	2 (0.014)	-	-	49.7

Table 8.24 Stepwise regression analysis of the osteoporotic fracture toughness results from the disk samples in the AL direction in relation to the 12 independent variables.

OP Disks AL	$\rho_{App.}$ (g cm^{-3})	$\rho_{Mat.}$ (g cm^{-3})	WF (%)	MC_{HYD} (%)	HHL (m/m)	HLNL (m/m)	HLKNL (m/m)	r^2 value (%)
K_Q	1 (<0.001)	-	-	-	-	-	-	75.9
	1 (<0.001)	-	-	-	-	2 (0.048)	-	81.5
	1 (<0.001)	-	-	3 (0.093)	-	2 (0.012)	-	85.0
K_C	1 (<0.001)	-	-	-	-	-	-	76.1
	1 (<0.001)	-	-	-	-	2 (0.109)	-	79.9
	1 (<0.001)	-	-	3 (0.032)	-	2 (0.012)	-	85.7
J_Q	-	-	-	-	-	-	-	-
J_C	-	-	-	-	1 (0.090)	-	-	19.2
	-	-	2 (0.031)	-	1 (0.016)	-	-	44.4
	-	3 (0.074)	2 (0.011)	-	1 (0.007)	-	-	57.9
	-	3 (0.052)	2 (0.007)	-	1 (0.007)	-	4 (0.080)	68.5
	-	3 (0.082)	2 (0.009)	-	1 (0.002)	5 (0.093)	4 (0.019)	76.6
G_Q	1 (<0.001)	-	-	-	-	-	-	58.5
	1 (<0.001)	-	-	-	-	2 (0.081)	-	66.4
G_C	1 (<0.001)	-	-	-	-	-	-	60.1

The results of the osteoarthritic group differ from both the equine and the osteoporotic groups, with the dominant independent variable falling equally between the porosity and the apparent density of the samples. There is variation from the previous groups in the other independent variables as well, with the collagen cross-links that were seen being either the levels of pentosidine or LysPyr. Although the levels of pentosidine were seen in the osteoporotic group to have a significant effect it was the alternative mature cross-link OHPyr in the osteoporotic group that was seen not LysPyr.

Table 8.25 Stepwise regression analysis of the osteoarthritic fracture toughness results from the beam samples in relation to the 12 independent variables.

OA Beams Ac	$\rho_{App.}$ (g cm^{-3})	Porosity (%)	WF (%)	r^2 value (%)
K_Q	1 (<0.001)	-	-	69.0
	1 (0.001)	-	2 (0.007)	84.4
K_C	1 (<0.001)	-		71.9
	1 (0.001)	-	2 (0.007)	81.6
J_Q	-	-	-	-
J_C	1 (0.142)	-	-	17.06
G_Q	-	-	1 (0.002)	56.5
	-	2 (0.017)	1 (0.007)	74.6
G_C	1 (0.003)	-	-	52.9
	1 (0.020)	-	2 (0.029)	70.0
OA Beams AL	Porosity (%)	OC_{HYD} (%)	LysPyr (m/m)	r^2 value (%)
K_Q	1 (<0.001)	-	-	77.6
	1 (<0.001)	-	2 (0.108)	84.1
K_C	1 (<0.001)	-	-	81.6
	1 (<0.001)	-	2 (0.054)	88.8
J_Q	-	1 (0.101)	-	27.1
J_C	-	-	-	-
G_Q	1 (0.002)	-	-	65.9
	1 (0.002)	-	2 (0.109)	75.8
G_C	1 (0.002)	-	-	68.72
	1 (0.001)	-	2 (0.042)	81.92

Table 8.26 Stepwise regression analysis of the osteoarthritic fracture toughness results from the disk samples in the Ac direction, in relation to the 12 independent variables.

OA Disks Ac	$\rho_{App.}$ (g cm^{-3})	Porosity (%)	$\rho_{Mat.}$ (g cm^{-3})	WF (%)	MC_{HYD}	HLNL (m/m)	LysPyr (m/m)	fmoles Pentosidine / pmole collagen	r^2 value (%)
K_Q	-	1 (0.004)	-	-	-	-	-	-	77.9
	-	1 (0.001)	-	-	-	-	2 (0.038)	-	91.4
	-	1 (<0.001)	-	-	-	-	2 (0.004)	3 (0.020)	98.1
	-	1 (0.005)	-	-	4 (0.14)	-	2 (0.004)	3 (0.013)	99.2
	-	1 (0.003)	5 (0.053)	-	4 (0.027)	-	2 (0.002)	3 (0.006)	99.9
	6 (0.022)	1 (0.016)	5 (0.011)	-	4 (0.047)	-	2 (0.004)	3 (0.003)	100
K_C	1 (0.012)	-	-	-	-	-	-	-	67.6
	1 (0.016)	-	-	-	-	-	-	2 (0.138)	80.0
	1 (0.006)	-	-	-	-	-	3 (0.047)	2 (0.033)	93.4
	1 (0.017)	-	-	4 (0.081)	-	-	3 (0.015)	2 (0.012)	97.9
J_Q	-	-	1 (0.086)	-	-	-	-	-	41.2
J_C	1 (0.085)	-	-	-	-	-	-	-	41.4
	1 (0.017)	-	-	2 (0.070)	-	-	-	-	71.5
G_Q	-	1 (0.027)	-	-	-	-	-	-	58.6
	-	1 (0.006)	-	-	-	-	2 (0.022)	-	86.8
	-	1 (0.002)	-	-	-	-	2 (0.004)	3 (0.033)	96.3
G_C	-	-	-	-	-	-	-	1 (0.073)	43.95
	-	-	-	-	-	2 (0.039)	-	1 (0.010)	77.9

Table 8.27 Stepwise regression analysis of the osteoarthritic fracture toughness results from the disk samples in the AL direction, in relation to the 12 independent variables.

OA Disks AL	$\rho_{App.}$ (g cm^{-3})	Porosity (%)	OC_{HYD} (%)	LysPyr (m/m)	r^2 value (%)
K_Q	1 (0.045)	-	-	-	91.2
	1 (0.067)	-	-	2 (0.081)	99.9
K_C	-	1 (0.013)	-	-	97.48
	-	1 (0.001)	2 (0.002)	-	100
J_Q	-	-	1 (0.100)	-	81.02
J_C	-	-	1 (0.021)	-	95.9
G_Q	1 (0.128)	-	-	-	76.1
G_C	1 (0.004)	-	-	-	99.3
	1 (0.004)	-	2 (0.046)	-	100

The r^2 values that were achieved for the disk samples were falsely high due to the low numbers of samples included in the analysis, and Table 8.25, Table 8.26 and Table 8.27 were inserted for qualitative acknowledgement of the principal variables and not for quantitative reasons.

It is of note that the principal variables from the stepwise regression analyses are the same as those which provided the strongest correlations and level of significance in the individual regression analysis, although there was some discordance within the additional variables which made up the full stepwise regressions.

The stepwise regression analysis from the three groups has highlighted the dominant independent variables which most affect the fracture toughness of both human and equine cancellous bone. Of the variables, it would appear clear that, for the K and G values, the dominant variable is the apparent density of the material, along with the porosity which is closely related to the apparent density. However, although the material properties such as apparent density would appear to have the most effect on the K and G fracture toughness parameters, a large percentage of the variation in the results

remains unexplained and it is the composition of the bone which goes some way to explaining the gap.

In all three groups, compositional and biochemical variables were present in the regressions, with the levels of collagen cross-linking in the osteoporotic and osteoarthritic bone providing substantial support to the regressions. However, the compositional variables and the cross-links that are seen differed between the groups with no single cross-link or compositional variable dominating.

The stepwise regression analysis for the J-integral results was unpredictable; on a number of occasions the apparent density was seen to be the dominant variable, while on others it was the organic content and collagen cross-link levels which dominated. It is clear that the variables which affect the energy absorption of the bone or the J-integral are distinct from those which determine the K and G fracture toughness parameters, and that the composition or structure of the bone may be more important than the actual density.

What is clear is that, in all cases, the fracture toughness of bone is not governed by one single variable and that the combination of a number of different material, compositional and biochemical properties of the bone work in unison to provide the overall properties of cancellous bone, and that the integrity of the collagen network is a crucial factor which should not be ignored.

8.2.5 The J-Integral

The J-Integral results with respect to the material properties were the inverse of the relationship that was seen for the K and G values. In order to try and explain these findings the method of calculation that was outlined in section 6.3.2.3 was considered with relation to the loading curves. For the results that would have been expected, i.e. K, G and J fracture toughness parameters all increasing with apparent density, the load displacement curves would have been expected to have behaved as shown in Figure 8.2. Each reduction in density of the sample corresponded to a lower failure load, which occurred at either the same or slightly reduced displacement, so as to produce regression plots as shown in Figure 8.3 and Figure 8.4 for the K_C and J_C fracture toughness parameters which, despite the J_C results not being statistically significant, displayed the positive relationship with density that would have been expected.

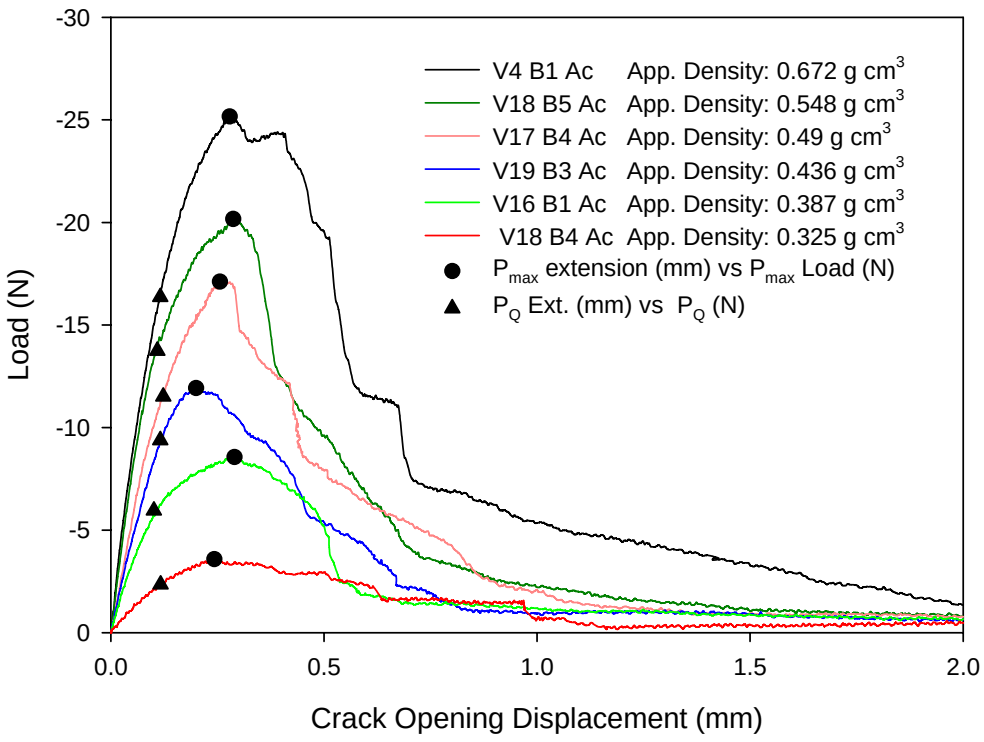

Figure 8.2 Load deformation curve comparisons from samples of the same initial notch length but with different apparent densities

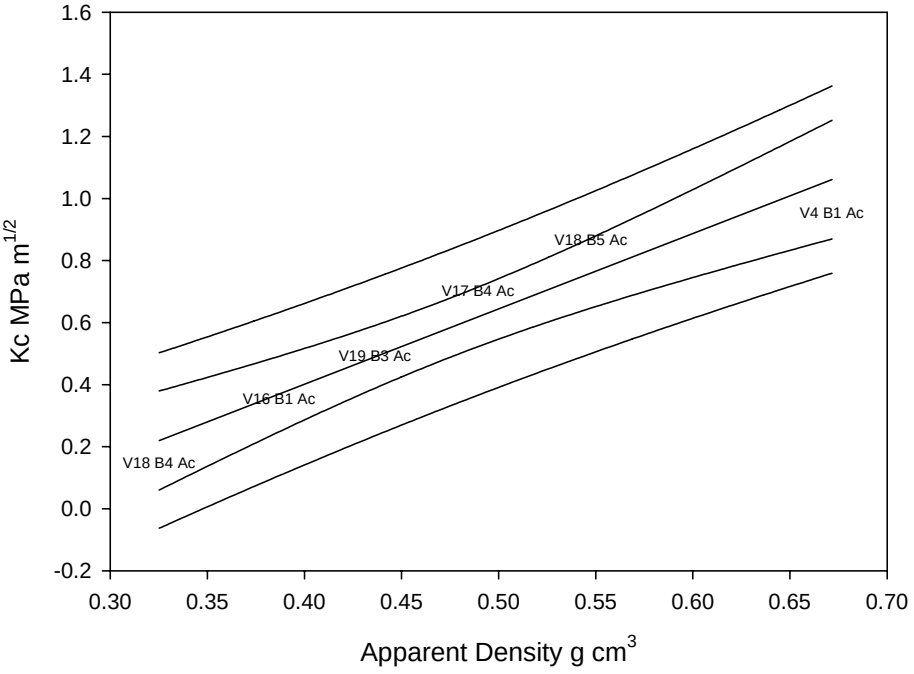

Figure 8.3 The regression plot for the K_C fracture toughness results in relation to apparent density, using the loading curves in Figure 8.2

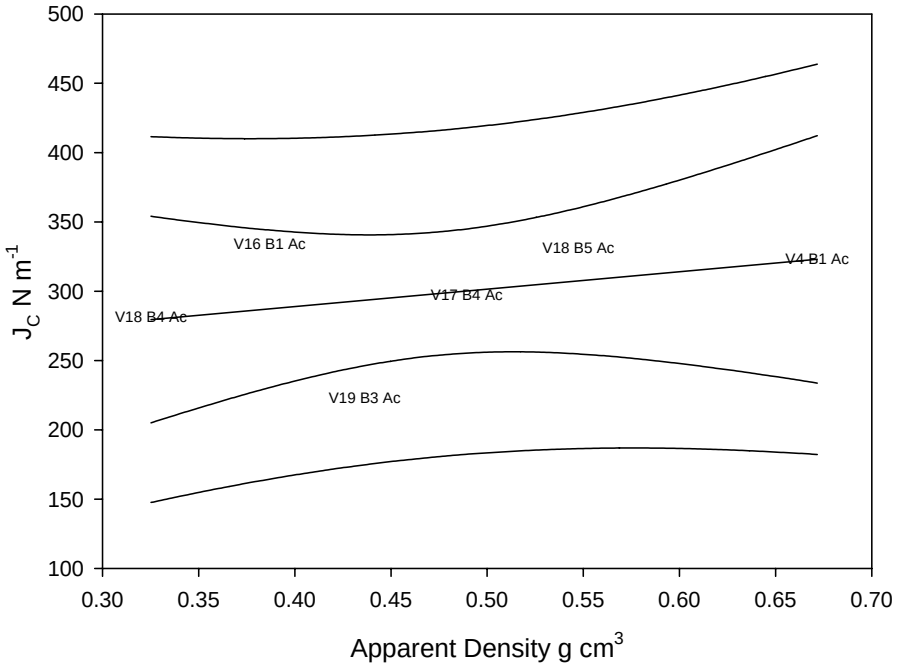

Figure 8.4 The regression plot for the J_C fracture toughness results in relation to apparent density, using the loading curves in Figure 8.2

The difference in the J-integral results originates when the loading curves are not in accordance with the nature of Figure 8.2, and the lower density samples have loading curves that demonstrate a greater displacement prior to failure or yield. The result is that a higher energy absorption is achieved prior to failure, which either equals or surpasses that of the higher density samples, causing the appearance of a negative relationship with apparent density. The reason this effect, which is only seen with the J-integral values, is that the K and G parameters are both based on the load, or the critical stress, whereas the J-integrals are based on the critical energies. In order to demonstrate that this is the effect that is occurring in this study, the extensions of P_Q and P_C at which the fracture toughness parameters were derived were compared against the apparent densities of the samples (Table 8.28).

Table 8.28 Pearson's correlation coefficients for the comparisons between the P_Q and P_C extensions with apparent density

	Beams Ac		Beams AL		Disks Ac		Disks AL	
	Ext. P_Q	Ext. P_{max}	Ext. P_Q	Ext. P_{max}	Ext. P_Q	Ext. P_{max}	Ext. P_Q	Ext. P_{max}
Osteoporotic								
$\rho_{App.}$	-0.131 0.313	-0.272 0.034	-0.344 0.009	-0.312 0.018	-0.377 0.063	-0.643 0.001	-0.185 0.346	-0.475 0.011
Equine								
$\rho_{App.}$	-0.360 0.004	-0.168 0.192	-0.450 0.001	-0.384 0.007	-0.405 0.069	-0.275 0.228	-0.248 0.254	-0.255 0.240
Osteoarthritic								
$\rho_{App.}$	-0.160 0.325	-0.233 0.148	-0.504 0.079	-0.399 0.177	-0.561 0.116	-0.629 0.069	0.260 0.534	0.364 0.375
All Samples								
$\rho_{App.}$	-0.187 0.017	-0.121 0.123	-0.422 <0.001	-0.383 <0.001	-0.430 0.001	-0.584 <0.001	-0.123 0.355	-0.345 0.007

The results of Table 8.28 clearly demonstrate that in all bar the Disks AL samples of the osteoarthritic group, the relationship between the apparent density with the P_Q and P_{max} extensions was negative and on the most part significant. This effect may be due to structural differences in the tissues, related to the change in density as

introduced in section 3.2.1.1, but as no structural analysis was undertaken in this study, it will remain unexplained.

8.3 Material and Compositional Comparisons

The composition and structure of cancellous bone varies greatly depending on the condition of the bone. In this section the aim is to compare and contrast the three different study cohorts, equine, osteoporotic and osteoarthritic, in terms of their material properties and composition. The material properties include variables such as apparent density, material density and porosity, and the compositional variables include the effects of the mineral and the organic content and the degree of collagen cross-linking. The aim is to enable the comparison with previous literature on the skeletal conditions to ensure the study groups are not different to those which have been studied previously and also to enable an understanding of what effects the conditions have on the tissue which might relate to the biomechanics.

8.3.1 Material Properties

Table 8.29 shows the range, mean and standard deviation of the material properties from the three different study groups and the ANOVA comparisons between the groups. The apparent densities and porosities of the samples from each group were significantly different, with the osteoporotic samples being lower in density and of higher porosity than either the osteoarthritic or the equine samples. The difference between the osteoarthritic samples and the equine samples was less significant but still showed the osteoarthritic samples to be of higher apparent density and lower porosity than the equine material. The comparisons between the material densities of the samples

showed there to be no significant difference between the groups, with all three having material densities within the region of 1.8 g cm^{-3}.

Table 8.29 Range, mean, standard deviation and ANOVA comparisons of the apparent densities, material densities, and porosities of the samples from the three study cohorts.

	Osteoporotic Samples	Osteoarthritic Samples	Equine Samples	ANOVA Comparison	p-value
No. of Samples	189	76	150		
Apparent Density (g/cm^{-3})					
Range	0.225 - 0.862	0.281 - 1.170	0.325 - 0.901	Osteoporotic vs. Osteoarthritic	<0.001
Mean	0.435	0.608	0.562	Osteoporotic vs. Equine	<0.001
St. Dev.	0.122	0.209	0.121	Osteoarthritic vs. Equine	0.035
Porosity (%)					
Range	39.33 - 87.7	16.39 - 84.96	41.7 - 82.33	Osteoporotic vs. Osteoarthritic	<0.001
Mean	75.66	65.47	68.57	Osteoporotic vs. Equine	<0.001
St. Dev.	8.79	14.24	8.59	Osteoarthritic vs. Equine	0.042
Material Density (g cm^{-3})					
Range	1.41 - 1.98	1.4 - 1.97	1.45 - 1.95	Osteoporotic vs. Osteoarthritic	0.174
Mean	1.82	1.8	1.81	Osteoporotic vs. Equine	0.418
St. Dev.	0.135	0.132	0.115	Osteoarthritic vs. Equine	0.412

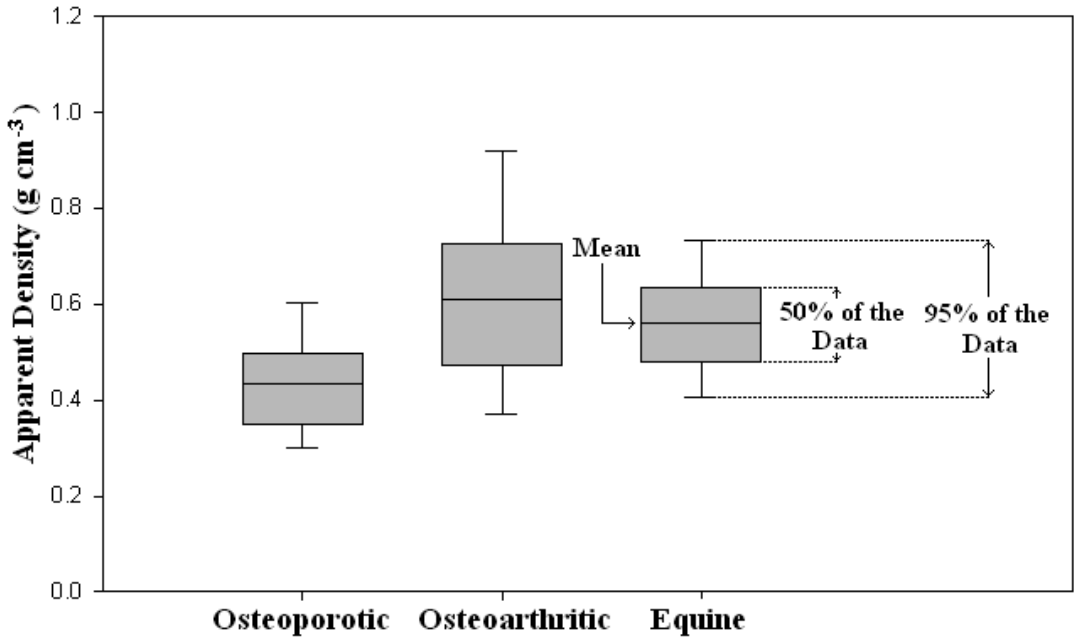

Figure 8.5 Box plot displaying the comparison between the apparent densities (g cm^{-3}) of the three study groups

Figure 8.5 to Figure 8.7 show the relationships between the three different study groups for apparent density, material density and porosity. The grey box represents the middle 50% of the data, with the horizontal line representing the mean, and the error bars indicating the area into which 95% of the data falls.

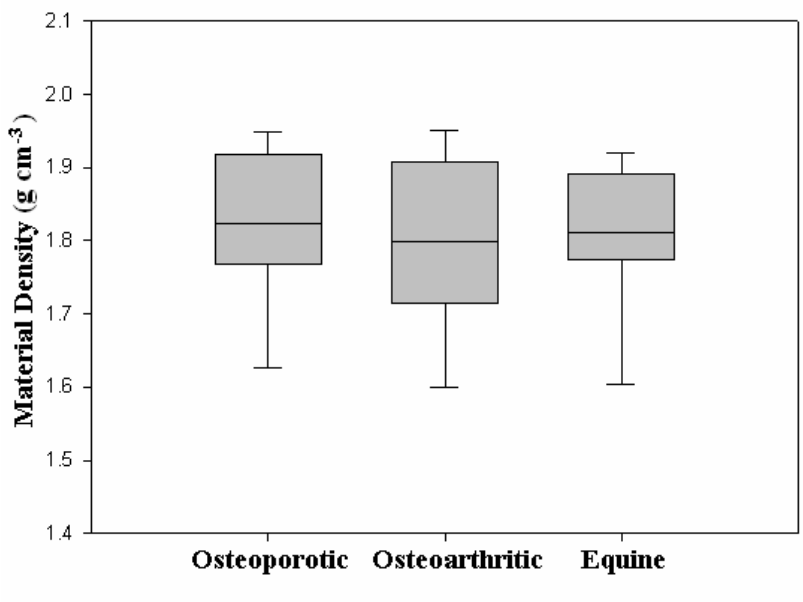

Figure 8.6 Box plot displaying the comparison between the Material Densities (g cm^{-3}) of the three study groups

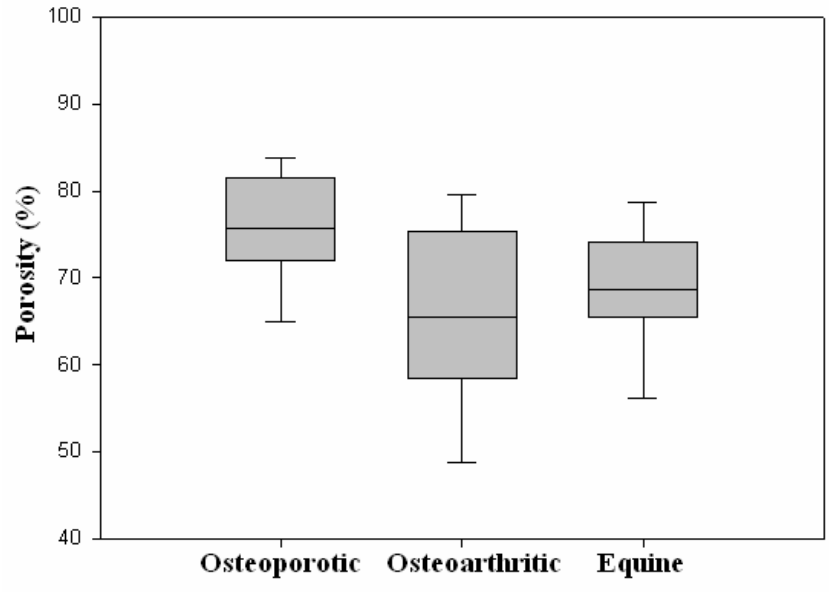

Figure 8.7 Box plot displaying the comparison between the porosities (%) of the three study groups

8.3.2. Intra-group Sample Comparisons

In order for the results of the mechanical tests on the different sample designs and orientations to be comparable, the material properties of the different sample designs and orientations were investigated to highlight any irregularities between them.

8.3.2.1 Osteoporotic samples

Table 8.30 Comparison between the material properties of the different sample designs and orientations of the osteoporotic group

OP	Beams All	Beams Ac	Beams AL	Disks All	Disks Ac	Disks AL
No. of Samples	118	61	57	61	31	30
Apparent Density						
Range	0.225 - 0.715	0.225 - 0.715	0.242 - 0.674	0.233 - 0.862	0.233 - 0.862	0.268 - 0.861
Mean	0.416	0.427	0.404	0.472	0.462	0.481
St. Dev.	0.099	0.103	0.093	0.152	0.155	0.150
Material Density						
Range	1.408 - 1.983	1.661 - 1.972	1.408 - 1.983	1.408 - 1.915	1.436 - 1.913	1.408 - 1.915
Mean	1.882	1.892	1.871	1.710	1.695	1.726
St. Dev.	0.085	0.063	0.103	0.142	0.139	0.144
Porosity (%)						
Range	52.14 - 87.70	59.53 - 87.70	52.14 - 87.22	39.33 - 86.90	41.83 - 86.90	39.33 - 85.01
Mean	77.73	77.32	78.17	71.66	71.94	71.39
St. Dev.	6.028	5.897	6.185	11.57	11.79	11.53

Ac: Across trabecular structure; AL Along trabecular structure

In order to highlight any statistically significant differences between the different groups shown in Table 8.30, and graphically in Figure 8.8 to Figure 8.10, ANOVA testing was performed. The material density and the porosity of the two samples designs were highly significantly different ($p<0.001$), with both of the variables being lower in the disk samples than in the beam samples. The apparent density was also significantly different ($p<0.05$) between the both the beams as a group and the beams AL when compared to the disk samples, but the beams AC were not significantly

different in density to the disk samples. The different sample orientations provided no difference, when considering intra-sample design.

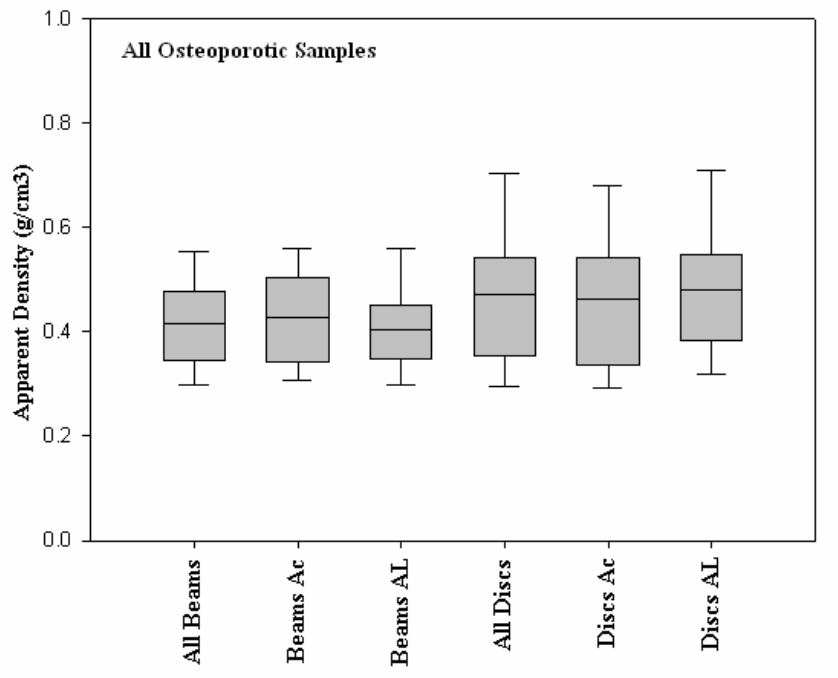

Figure 8.8 Comparison between the apparent densities of the different sample designs and orientations of the osteoporotic group

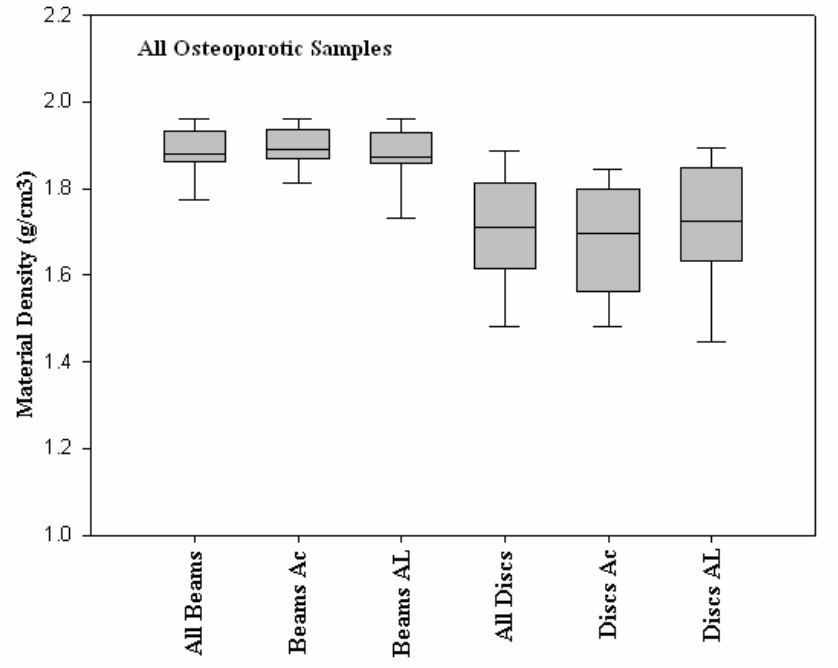

Figure 8.9 Comparison between the material density of the different sample designs and orientations of the osteoporotic group

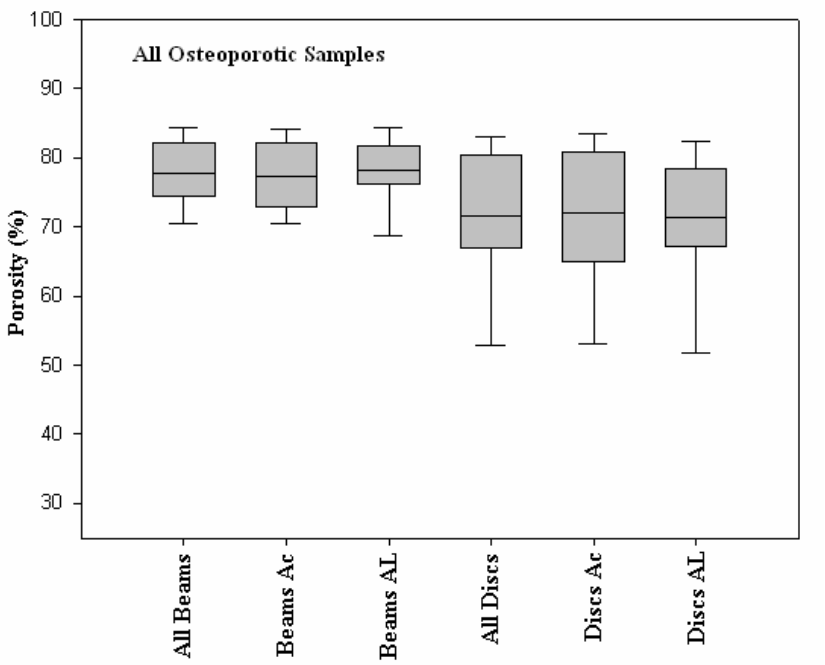

Figure 8.10 Comparison between the porosity of the different sample designs and orientations of the osteoporotic group

8.3.2.2 Osteoarthritic Group

Table 8.31 Comparison between the material properties of the different sample designs and orientations of the osteoarthritic group

OA	Beams All	Beams Ac	Beams AL	Disks All	Disks Ac	Disks AL
No. of Samples	55	41	14	21	11	10
Apparent Density						
Range	0.281 - 1.04	0.292 - 0.998	0.281 - 1.04	0.328 - 1.17	0.339 - 1.10	0.328 - 1.17
Mean	0.599	0.606	0.581	0.627	0.624	0.63
St. Dev.	0.184	0.176	0.210	0.264	0.267	0.276
Material Density						
Range	1.53 - 1.969	1.53 - 1.969	1.68 - 1.951	1.4 - 1.87	1.51 - 1.87	1.4 - 1.85
Mean	1.848	1.854	1.829	1.669	1.670	1.667
St. Dev.	0.098	0.102	0.087	0.119	0.106	0.137
Porosity (%)						
Range	34.7 - 85	34.7 - 84.5	38.5 - 85	16.4 - 81.9	27 - 81.9	16.4 - 79.5
Mean	67.1	66.9	67.8	61.5	61.8	61.0
St. Dev.	11.6	11.2	12.9	19.2	18.5	20.9

Ac: Across trabecular structure; AL Along trabecular structure

The results of the ANOVA testing for the osteoarthritic group (Table 8.31, Figure 8.11 to Figure 8.13) was discernibly different to that of the osteoporotic group. Neither the porosity nor the apparent density of either the sample designs or orientations were significantly different ($p>0.05$) from one another. The material density showed no differences between the intra-specimen design orientations, but when the disk and beam sample designs were compared, the disk samples had significantly reduced material densities.

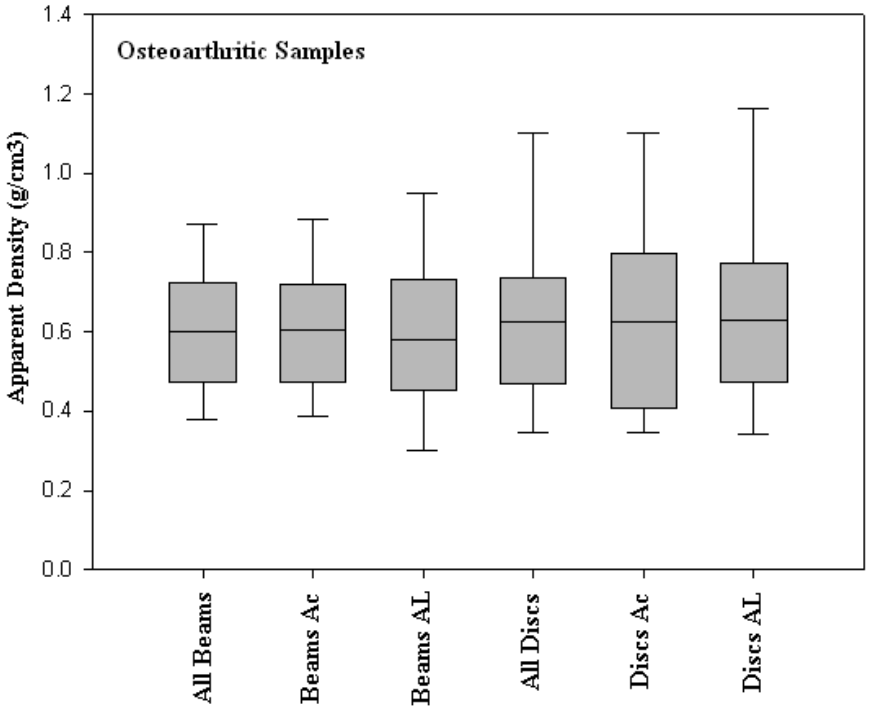

Figure 8.11 Comparison between the apparent densities of the different sample designs and orientations of the osteoarthritic group

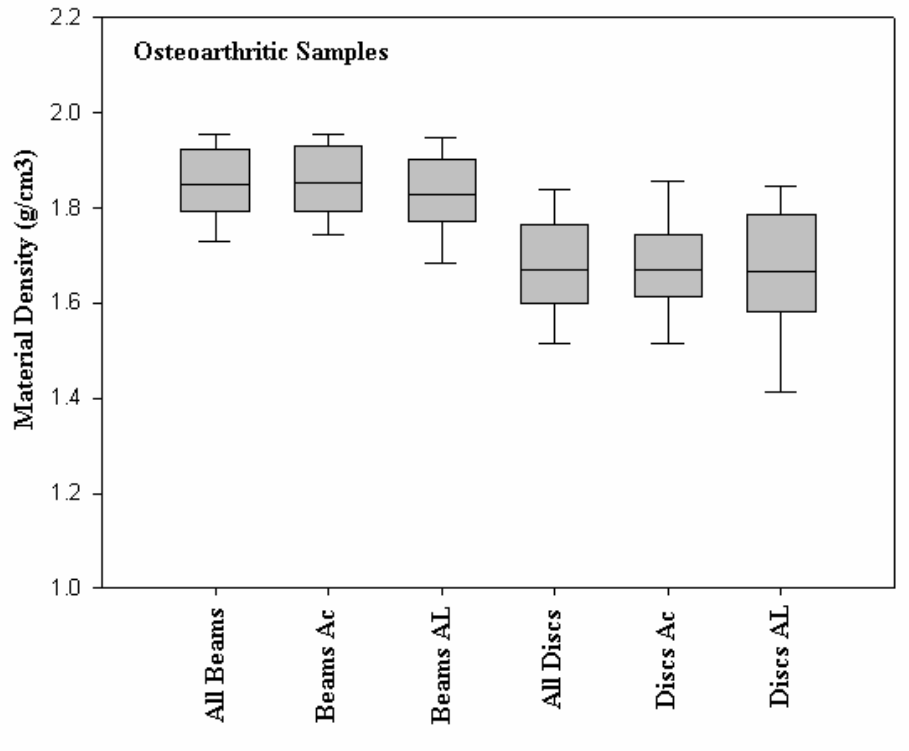

Figure 8.12 Comparison between the material densities of the different sample designs and orientations of the osteoarthritic group

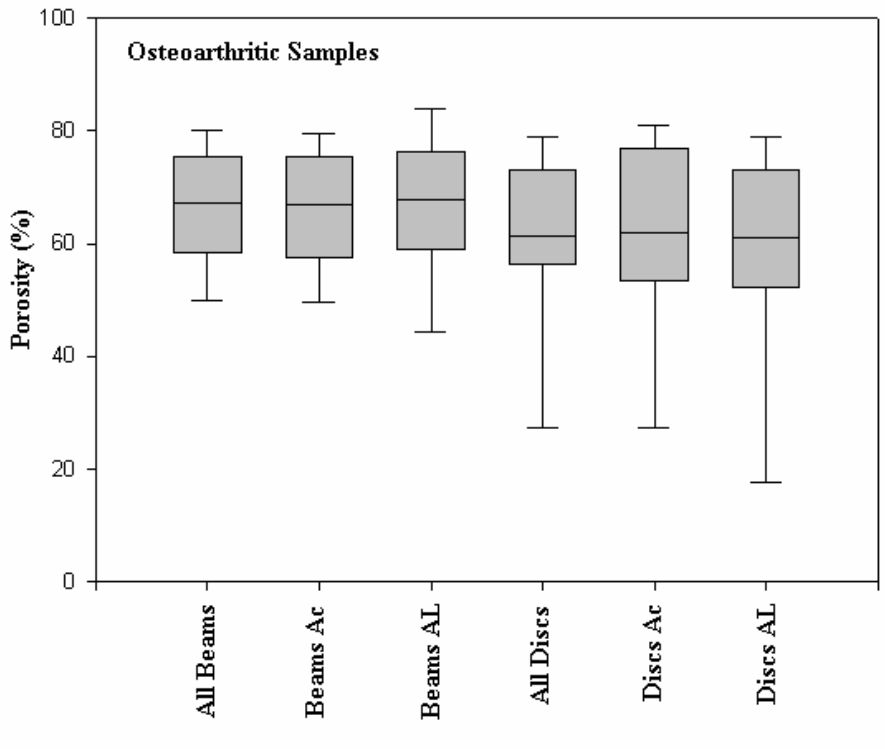

Figure 8.13 Comparison between the porosities of the different sample designs and orientations of the osteoarthritic group

8.3.2.3 Equine Group

Table 8.32 Comparison between the material properties of the different sample designs and orientations of the equine group

	Beams All	Beams Ac	Beams AL	Disks All	Disks Ac	Disks AL
No. of Samples	111	62	48	44	21	23
Apparent Density						
Range	0.325 - 0.83	0.325 - 0.672	0.435 - 0.83	0.479 - 0.901	0.521 - 0.901	0.479 - 0.786
Mean	0.518	0.479	0.57	0.672	0.689	0.656
St. Dev.	0.097	0.091	0.082	0.106	0.121	0.09
Material Density						
Range	1.455 - 1.95	1.455 - 1.944	1.604 - 1.95	1.501 - 1.894	1.501 - 1.889	1.556 - 1.894
Mean	1.855	1.85	1.86	1.704	1.699	1.708
St. Dev.	0.077	0.075	0.08	0.122	0.136	0.112
Porosity						
Range	0.483 - 0.823	0.620 - 0.823	0.483 - 0.771	0.417 - 0.747	0.417 - 0.724	0.524 - 0.747
Mean	0.719	0.740	0.692	0.601	0.587	0.613
St. Dev.	0.059	0.052	0.056	0.086	0.101	0.068

Ac: Across trabecular structure; AL Along trabecular structure

The results of the ANOVA comparisons within the equine group provided a number of statistically significant differences. The different sample designs had statistically significant differences ($p<0.001$) for all three variables that were investigated and, although the intra-specimen comparisons showed there to be no differences between the disk sample orientations and the material densities of the beam sample orientations, the apparent density and porosity of the beam samples were significantly different.

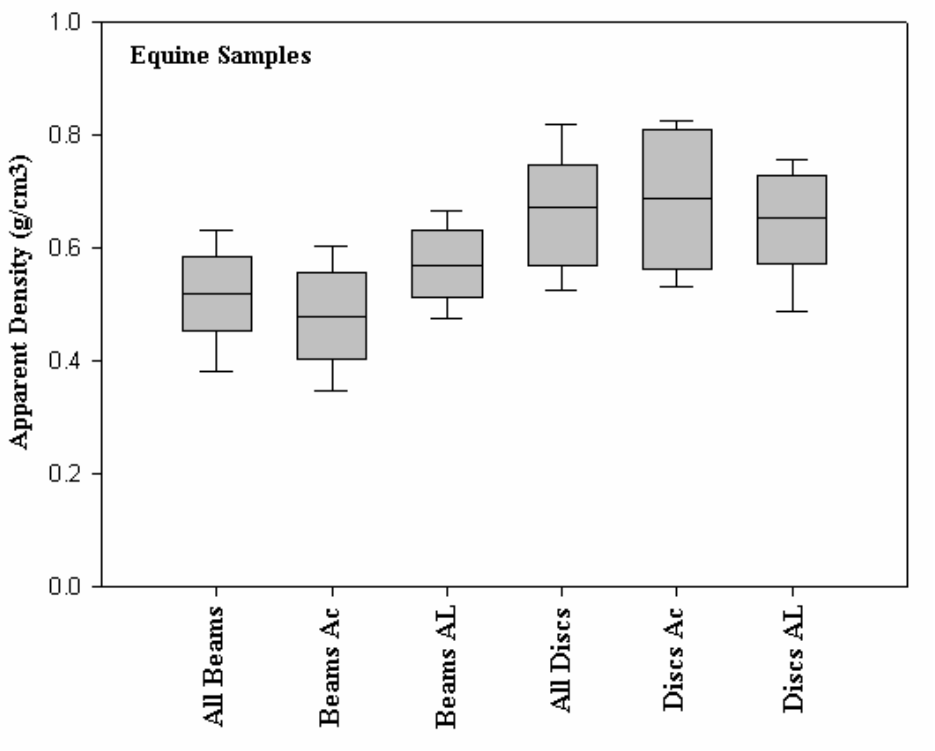

Figure 8.14 Comparison between the apparent densities of the different sample designs and orientations of the equine group

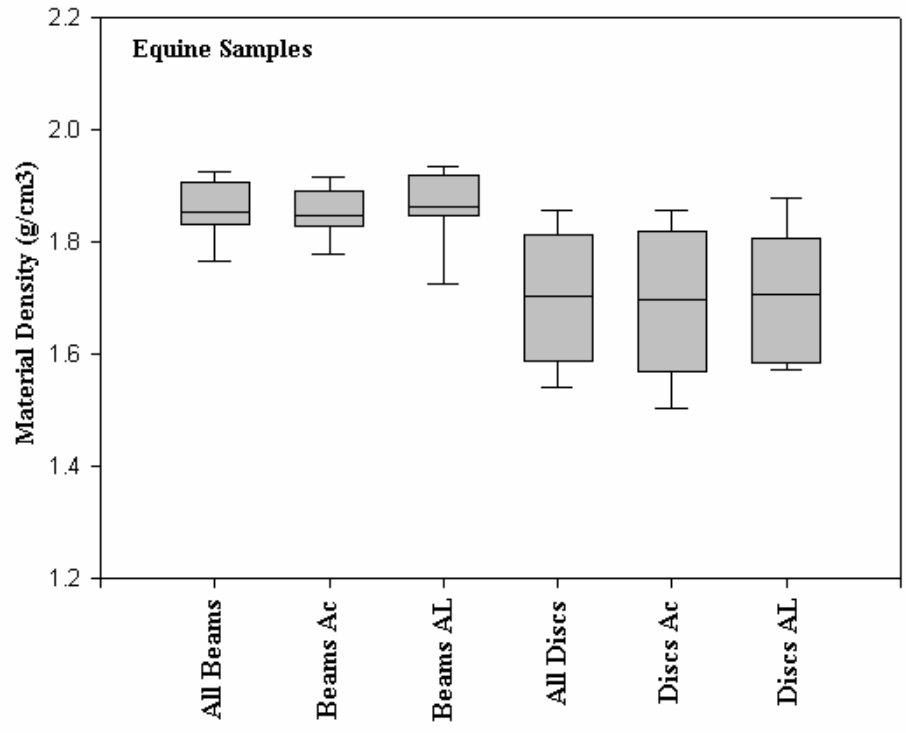

Figure 8.15 Comparison between the material densities of the different sample designs and orientations of the equine group

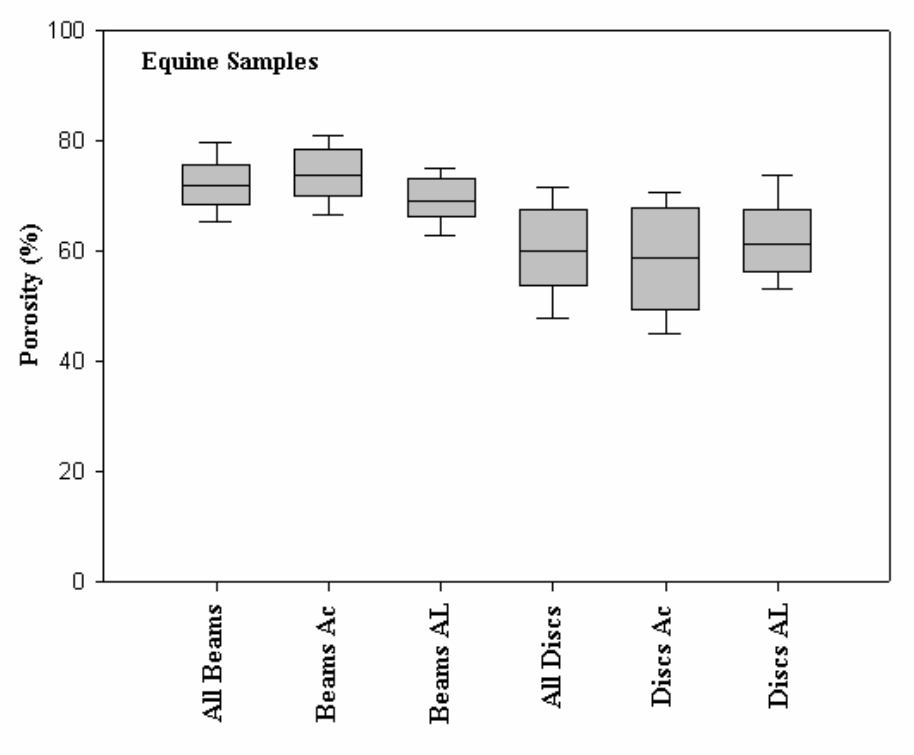

Figure 8.16 Comparison between the apparent densities of the different sample designs and orientations of the equine group

The differences between the different sample designs could be due to two different factors; the first is the sample source, or the area of bone the sample was prepared from. The effects of this are, however, likely to be minimal as the beam and disk samples were removed from the same slice of the femoral head, with the positions that they were extracted from being variable in each slice and head in an attempt to account for this source of error. The most likely source of the difference is experimental error caused by the nature of the sample designs. The cleaning process was very thorough to ensure all the marrow and fat were removed from the pores of the test samples, and in the case of the beam samples the dimensions enabled the jet washing process and the chloroform-methanol washes to permeate through the sample and perform the job. The disk samples, on the other hand, could be considered to have had

central portions, which due to the nature of cancellous bone structure, were like a closed cell foam, making the jet washing process and in some cases the chloroform-methanol washing processes ineffective, which may have affected the subsequent density measurements.

8.4 Compositional Properties

8.4.1 Mineral vs. Organic

Table 8.33 Range, mean, standard deviation and ANOVA comparisons of the compositions of the samples from the three study cohorts

	Osteoporotic Samples	Osteoarthritic Samples	Equine Samples	ANOVA Comparison	p-value
Water Fraction (%)					
Range	11.94 - 38.19	13.73 - 44.03	13.9 - 31.8	Osteoporotic vs. Osteoarthritic	0.019
Mean	18.8	20.3	19.6	Osteoporotic vs. Equine	0.081
St. Dev.	4.03	5.4	3.08	Osteoarthritic vs. Equine	0.178
Wet Mineral Content (%)					
Range	31.17 - 60.48	30.88 - 55.33	39.9 - 56.8	Osteoporotic vs. Osteoarthritic	<0.001
Mean	51.5	48.5	51.3	Osteoporotic vs. Equine	0.626
St. Dev.	3.2	4.71	2.57	Osteoarthritic vs. Equine	<0.001
Wet Organic Content (%)					
Range	7.14 - 39.97	25.08 - 47.30	26 - 32.3	Osteoporotic vs. Osteoarthritic	0.008
Mean	29.7	31.2	29.1	Osteoporotic vs. Equine	0.162
St. Dev.	4.67	2.41	1.25	Osteoarthritic vs. Equine	<0.001
Dry Mineral Content (%)					
Range	50.43 - 65.85	42.29 - 64.14	58.6 - 67	Osteoporotic vs. Osteoarthritic	<0.001
Mean	62.3	60.74	63.75	Osteoporotic vs. Equine	<0.001
St. Dev.	1.9	2.9	1.37	Osteoarthritic vs. Equine	<0.001
Dry Organic Content (%)					
Range	34.15 - 49.57	35.86 - 57.71	33 - 41.4	Osteoporotic vs. Osteoarthritic	<0.001
Mean	37.7	39.26	36.25	Osteoporotic vs. Equine	<0.001
St. Dev.	1.9	2.9	1.37	Osteoarthritic vs. Equine	<0.001

The mean, range and standard deviation of the compositional results are shown in Table 8.33 along with ANOVA comparison of the means between the different groups and, if the hydrated results are considered, the results support the differences seen in the pie charts (Figure 8.17). There was no significant difference between any of the hydrated compositional parameters between the osteoporotic and the equine samples, but the osteoarthritic samples were found to have significantly reduced mineral contents, and significantly increased organic contents.

Figure 8.17 shows pie charts of the average compositions of the samples from each of the three study groups, while also showing the difference in hydrated mineral and organic contents of the different sample groups. The results show that the composition of the equine samples and the osteoporotic samples differ only slightly; whereas there is a noticeable difference between the osteoarthritic samples and the osteoporotic and equine samples.

Figure 8.17 Pie-charts for the comparisons between the average compositions of three different study groups.
A). Osteoporotic B). Osteoarthritic C). Equine

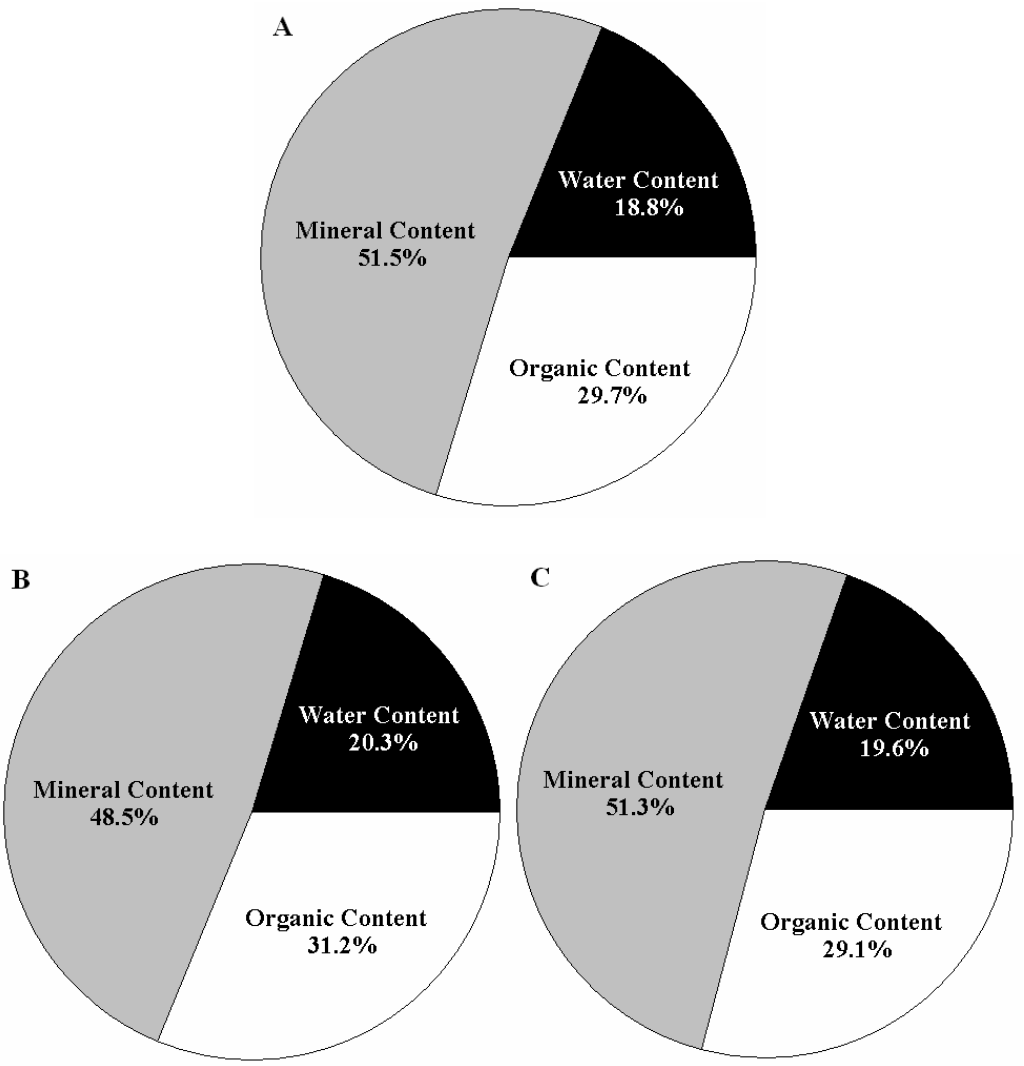

Table 8.33 also includes the dry mineral and dry organic contents, which indicates the percentage contents of each after dehydration of the sample. In this case all differences between groups were shown to be statistically significant with the osteoarthritic samples having the lowest mineral content and corresponding highest organic content in comparison to the other groups, with the bone from the equine sample displaying the highest mineral content and lowest organic content.

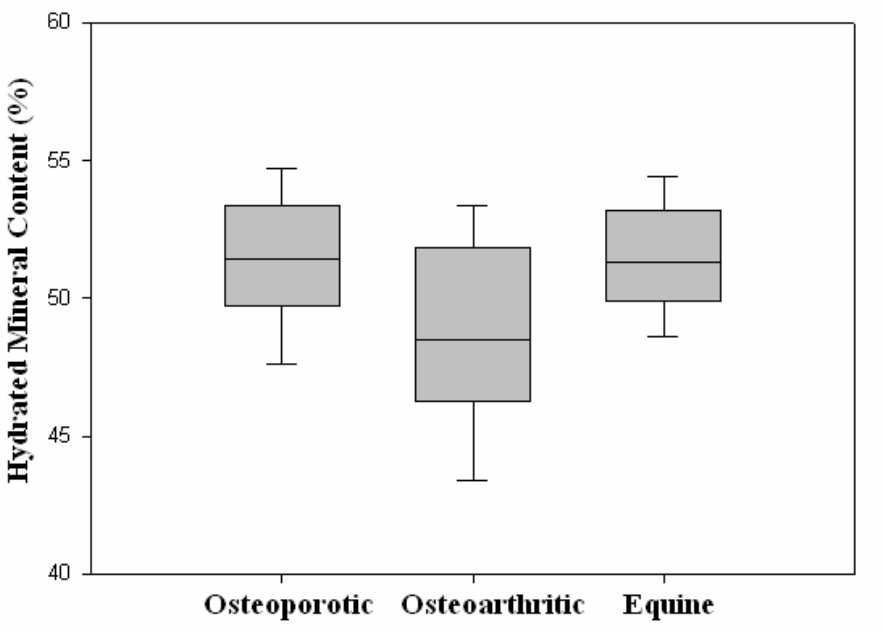

Figure 8.18 Box plot displaying the comparison between the hydrated mineral contents (%) of the three study groups

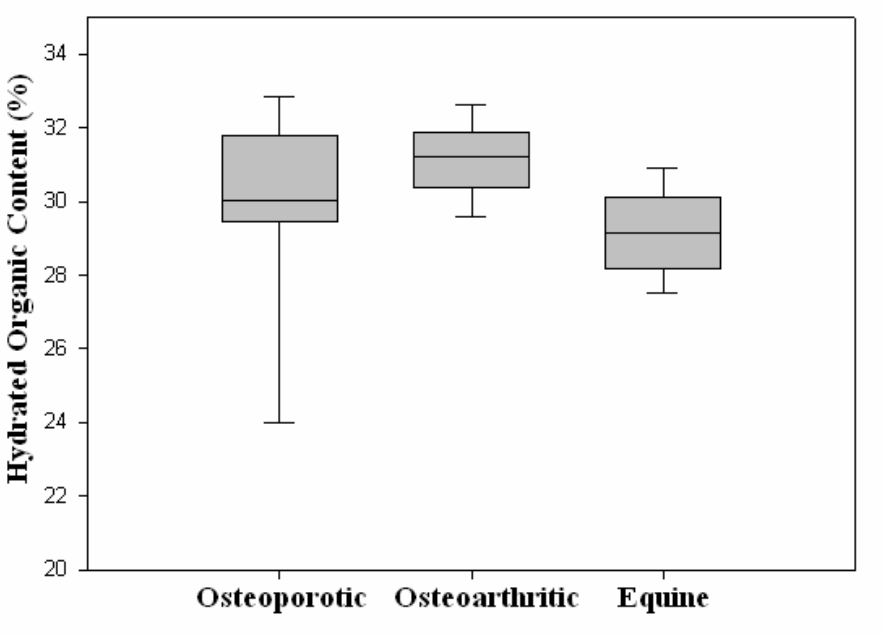

Figure 8.19 Box plot displaying the comparison between the Dry organic content (%) of the three study groups

8.5 Inter-material Property Relationship

The relationship between the three different material properties was investigated, as it has been shown previously that the loss of bone in osteoporosis is accompanied by a change in the material properties. The most obvious relationship was that the porosity and the apparent density of the bone were significantly inversely related (OP: $r = -0.964$, $p<0.001$; OA: $r = -0.980$, $p<0.001$; EQ: $r = -0.972$, $p<0.001$).

The remaining comparison was between the porosity and apparent density of the samples with their corresponding material density (Figure 8.20 to Figure 8.25).

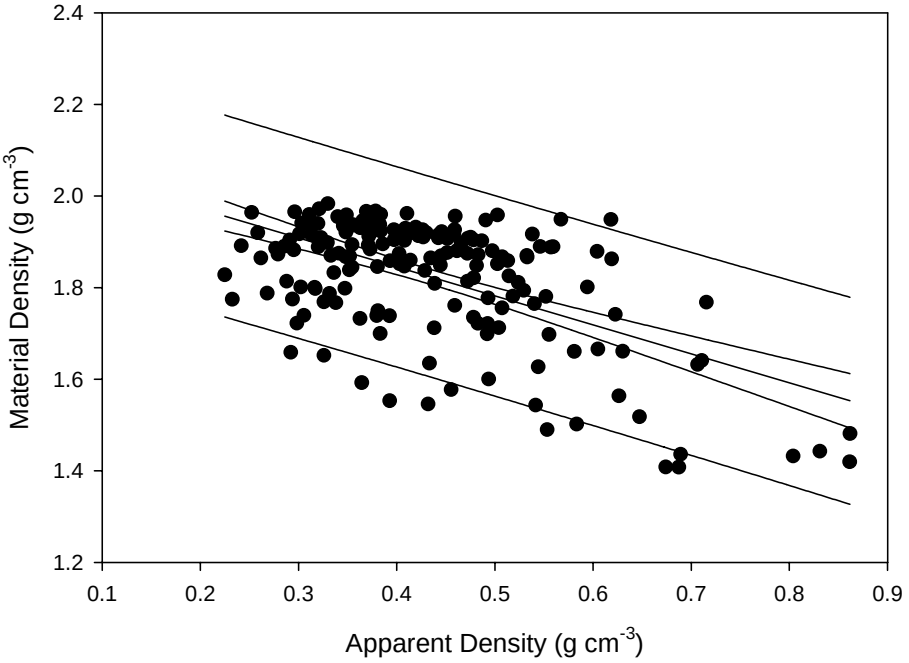

Figure 8.20 Linear regression between material density and apparent density of the osteoporotic samples

Material Density = 2.10 – 0.633(Apparent Density) r^2 = 32.8% p = <0.001

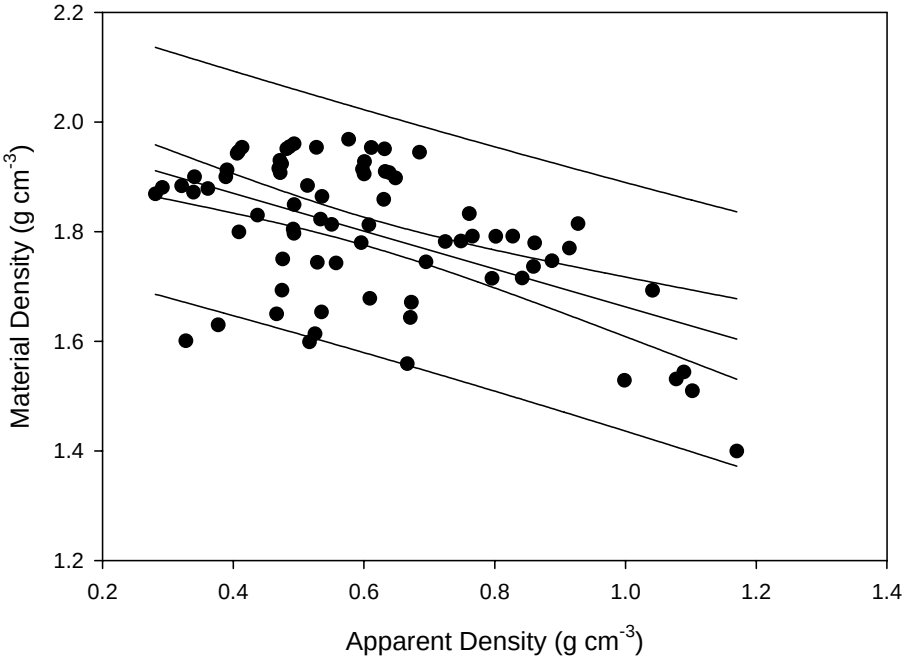

Figure 8.21 Linear regression between material density and apparent density of the osteoarthritic samples

Material Density = 2.01 – 0.345Apparent Density r^2 = 29.8% p = <0.001

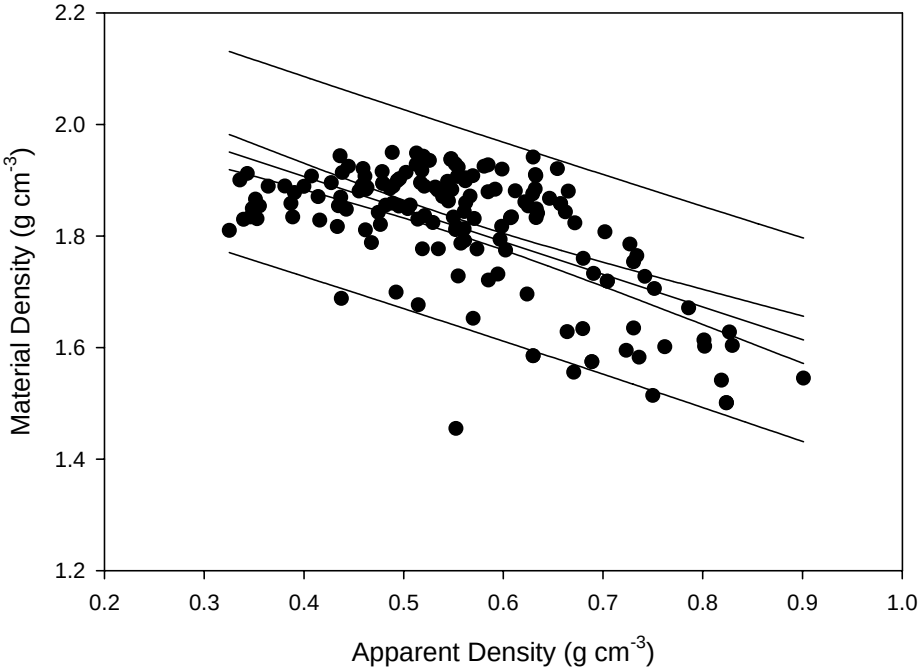

Figure 8.22 Linear regression between material density and apparent density of the Equine samples

Material Density = 2.14 – 0.585Apparent Density r^2 = 38.3% p = <0.001

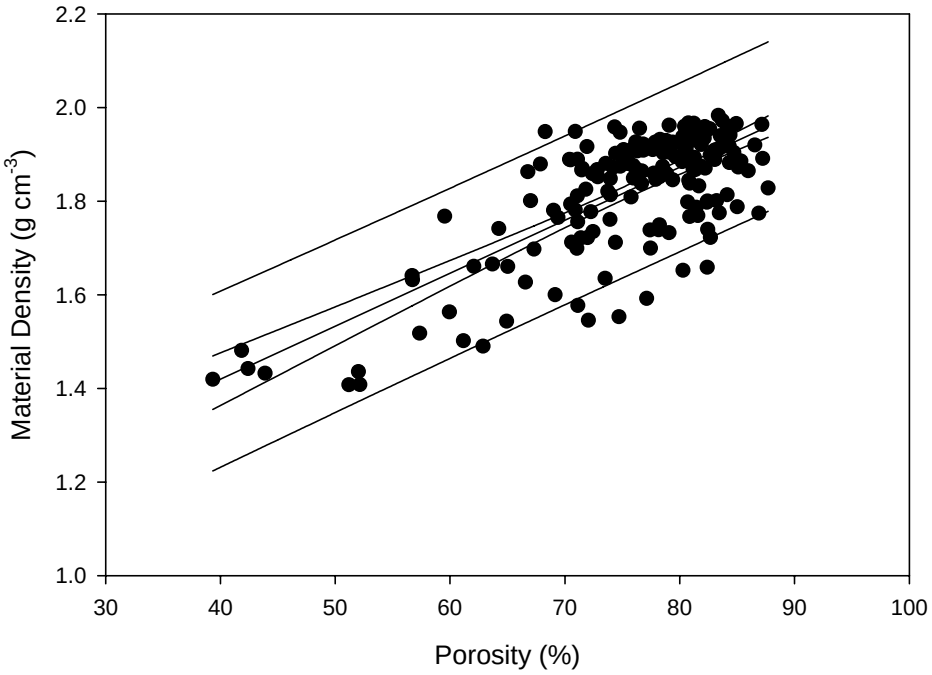

Figure 8.23 Linear regression between material density and porosity of the osteoporotic samples

Material Density = 0.967 + 0.011Porosity r^2 = 54.4% p = <0.001

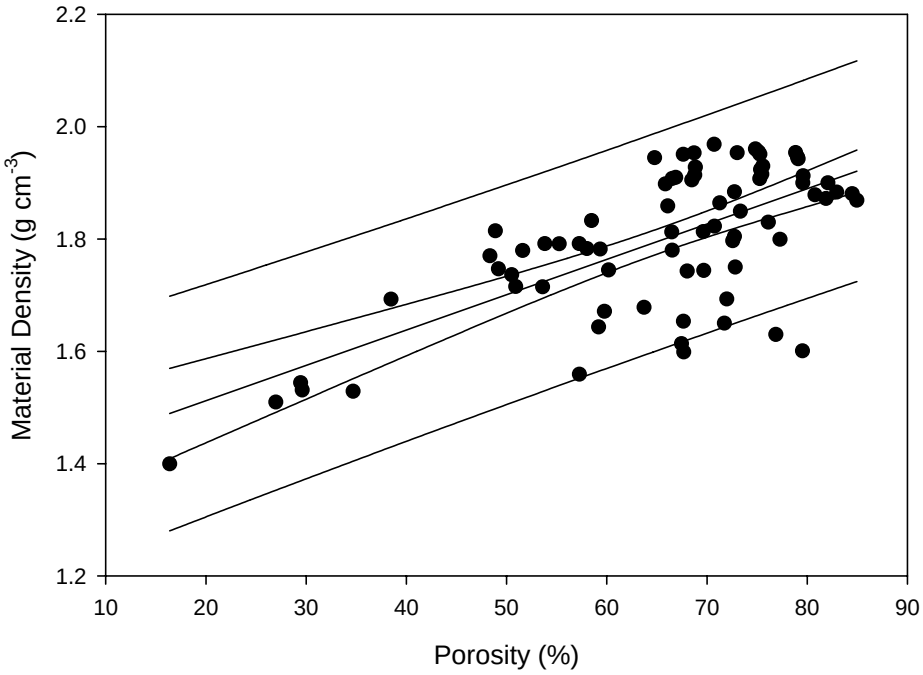

Figure 8.24 Linear regression between material density and porosity of the osteoarthritic samples

Material Density = 1.39 + 0.0063Porosity r^2 = 46.2% p = <0.001

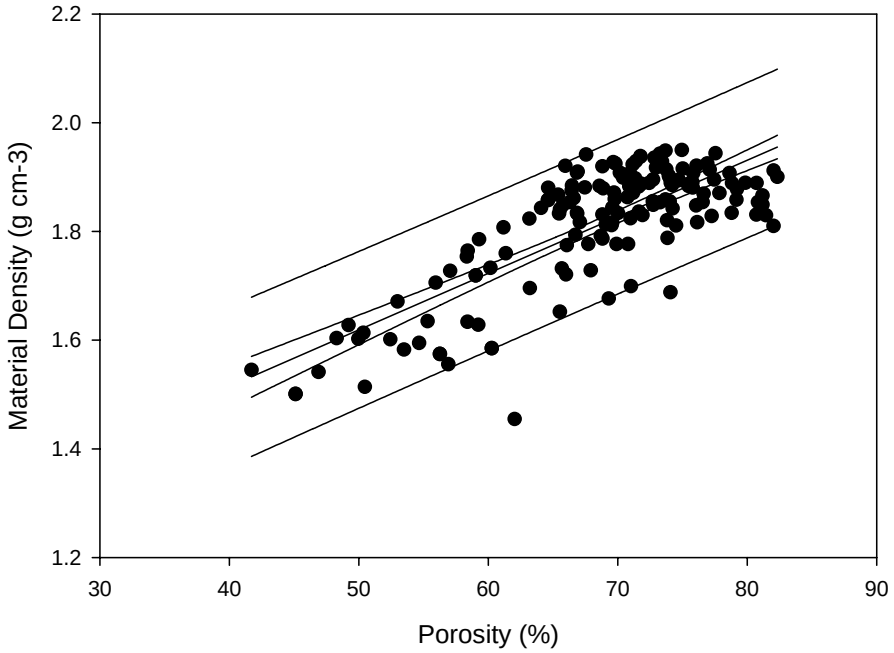

Figure 8.25 Linear regression between material density and porosity of the equine samples

Material Density = 1.10 + 0.0104Porosity r^2 = 60.8% p = <0.001

In each group the relationship demonstrated was the same, with a decrease in apparent density and an increase in porosity as the material density of the samples increased. The relationship was most pronounced for the comparison between the porosity and material density with r^2 values between 46.2 and 60.8% and high levels of significance ($p<0.001$). However the determination of the sample porosity is derived from equation 6.9 in which the porosity is equal to 1- (apparent density / material density) and therefore they should be closely related.

Table 8.34 Pearson's correlations between the compositional properties with respect to the material properties of the bone samples from the three groups

	WC	MC_{HYD}	OC_{HYD}	WC	MC_{HYD}	OC_{HYD}	WC	MC_{HYD}	OC_{HYD}	WC	MC_{HYD}	OC_{HYD}	WC	MC_{HYD}	OC_{HYD}
	Equine Beams Ac			Equine Beams AL			Equine Disks Ac			Equine Disks AL			All Equine		
$\rho_{App.}$ ($g\ cm^{-3}$)	0.101 0.433	-0.144 0.265	0.050 0.701	0.103 0.483	-0.269 0.061	0.260 0.071	0.060 0.795	-0.287 0.207	0.369 0.099	0.106 0.630	-0.212 0.343	0.068 0.758	-0.186 0.021	0.136 0.091	0.175 0.029
ρ_{Mat} ($g\ cm^{-3}$)	-0.479 <0.001	0.581 <0.001	-0.022 0.867	-0.508 <0.001	0.552 <0.001	0.114 0.437	-0.313 0.167	0.477 0.029	-0.120 0.604	-0.296 0.170	-0.008 0.970	0.476 0.022	-0.128 0.112	0.108 0.181	0.095 0.239
Porosity (%)	-0.208 0.104	0.277 0.030	-0.061 0.637	-0.214 0.139	0.362 0.011	-0.183 0.208	-0.154 0.506	0.367 0.102	-0.294 0.196	-0.177 0.418	0.151 0.502	0.114 0.604	0.124 0.123	-0.092 0.254	-0.115 0.156
	OP Beams Ac			OP Beams AL			OP Disks Ac			OP Disks AL			All OP		
$\rho_{App.}$ ($g\ cm^{-3}$)	0.091 0.498	0.143 0.284	-0.464 <0.001	0.096 0.486	-0.133 0.329	-0.087 0.535	0.088 0.636	0.198 0.286	-0.164 0.378	-0.050 0.795	0.157 0.415	-0.060 0.757	0.135 0.071	0.018 0.807	-0.129 0.085
ρ_{Mat} ($g\ cm^{-3}$)	-0.243 0.074	0.346 0.010	-0.110 0.425	-0.725 <0.001	-0.312 0.020	0.599 <0.001	-0.444 0.012	-0.308 0.092	0.470 0.008	-0.465 0.010	-0.162 0.392	0.477 0.008	-0.506 <0.001	-0.030 0.690	0.457 <0.001
Porosity (%)	-0.125 0.354	-0.080 0.554	0.429 0.001	-0.210 0.125	0.021 0.880	0.184 0.188	-0.181 0.329	-0.244 0.187	0.252 0.171	0.112 0.578	-0.002 0.994	-0.101 0.616	-0.243 0.001	-0.025 0.744	0.227 0.002
	OA Beams Ac			OA Beams AL			OA Disks Ac			OA Disks AL			All OA		
$\rho_{App.}$ ($g\ cm^{-3}$)	0.433 0.007	-0.495 0.002	0.006 0.970	0.607 0.028	-0.670 0.012	-0.407 0.189	0.610 0.061	-0.739 0.015	-0.070 0.848	0.415 0.267	-0.563 0.115	0.652 0.057	0.480 <0.001	-0.500 <0.001	-0.097 0.406
ρ_{Mat} ($g\ cm^{-3}$)	-0.590 <0.001	0.628 <0.001	-0.009 0.957	-0.808 0.001	0.886 <0.001	0.462 0.131	-0.552 0.098	0.681 0.030	0.035 0.924	-0.852 0.004	0.884 0.002	-0.097 0.804	-0.618 <0.001	0.630 <0.001	0.153 0.191
Porosity (%)	-0.484 0.002	0.545 <0.001	0 0.935	-0.649 0.016	0.714 0.006	0.450 0.142	-0.640 0.046	0.776 0.008	0.074 0.840	-0.085 0.841	0.157 0.710	-0.258 0.537	-0.553 <0.001	0.569 <0.001	0.126 0.283

8.6 Inter-material Property and Compositional Relationship

The Pearson's correlations between the material properties and hydrated compositional properties of the different test sample designs and orientations, for each of the three different groups, are shown in Table 8.34. The results vary between the different sample designs, orientations and groups, and on the whole the relationships between the variables are unclear. However, there is a clear positive correlation between the material density and the hydrated mineral content in both the equine and osteoarthritic groups, which is inverted in the osteoporotic group. The balance between the variables also differs depending on the groups, with the balance of the osteoarthritic groups and the equine groups being predominantly between the mineral and water contents, and the osteoporotic group being between the organic and the water contents.

Table 8.35 Pearson's correlations between the material properties and compositions of the test samples from the three groups

	MC_{DEHYD}	OC_{DEHYD}	MC_{DEHYD}	OC_{DEHYD}	MC_{DEHYD}	OC_{DEHYD}	MC_{DEHYD}	OC_{DEHYD}
	Equine Beams Ac		Equine Beams AL		Equine Disks Ac		Equine Disks AL	
$\rho_{App.}$ ($g\ cm^{-3}$)	-0.157 (0.227)	0.157 (0.227)	-0.404 (0.004)	0.404 (0.004)	-0.581 (0.006)	0.581 (0.006)	-0.201 (0.357)	0.201 (0.357)
ρ_{Mat} ($g\ cm^{-3}$)	0.470 (<0.001)	-0.470 (<0.001)	0.353 (0.013)	-0.353 (0.013)	0.521 (0.015)	-0.521 (0.015)	-0.300 (0.164)	0.300 (0.164)
Porosity (%)	0.267 (0.037)	-0.267 (0.037)	0.422 (0.003)	-0.422 (0.003)	0.582 (0.006)	-0.582 (0.006)	0.042 (0.851)	-0.042 (0.851)
	OP Beams Ac		OP Beams AL		OP Disks Ac		OP Disks AL	
$\rho_{App.}$ ($g\ cm^{-3}$)	0.407 (0.002)	-0.407 (0.002)	0.056 (0.683)	-0.056 (0.683)	0.222 (0.246)	-0.222 (0.246)	0.257 (0.187)	-0.257 (0.187)
ρ_{Mat} ($g\ cm^{-3}$)	0.335 (0.013)	-0.335 (0.013)	0.579 (<0.001)	-0.579 (<0.001)	0.241 (0.209)	-0.241 (0.209)	0.125 (0.252)	-0.125 (0.525)
Porosity (%)	-0.333 (0.011)	0.333 (0.011)	-0.072 (0.603)	0.072 (0.603)	-0.138 (0.477)	0.138 (0.477)	-0.244 (0.221)	0.244 (0.221)
	OA Beams Ac		OA Beams AL		OA Disks Ac		OA Disks AL	
$\rho_{App.}$ ($g\ cm^{-3}$)	-0.529 (0.001)	0.529 (0.001)	-0.352 (0.238)	0.352 (0.238)	-0.768 (0.01)	0.768 (0.010)	-0.751 (0.020)	0.751 (0.020)
ρ_{Mat} ($g\ cm^{-3}$)	0.705 (<0.001)	-0.705 (<0.001)	0.463 (0.111)	-0.463 (0.111)	0.724 (0.018)	-0.724 (0.018)	0.846 (0.004)	-0.846 (0.004)
Porosity (%)	0.583 (<0.001)	-0.583 (<0.001)	0.374 (0.208)	-0.374 (0.208)	0.806 (0.005)	-0.806 (0.005)	0.295 (0.477)	-0.295 (0.477)

In order to attempt to provide a better explanation for the relationships between these variables the dehydrated mineral and organic contents were compared (Table 8.35). The results show that the nature of the relationship between the mineral and organic content varies depending on the material properties. For the osteoarthritic and equine groups, the relationship between the mineral and organic content with respect to the apparent density and porosity are in agreement. For both groups, an increase in apparent density and corresponding reduction in porosity both lead to a reduction in the mineral content and an increase in the organic content. This is also in agreement with the previous results in this section which demonstrated that an increase in porosity and reduction in apparent density increased the material density, demonstrated in these results by an increase in material density increasing the mineral content.

The osteoporotic samples are in agreement with the two other groups about the nature of the relationship between the material density and mineral content, with an increase in material density corresponding to an increase mineral content. However, the relationship between the apparent density and porosity to the mineral and organic contents was the inverse of the other groups. The results in Table 8.35 show that for the osteoporotic samples, an increase in apparent density and the corresponding reduction in porosity lead to an increase in the mineral content of the bone, and a reduction in the organic content.

The results are also in disagreement with those of the previous section which showed the increase in apparent density correlating with a reduction in the mineral content which, based on the significant results of the material density and mineral content relationship, should have implied a reduction in the mineral content. The possible reasons for this difference will be discussed further later in this document.

8.7 Collagen Cross-link Comparison

The comparison between the collagen cross-linking within the groups was only performed on the two human groups, the osteoporotic and the osteoarthritic; the results of the analysis and comparison between the groups is shown in Table 8.36.

Table 8.36 Mean, range, standard deviation and ANOVA comparison between the collagen cross-linking within the osteoporotic and osteoarthritic samples.

	Osteoporotic Samples	Osteoarthritic Samples	ANOVA p-value
m/m HLNL			
Range	0.021 - 0.570	0.030 - 0.550	0.009
Mean	0.136	0.209	
St. Dev.	0.09	0.132	
m/m HHL			
Range	0.002 - 0.166	0.003 - 0.142	0.953
Mean	0.0384	0.038	
St. Dev.	0.0374	0.040	
m/m HLKNL			
Range	0.050 - 0.720	0.090 - 0.830	<0.001
Mean	0.180	0.327	
St. Dev.	0.114	0.191	
m/m OHPyr			
Range	0.095 - 0.735	0.210 - 1.160	0.051
Mean	0.353	0.444	
St. Dev.	0.150	0.227	
m/m LysPyr			
Range	0.010 - 0.443	0.070 - 0.420	0.905
Mean	0.173	0.176	
St. Dev.	0.088	0.095	
fmoles Pentosidine / pmole coll			
Range	4.78 - 66.56	2.23 - 78.85	0.150
Mean	22.52	16.25	
St. Dev.	13.04	20.69	

The results show that the levels of the immature cross-links HLKNL and HLNL were significantly greater in the osteoarthritic samples than the osteoporotic samples, a trend matched by the maturation of HLKNL, OHPyr cross-links which almost obtained significance. No significant difference was noted between the mature cross-links LysPyr and HHL contents nor the levels of pentosidine per mole of collagen between the groups although the levels of pentosidine per mole of collagen were

discernibly greater in the osteoporotic group than the osteoarthritic, despite failing to achieve significance.

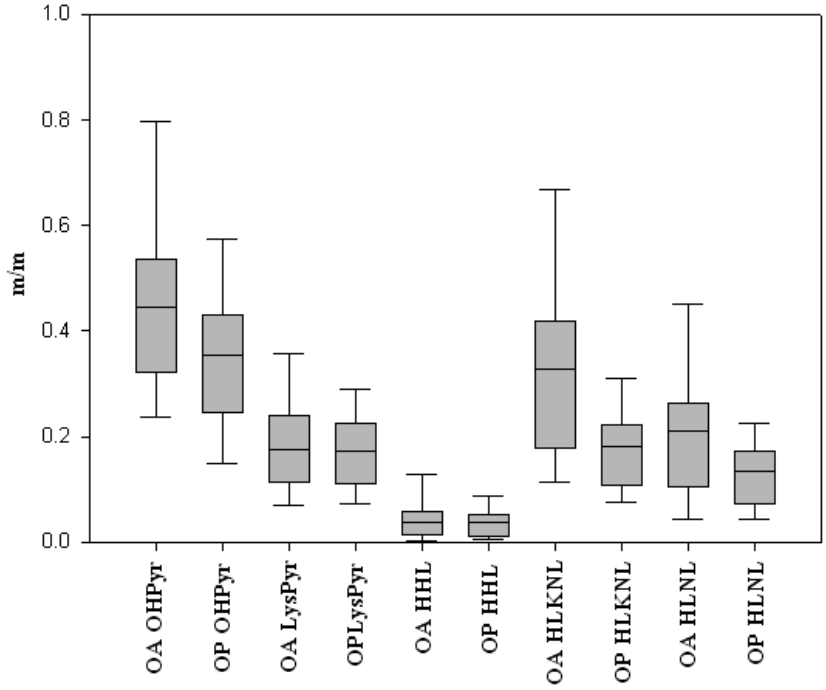

Figure 8.26 Box plot displaying the comparison between the collagen cross-linking of the osteoporotic and osteoarthritic study groups

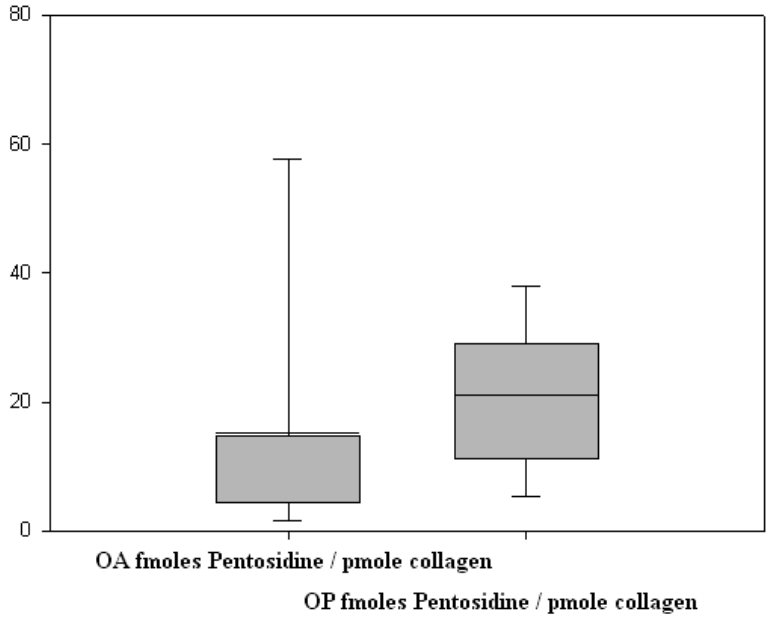

Figure 8.27 Box plot displaying the comparison between the fmoles Pentosidine / pmole collagen of the osteoporotic and osteoarthritic study groups

8.9 Biomechanics vs. QUS Assessments

The comparison between the biomechanical results and the QUS investigations was performed for both the compression testing results and the fracture toughness results. The analysis was only possible on the osteoarthritic group, and a section of the osteoporotic group; the comparisons were performed for each of the individual groups and with the osteoporotic and osteoarthritic groups in combination.

8.9.1 Compression Testing vs. Age and Clinical QUS

The relationships between the compressive mechanical properties and the age and clinical QUS measures obtained from the donor, provided a number of significant correlations as well as number of correlations which approached significance. (Table 8.37 to Table 8.39) For the individual groups the correlation with the age of the donor subject provided no significant or nearly significant correlations. The combination of the groups provided a larger spread of ages and sample size and for all bar two of the compressive mechanical parameters; ($E_{Contact}$ and $\varepsilon_{Ult.\ Platens}$) moderate, negative and significant correlations were seen.

For the osteoporotic group (Table 8.37) there was a number of significant correlations between the compressive mechanical results and the QUS assessments, with the distal radius, mid-shaft tibia and Calcaneus all providing a good degree of correlation ($r = 0.463 – 0.678$), although the level of significance varied ($p = 0.046 – 0.003$).

Table 8.37 Pearson's correlations between the compressive mechanical parameters, the age of the donor subject, and the QUS results obtained in-vivo on the donor subject for the osteoporotic group

Osteoporotic	$E_{Platens}$ (MPa)	$E_{Contact}$ (MPa)	$\varepsilon_{Yield\ Platens}$ (%)	$\varepsilon_{Ult.Platens}$ (%)	$\varepsilon_{Yield\ Contact}$ (%)	$\varepsilon_{Ult.Contact}$ (%)	σ_{Yield} (MPa)	$\sigma_{Ult.}$ (MPa)	Work to $Failure_{Platens}$ (Nmm^{-1})	Work to $Failure_{Contact}$ (Nmm^{-1})
Age	-0.152 (0.561)	0.052 (0.842)	*-0.295 (0.236)*	*0.205 (0.417)*	-0.300 (0.242)	*0.032 (0.898)*	-0.238 (0.312)	-0.196 (0.408)	-0.336 (0.147)	-0.260 (0.269)
DR SOS ($m\ s^{-1}$)	*0.382 (0.144)*	*0.232 (0.387)*	*0.469 (0.057)*	*0.585 (0.014)*	*-0.032 (0.924)*	*0.158 (0.562)*	0.402 (0.079)	0.432 (0.057)	0.286 (0.236)	0.479 (0.038)
DR T-score	0.325 (0.203)	0.240 (0.353)	0.362 (0.140)	0.427 (0.077)	-0.07 (0.806)	-0.15 (0.569)	0.349 (0.132)	0.374 (0.105)	0.239 (0.324)	0.412 (0.079)
PP SOS ($m\ s^{-1}$)	0.339 (0.184)	*0.032 (0.900)*	0.286 (0.249)	0.327 (0.185)	0.078 (0.766)	*0.055 (0.842)*	0.344 (0.138)	0.362 (0.116)	0.240 (0.309)	0.421 (0.073)
PP T-score	0.344 (0.177)	-0.019 (0.942)	0.298 (0.230)	0.333 (0.177)	0.046 (0.862)	-0.042 (0.872)	0.337 (0.146)	0.352 (0.128)	0.225 (0.340)	0.411 (0.080)
MT SOS ($m\ s^{-1}$)	0.584 (0.014)	*0.523 (0.037)*	*0.167 (0.562)*	0.113 (0.666)	*0.303 (0.253)*	-0.18 (0.496)	*0.491 (0.038)*	0.464 (0.045)	*0.126 (0.610)*	*0.295 (0.234)*
MT T-score	0.678 (0.003)	0.417 (0.096)	-0.002 (0.995)	0.083 (0.751)	-0.12 (0.671)	-0.06 (0.838)	0.498 (0.030)	0.510 (0.026)	0.049 (0.843)	0.308 (0.213)
BUA ($dB\ MHz^{-1}$)	0.390 (0.110)	*0.475 (0.054)*	*0.439 (0.068)*	0.276 (0.252)	*-0.341 (0.180)*	*0.235 (0.365)*	0.423 (0.056)	0.418 (0.059)	*0.134 (0.568)*	*0.392 (0.087)*
BUA T-score	0.392 (0.108)	0.439 (0.068)	0.397 (0.092)	0.267 (0.268)	-0.313 (0.220)	-0.181 (0.488)	0.437 (0.048)	0.431 (0.051)	0.096 (0.688)	0.347 (0.134)
VOS ($m\ s^{-1}$)	*0.550 (0.022)*	*0.373 (0.141)*	0.559 (0.013)	0.463 (0.046)	*0.077 (0.775)*	*0.032 (0.906)*	0.509 (0.018)	0.506 (0.019)	*0.272 (0.246)*	0.511 (0.021)
VOS T-score	0.480 (0.044)	0.195 (0.439)	0.560 (0.013)	0.464 (0.045)	0.041 (0.877)	0.012 (0.963)	0.510 (0.018)	0.506 (0.019)	0.198 (0.404)	0.512 (0.021)

Table 8.38 Pearson's correlations between the compressive mechanical parameters, the age of the donor subject, and the QUS results obtained in-vivo on the donor subject for the osteoarthritic group

Osteoarthritic	$E_{Platens}$ (MPa)	$E_{Contact}$ (MPa)	$\varepsilon_{Yield\ Platens}$ (%)	$\varepsilon_{Ult.Platens}$ (%)	$\varepsilon_{Yield\ Contact}$ (%)	$\varepsilon_{Ult.Contact}$ (%)	σ_{Yield} (MPa)	$\sigma_{Ult.}$ (MPa)	Work to $Failure_{Platens}$ (Nmm^{-1})	Work to $Failure_{Contact}$ (Nmm^{-1})
Age	-0.361 (0.380)	-0.411 (0.312)	-0.428 (0.290)	-0.520 (0.186)	-0.517 (0.234)	-0.187 (0.688)	-0.581 (0.131)	-0.571 (0.140)	-0.453 (0.307)	-0.565 (0.144)
DR SOS ($m\ s^{-1}$)	*0.192 (0.648)*	*0.195 (0.642)*	0.667 (0.071)	0.896 (0.003)	*0.440 (0.322)*	*0.458 (0.302)*	0.685 (0.061)	0.752 (0.032)	0.733 (0.061)	0.847 (0.008)
DR T-score	-0.012 (0.977)	-0.044 (0.917)	0.701 (0.053)	0.857 (0.007)	0.243 (0.6)	0.497 (0.256)	0.559 (0.149)	0.643 (0.086)	0.686 (0.089)	0.768 (0.026)
PP SOS ($m\ s^{-1}$)	0.187 (0.658)	*0.497 (0.210)*	0.760 (0.029)	*0.666 (0.071)*	-0.038 (0.936)	0.184 (0.693)	*0.603 (0.113)*	*0.592 (0.123)*	0.459 (0.301)	*0.627 (0.096)*
PP T-score	0.022 (0.958)	0.142 (0.737)	0.751 (0.032)	0.614 (0.105)	-0.164 (0.725)	0.177 (0.705)	0.456 (0.257)	0.473 (0.236)	0.423 (0.345)	0.498 (0.209)
MT SOS ($m\ s^{-1}$)	*-0.126 (0.764)*	*0.335 (0.419)*	0.632 (0.093)	0.582 (0.130)	-0.179 (0.701)	*-0.179 (0.703)*	0.362 (0.378)	0.410 (0.313)	0.332 (0.467)	0.518 (0.189)
MT T-score	0.089 (0.834)	0.361 (0.379)	0.557 (0.151)	0.531 (0.176)	-0.084 (0.858)	-0.064 (0.892)	0.405 (0.320)	0.431 (0.287)	0.332 (0.467)	0.505 (0.202)
BUA ($dB\ MHz^{-1}$)	-0.265 (0.525)	*-0.482 (0.227)*	-0.219 (0.601)	-0.564 (0.146)	0.197 (0.673)	-0.241 (0.603)	-0.487 (0.221)	-0.531 (0.176)	-0.487 (0.268)	-0.609 (0.109)
BUA T-score	-0.262 (0.530)	-0.41 (0.313)	-0.202 (0.632)	-0.563 (0.146)	0.089 (0.850)	-0.242 (0.602)	-0.485 (0.223)	-0.530 (0.177)	-0.486 (0.269)	-0.608 (0.110)
VOS ($m\ s^{-1}$)	0.191 (0.651)	*0.319 (0.440)*	0.138 (0.743)	-0.280 (0.501)	-0.084 (0.857)	*0.373 (0.410)*	0.170 (0.687)	-0.103 (0.809)	*0.2 (0.667)*	-0.267 (0.522)
VOS T-score	0.19 (0.651)	0.297 (0.476)	0.103 (0.808)	-0.281 (0.5)	-0.085 (0.857)	-0.352 (0.438)	0.009 (0.983)	-0.103 (0.808)	-0.199 (0.669)	-0.268 (0.521)

Table 8.39 Pearson's correlations between the compressive mechanical parameters, the age of the donor subject, and the QUS results obtained in-vivo on the donor subject for the combined osteoporotic and osteoarthritic group

Osteoporotic + Osteoarthritic	$E_{Platens}$ (MPa)	$E_{Contact}$ (MPa)	$\varepsilon_{Yield\ Platens}$ (%)	$\varepsilon_{Ult.Platens}$ (%)	$\varepsilon_{Yield\ Contact}$ (%)	$\varepsilon_{Ult.Contact}$ (%)	σ_{Yield} (MPa)	$\sigma_{Ult.}$ (MPa)	Work to $Failure_{Platens}$ (Nmm^{-1})	Work to $Failure_{Contact}$ (Nmm^{-1})
Age	-0.413 (0.040)	*-0.077 (0.705)*	*-0.305 (0.129)*	-0.337 (0.093)	-0.601 (0.002)	-0.422 (0.040)	-0.426 (0.024)	-0.405 (0.033)	-0.509 (0.007)	-0.463 (0.013)
DR SOS ($m\ s^{-1}$)	*0.297 (0.158)*	*0.224 (0.295)*	0.546 (0.005)	*0.680 (<0.001)*	0.242 (0.267)	0.254 (0.242)	0.533 (0.004)	0.580 (0.002)	0.506 (0.008)	0.598 (0.001)
DR T-score	0.201 (0.347)	0.133 (0.536)	0.508 (0.010)	0.640 (0.001)	0.226 (0.300)	0.282 (0.193)	0.465 (0.015)	0.511 (0.006)	0.503 (0.009)	0.561 (0.002)
PP SOS ($m\ s^{-1}$)	0.289 (0.170)	*0.130 (0.539)*	0.328 (0.110)	0.333 (0.103)	0.154 (0.472)	0.141 (0.511)	0.410 (0.034)	0.405 (0.036)	0.289 (0.143)	*0.365 (0.061)*
PP T-score	0.271 (0.20)	0.039 (0.851)	0.336 (0.101)	0.354 (0.083)	0.171 (0.424)	0.191 (0.371)	0.398 (0.040)	0.396 (0.041)	0.321 (0.103)	0.375 (0.054)
MT SOS ($m\ s^{-1}$)	*0.241 (0.259)*	*0.492 (0.015)*	*0.266 (0.209)*	0.297 (0.158)	*-0.164 (0.457)*	*-0.077 (0.721)*	*0.466 (0.017)*	*0.420 (0.033)*	0.219 (0.282)	*0.349 (0.080)*
MT T-score	0.226 (0.289)	0.335 (0.110)	0.124 (0.565)	0.254 (0.232)	-0.129 (0.559)	-0.090 (0.683)	0.405 (0.040)	0.400 (0.043)	0.161 (0.433)	0.309 (0.125)
BUA ($dB\ MHz^{-1}$)	0.376 (0.064)	0.358 (0.080)	*0.359 (0.072)*	0.137 (0.498)	0.249 (0.241)	0.283 (0.181)	*0.377 (0.048)*	0.338 (0.079)	0.274 (0.166)	0.311 (0.107)
BUA T-score	0.377 (0.063)	0.218 (0.295)	0.258 (0.203)	0.092 (0.654)	0.242 (0.255)	0.277 (0.190)	0.322 (0.095)	0.267 (0.170)	0.234 (0.241)	0.202 (0.302)
VOS ($m\ s^{-1}$)	0.466 (0.019)	0.333 (0.103)	*0.402 (0.041)*	0.138 (0.50)	*0.286 (0.176)*	0.205 (0.334)	*0.442 (0.019)*	0.386 (0.042)	0.318 (0.106)	0.355 (0.064)
VOS T-score	0.462 (0.020)	0.203 (0.329)	0.385 (0.052)	0.137 (0.505)	0.280 (0.185)	0.198 (0.355)	0.407 (0.032)	0.333 (0.084)	0.214 (0.284)	0.266 (0.248)

The comparisons between the osteoarthritic group (Table 8.38) and the clinical QUS measurements failed to provide the same degree of correlation as with the osteoporotic group. Only the distal radius provided any significant correlation, although the correlations that were achieved were high, r = 0.752 - 0.896, and with a high level of significance p = 0.032 - 0.003.

The results of the combination of the two groups were mixed (Table 8.39); the number of significant correlations was increased, but with the loss of some previously significant correlations from the individual groups. The distal radius provided good (r = 0.465 – 0.680) and significant correlations between 6 out of 10 of the mechanical parameters, with all QUS investigations, with the exception of BUA of the Calcaneus, providing significant correlations. The most notable of the mechanical parameters was the strength, which significantly correlated with 9 out of the 10 QUS investigations it was compared with, and was approaching significance for a further two.

It is of note that the correlations which were achieved between the QUS investigations and the compression testing results bore a close agreement with the correlations that were seen between the material properties the compression testing results, and the material properties with the QUS investigations (Section 8.10).

8.9.2 Fracture Toughness Testing vs. Age and QUS Investigations

The results for the fracture toughness parameters in comparison to the age and the QUS assessments from the donor subjects are shown in Table 8.40 to Table 8.45.

8.9.2.1 Age

For the individual groups in comparison to age, there are only two groups of samples which provide significant correlations, the osteoporotic beams Ac and the Osteoarthritic beams AL. In both cases the K and G values are found to reduce with the age of the donor, but as with the mechanical results vs. the material and compositional results in section 8.2.3 the J-integral results are the inverse, and increase with the age of the donor subject. This trend is seen in the non-significant correlations as well, but with a few exceptions.

For the combined group, the results are different to those seen in the individual groups; for all three sample designs there are significant correlations between the age of the donor and the fracture toughness parameters. In three out of the four sample designs, all six parameters K, G and J-integral show negative correlations with age, with the Disks Ac only being in agreement with the results of the individual groups. The reason for this may be due to the demographics of the two different groups being combined;, with the osteoarthritic group being significantly younger and with a higher number of male subjects, the results in comparison to age can be considered biased.

8.9.2.2 QUS Investigation

There are a number of significant correlations between the fracture toughness parameters and the QUS investigations for both the osteoporotic and osteoarthritic groups. The correlations are however sporadic, with no clear relationship between the

nature of the correlations, the QUS system utilised for either of the sample designs or orientations. For the osteoporotic group the best results were seen between the CUBA Clinical system and the K and G fracture toughness parameters from the disk Ac samples, with correlations ranging between r = 0.680 and 0.891 and high levels of significance ($p < 0.01$). The other three sample designs all failed even to approach significance, in comparison to the results of the CUBA clinical system, but both the beam and disk samples orientated in the AL direction achieved significant correlations with the QUS investigations of the proximal phalanx, but for the beam samples the correlation was negative in nature in contrast to the positive correlation seen with the disk samples.

For the osteoarthritic group the QUS assessment of the distal radius was the best performing investigation, with significant correlations seen in three out of the four sample designs and orientations, with a range of magnitudes from r = -0.360 to 0.798. The mid-shaft tibia and the proximal phalanx both achieved significant correlations with the mid-shaft tibia providing excellent correlations in comparison to the K and G values of the disk AL samples (r = 0.870 – 0.962). The CUBA Clinical system failed to produce a large number of significant correlations with the fracture toughness results but as with the mid-shaft tibia, the BUA and corresponding T-score correlated with the GQ value of the disk AL samples, but the correlations achieved were negative in nature (r = -0.866 and -0.832).

Table 8.40 Pearson's Correlations between the fracture toughness parameters from the beam samples and the age and QUS values obtain from the donor subjects for the OP group

OP Beams	Beams AC						Beams AL					
	K_Q	K_C	J_Q	J_C	G_Q	G_C	K_Q	K_C	J_Q	J_C	G_Q	G_C
Age	-0.354 (0.005)	-0.352 (0.005)	*0.447 (<0.001)*	0.293 (0.023)	-0.356 (0.005)	-0.358 (0.005)	*0.114 (0.409)*	*-0.045 (0.717)*	*-0.164 (0.231)*	*0.245 (0.069)*	0.148 (0.271)	*-0.032 (0.817)*
DR SOS (m s^{-1})	*0.1 (0.445)*	0.072 (0.584)	*-0.063 (0.641)*	-0.082 (0.537)	0.041 (0.756)	*-0.032 (0.796)*	*-0.221 (0.255)*	-0.215 (0.273)	*0.118 (0.552)*	*0.145 (0.467)*	*-0.182 (0.357)*	*-0.158 (0.426)*
DR T-score	0.272 (0.035)	0.245 (0.06)	-0.115 (0.39)	-0.185 (0.160)	0.204 (0.118)	0.180 (0.168)	-0.204 (0.299)	-0.192 (0.327)	0.016 (0.937)	-0.030 (0.881)	-0.122 (0.536)	-0.121 (0.539)
PP SOS (m s^{-1})	*0.158 (0.252)*	*0.141 (0.304)*	*-0.1 (0.481)*	-0.078 (0.575)	*0.11 (0.430)*	*0.089 (0.525)*	-0.397 (0.045)	-0.392 (0.048)	-0.123 (0.548)	*0.095 (0.652)*	-0.329 (0.101)	-0.333 (0.097)
PP T-score	0.238 (0.080)	0.236 (0.083)	-0.134 (0.340)	-0.145 (0.296)	0.193 (0.159)	0.200 (0.144)	-0.364 (0.068)	-0.360 (0.071)	-0.230 (0.259)	-0.074 (0.721)	-0.336 (0.093)	-0.342 (0.087)
MT SOS (m s^{-1})	0.277 (0.034)	0.253 (0.053)	-0.123 (0.36)	-0.196 (0.14)	*0.207 (0.113)*	0.170 (0.199)	*-0.179 (0.364)*	-0.134 (0.495)	-0.026 (0.894)	-0.012 (0.951)	*-0.182 (0.353)*	*-0.118 (0.552)*
MT T-score	0.263 (0.044)	0.239 (0.068)	-0.097 (0.473)	-0.169 (0.204)	0.171 (0.194)	0.152 (0.251)	-0.228 (0.243)	-0.191 (0.330)	0.031 (0.877)	0.107 (0.589)	-0.161 (0.412)	-0.143 (0.467)
BUA (dB MHz^{-1})	*0.385 (0.004)*	0.382 (0.004)	-0.224 (0.111)	-0.117 (0.405)	0.317 (0.020)	0.324 (0.017)	*0.122 (0.532)*	*0.035 (0.738)*	*-0.089 (0.657)*	*-0.265 (0.173)*	*0.1 (0.612)*	*0.031 (0.867)*
BUA T-score	0.382 (0.004)	0.390 (0.004)	-0.229 (0.103)	-0.117 (0.406)	0.324 (0.017)	0.332 (0.014)	0.063 (0.752)	0.026 (0.894)	-0.026 (0.894)	-0.239 (0.220)	0.043 (0.829)	0.021 (0.916)
VOS (m s^{-1})	0.348 (0.009)	0.349 (0.009)	-0.230 (0.097)	-0.082 (0.557)	0.313 (0.020)	0.323 (0.016)	*0.126 (0.519)*	*0.032 (0.858)*	*-0.217 (0.266)*	*-0.257 (0.186)*	*0.1 (0.618)*	-0.007 (0.970)
VOS T-score	*0.339 (0.011)*	0.349 (0.009)	-0.230 (0.097)	-0.081 (0.560)	0.313 (0.020)	0.323 (0.016)	0.093 (0.639)	0.028 (0.888)	-0.191 (0.330)	-0.244 (0.211)	0.044 (0.823)	-0.007 (0.970)

Table 8.41 Pearson's Correlations between the fracture toughness parameters from the disk samples and the age and QUS values obtain from the donor subjects for the OP group

OP Disks	Disks AC						Disks AL					
	K_Q	K_C	J_Q	J_C	G_Q	G_C	K_Q	K_C	J_Q	J_C	G_Q	G_C
Age	-0.139 (0.516)	-0.129 (0.547)	*0.266 (0.209)*	0.295 (0.162)	0.171 (0.434)	0.256 (0.238)	-0.283 (0.144)	-0.290 (0.134)	*-0.202 (0.294)*	0.350 (0.079)	-0.228 (0.242)	-0.242 (0.215)
DR SOS (m s^{-1})	0.530 (0.051)	*0.538 (0.047)*	*0.237 (0.395)*	*0.232 (0.404)*	0.288 (0.317)	*0.268 (0.355)*	*0.21 (0.421)*	*0.176 (0.497)*	*-0.319 (0.197)*	*-0.071 (0.772)*	*0.118 (0.654)*	*0.071 (0.781)*
DR T-score	0.500 (0.069)	0.498 (0.070)	-0.201 (0.472)	-0.198 (0.480)	0.260 (0.369)	0.230 (0.430)	0.118 (0.653)	0.082 (0.756)	-0.337 (0.171)	-0.040 (0.869)	0.042 (0.873)	-0.007 (0.980)
PP SOS (m s^{-1})	*0.293 (0.288)*	*0.263 (0.343)*	0.068 (0.809)	*-0.386 (0.155)*	*0.268 (0.354)*	*0.228 (0.435)*	0.719 (0.002)	*0.682 (0.004)*	*-0.338 (0.184)*	*-0.21 (0.405)*	*0.613 (0.012)*	*0.554 (0.026)*
PP T-score	0.185 (0.51)	0.169 (0.547)	0.092 (0.745)	-0.335 (0.222)	0.141 (0.630)	0.119 (0.685)	0.640 (0.008)	0.600 (0.014)	-0.370 (0.144)	-0.208 (0.407)	0.492 (0.053)	0.426 (0.1)
MT SOS (m s^{-1})	0.418 (0.121)	0.407 (0.132)	*-0.424 (0.115)*	*-0.519 (0.047)*	*0.276 (0.340)*	*0.263 (0.364)*	0.308 (0.265)	0.276 (0.319)	*-0.404 (0.121)*	*-0.276 (0.283)*	0.178 (0.525)	0.134 (0.634)
MT T-score	0.435 (0.106)	0.419 (0.120)	-0.370 (0.174)	-0.508 (0.053)	0.297 (0.303)	0.261 (0.367)	0.369 (0.176)	0.339 (0.216)	-0.304 (0.253)	-0.230 (0.374)	0.234 (0.401)	0.193 (0.490)
BUA (dB MHz^{-1})	*0.874 (<0.001)*	*0.891 (<0.001)*	*0.513 (0.051)*	-0.133 (0.637)	*0.852 (<0.001)*	*0.868 (<0.001)*	0.183 (0.481)	0.181 (0.486)	*-0.134 (0.596)*	*-0.276 (0.252)*	0.160 (0.539)	0.153 (0.558)
BUA T-score	0.852 (<0.001)	0.862 (<0.001)	0.463 (0.082)	-0.143 (0.610)	0.727 (0.003)	0.734 (0.003)	0.193 (0.459)	0.191 (0.462)	-0.141 (0.577)	-0.271 (0.262)	0.171 (0.512)	0.165 (0.527)
VOS (m s^{-1})	*0.778 (0.001)*	*0.78 (0.001)*	*0.285 (0.303)*	-0.290 (0.295)	*0.784 (0.001)*	*0.79 (0.001)*	0.082 (0.755)	0.082 (0.754)	-0.051 (0.842)	*-0.141 (0.567)*	0.063 (0.810)	0.066 (0.802)
VOS T-score	0.729 (0.002)	0.713 (0.003)	0.241 (0.388)	-0.291 (0.292)	0.702 (0.005)	0.680 (0.007)	0.082 (0.754)	0.082 (0.753)	-0.052 (0.838)	-0.130 (0.595)	0.064 (0.809)	0.066 (0.802)

Table 8.42 Pearson's Correlations between the fracture toughness parameters from the beam samples and the age and QUS values obtain from the donor subjects for the OA group

OA Beams	Beams AC						Beams AL					
	K_Q	K_C	J_Q	J_C	G_Q	G_C	K_Q	K_C	J_Q	J_C	G_Q	G_C
Age	-0.232 (0.156)	-2.33 (0.154)	-0.065 (0.699)	0.227 (0.165)	-0.263 (0.101)	-0.267 (0.096)	*-0.668 (0.013)*	-0.627 (0.002)	*0.164 (0.592)*	0.272 (0.369)	*-0.579 (0.038)*	-0.548 (0.053)
DR SOS (m s^{-1})	0.610 (<0.001)	0.645 (<0.001)	*-0.232 (0.162)*	-0.360 (0.024)	0.531 (<0.001)	0.556 (<0.001)	0.718 (0.002)	0.710 (0.002)	*-0.313 (0.321)*	-0.284 (0.175)	0.798 (0.010)	0.794 (0.009)
DR T-score	0.554 (<0.001)	0.593 (<0.001)	-0.204 (0.219)	-0.264 (0.104)	0.470 (0.002)	0.500 (0.001)	0.716 (0.001)	0.709 (0.001)	-0.44 (0.233)	-0.356 (0.132)	0.793 (0.007)	0.789 (0.006)
PP SOS (m s^{-1})	0.221 (0.176)	0.213 (0.194)	*-0.264 (0.627)*	-0.377 (0.018)	0.256 (0.111)	0.264 (0.1)	0.244 (0.295)	0.244 (0.302)	-0.579 (0.048)	*-0.595 (0.032)*	0.31 (0.421)	0.315 (0.421)
PP T-score	0.277 (0.087)	0.274 (0.092)	-0.046 (0.785)	-0.340 (0.034)	0.292 (0.067)	0.306 (0.055)	0.233 (0.313)	0.234 (0.302)	-0.572 (0.054)	-0.546 (0.041)	0.299 (0.442)	0.304 (0.443)
MT SOS (m s^{-1})	0.171 (0.340)	0.230 (0.198)	0.048 (0.795)	*0.045 (0.814)*	0.243 (0.166)	0.288 (0.098)	0.446 (0.108)	0.423 (0.102)	0.076 (0.836)	*0.089 (0.771)*	*0.456 (0.118)*	0.466 (0.126)
MT T-score	0.096 (0.594)	0.153 (0.395)	0.067 (0.718)	0.052 (0.775)	0.194 (0.271)	0.235 (0.181)	0.455 (0.102)	0.431 (0.096)	0.074 (0.820)	-0.070 (0.811)	0.482 (0.141)	0.474 (0.119)
BUA (dB MHz^{-1})	*0.476 (0.010)*	*0.418 (0.027)*	-0.253 (0.213)	-0.476 (0.012)	*0.345 (0.072)*	0.269 (0.167)	-0.517 (0.112)	-0.481 (0.097)	*0.158 (0.604)*	0.125 (0.401)	-0.480 (0.096)	-0.462 (0.07)
BUA T-score	0.408 (0.031)	0.371 (0.052)	-0.252 (0.214)	-0.475 (0.012)	0.313 (0.105)	0.270 (0.165)	-0.517 (0.113)	-0.481 (0.097)	-0.256 (0.686)	0.124 (0.399)	-0.479 (0.096)	-0.461 (0.071)
VOS (m s^{-1})	-0.330 (0.061)	-0.344 (0.05)	*-0.045 (0.793)*	-0.186 (0.30)	*-0.321 (0.064)*	*-0.345 (0.046)*	*-0.173 (0.574)*	*-0.205 (0.501)*	-0.366 (0.171)	*-0.409 (0.166)*	*-0.197 (0.518)*	*-0.245 (0.42)*
VOS T-score	-0.330 (0.061)	-0.344 (0.05)	-0.040 (0.829)	-0.186 (0.301)	-0.233 (0.186)	-0.248 (0.158)	-0.174 (0.646)	-0.171 (0.629)	-0.366 (0.172)	-0.404 (0.219)	-0.148 (0.578)	-0.141 (0.570)

Table 8. 43 Pearson's Correlations between the fracture toughness parameters from the disk samples and the age and QUS values obtain from the donor subjects for the OA group

OA Disks	Disks AC						Disks AL					
	K_Q	K_C	J_Q	J_C	G_Q	G_C	K_Q	K_C	J_Q	J_C	G_Q	G_C
Age	-0.349 (0.358)	-0.147 (0.705)	0.414 (0.268)	*0.247 (0.520)*	-0.287 (0.454)	*0.243 (0.528)*	-0.260 (0.573)	-0.325 (0.476)	*0.523 (0.228)*	*0.247 (0.594)*	-0.154 (0.741)	-0.288 (0.531)
DR SOS (m s^{-1})	0.695 (0.038)	0.540 (0.133)	*-0.472 (0.199)*	*-0.456 (0.217)*	0.645 (0.061)	0.300 (0.433)	0.622 (0.136)	0.753 (0.051)	0.116 (0.804)	*-0.126 (0.789)*	*0.367 (0.417)*	0.718 (0.069)
DR T-score	0.722 (0.028)	0.607 (0.083)	-0.346 (0.362)	-0.345 (0.363)	0.688 (0.041)	0.409 (0.274)	0.499 (0.254)	0.650 (0.114)	0.350 (0.442)	0.151 (0.747)	0.130 (0.782)	0.560 (0.191)
PP SOS (m s^{-1})	0.459 (0.213)	0.395 (0.293)	*-0.385 (0.306)*	*-0.295 (0.442)*	0.252 (0.513)	*0.095 (0.804)*	*-0.063 (0.890)*	0.209 (0.653)	-0.227 (0.625)	*-0.226 (0.628)*	*-0.311 (0.495)*	0.059 (0.900)
PP T-score	0.491 (0.179)	0.461 (0.212)	-0.239 (0.535)	-0.187 (0.629)	0.337 (0.376)	0.196 (0.613)	-0.044 (0.925)	0.200 (0.667)	-0.086 (0.855)	-0.068 (0.884)	-0.355 (0.434)	0.003 (0.995)
MT SOS (m s^{-1})	0.276 (0.472)	0.140 (0.719)	*-0.013 (0.963)*	0.030 (0.938)	0.314 (0.410)	*0.126 (0.742)*	*0.904 (0.013)*	*0.956 (0.003)*	*-0.071 (0.897)*	0.178 (0.736)	*0.636 (0.175)*	*0.887 (0.019)*
MT T-score	0.235 (0.543)	0.079 (0.840)	-0.040 (0.919)	0.011 (0.978)	0.272 (0.479)	0.006 (0.989)	0.962 (0.002)	0.924 (0.008)	-0.179 (0.734)	0.093 (0.861)	0.671 (0.145)	0.870 (0.024)
BUA (dB MHz^{-1})	0.319 (0.442)	0.303 (0.466)	*-0.454 (0.259)*	*-0.397 (0.329)*	*-0.11 (0.796)*	*-0.141 (0.737)*	*-0.620 (0.189)*	*-0.497 (0.316)*	*0.728 (0.101)*	*0.658 (0.155)*	*-0.866 (0.026)*	-0.780 (0.067)
BUA T-score	0.323 (0.436)	0.306 (0.461)	-0.452 (0.261)	-0.393 (0.336)	0.051 (0.904)	0.014 (0.974)	-0.585 (0.223)	-0.395 (0.438)	0.714 (0.111)	0.574 (0.233)	-0.832 (0.040)	-0.778 (0.069)
VOS (m s^{-1})	*-0.295 (0.441)*	*-0.33 (0.386)*	-0.297 (0.438)	-0.148 (0.703)	-0.487 (0.183)	-0.585 (0.098)	0.274 (0.599)	0.280 (0.591)	*-0.145 (0.784)*	0.040 (0.940)	0.153 (0.773)	0.150 (0.777)
VOS T-score	-0.216 (0.576)	-0.252 (0.514)	-0.296 (0.439)	-0.148 (0.704)	-0.487 (0.183)	-0.585 (0.098)	0.274 (0.60)	0.279 (0.592)	-0.076 (0.886)	0.040 (0.940)	0.152 (0.773)	0.149 (0.778)

The combination of the osteoarthritic samples from the same sample design and orientations improved the number of significant correlations achieved for the comparison between the fracture toughness parameters and the QUS investigations, with in particular the beam Ac samples providing a correlation with every QUS assessment. The results from the CUBA clinical system provided a number of significant correlations with all sample designs, orientation and fracture toughness parameters. The strongest correlations were seen between the J-integral values and either the BUA or its corresponding T-score; however the results from the disks orientated in the Ac direction were the inverse of the correlations seen with the other sample designs. The same inverse relationship is seen when the significant correlations from the VOS results of the CUBA clinical are compared with the J-integral values.

Of the Sunlight Omnisense investigations, the distal radius provided the greatest number of significant correlations, with the proximal phalanx also performing well, but in both cases the significant correlations were mainly between the beam samples and not the disks. The difference in the nature of the correlations seen in the BUA results is once again seen here with the disk Ac samples again showing the inverse of the relationship of the other three sample groups.

As with the compression testing results and the material properties (Section 8.10) vs. the QUS investigations, the greatest number and strongest results were seen when compared against the distal radius, calcaneal and mid-shaft tibia results. Although the results vary between the study group and the sample designs, it is clear that the ability of clinical QUS investigations to predict the density of the axial skeleton also enables the prediction of the mechanical properties due to the close link between the mechanics and the density of the material.

Table 8.44 Pearson's Correlations between the fracture toughness parameters from the beam samples and the age and QUS values obtain from the donor subjects for the OP and OA groups combined

OP + OA Beams	Beams AC						Beams AL					
	K_Q	K_C	J_Q	J_C	G_Q	G_C	K_Q	K_C	J_Q	J_C	G_Q	G_C
Age	-0.478 (<0.001)	-0.506 (<0.001)	-0.571 (<0.001)	*-0.539 (<0.001)*	-0.436 (<0.001)	-0.469 (<0.001)	-2.05 (0.092)	-0.321 (0.007)	*-0.653 (<0.001)*	*-0.639 (<0.001)*	*-0.045 (0.699)*	*-0.2 (0.10)*
DR SOS (m s^{-1})	0.281 (0.005)	0.275 (0.006)	-0.055 (0.597)	-0.090 (0.597)	0.267 (0.007)	0.264 (0.008)	0.369 (0.017)	0.375 (0.016)	*0.184 (0.251)*	*0.152 (0.343)*	0.359 (0.021)	0.357 (0.022)
DR T-score	0.388 (<0.001)	0.385 (<0.001)	0.897 (0.013)	0.017 (0.869)	0.339 (0.001)	0.342 (<0.001)	0.356 (0.022)	0.365 (0.019)	0.248 (0.119)	0.154 (0.338)	0.324 (0.039)	0.324 (0.039)
PP SOS (m s^{-1})	*0.235 (0.022)*	*0.224 (0.029)*	0.169 (0.108)	*0.134 (0.205)*	0.205 (0.046)	0.218 (0.034)	*-0.077 (0.630)*	*-0.071 (0.654)*	*0.055 (0.743)*	*0.077 (0.646)*	*-0.118 (0.475)*	*-0.114 (0.485)*
PP T-score	0.328 (0.001)	0.333 (0.001)	0.226 (0.032)	0.173 (0.098)	0.289 (0.004)	0.307 (0.002)	0.051 (0.758)	0.055 (0.742)	0.123 (0.454)	0.084 (0.611)	0.005 (0.976)	-0.001 (0.994)
MT SOS (m s^{-1})	*0.152 (0.149)*	*0.130 (0.221)*	*-0.161 (0.130)*	*-0.161 (0.130)*	*0.13 (0.218)*	*0.1 (0.339)*	*-0.063 (0.683)*	*-0.032 (0.885)*	-0.048 (0.764)	-0.025 (0.879)	*-0.084 (0.611)*	*-0.032 (0.845)*
MT T-score	0.087 (0.411)	0.065 (0.541)	-0.205 (0.054)	-0.207 (0.049)	0.061 (0.564)	0.044 (0.675)	-0.056 (0.726)	-0.040 (0.802)	-0.148 (0.356)	-0.099 (0.538)	-0.031 (0.847)	-0.021 (0.895)
BUA (dB MHz^{-1})	0.362 (<0.001)	0.397 (<0.001)	0.608 (<0.001)	0.621 (<0.001)	*0.288 (0.005)*	*0.311 (0.002)*	*0.214 (0.180)*	*0.179 (0.267)*	0.576 (<0.001)	0.425 (0.006)	*0.155 (0.332)*	*0.105 (0.515)*
BUA T-score	0.362 (<0.001)	0.398 (<0.001)	0.607 (<0.001)	0.621 (<0.001)	0.267 (0.009)	0.308 (0.003)	0.179 (0.264)	0.169 (0.291)	0.577 (<0.001)	0.425 (0.006)	0.112 (0.485)	0.100 (0.534)
VOS (m s^{-1})	0.197 (0.058)	0.228 (0.027)	0.431 (<0.001)	0.399 (<0.001)	0.152 (0.144)	0.187 (0.070)	*0.141 (0.378)*	0.102 (0.525)	*0.241 (0.128)*	*0.164 (0.301)*	*0.089 (0.587)*	0.042 (0.792)
VOS T-score	0.165 (0.112)	0.196 (0.058)	0.432 (<0.001)	0.373 (<0.001)	0.145 (0.162)	0.175 (0.089)	0.122 (0.449)	0.103 (0.524)	0.223 (0.160)	0.145 (0.366)	0.059 (0.714)	0.043 (0.791)

Table 8.45 Pearson's Correlations between the fracture toughness parameters from the disk samples and the age and QUS values obtain from the donor subjects for the OP and OA groups combined

OP + OA Beams	Disks AC						Disks AL					
	K_Q	K_C	J_Q	J_C	G_Q	G_C	K_Q	K_C	J_Q	J_C	G_Q	G_C
Age	*0.077 (0.670)*	-0.345 (0.049)	*0.577 (<0.001)*	*0.619 (<0.001)*	0.327 (0.068)	-0.213 (0.242)	-0.069 (0.688)	-0.427 (0.009)	*-0.614 (<0.001)*	*-0.626 (<0.001)*	*0.167 (0.330)*	-0.351 (0.036)
DR SOS (m s^{-1})	0.292 (0.157)	0.217 (0.297)	*-0.290 (0.160)*	*-0.205 (0.325)*	0.128 (0.552)	0.060 (0.782)	0.315 (0.125)	0.417 (0.038)	0.089 (0.665)	*0.130 (0.519)*	0.157 (0.455)	0.358 (0.079)
DR T-score	0.279 (0.177)	0.304 (0.139)	-0.339 (0.097)	-0.317 (0.123)	0.068 (0.753)	0.167 (0.435)	0.232 (0.264)	0.384 (0.058)	0.191 (0.350)	0.211 (0.290)	0.066 (0.753)	0.317 (0.123)
PP SOS (m s^{-1})	*0.3 (0.153)*	0.309 (0.142)	*-0.192 (0.371)*	-0.371 (0.074)	*0.197 (0.364)*	*0.217 (0.320)*	0.397 (0.055)	*0.564 (0.004)*	0.195 (0.350)	*0.219 (0.284)*	0.257 (0.226)	*0.436 (0.033)*
PP T-score	0.240 (0.259)	0.366 (0.079)	-0.182 (0.395)	-0.440 (0.031)	0.060 (0.785)	0.268 (0.216)	0.329 (0.117)	0.447 (0.029)	0.295 (0.152)	0.297 (0.140)	0.172 (0.423)	0.323 (0.124)
MT SOS (m s^{-1})	0.372 (0.074)	*0.249 (0.241)*	*-0.266 (0.207)*	*-0.259 (0.221)*	278 (0.199)	*0.190 (0.385)*	*0.390 (0.073)*	*0.449 (0.036)*	0.076 (0.731)	0.133 (0.536)	*0.221 (0.324)*	0.357 (0.103)
MT T-score	0.385 (0.063)	0.196 (0.358)	-0.204 (0.339)	-0.209 (0.326)	0.324 (0.132)	0.058 (0.792)	0.447 (0.037)	0.409 (0.059)	-0.067 (0.760)	-0.010 (0.964)	0.311 (0.159)	0.341 (0.120)
BUA (dB MHz^{-1})	*0.407 (0.048)*	*0.624 (0.001)*	-0.295 (0.162)	-0.652 (0.001)	*0.214 (0.328)*	0.523 (0.010)	-0.066 (0.760)	*0.276 (0.191)*	0.638 (0.001)	0.636 (<0.001)	*0.212 (0.319)*	*0.202 (0.341)*
BUA T-score	0.303 (0.150)	0.576 (0.003)	-0.292 (0.166)	-0.655 (0.001)	0.021 (0.923)	0.518 (0.011)	-0.064 (0.768)	0.262 (0.216)	0.639 (0.001)	0.637 (<0.001)	-0.201 (0.346)	0.163 (0.447)
VOS (m s^{-1})	*0.311 (0.139)*	*0.452 (0.027)*	*-0.295 (0.161)*	-0.574 (0.003)	*0.161 (0.466)*	*0.345 (0.106)*	0.018 (0.933)	0.247 (0.245)	0.345 (0.091)	0.350 (0.080)	*-0.148 (0.490)*	0.173 (0.418)
VOS T-score	0.288 (0.172)	0.409 (0.047)	-0.271 (0.200)	-0.575 (0.003)	0.131 (0.552)	0.284 (0.188)	0.018 (0.934)	0.247 (0.245)	0.347 (0.090)	0.351 (0.079)	-0.096 (0.654)	0.173 (0.418)

8.10 Material Properties vs. QUS

The results of the clinical aspect of this study demonstrated that there were significant correlations between the bone mineral density of the total hip and the clinical QUS investigation results. The aim of this section is to compare the material properties of the samples from the femoral heads with the results of the clinical QUS investigations.

Table 8.46 Pearson's correlation coefficients for the relationships between the averaged material properties of each osteoporotic individual vs. the clinical QUS results

Osteoporotic	$\rho_{App.}$	$\rho_{Mat.}$	Porosity
DR SOS (m s^{-1})	0.583 (0.009)	-0.236 (0.331)	-0.510 (0.026)
DR T-score	0.649 (0.003)	-0.288 (0.231)	-0.573 (0.010)
PP SOS (m s^{-1})	0.472 (0.041)	0.088 (0.720)	-0.399 (0.091)
PP T-score	0.516 (0.024)	0.077 (0.755)	-0.438 (0.061)
MT SOS (m s^{-1})	0.515 (0.024)	-0.522 (0.022)	-0.513 (0.025)
MT T-score	0.505 (0.028)	-0.553 (0.014)	-0.511 (0.025)
BUA (dB MHz^{-1})	0.552 (0.014)	0.173 (0.480)	-0.498 (0.030)
BUA T-score	0.555 (0.014)	0.198 (0.417)	-0.498 (0.030)
VOS (m s^{-1})	0.632 (0.004)	0.060 (0.806)	-0.586 (0.008)
VOS T-score	0.632 (0.004)	0.060 (0.806)	-0.586 (0.008)

The results for the osteoporotic individuals (Table 8.46) were surprising, with significant correlations seen between every QUS investigation which was performed and apparent density, with all bar the proximal phalanx showing equally good but inverted correlations with the porosity of the samples. The material density of the samples failed to provide any significant correlations, except with the mid-shaft tibia

which provide correlations of the same significance and strength as both the apparent density and porosity, although mimicking the porosity in nature.

The osteoarthritic samples were, however, not so well correlated with the material properties, but the low number of individuals within the osteoarthritic groups meant that the relationships had to be extremely strong in order for the correlations to appear strong and significant. The two QUS measurements which obtained significance were the SOS assessment of the distal radius and BUA of the calcaneus, with their corresponding T-scores.

Table 8.47 Pearson's correlation coefficients for the relationships between the averaged material properties of each osteoarthritic individual vs. the clinical QUS results

Osteoarthritic	$\rho_{App.}$	$\rho_{Mat.}$	Porosity
DR SOS (m s^{-1})	0.911 (0.002)	-0.557 (0.151)	-0.900 (0.002)
DR T-score	0.797 (0.018)	-0.498 (0.209)	-0.786 (0.021)
PP SOS (m s^{-1})	0.302 (0.467)	0.373 (0.363)	-0.223 (0.596)
PP T-score	0.313 (0.451)	0.335 (0.417)	-0.232 (0.580)
MT SOS (m s^{-1})	0.263 (0.570)	-0.201 (0.665)	-0.255 (0.580)
MT T-score	0.210 (0.651)	-0.182 (0.696)	-0.207 (0.655)
BUA (dB MHz^{-1})	0.852 (0.031)	-0.053 (0.920)	-0.795 (0.059)
BUA T-score	0.853 (0.031)	-0.045 (0.933)	-0.794 (0.059)
VOS (m s^{-1})	-0.164 (0.725)	0.440 (0.324)	0.179 (0.701)
VOS T-score	-0.164 (0.725)	0.440 (0.323)	0.179 (0.701)

Concluding Remarks

The results of this study demonstrate that the K and G fracture toughness of cancellous bone is governed predominantly by the apparent density of the material. This, however, is not exclusive, and a large percentage of the variation in the fracture toughness of cancellous bone can be attributed to the composition and particularly the condition and integrity of the collagen network. The J-integral for the cancellous bone material behaves very differently to the other material parameters, in that it would appear not to be governed by the apparent density as strongly as the K and G values, and that the composition and possibly the structure of the bone have more pronounced effects, although this could not be proved conclusively within this study as no investigations into the structure were performed.

The two different conditions that were investigated within this study have distinctly different effects on the cancellous bone of an individual. In osteoporosis it was found that, as expected, the apparent density of the bone was reduced, and the porosity was increased, whereas the osteoarthritic bone had a far higher apparent density than might normally have been expected. The composition of the bone within the two different conditions was also distinctly different, with the mineral content of the osteoarthritic bone being significantly lower than that of the osteoporotic bone, and the organic content being significantly higher. The same variation was seen in the collagen cross-linking within the bone of the two conditions; there were significant differences in the levels of the immature cross-links HLKNL and HLNL, but not in the mature cross-links, reflecting the increased bone metabolism which occurs in the conditions.

The basis behind the use of the QUS investigations to predict the mechanics of the bone at the femoral head was that QUS has been proven both in this study and in previous studies to have the ability to predict density at the axial skeleton. The hypothesis was that the strong relationship between the density and the fracture risk would be displayed in the relationships between QUS and the fracture mechanics. However, this was not the case and the relationships were, on the whole, quite poor. The fact is that whilst density may be the dominant factor, it is not the only factor and the QUS investigations may not be affected by the same variables as the fracture mechanics. In addition to this, the nature of the bone investigated by the Sunlight Omnisense system is different to that which was mechanically tested in this study; and in all the QUS investigations the measurements were from peripheral skeletal sites which in the case of the Sunlight Omnisense two of the three investigation sites could be considered non-load bearing (distal radius and proximal phalanx). This does not detract, however, from the fact that there were strong and significant correlations despite these error sources and the small population cohorts would indicate that this is a field which requires greater research.

Chapter 9: Discussion

9.1 Clinical Work Discussion

9.1.1 Introduction

The aims of the clinical work were to investigate the abilities of a number of different techniques to predict the DXA derived skeletal condition. The techniques under investigation were the osteoporosis risk factor questionnaires, ORAI, (S.M. Cadarette et al., 2000), OSIRIS (W.B. Sedrine et al., 2002), OST (L.K.H. Koh et al., 2001), pBW (K. Michaëlsson et al., 1996a), SCORE (E. Lydick et al. 1998), SOFSURF (D.M. Black et al., 1998); and two quantitative ultrasound systems with the capability between them to measure four peripheral skeletal sites. The work was performed not only to investigate the predictive abilities alongside the questionnaires, but also into the precision of the QUS systems and the relationship between skeletal sites. It is important to note that this study has not set out to find a replacement for DXA, but merely to find a suitable screening tool or screening strategy which would offer the clinician a more reliable referral criteria than is available currently.

The novel aspects within this area of the study are based around the comparison of all the questionnaires and the quantitative ultrasound results, in relation to the results provided by DXA. The comparisons have been performed previously within the literature but mainly on individual techniques; to the author's knowledge a wide scale review of the abilities in relation to each other within the same study cohort has not been attempted previously.

9.1.2 Precision Study

The reasons the precision study was performed were threefold; the first was that it enabled a comparison between the QUS systems and the measurement parameters both within the study and to the literature. The second was that it enabled the operator to gain experience of using the systems, and to ensure that in doing so the skill that was acquired was of a level acceptable to the manufacturers. The third was that by performing the initial precision study it was possible to monitor the quality of the investigations that were performed within the clinical environment that make up the large body of the results.

The precision of the two QUS systems and more specifically between the VOS/SOS results and the BUA results was discernibly different. The CV% results and the $_{RMS}$CV% results indicated that the level of BUA precision was inferior to that of the SOS and VOS results, for reasons highlighted in section 4.8.2.1. The determination of the $_{S}$CV%, which takes into account the magnitude and ranges of the measurement values, displayed a very different picture. The results of the $_{S}$CV% analysis demonstrated that the precision of BUA was, in fact, superior to that obtained for SOS at any of the three sites investigated by the Sunlight system, and depending on the study group was either inferior to or superior to the VOS results from the same CUBA device.

The initial precision study results on the individuals from group 1 were shown in table 7.1. For the Sunlight Omnisense system the distal radius and the proximal phalanx both displayed $_{RMS}$CV% that were better than the precision errors of the manufacturers' guidelines (table 4.10). However the precision error achieved for the CUBA Clinical system was ~1.5% below the standards set by the manufacturers, and the results for group 2 (table 7.2) were worse. The levels of precision that were achieved

were inferior to those that had been achieved in group 1 and in both the Sunlight Omnisense and the CUBA Clinical the levels of precision were inferior to the manufacturers' guidelines.

9.1.2.1 Alternative Error Sources

In both groups 1 and 2 the precision of the CUBA device was worse than the levels expected by the manufacturers, and the level of precision of the Sunlight system was also inferior when used in the clinical environment. Two possible sources of precision error were introduced in section 4.8.2.1, the first being repositioning and the second excess soft tissue or oedema.

Repositioning

Repositioning is a potential source of error for both the Sunlight and the CUBA systems. The Sunlight Omnisense's ROI selection method, of placing a mark on the patient's skin, ensures repeat measures are performed on the same area, reducing one source of repositioning error; however the system is 'operator dependant'. In order to perform a measurement, the operator is required to pass the probe over the measurement site in a controlled arc or path at roughly the same speed, any variation in arc length, speed of the probe movement or rotation of the probe head could potentially affect the results. The author believes this inherent potential for human error is the main source of the error for the Sunlight Omnisense results.

Before the study was undertaken, repositioning for the CUBA system was known to be a potential source of error and attempts were made to ensure the repositioning of the individuals was as close to the previous alignment as was possible. However, with small movements being shown to have effects of up to 9.2% (W.D.

Evans et al., 1995), the repositioning within this study must still be considered to have contributed to the precision error.

Oedema and Excess soft Tissue

The second potential source of error was either oedema or excess soft tissue at the measurement site. In the case of the study subjects for group 1, none of the individuals could be considered to have oedema or excess soft tissue, although it was more of an issue in group 2, as the BMI and weight values demonstrate in table 5.1

The effect of these two conditions on the Sunlight system is partly catered for by the system itself. In order for a measurement to be taken the probe has to be placed into close proximity to the bone at the measurement site. If the system adjudges that the distance is too great, it will not register a measurement as being performed. This feature of the system has its downsides; in a number of cases the probe was able to detect the bone beneath the surface, but only for a small portion of the arc over the measurement site. Although not a potential source of precision error, the resultant measurement was able to be completed with an impaired picture of the bone, as only a small area was investigated. This effect was found by the operator to occur mainly at the distal radius and the mid-shaft tibia, with the proximal phalanx measurement normally remaining free of this problem.

For the CUBA Clinical device this source of error was found to affect both groups. After the precision testing on group 1 had been performed, a potential source of error was highlighted via personal communication with McCue Plc. During the settling period and the measurement process a small force is applied to either side of the calcaneus, this ensures a good contact between the transducers and the skin, but in doing so compresses the surrounding soft tissue. This means that by the end of the

fourth of the quadruple measurements in group 1, and even after the first measurement on group 2, the resultant value is from a pulse that has travelled a shorter distance and through less soft tissue. With the potential effect of oedema on BUA being 14.2% (A. Johansen et al., 1997) the author considers this to have been a significant source of precision error.

The results of both of the studies provide a $_{RMS}$CV% level of precision which despite conflicting with the manufacturer's guidelines, is within the range that has been published previously by different study groups using the machines (tables 4.11 to 4.16). For the Sunlight Omnisense results, even the worst $_{RMS}$CV% errors obtained within group 2 for the proximal phalanx (1.06%) were within the range of the previous studies (0.2% - 1.22%), and at the distal radius and the mid-shaft tibia the level of precision achieved (0.48% and 0.74% respectively) were comparable to the average of the precisions presented in the literature (0.6% and 0.49% respectively).

For the CUBA Clinical the CV% and the $_{RMS}$CV% precision errors for both the BUA and the VOS were well below the average precision (5.52% and 4.52% for BUA and 0.75% and 0.42% for VOS) for the previous studies which utilised the CUBA system (W.C. Graafmans et al., 1996, J.C. Martin and D.M. Reid, 1996, S.L. Greenspan et al., 1997, C.F. Njeh et al., 2000, A. Stewart and D.M. Reid, 2000a), and were either comparable to or superior to the results from other calcaneal QUS systems.

It is clear from these results that the precision of QUS has the potential to be very high, when used in a controlled environment on well informed and normal individuals. The use of these QUS systems in reality is in situations that are far from perfect; the subjects are of all shapes and sizes from the general public, and the investigations are performed in a time restricted clinical environment. The effects of this

can be clearly seen between groups 1 and 2 within this study, with the precision error obtained for group 2 being inferior to that which was obtained for the normal subjects of group 1.

The results of the precision studies, both within this study and from the literature, give a clear demonstration of the reasons behind QUS being considered unable to monitor skeletal changes. With the annual changes within the skeleton being within the region of 0.5 - 2% in women depending on their menopausal status (C. Christiansen, 1995, C.M. Bono and T.A. Einhorn, 2003), and 0.3% in men (C.M. Bono and T.A. Einhorn, 2003), the amount of bone loss that could occur before QUS could be considered to have detected a significant difference renders it unsuitable. However this study has not set out to monitor skeletal changes, but to assess the diagnostic abilities and information contained within QUS investigation results for the prediction of the DXA derived condition of the axial skeleton.

9.1.3 Discriminatory Ability

The discriminatory ability within this study was investigated graphically and, by using Kappa indices, to provide a qualitative and quantitative demonstration of the agreement between techniques of the breakdown of the study population into the three classification groups.

9.1.3.1 Kappa Indices

The Kappa indices showed a range of results depending on the systems and sites being investigated. The best levels of agreement were seen between the results of the Sunlight system in group 1, with the Sunlight combined results in good or moderate

agreement with the distal radius (0.68) and mid-shaft tibia (0.5) results, although only fair for the proximal phalanx (0.24) and the agreement between the individual sites (0.12 - 0.19). This fair level of agreement was mimicked by the relationships between the lumbar spine and total hip DXA results (0.317 – 0.327), as well as between the VOS and the manufacturer's BUA results (0.18) from the CUBA system, with the agreement between the VOS and BUA results using the WHO guidelines classified as poor (0.001).

The comparisons between the QUS systems and DXA failed to perform any better and no results achieved any better than a fair level of agreement (>0.40) with the best agreement observed between the total hip result and the BUA calcaneus result using the WHO threshold, (group 1: 0.25, group 2: 0.208). It was noticeable that the WHO guidelines for the BUA results provided a better level of agreement with the DXA results than the manufacturer's guidelines. The strongest results for the comparison with DXA were found using the questionnaire systems, where all the Kappa index values that were obtained were better than those of the QUS systems. ORAI provided the best agreement with the total hip results (0.38), while SOFSURF was best in relation to the lumbar spine (0.325).

The better Kappa indices provided by the questionnaire systems for their agreement with DXA, compared with those of the QUS systems is mainly due to the nature of their calculation and origin. Their design and risk factor selections were maximised during their development for the sole purpose of predicting the DXA result, whereas the QUS investigations were designed to assess and diagnose the condition of a specific skeletal site irrespective of what might be occurring at the axial skeleton. Despite providing higher Kappa indices, the questionnaires are still within the fair

category of agreement, somewhat surprising considering their development. There are two potential reasons why the performances of the questionnaires were below what might have been expected. The first relates to the development studies of SOFSURF, (D.M. Black et al., 1998) SCORE, (E. Lydick et al., 1998) and OST (L.K.H. Koh et al., 2001) which were maximised for the prediction of DXA of the proximal femur and more specifically in the development of the SCORE and OST questionnaires the femoral neck; the other questionnaires were all developed using a combined DXA result which including the lumbar spine and the proximal femur. The second reason was the DXA T-score the questionnaires were developed to predict; in the development of the SCORE (E. Lydick et al., 1998) and ORAI (S.M.Cadarette et al., 2000) questionnaires, the DXA T-score the risk factors were predicting was set at -2 and not -2.5 as in the other studies. Both potential sources of irregularity in the results might explain the disagreement between the DXA and the questionnaire results; however questionnaire specific abnormality is not evident in the results.

9.1.3.2 Graphical Representations

The graphical representation of the discriminatory abilities goes some way to explaining the Kappa index results that were achieved. It is clear that the worst performing of all the investigations in comparison to DXA, the VOS results from the CUBA clinical system, are heavily over pessimistic with 80.1% of the individuals in group 2 and 70.7% of individuals from group 3 all being classified as osteoporotic. The BUA from the same system mimics these pessimistic results when using the manufacturer's guidelines, but reveals a much more realistic trend when the WHO guidelines are used. The opposite end of the scale is the proximal phalanx assessment

from the Sunlight system, which classified 81.3% of the group 2 individuals and 78.4% of the group 3 individuals as normal.

For the other measurement results and the questionnaire systems, the numbers within each of the classifications are very similar, although the questionnaire systems and the other Sunlight system results are all slightly optimistic in their classification. This gives rise to the question, why are the Kappa indices so poor? The reason is that although the numbers from each technique are the same, the individuals are different. One individual could be classified as osteoporotic using the BUA investigation, but osteopenic by their DXA result, and normal in relation to their proximal phalanx result; this highlights the previously mentioned problem that the human skeleton is not homogeneous in its condition at every site.

The Kappa indices calculated within this study for both groups 2 and 3 are in agreement with those in table 4.23 which shows the Kappa indices from previous studies within the literature. The results from C.R. Krestan et al. (2001) and I. Lernbass et al. (2002) were slightly superior to those achieved here, but were achieved using a different QUS system than in this study; the results from the study by A. Stewart and D.M. Reid (2000) who used the CUBA Clinical system, as in this study, found results that were comparable magnitude to those of this study. Unfortunately there is a lack of information within the literature with reference to the Kappa values for the Sunlight system and corresponding DXA values, but by using a different system to investigate the tibia, K.I.I. Kim et al., 2001 provided results that were superior to those achieved here.

With regards to the relationships seen in this study, both K.I.I. Kim et al., (2001), J. Damilakis et al., (2003b), showed similar optimistic trends within

investigations of the radius, phalanges and tibia with respect to investigations performed by DXA. The calcaneal BUA relationship to DXA was in agreement with I. Lernbass et al. (2002) as were the VOS results with V. Naganathan et al. (1999) who both demonstrated a pessimistic trend. However these were in contrast to the studies by A. Stewart and D.M. Reid (2000) and V. Naganathan et al. (1999) who showed optimistic trends for BUA, and I. Lernbass et al. (2002) and A. Stewart and D.M. Reid (2000) who showed optimistic results for VOS.

The variation of the relationships in comparison to the literature for the VOS calcaneal assessment results can be easily explained. It is clear from these results that the database within the CUBA Clinical system used in this study for calculation of the VOS T-score results is incorrect, and is providing much lower T-score values than required, and is therefore a source of bias that is affecting the results. The BUA results are harder to explain. The study by I. Lernbass et al. (2002) used a different technique, and a significantly smaller study group which may explain the differences, but the studies by V. Naganathan et al. (1999) and A. Stewart and D.M. Reid (2000) both used the same CUBA Clinical models in their investigations, and had population demographics which were similar to those used here. The differences in the studies were in the origins of the individuals recruited in the studies, the DXA system used by A. Stewart and D.M. Reid (2000), but mainly that the two studies included the femoral neck DXA results in their studies which were not considered here.

9.1.4 Inter-site Correlations

The inter-site correlations are the most published result with respect to the study of QUS and its relationship to the axial skeleton. They were included in this study not only for completeness, but also because very few studies, if any, have attempted to

investigate the correlations between the Questionnaire systems and either the QUS system results or the results from the DXA investigations. The difference between the Pearson's correlation results and the Kappa indices and analysis of the previous section is that it does not compare the paired results individually with relation to specific thresholds, but uses the relationship between each individual pair of results to form a linear relationship between the two techniques.

Not surprisingly, as all of the questionnaire systems use both age and weight as two of the most predictive risk factors in their calculations, with the obvious exclusion of pBW, the different questionnaire results are in close agreement with each other. The inter-questionnaire correlations are however not perfect due to the weightings of the variables and the additional risk factors used in certain questionnaires.

The Pearson's correlations between the questionnaires and the QUS results were highly significant ($p < 0.001$), with the exception of the mid-shaft tibia which failed to achieve significance in 4 out of the 6 correlations. The best correlations between the questionnaires and the QUS results were with the BUA results from the calcaneus ($r = 0.233 – 0.594$), followed closely by the SOS results at the proximal phalanx ($r = 0.220 – -0.574$), then the SOS from the distal radius ($r = 0.112 – -0.474$), VOS from the calcaneus ($r = -0.028 – -0.438$) and lastly the mid-shaft tibia ($r = -0.087 – -0.157$). The level of correlation could be considered moderate in most cases but approaching good for the comparison with BUA and both OSIRIS and SOFSURF.

The correlations between the questionnaire results and the DXA results provide a range of moderate and good correlations ($r = 0.330 – 0.658$), all of which were highly statistically significant ($p<0.001$). The correlations of the questionnaires with the results of the total hip ($r = 0.492 – 0.658$) are all greater than those seen for the lumbar spine (r

= 0.330 – 0.508), with OSIRIS and OST providing the highest correlations, r = 0.658 and r = 0.633 respectively. The same potential sources of error for the questionnaires (9.1.3.1), related to the DXA site and the DXA T-score level they were design to predict, apply with these results and may account for the improved correlations that were achieved between the OST, SCORE and SOFSURF questionnaires with the total hip in relation to those that were obtained versus the lumbar spine.

Only two previous studies have presented correlations between the questionnaire results and any skeletal investigation techniques; M. Ayers et al., (2000) provided correlations between SCORE and DXA of the lumbar spine (-0.33), femoral neck (-0.51) and total hip (-0.52) and A.W.C. Kung et al., (2003) provided correlations between OST and DXA of the femoral neck (0.62) and lumbar spine (0.49). The magnitudes of these correlations are in close agreement to those within this study and noticeably display better correlations between the questionnaire results and the proximal femur than the questionnaire results and the lumbar spine as seen in this study.

The correlations between the QUS investigations and the DXA results from both groups 1 and 2 all showed a high level of significance ($p<0.001$), with the exception of the relationship between the total hip and the mid-shaft tibia, within group 2 ($p = 0.070$). For the Sunlight Omnisense system the proximal phalanx provided the best correlations with the axial skeleton providing correlations of r = 0.318 and r = 0.340 with the lumbar spine and total hip respectively. The distal radius was second with correlations of r = 0.309 and r = 0.275 with the lumbar spine and total hip respectively, and the proximal tibia was third with correlations of r = 0.228 and r = 0.161 with the lumbar spine and total hip respectively. In comparison to the correlations within the literature shown in tables 4.18 to 4.21 the proximal phalanx correlations of

this study were comparable to the average correlations between the sites (Lumbar Spine: r = 0.35, Total Hip: r = 0.38) but both the distal radius (Lumbar Spine: r = 0.38, Total Hip: r = 0.36) and the mid-shaft tibia (Lumbar Spine: r = 0.39, Total Hip: r = 0.29) correlations from the literature were superior to those which were achieved in this study. The correlations between the lumbar spine and total hip DXA with the questionnaire systems were in fact better than those that were achieved with the Sunlight Omnisense system, with even the pBW results correlating better at the hip (r = 0.492) than any of the Sunlight systems investigations.

The level of correlations between the BUA and VOS results of the CUBA Clinical with the DXA results from the lumbar spine (BUA r = 0.527 - 0.568, VOS r = 0.473 - 0.481) and total hip DXA results (BUA r = 0.637 – 0.650, VOS r = 0.519 - 0.535) were consistently better than those of the Sunlight system with the DXA results and comparable to the questionnaire results in relation to the DXA results. The correlations between the calcaneal BUA results and either the lumbar spine or Total hip were at the top of the published range from within the literature (r = 0.26 - 0.83 and r = 0.31 - 0.68 respectively), as were the VOS results (r = 0.11 - 0.64 and 0.3 - 0.62).

The lack of strong correlations between the Sunlight Omnisense investigations and the DXA results is not due to the study demographics, as all the investigations were from the same study group, but due to the measurement sites it is used to investigate, and the nature of the ultrasound investigation itself. The Sunlight system uses an axial transmission method for the determination of the SOS through bone, meaning that the investigations are performed on areas of cortical bone. Although it has been shown that osteoporosis affects the cortical bone by thinning the outer cortex (C.M.Bono and T.A.Einhorn, 2003), the results within this study are correlations with either the lumbar

spine or the proximal femur, both of which are sites consisting mainly of cancellous bone. In addition to this, both the proximal phalanx and the distal radius are peripheral skeletal sites that can be considered to be non-load bearing, whereas the spine and proximal femur both undergo significant loading during the normal everyday physiological usage. The stronger correlations seen between the questionnaires and the axial skeletal sites are due to the reasons outlined in the previous sections, in that they have been developed and maximised specifically for the purpose of correlating with, and agreeing with, the condition of the axial skeleton. The CUBA clinical system is the opposite to the sunlight system, in that the site of investigation at the calcaneus is a load bearing site consisting of mainly cancellous bone, and as such the results provide a closer link to the spine and the proximal femur than the Sunlight Omnisense investigations. The importance of these correlations, and the fact they are significant in their nature, has little use within the clinical environment but serves to support the growing body of evidence that both the questionnaire systems and the QUS systems can predict the condition of the skeleton.

9.1.5 Diagnostic Ability

The investigation of the diagnostic ability enabled a direct comparison between the different questionnaires and QUS techniques with relation to their abilities to predict the condition of the axial skeleton. In virtually all of the questionnaire and QUS investigations from either of the study groups, the ability to predict a DXA T-score of -2.5 provided a higher AUC and therefore level of ability than they did when used to predict a T-score of -1. In addition to this the AUC values and diagnostic abilities were

noticeably higher when predicting the total hip as an individual site, than either of the other two investigations that were predicted for (DXA combined and Lumbar spine).

The results for both groups 1 and 2 show the abilities of the QUS systems with relation to DXA, with the BUA and the VOS results of the CUBA clinical system consistently providing either a moderate, good or in one case an excellent level (BUA vs. total hip AUC = 0.95) of diagnostic ability, and outperforming any of the Sunlight Omnisense investigations which, although providing one excellent level of ability (Sunlight combined vs. total hip AUC = 0.918), were mainly poor in their diagnostic ability. As mentioned at the end of the previous section, this is most likely due to the nature of the ultrasound technique used, the type of bone investigated and the peripheral, non-load bearing sites that were investigated.

The relationship between the results found in this study for the Sunlight Omnisense system measurement sites and those of previous studies shown in table 4.27 are very close. The Sunlight system has only been reported in one other study (J. Damilakis et al., 2003b) and the AUC results for both the proximal phalanx and the distal radius were almost identical when predicting for a T-scores of -2.5 or -1 at any axial skeletal site. It is of note that the alternative system for the investigation of the phalanges, the DBMSonic 1200 (IGEA, Carpi, Italy) which uses a transmission ultrasound method, provided far better AUC values (0.8-0.82) (J. Joly et al., 1999 and J.Y Reginster et al., 1998), out performing the Sunlight phalangeal investigations of both this study and the previous study (J. Damilakis et al., 2003b).

The range of BUA AUC results in this study obtained using the CUBA clinical (0.783 – 0.950), was virtually identical to the range of those seen previously in the literature (Table 4.24) for the prediction of osteoporosis irrespective of the axial skeletal

site for the CUBA clinical (0.76 – 0.90); as was the average AUC result for the prediction of osteoporosis in this study (0.831) compared to the CUBA clinical (0.825). However, in comparison to the average AUC of all the calcaneal investigation techniques together (0.798), the performance of the CUBA clinical is better. The AUC result for the prediction of a DXA T-score of -1 within this study ranged from 0.755 to 0.821 and averaging 0.791, better than either the previous CUBA clinical results from the literature (Range: 0.688 to 0.773, average: 0.74), and also the other calcaneal QUS devices (Range: 0.688 to 0.799, average: 0.769).

The VOS results of this study for the prediction of osteoporosis, irrespective of site and study group, provided a range of AUC results from 0.74 - 0.809, similar to the range from the literature (Table 4.25) for both the CUBA Clinical (AUC = 0.717 – 0.871) and the other calcaneal devices (AUC = 0.662 - 0.871), although the average AUC (0.766) was ever so slightly below the average AUC for the CUBA from the literature (0.803) and the AUC results from all the calcaneal devices (0.75). The volume of previous studies which have presented AUC results for calcaneal VOS prediction of a DXA T-score of -1 is small, however three of the four studies available used the CUBA Clinical providing a range of 0.68 to 0.783 at an average of 0.73, only slightly better than that which was achieved in this study (Range: 0.668 - 0.754, average: 0.718).

The consensus from the NOS (2002) on the use of QUS is that it may not be used to diagnose osteoporosis because the guidelines for the diagnosis of osteoporosis are based on DXA of the axial skeleton and the AUC results, Pearson's correlations and Kappa index results for a number of the investigations would support this. The study investigated purely the relationship to the axial skeleton, which due to the differences in the type of bone investigated, and the nature and position of the investigation sites is not

what the Sunlight system is best suited to do. However, the Sunlight investigations used in combination with one another provided both good and excellent (AUC: 0.843 – 0.918) results with respect to the total hip, and if the Sunlight system was used to predict the status of the forearm, a common area of osteoporotic fracture, the abilities may be significantly improved.

The diagnostic abilities of the CUBA Clinical system were considerably better than those of the Sunlight Omnisense system; the AUC results were mostly only moderate, although on the border line with the good classification. However, the performance of the BUA results with respect to the prediction of osteoporosis at the hip was the highest of any other investigation that was performed and even out performed the relationship between the DXA sites. This gives clear and strong support to the idea that calcaneal QUS assessments could be used to screen populations, with the ability of QUS extending beyond the prediction of the axial skeleton and provided a unique insight into the fracture risk of an individual (section 4.8.2.5) that in many cases is superior to that provided by DXA; the results of a screening scan from a calcaneal QUS device provide a significant amount of information on a patient's condition.

The only issue with the potential use of QUS as a screening method is related to the cost effectiveness of the technique, which unfortunately was not investigated in this study, but has been previously. The studies were, however, in disagreement, with the early studies by C.M. Langton et al. (1997, 1999) concluding that QUS was a cost effective method, while more recent studies by F. Marín et al. (2004) and M.F.V. Sim et al. (2005) found QUS not to be cost effective.

Questionnaire techniques have an advantage in one respect; their costs can be considered to be negligible. Although the questionnaires were consistently out

performed by the calcaneal BUA results, they possessed moderate levels of diagnostic ability with respect to the DXA combined and lumbar spine results (0.70 – 0.80), with the exception of pBW which could only manage poor diagnostic ability (0.60 – 0.70). However, as with the QUS results, the diagnostic abilities of the questionnaires to predict the total hip DXA results were notably improved, with good levels of ability obtained by every questionnaire including pBW for the prediction of a total hip DXA T-score of -2.5 (AUCs = 0.808 – 0.868), with high moderate and good diagnostic abilities for the other total hip DXA T-score thresholds results (AUC = 0.765 - 0.868). The magnitudes of the AUC results were in agreement with and slightly superior to the previous results within the literature (Tables 4.5 to 4.9).

The comparison between the different questionnaires based on the AUC results of the three different DXA thresholds and the three different sites (DXA combined, total hip and lumbar spine), would suggest that in order of ability, the questionnaires rank OSIRIS then OST, with SCORE and SOFSURF being hard to distinguish between, then ORAI and lastly pBW. These are in contrast to the only previous studies which offered any direct comparisons between the systems, and considered ORAI and SCORE to be equal (S.M. Cadarette et al., 2001), or SCORE to be superior to both OSIRIS and OST (F. Richy et al., 2004).

The disadvantages of the questionnaires as screening tools are that they are geared and developed for peri- and postmenopausal females which despite making up the largest proportion of the individuals requiring investigation, fail to take into consideration premenopausal women and male subject groups, or any younger individuals who suffer from the conditions that are listed in table 4.1 for the potential causes of secondary osteoporosis.

9.1.6 Threshold Selection

The premise behind performing the threshold selection element of this study was to attempt to find a particular threshold for each system, be it a questionnaire or a QUS investigation, which enabled the differentiation of individuals into those requiring further investigations, and those who did not. The three different methods that were investigated provided different outlooks on the differentiation method:

i). With the "best accuracy" ensuring as many patients as possible were correctly referred or excluded.

ii). The "best sensitivity and specificity" ensuring that cases of misdiagnosis were evenly split between the false negatives and false positives, while keeping incorrect referrals to a minimum.

iii). The "90% sensitivity method" ensured that the referral of as many as possible of the individuals whose DXA T-score was below the threshold level was correct.

In the process of doing the three sets of analysis it was clear that the nature of the screening tool that was required was important, and that the 90% sensitivity method which ensured that individuals with the condition were correctly selected was the preferred method. The results of this selection method varied depending on the DXA T-score level that was being predicted, with the number of misdiagnoses increasing, as the T-score that was being predicted was lowered, with the number of false negatives increasing as the threshold was reduced from -1 DXA T-score level to a DXA -2.5 T-score level. The author is not a clinician and is therefore not in the position to provide an insight into the levels at which an individual should require intervention by either hormone or drug therapies, but it would appear from these results that utilising the systems to differentiate between individuals with either osteopenia or osteoporosis from

normal, by predicting a DXA T-score of -1 provides the best screening strategy. This is, however, in contrast to the results of the diagnostic ability which showed that the diagnostic abilities of all the questionnaires and QUS investigations were better at predicting a DXA T-score of -2.5 than a DXA T-score of -1 for most sites. This may be due to the nature of the study cohort make-ups which contain a larger number of normal individuals than it does osteoporotic individuals, which may be affecting the results when examined at the different levels.

For the QUS systems the thresholds that are presented here have an additional advantage when being considered with respect to the number of incorrect referrals, any false positive results should in effect not be considered to be false positives. Section 4.8.2.5 of the literature review in this study clearly highlights that individuals with a reduced QUS result are at increased risk of fracture, so any individual who has no densitometry measure previously performed, but who receive a low QUS result, should be considered as at risk.

The thresholds that were developed for the questionnaire systems are very different depending on which of the threshold selection methods were used. The thresholds that were achieved for the best sensitivity and specificity method were very closely linked to those shown in table 4.4 and were values in the middle of the risk indices ranges. In contrast there was a marked difference in the threshold values obtained for the 90% sensitivity method in relation to those published in the literature for the techniques. This finding is quite surprising considering that the development studies by, K. Michaëlsson et al. (1996a), E. Lydick et al. (1998), S.M. Cadarette et al. (2000), L.K.H. Koh et al. (2001), and F. Salaffi et al. (2005) all provided cut-off values which demonstrated a 90% sensitivity. One explanation for the difference would be the

nature of the study populations, although most of the thresholds were either based on a Caucasian population as in this study or had been adapted previously to account for the differences in ethnicity. Another explanation involves an issue highlighted previously in the discussion on the Kappa indices (section 9.1.3.1), but also in later sections, and relates to the nature of the questionnaire's development, with different DXA investigations sites predicted for and also different T-score levels.

For the Sunlight Omnisense systems thresholds, the range within this study is discernibly different from both the manufacturer's recommended levels and the levels suggested by K.M. Knapp et al. (2004). These thresholds were designed with the purpose of diagnosing osteoporosis at the investigation sites, by ensuring the percentage of the study populations who were suffering from osteoporosis and osteopenia were identical to those for the DXA investigations of the axial skeleton. The thresholds that were provided for the diagnosis of osteoporosis and osteopenia were -2.6 and -1.4, -3.0 and -1.6, -3.0 and -2.3, for the distal radius, proximal phalanx and mid-shaft tibia respectively. When these thresholds were used for the differentiation of group 3 the results were poor, only 10 patients out of 45 were correctly diagnosed as osteoporotic using the distal radius with only 3 out of 45 correctly diagnosed at the proximal phalanx and the mid-shaft tibia. The same problem is demonstrated using the cut-off levels for osteopenia with only 57, 21 and 14 out of 144 patients being correctly diagnosed at the distal radius, proximal phalanx and mid-shaft tibia, respectively.

When the thresholds were used as they were supposed to be for the division of a population into three groups, so that the percentages of the populations within the groups matched those of the axial skeleton, the distal radius thresholds divided the study population neatly into three groups of the expected prevalence; however, the results for

both the mid-shaft tibia and proximal phalanx were not so good with the prevalence of osteoporosis in each case being far too low. The results of the threshold investigations in the study by K.M. Knapp et al. (2004) were produced to ensure the correct prevalence of osteoporosis was seen at each measurement site, so as to match the DXA determined prevalence. Therefore the thresholds K.M. Knapp et al. (2004) provided are very different to those which are required if the systems are to be used for the screening of a population with respect to DXA, as determined in this current study.

The threshold level analysis within the CUBA clinical system for the VOS results, provides results which are over and above those of the other systems with relation to ensuring the minimal number of misdiagnoses; however, the nature of the database within the CUBA system within this study means that comparisons with the literature are not feasible.

The threshold analyses results with respect to the BUA of the CUBA clinical system showed it to be the best system in its ability to reduce the numbers of misdiagnosed patients. A threshold of -1.5 and -2 was obtained for both the 90% sensitivity and best sensitivity and specificity determination methods. This value is in close agreement with the previous studies within the literature; the study of note is by C.M.Langton et al. (1999) who recommended a threshold of 63 dB MHz^{-1}, which equates to a T-score of between -1.58 and -1.64. The other T-score thresholds which have been suggested, but for different systems were either -1.61 or -1.45 (M.L.Frost et al. 2000) or -1.3 (J. Damilakis et al. 2001), all of which are in close resemblance to the threshold within this study.

The apparent superior performance of the techniques for the prediction of DXA T-scores below -1 is due to the nature of the study population. The numbers of

individuals within the population that have a DXA T-score of below -2.5 at any site, are far fewer than those who have a T-score of less than -2, and even fewer than those with a T-score below -1, as the previous group is included within the numbers. The effect is that when the prediction is attempted at a DXA T-score of -1, the number of potential false negatives is increased, but by using the 90% sensitivity method the larger group is ensured of correct diagnosis, and hence the number of misdiagnoses seen in the DXA T-score -1 prediction is lower than that for the DXA -2.5 T-score prediction.

9.1.7 Screening Strategy

As mentioned previously the screening strategy investigation was performed at the request of a member of the peer review process for the study published in Osteoporosis International. (R.B.Cook et al. 2005). The screening strategies were designed to enable the calculation of the lowest DXA T-score an individual is likely to obtain, using the QUS and Questionnaire results. The resultant value of the regression would enable the clinician to make a referral, with a higher degree of confidence than they would have had if they had used the referral criteria laid out by the different study groups (table 4.3).

The variables that are used within the equations are those which provide the greatest predictive ability of the DXA T-score and as such the variables that were selected are in keeping with the results of both the inter-site correlation and diagnostic abilities sections of this study. The best of the questionnaires, and the only one to provide any suitable level of diagnostic ability within the step wise regression, was OSIRIS, which provided the best inter-site correlations, and also consistently provided the highest AUC results. The same trend was seen for the QUS investigations, with

BUA and VOS providing the greatest predictive value, as they did consistently in the inter-site correlations and ROC analysis.

The last multi-parameter equation produced (equation 7.10) was a combination of the CUBA Clinical results, weight, and three questionnaires OSIRIS, OST and SOFSURF, and provided an r^2 of 46.8%. The three questionnaire systems and in particular, the final two provide very little in the way of additional predictive value (r^2: 45.3% to 46.8%) and apart from three variables are almost identical in their modes of calculation. As such equation 7.8 which utilises the results of the CUBA Clinical, weight and OSIRIS would be the best of the screening strategies presented in this study.

The two previous studies which have attempted to use calcaneal QUS as pre-screening systems both included an additional parameter into their strategies to aid in the differentiation; for P. Dargent-Molina et al. (2003) the additional parameter was weight, and for M. Gambacciani et al. (2004) it was a questionnaire system based on fracture risk. This is of interest as equation 7.8 from strategy three, which was considered to be the best of the equations, used both the calcaneal QUS investigation but also weight and OSIRIS which considers fracture history. Direct comparisons with the literature were not possible though, as the study by M. Gambacciani et al. (2004) was performed using phalangeal QUS and as the phalangeal assessment within this study provided little predictive ability and was excluded from any strategy results. The study by P. Dargent-Molina et al. (2003) used a different QUS device and was based on the presence of one of out of two risk factors, not a regression equation for the prediction of the minimum T-score.

9.1.8 Study Limitations

One of the most significant limitations within this study is the nature of the population that was investigated. The individuals that were investigated were all attending a DXA scanning clinic, to which they had been referred due the presence of one or more of the clinical risk factors outlined in tables 4.1 and 4.3. As such the population could be considered to be biased, with a greater likelihood of the individuals having low bone density or quality than might have been expected within the general public.

In addition to this, the questionnaires which were used in this study were based on self reported information from the volunteers, and not filled in from their medical records, with parameters such as weight and height not being measured but provided by the individual. The information contained within each completed questionnaire was checked by the researcher with the volunteer, but this still constitutes a potential source of inaccuracy within the questionnaires.

The numbers of individuals included in the study, in comparison to the validation studies of the questionnaire systems and a number of other studies on the abilities of QUS, were quite low. However in the author's opinion the numbers were enough to produce significant correlations and provide valid results.

9.2 In-Vitro Investigation Discussion

9.2.3 Compression Testing

The mechanical performance of cancellous bone as a cellular solid is comprehensively discussed by L.J.Gibson and M.F.Ashby, (1988, 1997, 2005). In their rigorous theoretical treatise, the authors presented results which predicted that the relationship between the apparent density of the sample with respect to both Young's modulus and strength is best provided by a power function of roughly 2. This was backed-up and supported by a large volume of literature which was reviewed in section 3.2.1.1, which showed that despite the range of powers extending from 1.06 to 3.46 for Young's modulus and 1.32 to 3.05 for strength, the average power from the previous studies also stood at 1.98 and 1.85 for the Young's modulus and strength respectively.

For the osteoporotic group, the results of the present study for the power function relationships were well within the range of the previous studies, although the Young's modulus was slightly below the previous average at 1.215 and 1.479 for the platens and contact extensometer readings respectively; the strength results were virtually spot on at 1.72. Whether the differences seen in the Young's modulus for the osteoporotic group were statistically significant is unknown and would form a source of future work to further investigate if this were the case and why the effects were occurring. Conversely, the results from the osteoarthritic groups were well below what would have been expected, with the Young's modulus obtaining power functions of 0.663 and 0.82, and the strength results only obtaining power functions of 1.27. The non-significant nature of the osteoarthritic relationships with Young's modulus and the lack of agreement with the previous results of the literature can be explained by the

lower number of samples which were tested, with only eight femoral heads available. Therefore the number of data points within each regression are reduced.

In addition to this, the studies within the literature are mainly based on the testing of cancellous bone from cadavers or bovine sources, which have been selected specifically to ensure that the bone is free of any conditions such as osteoarthritis and osteoporosis. Only one study B.Li & R.M.Aspden (1997b) presented any results of possible effects the conditions might have had but provided only linear function relationships from non-destructive testing results. These results indicated that the slope of the osteoarthritic regression was reduced, with the osteoporotic slope being similar to that of the normals, as seen in this study.

The relationships with respect to the other compression testing results and apparent density were very similar to those of this study. The yield stress provided significant power and linear function relationships with density for both the osteoporotic and osteoarthritic groups with the powers of the relationships being 1.73 and 1.07 respectively, with the osteoarthritic group showing the same reduced relationship as the strength and modulus results. The results within the literature (table 3.3) showed that the apparent density was only weakly related to the yield strain (r^2 = 0.48 - 0.49, D.L. Kopperdahl and T.M. Keaveny 1998) and ultimate strain (r = 0.271 - 0.35, K. Brear et al., 1988, I. Hvid et al., 1989) of a sample during compression testing. The results of this study were in contrast, depending on the extensometer; (which it was compared against), the platens extensometer provided strains which correlated significantly with apparent density for both the osteoarthritic and osteoporotic groups, with the strains of the osteoporotic group being in keeping with the previous studies, but the yield and ultimate strains of the osteoarthritic group were higher than those of the osteoporotic

group. In contrast, the strains obtained from the contact extensometer failed to achieve any level of correlation or significance within the osteoporotic group. The results are probably due to the errors introduced by platens testing and the end-effects introduced in section 3.2.1.5 and demonstrated in section 8.1.1. The strains are, on the whole, less reliably measured by platens testing than by a contact extensometer as the buckling and collapse of the trabeculae in contact with the platens will introduce strain increases. This degree of buckling and collapse will be closely related to the apparent density of the samples, with higher density samples having more support and connectivity between the trabeculae to prevent the buckling and collapse than a less dense sample. In contrast the contact extensometer results are free from these end effects and as such the errors associated with these end effects and density is not in evidence. The only contrast to this was the increased yield and ultimate strains of the osteoarthritic samples, which demonstrated a higher apparent density. The reasoning for this relates to the reduced mineral content of the bone which allows for the higher deflection of the samples.

The final compressive mechanical parameter which was investigated was the compressive toughness, or work to failure of the samples. In both the osteoporotic and osteoarthritic samples the relationship with apparent density was highly significant and both the power functions with respect to the study by I. Hvid at al. (1989), and the magnitudes of the linear regression slopes with respect to the studies by I. Hvid at al. (1989) and F. Linde et al. (1989) were of the same order of magnitude.

The effects of the sample porosity were, not surprisingly, the inverse of the results seen for the apparent density with correlations of similar magnitude and statistical significance.

The other material property of note was the material density, or the density of the actual trabeculae. For the osteoporotic group the correlations were on the whole poor and non-significant, with only the platens strain values and compressive toughness positively correlating with the material density and obtaining significance. As with the apparent density results, however, the osteoarthritic group behaved very differently, with 6 out of 10 of the mechanical parameters being highly significantly affected by the material density of the sample, and in most cases the correlations could be considered to be excellent (-0.767 to -0.900) and noticeably negative in nature. The negative relationship is in keeping with the results of section 8.4 which showed that the material density increases with the reduction in apparent density.

Unfortunately the composition of each specific compression core was not determined, but by using the results of the fracture toughness samples it is clear that the osteoarthritic samples have a lower mineral content, or mineralization, and a higher water and organic content in comparison to the osteoporotic bone. It was demonstrated by I. Hvid et al., (1985) and H. Follet et al., (2004) that the mineral content and the degree of mineralization both positively affect the mechanics of the bone tissue, and although both conditions investigated in this study have been shown to affect the composition of the bone, the differences are far more pronounced in the osteoarthritic group. The number of previous studies on the effects of collagen content and cross-linking on cancellous bone are very few. A.J. Bailey et al. (1999) demonstrated significant correlations between the percentage collagen content and the modulus, strength and work to failure cancellous bone in compression. Unfortunately the determination of the percentage collagen content using their methods was not performed for this study and neither was analysis using ashing, so no comparisons could be made.

However, the one other study by X. Banse et al. (2002b) demonstrated that it was the mature Ketoimine cross-links OH-Pyr and Lys-Pyr that weakly, but significantly, affected the ultimate strain. The results of this study were unable to provide any direct support for these results; however the stepwise regression analysis showed the collagen cross-link variables to significantly affect the yield and ultimate strains.

When the stepwise regression analysis is reviewed for the osteoporotic group, the dominant factor for every parameter except the yield and ultimate strains was the apparent density of the samples, followed by the porosity, with the material density and the collagen cross-linking analysis providing the additional variables in the analysis. For the osteoarthritic group the dominant variable is less easy to define and the collagen cross-linking within the tissue plays a far more prominent role. However the low number of samples within the osteoarthritic group may well have affected the analysis that was performed.

The variation in the mechanical properties of the bone within this study would appear to be due first and foremost to the apparent density, but with variations in the mineral and organic contents of the bone along with the degrees of collagen cross-linking playing significant roles. This may be more evident in the osteoarthritic bone where the mineral content is reduced at higher apparent densities, which may account for the reduced slopes and powers of the regressions with respect to apparent density.

The results of the compression testing within this study demonstrate that the samples of osteoporotic bone used behaved in a manner that was similar to, or the same as, that which had been previously found for normal cancellous bone. In contrast to this, the results of the compression testing of the cancellous bone from the osteoarthritic groups provided distinctly different results, with both the modulus and strength results

having reduced power functions and linear regression slopes, due to the combined effects of the material and compositional variables. However the volume of work within the literature on both osteoporosis and osteoarthritis is very small, and as such it is hard to be certain that the effects seen specifically for the osteoarthritic group are true.

9.2.4 Fracture Toughness Testing

The present fracture toughness tests are the first ever attempt to calculate / measure fracture toughness for cancellous bone (of any kind). Cancellous bone is a cellular solid capable at the macroscopic level of large deformations and elasto / plastic behaviour which is due to the microstructural deformations caused by the buckling/bending and rotation of the trabeculae.

The interesting point is that by all accounts the individual trabeculae are made up of the same semi-brittle material as standard bone matrix which comprises both the cortical and cancellous bone (Section 2 and 3.1). The tissue is therefore semi-brittle at the material level, but elasto/plastic at the macrostructural / macromechanical level. The presence of these large deformations is what discouraged researchers from applying institutional fracture mechanic methods in the calculation of K_{IC}.

There may be merits however in producing standard fracture toughness values for cancellous bone and therefore the approach taken was to produce toughness values from 2 different standard sample designs and orientations, and to test the validity of the tests by the standard methods.

9.2.4.1 Validity

For plane strain in particular, the validity of the fracture toughness results was tested using the guidelines laid out in ASTM standard E399-90, 'Standard Test method for Plane-Strain Fracture Toughness of Metallic Materials'. Initially the relationship between the maximum load (P_{max}) and the load at P_Q, a point determined using the guidelines from the standard and laid out in section 6.3.2.1 was examined. For all three groups and both sample designs and orientations, the results were above the 1.10 threshold value that was required to classify the results as valid measures of plane strain K_{IC}.

The second alternate check is the specimen strength ratio, based on equation 6.5, which relates to the specimen thickness requirements of the sample. Using the compressive yield strength of the samples, obtained using the regression analysis vs. apparent density from the compression testing results. The resultant values were below the limit of both the sample thickness and the initial notch length, suggesting that plane strain conditions existed. However the results of the literature review in section 3.2.3, demonstrated that the tensile yield strength of cancellous bone was 70% of the compressive yield strength. Recalculation of the specimen strength ratios using 70% of the compressive strength values still provided values below the limit of both the sample thickness and the initial notch length, once again suggesting that plane strain conditions exist.

Although the checks using homogenised micromechanical constants were verified for standards that have been suggested for the testing of metallic foams, but also wood and cortical bone, these standards are intended for homogeneous and mainly isotropic materials, not a '*composite, anisotropic, open porous cellular solid'*

T.M.Keaveny et al. (2001), and as such the validity of the results with respect to plane strain K_{IC} should be interpreted with caution.

There is a further limitation within this study which relates to the G fracture toughness values. The modulus values that were used in the calculation of the G values were determined using a compression core taken from the side of the same femoral head; however the core was orientated in the strong (Ac) direction. As such the calculation of the G values for the samples orientated in the AL direction should have been adjusted due to the anisotropy and they were not in this study, which may have adversely affected the G results for the AL orientated fracture toughness samples.

9.2.4.2 Fracture Toughness Results

The material property comparisons demonstrated that the apparent density of the osteoarthritic bone was significantly higher than that of the equine bone which was in turn significantly higher than the osteoporotic bone. As such the fracture toughness results would have been expected to show the same trends, but the comparison of the results from the different study groups highlighted a number of important differences and effects related to the material properties and composition of the bone samples.

Material Properties and Compositional Effects

Density and Porosity

The most influential parameter was predicted to be the apparent density of the material, with the relationships expected to be best explained by a power function of between 1 and 2 with relation to relative density (L.J. Gibson and M.F. Ashby, 1997a); a hypothesis which, when viewed in the form of the different sample designs and orientations, was weakly supported. However, combining the results from the different

study groups provided clear and significant proof that with relation to the critical stress intensity values (K), the power function relations to the apparent and relative densities were indeed between 1 and 2, averaging somewhere in the region of 1.6.

The results of the relationship between the critical strain energy release rate values and the density were even more variable between groups and sample designs than the critical stress intensity values. However, once again by using the study groups in combination the resultant powers of the logarithmic relationships with the apparent and relative densities bore a closer adherence between sample designs and orientations. In each cased the G power functions were higher than the corresponding K values, although this is unsurprising considering the determination of the G values was based on the square of the K values.

The results of the relationships between the J-integral values and the density were noticeably different to the relationships of the K and G values. The initial and most obvious difference was that for all the individual sample designs and groups the relationship was the inverse of that seen for the K and G values, but also the powers of the logarithmic relationships were visibly lower.

The reasons for the differences within the J-integral results are due to the values' inherent difference to the K and G values. The K and G values are both based on the load of fixed points on the curve, and as such the variation in the apparent density and other variables are positively related, as demonstrated by the positive power function relationships and correlations seen in this study. The J-integral on the other hand refers to the energy that is input into the system by the time there is onset in crack growth. The results clearly show that with a reduction in density, the deflection required to cause failure of the bone structure is increased with respect to higher density samples.

As such the energy that is required for the additional deflection is enough within this study to cause the lower density samples to present J_Q and J_C values which are equal to or higher than those of the higher density samples. The reason for this is most likely structural as at a density of above 350kg m^{-3} the structure can be considered to be a closed-cell foam of plates (L.J.Gibson, 1985, D.R.Carter and W.C.Hayes, 1977), whereas below this the structure gradually changes from the closed cell foam of plates to an open cell foam of rods or plates, eventually ending up with a structure dominated by rods (J.W.Pugh et al., 1973, J.L.Stone et al., 1983, L.J.Gibson, 1985). The different structures deform differently, in that the rods are able to bend and flex in loading far more than the plates, enabling the increased deflection prior to failure.

This is, however, not a bad effect; firstly the K and G fracture toughness values are reduced within the osteoporotic individuals as would be expected, and this contributes strongly to the increased risk of fracture that osteoporosis entails. Secondly the J-integral and the energy absorption of the tissue with reduced density enables it to withstand higher deflections in loading prior to a definite onset of crack growth and the structure failing, ensuring whatever structure and bone is remaining is kept intact.

The effects of porosity go hand in hand with those of apparent density, with the relationships being the inverse, but in most cases of equal significance and predictive ability; the material density, on the other hand, appeared to play only a secondary effect to apparent density, but mainly in conjunction with the compositional properties of the samples.

Composition

The nature of the relationship between the apparent density and the mineral and organic contents between the groups was different, with only the mineral and water contents of the osteoarthritic groups providing any strong and significant correlations with the fracture toughness parameters. However, when the dehydrated contents were investigated the fracture toughness parameters were significantly affected by the organic content as well. The fact that the correlations between the composition and the fracture toughness parameters were more pronounced in the osteoarthritic group is most likely to be an effect of the condition. The mineral content of the high apparent density bone is reduced with respect to normal bone, due to the increased turnover and bone matrix deposition associated with the disease preventing the full mineralization of the tissue.

The effects of mineral and organic content are, however, not evident within the groups themselves, as the variation in composition is comparatively small. The main effect was seen when the different groups were compared. The effects that were seen between the samples from the different groups could be partly explained by the variation in the material properties, but the main source of explanation lies in the composition. Fracture toughness values for cortical bone demonstrated a significant increase in the energy absorptive properties of antler in relation to human cortical bone (J.D. Currey et al. 1996), but lower crack initiation toughness, (D. Vashishth, 2004) and the reasoning for this was due to the reduced mineral content and increased organic content of the antler bone. The osteoarthritic bone was demonstrated in section 8.3.1 to have a significantly reduced mineral content, and significantly increased organic content with respect to the other two groups and as such the effects of the significantly higher apparent density of the osteoarthritic bone were nullified to a large extent with respect

to the K and G values as seen in these results, but the energy absorptive properties, such as expressed by the J-integral were significantly enhanced.

The results of the stepwise regression analysis for the three groups showed that it was either the apparent density or porosity which had the dominant effect on the K and G fracture toughness parameters. For the equine group the remaining variables consisted of the hydrated mineral and organic contents of the bone, but for the osteoporotic and osteoarthritic groups in which the collagen cross-linking analysis was performed, the overall percentages were out performed by the levels of collagen cross-links within the tissues. However there was no single cross-link which dominated in both of the groups and for the osteoporotic group the collagen cross-links were equally distributed between the sample designs and orientations. In contrast the osteoarthritic group appeared to be dominated by the mature Ketoimine cross-links Lys-Pyr, which was the only cross-link which did not appear in the osteoporotic analysis, but was one of the cross-links highlighted by X. Banse et al. (2002b) as affecting the compression testing results of cancellous bone.

The J-integral in the stepwise regressions was once again discernibly different to those of the K and G fracture toughness parameters. The apparent density on a number of occasions proved to be the dominant variable but in each case the r^2 was noticeably reduced in comparison to the other fracture toughness parameters and even the addition of other cross-link and compositional variables failed to satisfactorily explain the variation in the J-integral results. These findings lend further support to the idea that the variation in structure and its integrity with density may be playing an important role in the fracture mechanics which, in the case of this study, cannot be quantified or explained.

9.3 Material Property Investigations

The material properties of every sample which was prepared in this study were determined in order to explain and demonstrate the effects that they had on the mechanical parameters obtained from their mechanical testing. The samples were, however, prepared from three distinctly different sources of bone, either from osteoporotic or osteoarthritic human femoral heads, or the thoracic spines of two horses. Although there are clear differences between the groups the values and ranges that were obtained for the three different material properties were very similar to those outlined in section 2.1.2 by P. Zioupos et al (2000), F. Linde (1994) and E. Bonucci (2000).

The condition of the equine material was unknown in relation to skeletal conditions or diseases; however the vertebrae and vertebral discs were free of any macroscopic signs of disease, and were considered to be normal. The two skeletal conditions, osteoporosis and osteoarthritis are both known to adversely affect the bone tissue, and in distinctly different ways. The studies by B. Li and R.M. Aspden (1997 a,b,c) show that in osteoporosis, the apparent density of the bone is significantly reduced compared with normal bone, an effect which goes hand in hand with an increase in the porosity of the bone, findings which are unsurprising considering the definition and nature of the condition (section 4.3). Osteoarthritis, however, has the opposite effect on the apparent density of the bone, with significant increases in apparent density and reduction in porosity relative to normal bone. The results within this study are in close agreement with the studies by B. Li and R.M. Aspden (1997 a,b,c), not only in the effects seen in the conditions but also the resultant means and ranges of the variables within the study groups with regards to apparent density and porosity.

This study is, however, in disagreement with all three studies by B. Li and R.M. Aspden (1997 a,b,c), when the effects of the different conditions are viewed in relation to the material density. This study was unable to find any statistically significant difference between the material densities of the samples from the three different groups, with the means and ranges all being virtually identical. The previous studies all demonstrated a significant reduction in the material density seen in samples from osteoarthritic individuals and in one of the studies (B. Li and R.M. Aspden, 1997a) even the osteoporotic bone demonstrated a reduced material density. The differences between this study and B. Li and R.M. Aspden, (1997b,c), are inexplicable besides the demographics of the study populations and the slight differences in the site of the samples productions which have been shown previously to have effects (C.M. Schoenfeld et al., 1974, S.J. Brown et al., 2002). The study which demonstrated the differences for both the osteoarthritic and osteoporotic conditions determined the material density using 9mm x 1mm samples of bone from the subchondral bone plate of the femoral heads, which is far more compact than normal cancellous bone and therefore was not representative of the entire femoral head as used in this study.

9.4 Compositional Property Investigations

The compositional properties of the bone samples refer to the percentage relationships between their mineral, organic and water contents and the collagen cross-linking analysis. The results of the previous studies (B. Li and R.M. Aspden, 1997a,b,c), after the exclusion of B. Li and R.M. Aspden, (1997a) for the reasons outlined above, presented average mineral content, organic content and water content ranges from 52.6 to 56.9%, 29.2 to 29.5% and 13.9 to 16.9% respectively, for the osteoporotic samples,

virtually identical to the levels within this study. There was, however, a marked difference in the results of the osteoarthritic samples between the two B. Li and R.M. Aspden, (1997b,c) studies, but the average percentage compositions of 48.5%, 20.3% and 31.2% for the mineral, organic and water contents respectively within this study, were in close agreement to those from B. Li and R.M. Aspden, (1997b).

9.5 QUS vs. Material and Mechanical Properties.

9.5.1 Compression vs. QUS

SOS or VOS have been used for many years to provide an assessment of the Young's modulus of a material, and section 4.9.1 outlined the results of 4 studies which have utilised ultrasound measurements to determine the Young's modulus of cancellous bones, and a further 14 studies which have demonstrated a clear and significant link between the QUS results and mechanical properties, but using sample specific QUS investigations prior to mechanical testing. This study is different and novel in that the QUS investigations were performed in-vivo on the donor, and not directly on the mechanical samples under testing. It is also important to note that the studies by B. Li and R.M. Aspden, (1997c) and C.-C. Glüer et al., (1993) both demonstrate that the orientation of a sample with respect to the ultrasound path can substantially affect the results for both cortical and cancellous bone, and with the compression core of this study having been removed in the anterior-posterior alignment, the cores could be considered not to have been in the strongest direction.

Having demonstrated within the literature review that it is possible to determine the mechanical properties, and in particular Young's modulus, of cancellous bone from the SOS or VOS from an ultrasound test, and that the results have the potential to be affected by the bone orientation, it is important to consider the nature of

the investigations used in this study. The Sunlight Omnisense system has the ability to measure SOS, but the measurements are performed on the cortical bone of the measurement sites, although the nature of the ultrasound's pathway is along the length of the bone, which can be considered to mimic the alignment of the compression cores. The clinical relationships with axial skeletal density were found to be detrimentally affected by this different tissue macrostructure, but in relation to the in-vivo determined density in this study the correlations were good and as such the close link between the density and the biomechanics demonstrated in section 8.7.1.2 was expected to be seen in the correlations with the QUS. The CUBA clinical system produces both VOS and BUA for the calcaneus, by passing ultrasound pulses across it in the medio-lateral direction. The consistency in the sample orientation led to better clinical screening results and to good correlations with the in-vitro density measurements; this also offered a good chance of providing correlations with the biomechanical measurements.

For the osteoporotic group the correlations that were significant were in keeping with these predictions. The VOS results of the calcaneus provided 6 significant ($p < 0.05$) correlations with respect to the compressive properties ($E_{Platens}$ $r = 0.550$, $\varepsilon_{Yield\ Platens}$ $r = 0.559$, $\varepsilon_{Ultimate\ Platens}$ $r = 0.463$, σ_{Yield} $r = 0.509$, $\sigma_{Ultimate}$ $r = 0.506$, Work to Failure Contact $r = 0.511$) although the BUA results correlated poorly and only significantly with the yield strength ($r = 0.437$). The Sunlight system provided significant correlations with the compressive parameters with both the distal radius ($\varepsilon_{Ultimate\ Platens}$ $r = 0.585$ and Work to Failure Contact $r = 0.479$) and mid-shaft tibia (($E_{Platens}$ $r = 0.584$, $E_{Contact}$ $r = 0.523$, σ_{Yield} $r = 0.491$ and $\sigma_{Ultimate}$ $r = 0.464$). For the osteoarthritic group the only significant correlations obtained were between the distal radius investigations from

the Sunlight Omnisense system and the ultimate strain from the platens (r = 0.896), the ultimate strength (r = 0.752) and work to failure of the contact extensometer (r = 0.847).

Taking the two groups as one provided results which were discernibly different to either of the two individual groups. The distal radius investigations were the most prominent of the results, significantly correlating with 6 of the 10 compressive mechanical parameters. The joining of the two groups adversely affected the correlations which were obtained for the VOS calcaneus results with the compressive mechanical properties with significant correlations seen previously in the osteoporotic group failing to achieve significance. It was of particular note, however, the results from the joining of the two groups provided significant correlations between every one of the QUS investigations and the yield strength of the material, with only the BUA results not significantly correlating with the ultimate strength.

The results within section 8.8.1 were slightly disappointing in that there are only low numbers of significant correlations with respect to the mechanical results despite the agreements with orientation of the sample and the previously noted agreement with the in-vitro density.

9.5.2 QUS vs. Fracture Toughness

The strong and well accepted link between the QUS and the material properties, as well as the close link between the fracture risk of an individual and QUS results, should both provide support for the hypothesis that QUS has the potential to predict the fracture mechanics values for the bone in the femoral head.

The K and G fracture toughness results of both the osteoporotic beam and disk Ac samples, correlated significantly with the BUA and VOS results that were obtained

from the CUBA clinical system. The performance of the results from the Sunlight system was not as pronounced but the distal radius results significantly correlated with the K_Q and Kc values and the mid-shaft tibia results correlating with the K_Q and J_Q results. The results of the osteoporotic samples orientated in the AL direction were discernibly different form those of the Ac direction; the only significant correlations were seen between the K and G fracture toughness parameters and the proximal phalanx results, with the correlations between the K_Q and K_C results of the beam samples being inexplicably negative.

The results of the osteoarthritic group bore little resemblance to those of the osteoporotic group, and in addition to this there was little agreement between the sample designs of the same direction. However, a large number of significant correlations between the QUS parameters and the fracture toughness parameters were achieved. The best performing of the QUS investigations was the distal radius which obtained significant correlations with the K and G fracture toughness parameters of the beams in both orientations and the KQ and GQ values of the disks Ac. The performance of the proximal phalanx measurements was only significantly correlated with the JC and JQ values of the beam samples, while the mid-shaft tibia results only correlated with the K and G results of the disk samples in the AL direction; however these correlations were extremely good ($r = 0.870 – 0.956$). The performance of the CUBA results was mixed; significant correlations were obtained for the KQ, KC, JC of the Beam Ac samples in relation to the BUA, with VOS additionally correlating with the KC and GC results of the same group. However no significant correlations were obtained between any of the fracture toughness parameters from the disk Ac samples and the CUBA clinical QUS results. The only additional significant results were between the BUA

results and the GQ results of the disks AL, which mimicked the mid-shaft tibia results in that they were extremely good (r = -0.832 – -0.866) but inexplicably negative in nature.

The relatively low number of significant correlations within the results can be put down in part to the low number of individuals who were actually scanned and included in the analysis (20 osteoporotic and 8 osteoarthritic). It therefore seemed justifiable to combine the results of the two groups to provide an increased number and wider range of results. The combination had the effect of increasing the number of significant correlations that were obtained between the QUS and fracture toughness results; however, as seen with the compression testing results, some of the significant results of the individual groups were lost while new ones were gained. The most noticeable difference was that in the osteoporotic group there were no significant correlations between any of the QUS parameters and the J-integral, and only a few with the beam samples of the osteoarthritic group. The combinations of the results produced a number of highly significant correlations between the JQ and JC results, most notably between the BUA and VOS results of the CUBA clinical system.

This study shows that even in a comparatively small study group, the results obtained from the in-vivo assessment of an individual have the ability to predict a number of fracture toughness parameters obtained from the bone of the individual's femoral head. The results may have been influenced by factors other than the small sample size, the Sunlight Omnisense system may have suffered due to its modes of ultrasound for measurement only enabling the investigation of cortical bone, when the fracture toughness parameters investigated were all derived from cancellous bone. The CUBA Clinical on the other hand performs measurements on the load bearing

cancellous bone of the calcaneus, with the trabeculae orientated in the Ac direction and consequently this may constitute a reason for the increased numbers and strength of correlations with the Ac orientated samples.

In both study groups the numbers of individuals investigated were comparatively low with respect to the numbers within clinical trials of the abilities of QUS, and it is considered that the results of this study might have been improved by an increase in the number of participants. However the number of significant correlations seen within both the fracture toughness and compression testing studies, and the strong link with the in-vitro determined densities, indicate that QUS may have the potential to predict the mechanics of human skeletal tissue, and that further research into the capabilities of QUS is required.

9.5.3 QUS vs. Material Properties.

The results of the clinical work of this study demonstrate a clear and significant correlation between the density of the axial skeleton with relation to the result of a QUS investigation when both assessments were performed in-vivo, and not only did the clinical work demonstrate a good correlation but it also showed that the excellent potential of the QUS investigations to predict the density of the total hip DXA investigation. The results of the comparisons between the apparent densities of samples taken from the femoral heads and the in-vivo QUS investigations from the corresponding donor only proved to support these clinical findings, with respect to the determination of osteoporosis.

Table 8.46 demonstrated that when the average apparent density was taken for each individual of the osteoporotic group, every QUS investigation, and its

corresponding T-score, was significantly correlated to it, with the calcaneal assessments as in the clinical work providing the higher correlation, but with the distal radius results also providing similar levels of correlation. It is noticeable, though, that the VOS results of the calcaneus outperformed the corresponding BUA results, an inverse of the relationship seen during the clinical work. The mid-shaft tibia results were a surprise considering the poor performance which was achieved during the clinical work. The mid-shaft tibia SOS results correlated better than the proximal phalanx SOS results with respect to the porosity of the samples, and notably this was the only site which provided any correlation with the material density of the samples.

In contrast to the osteoporotic results the correlations between the osteoarthritic material properties and the QUS investigations were fewer in number, although the performances of note were the distal radius and the BUA results from the calcaneus, two of the highest performing investigations from the osteoporotic group, and also one of the best performing investigations with respect to the fracture toughness parameter of the osteoarthritic group. Once again the number of individuals within the osteoarthritic study group may have adversely affected the overall results.

However, when these results are considered in combination with those of the clinical studies, there is clear proof that QUS assessments of the peripheral skeleton and in particular those which occur on the calcaneus, have the potential to predict not only the material properties, such as the apparent density, but also by doing so the compressive and fracture mechanical properties of the bone.

Chapter 10: Conclusions

10.1 Clinical Studies.

The results of the clinical studies provide strong evidence and proof that clinical QUS, and in particular the calcaneal systems such as the CUBA Clinical, have the potential to offer a highly reliable screening tool for the prediction of the condition of the axial skeleton, with specific focus on the hip. The fact that QUS has been previously proven to predict fracture risk only serves to improve this, as any false positives need not be viewed as detracting from the screening technique as a whole.

The performance of the questionnaire systems within this study also provide strong evidence to support their use within the clinical environment, as they offer a low cost and reliable alternative to the all inclusive diagnostic guidelines laid out by a number of osteoporosis related societies. It should be noted, however, that the results of questionnaires should never be considered the definitive diagnosis, and clinicians should still use their discretion, as the questionnaires are based mainly on substantiated anthropometrical values and medical history and so ignore a large number of secondary sources of osteoporosis.

The potential use of the questionnaires in combination with the calcaneal QUS investigations provides a level of reliability over and above that for the individual techniques and would provide the clinician with a simple and easy method for the prediction of an individual's T-score.

10.2 In -Vitro Testing

The results of in-vitro testing of cancellous bone showed that both skeletal conditions investigated (osteoporosis and osteoarthritis) adversely affect the cancellous bone tissue but in distinctly different and virtually opposite manners. The compressive mechanical properties of the samples from the osteoporotic group bore the same relationships to variables such as apparent density as were previously laid out in the literature, but the effects of lower mineralization and mineral content within the osteoarthritic bone may well have adjusted the relationships seen, although this requires further work if it is to be fully substantiated.

The quantification of the fracture mechanical parameters for cancellous bone provides some new evidence for the effects of density variation on bone mechanical competence. The study proved the hypothesis of L.J. Gibson and M.F. Ashby (1997a) that the power function of the relationship between the stress intensity factor (K) would be dependent on density to a power of between 1 and 2, with the results of this study placing the power close to 1.5, the middle of the range.

The results also demonstrated that the change in structure that occurs in osteoporosis, and which had been seen previously in bone, has a marked effect on the fracture toughness of bone tissue, with the lower density rod structures able to absorb an increased energy prior to failure with respect to the denser plate-like structures. It was also noted that the effects of reducing the mineral content of cancellous bone were similar to those seen in cortical bone and antler, where initiation toughness such as K and G reduced with lower mineral content, but the energy absorption abilities such as the J-integral of the tissue significantly increased. The cancellous bone of this study showed such effects when comparing the osteoarthritic and osteoporotic tissue.

The performance of the QUS systems, in comparison to the biomechanics work and the in-vitro determined material properties, provided a number of significant correlations which the author believes would have been improved had the study cohorts of both the osteoporotic and osteoarthritic individuals been increased. The results with respect to the in-vitro determined material properties provides firm support that QUS could be safely used to predict or screen individuals for low bone density of their axial skeleton. In addition to this the number of significant correlations between the in-vitro determined compressive, and particularly the fracture mechanical properties, with respect to the clinical QUS investigation taken in-vitro, support the idea that QUS can predict fracture risk.

The results of the fracture toughness testing did, however, highlight the fact that the fracture mechanics of human cancellous bone, although dominated primarily by the apparent density of the material, are also reliant in a large part on the organic content and the integrity of the collagen network as well as the structural integrity of the cancellous bone network. As such, the author believes that the focus of therapies and diagnosis methods solely on density could be improved with respect to fracture risk if they were to consider the integrity of the collagen and cancellous bone networks. Therefore the ability of QUS to provide data which includes information on the structural integrity of the bone as well as its density should be reviewed by the governing bodies in order to provide useable guidelines for clinicians.

With respect to future work which the author considers to have come out of this study, any increase in the study population size of both the osteoporotic and osteoarthritic study groups would enable a better and clearer understanding of the effects of the variables. But more importantly it would allow for improved

investigations into the relationships between in-vivo QUS measurement values and the biomechanical properties of the cancellous bone.

The effects of the structure of the bone on the fracture mechanics would be an interesting field to substantiate the hypothesis made in this study that the J-integral results are being affected by the nature of the deformation of the structure over and above the apparent density.

References and Bibliography

R.A. Adler, M.T. Tran and V.I. Petkov. (2003) Performance of the Osteoporosis Self-Assessment Screening Tool for Osteoporosis in American Men. *Mayo Clinical Proceedings;* **Vol. 78,** p.723-727

M. Agren, A. Karellas, D. Leahey et al. (1991) Ultrasound Attenuation of the Calcaneus: A Sensitive and Specific Discriminator of Osteopenia in Postmenopausal Women. *Calcified Tissue International;* **Vol. 48,** p.240-244

O. Akkus, K.J. Jepsen and C.M. Rimnac (2000) Microstructural Aspects of the Fracture Process in Human Cortical Bone. *Journal of Materials Science;* **Vol. 35,** No. 24, p.6065-6074

B. Alberts, D. Bray, J. Lewis et al. (1994) Molecular Biology of the Cell. Chapter 19: Cell Junctions, Cell Adhesions, and the Extracellular Matrix; The Extracellular Matrix of Animals. 3rd Edition, Garland Publishing Inc., p.971-995

F.E. Alenfeld, C. Wüster, C. Funck et al. (1998) Ultrasound at the Proximal Phalanges in Healthy Women and Patients with Hip Fractures. *Osteoporosis International;* **Vol. 8,** p.393-398

M.J. Anderson, J.H. Keyak and H.B. Skinner (1992) Compressive Mechanical Properties of Human Cancellous Bone after Gamma Irradiation. *The Journal of Bone And Joint Surgery (American Volume);* **Vol. 74-A,** No. 5, p.747-752

E. Andrews, W. Sanders, L.J. Gibson (1999) Compressive and Tensile Behaviour of Aluminium Foams. *Materials Science and Engineering;* **Vol. A270,** p.113-124

R.B. Ashman, J.D. Corin and C.H. Turner (1987) Elastic Properties of Cancellous Bone Measurements by an Ultrasonic Technique. *Journal of Biomechanics;* **Vol. 20,** No. 10, p.979-986

R.B. Ashman, S.C. Corin, W.C. Van Buskirk et al. (1984) A Continuous Wave Technique for the Measurement of the Elastic Properties of Cortical Bone. *Journal of Biomechanics;* **Vol. 17,** p.349-361

R.B. Ashman and J.-Y. Rho (1988) Elastic Modulus of Trabecular Bone Material. *Journal of Biomechanics;* **Vol. 21,** p.177-181

P. Augat, T. Link, T.F. Lang et al. (1998) Anisotropy of the Elastic Modulus of Trabecular Bone Specimens from Different Anatomical Locations. *Medical Engineering & Physics;* **Vol. 20,** p.124-131

A.J. Bailey, S.F. Wotton, T.J. Sims et al. (1992) Post-translational Modifications in the Collagen of Human Osteoporotic Femoral Head. *Biochemical and Biophysical Research Communications;* **Vol. 185,** No. 3, p.801-805

A.J. Bailey, S.F. Wotton, T.J. Sims et al. (1993) Biochemical Changes in the Collagen of Human Osteoporotic Bone Matrix. *Connective Tissue Research;* **Vol. 29,** p.119-132

A.J. Bailey, R.G. Paul, L. Knott (1998) Mechanisms of Maturation and Aging of Collagen. *Mechanisms of Ageing and Development;* **Vol. 106,** p.1-56

A.J. Bailey and L. Knott (1999) Molecular Changes in Bone Collagen in Osteoporosis and Osteoarthritis in the Elderly. *Experimental Gerontology;* **Vol. 34,** p.337-351

A.J. Bailey, T.J. Sims, E.N. Ebbesen et al. (1999) Age-Related Changes in the Biochemical Properties of Human Cancellous Bone Collagen: Relationship to Bone Strength. *Calcified Tissue International;* **Vol. 65,** p.203-210

P.A. Ballard, D.W. Purdie, C.M. Langton et al. (1998) Prevalence of Osteoporosis and Related Risk Factors in UK Women in the Seventh Decade: Osteoporosis Case Findings By Clinical Referral Criteria Or Predictive Model? *Osteoporosis International;* **Vol.8,** p.535-539

X. Banse, J.P. Devogelaer, A. Lafosse et al. (2002a) Cross-link Profile of Bone Collagen Correlates with Structural Organization of Trabeculae. *Bone;* **Vol. 31,** No. 1, p.70-76

X. Banse, T.J. Sims and A.J. Bailey (2002) Mechanical Properties of Adult Vertebral Cancellous Bone: Correlation with Collagen Intermolecular Cross-Links. *Journal of Bone and Mineral Research;* **Vol. 17,** No. 9, p.1621-1628

D.T. Baran, A.M. Kelly, A. Karellas et al. (1988) Ultrasound Attenuation of the Os Calcis in Women with Osteoporosis and Hip Fractures. *Calcified Tissue International;* **Vol. 43,** p.138-142

D.T. Baran, C.K. McCarthy, D. Leahey et al. Broadband Ultrasound Attenuation of the Calcaneus Predicts Lumbar and Femoral Neck Density in Caucasian Women: A Preliminary Study. *Osteoporosis International;* **Vol. 1,** p.110-113

D.T. Baran, K.G. Faulkner, H.K. Genant et al. (1997) Diagnosis and Management of Osteoporosis: Guidelines for the Utilization of Bone Densitometry. *Calcified Tissue International;* **Vol. 61,** p.433-440

R. Barkmann, E. Kantorovich, C. Singal et al. (2000) A New Method for Quantitative Ultrasound Measurements at Multiple Skeletal Sites: First Results of Precision and Fracture Discrimination. *Journal of Clinical Densitometry;* **Vol. 3,** No. 1, p.1-7

H. Bart-Smith, A.-F. Bastawros, D.R. Mumm et al. (1998) Compressive Deformation and Yielding Mechanisms in Cellular Al Alloys Determined Using X-Ray Tomography and Surface Strain Mapping. *Acta Materiallia,* **Vol. 46,** No. 10, p.3583-3592

B. Bätge, J. Diebold, H. Stein et al. (1992) Compositional Analysis of the Collagenous Bone Matrix. A Study on Adult Normal and Osteopenic Bone Tissue. *European Journal of Clinical Investigation;* **Vol. 22,** p.805-812

D.C. Bauer, C.-C. Glüer, H.K. Genant et al. (1995) Quantitative Ultrasound and Vertebral Fracture in Postmenopausal Women. *Journal of Bone and Mineral Research;* **Vol. 10,** No. 3, p.353-358

D.C. Bauer, C.-C. Glüer, J.A. Cauley et al. (1997) Broadband Ultrasound Attenuation Predicts Fractures Strongly and Independently of Densitometry in Older Women. *Archives of Internal Medicine;* **Vol. 157,** No. 6, p.629-634

H.H. Bayraktar, E.F. Morgan, G.L. Niebur et al. (2004) Comparison of the Elastic and Yield Properties of Human Femoral Trabecular and Cortical Bone Tissue. *Journal of Biomechanics;* **Vol. 37,** p.27-35

R. Benzy and D.J. Green (1990) The Effect of Cell Size on the Mechanical Behaviour of Cellular Materials. *Acta Metallurgica et Materialia;* **Vol. 38,** No. 12, p.2517-2526

B.J. Biggerstaff. (2000) Comparing Diagnostic Tests: A Simple Graphic Using Likelihood Ratios. *Statistics in Medicine;* **Vol. 19,** p.649-663

F. Bini, A. Marinozzi, F. Marinozzi et al. (2002) Microtensile Measurements of Single Trabeculae Stiffness in Human Femur. *Journal of Biomechanics;* **Vol. 35,** p.1515-1519

D.M. Black, L. Palermo, J. Pearson et al. (2001) SOFSURF: A Simple, Useful Risk Factor System Can Identify The Large Majority of Women with Osteoporosis. *Bone;* **Vol. 23,** Issue 5, Suppl. 1, p.S605

G.M. Blake, C.-C. Glüer and I. Fogelman (1997) Bone Densitometry: Current Status and Future Prospects. *The British Journal of Radiology;* **Vol. 70,** Special Issue, p.S177-S186

F. Blanckaert, B. Cortet, P. Coquerelle et al. (1999) Ultrasound Velocity Through the Phalanges in Normal and Osteoporotic Patients. *Calcified Tissue International;* **Vol. 64,** p.28-33

S.L. Bonnick, C.C. Johnston, M. Kleerekoper et al. (2001) Importance of Precision in Bone Densitometry Measurements. *Journal of Clinical Densitometry;* **Vol. 4,** No. 2, p.105-110

C.M. Bono and T.A. Einhorn (2003) Overview of Osteoporosis: Pathophysiology and Determinants of Bone Strength. *European Spine Journal;* **Vol. 12,** (Suppl. 2), p.S90-S96

E. Bonucci (2000) Mechanical Testing of Bone and the Bone-Implant Interface. Chapter 1: Basic Composition and Structure of Bone. Edited by Y.H. An and R.A. Draughn. CRC Press LLC, p.3-17

P.M. Bossuyt, J.B. Reitsma, D.E. Bruns et al. (2003) Towards Complete and Accurate Reporting of Studies of Diagnostic Accuracy: The STARD Initiative. *Clinical Biochemistry;* **Vol. 36,** p.1-7

M.L. Bouxsein and S.E. Radloff (1997) Quantitative Ultrasound of the Calcaneus Reflects the Mechanical Properties of Calcaneal Trabecular Bone. *Journal of Bone and Mineral Research;* **Vol. 12,** No. 5, p.839-846

M.L. Bouxsein, B.S. Coan and S.C. Lee (1999) Prediction of the Strength of the Elderly Proximal Femur by Bone Mineral Density and Quantitative Ultrasound Measurements of the Heel and Tibia. *Bone;* **Vol. 25,** No. 1, p.49-54

K. Brear, J.D. Currey, S. Raines et al. (1988) Density and Temperature Effects on Some Mechanical Properties of Cancellous Bone. *Engineering in Medicine;* **Vol. 17,** No. 4, p.163-167

K. Brooke-Wavell, P.R. Jones and D.W. Pye. (1995) Ultrasound and Dual X-ray Absorptiometry Measurement of the Calcaneus: Influence of Region of Interest Location. *Calcified Tissue International;* **Vol. 57,** No. 1, p.20-24

C.U. Brown, Y.N. Yeni and T.L. Norman. (2000) Fracture Toughness is Dependent on Bone Location- A Study of the Femoral Neck, Femoral Shaft, and the Tibial Shaft. *Journal of Biomedical Materials Research;* **Vol. 49,** p.380-389

J.P. Brown, P. Pollintine, D.E.Powell et al. (2002) Regional Differences in Mechanical and Material Properties of Femoral Head Cancellous Bone in Health and Osteoarthritis. *Calcified Tissue International;* **Vol. 71,** p.227-234

J.P. Brown and R.G. Josse. (2002) 2002 Clinical Guidelines for the Diagnosis and Management of Osteoporosis in Canada. *Canadian Medical Association Journal;* **Vol. 167,** (Suppl. 10), p.S1-S34

W.T. Butler (1984) Matrix Molecules of Bone and Dentin. *Collagen Related Research;* **Vol. 4,** p.297

S.M. Cadarette, S.B. Jaglal and T.M. Murray. (1999) Validation of the Simple Calculated Osteoporosis Risk Estimation (SCORE) for Patient Selection for Bone Densitometry. *Osteoporosis International;* **Vol. 10,** p.85-90.

S.M. Cadarette, S.B. Jaglal, N. Kreiger, et al. (2000) Development and Validation of the Osteoporosis Risk Assessment Instrument to Facilitate Selection of Women for Bone Densitometry. *Canadian Medical Association Journal;* **Vol. 162,** Issue 9: p.1289-1294.

S.M. Cadarette, S.B. Jaglal, T.M. Murray et al. (2001) Evaluation of Decision Rules for Referring Women for Bone Densitometry by Dual-Energy X-ray Absorptiometry. *JAMA;* **Vol. 286,** No.1, p.57-63

S.M. Cadarette, W.J. McIsaac, G.A. Hawker et al. (2004) The Validity of Decision Rules for Selecting Women with Primary Osteoporosis for Bone Mineral Density Testing. *Osteoporosis International;* **Vol. 15,** p.361-366

D.R. Carter and W.C. Hayes (1977) The Compressive Behaviour of Bone as a Two-Phase Porous Structure. *Journal of Bone and Joint Surgery;* **Vol. 59-A,** p.954-962

C.H.M. Castro, M.M. Pinheiro and V.L. Szejnfeld (2000) Quantitative Ultrasound of the Calcaneus in Brazilian Caucasian Women: Normative Data are Similar to the Manufacturer's Normal Range. *Osteoporosis International;* **Vol. 11,** p.923-928

C. Cepollaro, S. Gonnelli, C. Pondrelli et al. (1997) The Combined Use of Ultrasound and Densitometry in the Prediction of Vertebral Fracture. *The British Journal of Radiology;* **Vol. 70,** p.691-696

A. Çetin, H. Ertürk, R. Çeliker et al. (2001) The role of quantitative ultrasound in predicting osteoporosis defined by dual energy X-ray absorptiometry. *Rheumatology International;* **Vol. 20,** p.55-59

J. Chalmers and K.C. Ho (1970) Geographical Variations in Senile Osteoporosis. *The Journal of Bone and Joint Surgery (British Edition);* **Vol. 52B,** No. 4, p.667-675

C. Chappard, C. Berger, C. Roux et al. (1999) Ultrasound Measurement on the Calcaneus: Influence of Immersion Time and Rotation of the Foot. *Osteoporosis International;* **Vol. 9,** p.318-326

S. Cheng, B. Fan, L. Wang et al. (1999) Factors Affecting Broadband Ultrasound Attenuation Results of the Calcaneus Using a Gel-Coupled Quantitative Ultrasound Scanning System. *Osteoporosis International;* **Vol. 10,** p.495-504

K. Choi, J.L. Kuhn, M.J. Ciarelli et al. (1989) The Elastic Modulus of Trabecular, Subchondral, and Cortical Bone Tissue. *Transactions of the 35th Orthopaedic Research Society;* **Vol. 14,** p.102

K. Choi, J.L. Kuhn, M.J. Ciarelli et al. (1990) The Elastic Moduli of Human Subchondral Trabecular, and Cortical Bone Tissue and the Size-dependency of Cortical Bone Modulus. *Journal of Biomechanics;* **Vol. 23,** p.1103-1113

C. Christiansen (1995) Osteoporosis: Diagnosis and Management Today and Tomorrow. *Bone;* **Vol. 17,** No. 5, Supplement, p.513S-516S

T. Ciarelli, S.A. Goldstein, J.L. Kuhn et al. (1991) Evaluation of Orthogonal Mechanical Properties and Density of Human Trabecular Bone from the Major Metaphyseal Regions with Materials Testing and Computed Tomography. *Journal of Orthopaedic Research;* **Vol. 9,** No. 5, p.674-682

M.A. Cimmino and M. Parodi (2005) Risk Factors for Osteoarthritis. *Seminars in Arthritis and Rheumatism;* p.29-34

D. Coggon, I. Reading, P. Croft et al. (2001) Osteoarthritis and Obesity. *International Journal of Obesity and Related Metabolic Disorders;* **Vol.25,** p.622-627

J.E. Compston, C. Cooper and J.A. Kanis (1995) Fortnightly Review: Bone Densitometry in Clinical Practice. *British Medical Journal;* **Vol. 310,** p.1507-1510

J.D. Currey (1969) The Mechanical Consequences of Variation in the Mineral Content of Bone. *Journal of Biomechanics;* **Vol. 2,** No. 1-A, p.1-11

.L. Cunningham, J.N. Fordham, T.A. Hewitt et al. (1996) Ultrasound Velocity and Attenuation at Different Skeletal Sites Compared with Bone Mineral Density Measured Using Dual Energy X-ray Absorptiometry. *The British Journal of Radiology;* **Vol. 69,** p.25-32

J.D. Currey, K. Brear and P. Zioupos (1996) The Effects of Aging and Chnages in Mineral Content in Degrading the Toughness of Human Femora. *Journal of Biomechanics;* **Vol. 29,** No. 2, p.257-260

J.E. Damilakis, E. Dretakis and N.C. Gourtsoyiannis (1992) Ultrasound Attenuation of the Calcaneus in the Female Population: Normative Data. *Calcified Tissue International;* **Vol. 51,** No. 3, p.180-183

J. Damilakis, K. Perisinakis, E. Vagios et al. (1998) Effect of Region of Interest Location on Ultrasound Measurements of the Calcaneus. *Calcified Tissue International;* **Vol. 63,** p.300-305

J.E. Damilakis, K. Perisinakis and C. Gourtsoyiannis. (2001) Imaging Ultrasonometry of the Calcaneus: Optimum T-Score Thresholds for the Identification of Osteoporotic Subjects. *Calcified Tissue International;* **Vol. 68,** No. 4, p.219-224

J. Damilakis, G. Papadokostakis, H. Vrahoriti et al. (2003a) Ultrasound Velocity Through the Cortex of Phalanges, Radius, and Tibia in Normal and Osteoporotic

Postmenopausal Women Using a New Multisite Quantitative Ultrasound Device. *Investigative Radiology;* **Vol. 38,** No. 4, p.207-211

J. Damilakis, G. Papadokostakis, K. Perisinakis et al. (2003b) Can Radial Bone Mineral Density and Quantitative Ultrasound Measurements Reduce the Number of Women Who Need Axial Density Skeletal Assessment? *Osteoporosis International;* **Vol. 14,** p.688-693

J. Damilakis, G. Papadokostakis, K. Perisinakis, et al. (2004) Discrimination of Hip Fractures by Quantitative Ultrasound of the Phalanges and the Calcaneus and Dual X-Ray Absorptiometry. *European Journal of Radiology;* **Vol. 50,** p.268-272

A. Devine, I.M. Dick, S.S. Dhaliwal et al. (2005) Prediction of Incident Osteoporotic Fractures in Elderly Women Using the Free Estradiol Index. *Osteoporosis International;* **Vol. 16,** p.216-221

A. Díez-Pérez, F. Marín, J. Vila et al. (2003) Evaluation of Calcaneal Quantitative Ultrasound in a Primary Care Setting as a Screening Tool for Osteoporosis in Postmenopausal Women. *Journal of Clinical Densitometry;* **Vol. 6,** No. 3, p.237 - 245

M. Ding, M. Dalstra, C.C. Danielsen et al. (1997) Age Variations in the Properties of Human Tibial Trabecular Bone. *Journal of Bone And Joint Surgery (British Volume);* **Vol. 79,** No. 6, p.995-1002

J. Dow, G. Lindsay and J. Morrison (1996) Biochemistry: Molecules, Cells and the Body. Chapter 15: The Structural Tissues. Addison-Wesley Publishers Ltd. p.455-479

W.M. Drake, M. McClung, C.F. Njeh et al. (2001) Multisite Bone Ultrasound Measurement on North American Female Reference Population. *Journal of Clinical Densitometry;* **Vol. 4,** No. 3, p.239-248

B. Drozdzowska, W. Pluskiewicz and F. de Terlizzi (2003) The Usefulness of Quantitative Ultrasound at the Hand Phalanges in the Detection of the Different Types of Nontraumatic Fractures. *Ultrasound in Medicine and Biology;* **Vol. 29,** No. 11, p.1545-1550

E.F.L. Dubois, J.P.W. van den Bergh, A.G.H. Smals et al. (2001) Comparison of Quantitative Ultrasound Parameters with Dual Energy X-ray Absorptiometry in pre- and Postmenopausal Women. *The Netherlands Journal of Medicine;* **Vol. 58,** p.62-70

A. Ekman, K. Michaëlsson, M. Petrén-Mallmin et al. (2001) DXA of the Hip and Heel Ultrasound but not Densitometry of the Fingers can Discriminate Female Hip Fracture Patients from Controls: A Comparison Between Four Different Methods. *Osteoporosis International;* **Vol. 12,** p.185-191

A. Ekman, K. Michaëlsson, M. Petrén-Mallmin, et al. (2002) Dual X-ray Absorptiometry of Hip, Heel Ultrasound, and Densitometry of Fingers Can Discriminate Male Patients with Hip Fractures from Control Subjects. *Journal of Clinical Densitometry;* **Vol. 5,** No. 1, p.79-85

W.D. Evans, E.A. Jones and G.M. Owen (1995) Factors Affecting the In-vivo Precision of Broad-band Ultrasonic Attenuation. *Physics in Medicine and Biology;* **Vol. 40,** p.137-151

G.F. Falasca, C. Dunston and Y.A. Banglawala. (2003) Further Validation of a Questionnaire to Identify Women Likely to Have Low Bone Density. *Journal of Clinical Densitometry;* **Vol. 6,** Issue 3: p.231-236.

G. Falgarone, R. Porcher, A. Duché et al. (2004) Discrimination of Osteoporotic Patients with Quantitative Ultrasound Using Imaging or Non-Imaging Device. *Joint Bone Spine;* **Vol. 71,** p.419-423

K.G. Faulkner, M.R. McClung, L.J. Coleman et al. (1994) Comparison of Broadband Ultrasound Attenuation to Single X-ray Absorptiometry Measurements at the Calcaneus in Postmenopausal Women. *Calcified Tissue International;* **Vol. 54,** p.90-97

D.T. Felson, A. Naimark, J. Anderson et al. (1987) The Prevalence of Knee Osteoarthritis in the Elderly. The Framingham Osteoarthritis Study. *Arthritis and Rheumatism;* **Vol. 30,** p.914-918

G.P. Feltrin, M. Nardin, A. Marangon, et al. (2000) Quantitative Ultrasound at the Hand Phalanges: Comparison with Quantitative Computed Tomography of the Lumber Spine in Postmenopausal Women. *European Radiology;* **Vol. 10,** p.826-831

Z. Feng, J. Rho, S. Han et al. (2000) Orientation and Loading Condition Dependence of Fracture Toughness in Cortical Bone. *Materials Science and Engineering C;* **Vol. 11,** p.41-46

A. Fitzpatrick (2002) Secondary Causes of Osteoporosis. *Mayo Clinical Proceedings;* **Vol. 77,** p. 453-468

L.H. Follet, G. Boivin, C. Rumelhart et al. (2004) The Degree of Mineralization is a Determinant of Bone Strength: A Study of Human Calcanei. *Bone;* **Vol. 34,** p.783-789

M.L. Frost, G.M. Blake and I. Fogelman (1999) Contact Quantitative Ultrasound: An Evaluation of Precision, Fracture Discrimination, Age-Related Bone Loss and Applicability of the WHO Criteria. *Osteoporosis International;* **Vol. 10,** p.441-449

S. Fujiwara, N. Masunari, G. Suzuki et al. (2001) Performance of Osteoporosis Risk Indices in a Japanese Population. *Current Therapeutic Research;* **Vol. 62,** Issue 8: p.586-594

M. Funke, L. Kopka, R. Vosshenrich et al. (1995) Broadband Ultrasound Attenuation in the Diagnosis of Osteoporosis: Correlation with Osteodensitometry and Fracture. *Radiology;* **Vol. 194,** p.77-81

P. Garnero, O. Borel, E. Gineyts et al. (2005) Extracellular Post-Translational Modifications of Collagen are Major Determinants of Biomechanical Properties of Fetal Bovine Cortical Bone. *Bone;* **Article in Press**

P. Gerdhem, H. Magnusson, M.K. Karlsson et al. (2002) Ultrasound of the Phalanges is Not Related to a Previous Fracture. *Journal of Clinical Densitometry;* **Vol. 5,** No. 2, p.159-166

P. Geusens, M.C. Hochberg, D.J.M. van der Voort et al. (2002) Performance of Risk Indices for Identifying Low Bone Density in Postmenopausal Women. *Mayo Clinical Proceedings;* **Vol. 77,** p.629-637

P. Ghosh (2003) Osteoarthritis: 2002 and Beyond. *Asia Pacific League of Associations for Rheumatology;* **Vol. 6,** p.83-88

R. Giardino, R. Rotini, F. Noia et al. (2002) Phalangeal Ultrasonography in Forearm Fracture Discrimination. *Biomedicine and Pharmacotherapy,* **Vol. 56,** p.332-338

L.J. Gibson (1985) The Mechanical Behaviour of Cancellous Bone. *Journal of Biomechanics;* **Vol. 18,** No. 5, p.317-328

L.J. Gibson and M.F. Ashby (1997a) Cellular Solids: Structure and Properties. Chapter 11: Cancellous Bone. 2nd Edition, Cambridge University Press, p.429 – 452

L.J. Gibson and M.F. Ashby (1997b) Cellular Solids: Structure and Properties. Chapter 5: The Mechanics of Foams: Basic Results. 2nd Edition, Cambridge University Press, p.175-231

L.J. Gibson and M.F. Ashby (1997c) Cellular Solids: Structure and Properties. Chapter 10: Wood. 2nd Edition, Cambridge University Press, p.387-428

L.J. Gibson (2005) Biomechanics of Cellular Solids. *Journal of Biomechanics;* **Vol. 38,** p.377-399

E.B.W. Giesen, M. Ding, M. Dalstra et al. (2001) Mechanical Properties of Cancellous Bone in the Human Mandibular Condyle are Anisotropic. *Journal of Biomechanics;* **Vol. 34,** p.799-803

A.S. Glas, J.G. Lijmer, M.H. Prins et al. (2003) The Diagnostic Odd Ratios: A Single Indicator of Test Performance. *Journal of Clinical Epidemiology;* **Vol. 56,** p.1129-1135

C.-C. Glüer, C.Y. Wu and G.K. Genant (1993) Broadband Ultarsound Attenaution Signals Depend on Trabecular Orientation: An In Vitro Study. *Osteoporosis International;* **Vol. 3,** p.185-191

C.-C. Glüer, G.M. Blake, Y. Lu et al. (1995) Accurate Assessment of Precision Errors: How to Measure the Reproducibility of Bone Densitometry Techniques. *Osteoporosis International;* **Vol. 5,** No. 4, p.262-270

C.-C. Glüer, G.M. Blake, Y. Lu, et al. (1995) Accurate Assessment of Precision Errors: How to Measure the Reproducibility of Bone Densitometry Techniques. *Osteoporosis International;* **Vol. 5,** No. 4, p.262-270

C.-C. Glüer, R. Eastell, D.M. Reid et al. (2004) Association of Five Quantitative Ultrasound Devices ad Bone Densitometry with Osteoporotic Vertebral Fractures in a Population-Based Sample: The OPUS Study. *Journal of Bone and Mineral Research;* **Vol. 19,** No. 5, p.782-793

S. Gnudi and C. Ripamonti (2004) Quantitative Ultrasound at the Phalanxes Discriminates Osteoporotic Women with Vertebral but not with Hip Fracture. *Ultrasound in Medicine and Biology;* **Vol. 30,** No. 3, p.357-361

S. Gonnelli, C. Cepollaro, D. Agnussei et al. (1995) Diagnostic Value of Ultrasound Analysis and Bone Densitometry as Predictors of Vertebral Deformity in Postmenopausal Women. *Osteoporosis International;* **Vol. 5,** p.413-418

W.C. Graafmans, A.v. Lingen, M.E. Ooms et al. (1996) Ultrasound Measurements in the Calcaneus: Precision and its Relation with Bone Mineral Density of the Heel, Hip, and Lumbar Spine. *Bone;* **Vol. 19,** No. 2, p.97-100

S. Grampp, M. Jergas, C.-C. Glüer et al. (1993) Radiologic Diagnosis of Osteoporosis: Current Methods and Perspectives. *Endocrine Radiology;* **Vol. 31,** No. 5, p.1133-1145

S. Grampp, H.K. Genant, A. Mathur et al. (1997) Comparisons of Noninvasive Bone Mineral Measurements in Assessing Age-Related Loss, Fracture Discrimination and Diagnostic Classification. *Journal of Bone and Mineral Research;* **Vol. 12,** No. 5, p.697-711

T. Greenhalgh (1997) How to Read a Paper: Papers that Report Diagnostic or Screening Tests. *BMJ;* **Vol. 315,** p.540-543

S.L. Greenspan, M.L. Bouxsein, M.E. Melton et al. (1997) Precision and Discriminatory Ability of Calcaneal Bone Assessment Technologies. *Journal of Bone and Mineral Research;* **Vol. 12,** No. 8, p.1303-1313

S.L. Greenspan, S. Cheng, P.D. Miller et al. (2001) Clinical Performance of a Highly Portable, Scanning Calcaneal Ultrasonometer. *Osteoporosis International;* **Vol. 12,** p.391-398

D.A. Grimes and K.F. Schulz. (2002) Uses and Abuses of Screening Tests. *The Lancet;* **Vol. 359,** p.881-884

G. Guglielmi, C.F. Njeh, F. de Terlizzi, et al. (2003) Phalangeal Quantitative Ultrasound, Phalangeal Morphometric Variables, and Vertebral Fracture Discrimination. *Calcified Tissue International;* **Vol. 72,** p.469-477

P. Hadji, O. Hars, Chr. Wüster et al. (1999) Stiffness Index Identifies Patients with Osteoporotic Fractures Better Than Ultrasound Velocity or Attenuation Alone. *Maturitas;* **Vol. 31,** p.221-226

M.A. Hakulinen, J.S. Day, J. Töyräs et al. (2005) Prediction of Density and Mechanical Properties of Human Trabecular Bone in Vitro by Using Ultrasound Transmission and Backscattering Measurements at 0.2-6.7 MHz Frequency Range. *Physics in Medicine and Biology;* **Vol. 50,** p.1629-1642

S. Han, J. Medige and I. Ziv (1996b) Combined Models of Ultrasonic Velocity and Attenuation for Predicting Trabecular Bone Strength and Mineral Density. *Clinical Biomechanics;* **Vol. 11,** No. 6, p.348-353

S. Han, J. Medige, K. Faran et al. (1997) The ability of Quantitative Ultrasound to Predict The Mechanical Properties of Trabecular Bone Under Different Strain Rates. *Medical Engineering and Physics;* **Vol. 19,** No. 8, p.742-747

D. Hans, P. Dargent-Molina, A.M. Schott et al. (1996) Ultrasonographic Heel Measurements to Predict Hip Fracture in Elderly Women: The EPIDOS Prospective Study. *The Lancet;* **Vol. 348,** p.511-514

D. Hans, S.K. Srivastav, C. Singal et al. (1999a) Does Combining the Results from Multiple Bone Sites Measured by a New Quantitative Ultrasound Device Improve Discrimination of Hip Fracture? *Journal of Bone and Mineral Research;* **Vol. 14,** No. 4, p.644-651

D. Hans, C. Wu, C.F. Njeh et al. (1999b) Ultrasound Velocity of Trabecular Bone Cubes Reflects Mainly Bone Density and Elasticity. *Calcified Tissue International;* **Vol. 64,** p.18-23

D. Hans, F. Hartl and M.A. Krieg (2003) Device-Specific Weighted T-score for two Quantitative Ultrasounds: Operational Propositions for the Management of Osteoporosis for 65 Years and Older Women in Switzerland. *Osteoporosis International;* **Vol. 14,** p.251-258

F. Hartl, A. Tyndall, M. Kraenzlin et al. (2002) Discriminatory ability of Quantitative Ultrasound Parameters and Bone Mineral Density in a Population-Based sample of Postmenopausal Women with Vertebral Fractures: Results of the Basel Osteoporosis Study. *Journal of Bone and Mineral Research;* **Vol. 17,** No. 2, p.321-330

Y.Q. He, B. Fan, D. Hans et al. (2000) Assessment of a new Quantitative Ultrasound Calcaneus Measurement: Precision and Discrimination of Hip Fractures in Elderly Women Compared with Dual X-ray Absorptiometry. *Osteoporosis International;* **Vol. 11,** p.354-360

R.J.M. Herd, G.M. Blake, T. Ramalingam et al. (1993) Measurements of Postmenopausal Bone Loss with a New Contact Ultrasound System. *Calcified Tissue International;* **Vol. 53,** p.153-157

R.J.M. Herd, G.M. Blake, C.G. Miller et al. (1994) The Ultrasonic Assessment of Osteopenia as Defined by Dual X-ray Absorptiometry. *The British Journal of Radiology;* **Vol. 67,** No. 799: p.631-635

J.L. Hernández, F. Marin, J. González-Macías et al. Discriminative Capacity of Calcaneal Quantitative Ultrasound and of Fracture Risk Factors in Postmenopausal Women with Osteoporotic Fractures. *Calcified Tissue International;* **Vol. 74,** p.357-365

M.-C. Ho Ba Tho, J.Y. Rho and R.B. Ashman (1997) Anatomical Variation of Human Cancellous Bone Mechanical Properties In-Vitro. *Studies in Health Technology and Informatics;* **Vol. 40,** p.157-173

R. Hodgskinson, J.D. Currey and G.P. Evans (1989) Hardness as an Indicator of the Mechanical Competence of Cancellous Bone. *Journal of Orthopaedic Research;* **Vol. 7,** p.754-758

R. Hodgskinson and J.D. Currey (1990) The Effect of Variation in Structure on the Young's Modulus of Cancellous Bone: A Comparison of Human and Non-Human Material. *Proceedings of the Institution of Mechanical Engineers;* **Vol. 204,** Part H, p.115-121

R. Hodgskinson and J.D. Currey (1990) Effects Structural Variation on Young's Modulus of Non-Human Cancellous Bone. *Proceedings of the Institution of Mechanical Engineers;* **Vol.204,** Part H, p.43-52

R. Hodgskinson, C.F. Njeh, J.D. Currey et al. (1997) The Ability of Ultrasound Velocity to Predict the Stiffness of Cancellous Bone In Vitro. *Bone;* **Vol. 21,** No. 2, p.183-190

C.J. Hosie, D.A. Smith, A.D. Deacon et al. (1987) Comparison of Broadband Ultrasound Attenuation of the Os Calcis and Quantitative Computed Tomography of the Distal Radius. *Clinical Physiology and Physiological Measurements;* **Vol. 8**, p.303-308

F.J. Hou, S.M. Lang, S.J. Hoshaw et al. (1998) Human Vertebral Body Apparent and Hard Tissue stiffness. *Journal of Biomechanics;* **Vol. 31,** p.1009-1015

J.S. Huang and L.J. Gibson (1991a) Fracture Toughness of Brittle Honeycombs. *Acta Metallurgica et Materialia;* **Vol. 39,** No. 7, p.1617 – 1626

J.S. Huang and L.J. Gibson (1991b) Fracture Toughness of Brittle Foams. *Acta Metallurgica et Materialia;* **Vol. 39,** No. 7, p.1627 – 1636

J.S. Huand and M.S. Chaing (1996) Effects of Microstructure, Specimen and Loading Geometries on K_{IC} of Brittle Honeycombs. *Engineering Fracture Mechanics;* **Vol. 54,** No. 6, p.813-821

J. Huopio, H. Kröger, R. Honkanen et al. (2004) Calcaneal Ultrasound Predicts Early Postmenopausal Fractures as well as Axial BMD. A Prospective Study of 422 Women. *Osteoporosis International;* **Vol. 15,** p.190-195

I. Hvid, N.C. Jensen, C. Bünger et al. (1985) Bone Mineral Assay: Its Relation to the Mechanical Strength of Cancellous Bone. *Engineering in Medicine;* **Vol. 14,** No. 2, p.79-83

I. Hvid, S.M. Bentzen, F. Linde (1989) X-Ray Quantitative Computed Tomography: The Relations to Physical Properties of Proximal Tibial Trabecular Bone Specimens. *Journal of Biomechanics;* **Vol. 22,** No. 8/9, p.837-844

A.A. Ismail, S.R. Pye, W.C. Cockerill et al. (2002) Incidence of Limb Fracture across Europe: Results from the European Prospective Osteoporosis Study (EPOS). *Osteoporosis International;* **Vol. 13,** p.565-571

M. Ito, A. Nishida, J. Kono et al. (2003) Which Bone Densitometry and Which Skeletal Site are Clinically Useful for Monitoring Bone Mass? *Osteoporosis International;* **Vol. 14,** p.959-964

K.S. Jensen, L. Mosekilde and L. Mosekilde (1990) A Model of Vertebral Trabecular Bone Architecture and its Mechanical Properties. *Bone;* **Vol. 11,** p.417-423

M. Jergas and H.K. Genant (1993) Current Methods and Recent Advances in the Diagnosis of Osteoporosis. *Arthritis and Rheumatism;* **Vol. 36,** No. 12, p.1649-1662

A. Johansen and M.D. Stone (1997) The Effect of Ankle Oedema on Bone Ultrasound Assessment at the Heel. *Osteoporosis International;* **Vol. 7,** p.44-47

A. Johansen, W. Evans and M. Stone. (1999) Bone Assessment In Elderly Women: What Does A Low Bone Ultrasound Result Tell Us About Bone Mineral Density? *Archives of Gerontology and Geriatrics;* **Vol. 28,** No. 3, p.239-246

J. Joly, R. Westhovens, H. Borghs et al. (1999) Reference Curve and Diagnostic Sensitivity for a New Ultrasound Device for the Phalanges, the DBMsonic 1200, in Belgian Women. *Osteoporosis International;* **Vol. 9,** p.284-289

J.M. Jordan, G. Luta, J.B. Renner et al. (1996) Ethnic Differences in Self-reported Functional Status in the Rural South: The Johnston County Osteoarthritis Project. *Arthritis Care and Research;* **Vol. 9,** p.483-491

J.M. Jordan, J.B. Renner, G. Luta et al. (1997) Hip Osteoarthritis Is Not Rare In African-Americans And Is Different Than In Caucasians. *Arthritis and Rheumatism;* **Vol. 40,** Suppl: S236

H.L. Jørgensen and C. Hassager (1997) Improved Reproducibility of Broadband Ultrasound Attenuation of the OS Calcis by using a Specific Region of Interest. *Bone;* **Vol. 21,** No. 1, p.109-112

H.L. Jørgensen, L. Warming, N.H. Bjarnason et al. (2001) How Does Quantitative Ultrasound Compare to Dual X-Ray Absorptiometry at Various Skeletal in Relation to the WHO Diagnosis Categories. *Clinical Physiology;* **Vol. 21,** No. 1, p.51-59

T.S. Kaneko, J.S. Bell, M.R. Pejcic et al. (2004) Mechanical Properties, Density and Quantitative CT Scan Data of Trabecular Bone with and without Metastases. *Journal of Biomechanics;* **Vol. 37,** p.523-530

J.A. Kanis, L.J. Melton, C. Christiansen et al. (1994) The Diagnosis of Osteoporosis. *The Journal of Bone and Mineral Research;* **Vol. 9,** p.1137-1141

J.A. Kanis (2002) Diagnosis of Osteoporosis and Assessment of Fracture Risk. *The Lancet;* **Vol. 359,** p.1929-1936

J.A. Kanis, E. Seeman, O. Johnell et al. (2005) The Perspective of The International Osteoporosis Foundation on The Official Positions of The International Society for Clinical Densitometry. *Osteoporosis International* **(Article In Press.)**

J.A. Kanis, F. Borgstrom, C. De Laet et al. (2005) Assessment of Fracture Risk. *Osteoporosis International;* **Vol.16,** p.581-589

S.J. Kaplan, W.C. Hayes and J.L. Stone (1985) Tensile Strength of Bovine Trabecular Bone. *Journal of Biomechanics;* **Vol. 18,** No. 9, p.723-727

M.K. Karlsson, Y. Duan, H. Ahlborg et al. (2001) Age, Gender, and Fragility Fractures are Associated with Differences in Quantitative Ultrasound Independent of Bone Mineral Density. *Bone;* **Vol. 28,** No. 1, p.118-122

J.J. Kaufman and T.A. Einhorn (1993) Ultrasound Assessment of Bone. *Journal of Bone and Mineral Research;* **Vol. 8,** No. 5, p.517-525

T.M. Keaveny, R.E. Borchers, L.J. Gibson et al. (1993) Trabecular Bone Modulus and Strength can Depend on Specimen Geometry. *Journal of Biomechanics;* **Vol. 26,** No. 8, p.991-1000

T.M. Keaveny, X.E. Guo, E.F. Wachtel et al. (1994a) Trabecular Bone Exhibits Fully Linear Elastic Behaviour and Yields at Low Strains. *Journal of Biomechanics;* **Vol. 27,** No. 9, p.1127-1136

T.M. Keaveny, E.F. Wachtel, C.M. Ford et al. (1994b) Differences Between the Tensile and Compressive Strengths of Bovine Tibial Trabecular Bone Depend on Modulus. *Journal of Biomechanics;* **Vol. 27,** No. 9, p.1137-1146

T.M. Keaveny, T.P. Pinilla, R.P. Crawford et al. (1997) Systemic and Random Errors in Compression Testing of Trabecular Bone. *Journal of Orthopaedic Research;* **Vol. 15,** p.101-110

T.M. Keaveny, E.F. Morgan, G.L. Niebur et al. (2001) Biomechanics of Trabecular Bone. *Annual Review of Biomedical Engineering;* **Vol. 3,** p.307-333

T.S. Keller (1994) Predicting the Compressive Mechanical Behaviour of Bone. *Journal of Biomechanics;* **Vol. 27,** No. 9, p.1159-1168

C.K. Kee (2000) Osteoarthritis: Manageable Scourge of Aging. *Rheumatology;* **Vol. 35,** p.199-208

R. Kent and J. Patrie (2005) Chest Deflection To Blunt Anterior Trauma Loading Is Sensitive To Age But Not To Load Distribution. *Forensic Science International;* **Vol. 149,** p.121-128

J.H. Keyak, I.Y. Lee and H.B. Skinner (1994) Correlations between Orthogonal Mechanical Properties and Density of Trabecular Bone: Use of Different Densitometric Measures. *Journal of Biomedical Materials Research;* **Vol. 28,** p.1329-1336

K.-T. Khaw, J. Reeve, R. Luben et al. (2004) Prediction of Total and Hip Fracture Risk in Men and Women by Quantitative Ultrasound of the Calcaneus: EPIC-Norfolk Prospective Population Study. *The Lancet;* **Vol. 363,** p.197-202

H. Kikugawa and T. Asaka. (2004) Effect of Long-Term Formalin Preservation on Bending Properties and Fracture Toughness of Bovine Compact Bone. *Materials Transactions;* **Vol. 45,** No. 10, p.3060-3064

K.I.I. Kim, I.-K. Han, H. Kim et al. (2001) How Reliable is the Ultrasound Densitometer for Community Screening to Diagnose Osteoporosis in Spine, Femur, and Forearm? *Journal of Clinical Densitometry;* **Vol. 4**, No. 2, p.159-165

K.M. Knapp, G.M. Blake, T.D. Spector et al. (2001) Multisite Quantitative Ultrasound: Precision, Age- and Menopause-Related Changes, Fracture Discrimination, and T-score Equivalence with Dual-Energy X-ray Absorptiometry. *Osteoporosis International;* **Vol. 12,** p.456-464

K.M. Knapp, G.M. Blake, T.D. Spector et al. (2002) Multisite Quantitative Ultrasound: Colles' Fracture Discrimination in Postmenopausal Women. *Osteoporosis International;* **Vol. 13,** p.474-479

K.M. Knapp, G.M. Blake, T.D. Spector et al. (2004) Can the WHO Definition of Osteoporosis be Applied to Multi-site Axial Transmission Quantitative Ultrasound? *Osteoporosis International;* **Vol. 15,** p.367-374

L. Knott and A.J. Bailey (1998) Collagen Cross-Links in Mineralizing Tissues: A Review of Their Chemistry, Function and Clinical Relevance. *Bone;* **Vol. 22,** No.3, p.181-187

L.K.H. Koh and D.C.E. Ng (2002) Osteoporosis risk factor assessment and Bone densitometry – Current Status and Future Trends. *Annals Academy of Medicine Singapore;* **Vol. 31,** Issue 1, p.37-42

L.K.H. Koh, W.B. Sedrine, T.P. Torralba et al. (2001) A Simple Tool to Identify Asian Women at Increased Risk of Osteoporosis. *Osteoporosis International;* **Vol. 12,** p.699-705

D.L. Kopperdahl and T.M. Keaveny (1998) Yield Strain Behaviour of Trabecular Bone. *Journal of Biomechanics;* **Vol. 31,** p.601-608

C.R. Krestan, S. Grampp, A. Resch-Holeczke et al. (2001) Diagnostic Disagreement of Imaging Quantitative Sonography of the Calcaneus with Dual X-ray Absorptiometry of the Spine and Femur. *American Journal of Roentgen;* **Vol. 177,** p.213-216

M.A. Krieg, J. Cornuz, C. Ruffieux et al. (2003) Comparison of Three Bone Ultrasounds for the Discrimination of Subjects with and Without Osteoporotic Fractures among 7562 Elderly Women. *Journal of Bone and Mineral Research;* **Vol. 18,** No. 7, p.1261-1266

H. Kröger, J. Jurvelin, I. Arnala et al. (1995) Ultrasound Attenuation of the Calcaneus in Normal Subjects and in Patients with Wrist Fracture. *Acta Orthopaedica Scandinavica;* **Vol. 66,** No. 1, p.47-52

J.L. Ku, S.A. Goldstein, K.W. Choi (1987) The Mechanical Properties of Single Trabeculae. *Transactions of the 33rd Orthopaedic Research Society;* **Vol. 12,** p.48

J.L. Kuhn, S.A. Goldstein, K.W. Choi (1989) Comparison of the Trabecular and Cortical Tissue Moduli from Human Iliac Crests. *Journal of Orthopaedic Research;* **Vol. 7,** p.876-884

A.W.C. Kung, A.Y.Y. Ho, W.B. Sedrine et al. (2003) Comparison of a Simple Clinical Risk Index and Quantitative Bone Ultrasound for Identifying Women at Increased Risk of Osteoporosis. *Osteoporosis International;* **Vol. 14,** p.716-721

A.J. Ladd, J.H. Kinney, D.L. Haupt et al. (1998) Finite-element Modeling of Trabecular Bone: Comparison with Mechanical Testing and Determination of Tissue Modulus. *Journal of Orthopaedic Research;* **Vol. 16,** p.622-628

C.M. Langton, S.B. Palmer, R.W. Porter (1984) The Measurement of Broadband Ultrasound Attenuation in Cancellous Bone. *Engineering in Medicine;* **Vol.13,** p.89-91

C.M. Langton, C.F. Njeh, R. Hodgskinson et al. (1996) Prediction of Mechanical Properties of the Human Calcaneus by Broadband Ultrasound Attenuation. *Bone;* **Vol. 18,** No. 6, p.495-503

C.M. Langton, P.A. Ballard, D.K. Langton et al. (1997) Maximising the Cost Effectiveness of BMD Referral for DXA using Ultrasound as a Selective Population Pre-screen. *Technology and Health Care;* **Vol. 5,** p.235-241

C.M. Langton and C.F. Njeh (1999) Acoustic and Ultrasonic Tissue Characterization – Assessment of Osteoporosis. *Proceedings of the Institution of Mechanical Engineers;* Part H, **Vol. 213,** p.261-269

C.M. Langton, D.K. Langton and S.A. Beardsworth (1999) Comparison of Accuracy and Cost Effectiveness of Clinical Criteria and BUA for Referral for BMD Assessment by DXA in Osteoporotic and Osteopenic Perimenopausal Subjects. *Technology and Health Care;* **Vol. 7,** p.319-330

P. Laugier (2004) An Overview of Bone Sonometry. *International Congress Series;* **Vol.1274,** p.23-32

S.C. Lee, B.S. Coan and M.L. Bouxsein (1997) Tibial Ultrasound Velocity Measured In Situ Predicts the Material Properties of Tibial Cortical Bone. *Bone;* **Vol. 21,** No. 1, p.119-125

B. Lees and J.C. Stevenson (1993) Preliminary Evaluation of a New Ultrasound Bone Densitometer. *Calcified Tissue International;* **Vol. 53,** p.149-152

I. Lernbass, A. Wutzl, J. Grisar et al. (2002) Quantitative Ultrasound in the Assessment of Bone Status of Patients Suffering from Rheumatic Diseases. *Skeletal Radiology;* **Vol. 31,** p.270-276

E. Lespessailles, A. Jullien, E. Eynard et al. (1998) Biomechanical properties of human os calcanei: relationships with bone density and fractal evaluation of bone microarchitecture. *Journal of Biomechanics;* **Vol. 31,** p.817-824

E.M. Lewiecki, D.L. Kendler, G.M. Kiebzak et al. (2004) Special Report on the official positions of the International Society for clinical Densitometry. *Osteoporosis International;* **Vol.15,** p.779-784

B. Li and R.M. Aspden (1997a) Composition and Mechanical Properties of Cancellous Bone from the Femoral Head of Patients with Osteoporosis and Osteoarthritis. *Journal of Bone and Mineral Research;* **Vol. 12,** No. 4, p.641-651

B. Li and R.M. Aspden (1997b) Mechanical and Material Properties of the Subchondral Bone Plate from the Femoral Head of Patients with Osteoarthritis or Osteoporosis. *Annals of the Rheumatic Diseases;* **Vol. 56,** p.247-254

B. Li and R.M. Aspden (1997c) Material Properties of Bone frome the Femoral Neck and Calcar Femorale of Patients with Osteoporosis and Osteoarthritis. *Osteoporosis International;* **Vol. 7,** p.450-456

B. Li, D. Marshall, M. Roe et al. (1999) The Electron Microscopic Appearance of the Subchondral Bone Plate in the Human Femoral Head in Osteoarthritis and Osteoporosis. *Journal of Anatomy;* **Vol. 195,** p.101-110

A.M. Lievense, S.M. Bierma-Zeinstra, A.P. Verhagen et al. (2002) Influence of Obesity on the Development of Osteoarthritis of the Hip: A Systemic Review. *Rheumatology;* **Vol. 41,** p.1155-1165

F. Linde, C.B. Gøthgen, I. Hvid et al. (1988) Mechanical Properties of Trabecular Bone by a Non-destructive Compression Testing Approach. *Engineering in Medicine;* **Vol. 17,** No. 1, p.23-29

F. Linde and I. Hvid. (1989) The Effect of Constraint on the Mechanical Behaviour of Trabecular Bone Specimens. *Journal of Biomechanics;* **Vol. 22,** No. 5, p.485-490

F. Linde, I. Hvid and B. Pongsoipetch. (1989) Energy Absorptive Properties of Human Trabecular Bone Specimens during Axial Compression. *Journal of Orthopaedic Research;* **Vol. 7,** No. 3, p.432-439

F. Linde, B. Pongsoipetch, L.H. Frich et al. (1990) Three-Axial Strain Controlled Testing Applied to Bone Specimens from the Proximal Tibial Epiphysis. *Journal of Biomechanics;* **Vol. 22,** No. 11, p.1167-1172

F. Linde, P. Nørgaard, I. Hvid et al. (1991) Mechanical Properties of Trabecular Bone. Dependency on Strain Rate. *Journal of Biomechanics;* **Vol. 24,** No. 9, p.803-809

F. Linde, I. Hvid and F. Madsen (1992) The Effect of Specimen Geometry on the Mechanical Behaviour of Trabecular Bone Specimens. *Journal of Biomechanics;* **Vol. 25,** No. 4, p.359-368

F. Linde (1994) Elastic and Viscoelastic Properteis of Trabecular Bone by a Compression Testing Approach. *Danish Medical Bulletin;* **Vol. 41,** No. 2, p.119-138

E.-M. Lochmüller, F. Eckstein, D. Kaiser et al. (1998) Prediction of Vertebral Failure Loads From Spinal and Femoral Dual-Energy X-ray Absorptiometry, and Calcaneal Ultrasound: An In Situ Analysis with Intact Soft Tissues. *Bone;* **Vol. 23,** No. 5, p.417-424

E.-M. Lochmüller, R. Müller, V. Kuhn et al. (2003) Can Novel Densitometric Techniques Replace or Improve DXA in Predicting Bone Strength in Osteoporosis at the Hip and Other Skeletal Sites? *Journal of Bone and Mineral Research;* **Vol. 18,** No. 5, p.906-912

F. López-Rodríguez, P. Mezquita-Raya, J. de Dois Luna et al. (2003) Performance of Quantitative Ultrasound in the Discrimination of Prevalent Osteoporotic Fractures in a Bone Metabolic Unit. *Bone;* **Vol. 32,** p.571-578

S.K. Maiti, M.F. Ashby and L.J. Gibson (1984) Fracture Toughness of Brittle Cellular Solids. *Scripta Metallurgica;* **Vol. 18,** p.213-217

C.L. Malik, S.M. Stover, R.B. Martin et al. (2003) Equine Cortical Bone Exhibits Rising R-Curve Fracture Mechanics. *Journal of Biomechanics;* **Vol. 36,** p.191-198

J.P. Mansell and A.J. Bailey (1998) Abnormal Cancellous Bone Collagen Metabolism in Osteoarthritis. *Journal of Clinical Investigation;* **Vol. 101,** p.1596-1603

J.P. Mansell and A.J. Bailey (2003) Increased Metabolism of Bone Collagen in Post-Menopausal Female Osteoporotic Femoral Heads. *The International Journal of Biochemistry and Cell Biology;* **Vol. 35,** p.522-529

F. Marín, J. López-Bastida, A. Díez-Pérez et al. (2004) Bone Mineral Density Referral for Dual-Energy X-ray Absorptiometry Using Quantitative Ultrasound as a Prescreening Tool in Postmenopausal Women from the General Population: A Cost-Effectiveness Analysis. *Calcified Tissue International;* **Vol. 74,** p.277-283

J.C. Martin and D.M. Reid (1996) Appendicular Measurements in Screening Women for Low Axial Bone Mineral Density. *The British Journal of Radiology;* **Vol. 69,** p.234-240

A. Massie, D.M. Reid and R.W. Porter. (1993) Screening for Osteoporosis: Comparison between Dual Energy X-Ray Absorptiometry and Broadband Ultrasound Attenuation in 1000 Perimenopausal Women. *Osteoporosis International;* **Vol. 3,** p.107-110

R.W. McCalden, J.A. McGeough and C.M. Court-Brown (1997) Age-Related Changes in The Compressive Strength of Cancellous Bone. *The Journal of Bone and Mineral Research;* **Vol. 79-A,** No. 3, p.421-427

E.V. McCloskey, S.A. Murray, C. Miller, et al. (1990) Broadband Ultrasound Attenuation in the Os Calcis: Relationship to Bone Mineral at Other Skeletal Sites. *Clinical Science;* **Vol. 78,** p.227-233

P.L. Mente and J.L. Lewis (1987) Young's Modulus of Trabecular Bone Tissue. *Transactions of the Orthopaedic Research Society;* **Vol. 12,** p. 49

P.L. Mente and J.L. Lewis (1989) Experimental Method for the Measurement of the Elastic Modulus of Trabecular Bone Tissue. *Journal of Orthopaedic Research;* **Vol. 7,** p.456-461

K. Michaëlsson, R. Bergström, H. Mallmin et al. (1996a) Screening for Osteopenia and Osteoporosis: Selection by Body Composition. *Maturitas;* **Vol. 25,** p.79

K. Michaëlsson, R. Bergström, H. Mallmin et al. (1996b) Screening for Osteopenia and Osteoporosis: Selection by Body Composition. *Osteoporosis International;* **Vol. 6,** Issue 2, p.120-126

S. Minisola, R. Rossa, A. Scarda et al. (1995) Quantitative Ultrasound Assessment of Bone in Patients with Primary Hyperparathyroidism. *Calcified Tissue International;* **Vol. 56,** p.526-528

A. Montagnani, S. Gonnelli, C. Cepollaro et al. (2001) Usefulness of Bone Quantitative Ultrasound in Management of Osteoporosis in Men. *Journal of Clinical Densitometry;* **Vol. 4,** No. 3, p.231-237

E.F. Morgan, H.H. Bayraktar and T.M. Keaveny (2003) Trabecular Bone Modulus-Density Relationships Depend on Anatomic Site. *Journal of Biomechanics;* **Vol. 36,** p.897-904

E.F. Morgan and T.M. Keaveny (2001) Dependence of Yield Strain of Human Trabecular Bone on Anatomic Site. *Journal of Biomechanics;* **Vol. 34,** p.569-577

M. Moris, A. Peretz, R. Tjeka et al. (1995) Quantitative Ultrasound Bone Measurements: Normal Values and Comparison with Bone Mineral Density by Dual X-ray Absorptiometry. *Calcified Tissue International;* **Vol. 576,** p.6-10

L. Mosekilde, A. Viidik and L. Mosekilde. (1985) Correlation between the Compressive Strength of Iliac and Vertebral Trabecular Bone in Normal Individuals. *Bone;* **Vol. 6,** No. 5, p.291-295

L. Mosekilde, L. Mosekilde and C.C. Danielsen (1987) Biomechanical competence of vertebral trabecular bone in relation to ash density and age in normal individuals. *Bone;* **Vol. 8,** No. 2, p.79-85.

R.F. Mould (1998) Introduction to Medical Statistics, 3rd Edition. Institute of Physics Publishing, Bristol and Philadelphia.

A. Nafei, C.C. Danielsen, F. Linde et al. (2000) Properties of Growing Ovine Bone: Part I: Mechanical and Physical Properties. *Journal of Bone and Joint Surgery;* **Vol. 82,** No. 6, p.910-921

V. Naganathan, L. March, D. Hunter et al. (1999) Quantitative Heel Ultrasound as a Predictor for Osteoporosis. *The Medical Journal of Australia;* **Vol. 171,** p.297-300

R.K. Nalla, J.J. Kruzic, J.H. Kinney et al. (2004) Effect of Aging on the Toughness of Human Cortical Bone: Evaluation by R-Curves. *Bone;* **Vol. 35,** p.1240-1246

National Osteoporosis Foundation (2003) Physician's guide to prevention and Treatment of Osteoporosis. National Osteoporosis Foundation, Washington D.C.

National Osteoporosis Society (2005) Position Statement on the Reporting of Dual Energy X-ray Absorptiometry (DXA) Bone Mineral Density Scans. National Osteoporosis Society, Bath

National Osteoporosis Society (2002) Use of Quantitative Ultrasound in the Management of Osteoporosis. National Osteoporosis Society, Bath

T.V. Nguyen, J.R. Center and J.A. Eisman (2004) Bone Mineral Density-Independent Association of Quantitative Ultrasound Measurements and Fracture Risk in Women. *Osteoporosis International;* **Vol. 15,** p.942-947

C.F. Njeh, C.W. Kuo, C.M. Langton et al. (1997) Prediction of Human Femoral Bone Strength Using Ultrasound Velocity and BMD: An in Vitro Study. *Osteoporosis International;* **Vol. 7,** p.471-477

C.F. Njeh, D. Hans, J. Li et al. (2000) Comparison of Six Calcaneal Quantitative Ultrasound Devices: Precision and Hip Fracture Discrimination. *Osteoporosis International;* **Vol. 11,** p.1051-1062

C.F. Njeh, C. Wu, B. Fan et al. (2000b) Estimation of Wrist Fracture Load Using Phalangeal Speed of Sound: An In Vitro Study. *Ultrasound in Medicine and Biology;* **Vol. 26,** No. 9, p.1517-1523

C.F. Njeh, M.B. Chen, B. Fan et al. (2001) Evaluation of a Gel-Coupled Quantitative Ultrasound Device for Bone Status Assessment. *Journal of Ultrasound in Medicine;* **Vol. 20,** p.1219-1228

T.L. Norman, D. Vashishth and D.B. Burr (1992) Effect of Groove on Bone Fracture Toughness. *Journal of Biomechanics;* **Vol. 25,** No. 12, p.1489-1492

T.L. Norman, S.V. Nivargikar and D.B. Burr. (1996) Resistance to Crack Growth in Human Cortical Bone is Greater in Shear than in Tension. *Journal of Biomechanics;* **Vol. 29,** No. 8, p.1023-1031

A. Odgaard, I. Hvid and F. Linde (1989) Compressive axial strain distributions in cancellous bone specimens. *Journal of Biomechanics;* **Vol. 22,** No. 8-9, p.829-835

A. Odgaard and F. Linde. (1991) The Underestimation of Young's Modulus in Compressive Testing of Cancellous Bone Specimens. *Journal of Biomechanics;* **Vol. 24,** No. 8, p.691-698

H. Oxlund, L. Mosekilde and G. Ørtoft (1996) Reduced Concentration of Collagen Reducible Cross Links in Human Trabecular Bone with Respect to Age and Osteoporosis. *Bone;* **Vol. 19,** No. 5, p.479-484

S. Palacios, C. Menendez, J. Calderon et al. (1993) Spine and Femur Density and Broadband Ultrasound Attenuation of the Calcaneus in Normal Spanish Women. *Calcified Tissue International;* **Vol. 52,** p.99-102

C.D. Papaloucas, R.J. Ward, C.J. Tonkin et al. (2005) Cancellous Bone Changes in Hip Osteoarthritis: A Short-term Longitudinal Study Using Fractal Signature Analysis. *Osteoarthritis and Cartilage;* **Vol. 13,** p.998-1003

H.M. Park, W.B. Sedrine, J.Y. Reginster et al. (2003) Korean Experience with the OSTA Risk Index for Osteoporosis. *Journal of Clinical Densitometry;* **Vol. 6,** Issue 3, p.247-250

E.P. Paschalis, E. Stone, G. Lyritis et al. (2004) Bone Fragility and Collagen Cross-Links. *Journal of Bone and Mineral Research;* **Vol. 19,** No. 12, p.2000-2004

J.B. Phelps, G.B. Hubbard, X.D. Wang et al. (2000) Microstructural Heterogeneity and the Fracture Toughness of Bone. *Journal of Biomedical Materials Research;* **Vol. 51,** p.735-741

M.M. Pinheiro, C.H.M. Castro, A. Frisoli Jr. et al. (2003) Discriminatory Ability of Quantitative Ultrasound Measurements is Similar to Dual-Energy X-ray Absorptiometry in a Brazilian Women Population With Osteoporotic Fractures. *Calcified Tissue International;* **Vol. 73,** p.555-564

S.M.F. Pluijm, W.C. Graafmans, L.M. Bouter et al. (1999) Ultrasound Measurements for the Prediction of Osteoporotic Fractures in Elderly People. *Osteoporosis International;* **Vol. 9,** p.550-556

N.A. Pocock (1998) Quantitative Diagnostic Methods in Osteoporosis: A Review. *Australasian Radiology;* **Vol. 42,** p.327-334

V. Poll, C. Cooper and M.I.D. Cawley (1986) Broadband Ultrasound Attenuation in the Os Calcis and Single Photon Absorptiometry in the Distal Forearm: A Comparative Study. *Clinical Physiology and Physiological Measurements;* **Vol. 7,** p.375-379

S.H. Prins, J. Lauritzenm H.L. Jørgensen et al. (1999) Hip Fracture Discrimination by Imaging Ultrasound Measurements of the Calcaneus. *Clinical Physiology;* **Vol. 19,** No. 5, p.419-425

J.W. Pugh, R.M. Rose and E.L. Radin (1973) Elastic and Viscoelastic Properties of Trabecular Bone: Dependence on Structure. *Journal of Biomechanics;* **Vol. 6,** p.475-485

J.Y. Reginster, M. Dethor, H. Pirenne et al. (1998) Reproducibility and Diagnostic Sensitivity of Ultrasonometry of the Phalanges to Assess Osteoporosis. *International Journal of Gynecology and Obstetrics;* **Vol. 63,** p.21-28

J.Y. Reginster, W.B. Sedrine, P. Viethel et al. (2004) Validation of OSIRIS, a Prescreening Tool for the Identification of Women with an Increased Risk of Osteoporosis. *Gynecological Endocrinology;* **Vol. 18,** Issue 1, p.3-8

D.M. Reid and J. Harvie (1997) Secondary Osteoporosis. Baillière's Clinical *Endocrinology and Metabolism;* **Vol. 11,** No. 1, p.83-99

H. Resch, P. Pietschmann, P. Bernecker et al. (1990) Broadband Ultrasound Attenuation: A New Diagnostic Method in Osteoporosis. *American Journal of Roentgenology;* **Vol.155,** No. 4, p.825-828

J.-Y. Rho, R.B. Ashman and C.H. Turner (1993) Young's Modulus of Trabecular and Cortical Bone Material: Ultrasonic and Microtensile Measurements. *Journal of Biomechanics;* **Vol. 26,** No. 2, p.111-119

J.-Y. Rho, L. Kuhn-Spearing and P. Zioupos (1998) Mechanical Properties and the Hierarchical Structure of Bone. *Medical Engineering and Physics;* **Vol. 20,** p.92-102

J.-Y. Rho, M.E. Roy II, T.Y. Tsui et al. (1999) Elastic Properties of Microstructural Components of Human Bone Tissue as Measured by Nanoindentation. *Journal of Biomedical Materials Research;* **Vol. 44,** p.1-7

J.Y. Rho, P. Zioupos, J.D. Currey et al. (2002) Microstructural elasticity and regional heterogeneity in human femoral bone of various ages examined by nano-indentation. *Journal of Biomechanics;* **Vol. 35,** p.189-198

J.R. Rice (1968) A Path Independent Integral and the Approximate Analysis of Strain Concentration by Notches and Cracks. *Journal of Applied Mechanics;* **Vol. 35,** p.379-386

F. Richy, M. Gourlay, P.D. Ross et al. (2004) Validation and Comparative Evaluation of the Osteoporosis Self-Assessment Tool (OST) in a Caucasian Population from Belgium. *Quarterly Journal of Medicine;* **Vol. 97,** Issue 1, p.39-46

B.L. Riggs and L.J. Melton (1986) Involutional Osteoporosis. *New England Journal of Medicine;* **Vol. 314,** p.1676-1686

B.L. Riggs and L.J. Melton (1992) The Prevention and Treatment of Osteoporosis. *New England Journal of Medicine;* **Vol. 327,** p.620-627

L. Røhl, E. Larsen, F. Linde et al. (1991) Tensile and Compressive Properties of Cancellous Bone. *Journal of Biomechanics;* **Vol. 24,** No. 12, p.1143-1149

L. Rosenthall, A. Tenenhouse and J. Caminis (1995) A Correlative Study of Ultrasound Calcaneal and Dual-Energy X-Ray Absorptiometry Bone Measurements of the Lumbar Spine and Femur in 1000 Women. *European Journal of Nuclear Medicine;* **Vol. 22,** No. 5, p.402-406

P. Ross, C. Huang, J. Davis et al. (1995) Predicting Vertebral Deformity Using Bone Densitometry at Various Skeletal Sites and Calcaneus Ultrasound. *Bone;* **Vol. 16,** No. 3, p.325-332

P. Rossman, J. Zagzebski, C. Mesina et al. (1989) Comparison of Speed of Sound and Ultrasound Attenuation in the Os Calcis to Bone Density of the Radius, Femur

and Lumbar Spine. *Clinical Physiology and Physiological Measurement;* **Vol. 10,** p.353-360

J.C. Runkle and J. Pugh (1975) The Micro-mechanics of Cancellous Bone Tissue. *Bull. Hosp. J. Dis;* **Vol. 36,** p.2-10

A.S. Russell and R.T. Morrison (2001) An Assessment of the New "SCORE" index as a predictor of Osteoporosis in Women. *Scandinavian Journal of Rheumatology;* **Vol. 30,** p.35-39

L.M. Salamone, E.Q. Krall, S. Harris et al. (1994) Comparison of Broadband Ultrasound Attenuation to Single X-ray Absorptiometry Measurements at the Calcaneus in Postmenopausal Women. *Calcified Tissue International;* **Vol. 54,** p.90-97

M.M.A. Saleh, H.L. Jøgensen and J.B. Lauritzen (2002) Odds Ratios for Hip- and Lower Forearm Fracture Using Peripheral Bone Densitometry; A Case-Control Study of Postmenopausal Women. *Clinical Physiology and Functional Imaging;* **Vol. 22,** No. 1, p.58-63

C.M. Schoenfeld, E.P. Lautenschlager and P.R. Meyer. (1974) Mechanical Properties of Human Cancellous Bone in the Femoral Head. *Medical and Biological Engineering;* **Vol. 12,** No. 3, p.313-317

J. Schneider, B. Bundschuh, C. Späth et al. (2004) Discrimination of Patients with and Without Vertebral Fractures as Measured by Ultrasound and DXA Osteodensitometry. *Calcified Tissue International;* **Vol. 74,** p.246-254

A.M. Schott, S. Weill-Engerer, D. Hans et al. (1995) Ultrasound discriminates patients with hip fracture equally well as dual energy X-ray absorptiometry and

independently of bone mineral density. *Journal Of Bone And Mineral Research;* **Vol. 10,** No. 2, p.243-249

W.B. Sedrine, T. Chevallier, B. Zegels et al. (2002) Development and Assessment of the Osteoporosis Index of Risk (OSIRIS) to Facilitate Selection of Women for Bone Densitometry. *Gynecological Endocrinology;* **Vol. 16,** p.245-250

W.B. Sedrine, J.P. Devogelaer, J.M. Kaufman et al. (2001) Evaluation of the Simple Calculated Osteoporosis Risk Estimation (SCORE) in a Sample of White Women from Belgium. *Bone;* **Vol. 29,** Issue 4, p.374-380

J.E. Shea and S.C. Miller (2005) Skeletal Function and Structure: Implications for Tissue-Targeted Therapeutics. *Advanced Drug Delivery Reviews;* **Vol. 57,** p.945-957

M.F.V. Sim, M.D. Stone, C.J. Phillips et al. (2005) Cost Effectiveness Analysis of using Quantitative Ultrasound as a Selective Pre-screen for Bone Densitomtery. *Technology and Health Care;* **Vol. 13,** p.75-85

T.J. Sims, N.C. Avery and A.J. Bailey (2000) Quantitative Determination of Collagen Cross-links. In Methods in Molecular Biology, Vol.139: Extracellular Matrix Protocols, Ed. C.H. Streuli and M.E. Grant, Humana Press p.11-27

H.A. Sørensen, N.R. Jørgensen, J.-E.B. Jeńsen et al. (2001) Comparison of Quantitative Ultrasound and Dual X-ray Absorptiometry in Estrogen-Treated Early Postmenopausal Women. *Journal of Clinical Densitometry;* **Vol. 4,** No. 2, p.97-104

M. Sosa, P. Saavedra and M. Muñoz-Torres et al. (2002) Quantitative Ultrasound Calcaneus Measurements: Normative Data and Precision in the Spanish Population. *Osteoporosis International;* **Vol. 13,** p.487-492

M.D. Stefano and G.C. Isaia (2002) Ability of Ultrasound Bone Profile Score (UBPS) to Discriminate Between Fractured and Not Fractured Osteoporotic Women. *Ultrasound in Medicine and Biology;* **Vol. 28,** No. 11/12, p.1485-1489

A. Stewart, D.M. Reid and R.W. Porter (1994) Broadband Ultrasound Attenuation and Dual Energy X-ray Absorptiometry in Patients with Hip Fractures: Which Technique Discriminates Fracture Risk? *Calcified Tissue International;* **Vol. 54,** p.466-469

A. Stewart, D.J. Torgerson and D.M. Reid (1996) Prediction of Fractures in Perimenopausal Women: A Comparison of Dual Energy X-ray Absorptiometry and Broadband Ultrasound Attenuation. *Annals of Rheumatic Diseases;* **Vol. 55,** p.140-142

A. Stewart and D.M. Reid (2000a) Precision of Quantitative Ultrasound: Comparison of Three Commercial Scanners. *Bone;* **Vol. 27,** No. 1, p.139-143

A. Stewart and D.M. Reid (2000b) Quantitatiev Ultrasound or Clinical Risk Factors – Which Best Identifies Women at Risk of Osteoporosis? *The British Journal of Radiology;* **Vol. 73,** p.165-171

J.L. Stone, G.S. Beaupre and W.C. Hayes (1983) Multiaxial Strength Characteristics of Trabecular Bone. *Journal of Biomechanics;* **Vol. 16,** p.743-752

T. Stürmer, K.-P Günther and H. Brenner (2000) Obesity, Overweight and Patterns of Osteoarthritis: The Ulm Osteoarthritis Study. *Journal of Clinical Epidemiology;* **Vol. 53,** p.307-313

H. Sugita, M. Oka, J. Toguchida et al. (1999) Anisotropy of Osteoporotic Cancellous Bone. *Bone;* **Vol. 24,** No. 5, p.513-516

G.D. Summers (2001) Osteoporosis in Men. *Radiography;* **Vol. 7,** p.119-123

Y. Tanabe and W. Bonfield. (1999) Effects of Initial Crack Length and Specimen Thickness on Fracture Toughness of Compact Bone. *JSME International Journal,* Series C; **Vol. 42,** 3, p.532-538

P.R. Townsend and R.M. Rose (1975) Buckling Studies of Single Human Trabeculae. *Journal of Biomechanics;* **Vol. 8,** p.199-201

A.M. Tromp, J.H. Smit, D.J.H. Deeg et al. (1999) Quantitative Ultrasound Measurements of the Tibia and Calcaneus in Comparison with DXA Measurements at Various Skeletal Sites. *Osteoporosis International;* **Vol. 9,** p.230-235

J.G. Truscott, M. Simpson, S.P. Stewart et al. (1992) Bone Ultrasonic Attenuation in Women: Reproducibility, Normal Variation and Comparison with Photon Absorptiometry. *Clinical Physiology And Physiological Measurements;* **Vol. 13,** p.29-36

E. Tsuda-Futami, D. Hans, C.F. Njeh et al. (1999) An Evaluation of a New Gel-coupled Ultrasound Device for the Quantitative Assessment of Bone. *The British Journal of Radiology;* **Vol. 72,** p.691-700

C.H. Turner (1989) Yield Behaviour of Bovine Cancellous Bone. *Journal of Biomechanical Engineering;* **Vol. 111,** No. 3, p.256-260

C.H. Turner and D.B. Burr (1993) Basic Biomechanical Measurements of Bone: A Tutorial. *Bone;* **Vol. 14,** p.595-608

C.H. Turner, M. Peacock, L. Timmerman et al. (1995) Calcaneal Ultrasonic Measurements Discriminate Hip Fracture Independently of Bone Mass. *Osteoporosis International;* **Vol. 5,** p.130-135

C.H. Turner, J.-Y. Rho, Y. Takano et al. (1999) The Elastic Properties of Trabecular and Cortical Bone Tissues are Similar: Results form Two Microscopic Measurement Techniques. *Journal of Biomechanics;* **Vol. 32,** p.437-441

D. Ulrich, T. Hildebrand, B. van Rietbergen et al. (1997) The Quality of Trabecular Bone Evaluated with Micro-computed Tomography, FEA and Mechanical Testing. *Studies in Health Technology and Informatics;* **Vol. 40,** p.97-112

W.J. Ungar, R. Josse, S. Lee et al. (2000) The Canadian SCORE™ Questionnaire. *Journal of Clinical Densitometry;* **Vol. 3,** Issue 3, p.269-280

D. Vanderschueren, S. Boonen and R. Bouillon (2000) Osteoporosis and Osteoporotic Fractures in Men: A Clinical Perspective. *Baillière's Clinical Endocrinology and Metabolism;* **Vol. 12,** No. 2, p.299-315

D. Vashishth (2004) Rising Crack-Growth-Resistance Behaviour in Cortical Bone: Implications for Toughness Measurements. *Journal of Biomechanics;* **Vol. 37,** p.943-946

D. Von Mühlen, A.V. Lunde, E. Barrett-Connor et al. (1999) Evaluation of the Simple Calculated Osteoporosis Risk Estimation (SCORE) in Older Caucasian Women: The Rancho Bernardo Study. *Osteoporosis International;* **Vol. 10,** p.79-84

L.S. Wallace, J.E. Ballard, D. Holiday et al. (2004) Evaluation of Decision Rules for Identifying Low Bone Density in Postmenopausal African-American Women. *Journal Of The National Medical Association;* **Vol. 96,** No. 3, p.290-296

X. Wang, J. Lankford and C.M. Agrawal (1994) Use of a Compact Sandwich Specimen to Evaluate Fracture Toughness and Interfacial Bonding Of Bone. *Journal of Applied Biomaterials;* **Vol. 5,** p.315-323

X. Wang and C.M. Agrawal (1996) Fracture Toughness of Bone Using a Compact Sandwich Specimen: Effects of Sampling Sites and Crack Orientations. *Journal of Biomedical Materials Research;* **Vol. 33,** p.13-21

X. Wang, R.A. Bank, J.M. TeKoppele et al. (2001) The Role of Collagen in Determining Bone Mechanical Properties. *Journal of Orthopaedic Research;* **Vol. 19,** p.1021-1026

X. Wang, X. Shen and C.M. Agrawal (2002) Age-Related Changes in the Collagen Network and Toughness of Bone. *Bone;* **Vol. 31,** No. 1, p.1-7

M. Weiss, A.B. Ben-Shlomo, P. Hagag et al. (2000) Reference Database for Bone Speed of Sound Measurements by a Novel Quantitative Multi-site Ultrasound Device. *Osteoporosis International;* **Vol. 11,** p.688-696

J.L. Williams and J.L. Lewis (1982) Properties and an Anisotropic Model of Cancellous Bone from the Proximal Tibial Epiphysis. *Journal of Biomechanical Engineering,* **Vol. 104,** p.50-56

R.L. Wixson, N. Elasky and J. Lewis. (1989) Cancellous Bone Material Properties in Osteoarthritic and Rheumatoid Total Knee Patients. *Journal of Orthopaedic Research;* **Vol. 7,** No. 6, p.885-892

World Health Organisation (1994) Assessment of Fracture Risk and its Application to Screening for Postmenopausal Osteoporosis. Technical Report Series 843, WHO, Geneva.

C. Wu, D. Hans, Y. He et al. (2000) Prediction of Bone Strength of Distal Forearm Using Radius Bone Mineral Density and Phalangeal Speed of Sound. *Bone;* **Vol. 26,** No. 5, p.529-533

C. Wüster, C. Albanese, D. De Aloysio et al. (2000) Phalangeal Osteosonogrammetry Study: Age-Related Changes, Diagnostic Sensitivity, and Discrimination Power. *Journal of Bone and Mineral Research;* **Vol. 15,** No. 8, p.1603-161

H. Young, S. Howey and D.W. Purdie. Broadband Ultrasound Attenuation Compared with Dual-Energy X-ray Absorptiometry in Screening for Postmenopausal Low Bone Density. *Osteoporosis International;* **Vol. 3,** p.160-164

P. Zioupos and J.D. Currey (1998) Changes in the Stiffness, Strength and Toughness of Human Cortical Bone with Age. *Bone;* **Vol. 22,** No. 1, p.57-66

P. Zioupos, J.D. Currey and A.J. Hamer (1999) The Role of Collagen in the Declining Mechanical Properties of Aging Human Cortical Bone. *Journal of Biomedical Materials Research;* **Vol. 45,** p.108-116

P. Zioupos, C.W. Smith and Y.H. An (2000) Mechanical Testing of Bone and the Bone-Implant Interface. Chapter 4: Factors Affecting Mechanical Properties of Bone. Edited by Y.H.An and R.A.Draughn. CRC Press LLC, p.65-86

P. Zioupos (2005) In-Vivo Fatigue Microcracks in Human Bone: Material Properties of the Surrounding Bone Matrix. *European Journal of Morphology;* **Vol. 42,** No. 1/2, p. 31-41